U.S. Department of Transportation
Federal Highway Administration

Publication No. FHWA NHI-06-089
December 2006

NHI Course No. 132012

SOILS AND FOUNDATIONS

Reference Manual – Volume II

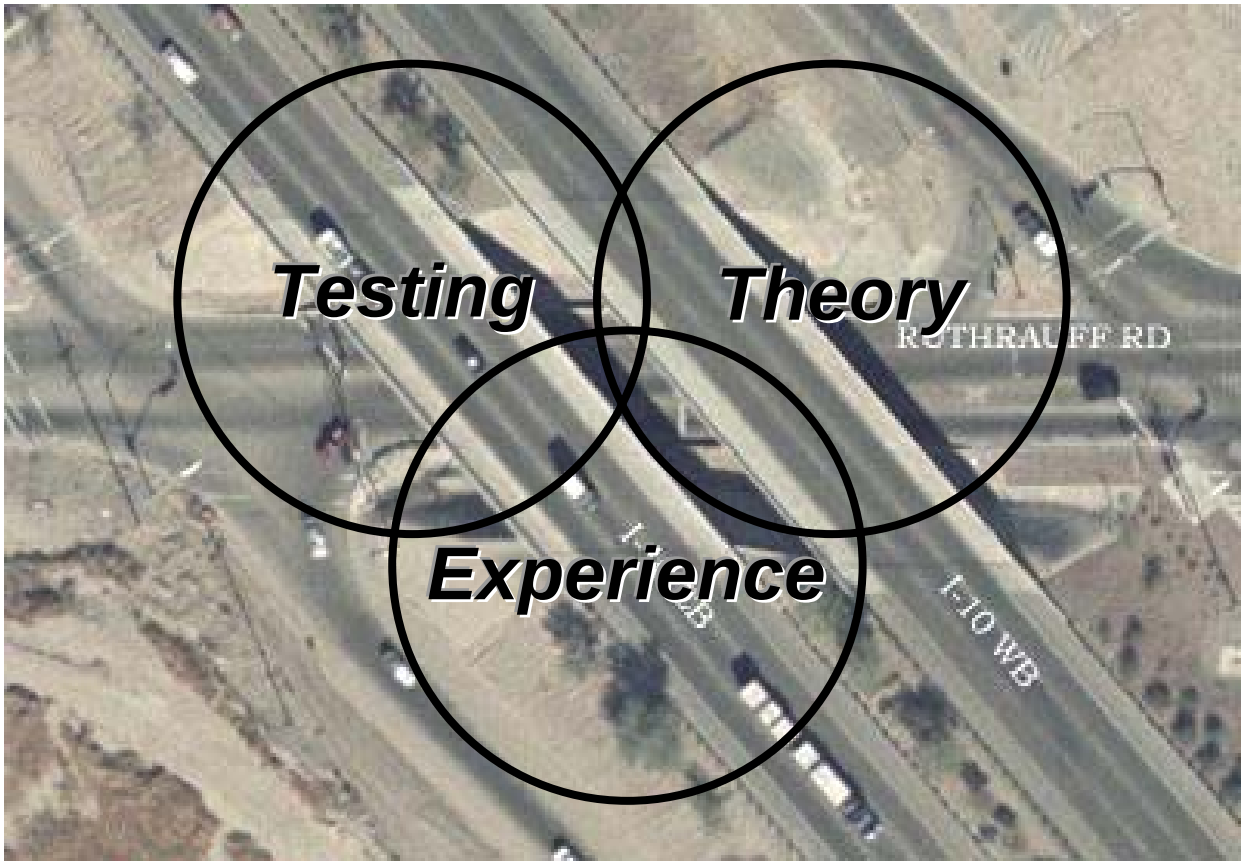

National Highway Institute

NOTICE

Technical Report Documentation Page

1. Report No.	2. Government Accession No.	3. Recipient's Catalog No.
FHWA-NHI–06-089		

4. Title and Subtitle	5. Report Date
SOILS AND FOUNDATIONS REFERENCE MANUAL – Volume II	December 2006 6. Performing Organization Code
7. Author(s) Naresh C. Samtani*, PE, PhD and Edward A. Nowatzki*, PE, PhD	8. Performing Organization Report No.
9. Performing Organization Name and Address Ryan R. Berg and Associates, Inc. 2190 Leyland Alcove, Woodbury, MN 55125 * NCS GeoResources, LLC 640 W Paseo Rio Grande, Tucson, AZ 85737	10. Work Unit No. (TRAIS) 11. Contract or Grant No. DTFH-61-02-T-63016
12. Sponsoring Agency Name and Address National Highway Institute U.S. Department of Transportation Federal Highway Administration, Washington, D.C. 20590	13. Type of Report and Period Covered 14. Sponsoring Agency Code

15. Supplementary Notes

FHWA COTR – Larry Jones

FHWA Technical Review – Jerry A. DiMaggio, PE; Silas Nichols, PE; Richard Cheney, PE; Benjamin Rivers, PE; Justin Henwood, PE.

Contractor Technical Review – Ryan R. Berg, PE; Robert C. Bachus, PhD, PE; Barry R. Christopher, PhD, PE

This manual is an update of the 3rd Edition prepared by Parsons Brinckerhoff Quade & Douglas, Inc, in 2000. Author: Richard Cheney, PE. The authors of the 1st and 2nd editions prepared by the FHWA in 1982 and 1993, respectively, were Richard Cheney, PE and Ronald Chassie, PE.

16. Abstract

The Reference Manual for Soils and Foundations course is intended for design and construction professionals involved with the selection, design and construction of geotechnical features for surface transportation facilities. The manual is geared towards practitioners who routinely deal with soils and foundations issues but who may have little theoretical background in soil mechanics or foundation engineering. The manual's content follows a project-oriented approach where the geotechnical aspects of a project are traced from preparation of the boring request through design computation of settlement, allowable footing pressure, etc., to the construction of approach embankments and foundations. Appendix A includes an example bridge project where such an approach is demonstrated. Recommendations are presented on how to layout borings efficiently, how to minimize approach embankment settlement, how to design the most cost-effective pier and abutment foundations, and how to transmit design information properly through plans, specifications, and/or contact with the project engineer so that the project can be constructed efficiently.

The objective of this manual is to present recommended methods for the safe, cost-effective design and construction of geotechnical features. Coordination between geotechnical specialists and project team members at all phases of a project is stressed. Readers are encouraged to develop an appreciation of geotechnical activities in all project phases that influence or are influenced by their work.

17. Key Words	18. Distribution Statement
Subsurface exploration, testing, slope stability, embankments, cut slopes, shallow foundations, driven piles, drilled shafts, earth retaining structures, construction.	No restrictions.

19. Security Classif. (of this report)	20. Security Classif. (of this page)	21. No. of Pages	22. Price
UNCLASSIFIED	UNCLASSIFIED	594	

Form DOT F 1700.7(8-72) Reproduction of completed page authorized

[THIS PAGE INTENTIONALLY BLANK]

PREFACE

This update to the Reference Manual for the Soils and Foundations course was developed to incorporate the guidance available from the FHWA in various recent manuals and Geotechnical Engineering Circulars (GECs). The update has evolved from its first two versions prepared by Richard Cheney and Ronald Chassie in 1982 and 1993, and the third version prepared by Richard Cheney in 2000.

The updated edition of the FHWA Soils and Foundations manual contains an enormous amount of information ranging from methods for theoretically based analyses to "rules of thumb" solutions for a wide range of geotechnical and foundation design and construction issues. It is likely that this manual will be used nationwide for years to come by civil engineering generalists, geotechnical and foundation specialists, and others involved in transportation facilities. That being the case, the authors wish to caution against indiscriminate use of the manual's guidance and recommendations. The manual should be considered to represent the minimum standard of practice. The user must realize that there is no possible way to cover all the intricate aspects of any given project. Even though the material presented is theoretically correct and represents the current state-of-the-practice, engineering judgment based on local conditions and knowledge must be applied. This is true of most engineering disciplines, but it is especially true in the area of soils and foundation engineering and construction. For example, the theoretical and empirical concepts in the manual relating to the analysis and design of deep foundations apply to piles installed in the glacial tills of the northeast as well as to drilled shafts installed in the cemented soils of the southwest. The most important thing in both applications is that the values for the parameters to be used in the analysis and design be selected by a geotechnical specialist who is intimately familiar with the type of soil in that region and intimately knowledgeable about the regional construction procedures that are required for the proper installation of such foundations in local soils.

General conventions used in the manual

This manual addresses topics ranging from fundamental concepts in soil mechanics to the practical design of various geotechnical features ranging from earthworks (e.g., slopes) to foundations (e.g., spread footings, driven piles, drilled shafts and earth retaining structures). In the literature each of these topics has developed its own identity in terms of the terminology and symbols. Since most of the information presented in this manual appears in other FHWA publications, textbooks and publications, the authors faced a dilemma on the regarding terminology and symbols as well as other issues. Following is a brief discussion on such issues.

- **Pressure versus Stress**

  The terms “pressure” and “stress” both have units of force per unit area (e.g., pounds per square foot). In soil mechanics “pressure” generally refers to an applied load distributed over an area or to the pressure due to the self-weight of the soil mass. “Stress,” on the other hand, generally refers to the condition induced at a point within the soil mass by the application of an external load or pressure. For example, “overburden pressure,” which is due to the self weight of the soil, induces “geostatic stresses” within the soil mass. Induced stresses cause strains which ultimately result in measurable deformations that may affect the behavior of the structural element that is applying the load or pressure. For example, in the case of a shallow foundation, depending upon the magnitude and direction of the applied loading and the geometry of the footing, the pressure distribution at the base of the footing can be uniform, linearly varying, or non-linearly varying. In order to avoid confusion, the terms “pressure” and “stress” will be used interchangeably in this manual. In cases where the distinction is important, clarification will be provided by use of the terms “applied” or “induced.”

- **Symbols**

  Some symbols represent more than one geotechnical parameter. For example, the symbol C_c is commonly used to identify the coefficient of curvature of a grain size distribution curve as well as the compression index derived from consolidation test results. Alternative symbols may be chosen, but then there is a risk of confusion and possible mistakes. To avoid the potential for confusion or mistakes, the Table of Contents contains a list of symbols for each chapter.

- **Units**

  English units are the primary units in this manual. SI units are included in parenthesis in the text, except for equations whose constants have values based on a specific set of units, English or SI. In a few cases, where measurements are conventionally reported in SI units (e.g., aperture sizes in rock mapping), only SI units are reported. English units are used in example problems. Except where the units are related to equipment sizes (e.g., drill rods), all unit conversions are “soft,” i.e., approximate. Thus, 10 ft is converted to 3 m rather than 3.05 m. The soft conversion for length in feet is rounded to the nearest 0.5 m. Thus, 15 ft is converted to 4.5 m not 4.57 m.

- **Theoretical Details**

  Since the primary purpose of this manual is to provide a concise treatment of the fundamental concepts in soil mechanics and an introduction to the practical design of various geotechnical features related to highway construction, the details of the theory underlying the methods of analysis have been largely omitted in favor of discussions on the application of those theories to geotechnical problems. Some exceptions to this general approach were made. For example, the concepts of lateral earth pressure and bearing capacity rely too heavily on a basic understanding of the Mohr's circle for stress for a detailed presentation of the Mohr's circle theory to be omitted. However, so as not to encumber the text, the basic theory of the Mohr's circle is presented in Appendix B for the reader's convenience and as an aid for the deeper understanding of the concepts of earth pressure and bearing capacity.

- **Standard Penetration Test (SPT) N-values**

  The SPT is described in Chapter 3 of this manual. The geotechnical engineering literature is replete with correlations based on SPT N-values. Many of the published correlations were developed based on SPT N-values obtained with cathead and drop hammer methods. The SPT N-values used in these correlations do not take in account the effect of equipment features that might influence the actual amount of energy imparted during the SPT. The cathead and drop hammer systems typically deliver energy at an estimated average efficiency of 60%. Today's automatic hammers generally deliver energy at a significantly higher efficiency (up to 90%). When published correlations based on SPT N-values are presented in this manual, they are noted as N_{60}-values and the measured SPT N-values should be corrected for energy before using the correlations.

  Some researchers developed correction factors for use with their SPT N-value correlations to address the effects of overburden pressure. When published correlations presented in this manual are based upon values corrected for overburden they are noted as $N1_{60}$. Guidelines are provided as to when the N_{60}-values should be corrected for overburden.

- **Allowable Stress Design (ASD) and Load and Resistance Factor Design (LRFD) Methods**

  The design methods to be used in the transportation industry are currently (2006) in a state of transition from ASD to LRFD. The FHWA recognizes this transition and has developed separate comprehensive training courses for this purpose. Regardless of whether the ASD or LRFD is used, it is important to realize that the fundamentals of soil mechanics, such as the

determination of the strength and deformation of geomaterials do not change. The only difference between the two methods is the way in which the uncertainties in loads and resistances are accounted for in design. Since this manual is geared towards the fundamental understanding of the behavior of soils and the design of foundations, ASD has been used because at this time most practitioners are familiar with that method of design. However, for those readers who are interested in the nuances of both design methods Appendix C provides a brief discussion on the background and application of the ASD and LRFD methods.

ACKNOWLEDGEMENTS

The authors would like to acknowledge the following events and people that were instrumental in the development of this manual.

- Permission by the FHWA to adapt the August 2000 version of the Soils and Foundations Workshop Manual.

- Provision by the FHWA of the electronic files of the August 2000 manual as well as other FHWA publications.

- The support of Ryan R. Berg of Ryan R. Berg and Associates, Inc. (RRBA) in facilitating the preparation of this manual and coordinating reviews with the key players.

- The support provided by the staff of NCS Consultants, LLC, (NCS) - Wolfgang Fritz, Juan Lopez and Randy Post (listed in alphabetical order of last names). They prepared some graphics, some example problems, reviewed selected data for accuracy with respect to original sources of information, compiled the Table of Contents, performed library searches for reference materials, and checked internal consistency in the numbering of chapter headings, figures, equations and tables.

- Discussions with Jim Scott (URS-Denver) on various topics and his willingness to share reference material are truly appreciated. Dov Leshchinsky of ADAMA Engineering provided copies of the ReSSA and FoSSA programs which were used to generate several figures in the manual as well as presentation slides associated with the course presentation. Robert Bachus of Geosyntec Consultants prepared Appendices D and E. Allen Marr of GeoComp Corporation provided photographs of some laboratory testing equipment. Pat Hannigan of GRL Engineers, Inc. reviewed the driven pile portion of Chapter 9. Shawn Steiner of ConeTec, Inc. and Salvatore Caronna of gINT Software prepared the Cone Penetration Test (CPT) and boring logs, respectively, shown in Chapter 3 and Appendix A. Robert (Bob) Meyers (NMDOT), Ted Buell (HDR-Tucson) and Randy Simpson (URS-Phoenix) provided comments on some sections (particularly Section 8.9).

- Finally, the technical reviews and recommendations provided by Jerry DiMaggio, Silas Nichols, Benjamin Rivers, Richard Cheney (retired) and Justin Henwood of the FHWA, Ryan Berg of RRBA, Robert Bachus of GeoSyntec Consultants, Jim Scott of URS, and Barry Christopher of Christopher Consultants, Inc., are gratefully acknowledged.

SPECIAL ACKNOWLEDGEMENTS

A special acknowledgement is due of the efforts of Richard Cheney and Ronald Chassie for their work in the preparation of the previous versions of this manual. It is their work that made this course one of the most popular FHWA courses. Their work in developing this course over the past 25 years is acknowledged.

With respect to this manual, the authors wish to especially acknowledge the in-depth review performed by Jerry DiMaggio and time he spent in direct discussions with the authors and other reviewers. Such discussions led to clarification of some existing guidance in other FHWA manuals as well as the introduction of new guidance in some chapters of this manual.

SI CONVERSION FACTORS				
APPROXIMATE CONVERSIONS FROM SI UNITS				
Symbol	**When You Know**	**Multiply By**	**To Find**	**Symbol**
LENGTH				
mm	millimeters	0.039	inches	in
m	meters	3.28	feet	ft
m	meters	1.09	yards	yd
Km	kilometers	0.621	miles	mi
AREA				
mm^2	square millimeters	0,0015	square inches	in^2
m^2	square meters	10.758	square feet	ft^2
m^2	square meters	1.188	square yards	yd^2
ha	hectares	2.47	acres	ac
km^2	square kilometers	0.386	square miles	mi^2
VOLUME				
ml	milliliters	0.034	fluid ounces	fl oz
l	liters	0.264	gallons	gal
m^3	cubic meters	35.29	cubic feet	ft^3
m^3	cubic meters	1.295	cubic yards	yd^3
MASS				
g	grams	0.035	ounces	oz
kg	kilograms	2.205	pounds	lb
Tones	tonnes	1.103	US short tons	tons
TEMPERATURE				
ºC	Celsius	1.8ºC + 32	Fahrenheit	ºF
WEIGHT DENSITY				
kN/m^3	kilonewtons / cubic meter	6.36	Pound force / cubic foot	pcf
	FORCE and PRESSURE or STRESS			
N	newtons	0.225	pound force	lbf
kN	kilonewtons	225	pound force	lbf
kPa	kilopascals	0.145	pound force / square inch	psi
kPa	kilopascals	20.88	pound force / square foot	psf
PERMEABILITY (VELOCITY)				
cm/sec	centimeter/second	1.9685	feet/minute	ft/min

[THIS PAGE INTENTIONALLY BLANK]

SOILS AND FOUNDATIONS
VOLUME II

TABLE OF CONTENTS

LIST OF FIGURES

LIST OF TABLES

LIST OF SYMBOLS

Chapter 8

A	Angular distortion
A'	Effective footing area
AASHTO	American Association of State Highway and Transportation Officials
ASD	Allowable stress design
B	Width
B'_f	Effective footing width
b_c, b_γ, b_q	Base inclination correction factors
B_f	Footing width
B_f*	Modified footing width for bearing capacity analysis of footings on sands
c	Cohesion of soil
c*	Reduced effective cohesion for punching shear
C_1	Correction factor for embedment depth
C_2	Correction factor for time-dependent settlement increase
C_c	Compression indices
C_d	Shape and rigidity factors
$C_{w\gamma}$, C_{wq}	Groundwater correction factors
D_f	Depth of embedment
D_I	Maximum depth of strain influence
D_{IP}	Depth to maximum strain influence factor
DL	Dead load
d_o	Depth of influence of footing
DOSI	Depth of Significant Influence
d_q	Embedment depth correction factor
D_r	Relative density of sand
D_w	Depth of water table
E	Elastic modulus of soil
e_B	Eccentricity in direction of footing width
e_L	Eccentricity in direction of footing length
E_m	Young's modulus of rock mass
e_o	Initial void ratio
f	Lateral extent of influence of footing
FD	Foundation design specialist
FHWA	Federal Highway Administration
FS	Factor of safety
ft	Foot
GT	Geotechnical specialist
H_c	Thickness of soil layer considered
IGM	Intermediate geomaterial
I_z	Strain influence factor
I_{ZB}	Strain influence factor at footing elevation
I_{ZP}	Maximum strain influence factor
kPa	Kilopascal
L	Length

L'_f	Effective footing length
L_f	Footing length
LL	Live load
LRFD	Load resistance factor design
MPa	Megapascal
MSE	Mechanically stabilized earth
n	Number of soil layers
N	SPT blow count value
$N1_{60}$	SPT blow count corrected for depth and hammer efficiency
N_c, N_q, N_γ	Bearing capacity factors
N_{cq}, $N_{\gamma q}$	Bearing capacity factors modified for sloping ground surface
N_s	Slope stability factor
OCR	Overconsolidation ratio
P	Applied footing load
p_o	Effective overburden pressure
p_{op}	effective stress at depth of peak strain influence factor
psf	Pounds per square foot
q	Uniform surcharge pressure at the base of the footing
q_{all}	Allowable bearing capacity
q_{eq}	Equivalent uniform bearing pressure
q_{max}	Maximum bearing pressure under the footing
q_{min}	Minimum bearing pressure under the footing
$q_{ult\ gross}$	Gross ultimate bearing capacity
$q_{ult\ net}$	Net ultimate bearing capacity
q_{ult}	Ultimate bearing capacity
RQD	Rock quality designation
S	Settlement
S, 2S, 3S	Settlement contours
s_c, s_q, s_γ	Shape correction factors
S_i	Settlement of i-th soil layer
SL	Distance between adjacent foundations (span length)
SLS	Serviceability limit state
S_t	Sensitivity of clay
ST	Structural specialist
t	time
tsf	Tons per square foot
ULS	Ultimate limit state
X	Modification factor for determination of elastic modulus
z_i	Depth to soil layer i
α	Footing inclination from horizontal
γ	Unit weight of soil
γ'	Effective unit weight of soil
γ_a	Unit weight of soil above the footing
γ_b	Submerged unit weight of soil
δ	Differential settlement
δ_v	Vertical settlement at surface

ΔH	Consolidation settlement
ΔH_i	Settlement factor for soil layer i
Δp	Net load intensity at foundation depth
ν	Poisson's ratio
ϕ	Angle of internal friction
ϕ^*	Reduced effective soil friction angle for punching shear
ϕ'	Effective angle of internal friction

Chapter 9

A	Cross-sectional area of the pile
AASHTO	American Association of State Highway and Transportation Officials
A_p	Cross-sectional area of an unplugged pile
API	American Petroleum Institute
a_s	Acceleration of the drilled corresponding to F_{so}
A_s	Shaft surface area
ASD	Allowable stress design
A_{si}	Pile interior surface area
ASTM	American Society for Testing and Materials
A_t	Pile toe area
A_t	Tip area of rock socket
b	Pile diameter or width
B	Width of the pile group
BPF	Blows per foot
C	Wave propagation velocity of pile material
c_a	Pile adhesion
C_d	Pile perimeter at depth d
C_F	Correction factor for K_δ when $\delta \neq \phi$
CIDH	Cast-in-drilled hole
CIP	Cast-in-place
COR	Coefficient of restitution
cps	counts per second
CPT	Cone penetration test
CSL	Cross-hole sonic logging
CSLT	Cross-hole sonic logging tomography
c_u	Average undrained shear strength
c_{u1}	Weighted average of the undrained shear strength over the depth of pile embedment for the cohesive soils along the pile group perimeter
c_{u2}	Average undrained shear strength of the cohesive soils at the base of the pile group to a depth of 2B below pile toe level
D	Pile embedment length
d	Center to center distance
d	Depth
D	Diameter of the shaft
D	Distance from ground surface to bottom of clay layer or pile toe
D_R	Diameter of rock socket
E	Modulus of elasticity of pile material

E_i	Intact rock modulus
E_m	Rock mass modulus
E_n	Driving energy
EN	Engineering News
E_r	Manufacturer's rated hammer energy
f'_c	28-day compressive strength of concrete
FHWA	Federal Highway Administration
f_{pe}	Pile prestress
FS	Factor of safety
f_s	Unit shaft resistance
f_{si}	Interior unit shaft resistance
f_{si}	Ultimate unit load transfer in side resistance
f_{so}	Exterior unit shaft resistance
F_{so}	Force measured by the load cell at the point at which the slope of the rebound curve is zero
f_{so}	Ultimate unit shaft resistance
f_y	Yield stress of steel
g	Acceleration of gravity
GDL	Gamma-gamma density logging
H	Distance of ram fall
I_f	Influence factor for group embedment
IGM	Intermediate geomaterial
IR	Impulse response
k	Constant which varies from 0.1 to 1 based on hammer type
K_s	Earth pressure coefficient
K_δ	Coefficient of lateral earth pressure at depth d
L	Effective length of the pile
L_R	Length of rock socket
LRFD	Load and resistance factor design
LVDT	Linear variable displacement transducer
M	Mean
n	Number of piles in group
N	Number of layers used in the analysis
N	SPT blows per foot
N′	SPT value corrected for overburden pressure
N'_q	Bearing capacity factor
$\overline{N}'$	Average corrected SPT $N1_{60}$ value within depth B below pile toe
$\overline{N}1$	Average corrected SPT $N1_{60}$ for each soil layer
N1	Overburden corrected blowcount
$N1_{60}$	Overburden-normalized energy-corrected blowcount
N_{60}	Energy-corrected SPT-N value adjusted to 60% efficiency
N_b	Number of hammer blows per 1 inch final penetration
N_c	Bearing capacity factor
NCHRP	National Cooperative of Highway Research Program
NDT	Non-destructive test
NML	Neutron moisture logging

N_t	Toe bearing capacity coefficient
P	Safe pile load
p_a	Atmospheric pressure (2.12ksf or 101kPa)
p_d	Average effective overburden pressure at the midpoint of each soil layer
p_d	Effective overburden pressure at the center of depth increment Δd
PDA	Pile driving analyzer
p_f	Design foundation pressure
p_o	Effective overburden pressure
p_o	Effective overburden stress at depth z_i
PSL	Perimeter sonic logging
p_t	Effective overburden pressure at the pile toe
PVC	Polyvinyl chloride
Q	Test load
Q_a	Allowable geotechnical soil resistance
Q_a	Design load
QA	Quality assurance
Q_{avg}	Average load in the pile
Q_h	Applied Pile Head Load
Q_s	Ultimate skin capacity
Q_{sr}	Ultimate side resistance in rock
q_{SR}	Unit skin resistance of rock
Q_t	Ultimate tip (base or end) capacity
q_L	Limiting unit toe resistance
q_t	Unit toe resistance or unit end bearing
Q_{tr}	Ultimate tip resistance in rock
q_{tr}	Unit tip resistance of rock
Q_u	Ultimate geotechnical pile capacity or ultimate axial load or ultimate pile capacity
q_u	Uniaxial compressive strength of rock
Qu	Ultimate capacity of each individual pile in the pile group
Q_{ug}	Ultimate capacity of the pile group
Q_{ult}	Ultimate axial capacity
R	Total soil resistance against the pile
R_1, R_2	Deflection readings at measuring points
RQD	Rock quality designation
R_s	Total skin resistance
R_s	Ultimate shaft resistance
R_{s1}, R_{s2}, R_{s3}	Resistance in different soil layers
R_t	Total toe resistance
R_t	Ultimate toe resistance
R_t (max)	Maximum ultimate toe resistance
R_t	Estimated toe resistance
R_t	Pile toe resistance
R_T	Total static resistance of the drilled shaft
R_u	Ultimate pile capacity
R_{ult}	Delivered hammer energy for an assigned driving soil resistance

s	Estimated total settlement
S	Pile penetration per blow
SD	Standard deviation
SE	Sonic echo
s_f	Settlement at failure
SPT	Standard penetration test
SRD	Soil resistance to driving
s_{ui}	Undrained shear strength in a layer Δz_i
s_{ut}	Undrained shear strength of the soil at the tip of the shaft
s_u	Undrained shear strength
TL	Temperature logging
TTI	Texas Transportation Institute
u_k	Hydrostatic pore water pressure
US	Ultra-seismic
u_s	Excess pore water pressure
V	Computed velocity
V	Volume per foot for pile segment
V_C	Theoretical compression wave velocity in concrete
VR	Velocity reductions
W	Weight of pile
W	Weight of ram
W	Weight of shaft
WEA	Wave equation analysis
w_p	Weight of the plug
W_s	Total weight of the drilled shaft
WSDOT	Washington State Department of Transportation
z	Depth of the penetration
Z	Length of the pile group
z_i	Depth to the center of the i^{th} layer
α_i	Adhesion factor in a layer Δz_i
α_t	Dimensionless factor dependent on pile depth-width relationship
δ	Interface friction angle between pile and soil
η_g	Pile group efficiency
Ψ	Ratio of undrained shear strength of soil to effective overburden pressure
Δ	Elastic deformation
Δd	Length if pile segment
ΔL	Elastic shortening of the pile
ΔL	Length of pile between two measured points under no load condition
Δz	Thickness if layer i
α	Adhesion factor
α_E	Reduction factor to account for jointing in rock
β	Bjerrum-Burland beta coefficient
ϕ'	Effective soil friction angle
ϕ	Soil friction angle
γ'_i	Effective unit weight of the i^{th} layer

σ_a	AASHTO allowable working stress
ω	Angle of pile taper measured from the vertical

Chapter 10

AASHTO	American Association of State Highway and Transportation Officials
ASTM	American Society for Testing and Materials
B	Base width
c'	Effective cohesion
c_a	adhesion between concrete and soil
CIP	Cast-in-place
c_w	Wall adhesion
e	Eccentricity
ERS	Earth retaining structures
FHWA	Federal Highway Administration
FS_{bc}	Factor of safety against bearing capacity failure
FS_s	Factor of safety against sliding
H	Height of retaining wall
h_w	Distance from ground surface to water table
K	Ratio of horizontal to vertical stress
K_a	Coefficient of active earth pressure
K_{ac}	Coefficient of active earth pressure adjusted for wall adhesion
K_o	Coefficient of lateral earth pressure "at rest"
K_p	Coefficient of passive earth pressure
K_{pc}	Coefficient of passive earth pressure adjusted for wall adhesion
$\overline{m}$	Coefficient to relate wall height to distance of load from retaining wall
$\overline{n}$	Coefficient to relate wall height to depth from ground surface
MSE	Mechanically stabilized earth
OCR	Over consolidation ratio
p_0	Vertical pressure at a given depth
p_a'	Active effective pressure
p_h	Lateral earth pressure at a given depth
p_p'	Passive effective pressure
q, q_s	Vertical surcharge load
Q_1, Q_2,Q_p	Surcharge loads
q_{eq}	Equivalent uniform bearing pressure
q_{max}	Maximum bearing pressure
q_{min}	Minimum bearing pressure
SOE	Support of excavation
u	Pore water pressure
W	Weight at base of wall
Y	Horizontal deformation of retaining wall
z	Depth from surface
z_w	Depth from water table
β	Angle of slope
θ	Slope of wall backface
Ω	Dimensionless coefficient

Δp_h	Increase in lateral earth pressure due to vertical surcharge
δ	Wall friction
δ_b	friction angle between soil and base
γ'	Effective soil unit weight
γ	Soil unit weight
γ_{sat}	Saturated soil unit weight
γ_w	Unit weight of water
ϕ	Angle of internal friction of soil
ϕ'	Effective (drained) friction angle

[THIS PAGE INTENTIONALLY BLANK]

CHAPTER 8.0
SHALLOW FOUNDATIONS

Foundation design is required for all structures to ensure that the loads imposed on the underlying soil will not cause shear failures or damaging settlements. The two major types of foundations used for transportation structures can be categorized as "shallow" and "deep" foundations. This chapter first discusses the general approach to foundation design including consideration of alternative foundations to select the most cost-effective foundation. Following the general discussion, the chapter then concentrates on the topic of shallow foundations.

8.01 Primary References:

The two primary references for shallow foundations are:

FHWA (2002c). *Geotechnical Engineering Circular 6 (GEC 6), Shallow Foundations*. Report No. FHWA-SA-02-054, Author: Kimmerling, R. E., Federal Highway Administration, U.S. Department of Transportation.

AASHTO (2004 with 2006 Interims). *AASHTO LRFD Bridge Design Specifications,* 3rd Edition, American Association of State Highway and Transportation Officials, Washington, D.C.

8.1 GENERAL APPROACH TO FOUNDATION DESIGN

The duty of the foundation design specialist is to establish the most economical design that safely conforms to prescribed structural criteria and properly accounts for the intended function of the structure. Essential to the foundation engineer's study is a rational method of design, whereby various foundation types are systematically evaluated and the optimum alternative selected. The following foundation design approach is recommended:

1. Determine the direction, type and magnitude of foundation loads to be supported, tolerable deformations and special constraints such as:

    a. Underclearance requirements that limit allowable total settlement.
    b. Structure type and span length that limits allowable deformations and angular distortions.
    c. Time constraints on construction.
    d. Extreme event loading and construction load requirements.

In general, a discussion with the structural engineer about a preliminary design will provide this information and an indication of the flexibility of the constraints.

2. Evaluate the subsurface investigation and laboratory testing data with regard to reliability and completeness. The design method chosen should be commensurate with the quality and quantity of available geotechnical data, i.e., **don't use state-of-the-art computerized analyses if you have not performed a comprehensive subsurface investigation to obtain reliable values of the required input parameters.**

3. Consider alternate foundation types where applicable as discussed below.

8.1.1 Foundation Alternatives and Cost Evaluation

As noted earlier, the two major alternate foundation types are the "shallow" and "deep" foundations. Shallow foundations are discussed in this chapter. Deep foundation alternatives including piles and drilled shafts are discussed in the next chapter. Proprietary foundation systems should not be excluded as they may be the most economical alternative in a given set of conditions. Cost analyses of all feasible alternatives may lead to the elimination of some foundations that were otherwise qualified under the engineering study. Other factors that must be considered in the final foundation selection are the availability of materials and equipment, the qualifications and experience of local contractors and construction companies, as well as environmental limitations/considerations on construction access or activities.

Whether it is for shallow or deep foundations, it is recommended that foundation support cost be defined as the total cost of the foundation system divided by the load the foundation supports in tons. Thus, the cost of the foundation system should be expressed in terms of **dollars per ton load** that will be supported. For an equitable comparison, the total foundation cost should include all costs associated with a given foundation system including the need for excavation or retention systems, environmental restrictions on construction activities, e.g., vibrations, noise, disposal of contaminated excavated spoils, pile caps and cap size, etc. For major projects, if the estimated costs of alternative foundation systems during the design stage are within 15 percent of each other, then alternate foundation designs should be considered for inclusion in contract documents. If alternate designs are included in the contract documents, both designs should be adequately detailed. For example, if two pile foundation alternatives are detailed, the bid quantity pile lengths should reflect the estimated pile lengths for each alternative. Otherwise, material costs and not the installed foundation

cost will likely determine the low bid. Use of alternate foundation designs will generally provide the most cost effective foundation system.

A conventional design alternate should generally be included with a proprietary design alternate in the final project documents to stimulate competition and to anticipate value engineered proposals from contractors.

8.1.2 Loads and Limit States for Foundation Design

Foundations should be proportioned to withstand all anticipated loads safely including the permanent loads of the structure and transient loads. Most design codes specify the types of loads and load combinations to be considered in foundation design, e.g., AASHTO (2002). These load combinations can be used to identify the "limit" states for the foundation types being considered. A limit state is reached when the structure no longer fulfills its performance requirements. There are several types of limit states that are related to maximum load-carrying capacity, serviceability, extreme event and fatigue. Two of the more common limit states are as follows:

- An **ultimate limit state** (ULS) corresponds to the maximum load-carrying capacity of the foundation. This limit state may be reached through either structural or geotechnical failure. An ultimate limit state corresponds to collapse. The ultimate state is also called the **strength limit state** and includes the following failure modes for shallow foundations:
    - bearing capacity of soil exceeded,
    - excessive loss of contact, i.e., eccentricity,
    - sliding at the base of footing,
    - loss of overall stability, i.e.,, global stability,
    - structural capacity exceeded.

- A **serviceability limit state** (SLS) corresponds to loss of serviceability, and occurs before collapse. A serviceability limit state involves unacceptable deformations or undesirable damage levels. A serviceability limit state may be reached through the following mechanisms:
    - Excessive differential or total foundation settlements,
    - Excessive lateral displacements, or
    - Structural deterioration of the foundation.

The serviceability limit state for transportation structures is based upon economy and the quality of ride. The cost of limiting foundation movements should be compared to the cost of designing the superstructure so that it can tolerate larger movements, or of correcting the consequences of movements through maintenance, to determine minimum life cycle cost. More stringent criteria may be established by the owner.

All relevant limit states must be considered in foundation design to ensure an adequate degree of safety and serviceability. Therefore, all foundation design is geared towards addressing the ULS and the SLS. In this manual, the allowable stress design (ASD) approach is used. Further discussion on ASD and other design methods such as the Load and Resistance Factor Design (LRFD) can be found in Appendix C.

8.2 TYPES OF SHALLOW FOUNDATIONS

The geometry of a typical shallow foundation is shown in Figure 8-1. Shallow foundations are those wherein the depth, D_f, of the foundation is small compared to the cross-sectional size (width, B_f, or length, L_f). This is in contradistinction to deep foundations, such as driven piles and drilled shafts, whose depth of embedment is considerably larger than the cross-section dimension (diameter). The exact definition of shallow or deep foundations is less important than an understanding of the theoretical assumptions behind the various design procedures for each type. Stated another way, it is important to recognize the theoretical limitations of a design procedure that may vary as a function of depth, such as a bearing capacity equation. Common types of shallow foundations are shown in Figures 8-2 through 8-9.

8.2.1 Isolated Spread Footings

Footings with L_f/B_f ratio less than 10 are considered to be isolated footings. Isolated spread footings (Figure 8-2) are designed to distribute the concentrated loads delivered by a single column to prevent shear failure of the soil beneath the footing. The size of the footing is a function of the loads distributed by the supported column and the strength and compressibility characteristics of the bearing materials beneath the footing. For bridge columns, isolated spread footings are typically greater than 10 ft by 10 ft (3 m by 3 m). These dimensions increase when eccentric loads are applied to the footing. Structural design of the isolated footing includes consideration for moment resistance at the face of the column in the short direction of the footing, as well as shear and punching around the column.

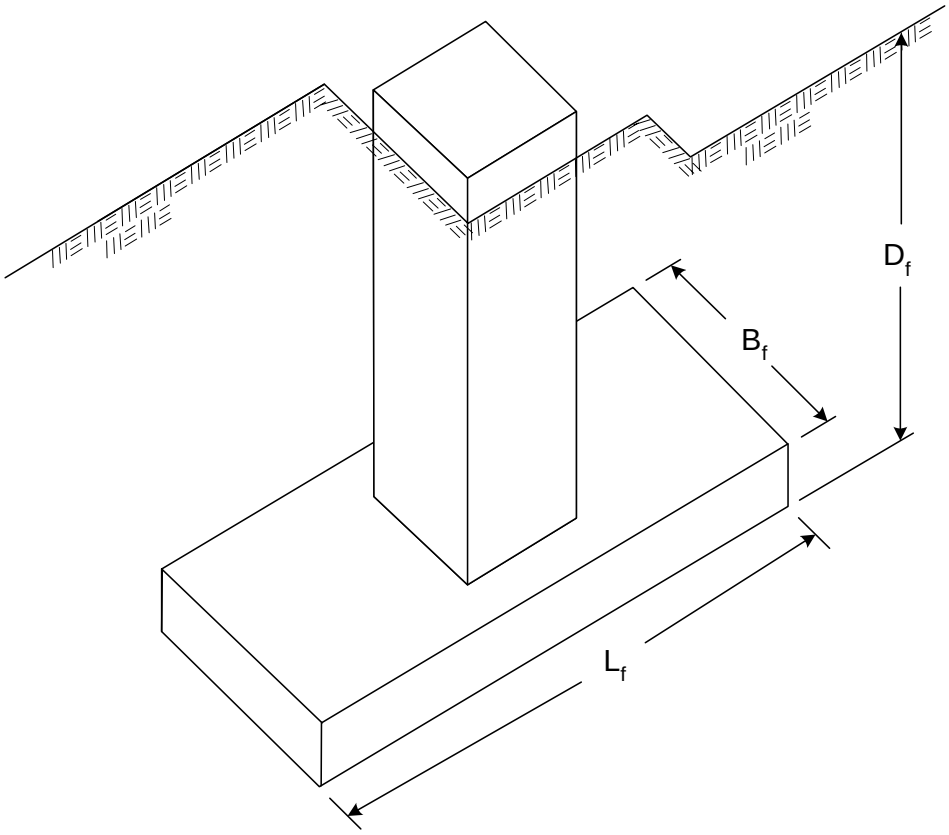

Figure 8-1. Geometry of a typical shallow foundation (FHWA, 2002c, AASHTO 2002).

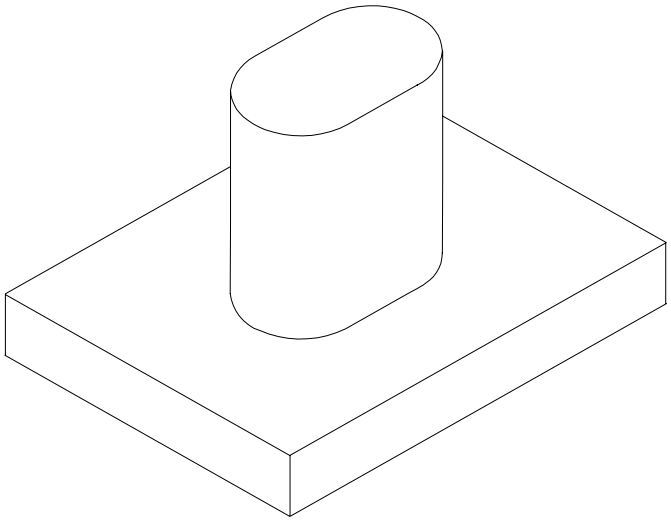

Figure 8-2. Isolated spread footing (FHWA, 2002c).

8.2.2 Continuous or Strip Footings

The most commonly used type of foundation for buildings is the continuous strip footing (Figure 8-3). For computation purposes, footings with an L_f/B_f ratio ≥ 10 are considered to be continuous or strip footings. Strip footings typically support a single row of columns or a bearing wall to reduce the pressure on the bearing materials. Strip footings may tie columns together in one direction. Sizing and structural design considerations are similar to those for isolated spread footings with the exception that plane strain conditions are assumed to exist in the direction parallel to the long axis of the footing. This assumption affects the depth of significant influence (DOSI), i.e., the depth to which applied stresses are significantly felt in the soil. For example, in contrast with isolated footing where the DOSI is between 2 to 4 times the footing width, the DOSI in the case of the strip footings will always be at least 4 times the width of the footing as discussed in Section 2.4.1 of Chapter 2. The structural design of strip footings is generally governed by beam shear and bending moments.

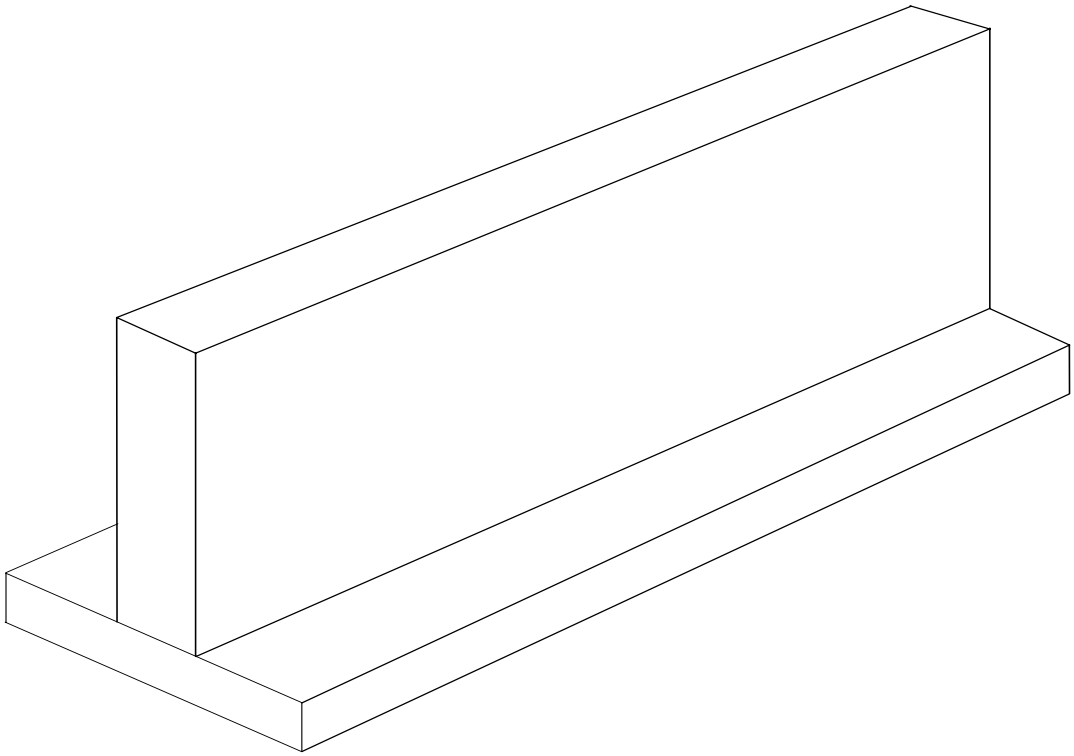

Figure 8-3. Continuous strip footing (FHWA, 2002c).

8.2.3 Spread Footings with Cantilevered Stemwalls

An earth retaining system consisting of a spread footing supporting a cantilevered retaining wall is frequently used to resist lateral loads applied by a backfill and other external loads that may be acting on top of the backfill (refer to Figures 8-4 and 8-5). The system must offer resistance to both vertical and horizontal loads as well as to overturning moments. The spread footing is designed to resist overturning moments and vertical eccentric loads caused by the lateral earth pressures and the horizontal components of the externally applied loads acting on the cantilever stemwall. The wall itself is designed as a simple cantilevered structure to resist the lateral earth pressures imposed by the backfill and other external loads that may be applied on top of the backfill.

8.2.4 Bridge Abutments

Bridge abutments are required to perform numerous functions, including the following:

- Retain the earthen backfill behind the abutment.
- Support the superstructure and distribute the loads to the bearing materials below the spread footing, assuming that a spread footing is the foundation system chosen for the abutment.
- Provide a transition from the approach embankment to the bridge deck.
- Depending on the structure type, accommodate shrinkage and temperature movements within the superstructure.

Spread footings with cantilevered stemwalls are well suited to perform these multiple functions. The general arrangement of a bridge abutment with a spread footing and a cantilevered stemwall is shown in Figures 8-4 and 8-5. In the case of weak soils at shallow depths, deep foundations, such as drilled shafts or driven piles, are often used to support the abutment. There are several other abutment types such as those that use mechanically stabilized earth (MSE) walls with spread foundations on top or with deep foundation penetrating through the MSE walls. Several different types of bridge abutments are shown in Figure 7-2 in Chapter 7.

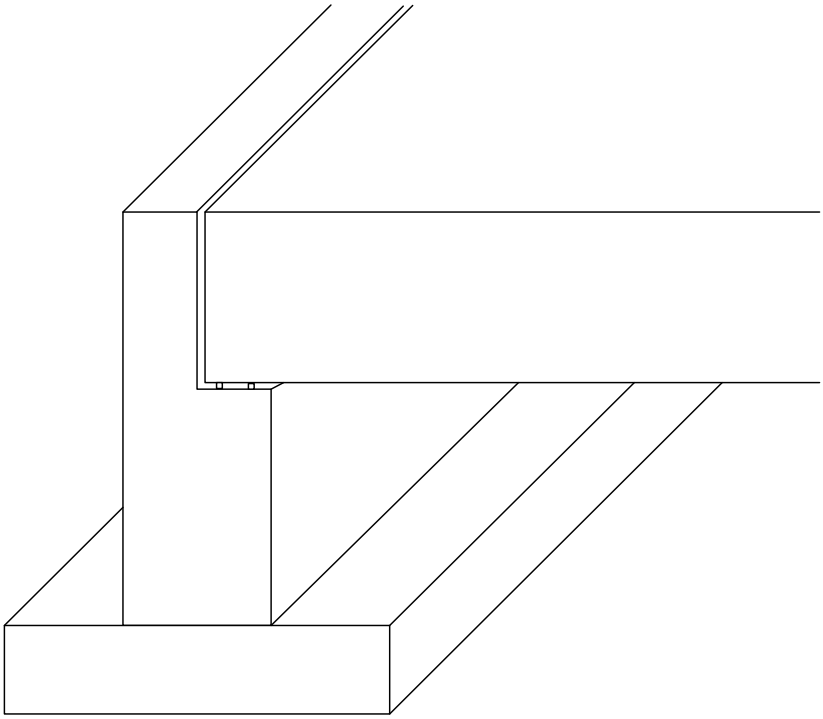

Figure 8-4. Spread footing with cantilever stemwall at bridge abutment.

Figure 8-5. Abutment/wingwall footing, I-10, Arizona.

8.2.5 Retaining Structures

The foundations for semi-gravity concrete cantilever retaining walls (inverted "T" walls) are essentially shallow spread footings. The wall derives its ability to resist loads from a combination of the dead weight of the backfill on the heel of the wall footing and the structural cantilever of the stem (Figure 8-6).

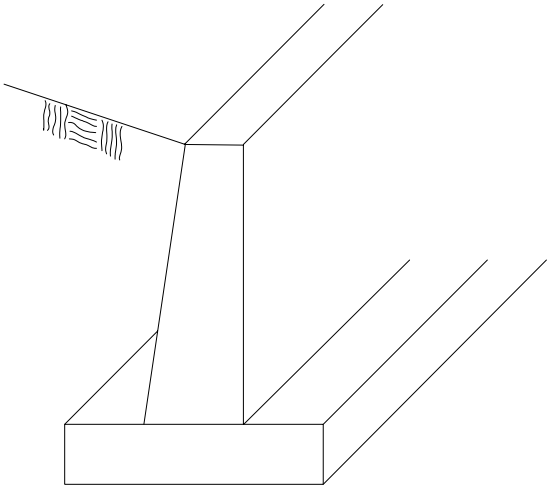

Figure 8-6. Footing for a semi-gravity cantilever retaining wall (FHWA, 2002c).

8.2.6 Building Foundations

When a building stemwall is buried, partially buried or acts as a basement wall, the stemwall resists the lateral earth pressures of the backfill. Unlike bridge abutments where the bridge structure is usually free to move horizontally on the abutment or the semi-gravity cantilever wall, the tops or the ends of the stemwalls in buildings are frequently restrained by other structural members such as beams, floors, transverse interior walls, etc. These structural members provide lateral restraint that affects the magnitude of the design lateral earth pressures

8.2.7 Combined Footings

Combined footings are similar to isolated spread footings except that they support two or more columns and are rectangular or trapezoidal in shape (Figure 8-7). They are used primarily when the column spacing is non-uniform (Bowles, 1996) or when isolated spread footings become so closely spaced that a combination footing is simpler to form and construct. In the case of bridge abutments, an example of a combined footing is the so-called

"spill-through" type abutment (Figure 8-8). This configuration was used during some of the initial construction of the Interstate Highway System on new alignments where spread footings could be founded on competent native soils. Spill-through abutments are also used at stream crossings to make sure that foundations are below the scour depth of the stream.

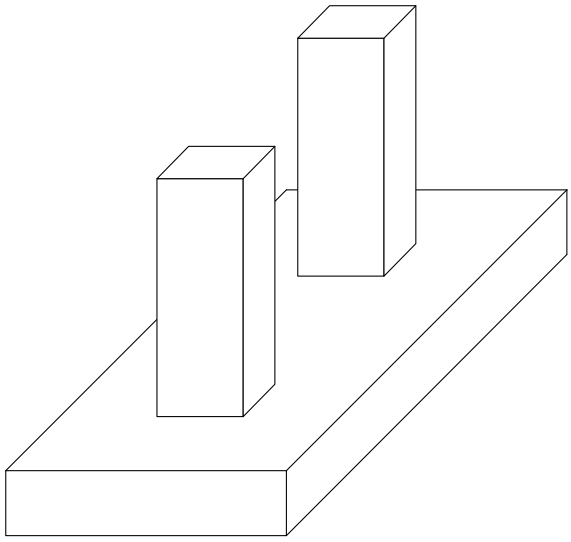

Figure 8-7. Combined footing (FHWA, 2002c).

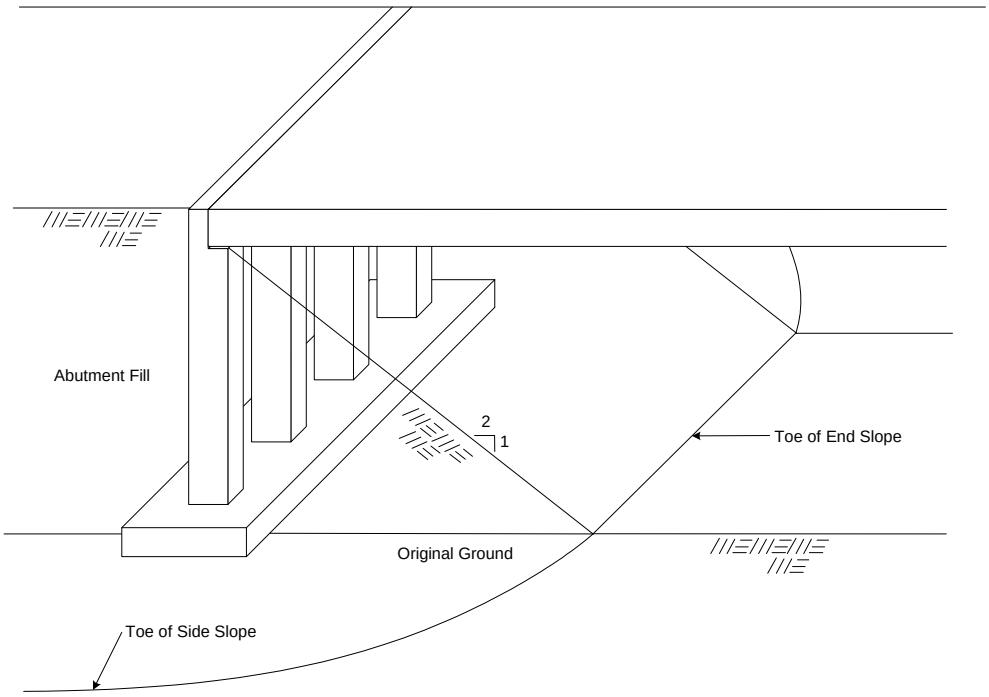

Figure 8-8. Spill-through abutment on combination strip footing (FHWA, 2002c).

Due to the frame action that develops with combined footings, they can be used to resist large overturning or rotational moments in the longitudinal direction of the column row.

There are a number of approaches for designing and constructing combined footings. The choice depends on the available space, load distribution among the columns supported by the footing, variations of soil properties supporting the footing, and economics.

8.2.8 Mat Foundations

A mat foundation consists of a single heavily reinforced concrete slab that underlies the entire structure or a major portion of the structure. Mat foundations are often economical when spread footings would cover more than about 50 percent of the plan area of the structure's footprint (Peck, *et al.,* 1974). A mat foundation (Figure 8-9) typically supports a number of columns and/or walls in either direction or a uniformly distributed load such as that imposed by a storage tank. The principal advantage of a mat foundation is its ability to bridge over local soft spots, and to reduce differential movement.

Structures founded on relatively weak soils may be supported economically on mat foundations. Column and wall loads are transferred to the foundation soils through the mat foundation. Mat foundations distribute the loads over a large area, thus reducing the intensity of contact pressures. Mat foundations are designed with sufficient reinforcement and thickness to be rigid enough to distribute column and wall loads uniformly. Although differential settlements may be minimized by the use of mat foundations, greater uniform settlements may occur because the zone of influence of the applied stress may extend to considerable depth due to the larger dimensions of the mat. Often a mat also serves as the base floor level of building structures.

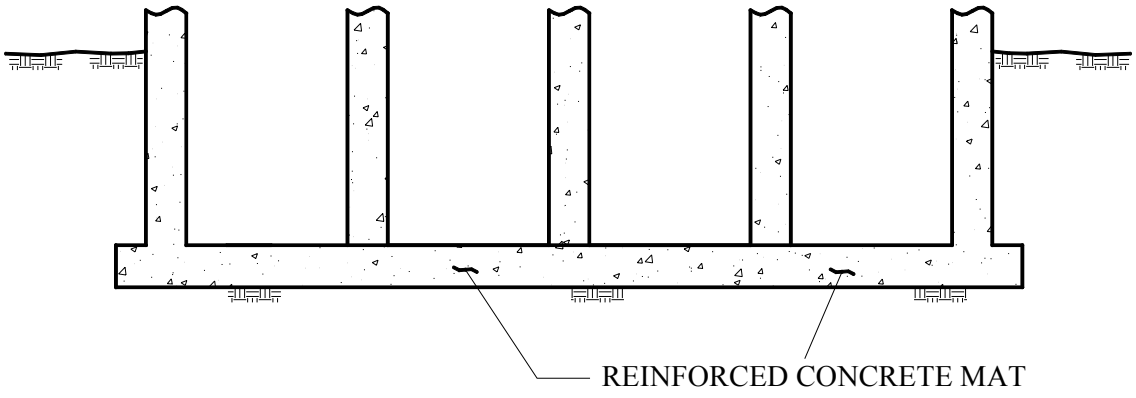

Figure 8-9. Typical mat foundation (FHWA, 2002c).

Mat foundations have limited applicability for bridge support, except where large bridge piers, such as bascules or other movable bridge supports, bear at relatively shallow depth without deep foundation support. This type of application may arguably be a deep foundation, but the design of such a pier may include consideration of the base of the bascule pier as a mat. Discussion of mat foundation design is included in FHWA (2002c).

A more common application of mat foundations for transportation structures includes lightly loaded rest area or maintenance facilities such as small masonry block structures, sand storage bins or sheds, or box culverts constructed as a continuous structure.

8.3 SPREAD FOOTING DESIGN CONCEPT AND PROCEDURE

The geotechnical design of a spread footing is a two-part process. First the allowable soil bearing capacity must be established to ensure stability of the foundation and determine if the proposed structural loads can be supported on a reasonably sized foundation. Second, the amount of settlement due to the actual structural loads must be predicted and the time of occurrence estimated. Experience has shown that settlement is usually the controlling factor in the decision to use a spread footing. This is not surprising since structural considerations usually limit tolerable settlements to values that can be achieved only on competent soils not prone to a bearing capacity failure. Thus, the **allowable bearing capacity** of a spread footing is defined as the lesser of:

- The applied stress that results in a shear failure divided by a suitable factor of safety (FS); this is a criterion based on an **ultimate limit state** (ULS) as discussed previously.
  or
- The applied stress that results in a specified amount of settlement; this is a criterion based on a **serviceability limit state** (SLS) as discussed previously.

Both of the above considerations are a function of the least lateral dimension of the footing, typically called the footing width and designated as B_f as shown in Figure 8-1. The effect of footing width on allowable bearing capacity and settlement is shown conceptually in Figure 8-10. The allowable bearing capacity of a footing is usually controlled by shear-failure considerations for narrow footing widths as shown in Zone A in Figure 8-10. As the footing width increases, the allowable bearing capacity is limited by the settlement potential of the soils supporting the footing within the DOSI which is a function of the footing width as discussed in Section 2.4 of Chapter 2. Stated another way, as the footing width increases, the stress increase "felt" by the soil may decrease but the effect of the applied stress will extend

more deeply below the footing base. Therefore, settlements may increase depending on the type of soils within the DOSI. This is schematically shown in Zone B in Figure 8-10.

The concept of decreasing allowable bearing capacity with increasing footing width for the settlement controlled cases is an important concept to understand. In such cases, the allowable bearing capacity is the value of the applied stress at the footing base that will result in a given settlement. Since the DOSI increases with increasing footing width, the only way to limit the settlements to a certain desired value is by reducing the applied stress. The more stringent the settlement criterion the less the stress that can be applied to the footing which in turn means that the allowable bearing capacity is correspondingly less. This is conceptually illustrated in Figure 8-10 wherein it is shown that decreasing the settlement, i.e., going from 3S to 2S to S decreases the allowable bearing capacity at a given footing width. An example of the use of the chart is presented in Section 8.8.

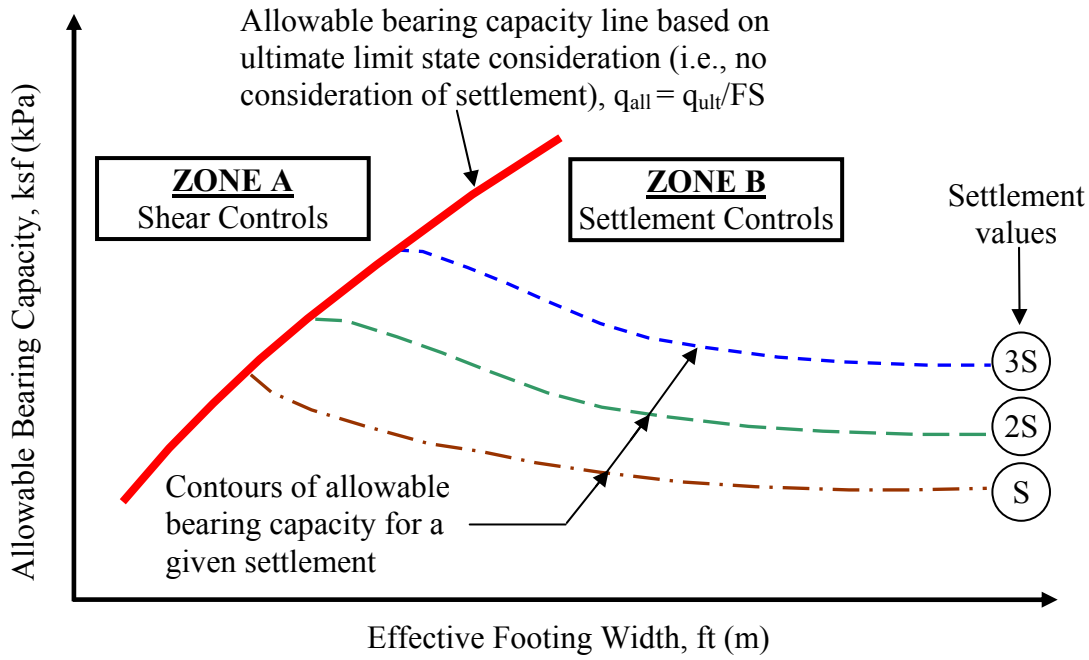

Figure 8-10. Shear failure versus settlement considerations in evaluation of allowable bearing capacity.

The design process flow chart for a bridge supported on spread footings is shown in Figure 8-11. In the flow chart, the foundation design specialist is a person with the skills necessary to address both geotechnical and structural design. Section 8.4 discusses the bearing capacity aspects while Section 8.5 discusses the settlement aspects of shallow foundation design.

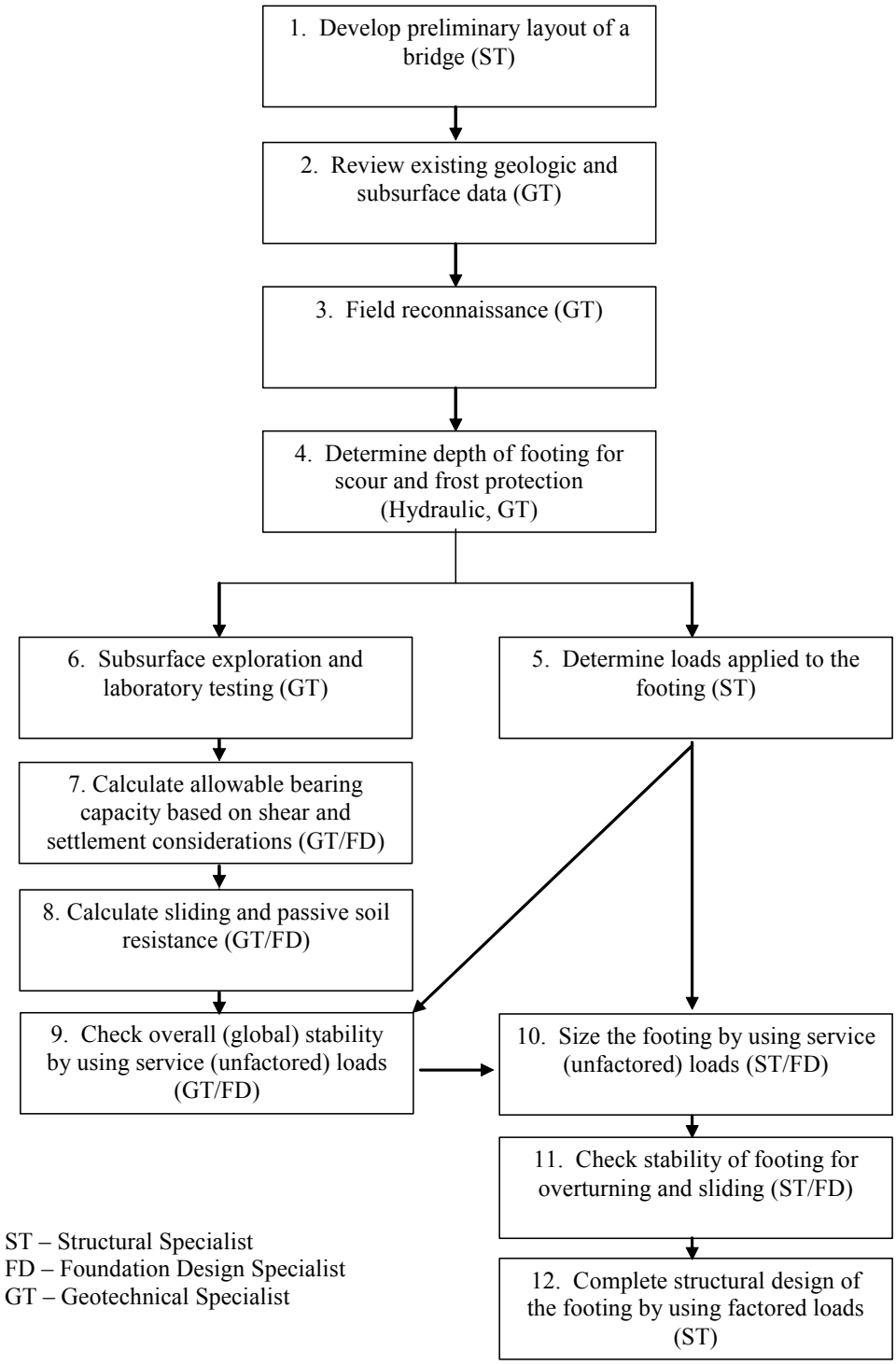

Figure 8-11. Design process flow chart – bridge shallow foundation (modified after FHWA, 2002c).

8.4 BEARING CAPACITY

This section discusses bearing capacity theory and its application toward computing allowable bearing capacities for shallow foundations.

A foundation failure will occur when the footing penetrates excessively into the ground or experiences excessive rotation (Figure 8-12). Either of these excessive deformations may occur when,

(a) the shear strength of the soil is exceeded, and/or

(b) large uneven settlement and associated rotations occur.

The failure mode that occurs when the shear strength is exceeded is known as a bearing capacity failure or, more accurately, an **ultimate bearing capacity failure**. Often, large settlements may occur prior to an ultimate bearing capacity failure and such settlements may impair the serviceability of the structure, i.e., the ultimate limit state (ULS) has not been exceeded, but the serviceability limit state (SLS) has. In this case, to control the settlements within tolerable limits, the footprint and/or depth of the structure below the ground may be dimensioned such that the imposed bearing pressure is well below the ultimate bearing capacity.

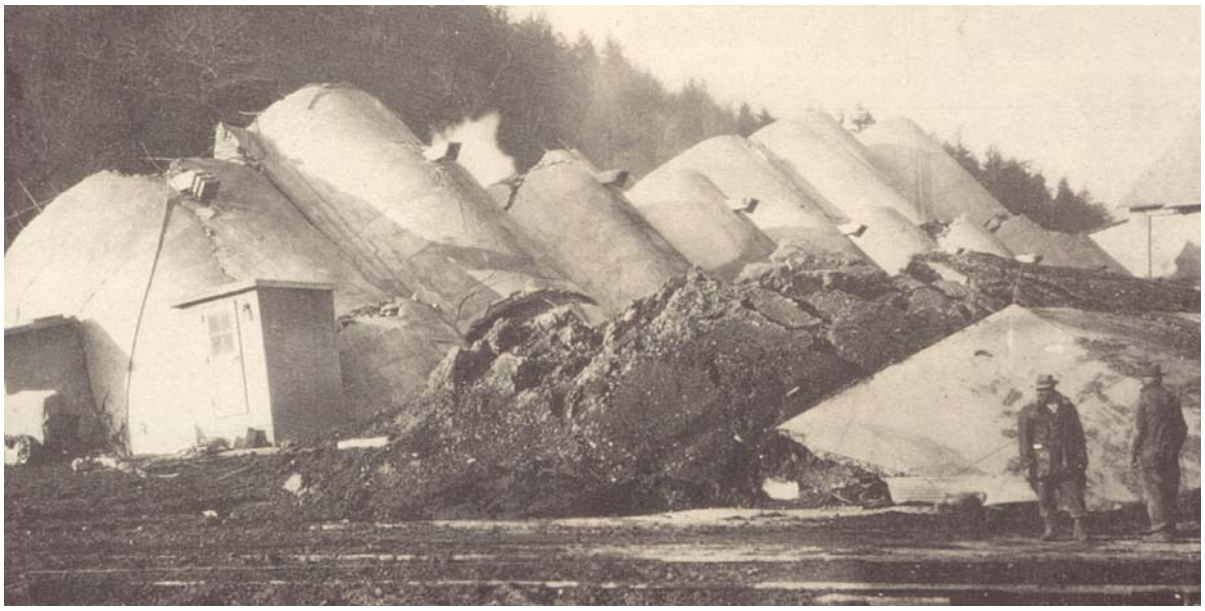

Figure 8-12. Bearing capacity failure of silo foundation (Tschebotarioff, 1951).

8.4.1 Failure Mechanisms

The type of bearing capacity failure is a function of several factors such as the type of the soil, the density (or consistency) of the soil, shape of the loaded surface, etc. This section discusses three failure mechanisms.

8.4.1.1 General Shear

When a footing is loaded to the ultimate bearing capacity, a condition of plastic flow develops in the foundation soils. As shown in Figure 8-13, a triangular wedge beneath the footing, designated as Zone I, remains in an elastic state and moves down into the soil with the footing. Although only a single failure surface (CD) is shown in Zone II, radial shear develops throughout Zone II such that radial lines of failure extending from the Zone I boundary (CB) change length based on a logarithmic spiral until they reach Zone III. Although only a single failure surface (DE) is shown in Zone III, a passive state of stress develops throughout Zone III at an angle of $45^o - (\phi'/2)$ from the horizontal. This configuration of the ultimate bearing capacity failure, with a well-defined failure zone extending to the surface and with bulging of the soil occurring on both sides of the footing, is called a "general shear" type of failure. General shear-type failures (Figure 8-14a) are believed to be the prevailing mode of failure for soils that are relatively incompressible and reasonably strong.

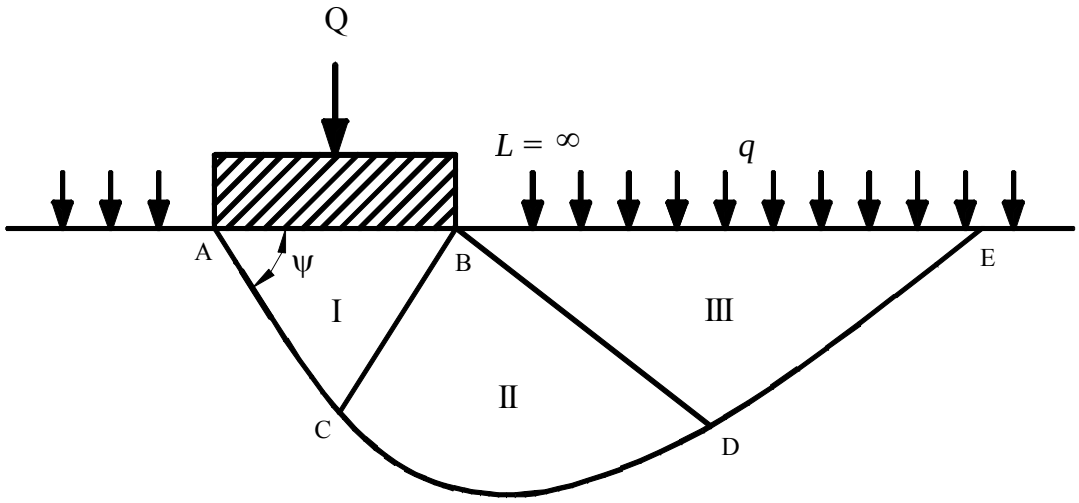

Figure 8-13. Boundaries of zone of plastic equilibrium after failure of soil beneath continuous footing (FHWA, 2002c).

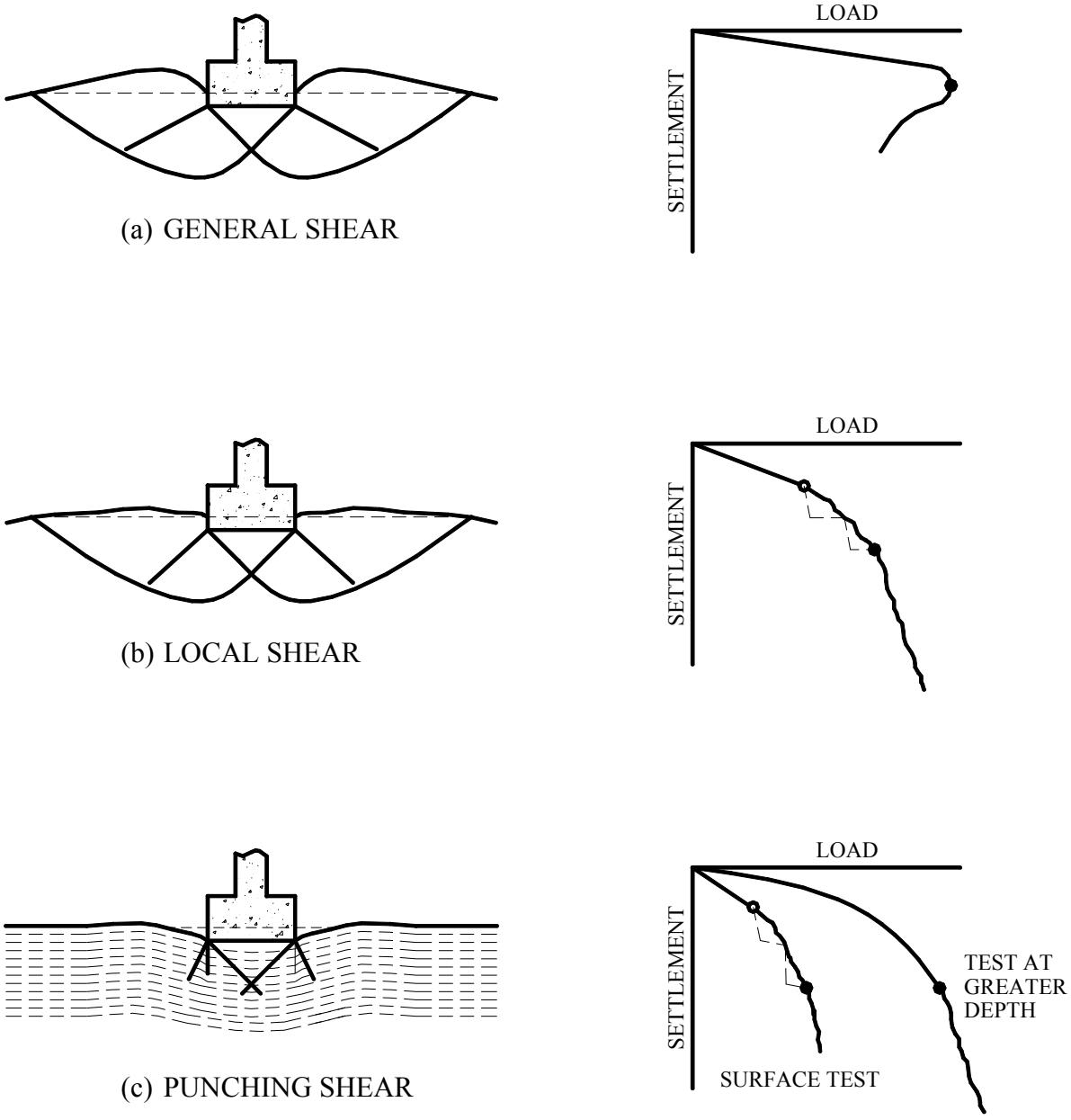

Figure 8-14. Modes of bearing capacity failure (after Vesic, 1975) (a) General shear (b) Local shear (c) Punching shear

8.4.1.2 Local Shear

Local shear failure is characterized by a failure surface that is similar to that of a general shear failure but that does not extend to the ground surface. In the case of a local shear failure the failure zone ends somewhere in the soil below the footing (Figure 8-14b). Local shear failure is accompanied by vertical compression of soil below the footing and visible bulging of soil adjacent to the footing, but not by sudden rotation or tilting of the footing. Local shear failure is a transitional condition between general and punching shear failure. Local shear failures may occur in soils that are relatively loose compared to soils susceptible to general shear failure.

8.4.1.3 Punching Shear

Punching shear failure is characterized by vertical shear around the perimeter of the footing and is accompanied by a vertical movement of the footing and compression of the soil immediately below the footing. The soil outside the loaded area is not affected significantly (Figure 8-14c). The ground surface adjacent to the footing moves downward instead of bulging as in general and local shear failure. Punching shear failure generally occurs in loose or compressible soils, in weak soils under slow (drained) loading, and in dense sands for deep footings subjected to high loads.

Note that from a perspective of bridge foundation design, soils so obviously weak as to experience local or punching shear failure modes should be avoided for supporting shallow foundations. Additional guidance on dealing with soils that fall in the intermediate or local shear range of behavior is provided in Section 8.4.5.

8.4.2 Bearing Capacity Equation Formulation

In essence, the bearing capacity failure mechanism is similar to the embankment slope failure mechanism discussed in Chapter 6. In the case of footings, the ultimate bearing capacity is equivalent to the stress applied to the soil by the footing that causes shear failure to occur in the soil below the footing base. For a concentrically loaded rigid strip footing with a rough base on a level homogeneous foundation material without the presence of water, the gross ultimate bearing capacity, q_{ult}, is expressed as follows (after Terzaghi, 1943):

$$q_{ult} = \underbrace{c\,(N_c)}_{\text{“Cohesion” term}} + \underbrace{q\,(N_q)}_{\text{“Surcharge” term}} + \underbrace{0.5\,(\gamma)(B_f)(N_\gamma)}_{\text{Foundation soil “Weight” term}} \qquad 8\text{-}1$$

where: c = cohesion of the soil (ksf) (kPa)

q = total surcharge at the base of the footing = $q_{appl} + \gamma_a D_f$ (ksf) (kPa)

q_{appl} = applied surcharge (ksf)(kPa)

γ_a = unit weight of the overburden material above the base of the footing causing the surcharge pressure (kcf) (kN/m^3)

D_f = depth of embedment (ft) (m) (Figure 8-1)

γ = unit weight of the soil under the footing (kcf) (kN/m^3)

B_f = footing width, i.e., least lateral dimension of the footing (ft) (m) (Figure 8-1)

N_q = bearing capacity factor for the "surcharge" term (dimensionless)

$$= e^{\pi \tan\phi} \tan^2\left(45° + \frac{\phi}{2}\right) \qquad 8\text{-}2$$

N_c = bearing capacity factor for the "cohesion" term (dimensionless)

$$= (N_q - 1)\cot\phi \qquad \text{for } \phi > 0° \qquad 8\text{-}3$$

$$= 2 + \pi = 5.14 \qquad \text{for } \phi = 0° \qquad 8\text{-}4$$

N_γ = bearing capacity factor for the "weight" term (dimensionless)

$$= 2\,(N_q + 1)\tan(\phi) \qquad 8\text{-}5$$

Many researchers proposed different expressions for the bearing capacity factors, N_c, N_q, and N_γ. The expressions presented above are those used by AASHTO (2004 with 2006 Interims). These expressions are a function of the friction angle, ϕ. Table 8-1 can be used to estimate friction angle, ϕ, from corrected SPT N-value, $N1_{60}$, for cohesionless soils. Otherwise, the friction angle can be measured directly by laboratory tests or in situ testing. The values of N_c, N_q, and N_γ as computed for various friction angles by Equations 8-3/8-4, 8-2, and 8-5, respectively are included in Table 8-1 and in Figure 8-15. Computation of ultimate bearing capacity is illustrated in Example 8-1.

Table 8-1
Estimation of friction angle of cohesionless soils from Standard Penetration Tests (after AASHTO, 2004 with 2006 Interims; FHWA, 2002c)

Description	Very Loose	Loose	Medium	Dense	Very Dense
Corrected SPT $N1_{60}$	0	4	10	30	50
Approximate ϕ, degrees*	25 – 30	27 – 32	30 – 35	35 – 40	38 – 43
Approximate moist unit weight, (γ) pcf*	70 – 100	90 – 115	110 – 130	120 – 140	130 – 150
* Use larger values for granular material with 5% or less fine sand and silt. Note: Correlations may be unreliable in gravelly soils due to sampling difficulties with split-spoon sampler as discussed in Chapter 3.					

Table 8-2
Bearing Capacity Factors (AASHTO, 2004 with 2006 Interims)

ϕ	N_c	N_q	N_γ	ϕ	N_c	N_q	N_γ
0	5.14	1.0	0.0	23	18.1	8.7	8.2
1	5.4	1.1	0.1	24	19.3	9.6	9.4
2	5.6	1.2	0.2	25	20.7	10.7	10.9
3	5.9	1.3	0.2	26	22.3	11.9	12.5
4	6.2	1.4	0.3	27	23.9	13.2	14.5
5	6.5	1.6	0.5	28	25.8	14.7	16.7
6	6.8	1.7	0.6	29	27.9	16.4	19.3
7	7.2	1.9	0.7	30	30.1	18.4	22.4
8	7.5	2.1	0.9	31	32.7	20.6	26.0
9	7.9	2.3	1.0	32	35.5	23.2	30.2
10	8.4	2.5	1.2	33	38.6	26.1	35.2
11	8.8	2.7	1.4	34	42.2	29.4	41.1
12	9.3	3.0	1.7	35	46.1	33.3	48.0
13	9.8	3.3	2.0	36	50.6	37.8	56.3
14	10.4	3.6	2.3	37	55.6	42.9	66.2
15	11.0	3.9	2.7	38	61.4	48.9	78.0
16	11.6	4.3	3.1	39	67.9	56.0	92.3
17	12.3	4.8	3.5	40	75.3	64.2	109.4
18	13.1	5.3	4.1	41	83.9	73.9	130.2
19	13.9	5.8	4.7	42	93.7	85.4	155.6
20	14.8	6.4	5.4	43	105.1	99.0	186.5
21	15.8	7.1	6.2	44	118.4	115.3	224.6
22	16.9	7.8	7.1	45	133.9	134.9	271.8

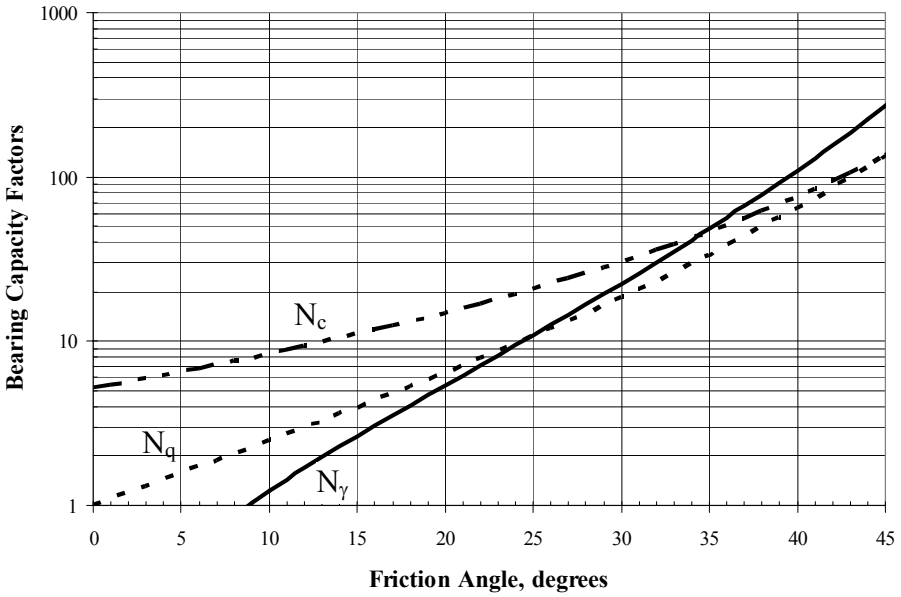

Figure 8-15. Bearing capacity factors versus friction angle.

Example 8-1: Determine the ultimate bearing capacity for a rigid strip footing with a rough base having the dimensions shown in the sketch below. Assume that the footing is concentrically loaded and that the total unit weight below the base of the footing is equal to the total unit weight above the base of the footing, i.e., in terms of the symbols used previously, $\gamma = \gamma_a$. First assume that the ground water table is well below the base of the footing and therefore it has no effect on the bearing capacity. Then, assume that the groundwater table is at the base of the footing and recompute the ultimate bearing capacity.

.

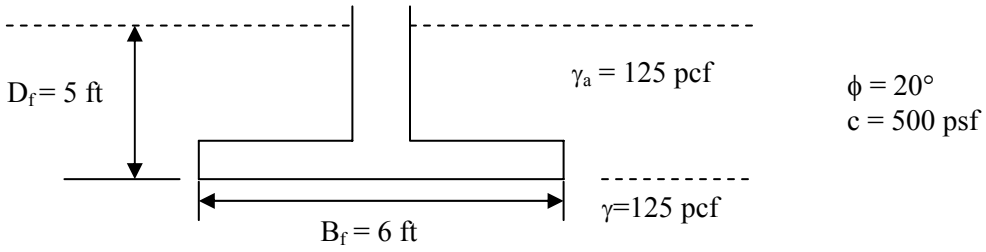

Solution:

Assume a general shear condition and enter Table 8-2 for ϕ= 20° and read the bearing capacity factors as follows:

N_c = 14.8, N_q = 6.4, N_γ = 5.4. These values can also be read from Figure 8-15.

$$q_{ult} = c(N_c) + \gamma_a (D_f)(N_q) + 0.5(\gamma)(B_f)(N_\gamma)$$

q_{ult} = (500 psf)(14.8) + (125 pcf) (5 ft) (6.4) + 0.5(125 pcf) (6 ft)(5.4)
= 7,400 psf + 4,000 psf + 2,025 psf
q_{ult} = 13,425 psf

Effect of water: If the ground water table is at the base of the footing, i.e., a depth of 5 ft from the ground surface, then effective unit weight should be used in the "weight" term as follows:

q_{ult} = (500 psf)(14.8) + (125 pcf) (5 ft) (6.4) + 0.5(125 pcf - 62.4 pcf) (6 ft)(5.4)
= 7,400 psf + 4,000 psf + 1,014 psf
q_{ult} = 12,414 psf

Sections 8.4.2.1 and 8.4.3.2 further discuss the effect of water on ultimate bearing capacity.

8.4.2.1 Comparative Effect of Various Terms in Bearing Capacity Formulation

In Equation 8-1, the first term is called the "cohesion" term, the second term is called the "surcharge" term since it represents the loads above the base of the footing, and the third term is called the "weight" term since it represents the weight of the foundation soil in the failure zone below the base of the footing. Consider now the effect that each of these terms has on the computed value of the ultimate bearing capacity (q_{ult}).

- **Purely cohesive soils, $\phi = 0$ (corresponds to undrained loading)**: In this case, the last term is zero ($N_\gamma = 0$ for $\phi = 0$) and the first term in Equation 8-1 is a constant. Therefore the ultimate bearing capacity is a function of only the cohesion as it appears in the cohesion term in Equation 8-1 and the depth of embedment of the footing as it appears in the surcharge term in Equation 8-1. For this case, the footing width has no influence on the ultimate bearing capacity.

- **Purely frictional or cohesionless soils, $c = 0$ and $\phi > 0$**: In this case, there will be large changes in ultimate bearing capacity when properties and/or dimensions are changed. The embedment effect is particularly important. Removal of the soil over an embedded footing, either by excavation or scour, can substantially reduce its ultimate bearing capacity and result in a lower factor of safety than required by the design. Removal of the soil over an embedded footing can also cause greater settlement than initially estimated. Similarly, a rise in the ground water level to the ground surface will reduce the effective unit weight of the soil by making the soil buoyant, thus reducing the surcharge and unit weight terms by essentially one-half.

Table 8-3 shows how bearing capacity can vary with changes in physical properties or dimensions. Notice that for a given value of cohesion, the effect of the variables on the bearing capacity in cohesive soils is minimal. Only the embedment depth has an effect on bearing capacity in cohesive soils. Also note that a rise in the ground water table does not influence cohesion. Interparticle bonding remains virtually unchanged unless the clay is reworked or the clay contains minerals that react with free water, e.g., expansive minerals.

Table 8-3 also shows that for a given value of internal friction angle, the effect on cohesionless soils is significant when dimensions are changed and/or a rise in the water table takes place. The embedment effect is particularly important. Removal of soil from over an embedded footing, either by excavation or scour, can substantially reduce the ultimate bearing capacity and possibly cause catastrophic shear failure. Rehabilitation or repair of an existing spread footing often requires excavation of the soil above the footing. If the effect of this removal on bearing capacity is not considered, the footing may move downward resulting in structural distress.

Table 8-3
Variation in bearing capacity with changes in physical properties or dimensions

Properties and Dimensions	Cohesive Soil	Cohesionless Soil
$\gamma = \gamma_a$ = effective unit weight γ' = effective unit weight; D_f = embedment depth B_f = footing width (assume continuous footing)	$\phi = 0$ c = 1,000 psf q_{ult} (psf)	$\phi = 30^o$ c = 0 q_{ult} (psf)
A. Initial situation: γ = 120 pcf, D_f = 0', B_f = 5' deep water table	5,140	6,720
B. Effect of embedment: γ = 120 pcf,, D_f = 5', B_f = 5', deep water table	5,740	17,760
C. Effect of width: γ = 120 pcf, D_f = 0', B_f = 10' deep water table	5,140	13,440
D. Effect of water table at surface: γ' = 57.6 pcf, D_f = 0', B_f = 5'	5,140	3,226

8.4.3 Bearing Capacity Correction Factors

A number of factors that were not included in the derivations discussed earlier influence the ultimate bearing capacity of shallow foundations. Note that Equation 8-1 assumes a rigid strip footing with a rough base, loaded through its centroid, that is bearing on a level surface of homogeneous soil. Various correction factors have been proposed by numerous investigators to account for footing shape adjusted for eccentricity, location of the ground water table, embedment depth, sloping ground surface, an inclined base, the mode of shear, local or punching shear, and inclined loading. The general philosophy of correcting the theoretical ultimate bearing capacity equation involves multiplying each of the three terms in the bearing capacity equation by empirical factors to account for the particular effect. Each correction factor includes a subscript denoting the term to which the factor should be applied: "c" for the cohesion term, "q" for the surcharge term, and "γ" for the weight term. Each of these factors and suggestions for their application are discussed separately below. In most cases these factors may be used in combination.

The general form of the ultimate bearing capacity equation, including correction terms, is:

$$q_{ult} = cN_c s_c b_c + qN_q C_{wq} s_q b_q d_q + 0.5\gamma B_f N_\gamma C_{w\gamma} s_\gamma b_\gamma \qquad 8\text{-}6$$

where: s_c, s_γ and s_q are **shape correction factors**

b_c, b_γ and b_q are **base inclination correction factors**

$C_{w\gamma}$ and C_{wq} are **groundwater correction factors**

d_q is an **embedment depth correction factor** to account for the shearing resistance along the failure surface passing through cohesionless material above the bearing elevation. Recall that the embedment is modeled as a surcharge pressure applied at the bearing elevation. To be theoretically correct, the "q" in the surcharge term consists of two components, one the embedment depth surcharge to which the correction factor applies, the other an applied surcharge such as the traffic surcharge to which the correction factor, by definition, does not apply. Therefore, theoretically the "q" in the surcharge term should be replaced with $(q_a + \gamma D_f\, d_q)$ where q_a is defined as an applied surcharge for cases where applied surcharge is considered in the analysis;

N_c, N_q and N_γ are **bearing capacity factors** that are a function of the friction angle of the soil. N_c, N_q and N_γ can be obtained from Table 8-2 or Figure 8-15 or they can be computed by Equation 8-3/8-4, 8-2 and 8-5, respectively. As discussed in Section 8.4.3.6, N_c and N_γ are replaced with N_{cq} and $N_{\gamma q}$ for the case of sloping ground or when the footing is located near a slope. In these cases the N_q term is omitted.

The following sections provide guidance on the use of the bearing capacity correction factors, and whether or not certain factors should be used in combination.

8.4.3.1 Footing Shape (Eccentricity and Effective Dimensions)

The following two issues are related to footing shape:

- Distinguishing a strip footing from a rectangular footing. The general bearing capacity equation is applicable to strip footings, i.e., footings with $L_f/B_f \geq 10$. Therefore, footing shape factors should be included in the equation for the ultimate bearing capacity for rectangular footings with L_f/B_f ratios less than 10.

- Use of the effective dimensions of footings subjected to eccentric loads. Eccentric loading occurs when a footing is subjected to eccentric vertical loads, a combination

of vertical loads and moments, or moments induced by shear loads transferred to the footing. Abutments and retaining wall footings are examples of footings subjected to this type of loading condition. Moments can also be applied to interior column footings due to skewed superstructures, impact loads from vessels or ice, seismic loads, or loading in any sort of continuous frame. Eccentricity is accounted for by distributing the non-uniform pressure distribution due to the eccentric load as an equivalent uniform pressure over an "effective area" that is smaller than the actual area of the original footing such that the point of application of the eccentric load passes through the centroid of the "effective area." The eccentricity correction is usually applied by reducing the width (B_f) and length (L_f) such that:

$$B'_f = B_f - 2e_B \quad 8\text{-}7$$

$$L'_f = L_f - 2e_L \quad 8\text{-}8$$

where, as shown in Figure 8-16, e_B and e_L are the eccentricities in the B_f and L_f directions, respectively. These eccentricities are computed by dividing the applied moment in each direction by the applied vertical load. It is important to maintain consistent sign conventions and coordinate directions when this conversion is done. The reduced footing dimensions B'_f and L'_f are termed the effective footing dimensions. When eccentric load occurs in both directions, the equivalent uniform bearing pressure is assumed to act over an effective fictitious area, A', where (AASHTO, 2004 with 2006 Interims):

$$A' = B'_f L'_f \quad 8\text{-}9$$

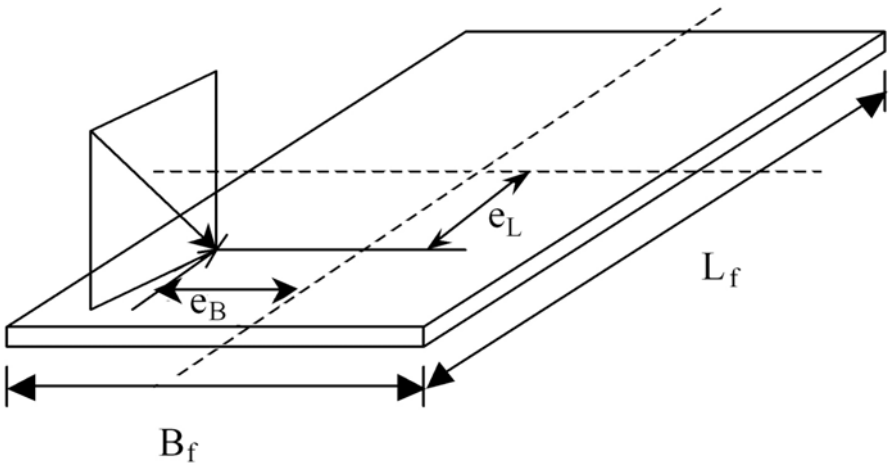

Figure 8-16. Notations for footings subjected to eccentric, inclined loads (after Kulhawy, 1983).

The concept of an effective area loaded by an equivalent uniform pressure is an approximation made to account for eccentric loading and was first proposed by Meyerhof (1953). Therefore, the equivalent uniform pressure is often referred to as the "**Meyerhof pressure**." The concept of equivalent footing and Meyerhof pressure is used for geotechnical analysis during sizing of the footing, i.e., bearing capacity and settlement analyses. However, the structural design of a footing should be performed using the actual trapezoidal or triangular pressure distributions that model the pressure distribution under an eccentrically loaded footing more conservatively. A comparison of the two loading distributions is shown in Figure 8-17.

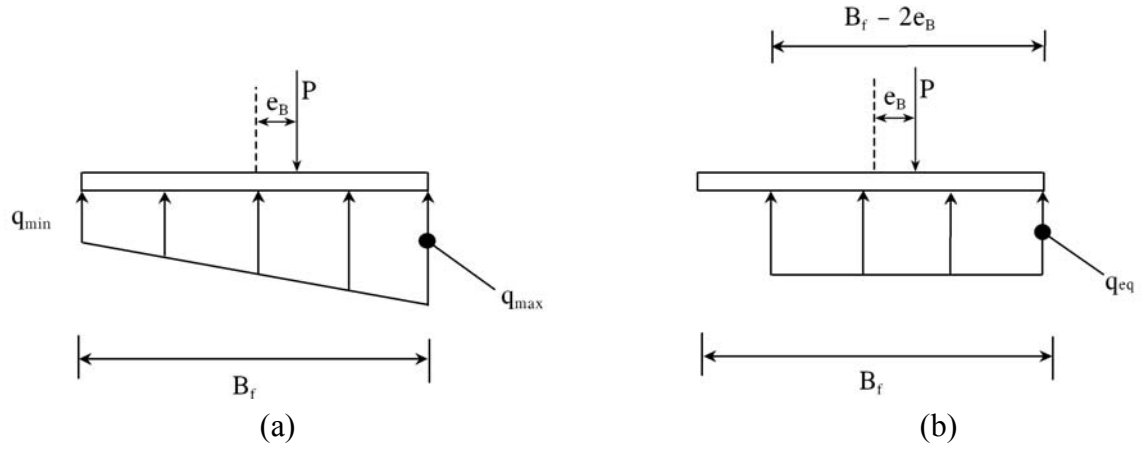

Figure 8-17. Eccentrically loaded footing with (a) Linearly varying pressure distribution (structural design), (b) Equivalent uniform pressure distribution (sizing the footing).

Limiting eccentricities are defined to ensure that zero contact pressure does not occur at any point beneath the footing. These limiting eccentricities vary for soil and rock. Footings founded on soil should be designed such that the eccentricity in any direction (e_B or e_L) is less than one-sixth (1/6) of the actual footing dimension in the same direction. For footings founded on rock, the eccentricity should be less than one-fourth (1/4) of the actual footing dimension. If the eccentricity does not exceed these limits, a separate calculation for stability with respect to overturning need not be performed. If eccentricity does exceed these limits, the footing should be resized.

The shape correction factors are summarized in Table 8-4. For eccentrically loaded footings, AASHTO (2004 with 2006 Interims) recommends use of the effective footing dimensions, B'_f and L'_f, to compute the shape correction factors. However, in routine foundation design, use of the effective footing dimensions is not practical since the effective dimensions will

change for various load cases. Besides, the difference in the computed shape correction factors for actual and effective footing dimensions will generally be small. Therefore the geotechnical engineer should make reasonable assumptions about the footing shape and dimensions and compute the correction factors by using the equations in Table 8-4.

Table 8-4
Shape correction factors (AASHTO, 2004 with 2006 Interims)

Factor	Friction Angle	Cohesion Term (s_c)	Unit Weight Term (s_γ)	Surcharge Term (s_q)
Shape Factors, s_c, s_γ, s_q	$\phi = 0$	$1+\left(\frac{B_f}{5L_f}\right)$	1.0	1.0
	$\phi > 0$	$1+\left(\frac{B_f}{L_f}\right)\left(\frac{N_q}{N_c}\right)$	$1-0.4\left(\frac{B_f}{L_f}\right)$	$1+\left(\frac{B_f}{L_f}\tan\phi\right)$
Note: Shape factors, s, should not be applied simultaneously with inclined loading factors, i. See Section 8.4.3.5.				

8.4.3.2 Location of the Ground Water Table

If the ground water table is located within the potential failure zone above or below the base of a footing, buoyant (effective) unit weight should be used to compute the overburden pressure. A simplified method for accounting for the reduction in shearing resistance is to apply factors to the two terms in the bearing capacity equation that include a unit weight term. Recall that the cohesion term is neither a function of soil unit weight nor effective stress. The ground water factors may be computed by interpolating values between those provided in Table 8-5 (D_W = depth to water from ground surface).

Table 8-5
Correction factor for location of ground water table
(AASHTO, 2004 with 2006 Interims)

D_W	$C_{w\gamma}$	C_{wq}
0	0.5	0.5
D_f	0.5	1.0
$> 1.5B_f + D_f$	1.0	1.0
Note: For intermediate positions of the ground water table, interpolate between the values shown above.		

8.4.3.3 Embedment Depth

Because the effect on bearing capacity of the depth of embedment was accounted for by considering it as an equivalent surcharge applied at the footing bearing elevation, the effect of the shearing resistance due to the failure surface actually passing through the footing embedment cover was neglected in the theory. If the backfill or cover over the footing is known to be a high-quality, compacted granular material that can be assumed to remain in place over the life of the footing, additional shearing resistance due to the backfill can be accounted for by including in the surcharge term the embedment depth correction factor, d_q, shown in Table 8-6. Otherwise, the depth correction factor can be conservatively omitted.

Table 8-6
Depth correction factors
(Hansen and Inan, 1970; AASHTO, 2004 with 2006 Interims)

Friction Angle, ϕ (degrees)	D_f/B_f	d_q
32	1	1.20
	2	1.30
	4	1.35
	8	1.40
37	1	1.20
	2	1.25
	4	1.30
	8	1.35
42	1	1.15
	2	1.20
	4	1.25
	8	1.30
Note: The depth correction factor should be used only when the soils above the footing bearing elevation are as competent as the soils beneath the footing level; otherwise, the depth correction factor should be taken as 1.0.		

Spread footings should be located below the depth of frost potential due to possible frost heave considerations discussed in Section 5.7.3. Figure 5-29 may be used for preliminary guidance on depth of frost penetration. Similarly, footings should be located below the depth of scour to prevent undermining of the footing.

8.4.3.4 Inclined Base

In general, inclined footings for bridges should be avoided or limited to inclination angles, α, less than about 8 to 10 degrees from the horizontal. Steeper inclinations may require keys, dowels or anchors to provide sufficient resistance to sliding. For footings inclined to the horizontal, Table 8-7 provides equations for the correction factors to be used in Equation 8-6.

Table 8-7
Inclined base correction factors (Hansen and Inan, 1970; AASHTO, 2004 with 2006 Interims)

Factor	Friction Angle	Cohesion Term (c)	Unit Weight Term (γ)	Surcharge Term (q)
		b_c	b_γ	b_q
Base Inclination Factors, b_c, b_γ, b_q	$\phi = 0$	$1-\left(\frac{\alpha}{147.3}\right)$	1.0	1.0
	$\phi > 0$	$b_q-\left(\frac{1-b_q}{N_c \tan\phi}\right)$	$(1\text{-}0.017\alpha \tan\phi)^2$	$(1\text{-}0.017\alpha \tan\phi)^2$
ϕ = friction angle, degrees; α = footing inclination from horizontal, upward +, degrees				

8.4.3.5 Inclined Loading

A convenient way to account for the effects of an inclined load applied to the footing by the column or wall stem is to consider the effects of the axial and shear components of the inclined load individually. If the vertical component is checked against the available bearing capacity and the shear component is checked against the available sliding resistance, the inclusion of load inclination factors in the bearing capacity equation can generally be omitted. The bearing capacity should, however, be evaluated by using effective footing dimensions, as discussed in Section 8.4.3.1 and in the footnote to Table 8-4, since large moments can frequently be transmitted to bridge foundations by the columns or pier walls. **The simultaneous application of shape and load inclination factors can result in an overly conservative design.**

Unusual column geometry or loading configurations should be evaluated on a case-by-case basis relative to the foregoing recommendation before the load inclination factors are omitted. An example might be a column that is not aligned normal to the footing bearing surface. In this case, an inclined footing may be considered to offset the effects of the inclined load by providing improved bearing efficiency (see Section 8.4.3.4). Keep in mind that bearing surfaces that are not level may be difficult to construct and inspect.

8.4.3.6 Sloping Ground Surface

Placement of footings on or adjacent to slopes requires that the designer perform calculations to ensure that both the bearing capacity and the overall slope stability are acceptable. The bearing capacity equation should include corrections recommended by AASHTO as adapted from NAVFAC (1986b) to design the footings. Calculation of overall (global) stability is discussed in Chapter 6.

For sloping ground surface, Equation 8-6 is modified to include terms N_{cq} and $N_{\gamma q}$ that replace the N_c and N_γ terms. The modified version is given by Equation 8-10. There is no surcharge term in Equation 8-10 because the surcharge effect on the slope side of the footing is ignored.

$$q_{ult} = c(N_{cq})s_c b_c + 0.5\gamma B_f (N_{\gamma q}) C_{w\gamma} s_\gamma b_\gamma \qquad 8\text{-}10$$

Charts are provided in Figure 8-18 to determine N_{cq} and $N_{\gamma q}$ for footings on (Figure 8-18a) or close to (Figure 8-18d) slopes for cohesive ($\phi = 0^o$) and cohesionless ($c = 0$) soils. As indicated in Figure 8-18d, the bearing capacity is independent of the slope angle if the footing is located beyond a distance, 'b,' of two to six times the foundation width, i.e., the situation is identical to the case of horizontal ground surface.

Other forms of Equation 8-10 are available for cohesive soils ($\phi = 0^o$). However, because footings located on or near slopes consisting of cohesive soils, they are likely to have design limitations due to either settlement or slope stability, or both, the presentation of these equations is omitted here. The reader is referred to NAVFAC (1986a, 1986b) for discussions of these equations and their applications and limitations.

Equation 8-10, which includes the width term for cohesionless soils, is useful in designing footings constructed within bridge approach fills. In this case, obtain $N_{\gamma q}$ from Figure 8-18(c) or 8-18(f) and then compute the ultimate bearing capacity by using Equation 8-10.

8.4.3.7 Layered Soils

For layered soils, the reader is referred to the guidance provided in AASHTO (2004 with 2006 Interims).

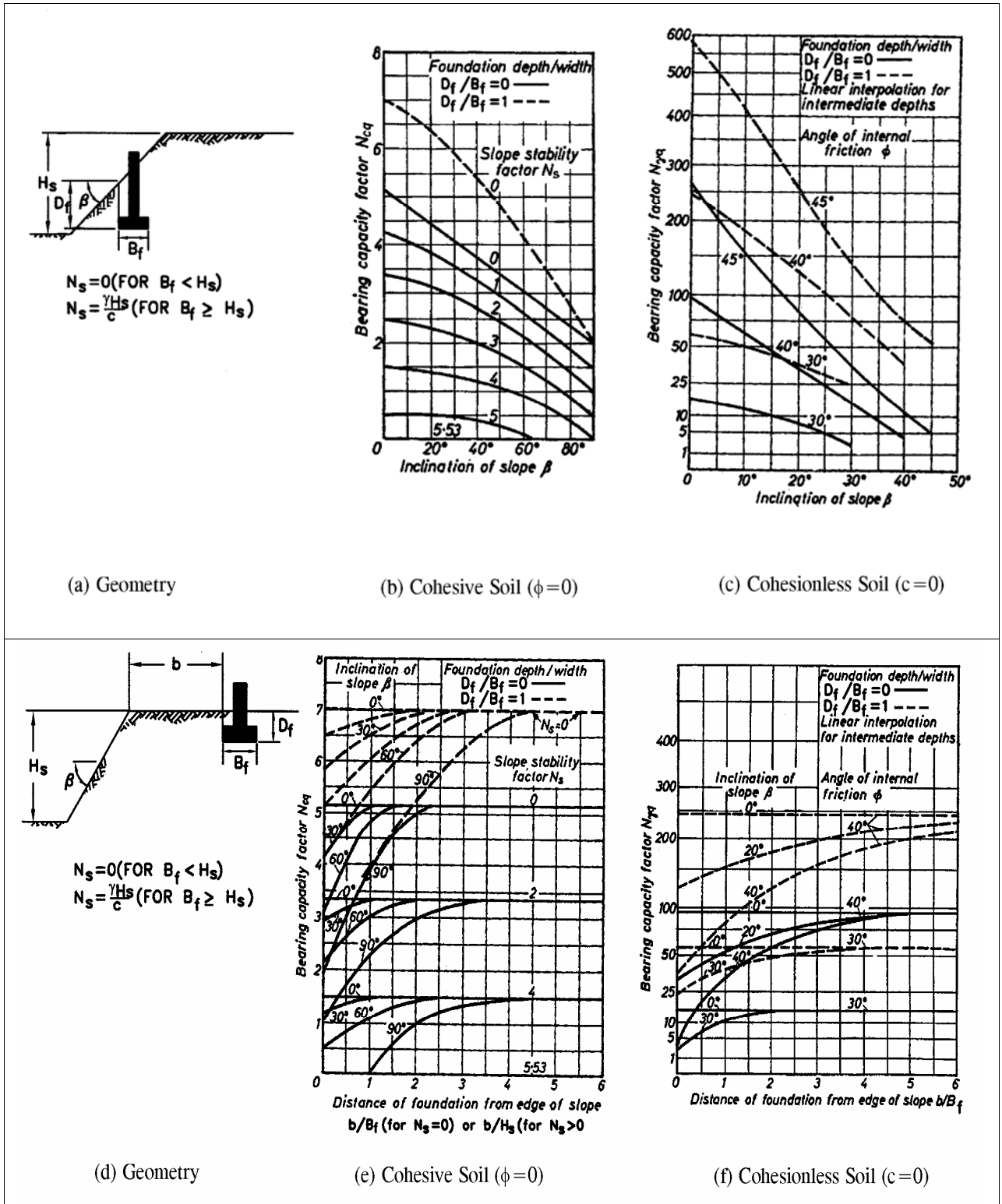

(a) Geometry

(b) Cohesive Soil ($\phi = 0$)

(c) Cohesionless Soil ($c = 0$)

(d) Geometry

(e) Cohesive Soil ($\phi = 0$)

(f) Cohesionless Soil ($c = 0$)

Figure 8-18. Modified bearing capacity factors for continuous footing on sloping ground (after Meyerhof, 1957, from AASHTO, 2004 with 2006 Interims)

8.4.4 Additional Considerations Regarding Bearing Capacity Correction Factors

The inherent or implied factor of safety of a settlement-limited allowable bearing capacity relative to the computed ultimate bearing capacity is usually large enough to render the magnitude of the application of the individual correction factors small. Some comments in this regards are as follows:

- AASHTO (2002) guidelines recommend calculating the shape factors, s, by using the effective footing dimensions, B'_f and L'_f. However, the original references (e.g., Vesic, 1975) do not specifically recommend using the effective dimensions to calculate the shape factors. Since the geotechnical engineer typically does not have knowledge of the loads causing eccentricity, it is recommended that the full footing dimensions be used to calculate the shape factors according to the equations given in Table 8-4 for use in computation of ultimate bearing capacity.

- Bowles (1996) also recommends that the shape and load inclination factors (s and i) should not be combined.

- In certain loading configurations, the designer should be careful in using inclination factors together with shape factors that have been adjusted for eccentricity (Perloff and Baron, 1976). The effect of the inclined loads may already be reflected in the computation of the eccentricity. Thus an overly conservative design may result.

Further, the bearing capacity correction factors were developed with the assumption that the correction for each of the terms involving N_c, N_γ and N_q can be found independently. The bearing capacity theory is an idealization of the response of a foundation that attempts to account for the soil properties and boundary conditions. Bearing capacity analysis of foundations is frequently limited by the geotechnical engineer's ability to determine material properties accurately as opposed to inadequacies in the theory used to develop the bearing capacity equations. Consider Table 8-2 and note that a one degree change in friction angle can result in a 10 to 15 percent change in the factors N_c, N_γ and N_q. Determination of the in situ friction angle to an accuracy of 1º is virtually impossible. Also note that the value of N_γ more than doubles when the friction angle increases from 35º to 40º. Clearly, the uncertainties in the material properties will control the uncertainty of a bearing capacity computation to a large extent. **The importance of the application of the correction factors is therefore secondary to adequate assessment of the inherent strength characteristics of the foundation soil through correctly performed field investigations and laboratory testing**.

Unfortunately, very few spread footings of the size used for bridge support have been load-tested to failure. Therefore, the evaluation of ultimate bearing capacity is based primarily on theory and laboratory testing of small-scale footings, with modification of the theoretical equations based on observation.

8.4.5 Local or Punching Shear

Several references, including AASHTO (2004 with 2006 Interims), recommend reducing the soil strength parameters if local or punching shear failure modes can develop. Figure 8-19 shows conditions when these modes can develop for granular soils. The recommended reductions are shown in Equations 8-11 and 8-12.

$$c^* = 0.67c \qquad 8\text{-}11$$

$$\phi^* = \tan^{-1}(0.67\tan\phi) \qquad 8\text{-}12$$

where: c^* = reduced effective stress soil cohesion for punching shear (tsf (MPa))
ϕ^* = reduced effective stress soil friction angle for punching shear (degrees)

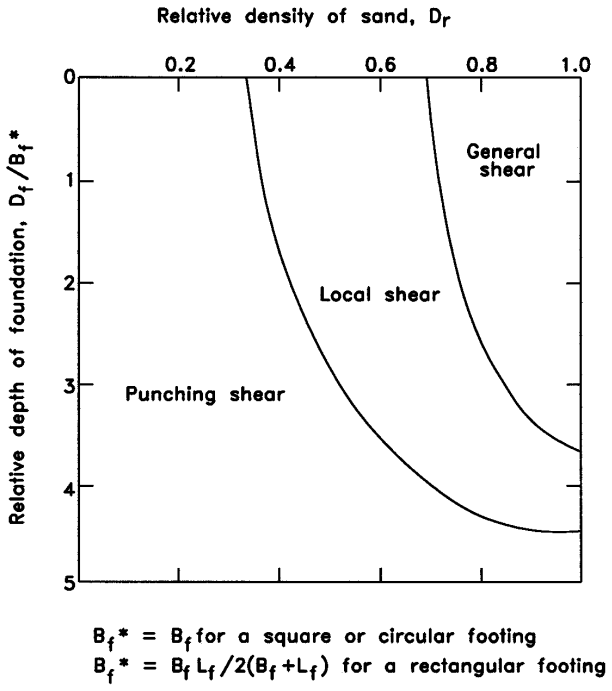

Figure 8-19. Modes of failure of model footings in sand (after Vesic, 1975; AASHTO, 2004 with 2006 Interims)

Soil types that can develop local or punching shear failure modes include loose sands, quick clays (i.e., clays with sensitivity, $S_t > 8$; see Table 3-12 in Chapter 3), collapsible sands and silts, and brittle clays (OCR > 4 to 8). As indicated in Section 3.12, **sensitivity of clay** is defined as the ratio of the peak undrained shearing strength to the remolded undrained shearing strength. These soils present potential "problem" conditions that should be identified through a comprehensive geotechnical investigation. In general, these problem soils will have other characteristics that make them unsuitable for the support of shallow foundations for bridges, including large settlement potential for loose sands, sensitive clays and collapsible soils. Brittle clays exhibit relatively high strength at small strains, but they generally undergo significant reduction in strength at larger strains (strain-softening). This behavior should be identified and quantified through the field and laboratory testing program and compared to the anticipated stress changes resulting from the shallow foundation and ground slope configuration under consideration.

Although local or punching shear failure modes can develop in loose sands or when very narrow footings are used, this local condition seldom applies to bridge foundations because spread footings are not used on obviously weak soils. In general, relatively large footing sizes are needed for structural stability of bridge foundations.

The geotechnical engineer may encounter the following two situations where the application of the one-third reduction according to Equation 8-12 can result in an unnecessarily over-conservative design.

- The first is when a footing bears on a cohesionless soil that falls in the local shear portion of Figure 8-19. Note that a one-third reduction in the tangent of a friction angle of 38 degrees, a common value for good-quality, compacted, granular fill, results in a 73 percent reduction in the bearing capacity factor N_q, and an 81 percent reduction in N_γ. Also note that Figure 8-19 does not consider the effect of large footing widths, such as those used for the support of bridges. **Therefore, provided that settlement potential is checked independently and found to be acceptable, spread footings on normally consolidated cohesionless soils falling within the local shear portion of Figure 8-19 should <u>not</u> be designed by using the one-third reduction according to Equation 8-12.**

- The second situation is when a spread footing bears on a compacted structural fill. The relative density of compacted structural fills as compared to compactive effort, i.e., percent relative compaction, indicates that for fills compacted to a minimum of 95 percent of maximum dry density as determined by AASHTO T 180, the relative

density should be at or above 75 percent (see Figure 5-33 in Chapter 5). This relationship is consistent with the excellent performance history of spread footings in compacted structural fills (FHWA, 1982). Therefore, the one-third reduction should not be used in the design of footings on compacted structural fills constructed with good quality, granular material.

8.4.6 Bearing Capacity Factors of Safety

The minimum factor of safety applied to the calculated ultimate bearing capacity will be a function of:

- The confidence in the design soil strength parameters c and ϕ,
- The importance of the structure, and
- The consequence of failure.

Typical minimum factors of safety for shallow foundations are in the range of 2.5 to 3.5. A minimum factor of safety against bearing capacity failure of 3.0 is recommended for most bridge foundations. This recommended factor of safety was selected through a combination of applied theory and experience. **Uncertainty in the magnitudes of the loads and the available soil bearing strength are combined into this single factor of safety.** The general equation to compute the allowable bearing capacity as a function of safety factor is:

$$q_{all} = \frac{q_{ult}}{FS} \qquad 8\text{-}13$$

where: q_{all} = allowable bearing capacity (ksf) (kPa)
q_{ult} = ultimate bearing capacity (ksf) (kPa)
FS = the applied factor of safety

8.4.6.1 Overstress Allowances

Allowable Strength Design (ASD) criteria permit the allowable bearing capacity to be exceeded for certain load groups (e.g., seismic) by a specified percentage that ranges from 25 to 50 percent (AASHTO, 2002). These overstress allowances are permitted for short-duration, infrequently occurring loads and may also be applied to calculated allowable bearing capacities. Construction loading is often a short-duration loading and may be considered for overstress allowances. **Overstress allowances should not be permitted for cases where soft soils are encountered within the depth of significant influence (DOSI) or durations are such that temporary loads may cause unacceptable settlements.**

8.4.7 Practical Aspects of Bearing Capacity Formulations

This section presents some useful practical aspects of bearing capacity formulations. Several interesting observations are made here that provide practical guidance in terms of implementation and interpretation of the bearing capacity formulation and computed results.

8.4.7.1 Bearing Capacity Computations

The procedure to be used to compute bearing capacity is as follows:

1. Review the structural plans to determine the proposed footing widths. In the absence of data assume a pier footing width equal to 1/3 the pier column height and an abutment footing width equal to 1/2 the abutment height.

2. Review the soil profile to determine the position of the groundwater table and the interfaces between soil layer(s) that exist within the appropriate depth below the proposed footing level.

3. Review soil test data to determine the unit weight, friction angle and cohesion of all of the impacted soils. In the absence of test data, estimate these values for coarse-grained granular soils from SPT N-values (refer to Table 8-3). NOTE SPT N-values in cohesive soils should not be used to determine shear strengths for final design since the reliability of SPT N-values in such soils is poor.

4. Use Equation 8-6 with appropriate correction factors to compute the ultimate bearing capacity. The general case (continuous footing) may be used when the footing length is 10 or more times the footing width. Also the bearing capacity factor N_γ will usually be determined for a rough base condition since most footings are poured concrete. However the smoothness of the contact material must be considered for temporary footings such as wood grillages (rough), or steel supports (smooth) or plastic sheets (smooth). The safety factor for the bearing capacity of a spread footing is selected both to limit the amount of soil strain and to account for variations in soil properties at footing locations.

5. The mechanism of the general bearing capacity failure is similar to the embankment slope failure mechanism. However, the footing analysis is a 3-dimensional analysis as opposed to the 2-dimensional slope stability analysis. The bearing capacity factors N_c, N_q and N_γ relate to the actual volume of soil involved in the failure zones. A

cursory study of the failure cross sections in Figure 8-13, discloses that the depth and lateral extent of the failure zones and the values of N_c, N_q and N_γ are determined by the dimensions of the wedge-shaped zone directly below the footing. As the friction angle increases, the depth and width of the failure zones increase, i.e., more soil is impacted and more shear resistance is mobilized, thereby increasing the bearing capacity.

6. Substantial downward movement of the footing is required to mobilize the shearing resistance within the entire failure zone completely. Besides providing a margin of safety on shear strength properties, the relatively large safety factor of 3 commonly used in the design of footings controls the amount of strain necessary to mobilize the allowable bearing capacity fully. Settlement analysis (Section 8.5) is recommended to compute the allowable bearing capacity corresponding to a specified limiting settlement. That allowable bearing capacity may result in a factor of safety with respect to ultimate bearing capacity much larger than 3.

7. In reporting the results of bearing capacity analyses, the footing width that was used to compute the bearing capacity should always be included. Most often the geotechnical engineer must assume a footing width since bearing capacity analyses are completed before structural design begins. It is recommended that bearing capacity be computed for a range of possible footing widths and those values be included in the foundation report with a note stating that if other footing widths are used, the geotechnical engineer should be contacted. The state of the practice today is for the geotechnical engineer to develop location-specific bearing capacity charts on which allowable bearing capacity is plotted versus footing width for a family of curves representing specific values of settlement. Refer to Figure 8-10 for a schematic example of such a chart.

8. The **net** ultimate bearing pressure is the difference between the gross ultimate bearing pressure and the pressure that existed due to the ground surcharge at the bearing depth before the footing was constructed, q (= $\gamma_a D_f$). The net ultimate bearing pressure can thus be computed by subtracting the ground surcharge (q) from Equation 8-6:

$$q_{ult\,net} = q_{ult} - q \qquad 8\text{-}14$$

$$q_{ult\,net} = cN_c s_c b_c + q(N_q - 1) C_{wq} s_q b_q d_q + 0.5\gamma B_f N_\gamma C_{w\gamma} s_\gamma b_\gamma \qquad 8\text{-}15$$

The structural designer will typically include the self-weight of the concrete footing and the backfill over the footing (approximately equal to $\gamma_a D_f$) in the loads that contribute to the applied bearing stress. Therefore, if the geotechnical engineer computes and reports a net ultimate bearing pressure, the effect of the surcharge directly over the footing area is counted twice. Reporting an allowable bearing capacity computed from a net ultimate bearing pressure is conservative and generally not recommended provided that a suitable factor of safety is maintained against bearing capacity failure. If the geotechnical engineer chooses to report an allowable bearing capacity computed from a net ultimate bearing pressure, this fact should be clearly stated in the foundation report.

8.4.7.2 Failure Zones

Certain practical information based on the geometry of the failure zone is as follows:

1. The bearing capacity of a footing is dependent on the strength of the soil within a depth of approximately 1.5 times footing width below the base of the footing unless much weaker soils exist just below this level, in which case a potential for punching shear failure may exist. Continuous soil samples and SPT N-values should be routinely specified within this depth. If the borings for a structure are done long before design, a good practice is to obtain continuous split spoon samples for the top 15 ft (4.5 m) of each boring where footings may be placed on natural soil. The cost of this sampling is minimal but the knowledge gained is great. At a minimum, continuous sampling to a depth of 15 ft (4.5 m) will generally provide the following information:

    a. thickness of existing topsoil.
    b. location of any thin zones of unsuitable material.
    c. accurate determination of depth of existing fill.
    d. improved ground water determination in the critical zone.
    e. representative samples in this critical zone to permit reliable determination of strength parameters in the laboratory and confident assessment of bearing capacity.

2. Often questions arise during excavation near existing footings as to the effect of soil removal adjacent to the footing on the bearing capacity of that footing. In general, for weaker soils the zone of lateral influence extends outside the footing edge less than twice the footing width. Reductions in bearing capacity can be estimated by

considering the effects of surcharge removal within these zones. The theoretical lateral extent of this zone is shown in Figure 8-20. This figure is also useful in determining the effects of ground irregularities on bearing capacity or the effects of footing loads on adjacent facilities.

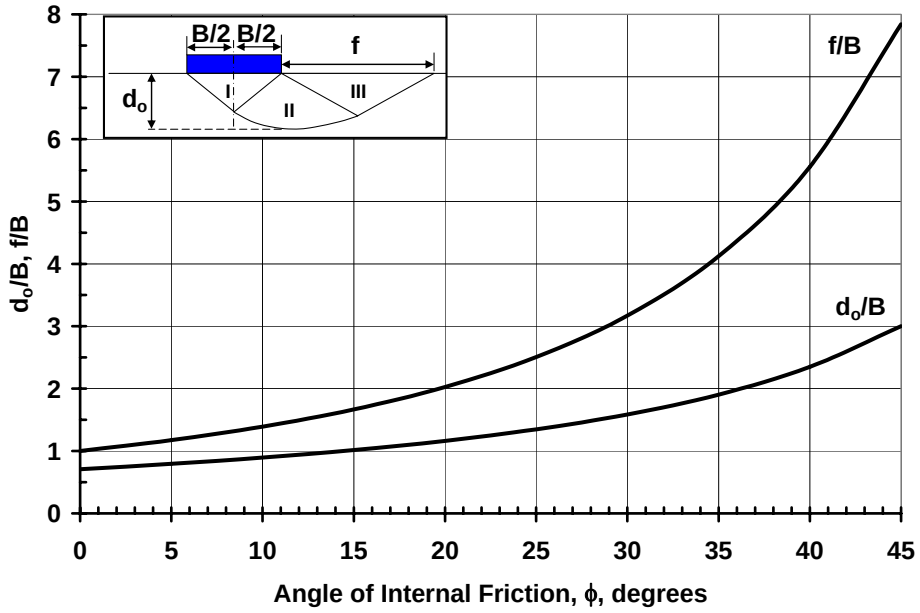

Figure 8-20. Approximate variation of depth (d_o) and lateral extent (f) of influence of footing as a function of internal friction angle of foundation soil.

As noted earlier, the general mechanism by which soils resist a footing load is similar to the foundation of an embankment resists shear failure. The load to cause failure must exceed the available soil strength within the failure zone. When failure occurs the footing plunges into the ground and causes an uplift of the soil adjacent to the sides of the footing. The resistance to failure is based on the soil strength and the amount of soil above the footing. Therefore, the bearing capacity of a footing can be increased by:

1. replacing or densifying the soil below the footing prior to construction.

2. increasing the embedment of the footing below ground, provided no weak soils exist within 1.5 times the footing width.

Common examples of improving bearing capacity are the support of temporary footings on pads of gravel or the embedment of mudsills a few feet below ground to support falsework. The design of these support systems is primarily done by bearing capacity analysis in which the results of subsurface explorations and testing are used. Structural engineers who review falsework designs should carefully check the soil bearing capacity at foundation locations.

8.4.8 Presumptive Bearing Capacities

Many building codes include provisions that arbitrarily limit the amount of loading that may be applied on various classes of soils by structures subject to code regulations. These limiting loads are generally based on bearing pressures that have been observed to result in acceptable settlements. The implication is that on the basis of experience alone it may be presumed that each designated class of soil will safely support the loads indicated without the structure undergoing excessive settlements. Such values listed in codes or in the technical literature are termed presumptive bearing capacities.

8.4.8.1 Presumptive Bearing Capacity in Soil

The use of presumptive bearing capacities for shallow foundations bearing in soils is not recommended for final design of shallow foundations for transportation structures, especially bridges. Guesses about the geology and nature of a site and the application of a presumptive value from generalizations in codes or in the technical literature are not a substitute for an adequate site-specific subsurface investigation and laboratory testing program. As an exception, presumptive bearing values are sometimes used for the preliminary evaluation of shallow foundation feasibility and estimation of footing dimensions for preliminary constructability or cost evaluations.

8.4.8.2 Presumptive Bearing Capacity in Rock

Footings on intact sound rock that is stronger and less compressible than concrete are generally stable and do not require extensive study of the strength and compressibility characteristics of the rock. However, site investigations are still required to confirm the consistency and extent of rock formations beneath a shallow foundation.

Allowable bearing capacities for footings on relatively uniform and sound rock surfaces are documented in applicable building codes and engineering manuals. Many different definitions for sound rock are available. **In simple terms, however, "sound rock" can generally be defined as a rock mass that does not disintegrate after exposure to air or water and whose discontinuities are unweathered, closed or tight, i.e., less than about 1/8 in (3 mm) wide and spaced no closer than 3 ft (1 m) apart.** Table 8-8 presents allowable bearing pressures for intact rock recommended in selected local building codes (Goodman, 1989). These values were developed based on experience in sound rock formations, with the intention of satisfying both bearing capacity and settlement criteria in order to provide a satisfactory factor of safety. However, the use of presumptive values may lead to overly conservative and costly foundations. In such cases, most codes allow for a

variance if the request is supported by an engineering report. Site-specific investigation and analysis is strongly encouraged.

In areas where building codes are not available or applicable, other recommended presumptive bearing values, such as those listed in Table 8-9, may be used to determine the allowable bearing pressure for sound rock. For footings designed by using these published values, the elastic settlements are generally less than 0.5 in (13 mm). Where the rock is reasonably sound, but fractured, the presumptive values listed in Tables 8-8 and 8-9 should be reduced by limiting the bearing pressures to tolerable settlements based on settlement analyses. Most building codes also provide reduced recommended bearing pressures to account for the degree of fracturing.

Peck, *et al.* (1974) presented an empirical correlation of presumptive allowable bearing pressure with Rock Quality Designation (RQD), as shown in Table 8-10. If the recommended value of allowable bearing pressure exceeds the unconfined compressive strength of the rock or allowable stress of concrete, the allowable bearing pressure should be taken as the lower of the two values. Although the suggested bearing values of Peck, *et al.* (1974) are substantially greater than most of the other published values and ignore the effects of rock type and conditions of discontinuities, they provide a useful guide for an upper-bound estimation as well as an empirical relationship between allowable bearing values and the intensity of fracturing and jointing (Table 8-10). Note that with a slight increase of the degree of fracturing of the rock mass, for example when the RQD value drops from 100 percent to 90 percent, the recommended bearing capacity value is reduced drastically from 600 ksf (29 MPa) to 400 ksf (19 MPa).

In no instance should the allowable bearing capacity exceed the allowable stress of the concrete used in the structural foundation. Furthermore, Peck, *et al.* (1974) also suggest that the average RQD for the bearing rock within a depth of the footing width (B_f) below the base of the footing should be used if the RQD values within the depth are relatively uniform. If rock within a depth of $0.5B_f$ is of poorer quality, the RQD of the poorer quality rock should be used to determine the allowable bearing capacity.

Table 8-8

Allowable bearing pressures for fresh rock of various types (Goodman, 1989)

Rock Type	Age	Location	Allowable Bearing Pressure tsf (MPa)
Massively bedded limestone[5]		U.K.[6]	80 (3.8)
Dolomite	L. Paleoz.	Chicago	100 (4.8)
Dolomite	L. Paleoz.	Detroit	20-200 (1.0 – 9.6)
Limestone	U. Paleoz.	Kansas City	20-120 (0.5 – 5.8)
Limestone	U. Paleoz.	St. Louis	50-100 (2.4 – 4.8)
Mica schist	Pre-Camb.	Washington	20-40 (0.5 – 1.9)
Mica schist	Pre-Camb.	Philadelphia	60-80 (2.9 – 3.8)
Manhattan schist	Pre-Camb.	New York	120 (5.8)
Fordham gneiss	Pre-Camb.	New York	120 (5.8)
Schist and slate	-	U.K.[6]	10-25 (0.5 – 1.2)
Argillite	Pre-Camb.	Cambridge, MA	10-25 (0.5 – 1.2)
Newark shale	Triassic	Philadelphia	10-25 (0.5 – 1.2)
Hard, cemented shale	-	U.K.[6]	40 (1.9)
Eagleford shale	Cretaceous	Dallas	13-40 (0.6 – 1.9)
Clay shale	-	U.K.[6]	20 (1.0)
Pierre shale	Cretaceous	Denver	20-60 (1.0 – 2.9)
Fox Hills sandstone	Tertiary	Denver	20-60 (1.0 – 2.9)
Solid chalk	Cretaceous	U.K.[6]	13 (0.6)
Austin chalk	Cretaceous	Dallas	30-100 (1.4 – 4.8)
Friable sandstone and claystone	Tertiary	Oakland	8-20 (0.4 – 1.0)
Friable sandstone (Pico formation)	Quaternary	Los Angeles	10-20 (0.5 – 1.0)

Notes:

[1] According to typical building codes; reduce values accordingly to account for weathering or unrepresentative fracturing

[2] Values from Thorburn (1966) and Woodward, Gardner and Greer (1972).

[3] When a range is given, it relates to usual range in rock conditions.

[4] Sound rock that rings when struck and does not disintegrate. Cracks are unweathered and open less than 10 mm.

[5] Thickness of beds greater than 3 ft (1 m), joint spacing greater than 2 mm; unconfined compressive strength greater than 160 tsf (7.7 MPa) (for a 4 in (100 mm) cube).

[6] Institution of Civil Engineers Code of Practice 4.

Table 8-9
Presumptive values of allowable bearing pressures for spread foundations on rock (modified after NAVFAC, 1986a, AASHTO 2004 with 2006 Interims)

Type of Bearing Material	Consistency In Place	Allowable Bearing Pressure tsf (MPa)	
		Range	Recommended Value for Use
Massive crystalline igneous and metamorphic rock: granite, diorite, basalt, gneiss, thoroughly cemented conglomerate (sound condition allows minor cracks)	Hard, sound rock	120-200 (5.8 - 9.6)	160 (7.7)
Foliated metamorphic rock: Slate, schist (sound condition allows minor cracks)	Medium-hard, sound rock	60-80 (2.9-3.8)	70 (3.4)
Sedimentary rock; hard cemented shales, siltstone, sandstone, limestone without cavities	Medium-hard, sound rock	30-50 (1.4-2.4)	40 (1.9)
Weathered or broken bedrock of any kind except highly argillaceous rock (shale). RQD less than 25	Soft rock	16-24 (0.8-1.2)	20 (1)
Compacted shale or other highly argillaceous rock in sound condition	Soft rock	16-24 (0.8-1.2)	20 (1)

Notes:

1. For preliminary analysis or in the absence of strength tests, design and proportion shallow foundations to distribute their loads by using presumptive values of allowable bearing pressure given in this table. Modify the nominal value of allowable bearing pressure for special conditions described in notes 2 through 8.
2. The maximum bearing pressure beneath the footing produced by eccentric loads that include dead plus normal live load plus permanent lateral loads shall not exceed the above nominal bearing pressure.
3. Bearing pressures up to one-third in excess of the nominal bearing values are permitted for transient live load from wind or earthquake. If overload from wind or earthquake exceeds one-third of nominal bearing pressures, increase allowable bearing pressures by one-third of nominal value.
4. Extend footings on soft rock to a minimum depth of 1.5 in (40 mm) below adjacent ground surface or surface of adjacent floor, whichever elevation is the lowest.
5. For footings on soft rock, increase allowable bearing pressures by 5 percent of the nominal values for each 1 ft (300 mm) of depth below the minimum depth specified in Note 4.
6. Apply the nominal bearing pressures of the three categories of hard or medium hard rock shown above where the base of the foundation lies on rock surface. Where the foundation extends below the rock surface, increase the allowable bearing pressure by 10 percent of the nominal values for each additional 1ft (300 mm) of depth extending below the surface.
7. For footings smaller than 3 ft (1 m) in the least lateral dimension, the allowable bearing pressure shall be the nominal bearing pressure multiplied by the least lateral dimension.
8. If the above-recommended nominal bearing pressure exceeds the unconfined compressive strength of intact specimen, the allowable pressure equals the unconfined compressive strength.

Table 8-10
Suggested values of allowable bearing capacity (Peck, *et al.*, 1974)

RQD (%)	Rock Mass Quality	Allowable Pressure ksf (MPa)
100	Excellent	600 (29)
90	Good	400 (19)
75	Fair	240 (12)
50	Poor	130 (6)
25	Very Poor	60 (3)
0	Soil-like	20 (1)

8.5 SETTLEMENT OF SPREAD FOOTINGS

The controlling factor in the design of a spread footing is usually tolerable settlement. Estimation of settlement may be routinely accomplished with adequate geotechnical data and knowledge of the structural loads. The accuracy of the estimation is only as good as the quality of the geotechnical data and the estimation of the actual loads. Settlements of spread footings are frequently overestimated by engineers for the following reasons:

1. The structural load causing the settlement is overestimated. In the absence of actual structural loads, geotechnical engineers conservatively assume that the footing pressure equals the maximum allowable soil bearing pressure.

2. Settlement occurring during construction is not subtracted from total predicted amounts (See discussion in Section 8.9 for more details).

3. Preconsolidation of the subsoil is not accounted for in the analysis. Preconsolidation may be due to a geologic load applied in past time or to removal of significant amounts of soil in construction prior to placement of the foundation. This error can cause a grossly overestimated settlement.

As explained in Chapter 7, there are two primary types of settlement, immediate (short-term) and consolidation (long-term). The procedures for computing these settlements under spread footings are similar to those under embankments as discussed in Chapter 7. The following sections illustrate the computation of immediate and consolidation settlements.

8.5.1 Immediate Settlement

As noted in Chapter 7, there are several methods available to evaluate immediate settlements. Modified Hough's method was introduced in Chapter 7 and was illustrated by an example. Modified Hough's method can also be applied to shallow foundations by using the same approach demonstrated in Chapter 7. Studies conducted by FHWA (1987) indicate that Modified Hough's procedure is conservative and over-predicts settlement by a factor of 2 or more. Such conservatism may be acceptable for the evaluation of the settlement of embankments due to reasons discussed in Chapter 7. However, in the case of shallow foundations such conservatism may lead to unnecessary use of costlier deep foundations in cases where shallow foundations may be viable. Therefore, use of a more rigorous procedure such Schmertmann's modified method (1978) is recommended for shallow foundations, and is presented here.

8.5.1.1 Schmertmann's Modified Method for Calculation of Immediate Settlements

An estimate of the immediate settlement, S_i, of spread footings can be made by using Equation 8-16 as proposed by Schmertmann, *et al.* (1978).

$$S_i = C_1 C_2 \, \Delta p \sum_{i=1}^{n} \Delta H_i \quad \text{where} \quad \Delta H_i = H_c \left(\frac{I_z}{XE} \right) \qquad 8\text{-}16$$

where: I_z = strain influence factor from Figure 8-21a. The dimension B_f represents the least lateral dimension of the footing after correction for eccentricities, i.e. use least lateral effective footing dimension. The strain influence factor is a function of depth and is obtained from the strain influence diagram. The strain influence diagram is easily constructed for the axisymmetric case ($L_f/B_f = 1$) and the plane strain case ($L_f/B_f \geq 10$) as shown in Figure 8-21a. The strain influence diagram for intermediate conditions can be determined by simple linear interpolation.

n = number of soil layers within the zone of strain influence (strain influence diagram).

Δp = ***net*** uniform applied stress (load intensity) at the foundation depth (see Figure 8-21b).

E = elastic modulus of layer i based on guidance provided in Table 5-16 in Chapter 5.

X = a factor used to determine the value of elastic modulus. If the value of elastic modulus is based on correlations with $N1_{60}$-values or q_c from Table 5-16 in Chapter 5, then use X as follows.

$X = 1.25$ for axisymmetric case ($L_f/B_f = 1$)
$X = 1.75$ for plane strain case ($L_f/B_f \geq 10$)

Use interpolation for footings with $1 < L_f/B_f \leq 10$

If the value of elastic modulus is estimated based on the range of elastic moduli in Table 5-16 or other sources use $X = 1.0$.

(a)

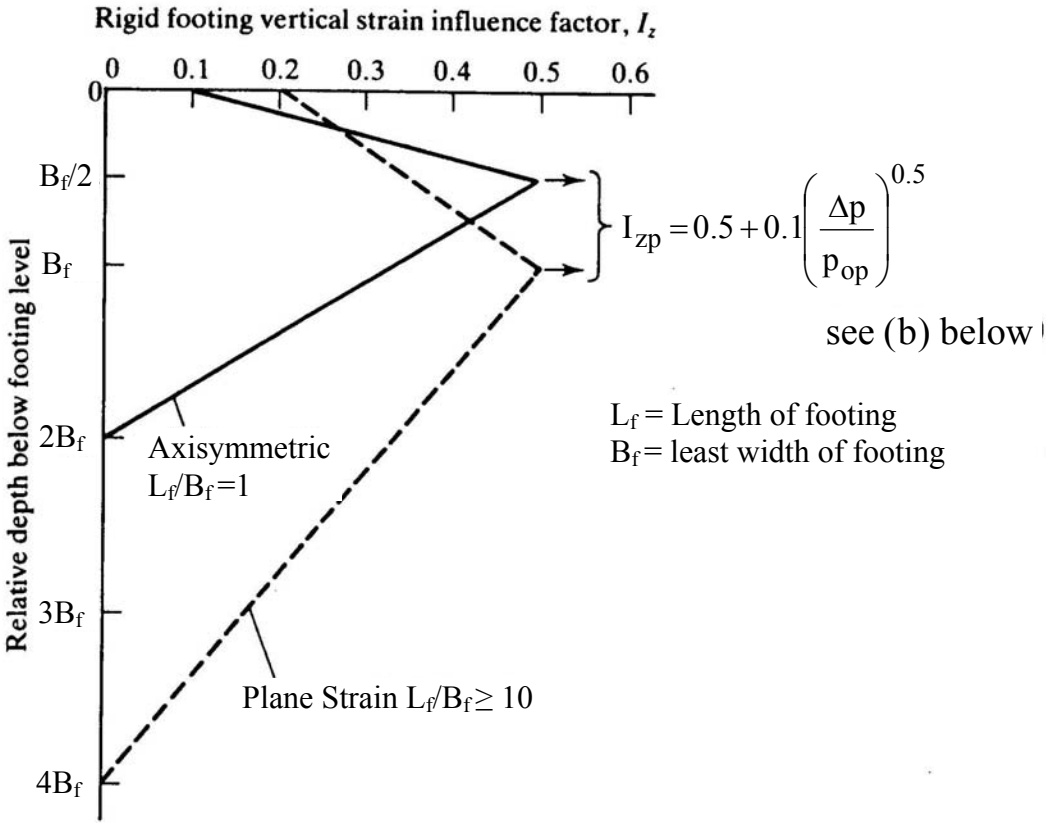

(b)

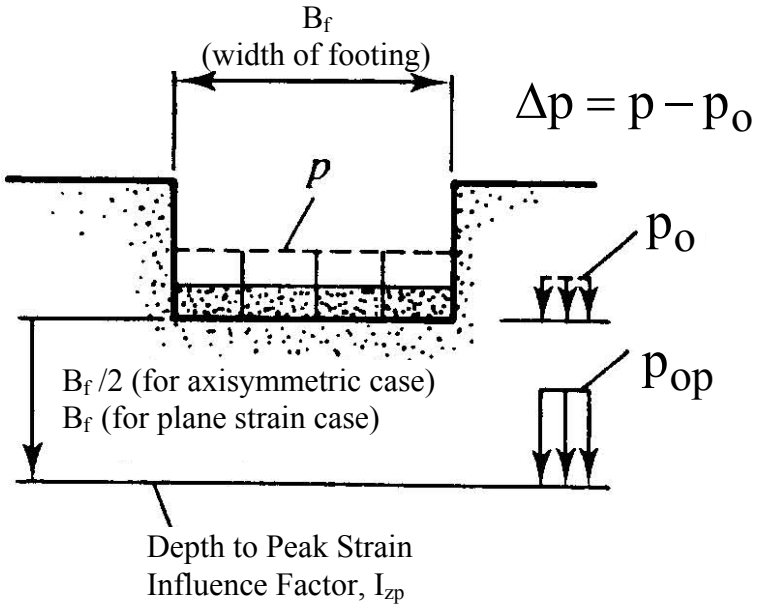

Figure 8-21. (a) Simplified vertical strain influence factor distributions, (b) Explanation of pressure terms in equation for I_{zp} (after Schmertmann, *et al.*, 1978).

C_1 = a correction factor to incorporate the effect of strain relief due to embedment where:

$$C_1 = 1 - 0.5\left(\frac{p_o}{\Delta p}\right) \geq 0.5 \qquad 8\text{-}17$$

where p_o is effective in-situ overburden stress at the foundation depth and Δp is the net foundation pressure as shown in Figure 8-21b

C_2 = a correction factor to incorporate time-dependent (creep) increase in settlement for t (years) after construction where:

$$C_2 = 1 + 0.2\log_{10}\left(\frac{t(\text{years})}{0.1}\right) \qquad 8\text{-}18$$

8.5.1.2 Comments on Schmertmann's Method

- **Effect of lateral strain**: Schmertmann and his co-workers based their method on the results of displacement measurements within sand masses loaded by model footings, as well as finite element analyses of deformations of materials with nonlinear stress-strain behavior that expressly incorporated Poisson's ratio. Therefore, the effect of the lateral strain on the vertical strain is included in the strain influence factor diagrams.

- **Effect of preloading:** The equations used in Schmertmann's method are applicable to normally loaded sands. If the sand was pre-strained by previous loading, then the actual settlements will be overpredicted. Schmertmann, *et al.* (1978) recommend a reduction in settlement after preloading or other means of compaction of half the predicted settlement. Alternatively, in case of preloaded soil deposits, the settlement can be computed by using the method proposed by D'Appolonia (1968, 1970), which includes explicit consideration of preloading.

- **C_2 correction factor**: The time duration, t, in Equation 8-18 is set to 0.1 years to evaluate the settlement immediately after construction, i.e., $C_2 = 1$. If long-term creep deformation of the soil is suspected then an appropriate time duration, t, can be used in the computation of C_2. **As explained in Sections 5.4.1 and 7.6, creep deformation is not the same as consolidation settlement.** This factor can have an important influence on the reported settlement since it is included in Equation 8-16 as a multiplier. For example, the C_2 factor for time durations of 0.1 yrs, 1 yr, 10 yrs and 50 yrs are 1.0, 1.2, 1.4 and 1.54, respectively. In cohesionless soils and unsaturated fine-grained cohesive

soils with low plasticity, time durations of 0.1 yr and 1 yr, respectively, are generally appropriate and sufficient for cases of static loads. Where consolidation settlement is estimated in addition to immediate settlement, $C_2 = 1$ should be used.

The use of Schmertmann's modified method to calculate immediate settlement is illustrated numerically in Example 8-2.

Example 8-2: A 6 ft x 24 ft footing is founded at a depth of 3 ft below ground elevation with the soil profile and average $N1_{60}$ values shown. Determine the settlement in inches (a) at the end of construction and (b) 1 year after construction. There is no groundwater. The footing is subjected to an applied stress of 2,000 psf.

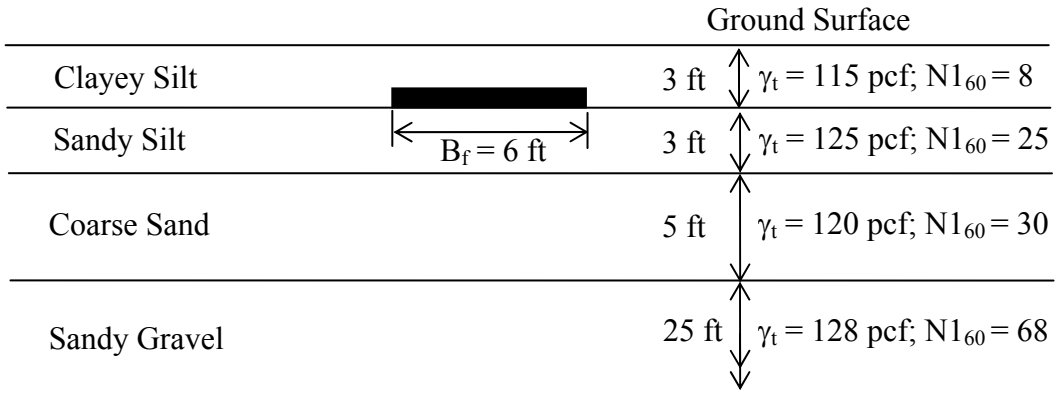

Solution:

Step 1: Begin by drawing the strain influence diagram. The L_f/B_f ratio for the footing is 24′/6′ = 4. From Figure 8-21(a), determine the value of the strain influence factor at the base of the footing, I_{ZB}, as follows:

$I_{ZB} = 0.1$ for axisymmetric case $(L_f/B_f = 1)$
$I_{ZB} = 0.2$ for plane strain case $(L_f/B_f \geq 10)$

Difference between axisymmetric L_f/B_f and plane strain $L_f/B_f = 9$
Difference between axisymmetric I_{ZB} and plane strain $I_{ZB} = 0.1$
Use linear interpolation for $L_f/B_f = 4$:

$\Delta(L_f/B_f)$ with respect to axisymmetric $L_f/B_f = 4\text{-}1 = 3$. Therefore

$$I_{ZB} = 0.1 + \frac{(0.2 - 0.1)}{9}(3) = 0.1 + \frac{0.1}{3} = 0.133$$

Step 2: Determine the maximum depth of influence, D_I, as follows:

$D_I = 2B_f$ for $L_f/B_f = 1$
$D_I = 4B_f$ for $L_f/B_f > 10$

By using linear interpolation $L_f/B_f = 4$ as before:

$\Delta (L_f/B_f)$ with respect to axisymmetric $L_f/B_f = 4\text{-}1 = 3$. Therefore

$$D_I = 2B_f + \frac{(4B_f - 2B_f)}{9}(3) = 2B_f + \frac{2B_f}{3} = \frac{6B_f + 2B_f}{3} = \frac{8B_f}{3}$$

$$D_I = \frac{8}{3}(6\,\text{ft}) = 16\,\text{ft}$$

Step 3: Determine the depth to the peak strain influence factor, D_{IP}, as follows:

From Figure 8-21(a) $D_{IP} = B_f/2$ for $L_f/B_f = 1$
$D_{IP} = B_f$ for $L_f/B_f > 10$

Use linear interpolation for $L_f/B_f = 4$:

$\Delta(L_f/B_f)$ with respect to axisymmetric $L_f/B_f = 4\text{-}1 = 3$. Therefore

$$D_{IP} = \frac{B_f}{2} + \frac{\left(B_f - B_f/2\right)}{9}(3) = \frac{B_f}{2} + \frac{B_f}{6} = \frac{3B_f + B_f}{6} = \frac{4B_f}{6}$$

$$D_{IP} = \frac{4}{6}(6\,\text{ft}) = 4\,\text{ft}$$

Step 4: Determine the value of the maximum strain influence factor, I_{ZP}, as follows:

$$I_{ZP} = 0.5 + 0.1\left(\frac{\Delta p}{p_{op}}\right)^{0.5}$$

$$\Delta p = 2{,}000\,\text{psf} - 3\,\text{ft}(115\,\text{pcf}) = 1{,}655\,\text{psf}$$

$$p_{op} = 3\,\text{ft}(115\,\text{pcf}) + 3\,\text{ft}(125\,\text{pcf}) + 1\,\text{ft}(120\,\text{pcf})$$

$$p_{op} = 345\,\text{psf} + 375\,\text{psf} + 120\,\text{psf} = 840\,\text{psf}$$

$$I_{ZP} = 0.5 + 0.1\sqrt{\frac{1{,}655\text{psf}}{840\text{psf}}} = 0.64$$

Step 5: Draw the I_Z vs. depth diagram as follows and divide it into convenient layers by using the following guidelines:

- The depth of the peak value of the strain influence is fixed. To aid in the computation, develop the layering such that one of the layer boundaries occurs at this depth even though it requires that an actual soil layer be sub-divided.
- Limit the top layer as well as the layer immediately below the peak value of influence factor, I_{zp}, to $2/3B_f$ or less to adequately represent the variation of the influence factor within D_{IP}.
- Limit maximum layer thickness to 10 ft (3 m) or less.
- Match the layer boundary with the subsurface profile layering.

In accordance with the above guidelines, the influence depth of 16 ft is divided into 4 layers as shown below. Since the strain influence diagram starts at the base of the footing, the thickness of Layer 1 corresponds to the thickness of the sandy silt layer shown in the soil profile. Likewise, Layer 4 corresponds to the thickness of the sandy gravel layer that has been impacted by the strain influence diagram. The sum of the thicknesses of Layers 2 and 3 correspond to the thickness of the coarse sand layer shown in the soil profile. The sub-division is made to account for the strain influence diagram going though its peak value within the coarse sand layer. The minimum and maximum layer thicknesses are 1 ft (Layer 2) and 8 ft (Layer 4), respectively. The layer boundaries are shown by solid lines while the layer centers are shown by dashed lines.

Step 6: Determine value of elastic modulus E_s from Table 5-16 from Chapter 5.

Layer 1: Sandy Silt: $E = 4N1_{60}$ tsf
Layer 2: Coarse Sand: $E = 10N1_{60}$ tsf
Layer 3: Coarse Sand: $E = 10N1_{60}$ tsf
Layer 4: Sandy Gravel: $E = 12N1_{60}$ tsf

Since the elastic modulus E_s is based on correlations with $N1_{60}$-values obtained from Table 5-16, calculate the X multiplication factor as follows:

$X = 1.25$ for $L_f/B_f = 1$
$X = 1.75$ for $L_f/B_f \geq 10$

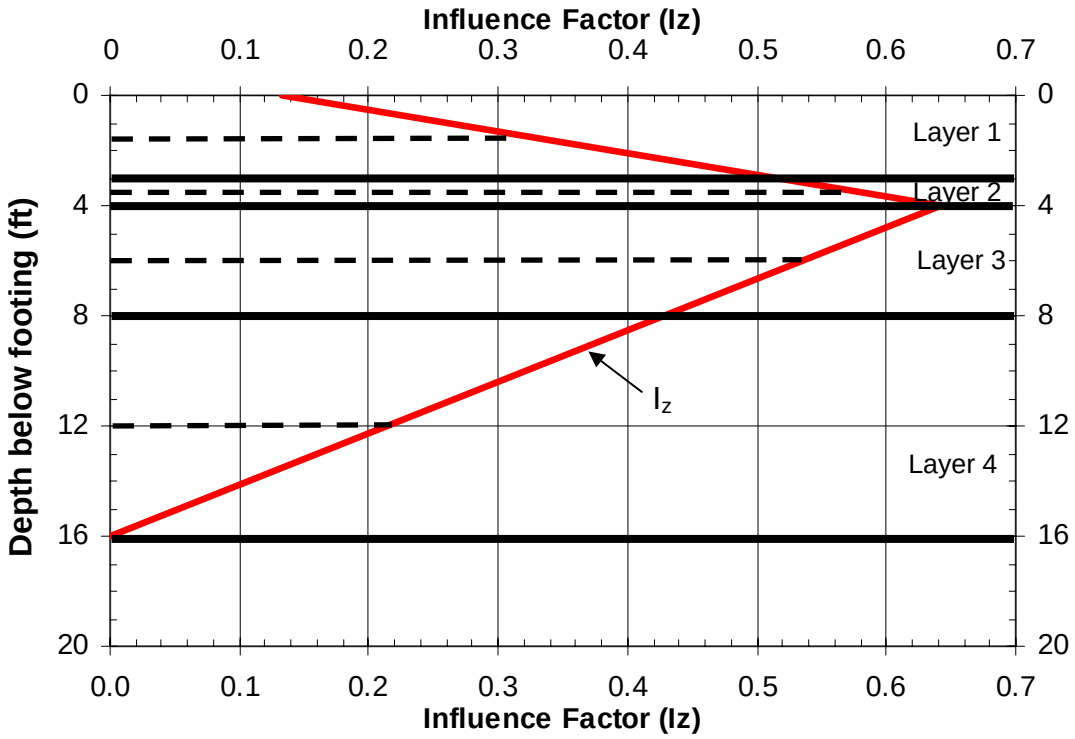

Use linear interpolation for $L_f/B_f = 4$

$\Delta\ (L_f/B_f)$ with respect to axisymmetric $L_f/B_f = 4\text{-}1 = 3$

$$X = 1.25 + \frac{(1.75 - 1.25)}{9}(3) = 1.42$$

Step 7: Using the thickness of each layer, H_c, and the relevant values for that particular layer, determine the settlement by setting up a table as follows:

Layer	H_c (inches)	$N1_{60}$	E (tsf)	XE (tsf)	Z_1 (ft)	I_Z at Z_i	$\Delta H_i = \frac{I_Z}{XE} H_c$ (in/tsf)
1	36	25	100	142	1.5	0.323	0.0819
2	12	30	300	426	3.5	0.577	0.0163
3	48	30	300	426	6	0.533	0.0601
4	96	68	816	1,159	12	0.213	0.0177
						$\Sigma H_i =$	**0.1760**

Step 8: Determine embedment factor (C_1) and creep factor (C_2) as follows:

a) Embedment factor

$$C_1 = 1 - 0.5\left(\frac{p_o}{\Delta p}\right) = 1 - 0.5\left(\frac{3\,\text{ft} \times 115\,\text{pcf}}{1655\,\text{psf}}\right) = 0.896$$

b) Creep Factor

$$C_2 = 1 + 0.2\log_{10}\left(\frac{t(\text{years})}{0.1}\right)$$

- For end of construction t(yrs) = 0.1 yr (1.2 months)

$$C_2 = 1 + 0.2\log_{10}\left(\frac{0.1}{0.1}\right) = 1.0$$

- For end of 1 year:

$$C_2 = 1 + 0.2\log_{10}\left(\frac{1}{0.1}\right) = 1.2$$

Step 9: Determine the settlement at end of construction as follows:

$$S_i = C_1 C_2 \Delta p \sum H_i$$

$$S_i = (0.896)(1.0)\left(\frac{1{,}655\text{psf}}{2{,}000\,\text{psf}/\text{tsf}}\right)\left(0.1760\frac{\text{in}}{\text{tsf}}\right)$$

$$S_i = 0.130\,\text{inches}$$

Step 10: Determine the settlement after 1 year as follows:

$$S_i = 0.130\,\text{inches}\left(\frac{1.2}{1.0}\right) = 0.156\,\text{inches}$$

8.5.1.3 Tabulation of Parameters in Schmertmann's Method

To facilitate computations, Table 8-11 presents a tabulation of the various parameters involved in computation of settlement by Schmertmann's method. This table was generated by using the linear interpolation scheme demonstrated in Example 8-2. Linear interpolation may be used for L_f/B_f values between those presented in Table 8-11.

Table 8-11

Values of parameters used in settlement analysis by Schmertmann's method

L_f/B_f	I_z at footing base, I_{ZB}	Depth to I_{zp}, D_{IP}	Depth of I_Z diagram, D_I	X factor	L_f/B_f	I_z at footing base, I_{ZB}	Depth to I_{zp}, D_{IP}	Depth of I_Z diagram, D_I	X factor
		Note 1	Note 1	Note 2			Note 1	Note 1	Note 2
1.00	**0.100**	**0.500**	**2.000**	**1.250**	**6.00**	**0.156**	**0.778**	**3.111**	**1.528**
1.25	0.103	0.514	2.056	1.264	6.25	0.158	0.792	3.167	1.542
1.50	0.106	0.528	2.111	1.278	6.50	0.161	0.806	3.222	1.556
1.75	0.108	0.542	2.167	1.292	6.75	0.164	0.819	3.278	1.569
2.00	**0.111**	**0.556**	**2.222**	**1.306**	**7.00**	**0.167**	**0.833**	**3.333**	**1.583**
2.25	0.114	0.569	2.278	1.319	7.25	0.169	0.847	3.389	1.597
2.50	0.117	0.583	2.333	1.333	7.50	0.172	0.861	3.444	1.611
2.75	0.119	0.597	2.389	1.347	7.75	0.175	0.875	3.500	1.625
3.00	**0.122**	**0.611**	**2.444**	**1.361**	**8.00**	**0.178**	**0.889**	**3.556**	**1.639**
3.25	0.125	0.625	2.500	1.375	8.25	0.181	0.903	3.611	1.653
3.50	0.128	0.639	2.556	1.389	8.50	0.183	0.917	3.667	1.667
3.75	0.131	0.653	2.611	1.403	8.75	0.186	0.931	3.722	1.681
4.00	**0.133**	**0.667**	**2.667**	**1.417**	**9.00**	**0.189**	**0.944**	**3.778**	**1.694**
4.25	0.136	0.681	2.722	1.431	9.25	0.192	0.958	3.833	1.708
4.50	0.139	0.694	2.778	1.444	9.50	0.194	0.972	3.889	1.722
4.75	0.142	0.708	2.833	1.458	9.75	0.197	0.986	3.944	1.736
5.00	**0.144**	**0.722**	**2.889**	**1.472**	**10.00**	**0.200**	**1.000**	**4.000**	**1.750**
5.25	0.147	0.736	2.944	1.486	**> 10**	**0.200**	**1.000**	**4.000**	**1.750**
5.50	0.150	0.750	3.000	1.500					
5.75	0.153	0.764	3.056	1.514					

Notes:

1. The depths are obtained by multiplying the value in this column by the footing width, B_f.

2. If elastic modulus is not based on SPT or CPT, then X=1.0. See Section 8.5.1.1 for a discussion on values of X factor.

Legend

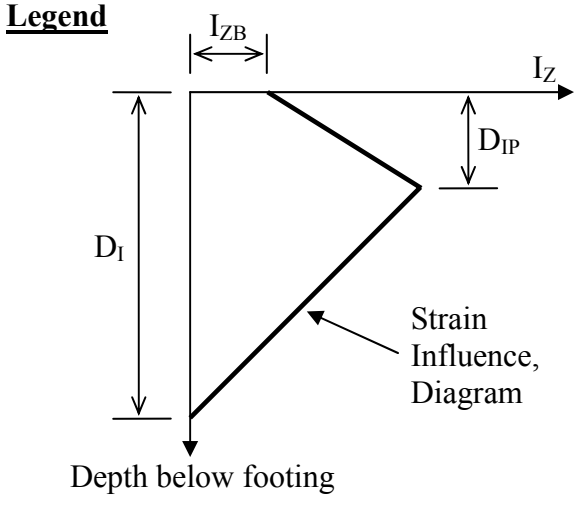

8.5.2 Obtaining Limiting Applied Stress for a Given Settlement

As indicated in Section 8.3, the allowable bearing capacity based on settlement considerations is defined as "the applied stress that results in a specified amount of settlement." Thus, the quantity of interest is often the limiting applied stress for a specified amount of settlement. In this case, Equation 8-16 can be inverted and solved to obtain the limiting applied stress, Δp, for a given settlement, S_i. By repeating the computation for a range of settlement values, the curves shown in Zone B of Figure 8-10 can be generated. It is important to realize that the applied stress computed by the inverted form of Equation 8-16 is a uniform stress. Consequently, that value of stress should be compared to the Meyerhof equivalent uniform pressure (q_{eq}) acting on an effective footing width as shown in Figure 8-17b and not the maximum stress (q_{max}) of the trapezoidal pressure distribution on the total footing width as shown in Figure 8-17a. It is for this reason that the X-axis of an allowable bearing capacity chart refers to an effective footing width and not total footing width.

8.5.3 Consolidation Settlement

The procedures to compute consolidation settlements discussed in Chapter 7 can be applied to spread footings also. The following example illustrates the method for determining consolidation settlement due to a load applied to a spread footing.

Example 8-3: Determine the settlement of the 10 ft × 10 ft square footing due to a 130 kip axial load. Assume the gravel layer is incompressible.

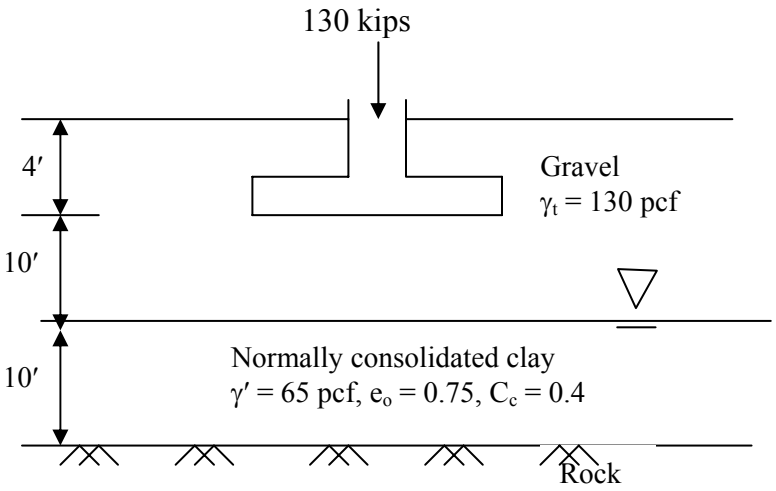

Solution:

Find overburden pressure, p_o, at center of clay layer

p_o = (14 ft × 130 pcf) + (5 ft × 65 pcf) = 2,145 psf

Find change in pressure (Δp) at center of clay layer due to applied load. Use the approximate 2:1 stress distribution method discussed in Section 2.5 of Chapter 2.

$$\Delta p = \frac{130\,\text{kips}}{(10\,\text{ft} + 15\,\text{ft})^2} = \frac{130\,\text{kips}}{625\,\text{ft}} = 0.208\,\text{ksf} = 208\,\text{psf}$$

Use Equation 7-2 to calculate the magnitude of consolidation settlement.

$$\Delta H = H \frac{C_c}{1 + e_o} \log_{10}\left(\frac{p_o + \Delta p}{p_o} \right)$$

$$\Delta H = 10\,\text{ft}\left(\frac{0.4}{1 + 0.75} \right) \log_{10}\left(\frac{2{,}145\,\text{psf} + 208\,\text{psf}}{2{,}145\,\text{psf}} \right) = 0.09\,\text{ft} = 1.1\,\text{in}$$

In reality, the magnitude of the total settlement of the foundation would be the sum of the consolidation settlement of the clay and the immediate settlement of the gravel. The gravel was assumed to be incompressible in this example. However, in practice, the component of the total settlement due to the immediate settlement of the gravel would be determined by using Schmertmann's method with only that portion of the strain influence diagram in the gravel being considered.

8.6 SPREAD FOOTINGS ON COMPACTED EMBANKMENT FILLS

Geotechnical engineers have long recognized the desirability of placing footings on engineered fills. In general, the load imposed by the weight of the fill is many times that of the imposed footing load. If adequate time is allowed for the foundation soils to settle under the fill load, subsequent application of a smaller structural load will result in negligible settlement of the structure. In bridge construction, common practice is to build the approach embankment excluding the area to be occupied by the abutment and allow settlement to occur prior to abutment construction. Details of the settlement of approach embankment fills are presented in Chapter 7.

Field evaluation of spread footings placed in or on engineered fills constructed of select granular material, show that spread footings provide satisfactory performance, i.e., minimal vertical and lateral displacements, if all relevant factors are considered in the design of the embankment and the footing. A performance evaluation of spread footings on compacted embankment fills was conducted through a joint study between FHWA and the Washington State Department of Transportation (FHWA, 1982). A visual inspection was made of the structural condition of 148 highway bridges supported by spread footings on engineered fills throughout the State of Washington. The approach pavements and other bridge appurtenances were also inspected for damage or distress that could be attributed to the use of spread footings on engineered fill. This review, in conjunction with detailed survey investigations of the foundation movement of 28 selected bridges, was used to evaluate the performance of spread footings on engineered fills. None of the bridges investigated displayed any safety problems or serious functional distress. The study concluded that spread footings can provide a satisfactory alternative to deep foundations, especially when high embankments of good quality borrow materials are constructed over satisfactory foundation soils. Further studies were made to substantiate the feasibility of using spread footings in lieu of more expensive deep foundation systems. Cost analyses showed that spread footings were 50 to 65 percent less expensive than the alternate choice of deep foundations. Studies of foundation movement showed that bridges easily tolerated differential settlements of 1 to 3 inches (25 to 75 mm) without serious distress.

In addition to the FHWA (1982) study which was limited to the bridges in the State of Washington, a nationwide study of 314 bridges was conducted (FHWA, 1985). The nationwide study arrived at similar conclusions. Unfortunately many agencies continue to disregard spread footings as alternative foundations for highway structures. Yet another study (NCHRP, 1983), states the following:

> "In summary, it is very clear that the tolerable settlement criteria currently used by most transportation agencies are extremely conservative and are needlessly restricting the use of spread footings for bridge foundations on many soils. Angular distortions of 1/250 of the span length and differential vertical movements of 2 to 4 inches (50 to 100 mm), depending on span length, appear to be acceptable, assuming that approach slabs or other provisions are made to minimize the effects of any differential movements between abutments and approach embankments. Finally, horizontal movements in excess of 2 inches (50 mm) appear likely to cause structural distress. The potential for horizontal movements of abutments and piers should be considered more carefully than is done in current practice."

It is recommended that **compacted structural fills used for supporting spread footings should be a select and specified material that includes sand- and gravel-sized particles. Furthermore, the fill should be compacted to a minimum relative compaction of 95% based on Modified Proctor compaction energy. This structural fill should extend for the entire embankment below the footing.** FHWA (2002c) notes that the Washington Department of Transportation (WSDOT) successfully used the gradation listed in Table 8-12 to design spread footings for the I-5 Kalama Interchange. WSDOT limited the maximum bearing pressures to 3 tsf (290 kPa) and the measured settlements were found to be less than 1.5 in (40 mm) within the fill. In addition to WSDOT, the Nevada Department of Transportation (NDOT) commonly uses spread foundations founded within compacted structural embankment fills.

Direct shear testing of materials such as those described in Table 8-12 is not practical on a project-by-project basis since such materials require large specialized test equipment. Therefore the design of spread footings on compacted sand and gravel is based on a combination of experience and the results of infrequent large-scale laboratory testing on specified gradations of select fill materials. Materials specifications are then developed based on the specified gradations to ensure good quality control during construction. This procedure helps ensure that the conclusions from the laboratory tests are valid for the construction practices used to place the fills.

Table 8-12
Typical specification of compacted structural fill used by WSDOT (FHWA, 2002c)

Sieve Size	Percent Passing
4" (100 mm)	100
2" (50 mm)	75 – 100
No. 4 (4.75 mm)	50 – 80
No. 40 (0.425 mm)	30 max
No. 200 (0.075 mm)	7 max
Sand Equivalent (See Note 1)	42 min
Notes: 1. See Section 5.3.4.1 in Chapter 5 for a discussion of sand equivalent test.	

8.6.1 Settlement of Footings on Structural Fills

Calculation of the settlement of a spread footing supported in or on an engineered fill requires an assumption about the compressibility of the fill material. Because structural fills should be constructed of good-quality granular materials and by following good construction techniques, the estimation of settlement lends itself to the application of the methods

discussed in this Chapter. To estimate settlements of footings in structural fills by Schmertmann's method, an assumption must be made about the SPT N-value that is representative of the engineered fill.

FHWA (1987) used a SPT N-value of 32 blows per foot corrected for overburden pressure as a representative value for estimating settlement in structural fills. This value of SPT N-value corresponds to a relative density, D_r, of approximately 85 percent at an overburden stress of about 1 tsf (100 kPa) (FHWA, 1987); this is confirmed by the data in Figure 5-23. Based on Figure 5-33 or Equation 5-21, this value of D_r is at approximately 97% relative compaction based on Modified Proctor compaction energy (ASTM D 1557). Under such compacted conditions, and in the absence of other SPT data in structural fills, the settlement of a footing supported on structural fill can be estimated by using an assumed corrected SPT N-value ($N1_{60}$) of 32. However, a relative compaction of 95% based on Modified Proctor compaction energy is often used. For this case, a corrected SPT N-value ($N1_{60}$) of 23 is more appropriate.

8.7 FOOTINGS ON INTERMEDIATE GEOMATERIALS (IGMs) AND ROCK

The assumption made in this chapter is that intermediate geomaterials (IGMs) are stiff and strong enough that bearing capacity and settlement considerations will generally not govern the design of a spread footing supported on such a material. If a settlement estimate is necessary for shallow foundations supported on an IGM or rock, a method based on elasticity theory is probably the best approach. As with any of the methods for estimating settlement that use elasticity theory, the accuracy of the values estimated for the elastic parameter(s) required by the method is a major factor in determining the reliability of the predicted settlements.

Equation 8-19 may be used to compute the settlement of a shallow spread footing founded on rock based on Young's modulus of the intact rock. In this equation, the stress applied at the top of the rock surface can be calculated by using the stress distribution methods presented in Chapter 2.

$$\delta_v = \frac{C_d \, \Delta p \, B_f (1 - \nu^2)}{E_m} \qquad 8\text{-}19$$

where: δ_v = vertical settlement at surface

C_d = shape and rigidity factors (Table 8-13)

Δp = change in stress at top of rock surface due to applied footing load
B_f = footing width or diameter
ν = Poisson's ratio (refer to Table 5-22 in Chapter 5)
E_m = Young's modulus of rock mass (see Section 5.12.1 in Chapter 5)

The elastic modulus of IGMs and some rocks may be measurable by in situ testing with equipment such as the pressuremeter (FHWA 1989a), the dilatometer (FHWA 1992b), and plate load tests or flat jacks. ASTM standards are available for each of these in situ tests and they provide details regarding performance and the interpretation of the test data. The method for determining elastic modulus based on RMR discussed in Chapter 5.

To preserve the stability of footings on IGMs or rock, the geotechnical engineer must evaluate the potential for a global stability failure and the potential of limitations of the allowable bearing capacity because of the presence of rock mass discontinuities. The bearing capacity of IGMs derived from sedimentary rock can dramatically decrease when the IGM is exposed to weathering and moisture.

Table 8-13
Shape and rigidity factors, C_d, for calculating settlements of points on loaded areas at the surface of a semi-infinite elastic half space (after Winterkorn and Fang, 1975)

Shape	Center	Corner	Middle of Short Side	Middle of Long Side	Average
Circle	1.00	0.64	0.64	0.64	0.85
Circle (rigid)	0.79	0.79	0.79	0.79	0.79
Square	1.12	0.56	0.76	0.76	0.95
Square (rigid)	0.99	0.99	0.99	0.99	0.99
Rectangle (length/width):					
1.5	1.36	0.67	0.89	0.97	1.15
2	1.52	0.76	0.98	1.12	1.30
3	1.78	0.88	1.11	1.35	1.52
5	2.10	1.05	1.27	1.68	1.83
10	2.53	1.26	1.49	2.12	2.25
100	4.00	2.00	2.20	3.60	3.70
1000	5.47	2.75	2.94	5.03	5.15
10000	6.90	3.50	3.70	6.50	6.60

8.8 ALLOWABLE BEARING CAPACITY CHARTS

The concept of an allowable bearing capacity chart was discussed in Section 8.3. The curves shown in Figure 8-10 can be obtained by performing computations for allowable bearing capacity and settlement for a range of values of footing widths by using the procedures described in Sections 8.4 to 8.7. This section presents an example bearing capacity chart and a step-by-step procedure to use such a chart for the sizing of footings.

Example 8-3: The abutments of a bridge will be founded on spread foundations similar to the configuration shown in Figure 8-4. The length, L_f, of the abutment footing is 130 ft. The minimum depth of embedment, D_f, of the footing base is 5 ft. The geotechnical engineer developed a bearing capacity chart based on site-specific subsurface data. This chart is shown in Figure 8-22. Determine the footing width, B_f, such that the settlement of the footing is less than or equal to 1 in.

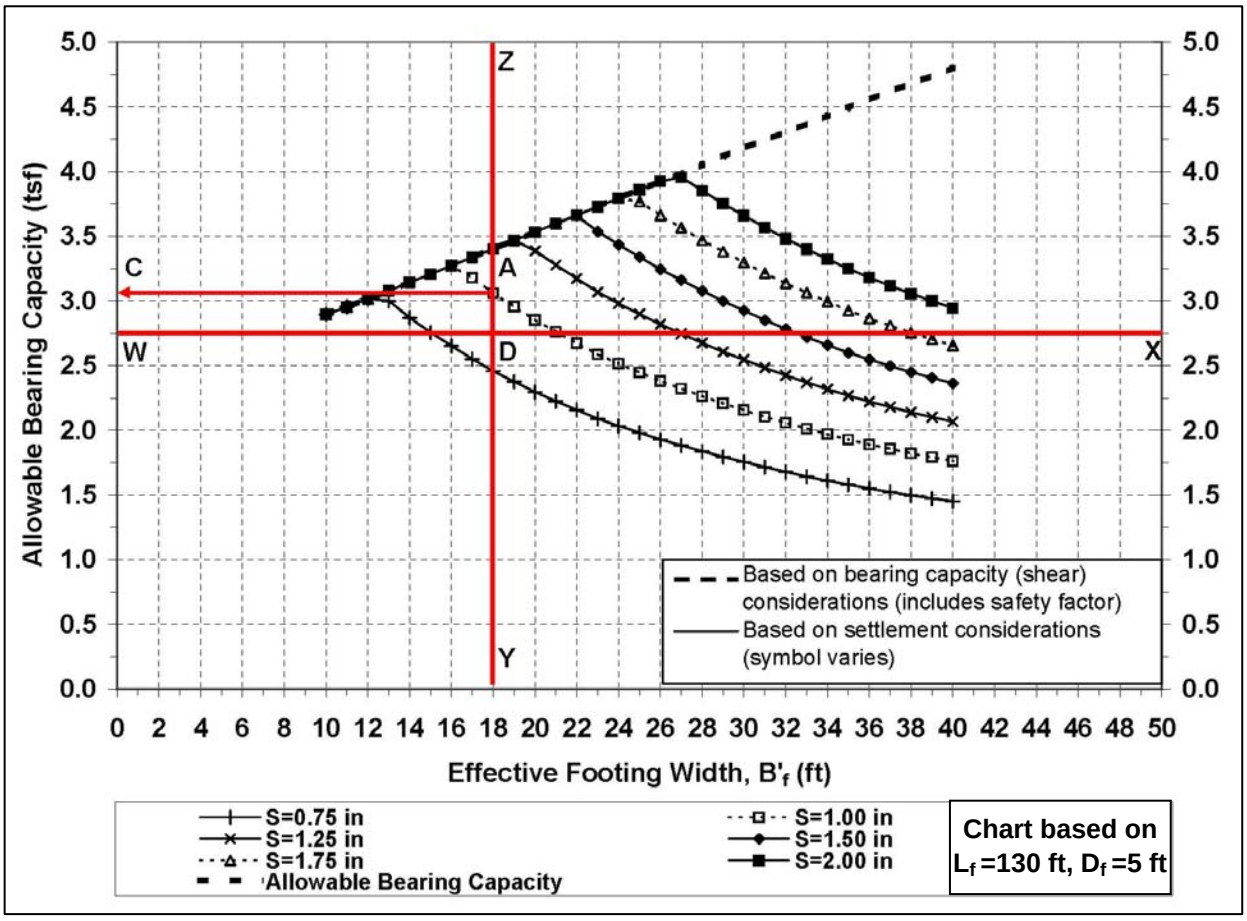

Figure 8-22. Example allowable bearing capacity chart.

Solution:

Step 1:

Assume a footing width, B_f, and compute the equivalent ***net*** uniform (Meyerhof) bearing pressure, q_{eu}, at the base of the footing. The equivalent net uniform bearing pressure, q_{eu}, is obtained by dividing the resultant vertical load, R, by the effective area, A', of the footing as follows:

$$q_{eu} = R/A'$$

The resultant vertical load, i.e., the vertical component of the resultant load, should be determined by using the unfactored dead load, plus the unfactored component of live and impact loads assumed to extend to the footing level (Section 4.4.7.2 of AASHTO, 2002). The effective area, A', is determined as follows based on Equation 8-7, 8-8 and 8-9:

$$A' = B'_f L'_f = (B_f - 2e_B)(L_f - 2e_L)$$

where e_B and e_L are the eccentricities of the resultant load, R, in the B_f and L_f directions, respectively, as indicated in Figure 8-16. The eccentricities, e_B and e_L should be such that they are less than $B_f/6$ and $L_f/6$, respectively to ensure that no uplift occurs anywhere within the base of the footing. In cases where there is no load eccentricity, the effective length, L'_f, and the effective width, B'_f, are equal to the actual length, L_f, and actual width, B_f, respectively.

For the example problem stated above, assume for the sake of illustration that the computed equivalent net uniform bearing pressure, q_{eu}, at the base of the footing is 2.75 tsf for a retaining wall footing that is 130 ft long ($L_f = L'_f$), has an effective width, B'_f, of 18 ft, and is embedded 5 ft.

Step 2:

Since the minimum required allowable bearing capacity has to be at least equal to the net equivalent uniform bearing pressure, q_{eu}, draw a horizontal line on the chart corresponding to the value of q_{eu}. Thus, for the example problem, draw a horizontal line WX on the chart corresponding to a value of 2.75 tsf as shown in Figure 8-22. This horizontal line will intersect the curves of equal settlement, e.g., S=0.75 in, S = 1.0 in and so on as shown in Figure 8-22.

Step 3:

Draw a vertical line YZ for the effective footing width, B'_f, of 18 ft. Like the horizontal line, WX, the vertical line, YZ, will intersect the curves of equal settlement, e.g., S=0.75 in, S = 1.0 in as shown in Figure 8-22.

Step 4:

From the point of intersection of the vertical line, YZ, with the appropriate acceptable settlement curve (1.00-in for this example) draw a horizontal line to the Y-axis to determine the allowable bearing capacity. By drawing the horizontal line, AC, it can be determined that the allowable bearing capacity corresponding to an effective footing width of 18 ft is approximately 3.2 tsf (see Point C in Figure 8-22). This value is greater than the q_{eu} value of 2.75 tsf and therefore the footing whose effective width, B'_f, is 18 ft is acceptable.

An alternative way to evaluate the acceptability of a footing size is to determine the estimated settlement corresponding to the computed equivalent net uniform bearing pressure, q_{eu}, and compare it with the acceptable settlement. From the bearing capacity chart for the example problem, it can be seen that at an effective footing width, B'_f, of 18 ft and a q_{eu} value of 2.75 tsf, the estimated settlement will be approximately 0.88 in (see Point D that falls between the S=0.75 in and S=1.00 in curves in Figure 8-22). This value of estimated settlement is less than the limiting settlement of 1 in and is therefore acceptable.

Step 5:

Repeat Steps 1 to 4 as necessary to optimize the footing design or to resize the footing based on the "available" allowable bearing capacity. In this example, the "available" allowable bearing capacity for an 18 ft wide footing is 3.2 tsf which is greater than the required value of 2.75 tsf. Thus, it is possible that the footing width can be reduced. During the optimization process, linear interpolation within the limits of the data presented in the chart is acceptable. However, extrapolation of data is not advisable.

8.8.1 Comments on the Allowable Bearing Capacity Charts

- A factor of safety, FS, against ultimate bearing capacity (shear) failure is included in the computations that yield the steeply rising line on the left side of the chart, i.e., the line that is based on bearing capacity considerations. Since the settlement based allowable bearing capacity curves plot on the right side of the bearing capacity line, the actual factor of safety against shear failure will be higher than the assumed minimum FS.

- The effective footing width, B'_f, on the X-axis of the charts represents the least lateral effective dimension of the footing. The footing size determined from the chart is a function of the depth of embedment of the footing, D_f, and the length of the footing, L_f. The depth of embedment, D_f, is the vertical distance between the lowest finished permanent ground surface above the footing to the base of the footing. Each bearing capacity chart is developed for a given footing length, L_f, and a minimum depth of embedment, D_f. Therefore, these quantities must be clearly labeled on the chart as shown in Figure 8-22. If the actual dimensions of D_f and/or L_f vary by more than ±10% from those noted on the charts then a new chart should be developed for the actual values of D_f and L_f.

- Finally, each bearing capacity chart should be specific to a given foundation element and should be developed based on location-specific geotechnical data. Consequently the charts should not be used for foundations at locations other than at which they are applicable.

8.9 EFFECT OF DEFORMATIONS ON BRIDGE STRUCTURES

Bridge foundations and other geotechnical features such as approach embankments should be designed so that their deformations (settlements and/or lateral movements) will not cause damage to the bridge structure. Uneven displacements of bridge abutments and pier foundations can affect the quality of ride and the safety of the traveling public as well as the structural integrity of the bridge. Such movements often lead to costly maintenance and repair measures. Therefore, it is important that the geotechnical specialist as well as the structural engineer fully understand the effect of deformations of geotechnical features on bridge structures.

FHWA (1985) and Duncan and Tan (1991) studied tolerable movements for bridges and found that "foundation movements would become intolerable for some other reason before reaching a magnitude that would create intolerable rider discomfort." The "other" reasons might include reduction of clearance at overpasses and drainage considerations, as discussed later. Therefore, if movements are within a tolerable range with regard to structural distress for the bridge superstructure, they will also be acceptable with respect to user comfort and safe vehicle operation. The severity of the consequences of uneven movements of bridge structures, superstructure as well as substructure, increases with the magnitude of the settlements and lateral movements. Both of these components of bridge movements are discussed below.

A. Settlement

Settlement can be subdivided into the following three components, which are illustrated in Figure 8-23 (Duncan and Tan, 1991):

1. **Uniform settlement**: In this case, all bridge support elements settle equally. Even though the bridge support elements settle equally, they can cause differential settlement with respect to the approach embankment and associated features such as approach slabs and utilities that are commonly located in or across the end-spans of bridges. Such differential settlement can create several problems. For example, it can reduce the clearance of the overpass, create a bump at the end of the bridge, change grades at the end of the bridge causing drainage problems, and distort underground utilities at the interfaces of the bridge and approaches.

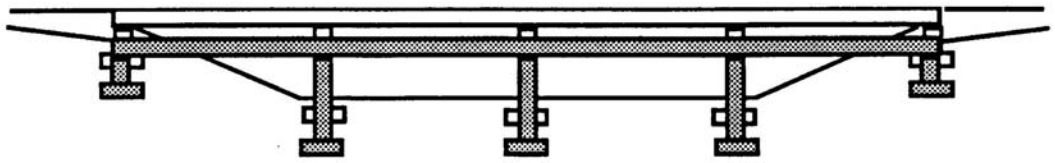

Uniform Settlement

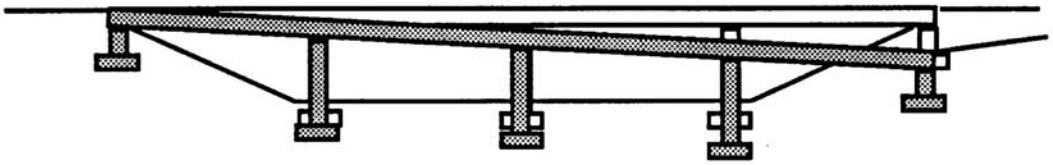

Tilt (Rotation)

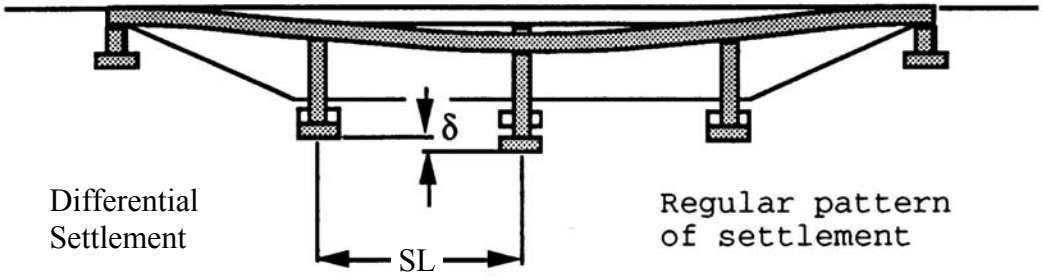

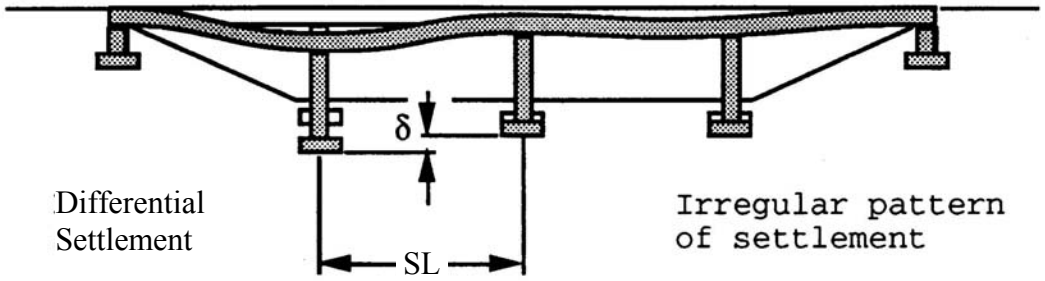

$$A = \text{Angular Distortion}$$

$$A = \frac{\text{Difference in Settlement Between Foundations}}{\text{Distance Between Foundations}} = \frac{\delta}{SL}$$

Figure 8-23. Components of settlement and angular distortion in bridges (after Duncan and Tan, 1991).

Although uniform settlements may be computed theoretically, from a practical viewpoint it is not possible for the bridge structure to experience truly uniform settlement due to a combination of many factors including, but not limited to, the variability of loads and soil properties

2. **Tilt or rotation**: Tilt or rotation occurs mostly in single span bridges with stiff superstructures. Tilt or rotation may not cause distortion of the superstructure and associated damage, but due to its differential movement with respect to the facilities associated with approach embankments, tilt or rotation can create problems similar to those of uniform settlement that were discussed above, e.g., a bump at the end of the bridge, drainage problems, and damage to underground utilities.

3. **Differential settlement**: Differential settlement directly results in deformation of the bridge superstructure. As shown in Figure 8-23, two different patterns of differential settlement can occur. These are:

    a. **Regular pattern**: In this case, the settlement increases progressively from the abutments towards the center of the bridge

    b. **Irregular pattern**: In this case, the settlement at each support location varies along the length of the bridge.

Both of the above patterns of settlement lead to angular distortion, which is defined as the ratio of the difference in settlement between two points divided by the distance between the two points. For bridge structures, the two points to evaluate the differential settlement are commonly selected as the distance between adjacent support elements, SL, as shown in Figure 8-23. Depending on the type of connections between the superstructure and support columns (pinned or fixed) and the locations of expansion and construction joints along the bridge deck (mid-span or elsewhere), the irregular pattern of differential settlement has the potential to create greater structural distress than the regular pattern of differential settlement. The distress may occur due to increased internal stresses associated with flexure and/or shear of the bridge superstructure and is generally manifested by cracks in the bridge deck and/or girders at support locations.

In addition to the problems they create in the bridge superstructure, differential settlements can create the same problems as uniform settlements discussed earlier, i.e., problems with bumps at the junctures with approach slabs, problems with drainage, problems with clearance at underpasses, etc.

B. Horizontal Movements

Horizontal movements cause more severe and widespread problems than do equal magnitudes of vertical settlement. The types of problems that arise as a result of differential horizontal movements between bridge decks and abutments, or between adjacent spans of bridges, include the following (Duncan and Tan, 1991):

- Shearing of anchor bolts,
- Excessive opening of expansion joints,
- Reduced effectiveness of expansion joints when clearance is reduced,
- Complete closing of expansion joints and jamming of bridge decks into abutments or adjacent spans,
- Shifting of abutments when expansion joints jam,
- Severe damage to abutment walls, approach slabs or bridge decks due to excessive loads when expansion joints jam,
- Distortion and damage to bearing devices,
- Excessive tilting of rockers,
- Damage to rail curbs, sidewalks and parapets.

C. Reliability of Estimation of Movements

All analytical methods used for estimating movements are based on certain assumptions. Therefore, there is an inherent uncertainty associated with the estimated values of movements. The uncertainty of estimated differential settlement is larger than the uncertainty of the estimated settlement at the two support elements used to calculate the differential settlement, e.g., between abutment and pier, or between piers. For example, if one support element settles less than the amount estimated while the other support element settles the amount estimated, the actual differential settlement will be larger than the difference between the two values of estimated settlement at the support elements. Duncan and Tan (1991) suggest the following assumptions to estimate the likely value of differential settlement:

- The settlement of any support element could be as large as the value calculated by using conservative procedures, and
- At the same time, the settlement of the adjacent support element could be zero.

Use of these conservative assumptions would result in an estimated maximum possible differential settlement equal to the largest settlement calculated at either end of any span.

8.9.1 Criteria for Tolerable Movements of Bridges

8.9.1.1 Vertical Movements

The FHWA (1985) study used the following definition of intolerable movement:

> "Movement is not tolerable if damage requires costly maintenance and/or repairs and a more expensive construction to avoid this would have been preferable."

This definition is somewhat subjective based on the cost and practical problems involved in the repair and maintenance or use of an alternative more expensive construction technique. FHWA (1985) studied data for 56 simple span bridges and 119 continuous span bridges and chose to express the definition for tolerable movement quantitatively in terms of limiting angular distortion as shown in Table 8-14.

Table 8-14
Tolerable movement criteria for bridges (FHWA, 1985; AASHTO 2002, 2004)

Limiting Angular Distortion, δ/SL	Type of Bridge
0.004	Multiple-span (continuous span) bridges
0.005	Single-span bridges
Note: δ is differential settlement, SL is the span length. The quantity, δ/SL, is dimensionless and is applicable when the same units are used for δ and SL, i.e., if δ is expressed in inches then SL should also be expressed in inches.	

For example, the criteria in Table 8-14 suggest that for a 100 ft (30 m) span, a differential settlement of 4.8 inches (120 mm) is acceptable for a continuous span and 6 inches (150 mm) is acceptable for a simple span.

Such relatively large values of differential settlements create concern for structural designers, who often arbitrarily limit the criteria to one-half to one-quarter of the values listed in Table 8-14. While there are no technical reasons for structural designers to set such arbitrary additional limits for the criteria listed in Table 8-14, there are often practical reasons based on the tolerable limits of deformation of other structures associated with a bridge, e.g., approach slabs, wingwalls, pavement structures, drainage grades, utilities on the bridge, deformations that adversely affect quality of ride, etc. Thus, the relatively large differential settlements based on Table 8-14, should be considered in conjunction with functional or performance criteria not only for the bridge structure itself but for all of the associated facilities. The following steps are suggested in this regard:

Step 1: Identify all possible facilities associated with the bridge structure, and the tolerance of those facilities to movements.

Step 2: Due to the inherent uncertainty associated with estimated values of settlement, determine the differential settlement by using the conservative assumptions described earlier. It is important that the estimation of differential settlement is based on a realistic evaluation of the sequence and magnitude of the loads as described in Section 8.9.2.

Step 3: Compare the differential settlement from Step 2 with the various tolerances identified in Step 1 and in Table 8-14. Based on this comparison identify the critical component of the facility. Review this critical component to check if it can be relocated or if it can be designed to more relaxed tolerances. Repeat this process as necessary for other facilities. In some cases, a simple re-sequencing of the construction of the facility based on the construction sequence of the bridge may help mitigate the issues associated with intolerable movements.

The above approach will help to develop project-specific limiting angular distortion criteria that may differ from the general guidelines listed in Table 8-14.

8.9.1.2 Horizontal Movements

Based on a survey of bridges, FHWA (1985) found that horizontal movements less than 1 in (25 mm) were almost always reported as being tolerable, while horizontal movements greater than 2 in (50 mm) were quite likely to be considered to be intolerable. Based on this observation, FHWA (1985) recommended that horizontal movements be limited to 1.5 in (38 mm). The data presented by FHWA (1985) showed that horizontal movements tended to be more damaging when they were accompanied by settlement than when they were not. The estimation of magnitude of horizontal movements should take into account the movements associated with considerations of slope instability and lateral squeeze as discussed in Chapter 6 and 7, respectively.

Abutments are often designed for active lateral earth pressure conditions, which require a certain amount of movement (see Chapter 9). Depending on the configuration of the bridge end spans and expansion joints, horizontal movements of an abutment can be restrained, however, such restraint can lead to an increase in the lateral earth pressures above the active earth pressures normally used in design. Design of expansion joints should allow for sufficient movement to keep earth pressures at or close to their design values and still allow the joints to perform properly under all temperature conditions.

8.9.2 Loads for Evaluation of Tolerable Movements Using Construction Point Concept

Most designers use the criteria described in Section 8.9.1 as if a bridge structure is instantaneously wished into place, i.e., all the loads are applied at the same time. In reality, loads are applied gradually as construction proceeds. Consequently, settlements will also occur gradually as construction proceeds. There are several critical construction points that should be evaluated separately by the designer. Table 8-15 illustrates this critical construction concept for a bridge abutment footing that was constructed as part of a 2-span bridge in the southwest United States. The prestressed concrete beam bridge is 64.4 ft (19.6 m) wide and 170 ft (52 m) long. The bridge is continuous with mechanically stabilized earth (MSE) walls wrapped around both of the abutments. The abutments are fixed for shear transfer through semi-integral diaphragms connected to spread footings on top of the MSE walls.

Even though the total settlement cited in Table 8-15 is 7.5 inches, in reality only 2.0 in is significant because it occurs progressively during the first 10 years the bridge is in service. (Note that immediately after construction the net settlement was estimated to be only 0.5 in even though the total settlement computed at this stage is 5.0 in)

The pier for this bridge is supported by a group of pipe piles and was estimated to experience a settlement of approximately 0.5 in. To compute the worst angular distortion, it was assumed that the pier would not experience settlement while the abutment would experience the full estimated settlement. Thus, the angular distortion criterion where 0 in settlement is assumed at the pier yields the following results for an 85 ft span (1/2 of the 170 ft long bridge):

- *With Construction Point Concept*

  Angular Distortion, A = (2.0 in – 0.0 in)/(85 ft x 12 in/ft) = 2.0 in/1,020 in = 0.002

  In this case, A is one-half of the limiting angular distortion of 0.004 as per Table 8-14. Therefore, the settlements are acceptable.

- *Without Construction Point Concept*

  Angular Distortion, A = (7.5 in – 0.0 in)/(85 ft x 12 in/ft) = 7.5 in/1,020 in = 0.0073

  Since A > 0.004, the angular distortion is deemed intolerable.

Table 8-15
Example of settlements evaluated at various critical construction points

Construction Point	Estimated Net Applied Stress[1] (psf)	Settlement (inches)[2]	Net Settlement (inches)
I. Embankment only	2,770	3.4	-
II. MSE Wall + Spread footing (no deck)	6,020	5.0	1.6 (during construction)
III. MSE Wall + Spread footing + Deck (DL + LL)	6,520	5.5	0.5 (= 5.5 – 5.0)
IV. MSE Wall + Spread Footing + Deck (DL+LL) + Creep[3]	6,520	7.5	2.0 (= 7.5 – 5.5)

Notes:

1. The 2 ft depth of embedment for the MSE wall was taken into account while estimating the net applied stress from new construction.

2. Settlement analyses were performed by using Schmertmann's method (1978) that allows for estimation of long-term (creep) settlement. In this project, relatively dry, low plastic fine grained soils were encountered that could possibly deform for some time after construction.

3. A time period of 1.5 months was assumed for each Point II and III analyses. For this duration, the creep component of the deformation was less than 5% of the settlements reported above for Point II and III. Conservatively, a time period of 10 years was assumed for the creep deformations for Point IV, after which it was assumed that no significant creep deformations would occur. Note, that the net settlement of 2.0 inches between construction Point III and IV is attributed entirely to creep settlement.

In this example, if the designer did not take into account the various construction points when evaluating settlement, then not only would the angular distortion criteria listed in Table 8-15 not be met but it would also likely lead to implementation of costly and unnecessary ground improvement measures. This approach was used successfully for 55 bridges constructed as part of the I25/I40 ("BIG I") traffic interchange in Albuquerque, NM. This critical construction point approach permitted the use of true bridge abutments, i.e., spread footings on top of MSE walls, on 28 of the 55 bridges on the BIG I project, which resulted in significant cost savings for the New Mexico Department of Transportation (NMDOT). The project was completed in 2001 and all of the bridges have performed well to date (2006).

A key point in evaluating settlements at critical construction points is that the approach requires close coordination between the structural and geotechnical specialists. In the case of the BIG I project, the structural specialist performed a realistic evaluation of the loads and construction sequence and communicated them to the geotechnical specialist, who then evaluated the settlements for those loads. As demonstrated by the above example, this approach resulted in a realistic evaluation of the deformation of the bridge structure. This critical construction point approach can also often help in making other decisions such as the need for costly ground improvement measures.

8.10 SPREAD FOOTING LOAD TESTS

Spread footing load tests can be used to verify both bearing capacity and settlement predictions. Briaud and Gibbens (1994) present the results of predicted and measured behavior of five spread footings on sand. Full scale tests have been done on predominantly granular soils. An example is the I-359 project in Tuscaloosa, Alabama where dead load was placed on 12 ft x 12 ft (3.7 m x 3.7 m) footings to create a foundation contact pressure of over 4 tsf (383 kPa). A settlement of 0.1 in (2.5 mm) was recorded when the footing concrete was placed. The greatest settlement recorded after application of the load was also approximately 0.1 in (2.5 mm). Spread footing load tests can help develop confidence in the use of such foundations for transportation structures.

8.11 CONSTRUCTION INSPECTION

Construction inspection requirements for shallow foundations are similar to those for other concrete structures. In some cases, agencies may have inspector checklists for construction of shallow foundations. Table 8-16 provides a summary of construction inspection check points for shallow foundations. Throughout construction, the inspector should check submittals for completeness before transmitting them to the engineer.

8.11.1 Structural Fill Materials

Fill requirements should be strictly adhered to because the fill must perform within expected limits with respect to strength and, more importantly, within tolerance for differential settlement. Sometimes the area for construction of the fill is small, such as behind abutment and wingwalls. In such situations, the use of hand compactors or smaller compaction equipment may be necessary.

When the construction of structural fills that will support shallow foundations is being monitored, particular attention should be paid to the following items:

- The material should be tested for gradation and durability at sufficient frequency to ensure that the material being placed meets the specification.

- The specified level of compaction must be obtained in the fill. Testing, if applicable, should be performed in accordance with standard procedures and at the recommended intervals or number of tests per lift.

If a surcharge fill is required for pre-loading, it should be verified that the unit weight of the surcharge fill meets the value assumed in the design.

Table 8-16

Inspector responsibilities for construction of shallow foundations

CONTRACTOR SET UP
• Review plans and specifications. • Review contractor's schedule. • Review test results and certifications for pre-approved materials, e.g., cement, coarse and fine aggregate. • Confirm that the contractor's stockpile and staging area are consistent with locations shown on plans. • Discuss anticipated ground conditions and potential problems with the contractor. • Review the contractor's survey results against the plans.
EXCAVATION
• Verify that excavation slopes and/or structural excavation support is consistent with the plans. • Confirm that limits of any required excavations are within right-of-way limits shown on the plans. • Confirm that all unsuitable materials, e.g., sod, snow, frost, topsoil, soft/muddy soils, are removed to the limits and depths shown on the plans and the excavation is backfilled with properly compacted granular material. **The in-place bearing stratum of soil or rock should be checked to verify the in-situ condition and the degree of improvement achieved by the contractor's preparation approach. Some soil types can become remolded and weakened from disturbance. If the conditions deviate from those anticipated in the geotechnical report and/or the plans and specifications, the geotechnical engineer should be consulted to determine if additional measures are necessary.** • Confirm that leveling and proof-rolling of the foundation area is consistent with the requirements of the specifications. Probing is recommended for verification of subgrade. • Confirm that contractor's excavation operations do not result in significant water ponding. • Confirm that existing drainage features, utilities, and other features are protected. • Identify areas not shown on the plans where unsuitable material exists and notify engineer.
SHALLOW FOUNDATION
• Approve footing foundation condition before concrete is poured. • Confirm reinforcement strength, size, and type consistent with the specifications. • Confirm consistency of the contractor's outline of the footing (footing size and bottom of footing depth) with the plans. • Confirm location and spacing of reinforcing steel consistent with the plans. • Confirm water/cement ratio and concrete mix design consistent with the specifications. • Record concrete volumes poured for the footing. • Confirm appropriate concrete curing times and methods as provided in the specifications. • Confirm that concrete is not placed on ice, snow, or otherwise unsuitable ground. • Confirm that concrete is being placed in continuous horizontal layers and that the time between successive layers is consistent with the specifications.
POST INSTALLATION
• Verify pay quantities.

8.11.2 Monitoring

The elevations of constructed foundations should be checked before and after the structural load is applied. The measurements made at those times will serve as a baseline for the long-term monitoring of the bridge. Subsequently, additional survey measurements should be made to confirm satisfactory performance or to identify whether potentially harmful settlements are occurring. It may be important to check the completion of fill settlements before foundation construction if the fill was constructed over soft compressible soils. As indicated in Chapter 7, settlement plates, horizontal inclinometers, or other types of instrumentation are typically installed in such cases. The lateral displacement potential can be greater than the vertical movements; therefore, if conditions warrant, monitoring may also include complete survey coordinates and possibly more accurate instrumentation.

Monitoring may also be necessary to evaluate the impact of the new construction on neighboring facilities or the ground surface. Such concerns could be monitored with simple survey tag lines with benchmarks and monitoring hubs and telltales to measure lateral deviations and vertical subsidence/heave. Greater reliability may require more sophisticated instrumentation, such as inclinometers, strain gages, extensometers and tiltmeters. Surveys of the pre-construction condition of neighboring structures should be conducted, particularly in congested urban areas. The instrumentation program should be developed with a consideration of the anticipated performance, risks and potential consequences. Parameters should be identified that are critical to project success and appropriate instrumentation selected. A key to successful use of instrumentation is to measure, plot and interpret the data in a timely manner to be able to take corrective measures, if needed.

[THIS PAGE INTENTIONALLY BLANK]

CHAPTER 9.0
DEEP FOUNDATIONS

Foundation design and construction involves assessment of factors related to engineering and economics. As discussed in Chapter 8, the selection of the most feasible foundation system requires consideration of both shallow and deep foundation types in relation to the characteristics and constraints of the project and site conditions. Situations commonly exist where shallow foundations are inappropriate for support of structural elements. These situations may be related either to the presence of unsuitable soil layers in the subsurface profile, adverse hydraulic conditions, or intolerable movements of the structure. Deep foundations are designed to transfer load through unsuitable subsurface layers to suitable bearing strata. Typical situations that require the use of deep foundations are shown in Figure 9-1 and briefly discussed below.

- Figure 9-1(a) shows the most common case in which the upper soil strata are too compressible or too weak to support heavy vertical loads. In this case, deep foundations transfer loads to a deeper dense stratum and act as toe bearing foundations. In the absence of a dense stratum within a reasonable depth, the loads must be gradually transferred, mainly through soil resistance along shaft, Figure 9-1(b). An important point to remember is that deep foundations transfer load through unsuitable layers to suitable layers. **The foundation designer must define at what depth suitable soil layers begin in the soil profile**.

- Deep foundations are frequently needed because of the relative inability of shallow footings to resist inclined, lateral, or uplift loads and overturning moments. Deep foundations resist uplift loads by shaft resistance, Figure 9-l(c). Lateral loads are resisted either by vertical deep foundations in bending, Figure 9-l(d), or by groups of vertical and battered foundations, which combine the axial and lateral resistances of all deep foundations in the group, Figure 9-l(e). Lateral loads from overhead highway signs and noise walls may also be resisted by groups of deep foundations, Figure 9-1(f).

- Deep foundations are often required when scour around footings could cause loss of bearing capacity at shallow depths, Figure 9-l(g). In this case the deep foundations must extend below the depth of scour and develop the full capacity in the support zone below the level of expected scour. FHWA (2001c) scour guidelines require the geotechnical analysis of bridge foundations to be performed on the basis that all stream bed materials in the scour prism have been removed and are not available for bearing or lateral support. Costly damage and the need for future underpinning can be avoided by properly designing for scour conditions.

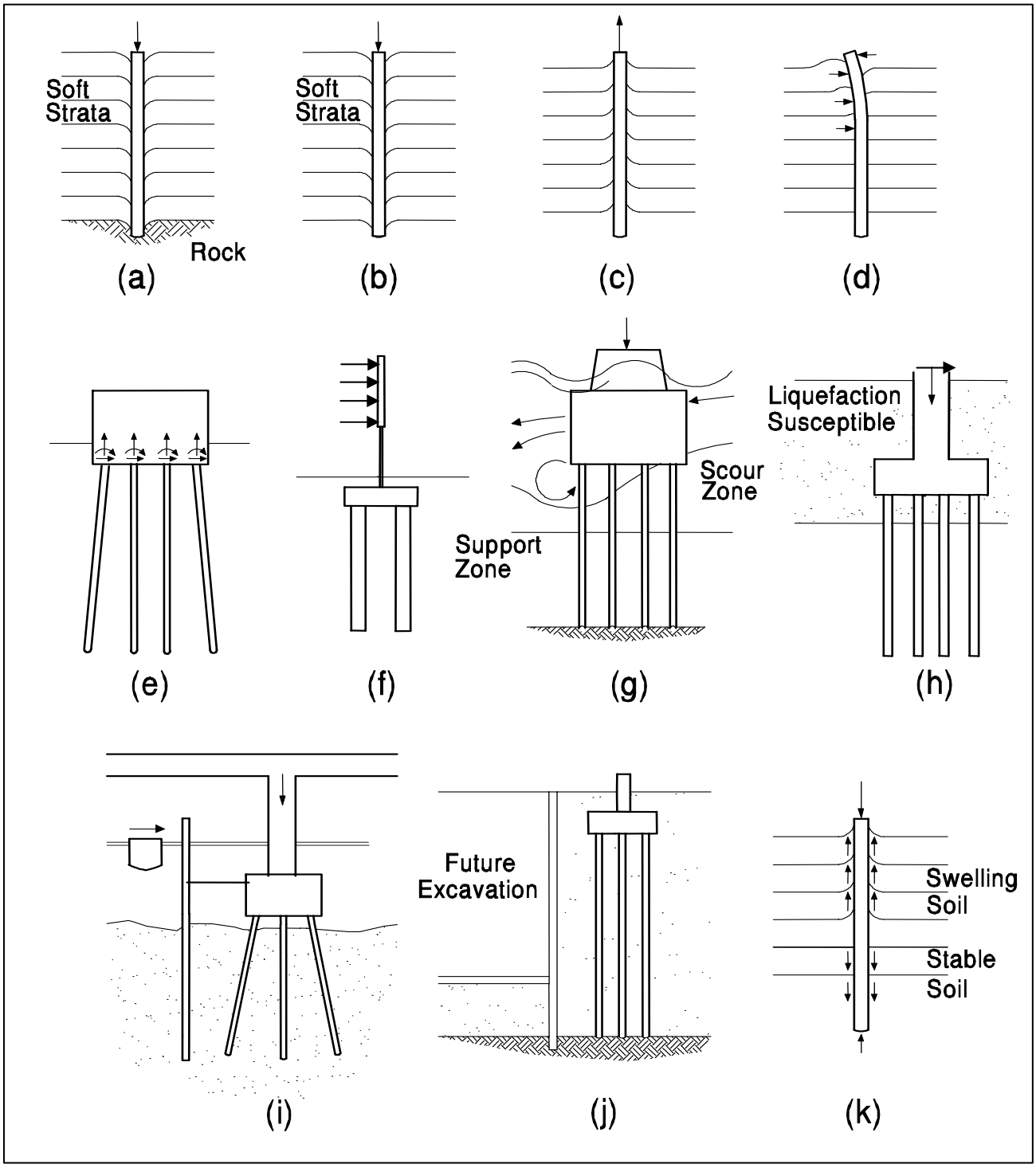

Figure 9-1. Situations in which deep foundations may be needed (Vesic, 1977; FHWA, 2006a).

- Soils subject to liquefaction in a seismic event may also dictate that a deep foundation be used, Figure 9-1(h). Seismic events can induce significant lateral loads to deep foundations. During a seismic event, liquefaction-susceptible soils offer less lateral resistance as well as reduced shaft resistance to a deep foundation. Liquefaction effects on deep foundation performance must be considered for deep foundations in seismic areas.

- Deep foundations are often used as fender systems to protect bridge piers from vessel impact, Figure 9-1(i). Fender system sizes and group configurations vary depending upon the magnitude of vessel impact forces to be resisted. In some cases, vessel impact loads must be resisted by the bridge pier foundation elements. Single deep foundations may also be used to support navigation aids.

- In urban areas, deep foundations may occasionally be needed to support structures adjacent to locations where future excavations are planned or could occur, Figure 9-1(j). Use of shallow foundations in these situations could require future underpinning in conjunction with adjacent construction.

- Deep foundations are used in areas of expansive or collapsible soils to resist undesirable seasonal movements of the foundations. Deep foundations under such conditions are designed to transfer foundation loads, including uplift or downdrag, to a level unaffected by seasonal moisture movements, Figure 9-1(k).

9.1 TYPES OF DEEP FOUNDATIONS AND PRIMARY REFERENCES

There are numerous types of deep foundations. Figure 9-2 shows a deep foundation classification system based on type of material, configuration, installation technique and equipment used for installation. This chapter discusses the driven pile and drilled shaft foundation types based on the information in the following primary references:

FHWA (2006a) *Design and Construction of Driven Pile Foundations - Vol. I and II*, Report No. FHWA-NHI-05-042 and FHWA-NHI-05-043, Authors: Hannigan, P.J., G.G. Goble, G. Thendean, G.E. Likins and F. Rausche., Federal Highway Administration, U.S. Department of Transportation.

FHWA (1999). *Drilled Shafts: Construction Procedures and Design Methods*. Report No. FHWA-IF-99-025, Authors: O'Neill, M. W. and Reese, L. C. Federal Highway Administration, U.S. Department of Transportation.

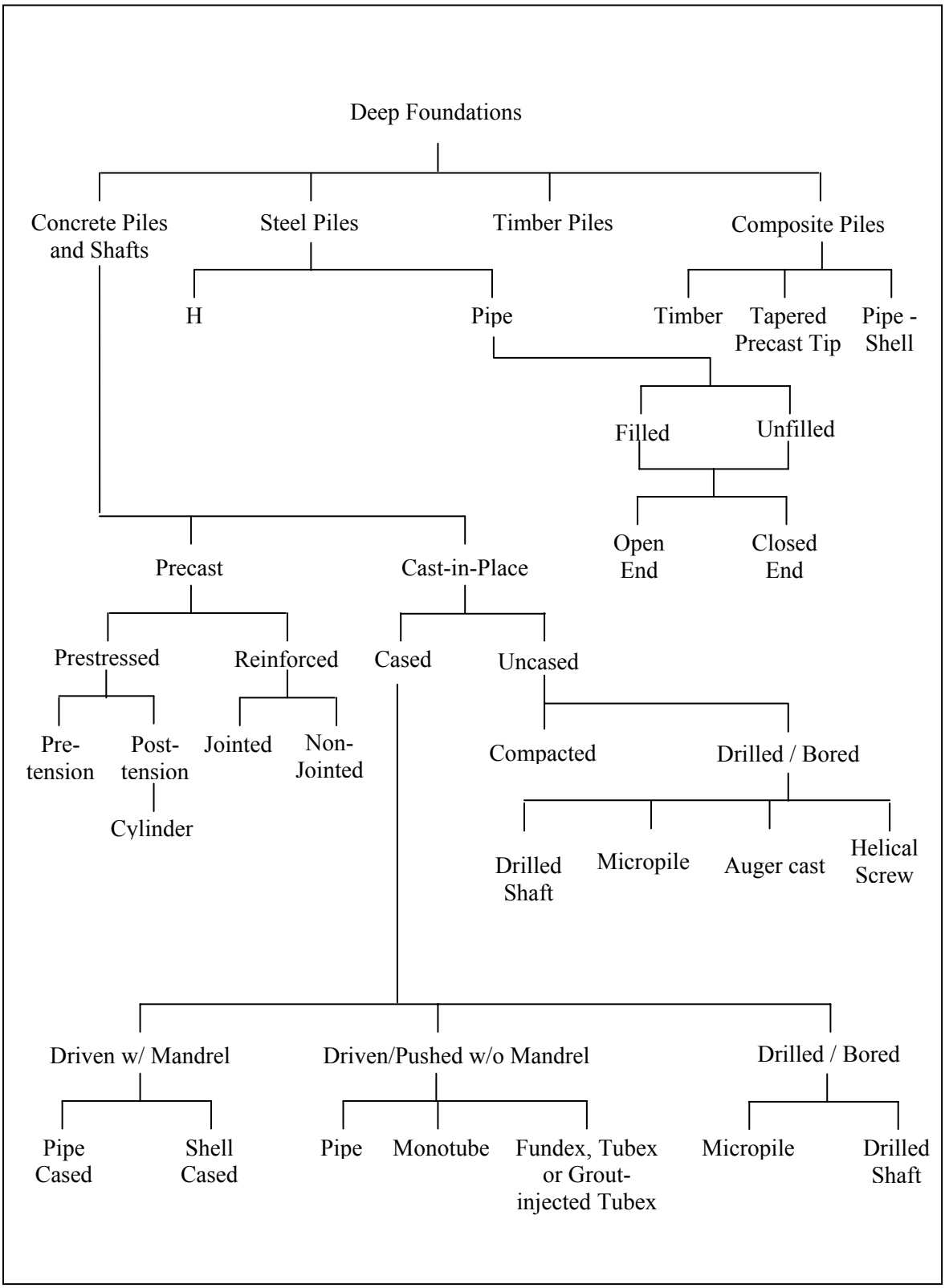

Figure 9-2. Deep foundation classification system (after FHWA, 2006a).

Micropiles and auger-cast piles are rapidly gaining in popularity as viable types of deep foundations for transportation structures. These types of piles are not addressed in this chapter. Guidance for these types of piles can be found in the following FHWA manuals.

FHWA (2005a). "Micropile Design and Construction," Report No. FHWA NHI-05-039, Authors: Sabatini, P.J., Tanyu, B., Armour., P., Groneck, P., and Keeley, J., National Highway Institute, Federal Highway Administration, U.S. Department of Transportation.

FHWA (2006c) "Geotechnical Engineering Circular No. 8, Continuous Flight Auger Piles," Authors: Brown, D. and Dapp, S., Federal Highway Administration, U.S. Department of Transportation.

9.1.1 Selection of Driven Pile or Cast-in-Place (CIP) Pile Based on Subsurface Conditions

For many years the use of a deep foundation has meant security to many designers. For example, the temptation to use driven piles under every facility is great because detailing of plans is routine, quantity estimate is neat, and safe structural support is apparently assured. Often, designers do not consider other pile alternatives such as cast-in-place (CIP) piles. Figure 9-2 shows a variety of CIP pile types. The most common CIP pile type is the drilled shaft which, as indicated earlier, is the only CIP pile type discussed in this chapter. The selection of appropriate pile types for any project should include a consideration of subsurface conditions as the first step. Table 9-1 provides a discussion of driven pile versus drilled shafts for various subsurface conditions. Sections 9.2 to 9.9 discuss the details of the driven pile foundation systems while Sections 9.10 to 9.14 discuss the CIP pile types with emphasis on drilled shafts.

9.1.2 Design and Construction Terminology

Just as with the design of other geotechnical features, there is a specific terminology associated with design of various deep foundations. Examples of terminology are "static pile capacity," "ultimate pile capacity," "allowable pile capacity," "driving capacity," "restrike capacity," "shaft resistance in piles," "side resistance in drilled shafts," "toe resistance for piles," "base or tip resistance for drilled shafts," etc. This terminology has been ingrained in the technical literature, FHWA manuals, various text books and AASHTO. Herein, the terminology in various primary references listed above will be used for driven piles and drilled shafts. The first time a specific phrase or term appears in the text, it will be highlighted in **bold text**.

For all deep foundations, the capacity of the foundation is a function of the geotechnical and the structural aspects. The geotechnical aspect is a function of the resistance from the ground while

the structural aspect is a function of the structural section and the structural properties of the pile. In this chapter, the primary emphasis is on the geotechnical aspects of the deep foundations. Structural aspects are discussed only to the extent that they may be relevant, e.g., the structural capacity of a pile relative to the driving stresses induced during the driven pile installation process.

Table 9-1
Pile type selection based on subsurface and hydraulic conditions

Typical Problem	Recommendations
Boulders overlying bearing stratum	Use heavy nondisplacement driven pile with a reinforced tip or manufactured point and include contingent predrilling item in contract. Depending on the size of the boulders, large diameter drilled shaft may be feasible.
Loose cohesionless soil	Use tapered pile to develop maximum skin friction. For drilled shafts, side-support in form of casing or slurry will be required making it costlier than the driven pile option
Negative shaft resistance	Use smooth steel pile to minimize drag adhesion, and avoid battered piles. Minimize the magnitude of drag force when possible. In case of drilled shafts use casing to minimize drag load.
Deep soft clay	Use rough concrete pile to increase adhesion and rate of pore water dissipation. Drilled shaft is possible but side-support in form of casing or slurry will be required making it costlier than driven pile option.
Artesian Pressure	Do not use mandrel driven thin-wall shells as generated hydrostatic pressure may cause shell collapse; pile heave common to closed-end pipe. In case of drilled shaft, a slurry drilling will be required.
Scour	Do not use tapered piles unless large part of taper extends well below scour depth. Design permanent pile capacity to mobilize soil resistance below scour depth. Large drilled shaft is likely a better option compared to a group of piles.
Coarse Gravel Deposits	Use precast concrete piles where hard driving expected in coarse soils. DO NOT use H-piles or open end pipes as nondisplacement piles will penetrate at low blow count and cause unnecessary overruns. Drilled shaft is likely a better option for coarse gravel deposit.

9.2 DRIVEN PILE DESIGN-CONSTRUCTION PROCESS

The driven pile design and construction process has aspects that are unique in all of structural design. Because the driving characteristics are related to pile capacity for most soils, they can be used to improve the accuracy of the pile capacity estimate. In general, the various methods of determining pile capacity from dynamic data such as driving resistance with wave equation analysis and dynamic measurements are considerably more accurate than the static analysis methods based on subsurface exploration information. **It must be clearly understood that the static analysis based on the subsurface exploration information usually has the function of providing an *estimate* of the pile length prior to field installation. The final driving criterion is usually a blow count that is established after going to the field and the individual pile penetrations may vary depending on the soil variability. Furthermore, pile driveability is a very important aspect of the process and must be considered during the design phase.**

The key point to understand in a driven pile design is that the pile should be designed such that it (a) can be driven to the design depth without damage, and (b)sustain the loads with the design factor of safety during the service life of the structure. If the design is completed and the piles cannot be driven, large costs can be generated. It is absolutely necessary that the design and construction phases be linked in a way that does not exist elsewhere in construction.

The driven pile design-construction process is outlined in the flow chart of Figure 9-3. This flow chart will be discussed block by block using the numbers in the blocks as a reference and it will serve to guide the designer through all of the tasks that must be completed.

Block 1: Establish Global Project Performance Requirements

The first step in the entire process is to determine the general structure requirements.

1. Is the project a new bridge, a replacement bridge, a bridge renovation, a retaining wall, a noise wall, or sign or light standard?

2. Will the project be constructed in phases or all at one time?

3. What are the general structure layout and approach grades?

4. What are the surficial site characteristics?

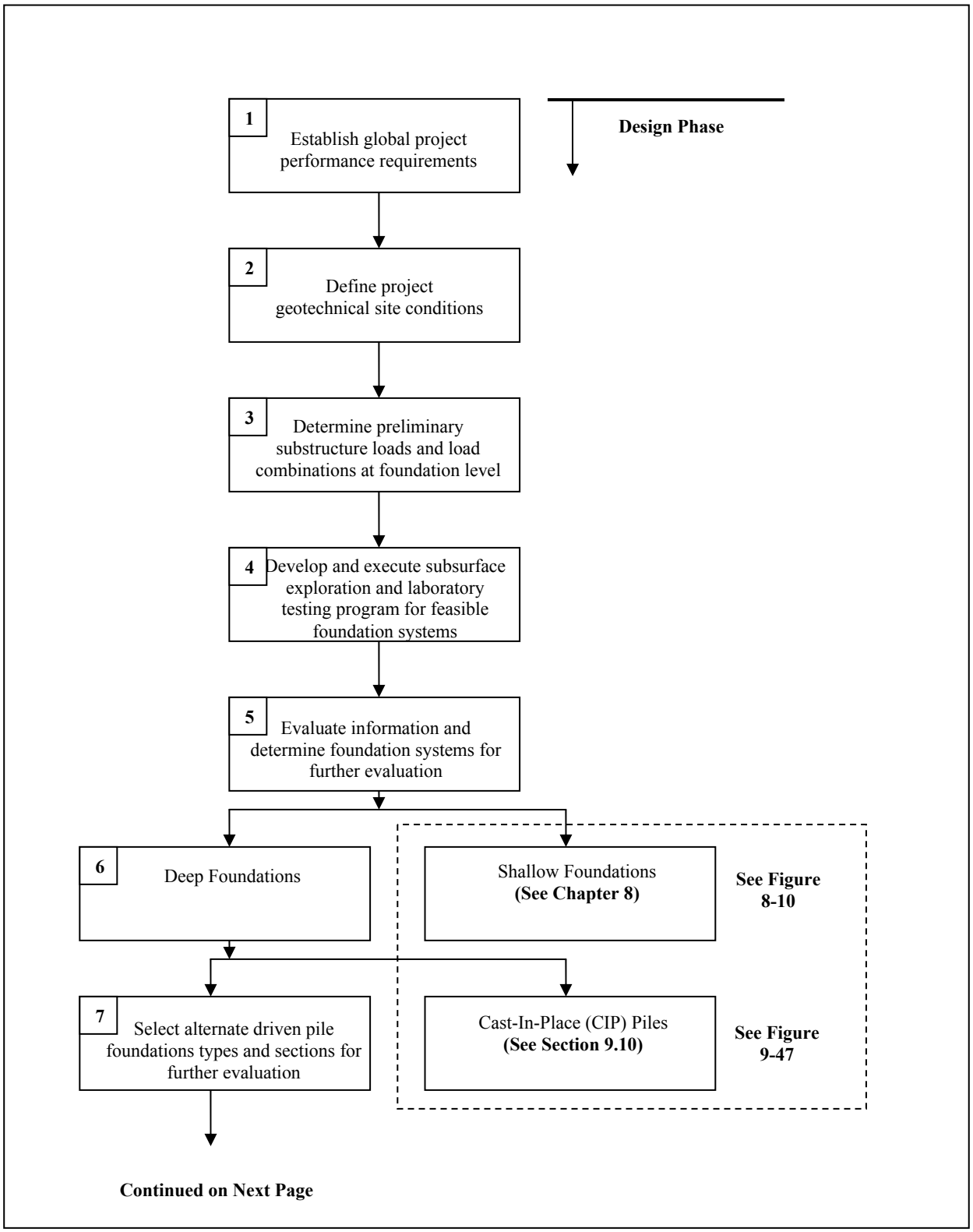

Figure 9-3. Driven pile design and construction process (after FHWA 2006a).

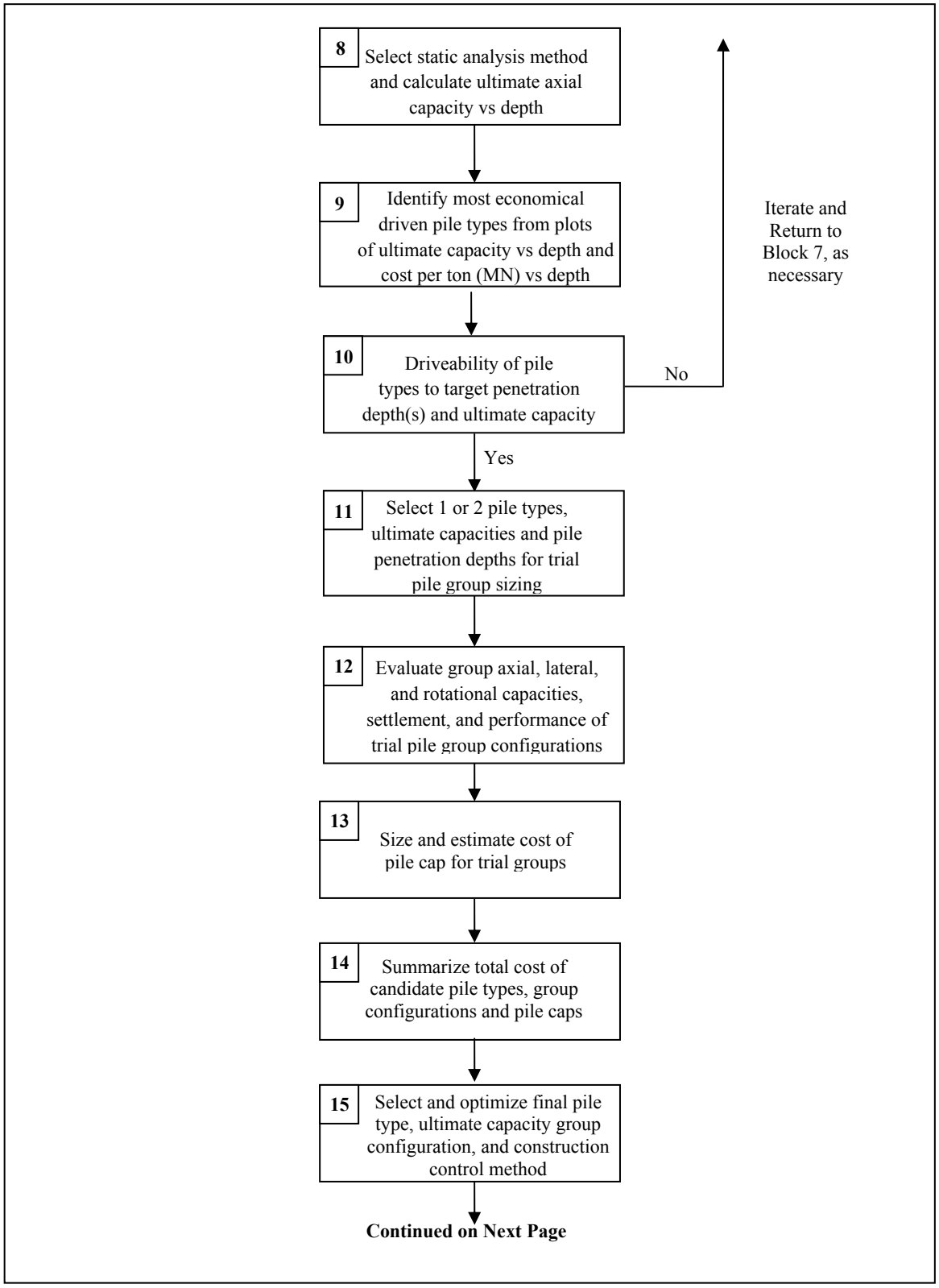

Figure 9-3 (Continued). Driven pile design and construction process (after FHWA 2006a).

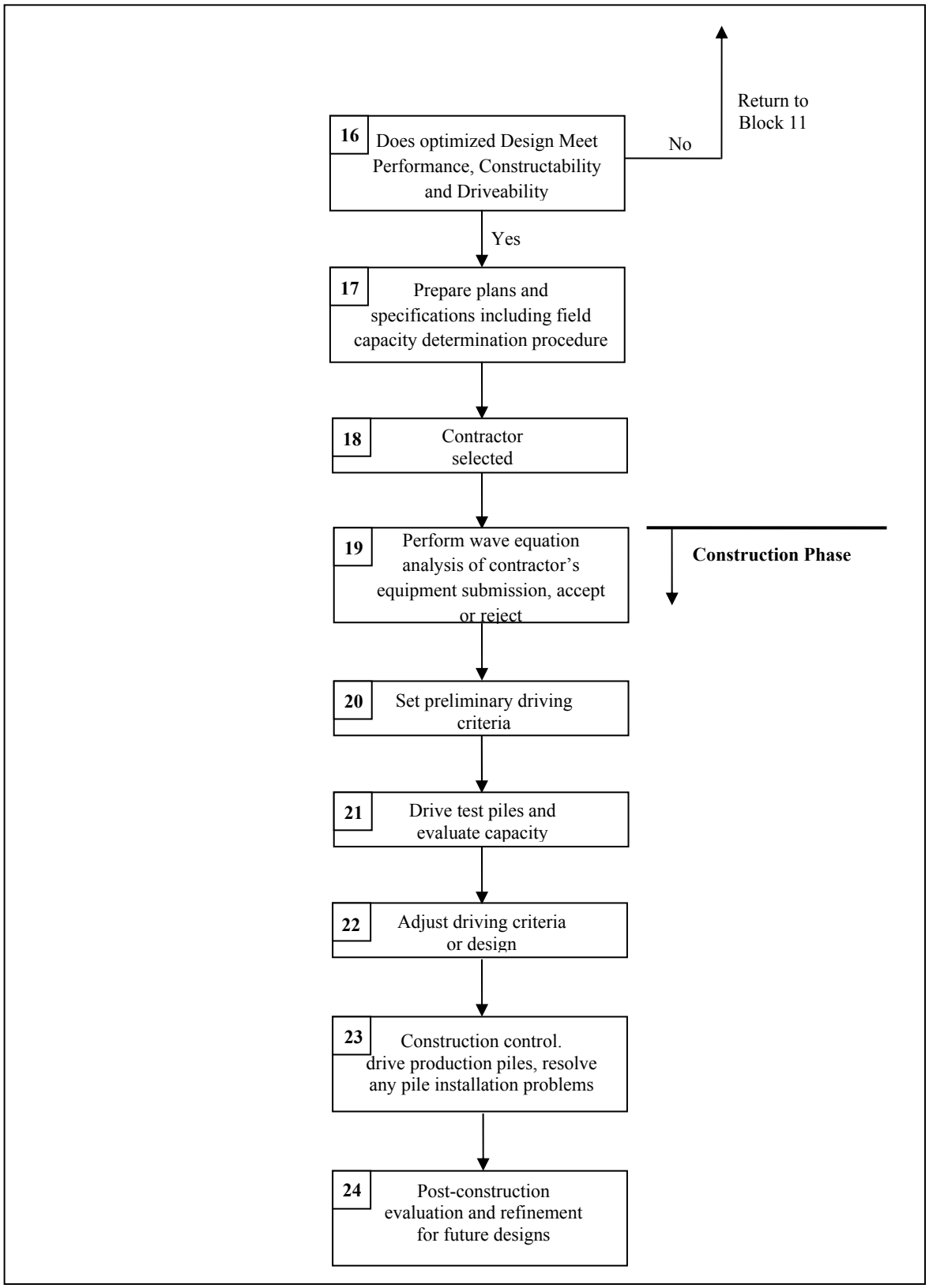

Figure 9-3 (Continued). Driven pile design and construction process (after FHWA 2006a).

5. Is the structure subjected to any special design events such as seismic, scour, downdrag, debris loading, vessel impact, etc.? If there are special design events, the design requirements should be reviewed at this stage so that these can be factored into the site investigation.

6. What are the approximate foundation loads? What are the deformation or deflection requirements (total settlement, differential settlement, lateral deformations, tolerances)?

7. Are there site environmental issues that must be considered in the design (specific limitation on noise, vibrations, etc.)?

Block 2: Define Project Geotechnical Site Conditions

A great deal can be learned about the foundation requirements with even a very general understanding of the site geology. For small structures, this may involve only a very superficial investigation such as a visit to the site. The foundation design for very large structures may require extensive geologic studies and review of geologic maps. Based on the geologic studies, the project team should consider possible modifications in the structure that may be desirable for the site under consideration

Frequently there is information available on foundations that have been constructed in the area. This information can be of assistance in avoiding problems. Both subsurface exploration information and foundation construction experience should be collected ***prior*** to beginning the foundation design. Unfortunately, this step is not often done in practice.

Block 3: Determine Preliminary Substructure Loads and Load Combinations at the Foundation Level

Substructure loads and reasonable vertical and lateral deformation requirements should be established at this time. This issue was considered in Block 1. The result of that effort has probably matured in the intervening time which might be quite long for some projects and is now better defined. It is imperative that the foundation specialist obtain a completely defined and unambiguous set of foundation loads and performance requirements in order to proceed through the foundation design process. Accurate load information and performance criteria are essential in the development and implementation of an adequate subsurface exploration program for the planned structure.

Block 4: Develop and Execute Subsurface Exploration Program for Feasible Foundation Systems

Based on the information obtained in Blocks 1-3, it is possible to make decisions regarding the necessary information that must be obtained for the feasible foundation systems at the site. The subsurface exploration program and the associated laboratory testing must meet the needs of the design problem that is to be solved at a cost consistent with the size and importance of the structure. The results of the subsurface exploration program and the laboratory testing are used to prepare a subsurface profile and identify critical cross sections. These tasks are covered in greater detail in Chapters 3, 4, and 5.

Block 5: Evaluate Information and Select Candidate Foundation Systems

The information collected in Blocks 1-4 must be evaluated and candidate foundation systems selected for further consideration. The first question to be decided is whether a shallow or a deep foundation is required. This question will be answered based primarily on the strength and compressibility of the site soils, the proposed loading conditions, scour depth, the project performance criteria and the foundation cost. If settlement and scour are not a problem for the structure, then a shallow foundation will probably be the most economical solution. Ground improvement techniques in conjunction with shallow foundations should also be evaluated. Shallow and deep foundation interaction with approach embankments must also be considered. If the performance of a shallow foundation exceeds the limitations imposed by the structure performance criteria, a deep foundation must be used. The design of ground improvement techniques is not covered in this manual and can be found in FHWA (2006b). Information on design considerations for shallow foundations can be found in Chapter 8.

Block 6: Deep Foundations

The decision on deep foundation type is now between driven piles and other deep foundation systems. These other deep foundation systems are primarily drilled shafts, but would also include micropiles, auger cast piles, and other drilled-in deep foundation systems as shown in Figure 9-2. The questions that must be answered in deciding between driven piles and other deep foundation systems will center on the relative costs of available, possible systems. Foundation support cost can be conveniently calculated based on a cost per unit of load carried. In addition, constructability must be considered. Design guidance on drilled shafts can be found in Section 9.10 of this chapter. Guidance for other deep foundation systems such as micro-piles and auger cast piles can be found in the references listed in Section 9.1.

Block 7: Select Candidate Driven Pile Types for Further Evaluation

At this point on the flow chart, the primary concern is for the design of a driven pile foundation. The pile type must be selected consistent with the applied load per pile. Consider this problem. The general magnitude of the column or pier loads is known from the information obtained in Blocks 1 and 3. However, a large number of combinations of pile capacities and pile types can satisfy the design requirements. Should twenty, 225 kip (1000 kN) capacity piles be used to carry a 4,500 kip (20,000 kN) load, or would it be better to use ten, 450 kip (2,000 kN) capacity piles? This decision should consider both the structural capacity of the pile and the realistic geotechnical capacities of the pile type for the soil conditions at the site, the cost of the available alternative piles, and the capability of available construction contractors to drive the selected pile. Of course, there are many geotechnical factors that must also be considered. At this point in the design process, 2 to 5 candidate pile types and/or sections that meet the general project requirements should be selected for further evaluation. Pile type and selection considerations are covered in Section 9.3.

At this stage the loads must also be firmly established. In Block 1, approximate loads were determined, which were refined in Block 3. At the early stages of the design process the other aspects of the total structural design were probably not sufficiently advanced to establish the final design loads. By the time that Block 6 has been reached, the structural engineer should have finalized the various loads. One common inadequacy that is sometimes discovered when foundation problems arise is that the foundation loads were never really accurately defined at the final stage of the foundation design.

If there are special design events to be considered, they must be included in the determination of the loads. Vessel impact will be evaluated primarily by the structural engineer and the results of that analysis will give pile loads for that case. There may be stiffness considerations in dealing with vessel impact since the design requirement is basically a requirement that some vessel impact energy be absorbed by the foundation system.

Scour presents a different requirement. The loads due to the forces from the stream must be determined as specified in the AASHTO (2002), Section 3.18. The requirements of this AASHTO section should be included in the structural engineer's load determination process. The depth of scour must also be determined as directed in AASHTO (2002), Section 4.3.5. In the design process, it must be assured that the pile will still have adequate capacity after scour.

In many locations in the country, seismic loads will be an important contributor to some of the critical pile load conditions. Since the 1971 San Fernando Earthquake, significant emphasis has

been placed on seismic design considerations in the design of highway bridges. The AASHTO Standard Specifications for Highway Bridges has been substantially expanded to improve the determination of the seismic loads. Usually the structural engineer will determine the seismic requirements. Frequently the behavior of the selected pile design will affect the structural response and hence the pile design loads. In this case, there will be another loop in the design process that includes the structural engineer. The geotechnical engineer should review the seismic design requirements in Division I-A of AASHTO (2002) for a general understanding of the design approach.

Block 8: Select Static Analysis Method and Calculate Ultimate Capacity vs Depth

A static analysis method(s) applicable to the pile type(s) under consideration and the soil conditions at the site should now be selected. Static analysis methods are covered in detail in Section 9.4. The ultimate axial capacity versus depth should then be calculated for all candidate pile types and sections.

Block 9: Identify Most Economical Candidate Pile Types and/or Sections

The next step is to develop and evaluate plots of the ultimate axial static capacity versus pile penetration depth and the pile support cost versus pile penetration depth for each candidate pile type and/or section. The support cost, which is the cost per ton (kN) supported, is the ultimate capacity at a given penetration depth divided by the pile cost to reach that penetration depth. The pile cost can be calculated from the unit cost per ft (m) multiplied by the pile length to the penetration depth. These plots should be evaluated to identify possible pile termination depths to obtain the lowest pile support cost. This process is briefly discussed in Section 9.3.

Block 10: Calculate Driveability of Candidate Pile Types

Candidate pile types should now be evaluated for driveability. Can the candidate pile type and/or section be driven to the required capacity and penetration depth at a reasonable pile penetration resistance (blow count) without exceeding allowable driving stresses for the pile material? This analysis is performed by using the wave equation theory. All of the necessary information is available except the hammer selection. Since the hammer to be used on the job will be known only after the contractor is selected, possible hammers must be identified to make sure that the pile is driveable to the capacity and depth required.

Pile driveability, wave equation analysis and allowable pile driving stresses are discussed in Section 9.9.

If candidate pile types or sections do not meet driveability requirements they are dropped from further evaluation or modified sections must be chosen and evaluated. For H-piles and pipe piles it may be possible to increase the pile section without increasing the soil resistance to driving. For concrete piles an increase in section usually means a larger pile size. Therefore, an increase in soil resistance must also be overcome. Hence, some section changes may cause the design process to revisit Block 8. If all candidate pile types fail to meet driveability requirements, the design process must return to Block 7 and new candidate pile types must be selected.

Block 11: Select 1 or 2 Final Candidate Pile Types for Trial Group Sizing

The most viable candidate pile types and/or sections from the cost and driveability evaluations in Blocks 9 and 10 should now be evaluated for trial group sizing by using the final loads and performance requirements. Multiple pile penetration depths and the resulting ultimate capacity at those depths should be used to establish multiple trial pile group configurations for each candidate pile type. These trial configurations should then be carried forward to Block 13.

Block 12: Evaluate Capacity, Settlement, and Performance of Trial Groups

The trial group configurations should now be evaluated for axial group capacity, group uplift, group lateral load performance, and settlement. These computations and analysis procedures are described in Section 9.6.

Block 13: Size and Estimate Pile Cap Cost for Trial Groups

The size and thickness of the pile cap for each trial group should be evaluated, and the resulting pile cap cost estimated. It is not necessary to design the cap reinforcement at this time only to determine cap size. Pile cap cost is a key component in selecting the most cost effective pile type and should not be overlooked.

Block 14: Summarize Total Cost of Final Candidate Piles

The total cost of each candidate pile should now be determined. A given pile type may have several total cost options depending upon the pile penetration depths, ultimate capacities, group configurations, and pile cap sizes carried through the design process. The cost of any special construction considerations and environmental restrictions should also be included in the total cost for each candidate pile.

Block 15: Select and Optimize Final Pile Type, Capacity, and Group Configuration

Select the final pile foundation system including pile type, section, length, ultimate capacity and group configuration for final design. A complete evaluation of lateral and rotational resistance of the group should be performed. The design should be optimized for final structure loads, performance requirements, and construction efficiency.

Block 16: Does Optimized Design Meet All Requirements?

The final pile type, section, capacity and group configuration optimized in Block 15 should be evaluated so that all performance requirements have been achieved. If the optimization process indicates that a reduced pile section can be used, the driveability of the optimized pile section must be checked by a wave equation driveability analysis. This analysis should also consider what influence the group configuration and construction procedures (e.g., cofferdams, etc.) may have on pile installation conditions.

Block 17: Prepare Plans and Specifications, Set Field Capacity Determination Procedure

When the design has been finalized, plans and specifications can be prepared and the procedures that will be used to verify pile capacity can be defined. It is important that all of the quality control procedures are clearly defined for the bidders to avoid claims after construction is underway. In the past a pile load specified on the basis of dynamic formulae was a design or working load since a factor of safety is contained in the formula. Modern methods for determining pile capacity always use ultimate loads with a factor of safety (or in LRFD a resistance factor) selected and applied. This modern approach should also be made clear in the project specifications so that the contractor has no question regarding the driving requirements. Procedures should be in place that address commonly occurring pile installation issues such as obstructions and driveability.

Block 18: Contractor Selection

After the bidding process is complete, a contractor is selected. The contractor should be qualified and experienced in the installation of driven piles for the type of structure being built.

Block 19: Perform Wave Equation Analysis of Contractor's Equipment Submission

At this point the engineering effort shifts to the field. The contractor will submit a description of the pile driving equipment that he intends to use on the project for the engineer's evaluation. Wave equation analyses are performed to determine the driving resistance that must be achieved in the field to meet the required capacity and pile penetration depth. Driving stresses are determined and evaluated. If all conditions are satisfactory, the equipment is approved for driving. Some design specifications make this information advisory to the contractor rather than mandatory. Section 9.8 provides additional information in this area.

On smaller projects, a dynamic formula may be used to evaluate driveability. In this case, the modified Gates Formula should be used. If a dynamic formula is used, then driveability and hammer selection will be based on the driving resistance given by the formula only, since stresses are not determined. Dynamic formula usage is covered in Section 9.9.

Block 20: Set Preliminary Driving Criteria

Based on the results of the wave equation analysis of Block 19 (or on smaller projects the modified Gates Formula) and any other requirements in the design, the preliminary driving criteria can be set.

Block 21: Drive Test Pile and Evaluate Capacity

The test pile(s)**,** if required**,** are driven to the preliminary criteria developed in Block 19. Driving requirements may be defined by penetration depth, driving resistance, dynamic monitoring results or a combination of these conditions. The capacity can be evaluated by driving resistance from wave equation analysis, the results of dynamic monitoring, static load test, the modified Gates Formula, or a combination of these. Dynamic monitoring is described in Section 9.9. Static load test procedures are discussed in greater detail at the end of this chapter.

Block 22: Adjust Driving Criteria or Design

At this stage the final conditions can be set or, if test results from Block 21 indicate the capacity is inadequate, the driving criteria may have to be changed. In a few cases, it may be necessary to make changes in the design that will return the process as far back as Block 8.

In some cases, it is desirable to perform preliminary field testing before final design. When the job is very large and the soil conditions are difficult, it may be possible to achieve substantial

cost savings by having results from a design stage test pile program, including actual driving records at the site, as part of the bid package.

Block 23: Construction Control

After the driving criteria are set, the production pile driving begins. Quality control and assurance procedures have been established and are applied. Problems may arise and must be handled as they occur in a timely fashion.

Block 24: Post-Construction Evaluation and Refinement of Design

After completion of the foundation construction, the design should be reviewed and evaluated for its effectiveness in satisfying the design requirements and also its cost effectiveness.

9.3 ALTERNATE DRIVEN PILE TYPE EVALUATION

The selection of appropriate driven pile types for any project involves the consideration of several design and installation factors including pile characteristics, subsurface conditions and performance criteria. This selection process should consider the factors listed in Table 9-1, Table 9-2 and Table 9-3. Table 9-2 summarizes typical pile characteristics and uses. Table 9-3 presents the placement effects of pile shape characteristics.

Table 9-2
Typical piles and their range of loads and lengths

Type of Pile	Typical Axial Design Loads	Typical Lengths
Timber	20-110 kips (100 – 500 kN)	15-120 ft (5-37 m)*
Precast / Prestressed Reinforced Concrete	90-225 kips (400-1,000 kN) for reinforced 90-1000 kips (400-4,500 kN) for prestressed	30-50 ft (10-15m) for reinforced 50-130 ft (15-40m) for prestressed
Steel H	130-560 kips (600-2,500 kN)	15-130 ft (5-40 m)
Steel Pipe (without concrete core)	180-560 kips (800-2,500 kN)	15-130 ft (5-40 m)
Steel Pipe (with concrete core)	560-3400 kips (2,500-15,000 kN)	15-130 ft (5-40 m)
* 15-75 ft (5-23 m) for Southern Pine; 15-120 ft (5-37 m) for Douglas Fir		

Table 9-3
Pile type selection pile shape effects

Shape Characteristics	Pile Types	Placement Effects
Displacement	Steel Pipe (Closed end), Precast Concrete	• Increase lateral ground stress • Densify cohesionless soils, remolds and weakens cohesive soils temporarily • Set-up time may be 6 months in clays for pile groups
Nondisplacement	Steel H, Steel Pipe (Open end)	• Minimal disturbance to soil • Not suited for friction piles in coarse granular soils. Piles often have low driving resistances in these deposits making field capacity verification difficult thereby often resulting in excessive pile lengths.
Tapered	Timber, Monotube, Tapertube, Thin-wall shell	• Increased densification of soils with less disturbance, high capacity for short length in granular soils

In addition to the considerations provided in the Tables 9-1, 9-2 and 9-3, the problems posed by the specific project location and topography must be considered in any pile selection process. Following are some of the problems usually encountered:

1. Noise and vibration from driven pile installation may affect pile type selection, and require special techniques such as predrilling and/or vibration monitoring of adjacent structures.

2. Remote areas may restrict driving equipment size and, therefore, pile size.

3. Local availability of certain materials and the capability of local contractors may have decisive effects on pile selection.

4. Waterborne operations may dictate use of shorter pile sections due to pile handling limitations.

5. Steep terrain may make the use of certain pile equipment costly or impossible.

9.3.1 Cost Evaluation of Alternate Pile Types

Often several different pile types meet all the requirements for a particular structure. In such cases, the final choice should be made on the basis of a cost analysis that assesses the over-all cost of the foundation alternatives. This requires that candidate pile types be

carried forward in the design process for determination of the pile section requirements for design loads and constructability. The cost analysis for the candidate pile types should include uncertainties in execution, time delays, cost of load testing programs, as well as the differences in the cost of pile caps and other elements of the structure that may differ among alternatives. For major projects, alternate foundation designs should be considered for inclusion in the contract documents if there is a potential for cost savings.

For driven pile foundation projects, the total foundation cost can be separated into three major components as follows:

- The pile cost
- The pile cap cost, and
- The construction control method cost

For most pile types, the pile cost can usually be assumed as linear with depth based on unit price. However, this may not be true for very long concrete piles or long, large section steel piles. These exceptions may require the cost analysis to reflect special transportation, handling, or splicing costs for concrete piles or extra splice time and cost for steel piles. Table 9-4 presents cost savings recommendations to be considered during the evaluation of pile foundations. Expressing the cost of candidate pile types in terms of dollars per ton capacity would allow comparison of alternative pile types in a rational manner. Details of this approach, i.e., expressing costs in $/ton, are presented in FHWA (2006a).

9.4 COMPUTATION OF PILE CAPACITY

Once the allowable structural load has been determined for prospective pile alternates, the pile length required to support that load must be determined. For many years this length determination was considered part of the "art of foundation engineering." In recent years more rational analytic procedures have been developed. Static analyses provide a useful design tool to select the most economical pile alternates. The methods that follow are established procedures that account for the variables in pile length determination. The "art" remains in selecting appropriate soil strength values for the conditions and ascertaining the effects of pile installation on these values. For the typical project two static analyses will be required; the first to determine the length required for permanent support of the structures, and the second to determine the soil resistance to be overcome during driving to achieve the estimated length. It must be stressed that each new site represents a new problem with unique conditions. Experience with similar sites should not replace but should refine the rational analysis methods presented herein. This section discusses the concept of static capacity of the pile based on a rational approach.

Table 9-4. Cost savings recommendations for pile foundations (FHWA, 2006a)

Factor	Inadequacy of Older Methods	Cost Saving Recommendations	Remarks
A. Design structural load capacity of piles.	1. Allowable pile material stresses may not address site-specific considerations.	1. Use realistic allowable stresses for pile materials in conjunction with adequate construction control procedures, (i.e., load testing, dynamic pile monitoring and wave equation). 2. Determine potential pile types and carry candidate pile types forward in the design process. 3. Optimize pile size for loads.	1. Rational consideration of Factors A and B may decrease cost of a foundation by 25 percent or more. 2. Significant cost savings can be achieved by optimization of pile type and section for the structural loads with consideration of pile driveability requirements.
B. Design geotechnical capacity of soil and rock to carry load transferred by piles.	1. Inadequate subsurface explorations and laboratory testing. 2. Rules of thumb and prescribed values used in lieu of static design may result in overly conservative designs. 3. High potential for change orders and claims.	1. Perform thorough subsurface exploration including in-situ and laboratory testing to determine design parameters. 2. Use rational and practical methods of design. 3. Perform wave equation driveability analysis. 4. Use design stage pile load testing on large pile driving projects to determine load capacities (load tests during design stage).	1. Reduction of safety factor can be justified because some of the uncertainties about load carrying capacities of piles are reduced. 2. Rational pile design will generally lead to shorter pile lengths and/or smaller number of piles.
C. Alternate foundation design.	1. Alternate foundation designs are rarely used even when possibilities of cost savings exist by allowing alternates in contract documents.	1. For major projects, consider inclusion of alternate foundation designs in the contract documents if estimated costs of feasible foundation alternatives are within 15 percent of each other.	1. Alternative designs often generate more competition which can lead to lower costs.
D. Plans and specifications.	1. Unrealistic specifications. 2. Uncertainties due to inadequate subsurface explorations force the contractors to inflate bid prices.	1. Prepare detailed contract documents based on thorough subsurface explorations, understanding of contractors' difficulties and knowledge of pile techniques and equipment. 2. Provide subsurface information to the contractor.	1. Lower bid prices will result if the contractor is provided with all the available subsurface information. 2. Potential for contract claims is reduced with realistic specifications.
E. Construction determination of pile load capacity during installation.	1. Often used dynamic formulas such as Engineering News formula are unreliable. Correlations between load capacities determined from Engineering News formula and static load tests indicate safety factors ranging from less than 1 (i.e. failure) to about 20 (i.e. excessive foundation cost).	1. Eliminate use of dynamic formulas for construction control as experience is gained with the wave equation analysis. 2. Use wave equation analysis coupled with dynamic monitoring for construction control and load capacity evaluation. 3. Use pile load tests on projects to substantiate capacity predictions by wave equation and dynamic monitoring.	1. Reduced factor of safety may allow shorter pile lengths and/or smaller number of piles. 2. Pile damage due to excessive driving can be eliminated by using dynamic monitoring equipment. 3. Increased confidence and lower risk results from improved construction control.

The **static capacity** of a pile can be defined as the sum of soil/rock resistances along the pile shaft and at the pile toe available to support the imposed loads on the pile. Static analyses are performed to determine the ultimate capacity of an individual pile and of a pile group as well as the deformation response of a pile group to the applied loads. The **ultimate capacity** of an individual pile and of a pile group is defined as the smaller of:

(1) the capacity of the surrounding soil/rock medium to support the loads transferred from the pile(s) or,

(2) the structural capacity of the pile(s).

Soil-structure interaction analysis methods are used to determine the deformation response of piles and pile groups to lateral loads; such methods can also be used for deformation evaluation under vertical loads. The results from these analyses as well as the results of static analysis of pile group settlement are compared to the performance criteria established for the structure.

The ultimate geotechnical pile capacity, Q_u, of a pile in homogeneous soil may be expressed as follows in terms of the **shaft (commonly knows as "skin") resistance**, R_s, **toe resistance**, R_t, and the weight, W, of the pile:

$$Q_u = R_s + R_t - W \qquad 9\text{-}1$$

In most cases, such as H-Piles and open ended pipe piles, the weight W is small compared to the shaft and toe resistance and is neglected. However, the weight of pipe piles, particularly large diameter pipes, filled with concrete may be significant and may be included in the analysis. In this chapter, the W term is neglected. Equation 9-1, without the W term, may also be expressed in the form

$$Q_u = f_s A_s + q_t A_t \qquad 9\text{-}2$$

where f_s is the **unit shaft resistance** over the shaft surface area, A_s, and q_t is the **unit toe resistance** over the pile toe area, A_t. The above equations for pile bearing capacity assume that both the pile toe and the pile shaft have moved sufficiently with respect to the adjacent soil to simultaneously develop the ultimate shaft and toe resistances. Generally, the displacement needed to mobilize the shaft resistance is smaller than that required to mobilize the toe resistance. This simple rational approach has been commonly used for all piles except very large diameter piles where such an approach may not be valid.

Figure 9-4 illustrates typical load transfer profiles for a single pile. The load transfer distribution can be obtained from a static load test where strain gages or telltale rods are attached to a pile at different depths along the pile shaft. Figure 9-4 shows the measured ultimate axial load, Q_u, in the pile plotted against depth. **The shaft resistance transferred to the soil is represented by R_s, and R_t represents the resistance at the pile toe.** In Figure 9-4(a), the load transfer distribution for a pile with no shaft resistance is illustrated. In this case the full axial load at the pile head is transferred to the pile toe. In Figure 9-4(b), the axial load versus depth for a uniform shaft resistance distribution typical of a cohesive soil is illustrated. Figure 9-4(c) presents the axial load in the pile versus depth for a triangular shaft resistance distribution typical of cohesionless soils.

9.4.1 Factors of Safety

The results of static analyses yield a **geotechnical ultimate pile capacity**, Q_u. The **allowable geotechnical soil resistance** (**geotechnical pile design load**), Q_a, is selected by dividing the **geotechnical ultimate pile capacity**, Q_u, by a **factor of safety** as follows.

$$Q_a = \frac{Q_u}{\text{Factor of Safety}} \qquad 9\text{-}3$$

The range of the factor of safety, FS, has depended primarily upon the reliability of the particular method of static analysis with consideration of the following items:

1. The level of confidence in the input parameters. The level of confidence is a function of the type and extent of the subsurface exploration and laboratory testing of soil and rock materials.

2. Variability of the soil and rock.

3. Method of static analysis.

4. Effects of and consistency of the proposed pile installation method.

5. Level of construction control (static load test, dynamic analysis, wave equation analysis, Gates dynamic formula).

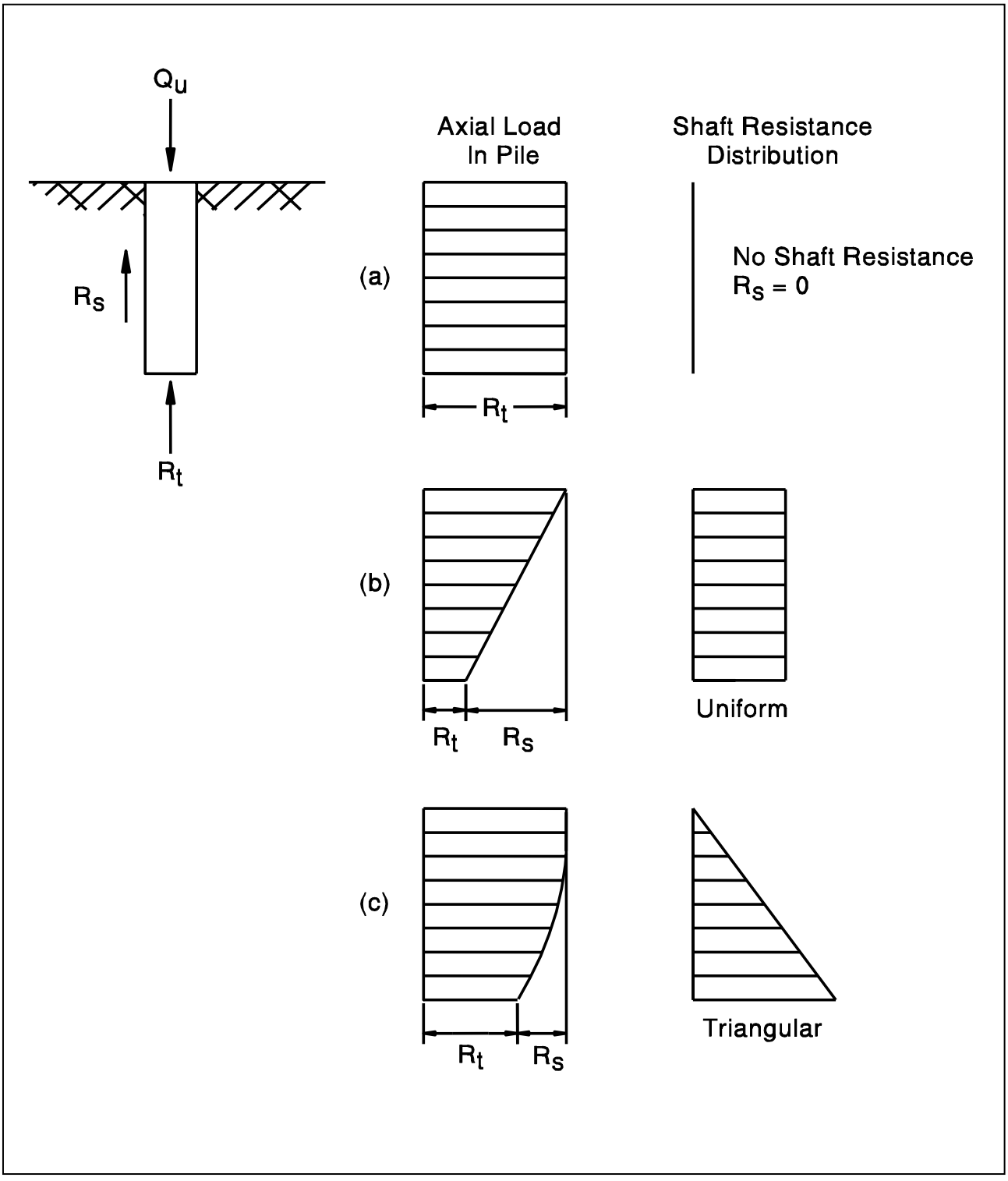

Figure 9-4. Typical load transfer profiles (FHWA, 2006a).

A large number of static analysis methods are documented in the literature with specific recommendations on the factor of safety to be used with each method. These recommended factors of safety have routinely disregarded the influence of the construction control method used to complement the static analysis computation. As part of the overall design process, it is important that the foundation designer qualitatively assess the validity of the chosen design analysis method and the reliability of the geotechnical design parameters.

While the range of static analysis factors of safety in the past was from 2 to 4, most of the static analysis methods recommended a factor of safety of 3. As foundation design loads increased over time, the use of higher factors of safety often resulted in pile installation problems. In addition, experience has shown that construction control methods have a significant influence on pile capacity. Therefore, **the factor of safety used in a static analysis calculation should be based upon the construction control method specified**. Provided that the procedures recommended in this manual are used for the subsurface exploration and analysis, the factors of safety in Table 9-5 are recommended based on the specified construction control method. The factor of safety for other test methods not included in Table 9-5 should be determined by the individual designer.

Table 9-5. Recommended factor of safety based on construction control method

Construction Control Method	Factor of Safety
Static load test with wave equation analysis	2.00
Dynamic testing with wave equation analysis	2.25
Indicator piles with wave equation analysis	2.50
Wave equation analysis	2.75
Gates dynamic formula	3.50

The pile design load should be supported by soil resistance developed only in soil layers that contribute to long term load support. The soil resistance from soils subject to scour, or from soil layers above soft compressible soils should not be considered. The following example problem will be used to clarify the use of the factor of safety in static pile capacity calculations for determination of the pile design load as well as for determination of the soil resistance to pile driving.

Consider a pile to be driven through the soil profile described in Figure 9-5. The proposed pile type penetrates through a sand layer subject to scour in the 100-year flood into an underlying very soft clay layer unsuitable for long term support and then into competent support materials. The soil resistances from the scour-susceptible sand layer and soft clay layer do not contribute to long term load support and should not be included in the soil resistance for support of the design load. In this example, static load testing with wave equation analysis will be used for construction control. Therefore, a factor of safety of 2.0 should be applied to the ultimate soil resistance calculated in suitable support layers in the static analysis. It should be noted that this approach is for scour conditions under the 100-year or overtopping flood events and that a different approach would apply for the superflood or 500-year event. For a superflood, a minimum factor of safety of 1.0 is used. This minimum factor of safety is determined by dividing the maximum pile load by the sum of the shaft and toe resistances available below scour depth.

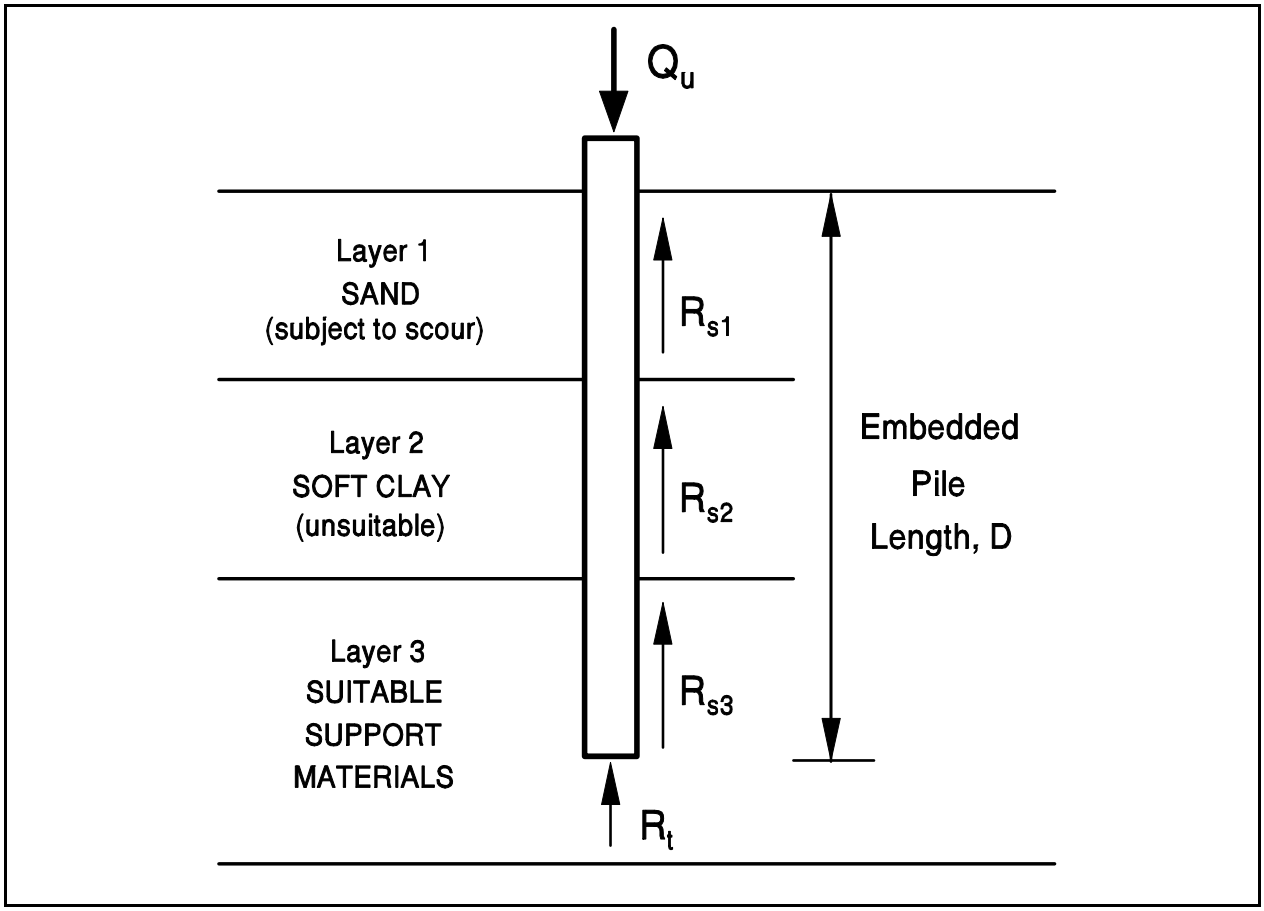

Figure 9-5. Soil profile for factor of safety discussion (FHWA, 2006a).

In the static analysis, a trial pile penetration depth is chosen and an ultimate pile capacity, Q_u, is calculated. This ultimate capacity includes the soil resistance calculated from all soil layers including the shaft resistance in the scour susceptible layer, R_{s1}, the shaft resistance in the unsuitable soft clay layer, R_{s2} as well as the resistance in suitable support materials along the pile shaft, R_{s3}, and at the pile toe resistance, R_t.

$$Q_u = R_{s1} + R_{s2} + R_{s3} + R_t$$

The design load, Q_a, is the sum of the soil resistances from the suitable support materials divided by a factor of safety, FS. As noted earlier, a factor of safety of 2.0 is used in the equation below because of the planned construction control with static load testing. Therefore,

$$Q_a = (R_{s3} + R_t) / (FS=2)$$

The design load may also be expressed as the sum of the ultimate capacity minus the calculated soil resistances from the scour susceptible and unsuitable layers divided by the factor of safety. In this alternative approach, the design load is expressed as follows:

$$Q_a = (Q_u - R_{s1} - R_{s2}) / (FS=2)$$

The result of the static analysis is then the estimated pile penetration depth, D, the design load for that penetration depth, Q_a, and the calculated ultimate capacity, Q_u.

For preparation of construction plans and specifications, the **calculated geotechnical ultimate capacity**, Q_u, is specified. Note that if the construction control method changes after the design stage, the required ultimate capacity and the required pile penetration depth for the ultimate capacity will also change. This is apparent when the previous equation for the design load is expressed in terms of the ultimate capacity as follows:

$$Q_u = R_{s1} + R_{s2} + (Q_a)(FS=2)$$

A static analysis should also be used to calculate the **soil resistance to driving**, SRD, that must be overcome to reach the estimated pile penetration depth necessary to develop the ultimate capacity. This information is necessary for the designer to select a pile section with the driveability to overcome the anticipated soil resistance and for the contractor to properly size equipment. Driveability aspects of design are discussed in Section 9.9.

In the SRD calculation, a factor of safety is not used. The soil resistance to driving is the sum of the soil resistances from the scour susceptible and unsuitable layers plus the soil resistance in the suitable support materials to the estimated penetration depth.

$$SRD = R_{s1} + R_{s2} + R_{s3} + R_t$$

Soil resistances in this calculation should be the resistance at the time of driving. Hence time dependent changes in soil strengths due to **soil setup or relaxation** should be considered (see Table 5-8 in Chapter 5 for brief explanation of these terms and Section 9.5.5 for more discussion). For the example presented in Figure 9-5, the driving resistance from the unsuitable clay layer would be reduced by the sensitivity of the clay. Therefore, R_{s2} would be R_{s2} / 2 for a clay with a sensitivity of 2. The soil resistance to driving to depth D would then be as follows

$$SRD = R_{s1} + R_{s2}/2 + R_{s3} + R_t$$

This example problem considers only the driving resistance at the final pile penetration depth. In cases where piles are driven through hard or dense layers above the estimated pile penetration depth, the soil resistance to penetrate these layers should also be calculated. Additional information on the calculation of time dependent soil strength changes is provided in Section 9.9 of this chapter.

The concepts discussed above are illustrated numerically in Example 9-1:

Example 9-1: Find the ultimate capacity and driving capacity for the pile from the data listed in the profile. The hydraulic specialist determined that the sand layer is susceptible to scour. The geotechnical specialist determined that the soft clay layer is unsuitable for providing resistance.

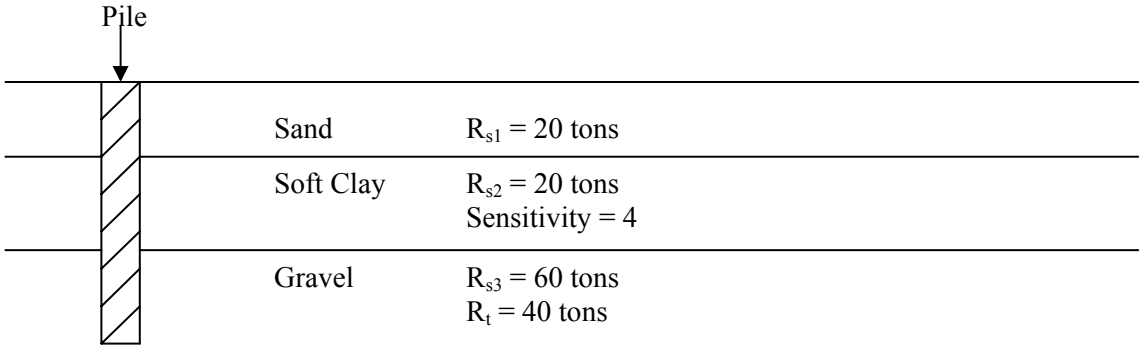

Solution:

Ultimate capacity $= R_{s3} + R_t$
$= 60 \text{ tons} + 40 \text{ tons} = 100 \text{ tons}$

Driving capacity $= R_{s1} + (R_{s2}/\text{Sensitivity}) + R_{s3} + R_t$
$$= 20\,\text{tons} + \frac{20\,\text{tons}}{4} + 60\,\text{tons} + 40\,\text{tons} = 125\ \text{tons}$$

9.5 DESIGN OF SINGLE PILES

Numerous static analysis methods are available for calculating the ultimate capacity of a single pile. The following sections of this chapter will present recommended analysis methods for piles in cohesionless, cohesive, and layered soil profiles. For additional methods based on N-values, and cone penetration test results the reader is referred to FHWA (2006a). Regardless of the method used to evaluate the static capacity of a pile, it must be understood that the factor of safety is not based on the method of analysis but on the construction control as discussed in Section 9.4. Furthermore, the pile length determined from a static analysis is just an *estimate* prior to going into the field.

9.5.1 Ultimate Geotechnical Capacity of Single Piles in Cohesionless Soils

The geotechnical ultimate capacity of a single pile in a cohesionless soil is the sum of shaft and toe resistances ($Q_u = R_s + R_t$). The calculation assumes that the shaft resistance and toe bearing resistance can be determined separately and that these two factors do not affect each other. The Nordlund method is recommended herein for computation of ultimate capacity of single piles in cohesionless soils.

9.5.1.1 Nordlund Method

The Nordlund method (1963) is based on field observations and considers pile taper and soil displacement in calculating the shaft resistance. The method also accounts for the differences in soil-pile coefficient of friction for different pile materials. The method is based on the results of several load test programs in cohesionless soils. Several pile types were used in these test programs including timber, H, closed end pipe, Monotubes and Raymond step-taper piles. These piles, which were used to develop the method's design curves, had pile widths generally in the range of 10 to 20 inches (250 to 500 mm). The Nordlund Method tends to overpredict pile

capacity for piles with widths larger than 24 inches (600 mm) and all sizes of open-ended pipe piles.

According to the Nordlund method, the geotechnical ultimate capacity, Q_u, of a pile in cohesionless soil is the sum of the shaft resistance, R_s and the toe resistance, R_t. Nordlund suggests the shaft resistance is a function of the following variables:

1. The friction angle of the soil.
2. The friction angle on the sliding surface between pile material and soil, i.e., the interface friction angle
3. The taper of the pile.
4. The effective unit weight of the soil.
5. The pile length.
6. The minimum pile perimeter.
7. The volume of soil displaced.

The Nordlund equation for computing the geotechnical ultimate capacity of a pile is as follows (see Figure 9-6 for illustration of variables):

$$Q_u = \sum_{d=0}^{d=D} K_\delta \, C_F \, p_d \, \frac{\sin(\delta + \omega)}{\cos \omega} \, C_d \, \Delta d + \alpha_t \, N'_q \, A_t \, p_t \qquad 9\text{-}4$$

where:
- d = depth.
- D = embedded length of the pile.
- K_δ = coefficient of lateral earth pressure at depth d.
- C_F = correction factor for K_δ when $\delta \neq \phi$.
- p_d = effective overburden pressure at the center of depth increment Δd.
- δ = interface friction angle between pile and soil.
- ω = angle of pile taper from vertical.
- ϕ = soil friction angle.
- C_d = pile perimeter at depth d.
- Δd = length of pile segment.
- α_t = dimensionless factor dependent on pile depth-width relationship.
- N'_q = bearing capacity factor.
- A_t = pile toe area.
- p_t = effective overburden pressure at the pile toe.

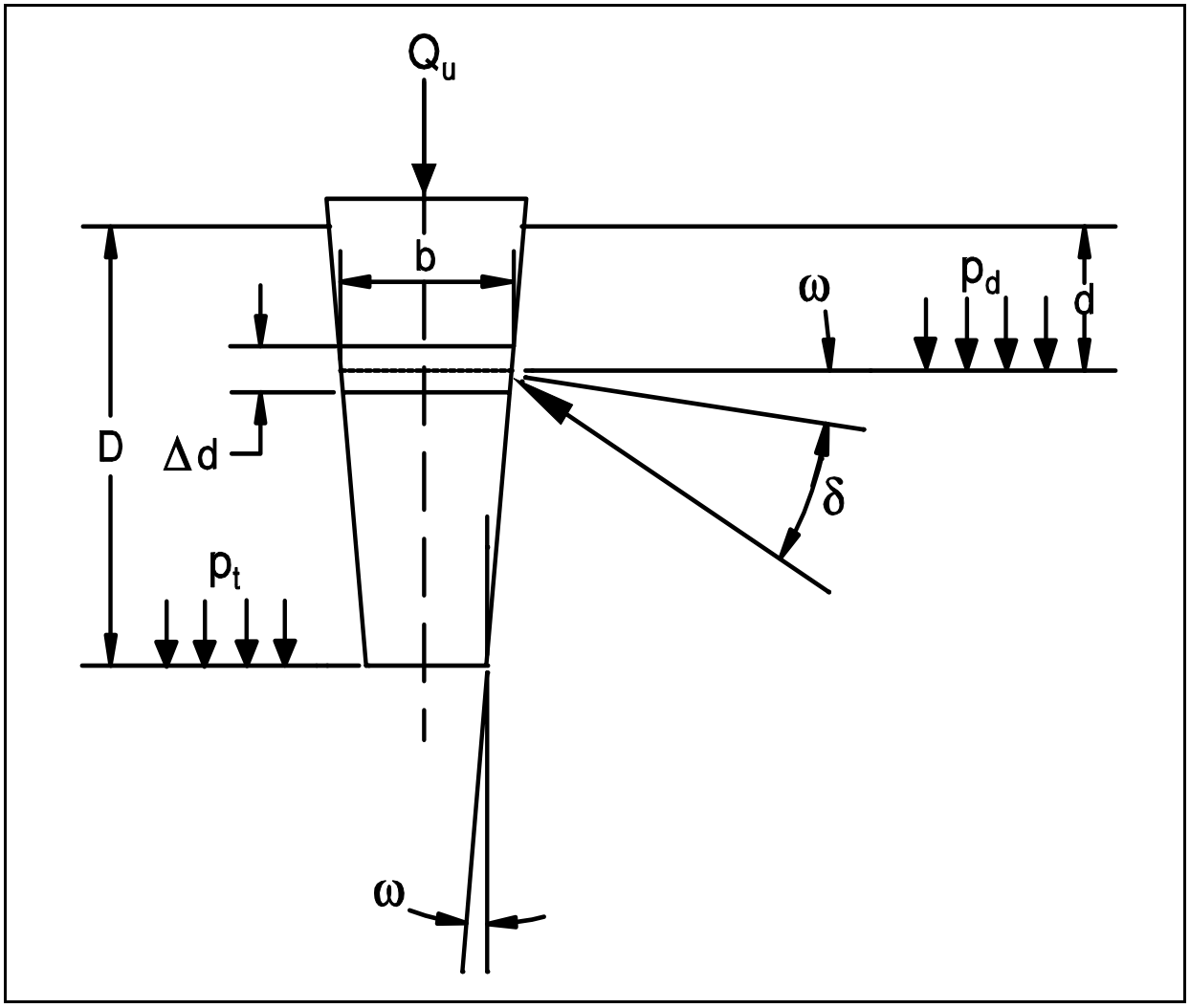

Figure 9-6. Nordlund's general equation for ultimate pile capacity (after Nordlund, 1979).

For a pile of uniform cross section (ω=0) and embedded length D, driven in soil layers of the same effective unit weight and friction angle, the Nordlund equation becomes:

$$Q_u = K_\delta C_F p_d \sin\delta C_d D + \alpha_t N'_q A_t p_t \qquad 9\text{-}5$$

The soil friction angle ϕ influences most of the calculations in the Nordlund method. In the absence of laboratory test data, ϕ can be estimated from corrected SPT N1 values. Therefore, Equation 3-3 in Chapter 3 should be used for correcting field N values. The corrected SPT $N1_{60}$ values may then be used in Table 8-1 of Chapter 8 to estimate the soil friction angle, ϕ.

Nordlund (1979) updated the method but did not place a limiting value on the shaft resistance. However, Nordlund recommended that the effective overburden pressure at the pile toe, p_t, used for computing the pile toe resistance be limited to 3 ksf (150 kPa).

STEP BY STEP PROCEDURE FOR USING NORDLUND METHOD

Steps 1 through 6 are for computing the shaft resistance and steps 7 through 9 are for computing the pile toe resistance.

STEP 1 Delineate the soil profile into layers and determine the ϕ angle for each layer.

a. Construct p_o diagram using procedure described in Chapter 2.

b. Using Figure 3-24, correct SPT field N values for overburden pressure and obtain corrected SPT $N1_{60}$ values. Delineate soil profile into layers based on corrected SPT $N1_{60}$ values.

c. Determine ϕ angle for each layer from laboratory or in-situ test data.

d. In the absence of laboratory or in-situ test data, determine the average corrected SPT $N1_{60}$ value, $\bar{N}1$, for each soil layer and estimate ϕ angle from Table 8-1 in Chapter 8.

STEP 2 Determine δ, the interface friction angle between the pile and soil based on displaced soil volume, V, and the soil friction angle, ϕ.

a. Compute volume of soil displaced per unit length of pile, V.

b. Enter Figure 9-7 with V and determine δ/ϕ ratio for pile type under consideration. Note that δ/ϕ may be greater than 1.0 for taper piles to account for the development of passive resistance along the length of the pile due to pile taper.

c. Calculate δ from δ/ϕ ratio.

STEP 3 Determine the coefficient of lateral earth pressure, K_δ, for each ϕ angle.

a. Determine K_δ for ϕ angle based on displaced volume, V, and pile taper angle, ω, by using either Figure 9-8, 9-9, 9-10, or 9-11 and the appropriate procedure described in Step 3b, 3c, 3d, or 3e.

b. If the displaced volume is 0.1, 1.0 or 10.0 ft^3/ft, which corresponds to one of the curves provided in Figures 9-8 through 9-11, and the ϕ angle is one of those provided, K_δ can be determined directly from the appropriate figure.

c. If the displaced volume is 0.1, 1.0 or 10.0 ft^3/ft, which corresponds to one of the curves provided in Figures 9-8 through 9-11, but the ϕ angle is other than those provided, use linear interpolation to determine K_δ for the required ϕ angle. Tables 9-6a and 9-6b also provide interpolated K_δ values at selected displaced volumes versus ϕ angle for uniform piles ($\omega = 0$).

d. If the displaced volume is other than 0.1, 1.0 or 10.0 ft^3/ft, which corresponds to one of the curves provided in Figures 9-8 through 9-11, and the ϕ angle corresponds to one of those provided, use log linear interpolation to determine K_δ for the required displaced volume. Tables 9-6a and 9-6b also provide interpolated K_δ values at selected displaced volumes versus ϕ angle for uniform piles ($\omega = 0$).

e. If the displaced volume is other than 0.1, 1.0 or 10.0 ft^3/ft, which correspond to one of the curves provided in Figures 9-8 through 9-11, and the ϕ angle is other than one of those provided, first use linear interpolation to determine K_δ for the required ϕ angle at the displaced volume curves provided for 0.1, 1.0 or 10.0 ft^3/ft. Then use log linear interpolation to determine K_δ for the required displaced volume. Tables 9-6a and 9-6b also provide interpolated K_δ values at selected displaced volumes versus ϕ angle for uniform piles ($\omega = 0$).

STEP 4 Determine the correction factor, C_F, to be applied to K_δ if $\delta \neq \phi$.

Use Figure 9-12 to determine the correction factor for each K_δ. Enter figure with ϕ angle and δ/ϕ value to determine C_F.

STEP 5 Compute the average effective overburden pressure at the midpoint of each soil layer, p_d (ksf).

Note: A limiting value is not applied to p_d.

STEP 6 Compute the shaft resistance in each soil layer. Sum the shaft resistance from each soil layer to obtain the ultimate shaft resistance, R_s (kips). For a pile of uniform cross-section embedded in a uniform soil profile

$$R_s = K_\delta C_F p_d \sin\delta C_d D \qquad 9\text{-}6$$

For H-piles in cohesionless soils, the "box" area should generally be used for shaft resistance calculations, i.e., the pile perimeter C_d should be considered as two times flange width plus two times the section height. Additional discussion on the behavior of open pile sections is presented in Section 9.5.4.

STEP 7 Determine the α_t coefficient and the bearing capacity factor, N'_q, from the ϕ angle near the pile toe.

a. Enter Figure 9-13(a) with ϕ angle near pile toe to determine α_t coefficient based on pile length to diameter ratio.

b. Enter Figure 9-13(b) with ϕ angle near pile toe to determine, N'_q.

c. If ϕ angle is estimated from SPT data, compute the average corrected SPT $N1_{60}$ value over the zone from the pile toe to 3 diameters below the pile toe.

STEP 8 Compute the effective overburden pressure at the pile toe, p_t (ksf).

Note: The limiting value of p_t is 3 ksf (150 kPa).

STEP 9 a. Compute the ultimate toe resistance, R_t (kips).

$$R_t = \alpha_t N'_q A_t p_t \qquad 9\text{-}7a$$

b. Compute the maximum ultimate toe resistance, R_t (max)

$$R_t \text{ (max)} = q_L A_t \qquad 9\text{-}7b$$

q_L value is obtained as follows:

1. Enter Figure 9-14 with ϕ angle near pile toe determined from laboratory or in-situ test data.

2. Enter Figure 9-14 with ϕ angle near the pile toe estimated from Table 8-1 in Chapter 8 and the average corrected SPT N1 near toe as described in Step 7.

c. Use lesser of the two R_t values obtained from Equations 9-7a and 9-7b.

For steel H and unfilled open end pipe piles, use only steel cross section area at pile toe unless there is reasonable assurance and previous experience that a soil plug will form at the pile toe. The assumption of a soil plug would allow the use of a box area at H pile toe and total pipe cross section area for open end pipe pile. Additional discussion on the behavior of open pile sections is presented in Section 9.5.4.

STEP 10 Compute the ultimate geotechnical pile capacity, Q_u (kips).

$$Q_u = R_s + R_t$$

STEP 11 Compute the allowable geotechnical soil resistance, Q_a (kips).

$$Q_a = \frac{Q_u}{\text{Factor of Safety}}$$

The factor of safety used in the calculation should be based upon the construction control method to be specified. Recommended factors of safety based on construction control method are listed in Table 9-5.

The concepts discussed above are illustrated numerically in Example 9-2.

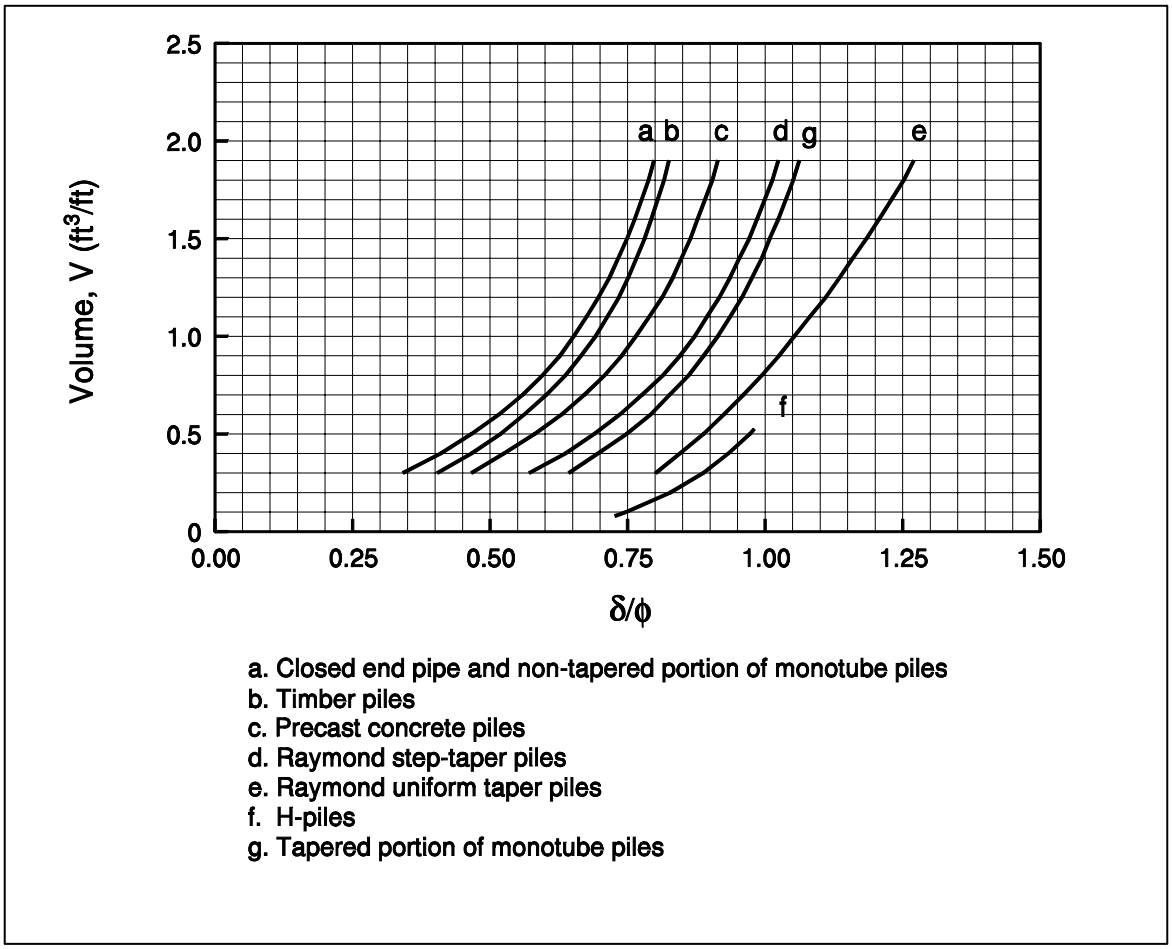

Figure 9-7. Relationship of δ/ϕ and pile soil displacement, V, for various types of piles (after Nordlund, 1963).

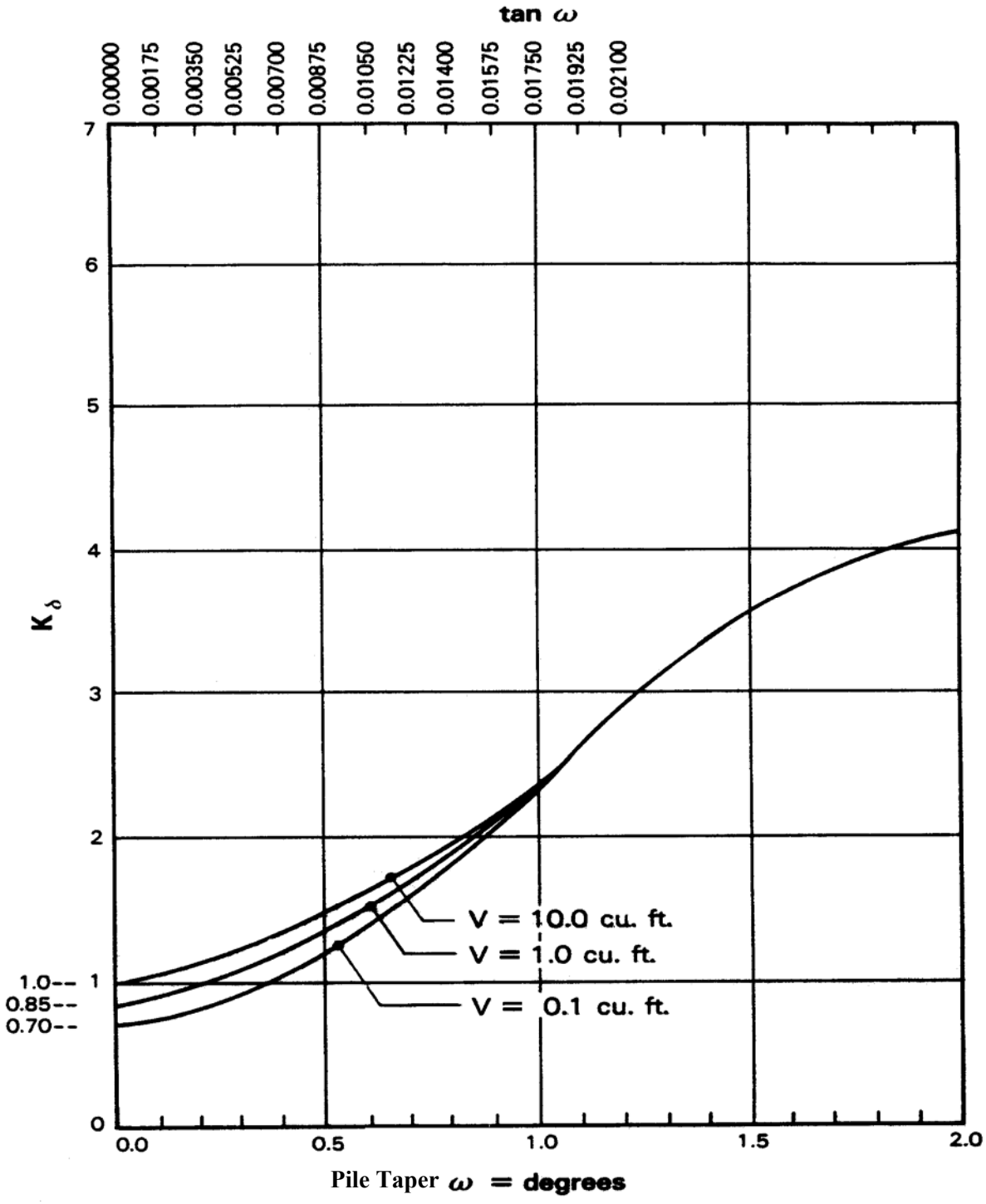

Figure 9-8. Design curves for evaluating K_δ for piles when $\phi = 25°$ (after Nordlund, 1963).

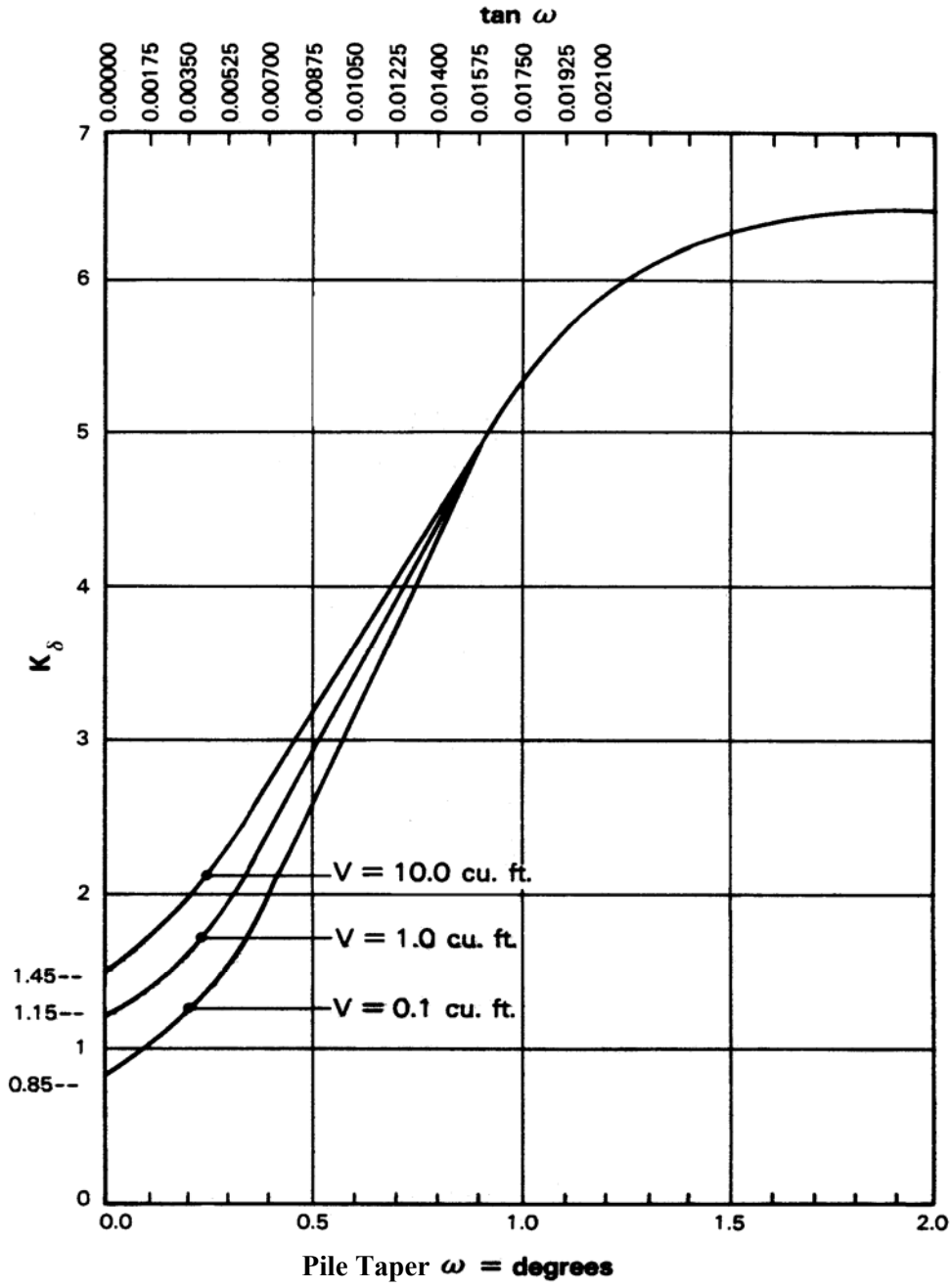

Figure 9-9. Design curves for evaluating K_δ for piles when $\phi = 30°$ (after Nordlund, 1963).

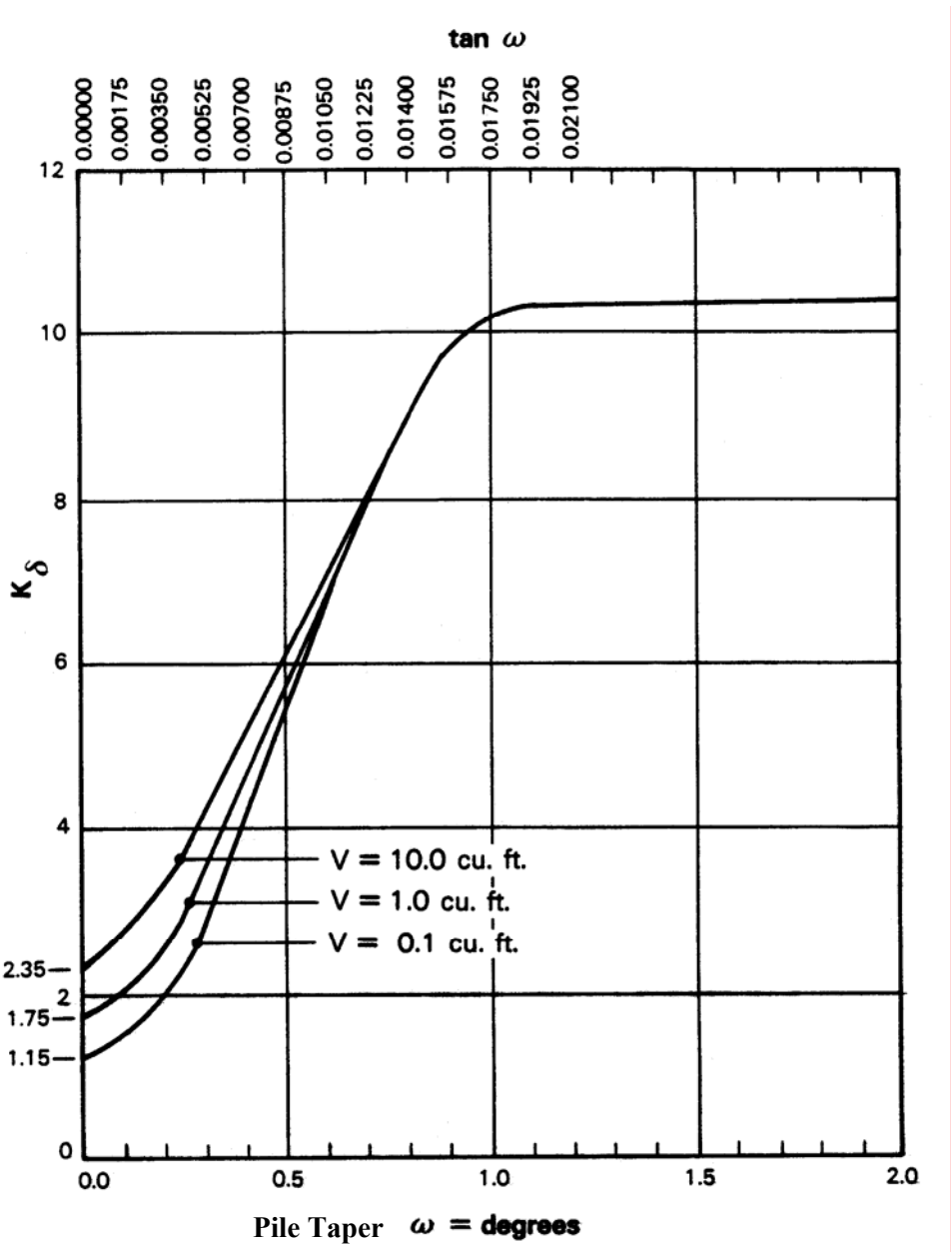

Figure 9-10. Design curves for evaluating K_δ for piles when $\phi = 35°$ (after Nordlund, 1963).

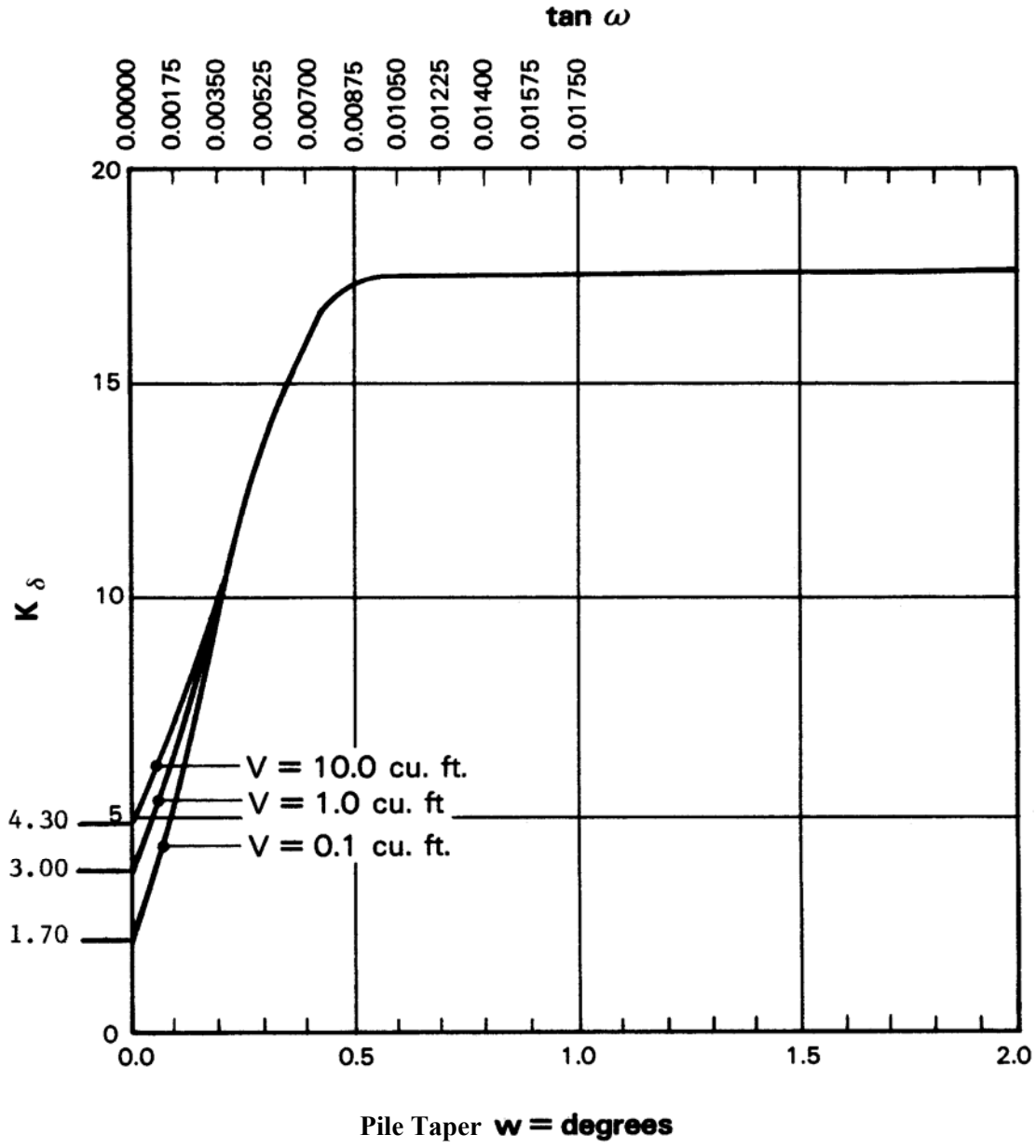

Figure 9-11. Design curves for evaluating K_δ for piles when $\phi = 40°$ (after Nordlund, 1963).

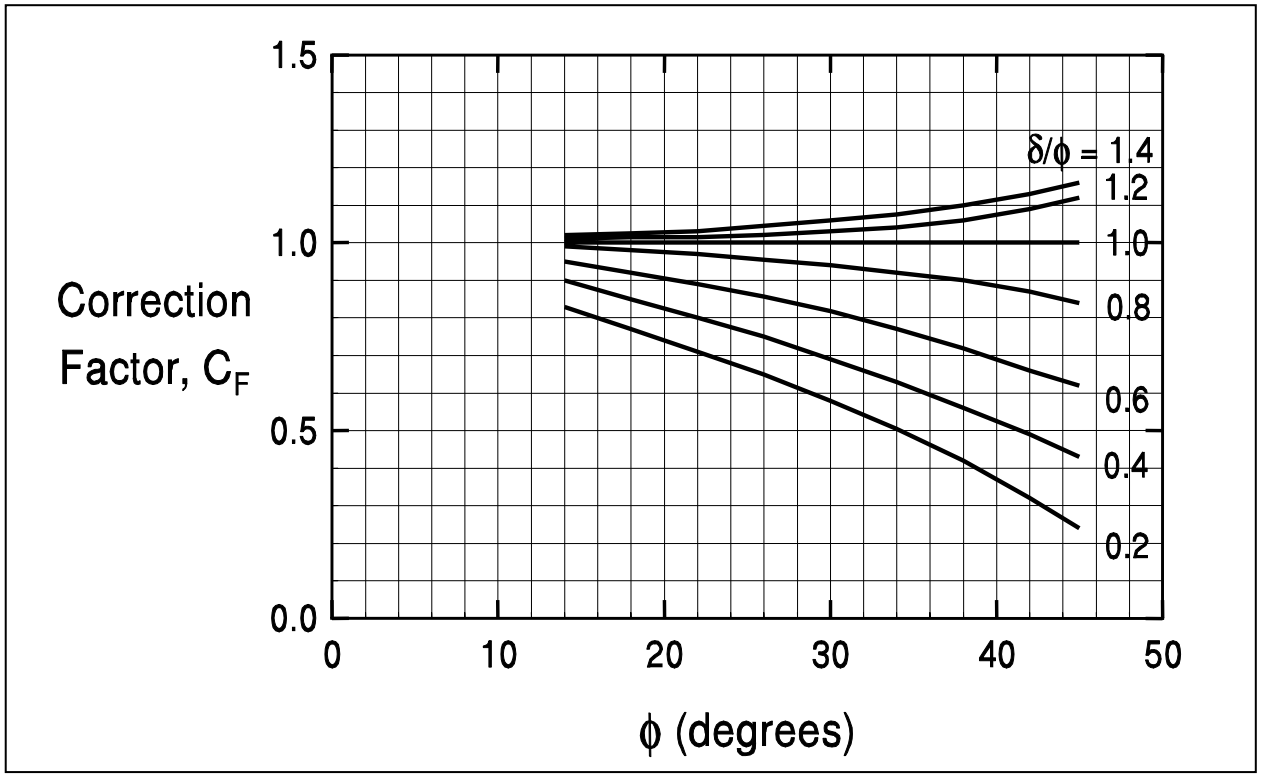

Figure 9-12. Correction factor, C_F for K_δ when $\delta \neq \phi$ (after Nordlund, 1963).

Table 9-6(a)

Design table for evaluating K_δ for piles when $\omega = 0°$ and V = 0.10 to 1.00 ft^3/ft (FHWA, 2006a)

ϕ	Displaced Volume –V (ft^3/ft)									
	0.10	0.20	0.30	0.40	0.50	0.60	0.70	0.80	0.90	1.00
25	0.70	0.75	0.77	0.79	0.80	0.82	0.83	0.84	0.84	0.85
26	0.73	0.78	0.82	0.84	0.86	0.87	0.88	0.89	0.90	0.91
27	0.76	0.82	0.86	0.89	0.91	0.92	0.94	0.95	0.96	0.97
28	0.79	0.86	0.90	0.93	0.96	0.98	0.99	1.01	1.02	1.03
29	0.82	0.90	0.95	0.98	1.01	1.03	1.05	1.06	1.08	1.09
30	0.85	0.94	0.99	1.03	1.06	1.08	1.10	1.12	1.14	1.15
31	0.91	1.02	1.08	1.13	1.16	1.19	1.21	1.24	1.25	1.27
32	0.97	1.10	1.17	1.22	1.26	1.30	1.32	1.35	1.37	1.39
33	1.03	1.17	1.26	1.32	1.37	1.40	1.44	1.46	1.49	1.51
34	1.09	1.25	1.35	1.42	1.47	1.51	1.55	1.58	1.61	1.63
35	1.15	1.33	1.44	1.51	1.57	1.62	1.66	1.69	1.72	1.75
36	1.26	1.48	1.61	1.71	1.78	1.84	1.89	1.93	1.97	2.00
37	1.37	1.63	1.79	1.90	1.99	2.05	2.11	2.16	2.21	2.25
38	1.48	1.79	1.97	2.09	2.19	2.27	2.34	2.40	2.45	2.50
39	1.59	1.94	2.14	2.29	2.40	2.49	2.57	2.64	2.70	2.75
40	1.70	2.09	2.32	2.48	2.61	2.71	2.80	2.87	2.94	3.0

Table 9-6(b)

Design table for evaluating K_{δ} for piles when $\omega = 0°$ and V = 1.0 to 10.0 ft^3/ft (FHWA, 2006a)

ϕ	Displaced Volume –V (ft^3/ft)									
	1.0	2.0	.3.0	4.0	5.0	6.0	7.0	8.0	9.0	10.0
25	0.85	0.90	0.92	0.94	0.95	0.97	0.98	0.99	0.99	1.00
26	0.91	0.96	1.00	1.02	1.04	1.05	1.06	1.07	1.08	1.09
27	0.97	1.03	1.07	1.10	1.12	1.13	1.15	1.16	1.17	1.18
28	1.03	1.10	1.14	1.17	1.20	1.22	1.23	1.25	1.26	1.27
29	1.09	1.17	1.22	1.25	1.28	1.30	1.32	1.33	1.35	1.36
30	1.15	1.24	1.29	1.33	1.36	1.38	1.40	1.42	1.44	1.45
31	1.27	1.38	1.44	1.49	1.52	1.55	1.57	1.60	1.61	1.63
32	1.39	1.52	1.59	1.64	1.68	1.72	1.74	1.77	1.79	1.81
33	1.51	1.65	1.74	1.80	1.85	1.88	1.92	1.94	1.97	1.99
34	1.63	1.79	1.89	1.96	2.01	2.05	2.09	2.12	2.15	2.17
35	1.75	1.93	2.04	2.11	2.17	2.22	2.26	2.29	2.32	2.35
36	2.00	2.22	2.35	2.45	2.52	2.58	2.63	2.67	2.71	2.74
37	2.25	2.51	2.67	2.78	2.87	2.93	2.99	3.04	3.09	3.13
38	2.50	2.81	2.99	3.11	3.21	3.29	3.36	3.42	3.47	3.52
39	2.75	3.10	3.30	3.45	3.56	3.65	3.73	3.80	3.86	3.91
40	3.00	3.39	3.62	3.78	3.91	4.01	4.10	4.17	4.24	4.30

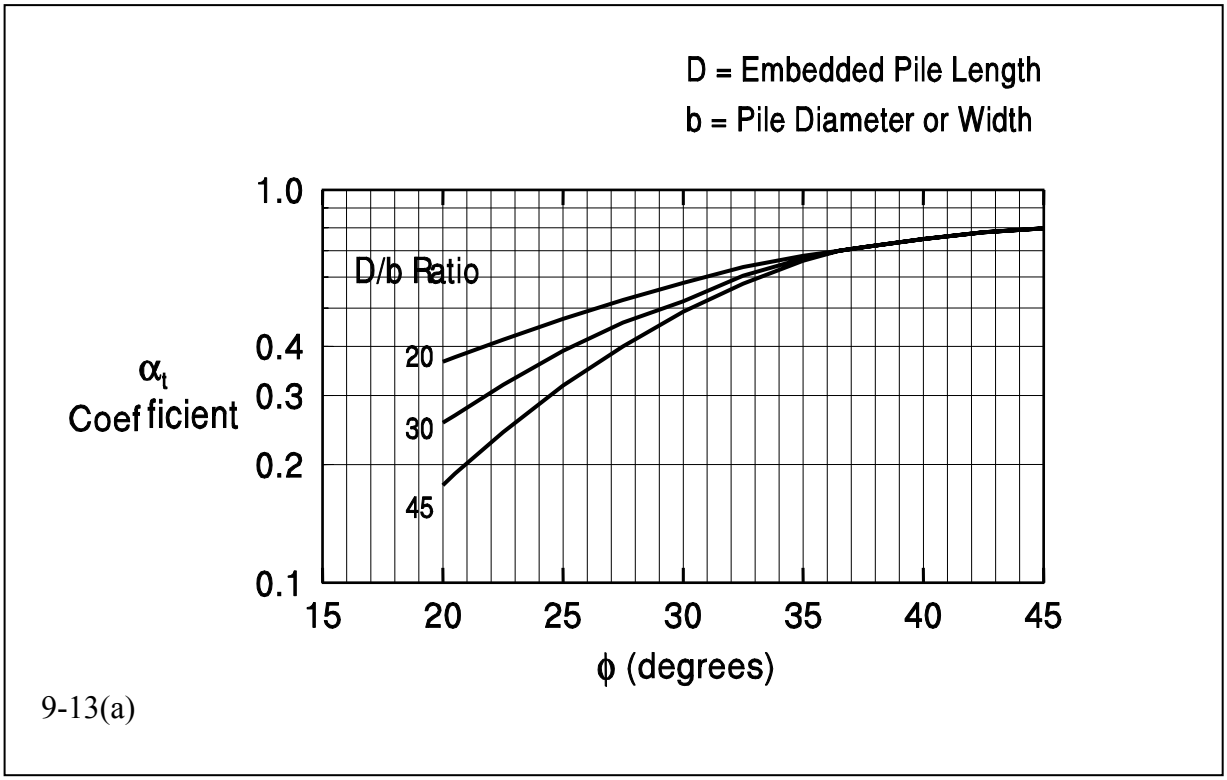

9-13(a)

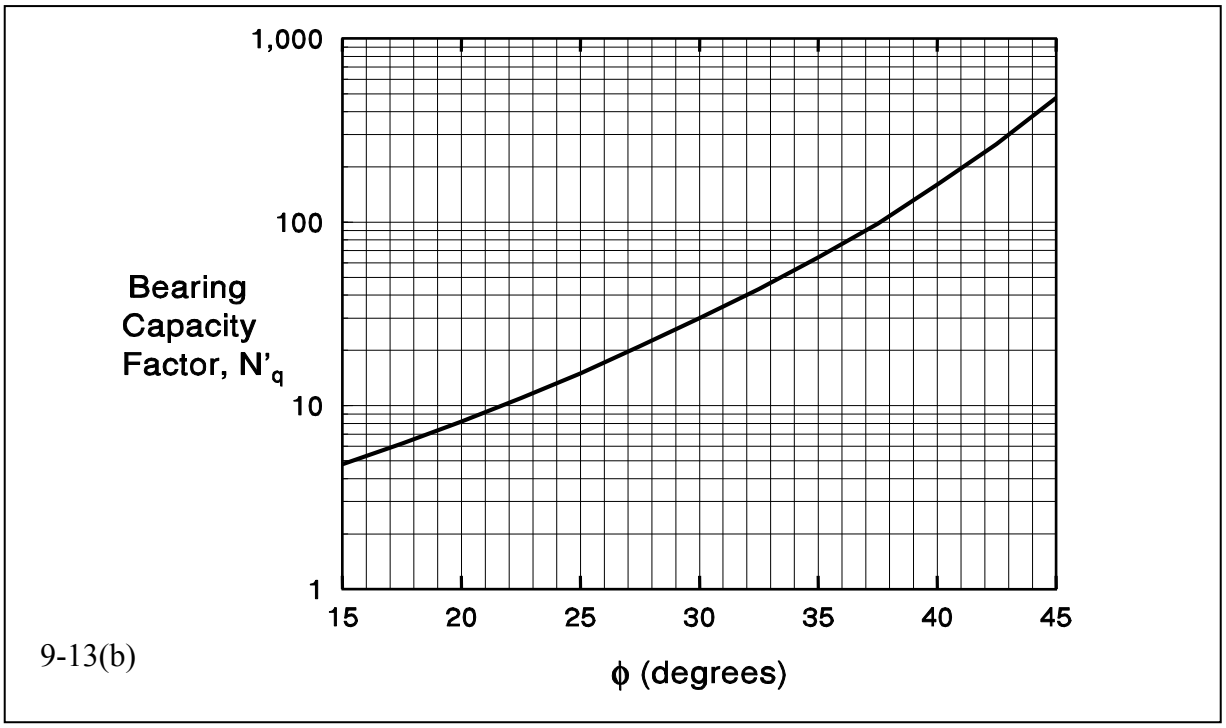

9-13(b)

Figure 9-13. Chart for estimating α_t coefficient and bearing capacity factor N'_q (FHWA, 2006a).

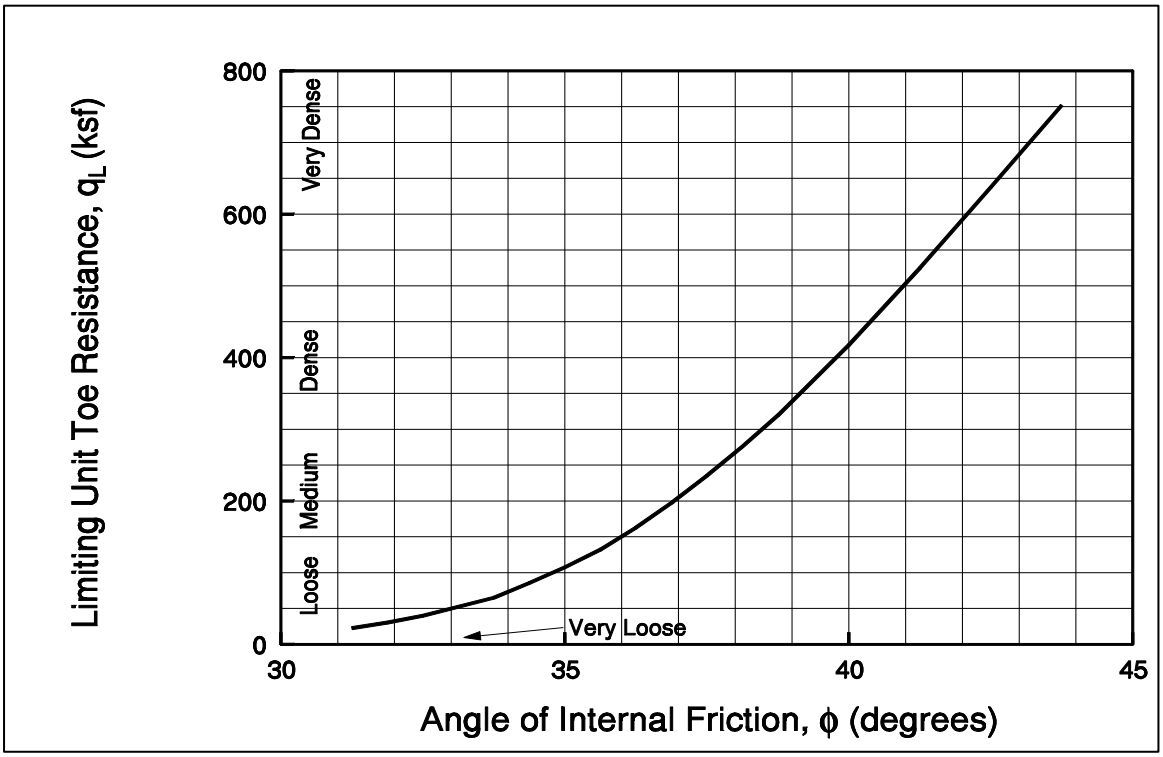

Figure 9-14. Relationship between maximum unit pile toe resistance and friction angle for cohesionless soils (after Meyerhof, 1976).

Example 9-2: Determine the ultimate geotechnical pile capacity, Q_u, for the 1 sq ft precast concrete pile

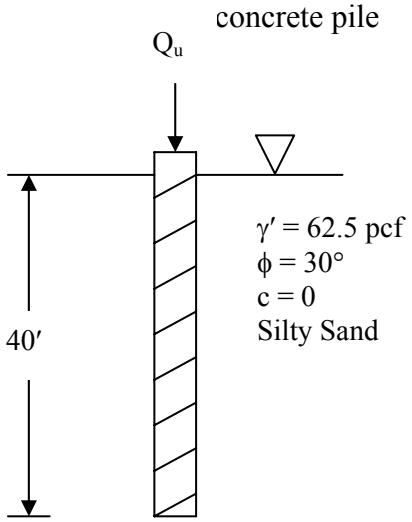

Since $\omega = 0$, use Equation 9-5

$Q_u = K_\delta C_F p_d \sin\delta C_d D + A_t \alpha_t p_t N'_q$

where the following terms are known from the problem

$A_t = 1$ sq.ft
$p_t = 40\ \gamma' = 2{,}500$ psf
$p_d = 20\ \gamma' = 1{,}250$ psf
$\omega = 0°$, $D = 40$ ft, $C_d = 4$ ft

Solution:

Find Shaft Resistance, R_S:

Use Figures 9-7, 9-9, and 9-12 with $\phi = 30°$

From Figure 9-7 – For V = 1 ft^3/ft, and curve "c" for precast concrete piles;

$\frac{\delta}{\phi} = 0.76$, Since $\phi = 30°$, $\delta = 22.8°$

From Figure 9-9 – For $\omega = 0$, V = 1 ft^3/ft; $K_\delta = 1.15$

From Figure 9-12 – For $\frac{\delta}{\phi} = 0.76$; $C_F = 0.9$

$R_s = K_\delta C_F p_d \sin\delta C_d D$ Equation 9-6

$R_s = (1.15)(0.9)(1{,}250\text{ psf})(\sin 22.8°)(4\text{ ft})(40\text{ ft}) = 80{,}216$ lbs

$R_s = 40.1$ tons

Find Toe Resistance, R_t:

Use Figure 9-13(b) to find N'_q and α_t for $\phi = 30°$

$N'_q = 30$; $\alpha_t = 0.5$ (for $\frac{D}{B} = 40$)

$R_t = A_t \alpha_t p_t N'_q = (1\text{ ft}^2)(0.5)(2{,}500\text{ psf})\ 30 = 37{,}500$ lbs $= 18.75$ tons Equation 9-7a

Check limiting point resistance from Figure 9-14, $q_L \approx 10$ ksf ≈ 5 tsf

$R_t = q_L A_t = (5\text{ tsf})(1\text{ ft}^2) = 5$ tons $\therefore R_t = 5$ tons Equation 9-7b

Compute Ultimate Capacity, Q_u:

$Q_u = R_s + R_t = 40.1 + 5 = 45.1$ tons

9.5.2 Ultimate Geotechnical Capacity of Single Piles in Cohesive Soils

The ultimate geotechnical capacity of a pile in cohesive soil may also be expressed as the sum of the shaft and toe resistances or $Q_u = R_s + R_t$. The shaft and toe resistances can be calculated from static analysis methods using soil boring and laboratory test data in either total stress or effective stress methods. The α-method is a total stress method that uses undrained soil shear strength parameters for calculating static pile capacity in cohesive soil. The α-method will be presented in Section 9.5.2.1. The effective stress method, or β-method, uses drained soil strength parameters for capacity calculations. Since the effective stress method may be used for calculating static pile capacity in cohesive as well as cohesionless soils, this method will be presented in Section 9.5.2.2. Alternatively, in-situ CPT test results can also be used to calculate pile capacity in cohesive soils from cone sleeve friction and cone tip resistance values. CPT-based methods as well as other methods are discussed in FHWA (2006a).

The shaft resistance of piles driven into cohesive soils is frequently as much as 80 to 90% of the total capacity. Therefore, it is important that the shaft resistance of piles in cohesive soils be estimated as accurately as possible.

9.5.2.1 Total Stress – α-method

For piles in clay, a total stress analysis is often used where ultimate capacity is calculated from the undrained shear strength of the soil. This approach assumes that the shaft resistance is independent of the effective overburden pressure and that the unit shaft resistance can be expressed in terms of an empirical adhesion factor times the undrained shear strength.

Shaft Resistance

The unit shaft resistance, f_s, is equal to the adhesion, c_a, which is the shear stress between the pile and soil at failure. This may be expressed in equation form as:

$$f_s = c_a = \alpha\, c_u \qquad 9\text{-}8$$

in which α is an empirical factor applied to the average undrained shear strength, c_u, of undisturbed clay along the embedded length of the pile. The coefficient α depends on the nature and strength of the clay, magnitude of load, pile dimension, method of pile installation, and time effects. The values of α vary within wide limits and decrease rapidly with increasing shear strength.

The adhesion factor, α, is a function of the soil stratigraphy and pile embedment. Three common cases are as follows:

- Case 1: Piles driven into stiff clays through overlying sands or sandy gravels
- Case 2: Piles driven into stiff clays through overlying soft clays
- Case 3: Piles driven into stiff clays without overlying different strata

Figure 9-15 presents the adhesion factor, α, versus the undrained shear strength of the soil as a function of unique soil stratigraphy and pile embedment for Case 1 and Case 2. The adhesion factor from these soil stratigraphy cases should be used only for determining the adhesion in a stiff clay layer in that specific condition as follows:

- **Case 1**: The top graph in Figure 9-15 may be used to select the adhesion factor when piles are driven through a sand or sandy gravel layer and into an underlying stiff clay stratum. This case results in the highest adhesion factors as granular material is dragged into the underlying clays. The greater the pile penetration into the clay stratum, the less influence the overlying granular stratum has on the adhesion factor. Therefore, for the same undrained shear strength, the adhesion factor decreases with increased pile penetration into the clay stratum.

- **Case 2**: The bottom graph in Figure 9-15 should be used to select the adhesion factor when piles are driven through a soft clay layer overlying a stiff clay layer. In this case, the soft clay is dragged into the underlying stiff clay stratum thereby reducing the adhesion factor of the underlying stiff clay soils. The greater the pile penetration into the underlying stiff clay soils, the less the influence the overlying soft clays have on the stiff clay adhesion factor. Therefore, the stiff clay adhesion factor increases with increasing pile penetration into the stiff clay soils.

Figure 9-16 presents the adhesion factor, α, versus the undrained shear strength of the soil for piles driven in stiff clays without any different overlying strata, i.e., Case 3. In stiff clays, a gap often forms between the pile and the soil along the upper portion of the pile shaft. In this case, the shallower the pile penetration into a stiff clay stratum the greater the effect the gap has on the shaft resistance that develops. Hence, the adhesion factor for a given shear strength is reduced at shallow pile penetration depths and increased at deeper pile penetration depths.

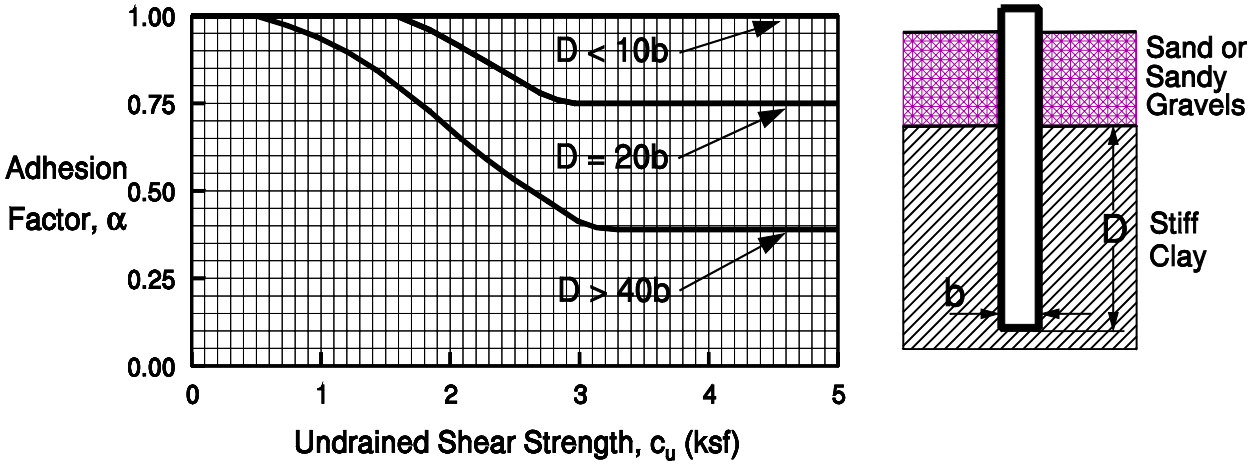

(a)

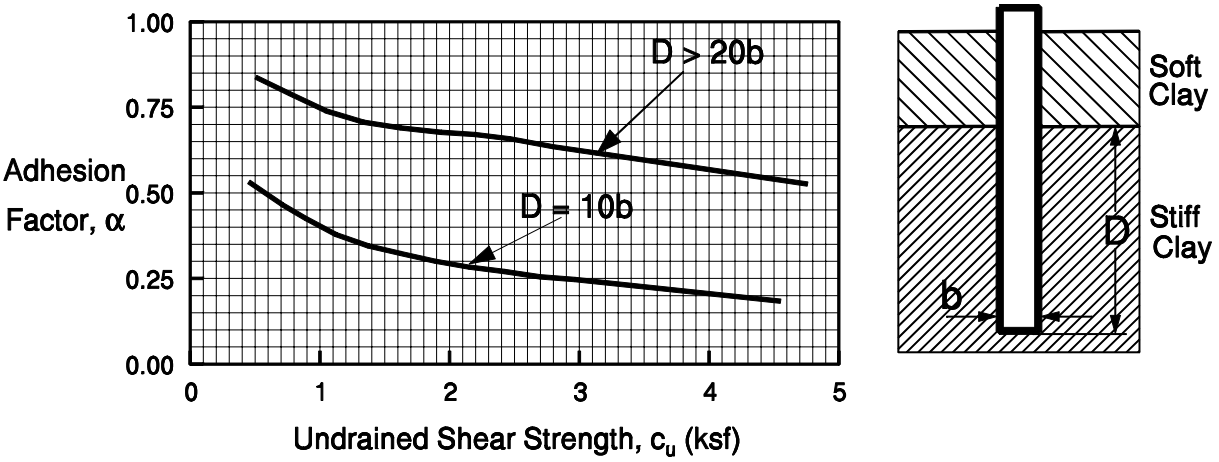

(b)

Figure 9-15. Adhesion values for driven piles in mixed soil profiles, (a) Case 1: piles driven through overlying sands or sandy gravels, and (b) Case 2: piles driven through overlying weak clay (Tomlinson, 1980).

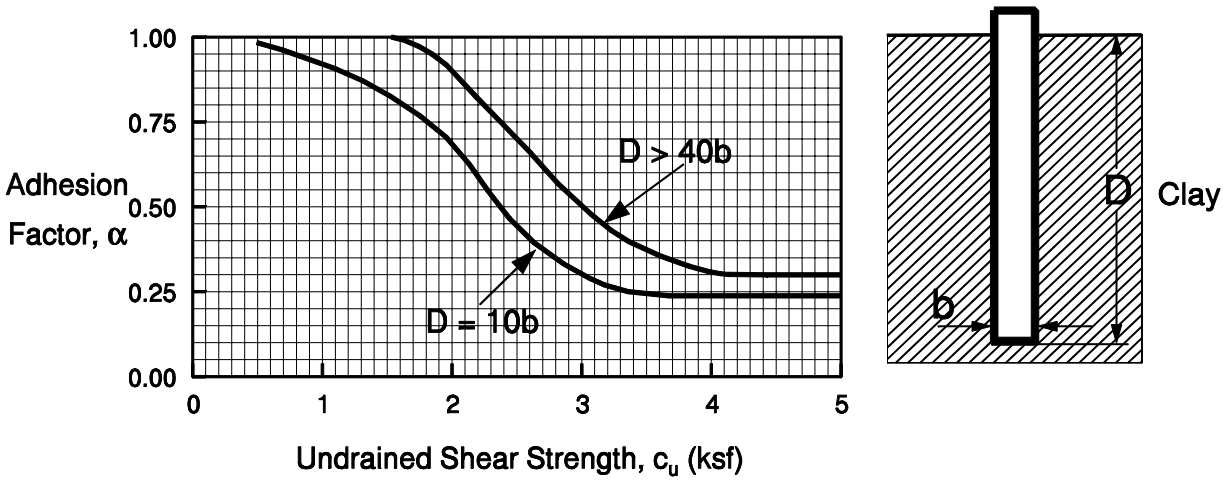

Figure 9-16. Adhesion values for driven piles in stiff clays without different overlying strata (Case 3) (Tomlinson, 1980).

The following should be considered by the designer while using Figures 9-15 and 9-16:

- For a soil profile consisting of clay layers of significantly different consistencies such as soft clays over stiff clays, adhesion factors should be determined for each individual clay layer.

- In clays with large shrink-swell potential, static capacity calculations should ignore the shaft resistance from the adhesion in the shrink-swell zone. During dry times, shrinkage will create a gap between the clay and the pile in this zone, therefore the shaft resistance should not be relied upon for long term support.

- In cases where either Figures 9-15b or 9-16 could be used, the inexperienced user should select and use the smaller value obtained from either figure. All users should confirm the applicability of a selected design chart in a given soil condition with local correlations between static capacity calculations and static load tests results.

- In the case of H piles in cohesive soils, the shaft resistance should not be calculated from the surface area of the pile, but rather from the sub-divided perimeter area of the four sides. The shaft resistance for H-piles in cohesive soils consists of the sum of the adhesion, c_a, times the flange surface area along the exterior of the two flanges, plus the undrained shear strength of the soil, c_u, times the section height surface area of the two remaining sides. This computation can be approximated by determining the adhesion and multiplying the

adhesion by the H-pile "box perimeter" area. Further discussion on this topic is included in Section 9.5.4.

Toe Resistance

The unit toe resistance in a total stress analysis for homogeneous cohesive soil is as follows:

$$q_t = c_u N_c \qquad 9\text{-}9$$

The term N_c is a dimensionless bearing capacity factor that depends on the pile diameter and the depth of embedment and c_u is the undrained shear strength of the material at and below the toe of the pile. The bearing capacity factor, N_c, is usually taken as 9 for deep foundations.

It should be remembered that the movement required to mobilize the toe resistance is several times greater than that required to mobilize the shaft resistance. At the movement required to fully mobilize the toe resistance, the shaft resistance may have decreased to a residual value. Therefore, the contribution of the toe resistance to the ultimate pile capacity in cohesive soils is sometimes ignored except in hard cohesive deposits such as glacial tills.

STEP BY STEP PROCEDURE FOR - "α-METHOD"

STEP 1 Delineate the soil profile into layers and determine the adhesion, c_a, from Figure 9-15 and 9-16 as appropriate. for each layer.

Enter the appropriate figure with the undrained shear strength of the soil, c_u, and determine adhesion or adhesion factor based on the ratio of the embedded pile length in clay, D, and the pile diameter, b. Use the D/b curve for the appropriate soil and embedment condition.

STEP 2 For each soil layer, compute the unit shaft resistance, f_s in ksf (kPa).

$$f_s = c_a = \alpha\, c_u$$

where: c_a = adhesion and α = adhesion factor.

STEP 3 Compute the shaft resistance in each soil layer and the ultimate shaft resistance, R_s, in kips (kN), from the sum of the shaft resistance from each layer.

$$R_s = f_s A_s \qquad 9\text{-}10$$

where: A_s = pile-soil surface area in ft^2 (m^2) = (pile perimeter) x (length).

STEP 4 Compute the unit toe resistance, q_t in ksf (kPa).

$$q_t = 9\, c_u$$

where: c_u = undrained shear strength of soil at the pile toe in ksf (kPa)

STEP 5 Compute the ultimate toe resistance, R_t in kips (kN).

$$R_t = q_t A_t \qquad 9\text{-}11$$

where: A_t = Area of pile toe in ft^2 (m^2).

STEP 6 Compute the ultimate geotechnical pile capacity, Q_u in kips (kN).

$$Q_u = R_s + R_t$$

STEP 7 Compute the allowable geotechnical soil resistance, Q_a in kips (kN).

$$Q_a = \frac{Q_u}{\text{Factor of Safety}}$$

The factor of safety in this static calculation should be based on the specified construction control method as described in Section 9.4 of this chapter. Factors of safety for various construction control methods are listed in Table 9-5.

9.5.2.2 Effective Stress – β-method

Static capacity calculations in cohesionless, cohesive, and layered soils can also be performed by using an effective stress based method. Effective stress based methods were developed to model the long term drained shear strength conditions. Therefore, the effective soil friction angle, ϕ', should be used in parameter selection.

In an effective stress analysis, the unit shaft resistance is calculated from the following expression:

$$f_s = \beta \, p_o \qquad 9\text{-}12$$

where: β = Bjerrum-Burland beta coefficient = $K_s \tan \delta$.
p_o = average effective overburden pressure along the pile shaft, in ksf (kPa).
K_s = earth pressure coefficient.
δ = interface friction angle between pile and soil.

The unit toe resistance is calculated from:

$$q_t = N_t \; p_t \qquad 9\text{-}13$$

where: N_t = toe bearing capacity coefficient.
p_t = effective overburden pressure at the pile toe in ksf (kPa).

Recommended ranges of β and N_t coefficients as a function of soil type and ϕ' angle from Fellenius (1991) are presented in Table 9-7. Fellenius (1991) notes that factors affecting the β and N_t coefficients consist of the soil composition including the grain size distribution, angularity and mineralogical origin of the soil grains, the original soil density and density due to the pile installation technique, the soil strength, as well as other factors. Even so, β coefficients are generally within the ranges provided and seldom exceed 1.0.

Table 9-7
Approximate range of β and N_t coefficients (Fellenius, 1991)

Soil Type	ϕ'	β	N_t
Clay	25 – 30	0.23 - 0.40	3 - 30
Silt	28 – 34	0.27 - 0.50	20 - 40
Sand	32 – 40	0.30 - 0.60	30 - 150
Gravel	35 – 45	0.35 - 0.80	60 - 300

For sedimentary cohesionless deposits, Fellenius (1991) that states N_t ranges from about 30 to a high of 120. In very dense non-sedimentary deposits such as glacial tills, N_t can be much higher, but it can also approach the lower bound value of 30. In clays, Fellenius (1991) notes that the toe resistance calculated by using an N_t of 3 is similar to the toe resistance calculated from an analysis where undrained shear strength is used. Therefore, the use of a relatively low value of the N_t coefficient in clays is recommended unless local correlations suggest higher values are appropriate.

Graphs of the ranges in β and N_t coefficients versus the range in ϕ' angle as suggested by Fellenius are presented in Figure 9-17 and 9-18, respectively. These graphs may be helpful in selection of β or N_t. The inexperienced user should select conservative β and N_t coefficients. As with any design method, the user should also confirm the appropriateness of a selected β or N_t coefficient in a given soil condition with local correlations between static capacity calculations and static load tests results.

It should be noted that the effective stress method places no limiting values on either the shaft or toe resistance.

STEP BY STEP PROCEDURE FOR THE EFFECTIVE STRESS METHOD

STEP 1 Delineate the soil profile into layers and determine ϕ' angle for each layer.

a. Construct p_o diagram by using previously described procedures in Chapter 2.

b. Divide soil profile throughout the pile penetration depth into layers and determine the effective overburden pressure, p_o, in ksf (kPa) at the midpoint of each layer.

c. Determine the ϕ' angle for each soil layer from laboratory or in-situ test data.

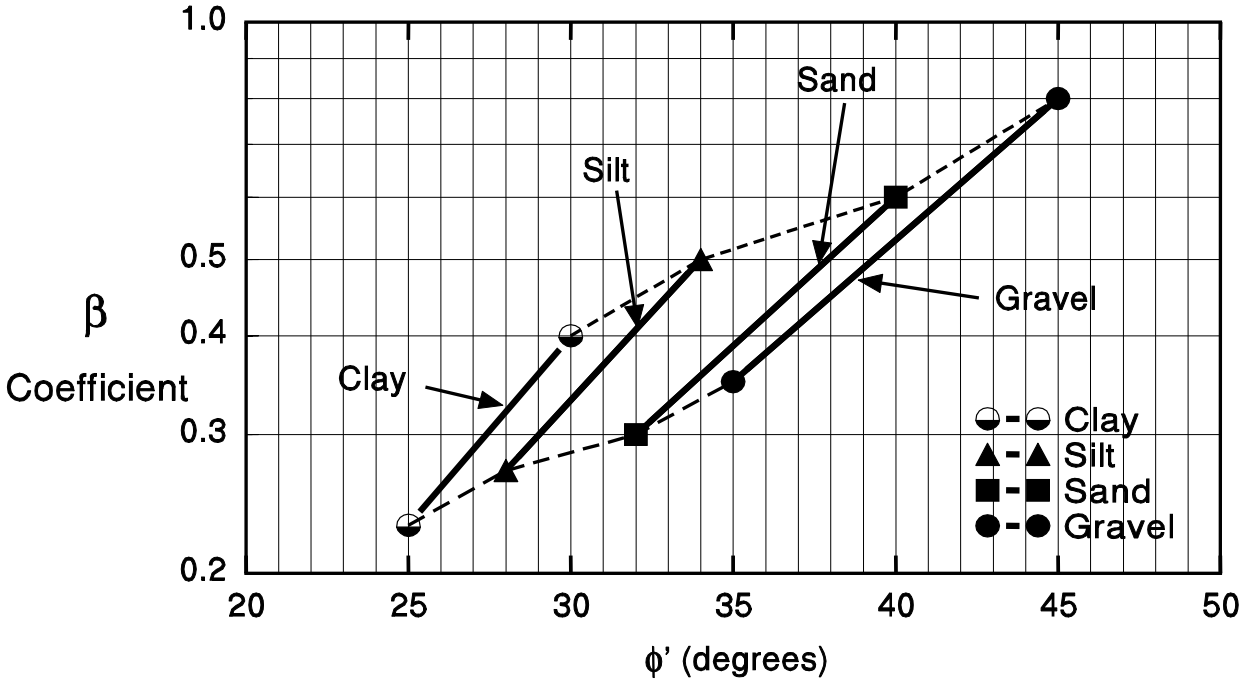

Figure 9-17. Chart for estimating β coefficient as a function of soil type ϕ' (after Fellenius, 1991).

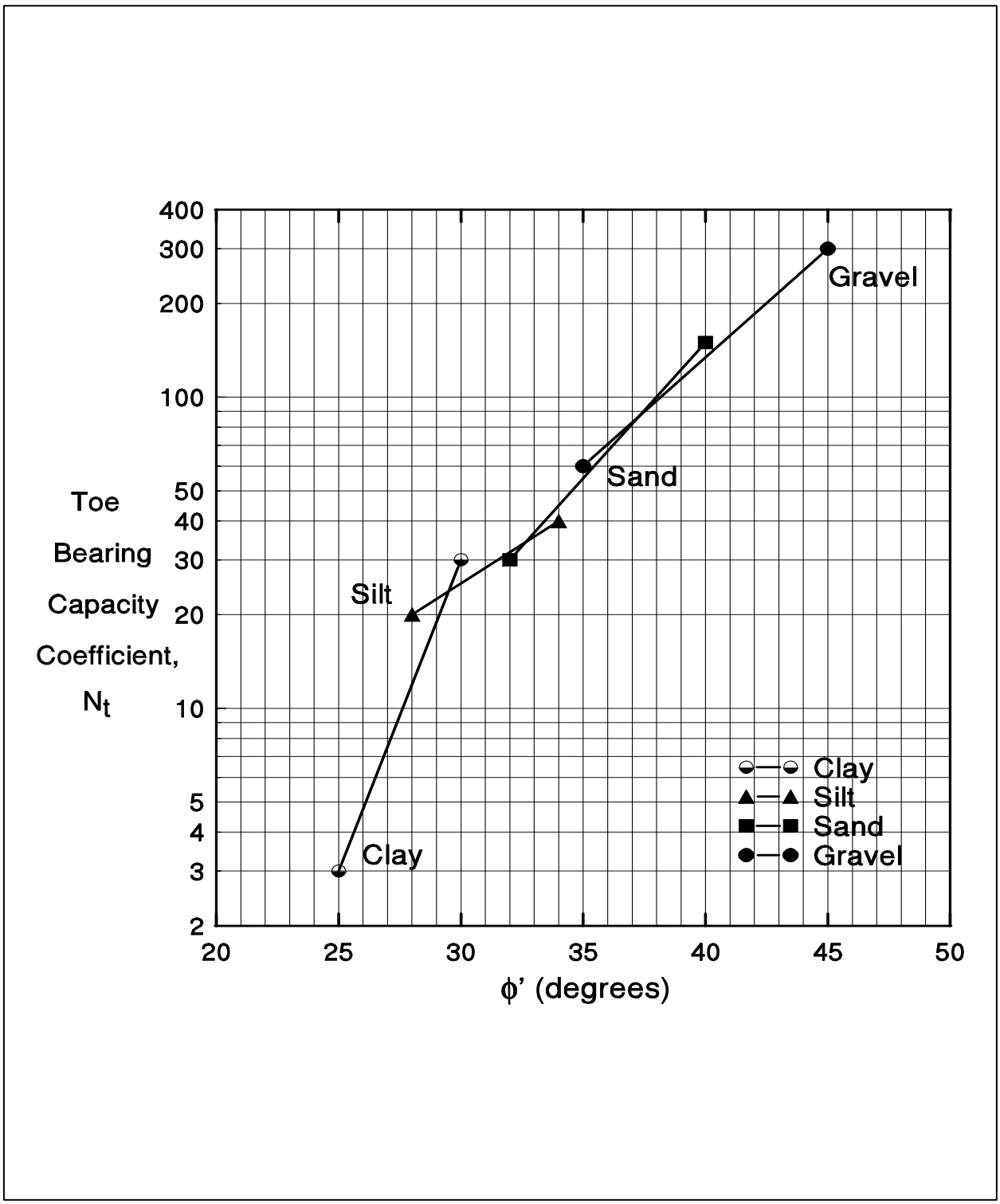

Figure 9-18. Chart for estimating N_t coefficients as a function of soil type ϕ' angle (after Fellenius, 1991).

d. In the absence of laboratory or in-situ test data for cohesionless layers, determine the average corrected SPT N1 value for each layer and estimate ϕ' angle from Table 8-1 in Chapter 8.

STEP 2 Select the β coefficient for each soil layer.

a. Use local experience to select β coefficient for each layer.

b. In the absence of local experience, use Table 9-7 or Figure 9-17 to estimate the β coefficient from the ϕ' angle for each layer.

STEP 3 For each soil layer compute the unit shaft resistance, f_s in ksf (kPa).

$$f_s = \beta \, p_o$$

STEP 4 Compute the shaft resistance in each soil layer and the ultimate shaft resistance, R_s in kips (kN) from the sum of the shaft resistance from each soil layer.

$$R_s = \Sigma \, f_s \, A_s$$

where: A_s = pile-soil surface area in ft^2 (m^2) = (pile perimeter) x (length).

STEP 5 Compute the unit toe resistance, q_t in ksf (kPa).

$$q_t = N_t \, p_t$$

a. Use local experience to select N_t coefficient.

b. In the absence of local experience, estimate N_t from Table 9-7 or Figure 9-18 based on ϕ' angle.

c. Calculate the effective overburden pressure at the pile toe, p_t in ksf (kPa).

STEP 6 Compute the ultimate toe resistance, R_t in kips (kN).

$$R_t = q_t \, A_t$$

where: A_t = area of the pile toe in m^2 (ft^2).

STEP 7 Compute the ultimate geotechnical pile capacity, Q_u in kips (kN).

$$Q_u = R_s + R_t$$

STEP 8 Compute the allowable geotechnical soil resistance, Q_a in kips (kN).

$$Q_a = \frac{Q_u}{\text{Factor of Safety}}$$

The factor of safety in this static calculation should be based on the specified construction control method as described in Section 9.4 of this chapter. Recommended factors of safety based on construction control methods are listed in Table 9-5

The concepts discussed above are illustrated numerically in Example 9-3.

Example 9-3: Determine the required pile length to resist a 40 tons load with a safety factor of 2. Assume no toe resistance for the 1 ft^2 precast concrete pile. Site specific tests have indicated that the adhesion may be assumed equal to cohesion.

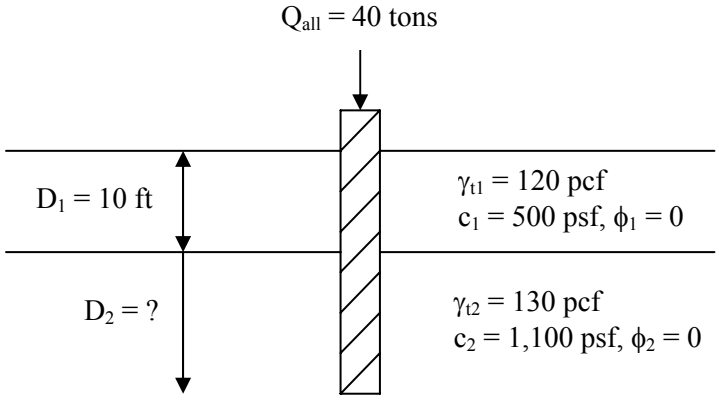

Solution:

$Q_u = R_{s1} + R_{s2}$ (Note: No toe resistance, i.e. 9 $c_u A_t = 0$)

$Q_u = c_{a1} A_{s1} + c_{a2} A_{s2}$

$Q_u = c_{a1} C_{d1} D_1 + c_{a2} C_{d2} D_2$

where C_{d1} and C_{d2} are pile perimeters within depths D_1 and D_2

$C_{d1} = C_{d2} = 4 \times 1 \text{ ft} = 4 \text{ ft}$

From the problem statement, for site-specific conditions, adhesion = cohesion. Therefore,

$c_{a1} = c_1 = 500 \text{ psf}$

$c_{a2} = c_2 = 1{,}100 \text{ psf}$

$Q_u = 40 \text{ tons} \times FS = 40 \text{ tons x } 2 = 80 \text{ tons}$

$80 \text{ tons} = (500 \text{ psf})(4 \text{ ft})(10 \text{ ft}) + (1{,}100 \text{ psf})(4 \text{ ft})D_2$

$80 \text{ tons} = 20{,}000 \text{ lbs} + 4{,}400 \, D_2 \text{ lbs/ft}$

$80 \text{ tons} = 10 \text{ tons} + 2.2 \, D_2 \text{ tons/ft}$

Solve for D_2,

$$D_2 = \frac{80 \text{ tons} - 10 \text{ tons}}{2.2 \text{ tons/ft}} \approx 32 \text{ ft}$$

$\therefore$ Total pile length required = 32 ft + 10 ft $\approx$ 42 ft

9.5.3 Ultimate Geotechnical Capacity of Single Piles in Layered Soils

The ultimate capacity of piles in layered soils can be calculated by combining the methods previously described for cohesionless and cohesive soils. For example, a hand calculation combining the Nordlund method from Section 9.5.1.1 for cohesionless soil layers with the α-method from Section 9.5.2.1 for cohesive soil layers could be used. The effective stress method as described in Section 9.5.2.2 could also be used for layered soil profiles.

9.5.4 Plugging of Open Pile Sections

Open pile sections include open end pipe piles and H-piles. The use of open pile sections has increased, particularly where special design events dictate large pile penetration depths. When open pile sections are driven, they may behave as low displacement piles and "cookie cut" through the soil, or act as displacement piles if a soil plug forms near the pile toe. It is generally desired that open sections remain unplugged during driving and plugged under static loading conditions.

Stevens (1988) reported that plugging of pipe piles in clays does not occur during driving if pile accelerations along the plug zone are greater than 22g. Holloway and Beddard (1995) reported that hammer blow size influenced the dynamic response of the soil plug. With a large hammer blow, the plug "slipped" under the dynamic event whereas under a lesser hammer blow the pile encountered toe resistance typical of a plugged condition. From a design perspective, these cases indicate that pile penetration of open sections can be facilitated if the pile section is designed to accommodate a large pile hammer. Wave equation analyses can provide calculated accelerations at selected pile segments.

Static pile capacity calculations must determine whether an open pile section will exhibit plugged or unplugged behavior. Studies by O'Neill and Raines (1991), Raines, *et al.* (1992), as well as Paikowsky and Whitman (1990) suggest that plugging of open pipe piles in medium dense to dense sands generally begins at a pile penetration-to-pile-diameter ratio of 20, but can occur in cases where the ratio is as high as 35. For pipe piles in soft to stiff clays, Paikowsky and Whitman (1990) reported plugging occurs at penetration-to-pile-diameter ratios of 10 to 20.

The above studies suggest that plugging in any soil material is probable under static loading conditions once the penetration-to-pile-diameter ratio exceeds 20 in dense sands and clays, or 20 to 30 in medium sands. An illustration of the difference in the soil resistance mechanism that develops on a pipe pile with an open and plugged toe condition is presented in Figure 9-19. Paikowsky and Whitman (1990) recommend that the static capacity of an open end pipe pile be calculated from the lesser of the following equations:

Plugged Condition:
$$Q_u = f_{so} A_s + q_t A_t \qquad 9\text{-}15a$$

Unplugged Condition:
$$Q_u = f_{so} A_s + f_{si} A_{si} + q_t A_p - w_p \qquad 9\text{-}15b$$

where: Q_u = ultimate pile capacity in kips (kN).
f_{so} = exterior unit shaft resistance in ksf (kPa).

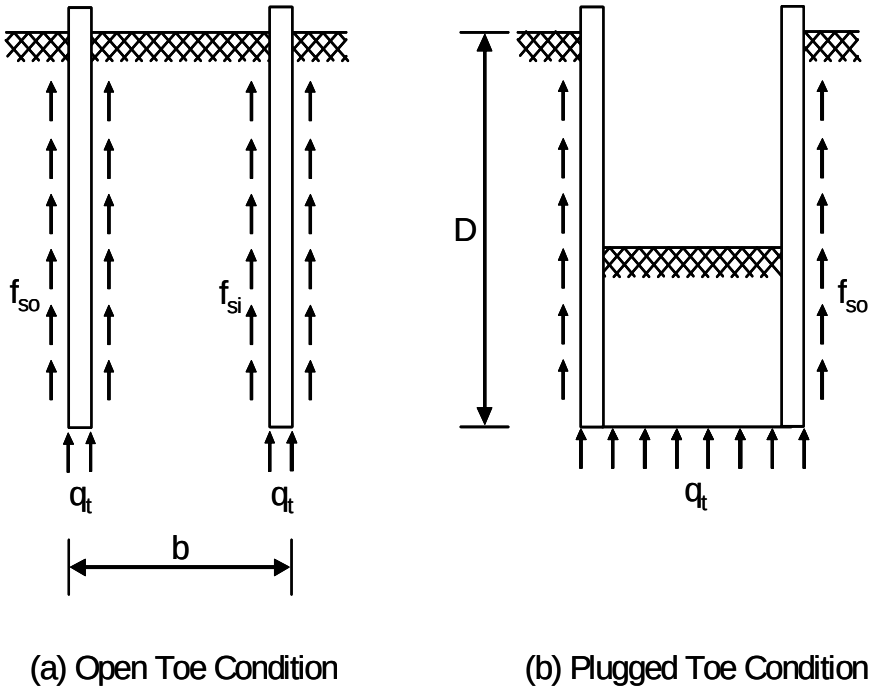

Figure 9-19. Plugging of open end pipe piles (after Paikowsky and Whitman, 1990).

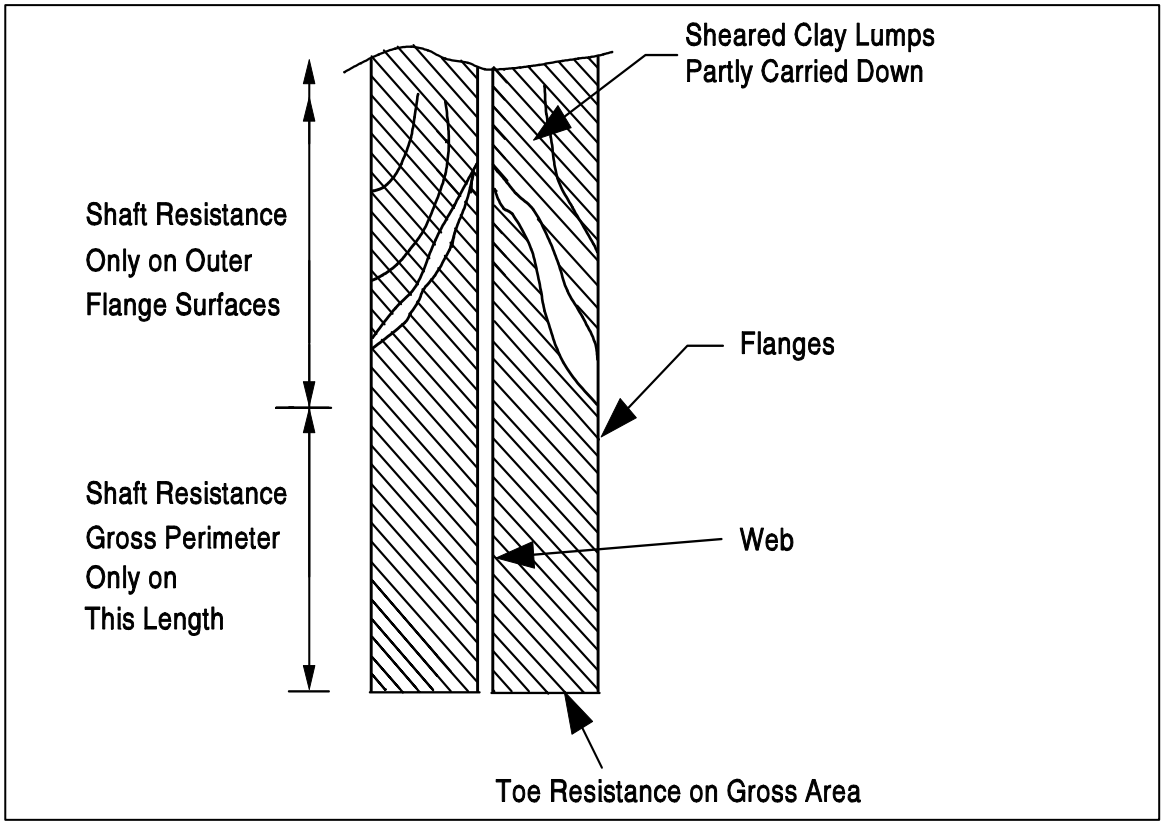

Figure 9-20. Plugging of H-piles (FHWA, 2006a).

A_s = pile exterior surface area in ft^2 (m^2)
f_{si} = interior unit shaft resistance in ksf (kPa)
A_{si} = pile interior surface area in ft^2 (m^2)
q_t = unit toe resistance in ksf (kPa)
A_t = toe area of a plugged pile in ft^2 (m^2)
A_p = cross sectional area of an unplugged pile in ft^2 (m^2)
w_p = weight of the plug in kips (kN)

Static pile capacity calculations for open end pipe piles in cohesionless soils should be performed by using the Paikowsky and Whitman (1990) equations. Toe resistance should be calculated by using the Tomlinson limiting unit toe resistance of 105 ksf (5000 kPa), once Meyerhof's limiting unit toe resistance, determined from Figure 9-14, exceeds 105 ksf (5000 kPa). For open end pipe piles in predominantly cohesive soils, the Tomlinson equation should be used.

The soil stresses and displacements induced by driving an open pile section and a displacement pile section are not the same. Hence, a lower unit toe resistance, q_t, should be used for calculating the toe capacity of open end pipe piles compared to a typical closed end condition. The value of the interior unit shaft resistance in an open end pipe pile is typically on the order of 1/3 to 1/2 the exterior unit shaft resistance, and is influenced by soil type, pile diameter, and pile shoe configuration. These factors will also influence the length of the soil plug that may develop.

For open end pipe piles in cohesionless soils, Tomlinson (1994) recommends that the static pile capacity be calculated using a limiting value of 105 ksf (5000 kPa) for the unit toe resistance, regardless of the pile size or soil density. Tomlinson states that higher unit toe resistances do not develop, because yielding of the soil plug rather than bearing capacity failure of the soil below the plug governs the capacity.

For open end pipe piles driven in stiff clays, Tomlinson (1994) recommends that the static pile capacity for cohesive soils be calculated as follows when field measurements confirm a plug is formed and carried down with the pile:

$$Q_u = 0.8\, c_a\, A_s + 4.5\, c_u\, A_t \qquad 9\text{-}16$$

where:
Q_u = ultimate pile capacity in kips (kN)
c_a = pile adhesion from Figure 9-15 in ksf (kPa)
A_s = pile-soil surface area in ft^2 (m^2)
c_u = average undrained shear strength at the pile toe in ksf (kPa)

A_t = toe area of a plugged pile in ft^2 (m^2)

The plugging phenomenon in H-piles can be equally difficult to analyze. However, the distance between flanges of an H-pile is smaller than the inside diameter of most open end pipe piles. Therefore, it can usually be assumed that an H-pile will be plugged under static loading conditions and the “box” area of the pile toe can be used for static calculation of the toe capacity in cohesionless and cohesive soils, i.e., area = flange width x section height. The toe capacity for H-piles driven to rock is usually governed by the pile structural strength. In that case, the toe capacity is calculated based on the steel cross sectional area, and should not include the area of a soil plug, if any.

For H-piles in cohesionless soils, arching between the flanges can usually be assumed, and the "box" perimeter can be used for shaft resistance calculations, i.e., perimeter = 2 x flange width + 2 x section height. In most cohesive soils, the shaft resistance is calculated from the sum of the adhesion, c_a, along the exterior of the two flanges plus the undrained shear strength of the soil, c_u, times the section height surface area of the two remaining sides of the "box" due to soil-to-soil shear along these two faces. Figure 9-20 illustrates that calculation of shear resistance for H-piles in stiff clays can still be problematic. Sheared clay lumps can develop above the plug zone, in which case the shaft resistance may develop only along the exterior surfaces of the flanges in the sheared lump zone.

The above discussions highlight the point that a higher degree of uncertainty often exists for static pile capacity calculations of open pile sections than for displacement piles. Soil plug formation and plug response is often different under static and dynamic loading. Such differences can complicate pile capacity evaluations of open pile sections with all dynamic methods (wave equation, dynamic testing, and dynamic formulas). Therefore, a static load test is recommended to verify calculated capacity for large diameter open end pipe piles, greater than 18 in (450 mm), or for H-piles designed to carry their load primarily in shaft resistance.

9.5.5 Time Effects on Pile Capacity

The soil is greatly disturbed when a pile is driven into the soil. As the soil surrounding the pile recovers from the installation disturbance, a time dependent change in pile capacity often occurs. Frequently piles driven in saturated clays, and loose to medium dense silts or fine sands gain capacity after driving has been completed. This phenomenon is called **soil setup**. Occasionally piles driven into dense saturated fine sands, dense silts, or weak laminated rocks such as shale, will exhibit a decrease in capacity after the driving has been completed. This phenomenon is called **relaxation**. Case history discussions on soil setup and relaxation may be found in Fellenius, *et al.* (1989), and Thompson and Thompson (1985), respectively.

9.5.5.1 Soil Setup

When saturated cohesive soils are compressed and disturbed due to pile driving, large excess pore water pressures develop. These excess pore water pressures are generated partly from the shearing and remolding of the soil and partly from radial compression as the pile displaces the soil. The excess pore water pressures cause a reduction in the effective stresses acting on the pile, and thus a reduction in the soil shear strength. The reduction in soil shear strength results in a reduced pile capacity during driving, and for a period of time afterwards.

After driving, the excess pore water pressures will dissipate primarily through radial flow of the pore water away from the pile. With the dissipation of pore water pressures, the soil reconsolidates and shear strength increases. This increase in soil shear strength results in an increase in the static pile capacity and is called **soil setup**. A similar decrease in resistance to pile penetration with subsequent soil setup may occur in loose to medium dense, saturated, fine grained sands or silts. The magnitude of the gain in capacity depends on soil characteristics, pile material and pile dimensions.

Because the pile capacity may increase after the end of driving, pile capacity assessments should be made from static load testing or **restriking** performed **after** equilibrium conditions in the soil have been re-established. The time for the return of equilibrium conditions is highly variable and depends on soil type and degree of soil disturbance. Piezometers installed within three diameters of the pile can be used to monitor pore pressure dissipation with time. Effective stress static pile capacity calculation methods can be used to evaluate the increase in capacity with time once pore pressures are quantified.

Static load testing or **restrike** testing of piles in fine grained soils should not be conducted until after pore pressures dissipate and return to equilibrium. In the absence of site-specific pore water

pressure data from piezometers, it is suggested that static load testing or restrking of piles in clays and other predominantly fine grained soils be delayed for at least two weeks after driving and preferably for a longer period. In sandy silts and fine sands, pore pressures generally dissipate more rapidly. In these more granular deposits, five days to a week is often a sufficient time delay.

FHWA (1996) calculated general soil setup factors based on the predominant soil type along the pile shaft. The **soil setup factor** was defined as the failure load from a static load test divided by the end-of-drive wave equation capacity. These results are presented in Table 9-20. The data base for this study was comprised of 99 test piles from 46 sites. The number of sites and the percentage of the data base in a given soil condition is included in the table. While these soil set-up factors may be useful for preliminary estimates, soil setup is better estimated based on site-specific data gathered from pile restriking, dynamic measurements, static load testing, and local experience.

Komurka, *et al.*, (2003) summarized the current practice in estimating and measuring soil setup in a report to the Wisconsin Highway Research Program. This report summarizes the mechanisms associated with soil setup development and reviews several empirical relationships for estimating set-up.

Table 9-8
Soil setup factors (after FHWA, 1996)

Predominant Soil Type Along Pile Shaft	Range in Soil Set-up Factor	Recommended Soil Set-up Factors*	Number of Sites and (Percentage of Data Base)
Clay	1.2 - 5.5	2.0	7 (15%)
Silt - Clay	1.0 - 2.0	1.0	10 (22%)
Silt	1.5 - 5.0	1.5	2 (4%)
Sand - Clay	1.0 - 6.0	1.5	13 (28%)
Sand - Silt	1.2 - 2.0	1.2	8 (18%)
Fine Sand	1.2 - 2.0	1.2	2 (4%)
Sand	0.8 - 2.0	1.0	3 (7%)
Sand - Gravel	1.2 - 2.0	1.0	1 (2%)
* Confirmation with local experience recommended			

9.5.5.2 Relaxation

The ultimate capacity of driven piles can also decrease with time following driving. This is known as **relaxation** and it has been observed in dense, saturated, fine grained soils such as non-cohesive silts and fine sands, as well as in some shales. In these cases, the driving process is believed to cause the dense soil near the pile toe to dilate, thereby generating negative excess

pore water pressures, i.e., suction. In accordance with the principle of effective stress, the negative pore water pressures temporarily increase the effective stresses acting on the pile, resulting in a temporarily higher soil strength and driving resistance. When these negative excess pore water pressures dissipate, the effective stresses acting on the pile decrease, as does the pile capacity. Relaxation in weak laminated rocks has been attributed to a release of locked-in horizontal stresses (Thompson and Thompson, 1985).

Because the pile capacity may decrease due to relaxation after the end of driving, pile capacity assessments from static load testing or restrking should be made after equilibrium conditions in the soil have been re-established. In the absence of site-specific pore water pressure data from piezometers, it is suggested that static load testing or restrking of piles in dense silts and fine sands be delayed for five days to a week after driving, or longer if possible. In relaxation-prone shales, it is suggested that static load testing or restrike testing be delayed a minimum of two weeks after driving.

Published cases of the relaxation magnitude of various soil types are quite limited. However, data from Thompson and Thompson (1985) as well as Hussein, *et al.* (1993) suggest relaxation factors for piles founded in some shales can range from 0.5 to 0.9. The **relaxation factor** is defined as the failure load from a static load test divided by the pile capacity at the end of initial driving. Relaxation factors of 0.5 and 0.8 have also been observed in two cases where piles were founded in dense sands and extremely dense silts, respectively. The importance of evaluating time dependent decreases in pile capacity for piles founded in these materials cannot be over emphasized.

9.5.6 Additional Design and Construction Considerations

The previous sections of this chapter addressed routine static analysis procedures for pile foundation design. However, the designer should be aware of additional design and construction considerations that can influence the reliability of static analysis procedures in estimating pile capacity. These issues include effects of predrilling or jetting, construction dewatering and soil densification on pile capacity. Pile-driving-induced vibrations can also influence the final design and results of static calculations if potential vibration levels dictate changes in pile type or installation procedures. These topics are outside the scope of this manual and the reader is referred to FHWA (2006a) for guidance.

9.5.7 The DRIVEN Computer Program

The FHWA developed the computer program DRIVEN in 1998 for calculation of static pile capacity. The DRIVEN program can be used to calculate the capacity of open and closed end pipe piles, H-piles, circular or square solid concrete piles, timber piles, and Monotube piles. The program results can be displayed in both tabular and graphical form. Analyses may be performed in either English or SI units and can be switched between units during analyses (FHWA, 1998b). The DRIVEN manual and software Version 1.2, released in March 2001, can be downloaded from www.fhwa.dot.gov/bridge/geosoft.htm.

In the DRIVEN program, the user inputs the soil profile consisting of the soil unit weights and strength parameters including the percentage strength loss during driving. For the selected pile type, the program calculates the pile capacity versus depth for the entire soil profile using the Nordlund and α-methods in cohesionless and cohesive layers, respectively. User-input percentage soil strength losses during driving are used to calculate the ultimate pile capacity at the time of driving as well as during restrike.

The DRIVEN program includes several analysis options that facilitate pile design. These options include:

- Soft compressible soils: The shaft resistance from unsuitable soil layers defined by the user is subtracted from the calculation of ultimate pile capacity.

- Scourable soils: Based on a user-input depth, the calculated shaft resistance from scourable soils due to local scour is subtracted from the calculation of ultimate pile capacity. In the case of channel degradation scour, the reduction in pile capacity from the loss of shaft resistance in the scour zone as well as the influence of the reduced effective overburden pressure from soil removal on the capacity calculated in the underlying layers is considered.

- Pile Plugging: DRIVEN handles pile plugging based on the recommendations presented in Section 9.5.4 of this manual.

The initial DRIVEN program screen is the Project Definition Screen illustrated in Figure 9-21. In this screen the user inputs the project information as well as the number of soil layers. Inputs for three water table elevations are provided. The water table at the time of drilling is used for correction of SPT N values for overburden pressure if that option is selected by the user. The

water table at the time of restrike / driving affects the effective overburden pressure in the static capacity calculations at those times. The static calculation at the time of driving includes soil strength losses. The restrike static calculations include the long term soil strength. The water table at the ultimate condition is used in the calculation of effective overburden pressure for the static capacity calculation under an extreme event.

The Soil Profile screen for a two layer soil profile is shown in Figure 9-22. A mouse click on the Select Graph Option will bring up the Cohesive Soil Layer Properties screen shown in Figure 9-23. The user can then select how the adhesion is calculated. The general adhesion option attributed to "Tomlinson 1979" in Figure 9-23 is based upon the data presented in Figure 9-16, i.e., piles without different overlying strata. The bottom option in the Cohesive Soil Layer Properties screen shown in Figure 9-23 allows the user to enter an adhesion value of their choice. This bottom option may be useful with the data presented in Figures 9-15 and 9-16 or site data from specific load test..

The Soil Profile screen for a two layer profile with cohesionless soil properties is presented in Figure 9-24. The user can input the same or different soil friction angles to be used in the shaft resistance and end bearing calculations in the layer. The user can also input SPT N values and let the program compute the soil friction angle from a correlation developed by Peck, *et al.* (1974) as shown in Figure 9-25. However, it is recommended that the user manually select the soil friction angle rather than use this program option as factors influencing the N value - ϕ angle correlation such as SPT hammer type and sample recovery are not considered by the program.

Both cohesive and cohesionless soil profile screens request the user to provide the percentage strength loss of the soil type during driving. This is sometimes difficult for the user to quantify. Insight into appropriate values of driving strength loss can be gathered from the soil setup factors presented in Section 9.5.5. The percent driving strength loss needed for input into DRIVEN can be then be calculated from:

$$\% \text{ Driving Strength Loss} = 1 - [1 / \text{setup factor}]$$

After the soil input has been entered, the user must select a pile type from a drop down menu located on the Soil Profile screen. A pile detail screen will appear for the pile type selected requesting additional information on the depth to the top of the pile and the pile properties. These DRIVEN screens are presented in Figure 9-26.

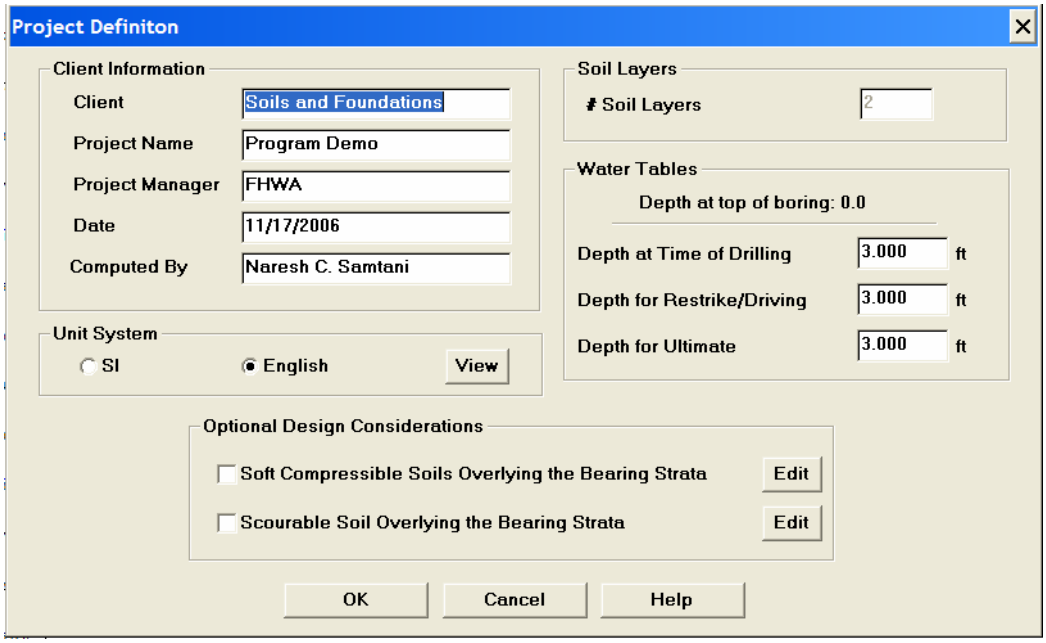

Figure 9-21. DRIVEN Project Definition screen.

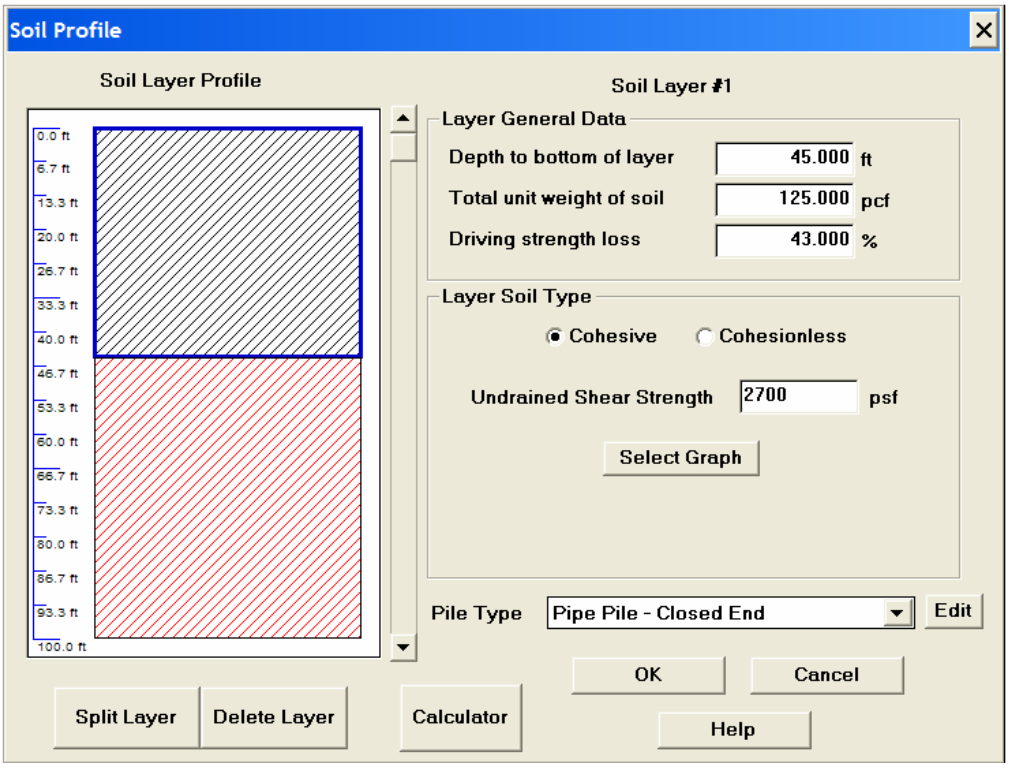

Figure 9-22. DRIVEN Soil Profile screen – cohesive soil.

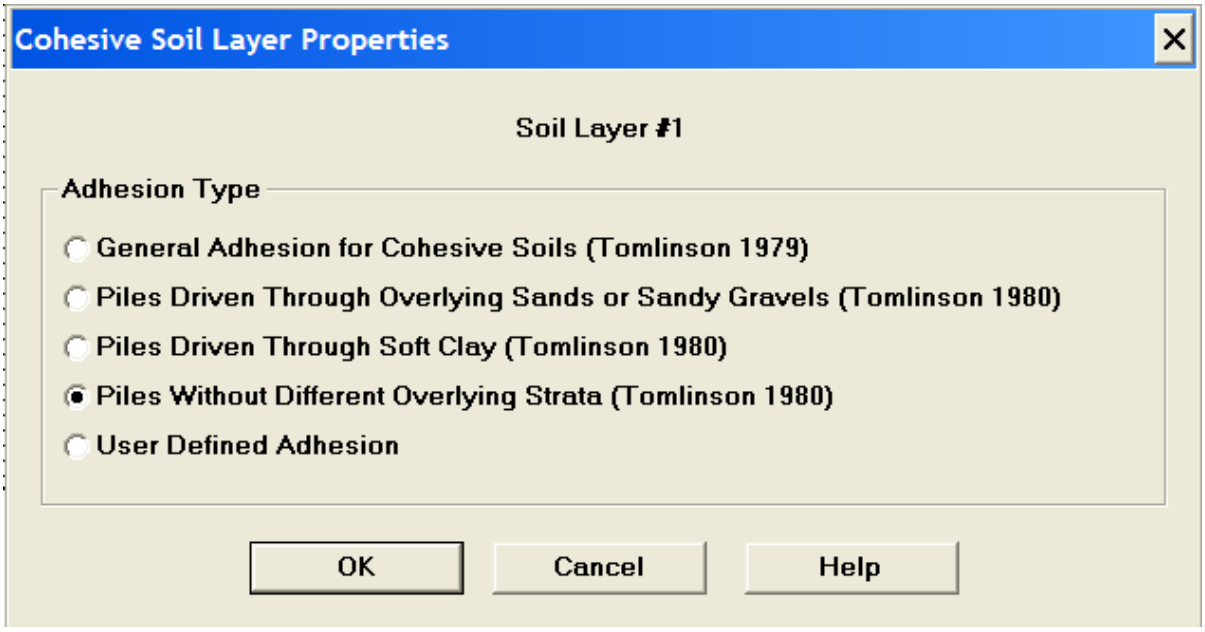

Figure 9-23. DRIVEN Cohesive Soil Layer Properties screen.

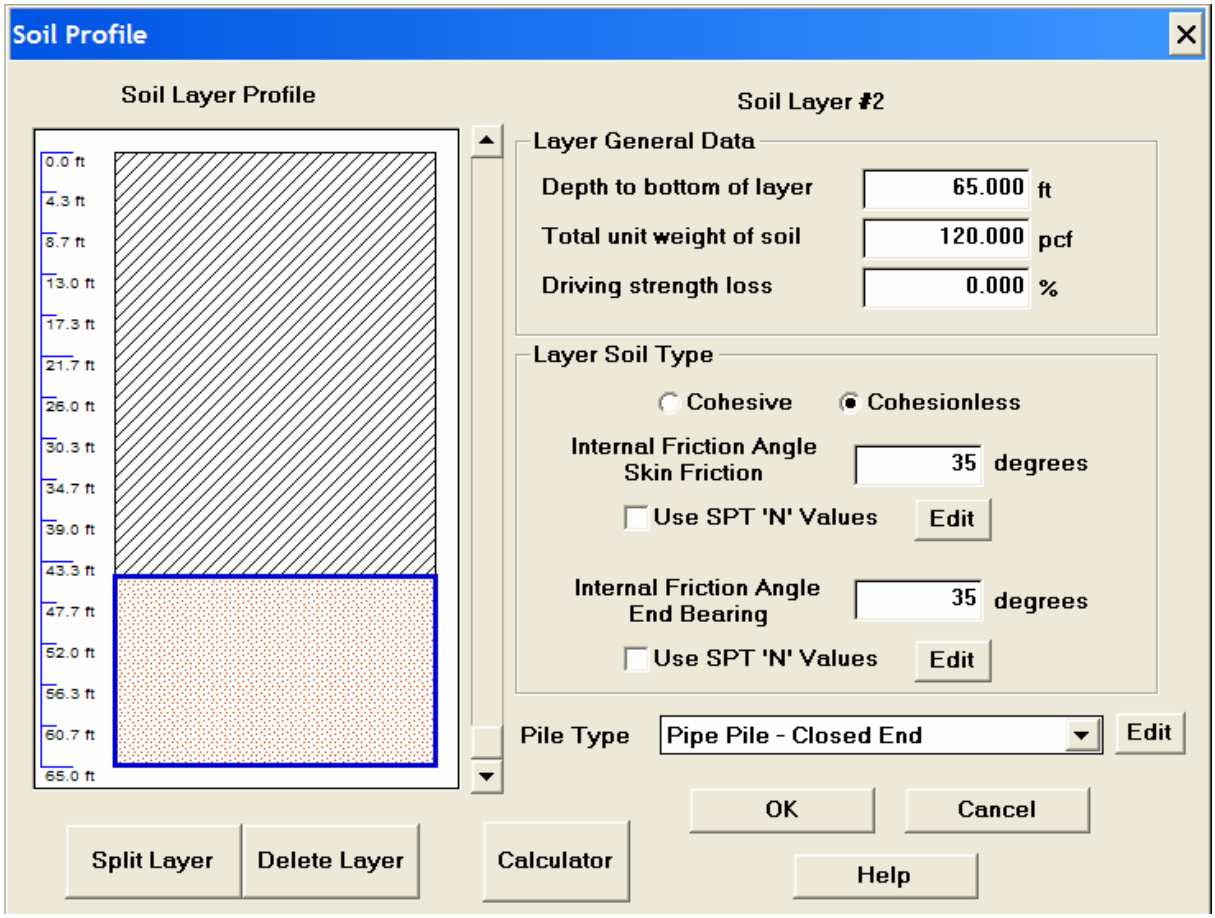

Figure 9-24. DRIVEN Soil Profile screen – cohesionless soil.

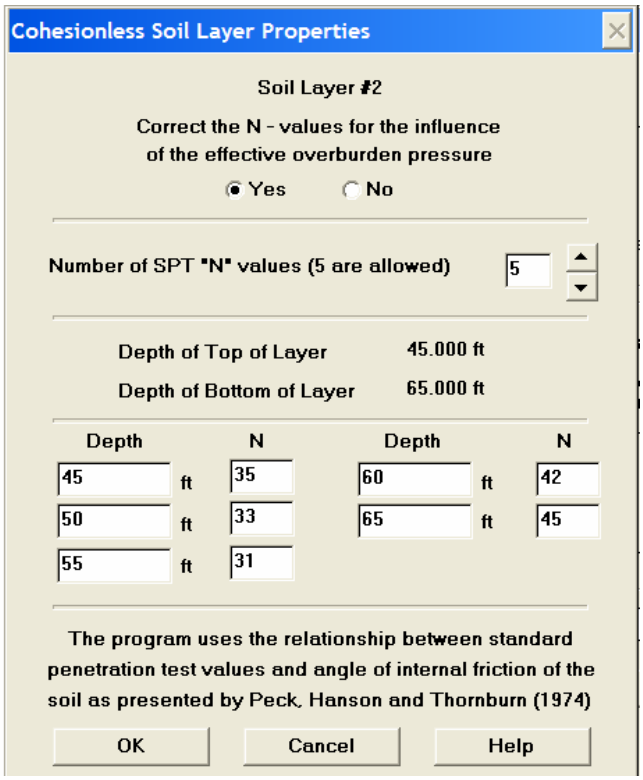

Figure 9-25. DRIVEN Cohesionless Soil Layer Properties screen.

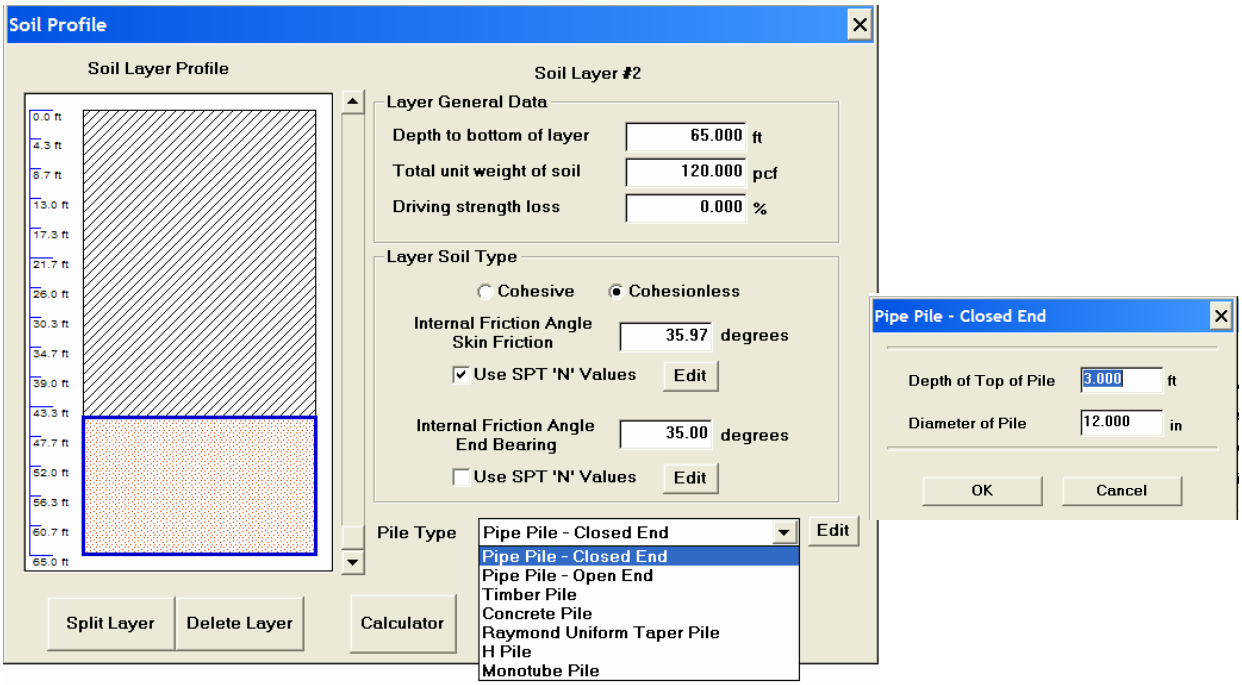

Figure 9-26. DRIVEN Soil Profile screen - Pile type selection drop down menu and pile detail screen.

Once all soil and pile information is entered, the user can review the static capacity calculations in tabular or graphical form by a mouse click on the appropriate icon in the program toolbar. The toolbar icons for tabular and graphical output are identified in Figure 9-27. The Output-Tabular screen is shown in Figure 9-28. A summary of the input data and the results of the analysis will be printed if the user clicks on the report button. Analysis output can also be presented graphically as shown in Figures 9-28 and 9-29 for driving and restrike static analyses, respectively. The ultimate capacity versus depth from shaft resistance, toe resistance, and the combined shaft and toe resistance can be displayed by clicking on "skin friction," "end bearing," and "total capacity" on the Plots menu of the Output-Graphical screen, capacity changes with time or from extreme events can be reviewed by clicking on "restrike," "driving," and "ultimate" on the Plot Set menu of the Output-Graphical screen.

The program also generates the soil input file required for a driveability study in the commonly used GRLWEAP wave equation program. The GRLWEAP file created by DRIVEN is compatible with the Windows versions of GRLWEAP. However, the DRIVEN file must be identified as a pre 2002 input file in the current version of GRLWEAP.

Additional DRIVEN program capabilities are described in the DRIVEN Program User's Manual by FHWA (1998b).

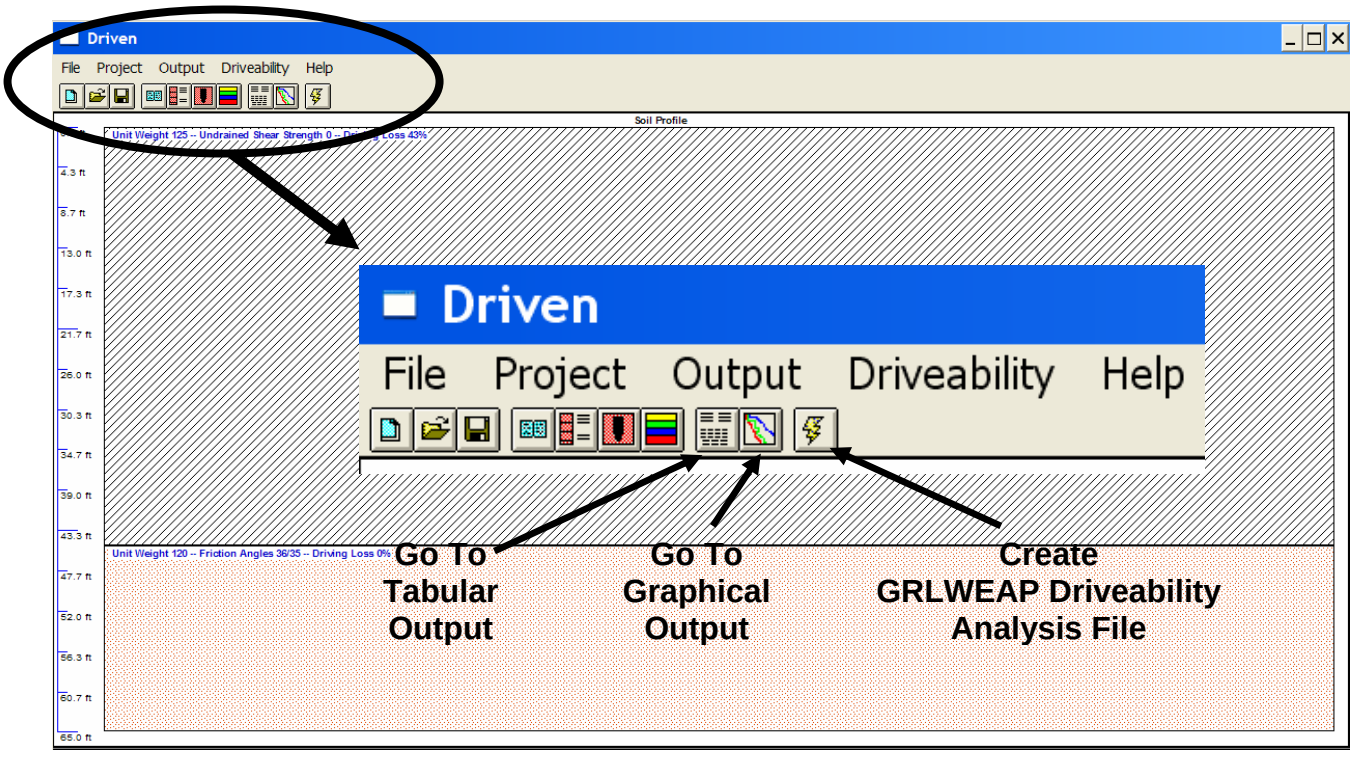

Figure 9-27. DRIVEN toolbar output and analysis options.

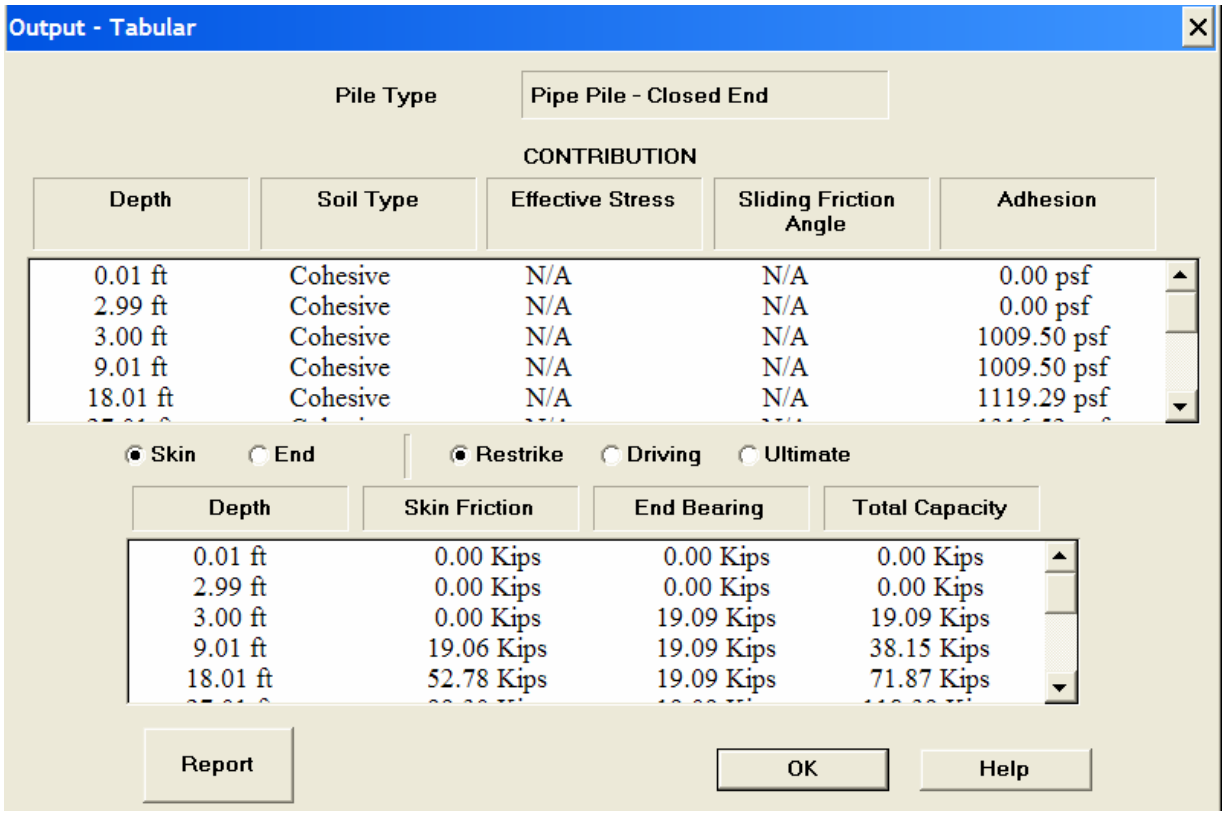

Figure 9-28. DRIVEN Output Tabular screen.

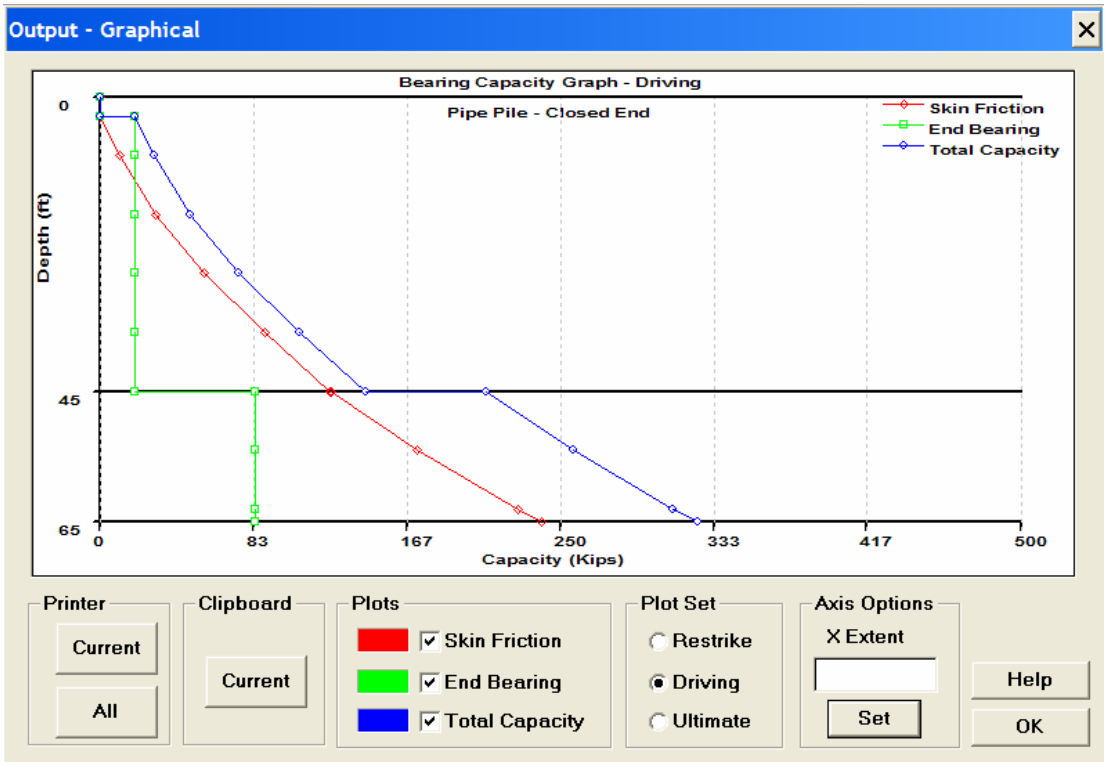

Figure 9-29. DRIVEN Output-Graphical screen for end of driving.

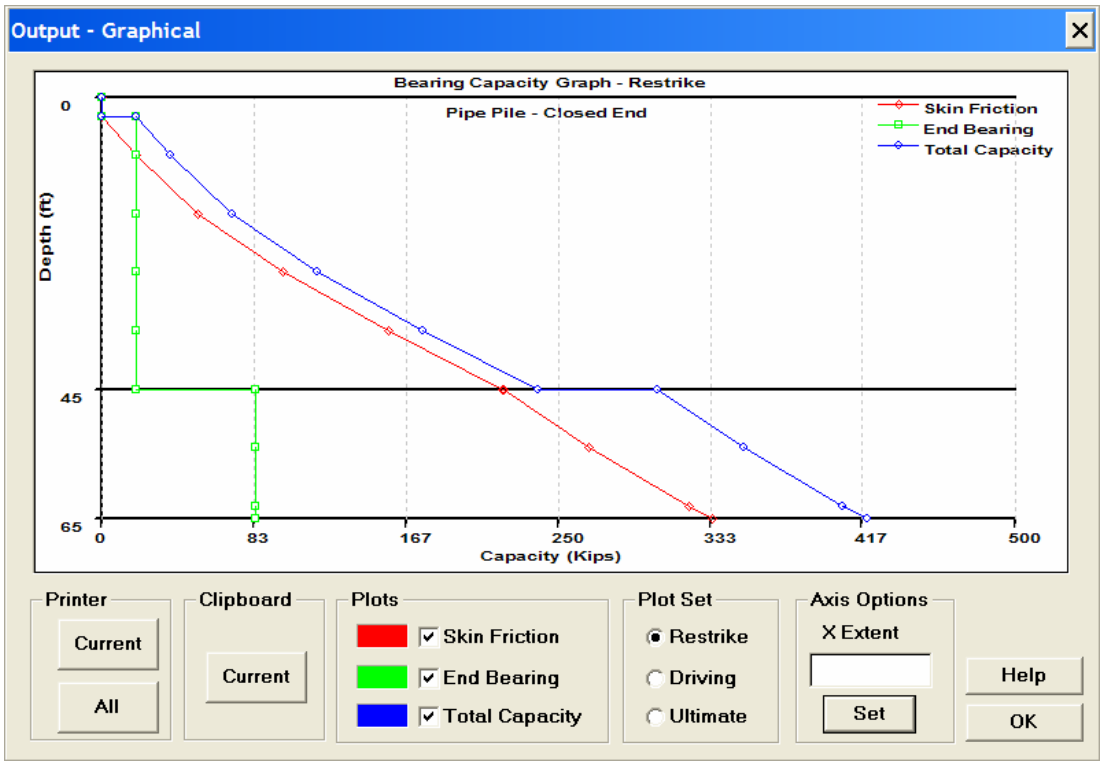

Figure 9-30. DRIVEN Output -Graphical screen for restrike.

9.5.8 Ultimate Capacity of Piles on Rock and in Intermediate Geomaterials (IGMs)

Pile foundations on rock are normally designed to carry large loads. For pile foundations driven to rock, which include steel H-piles, pipe piles or precast concrete piles, the exact area in contact with the rock, the depth of penetration into rock, as well as the quality of rock are largely unknown. Therefore, the determination of load capacity of driven piles on rock should be made on the basis of driving observations, local experience and load tests.

Rock Quality Designation (RQD) values can provide a qualitative assessment of rock mass as discussed in Chapter 3. Except for soft weathered rock, the structural capacity of toe bearing pile will generally be less than the capacity of rock of fair to excellent quality as described in Figure 3-17 in Chapter 3. The structural capacity, which is based on the allowable design stress for the pile material, will therefore govern the pile capacity in many cases.

Small diameter piles supported on fair to excellent quality rock may be loaded to their allowable structural capacity. Piles supported on soft weathered rock, such as shale or other types of very poor or poor quality rock, should be designed based on the results of pile load tests. Similarly, for driven piles that penetrate into soft rocks or IGMs, the ultimate capacity may include the contribution of shaft resistance if a static load test is performed to verify the magnitude of the shaft resistance.

9.6 DESIGN OF PILE GROUPS

The previous sections of this chapter dealt with design procedures for single piles. However piles for almost all highway structures are installed in groups due to the heavy foundation loads. This section of the chapter will address the foundation design procedures for evaluating the axial compression capacity of pile groups as well as the settlement of pile groups under axial compression loads. The axial compression capacity and settlement of pile groups are interrelated and are therefore presented in sequence.

The efficiency of a pile group in supporting the foundation load is defined as the ratio of the ultimate capacity of the group to the sum of the ultimate capacities of the individual piles comprising the group. This may be expressed in equation form as:

$$\eta_g = \frac{Q_{ug}}{nQ_u} \qquad 9\text{-}17$$

where: η_g = pile group efficiency
Q_{ug} = ultimate capacity of the pile group
n = number of piles in the pile group
Q_u = ultimate capacity of each individual pile in the pile group

If piles are driven into compressible cohesive soil or into dense cohesionless material underlain by compressible soil, then the ultimate axial compression capacity of a pile group may be less than that of the sum of the ultimate axial compression capacities of the individual piles. In this case, the pile group has a group efficiency of less than 1. In cohesionless soils, the ultimate axial compression capacity of a pile group is generally greater than the sum of the ultimate axial compression capacities of the individual piles comprising the group. In this case, the pile group has a group efficiency greater than 1.

The settlement of a pile group is likely to be many times greater than the settlement of an individual pile carrying the same per pile load as each pile in the group. Figure 9-31(a) illustrates that for a single pile, only a relatively small zone of soil around and below the pile toe is subjected to vertical stress. Figure 9-31(b) illustrates that for a pile group, a much larger zone of soil around and below the pile group is stressed. The settlement of the pile group may be large depending on the compressibility of the soils within the stressed zone.

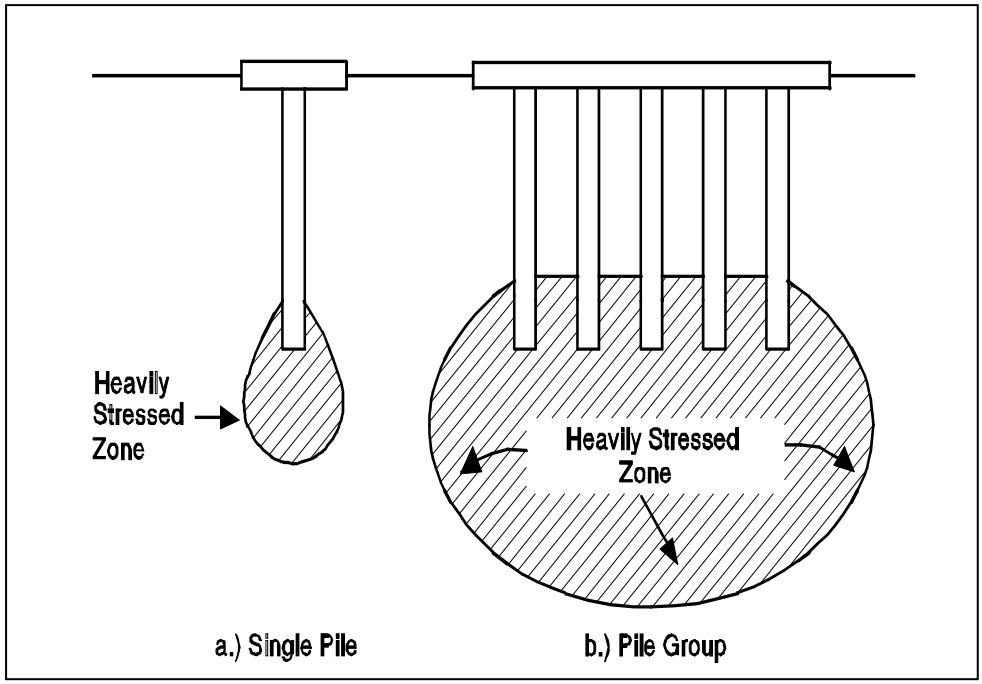

Figure 9-31. Stress zone from single pile and pile group (after Tomlinson, 1994).

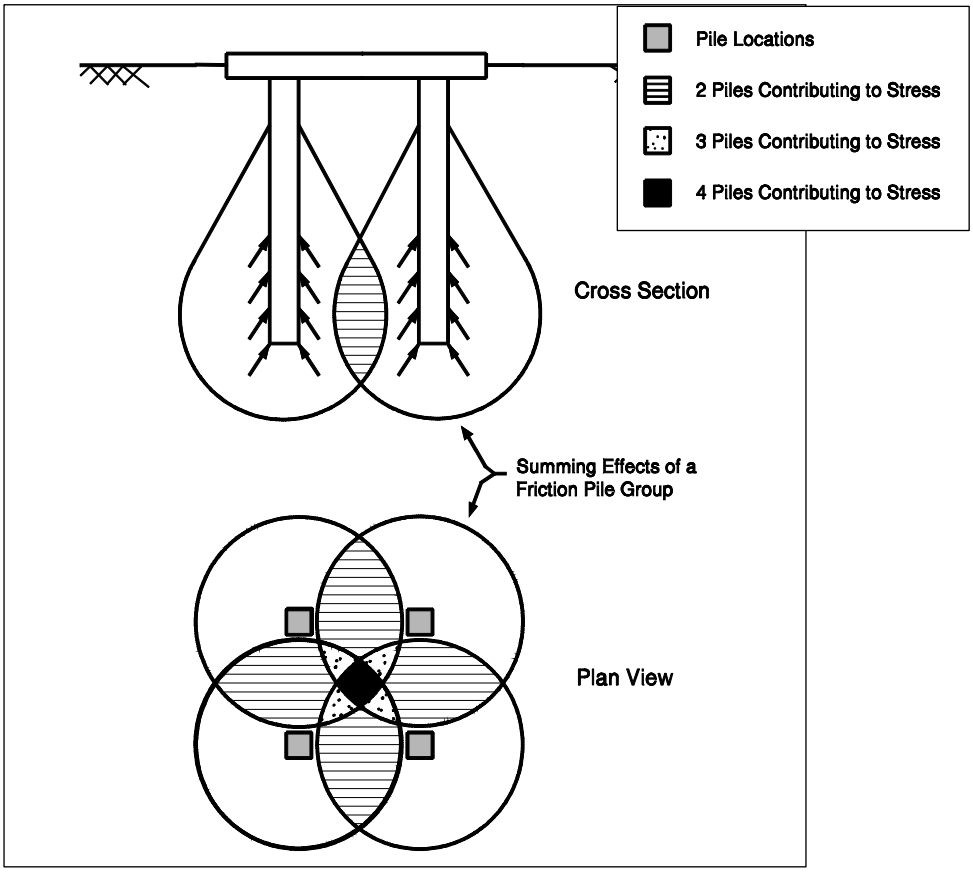

Figure 9-32. Overlap of stress zones for friction pile group (after Bowles, 1996).

The soil supporting a pile group is also subject to overlapping stress zones from individual piles in the group. The overlapping effect of stress zones for a pile group supported by shaft resistance is illustrated in Figure 9-32.

9.6.1 Axial Compression Capacity of Pile Groups

9.6.1.1 Cohesionless Soils

In cohesionless soils, the ultimate group capacity of driven piles with a center to center spacing of less than 3 pile diameters is greater than the sum of the ultimate capacity of the individual piles. The greater group capacity is due to the overlap of individual soil compaction zones around each pile, which increases the shaft resistance due to soil densification. Piles in groups at center to center spacings greater than three times the average pile diameter generally act as individual piles.

Design recommendations for estimating group capacity for driven piles in cohesionless soil are as follows:

1. The ultimate group capacity for driven piles in cohesionless soils not underlain by a weak deposit may be taken as the sum of the individual ultimate pile capacities, provided jetting or predrilling was not used in the pile installation process. Jetting or predrilling can result in group efficiencies less than 1. Therefore, jetting or predrilling should be avoided whenever possible or controlled by detailed specifications when necessary.

1. If a pile group founded in a firm bearing stratum of limited thickness is underlain by a weak deposit, then the ultimate group capacity is the smaller value of either the sum of the ultimate capacities of the individual piles, or the group capacity against block failure of an equivalent pier, consisting of the pile group and enclosed soil mass punching through the firm stratum into the underlying weak soil. From a practical standpoint, block failure in cohesionless soils can only occur when the center to center spacing of the piles is less than 2 pile diameters, which is less than the minimum center to center spacing of 2.5 diameters allowed by the AASHTO code (2002). The method shown for cohesive soils presented in the Section 9.6.1.3 may be used to evaluate the possibility of a block failure.

3. Piles in groups should not be installed at center to center spacings less than 3 times the average pile diameter. A minimum center to center spacing of 3 diameters is recommended to optimize group capacity and minimize installation problems.

9.6.1.2 Cohesive Soils

In the absence of negative shaft resistance, the group capacity in cohesive soil is usually governed by the sum of the ultimate capacities of the individual piles, with some reduction due to overlapping zones of shear deformation in the surrounding soil. Negative shaft resistance is described in Section 9.8 and often occurs when soil settlement transfers load to the pile. The AASHTO (2002) code states that the group capacity is influenced by whether or not the pile cap is in firm contact with the ground. If the pile cap is in firm contact with the ground, the soil between the piles and the pile group act as a unit.

The following design recommendations are for estimating ultimate pile group capacity in cohesive soils. The lesser of the ultimate pile group capacity, calculated from Steps 1 to 4, should be used.

1. For pile groups driven in clays with undrained shear strengths of less than 2 ksf (95 kPa) and for the pile cap not in firm contact with the ground, a group efficiency of 0.7 should be used for center to center pile spacings of 3 times the average pile diameter. If the center to center pile spacing is greater than 6 times the average pile diameter, then a group efficiency of 1.0 may be used. Linear interpolation should be used for intermediate center to center pile spacings.

2. For pile groups driven in clays with undrained shear strengths less than 2 ksf (95 kPa) and for the pile cap in firm contact with the ground, a group efficiency of 1.0 may be used.

3. For pile groups driven in clays with undrained shear strength in excess of 2 ksf (95 kPa), a group efficiency of 1.0 may be used regardless of the pile cap - ground contact.

4. Calculate the ultimate pile group capacity against block failure by using the procedure described in Section 9.6.1.3.

5. Piles in groups should not be installed at center to center spacings less than 3 times the average pile diameter and not less than 3 ft (1 m).

It is important to note that the driving of pile groups in cohesive soils can generate large excess pore water pressures. The excess pore water pressures can result in short term group efficiencies on the order of 0.4 to 0.8 for 1 to 2 months after installation. As these excess pore water pressures dissipate, the pile group efficiency will increase. Figure 9-33 presents observations on the dissipation of excess pore water pressure versus time for pile groups driven in cohesive soils.

Depending upon the group size, the excess pore water pressures typically dissipate within 1 to 2 months after driving. However, in very large groups, full excess pore water pressure dissipation may take up to a year.

If a pile group will experience the full group load shortly after construction, the foundation designer must evaluate the reduced group capacity that may be available for load support. In these cases, piezometers should be installed to monitor pore pressure dissipation with time. Effective stress capacity calculations can then be used to determine if the increase in pile group capacity versus time during construction meets the load support requirements.

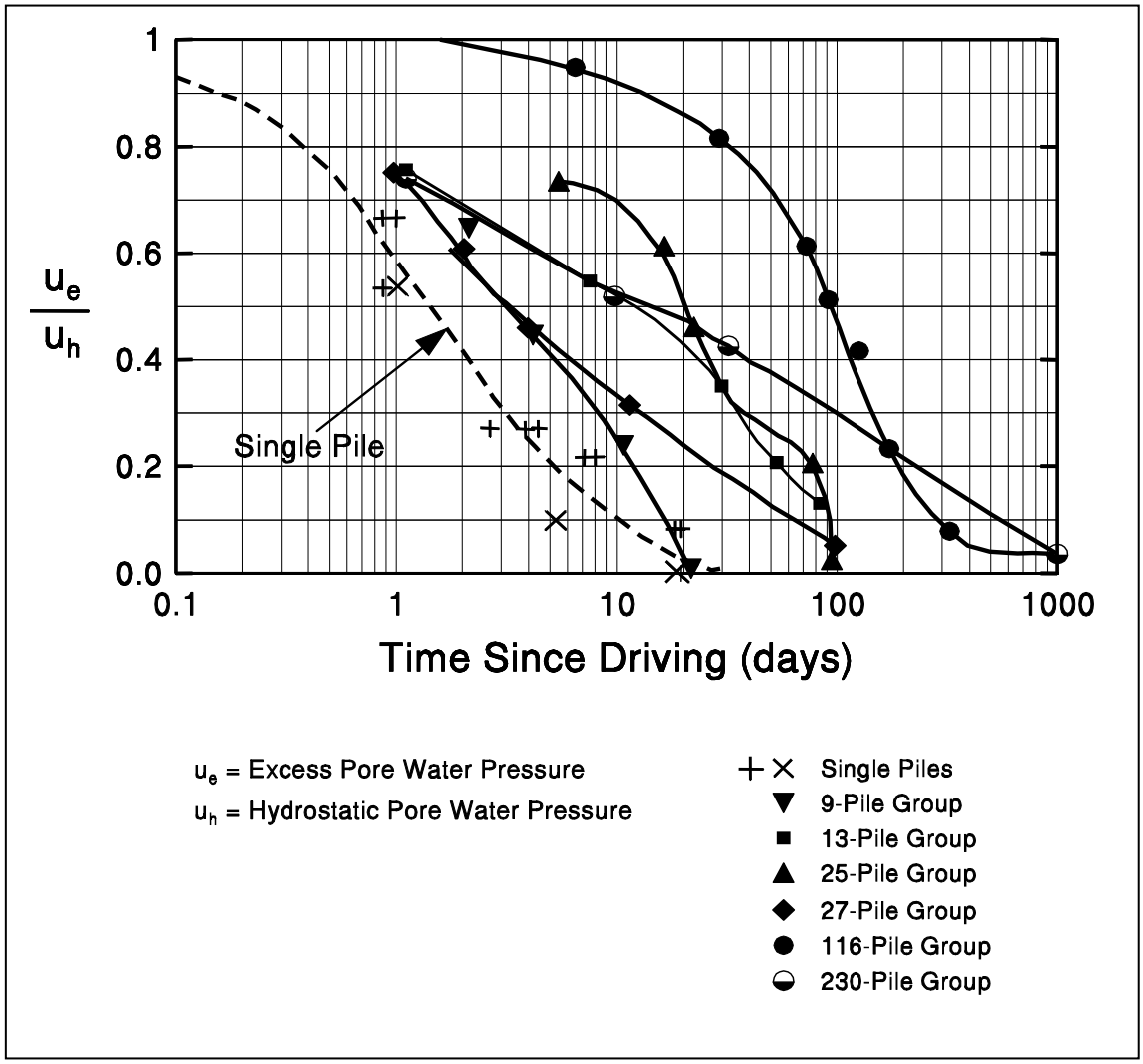

Figure 9-33. Measured dissipation of excess pore water pressure in soil surrounding full scale pile groups (after O'Neill, 1983).

9.6.1.3 Block Failure of Pile Groups

Block failure of pile groups is generally a design consideration only for pile groups in soft cohesive soils or in cohesionless soils underlain by a weak cohesive layer. For a pile group in cohesive soil as shown in Figure 9-34, the ultimate capacity of the pile group against a block failure is provided by the following expression:

$$Q_{ug} = 2D\,(B + Z)\,c_{u1} + B\,Z\,c_{u2}\,N_c \qquad 9\text{-}18$$

where:
- Q_{ug} = ultimate group capacity against block failure
- D = embedded length of piles
- B = width of pile group
- Z = length of pile group
- c_{u1} = weighted average of the undrained shear strength over the depth of pile embedment for the cohesive soils along the pile group perimeter
- c_{u2} = average undrained shear strength of the cohesive soils at the base of the pile group to a depth of 2B below pile toe level
- N_c = bearing capacity factor

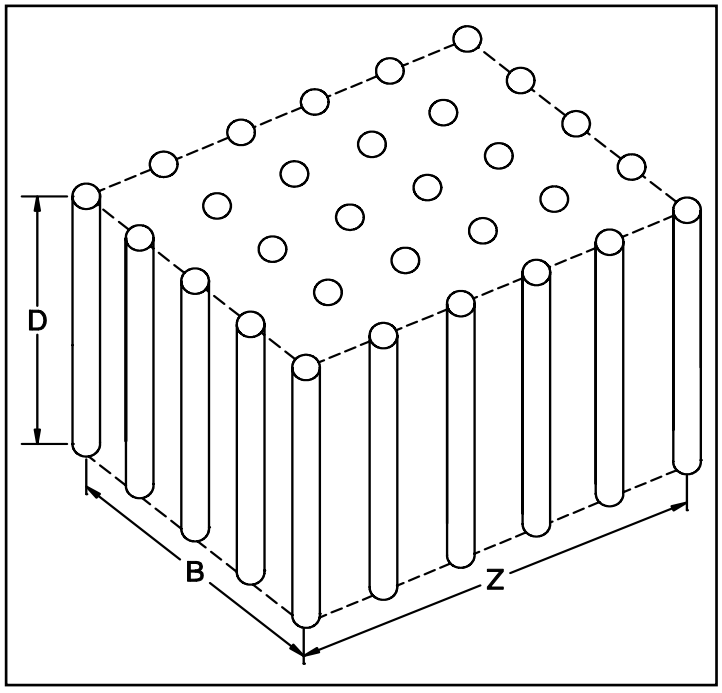

Figure 9-34. Three dimensional pile group configuration (after Tomlinson, 1994).

If a pile group will experience the full group load shortly after construction, the ultimate group capacity against block failure should be calculated by using the remolded or a reduced shear strength rather than the average undrained shear strength for c_{u1}.

The bearing capacity factor, N_c, for a rectangular pile group is generally 9. However, for pile groups with relatively small pile embedment depths and/or relatively large widths, N_c should be calculated from the following equation where the terms D, B and Z are as shown in Figure 9-34.

$$N_c = 5\left(1+\frac{D}{5B}\right)\left(1+\frac{B}{5Z}\right) \le 9 \qquad 9\text{-}19$$

In the evaluation of possible block failure of pile groups in cohesionless soils underlain by a weak cohesive deposit, the weighted average unit shaft resistance for the cohesionless soils should be substituted for c_{u1} in calculating the ultimate group capacity. The pile group base strength determined from the second part of the ultimate group capacity equation should be calculated by using the strength of the underlying weaker layer.

9.6.2 Settlement of Pile Groups

Pile groups supported in and underlain by cohesionless soils will produce only elastic or immeidate settlements. This means that the settlements will occur almost immediately as the pile group is loaded. Pile groups supported in and underlain by cohesive soils may produce both elastic settlements that will occur almost immediately and consolidation settlements that will occur over a period of time. In highly over-consolidated clays, the majority of the foundation settlement will occur almost immediately. Consolidation settlements will generally be the major source of foundation settlement in normally consolidated clays.

Methods for estimating settlement of pile groups are provided in the following sections. Methods for estimating single pile settlements are not provided in this document because piles are usually installed in groups.

9.6.2.1 Elastic Compression of Piles

The methods for computing pile group settlement discussed in the following sections consider soil settlements only and do not include the settlement caused by elastic compression of pile material due to the imposed axial load. Therefore, the elastic compression should also be computed and added to the group settlement estimates of soil settlement to obtain the total settlement. The elastic compression can be computed by the following expression:

$$\Delta = \frac{Q_a L}{A E} \qquad 9\text{-}20$$

where: Δ = elastic compression of pile material in inches (mm)
Q_a = design axial load in pile in kips (kN)
L = length of pile in inches (mm)
A = pile cross sectional area in in^2 (mm^2)
E = modulus of elasticity of pile material in ksi (kPa)

The modulus of elasticity for steel piles is 30,000 ksi (207,000 MPa). For concrete piles, the modulus of elasticity varies with concrete compressive strength and is generally on the order of 4,000 psi (27,800 MPa). The elastic compression of short piles is relatively small and can often be neglected in design.

9.6.2.2 Settlement of Pile Groups in Cohesionless Soils

Meyerhof (1976) recommended the settlement of a pile group in a homogeneous sand deposit not underlain by a compressible soil be conservatively estimated by the following expressions in U.S. units:

$$s = \frac{4\, p_f \sqrt{B}\, I_f}{\overline{N'}} \qquad \text{For silty sand, use: } s = \frac{8\, p_f \sqrt{B}\, I_f}{\overline{N'}} \qquad 9\text{-}21$$

where: s = estimated total settlement in inches
p_f = design foundation pressure in ksf = group design load divided by group area
B = width of pile group in ft
$\overline{N'}$ = average corrected SPT $N1_{60}$ value within a depth B below pile toe
I_f = influence factor for group embedment $= 1 - [\, D / 8B \,] \geq 0.5$
D = pile embedment depth in ft

9.6.2.3 Settlement of Pile Groups in Cohesive Soils

Terzaghi and Peck (1967) proposed that pile group settlements could be evaluated using an equivalent footing situated at a depth of D/3 above the pile toe. This concept is illustrated in Figure 9-35. For a pile group consisting of only vertical piles, the equivalent footing has a plan area (B)(Z) that corresponds to the perimeter dimensions of the pile group as shown in Figure 9-34. The pile group load over this plan area is then the bearing pressure transferred to the soil through the equivalent footing. The load is assumed to spread within the frustum of a pyramid of side slopes at 30º and to cause uniform additional vertical pressure at lower levels. The pressure at any level is equal to the load carried by the group divided by the plan area of the base of the frustum at that level. Once the equivalent footing dimensions have been established then the settlement of the pile group can be estimated by using the procedures described in Chapter 8 (Shallow Foundations).

Rather than fixing the equivalent footing at a depth of D/3 above the pile toe for all soil conditions, the depth of the equivalent footing should be adjusted based upon soil stratigraphy and load transfer mechanism to the soil. Figure 9-36 presents the recommended location of the equivalent footing for the following load transfer and soil resistance conditions:

a) toe bearing piles in hard clay or sand underlain by soft clay
b) piles supported by shaft resistance in clay
c) piles supported in shaft resistance in sand underlain by clay
d) piles supported by shaft and toe resistance in layered soil profile

Note that Figures 9-35 and 9-36 assume that the pile group consists only of vertical piles. If a group of piles contains battered piles, then they should be included in the determination of the equivalent footing width only if the stress zones from the battered piles overlap with those from the vertical piles.

9.7 DESIGN OF PILES FOR LATERAL LOAD

The interaction of a pile-soil system subjected to lateral load has long been recognized as a complex function of nonlinear response characteristics of both pile and soil. The theory and design method for analyzing laterally loaded piles is beyond the scope of this document. Guidance on lateral load analysis is provided in FHWA (1994). The program LPILE is commonly used to evaluate the behavior of single piles under lateral loads. FHWA (2006a) discusses the use of LPILE program for piles subjected to lateral loads.

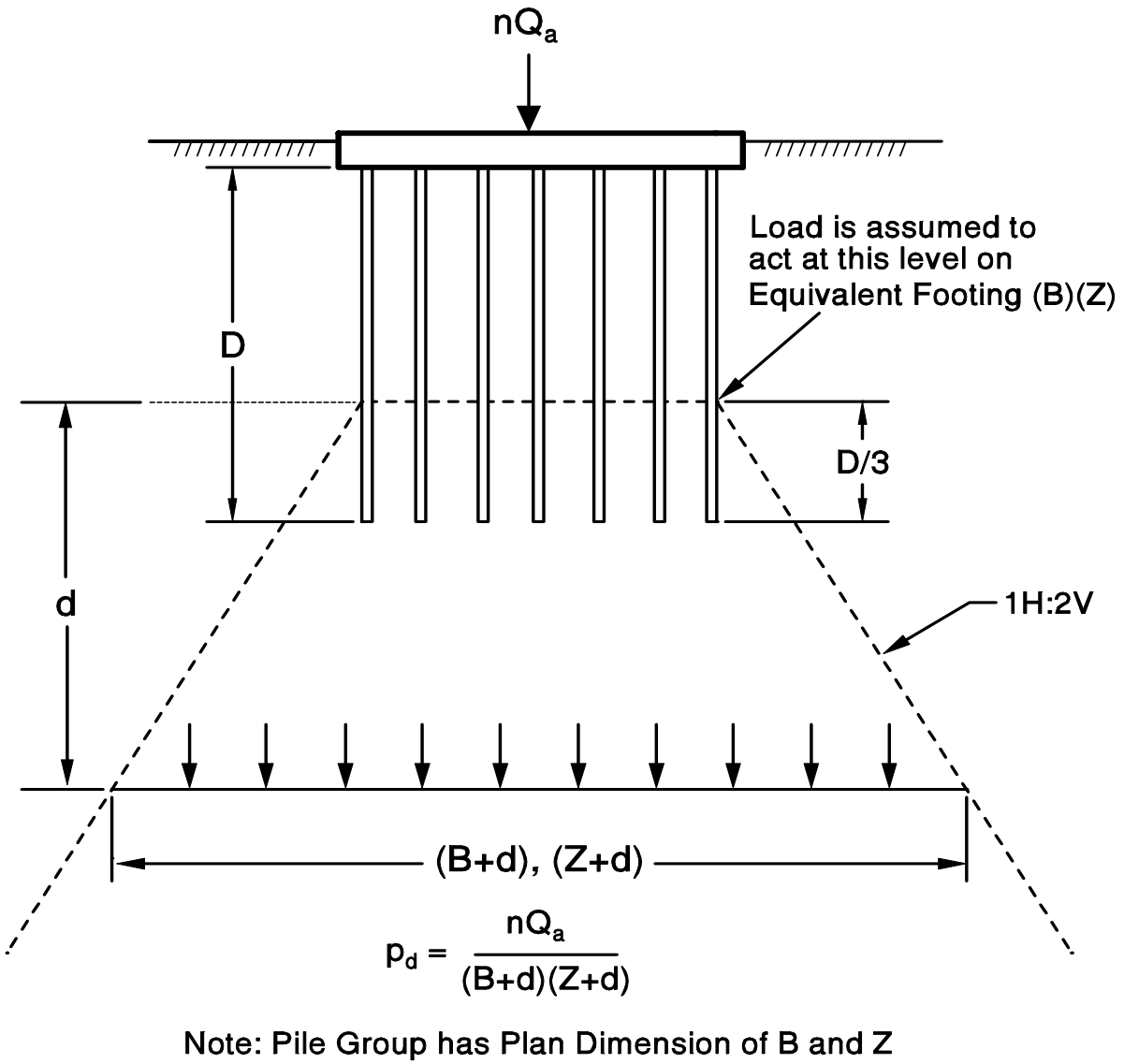

Figure 9-35. Equivalent footing concept (after Duncan and Buchignani, 1976).

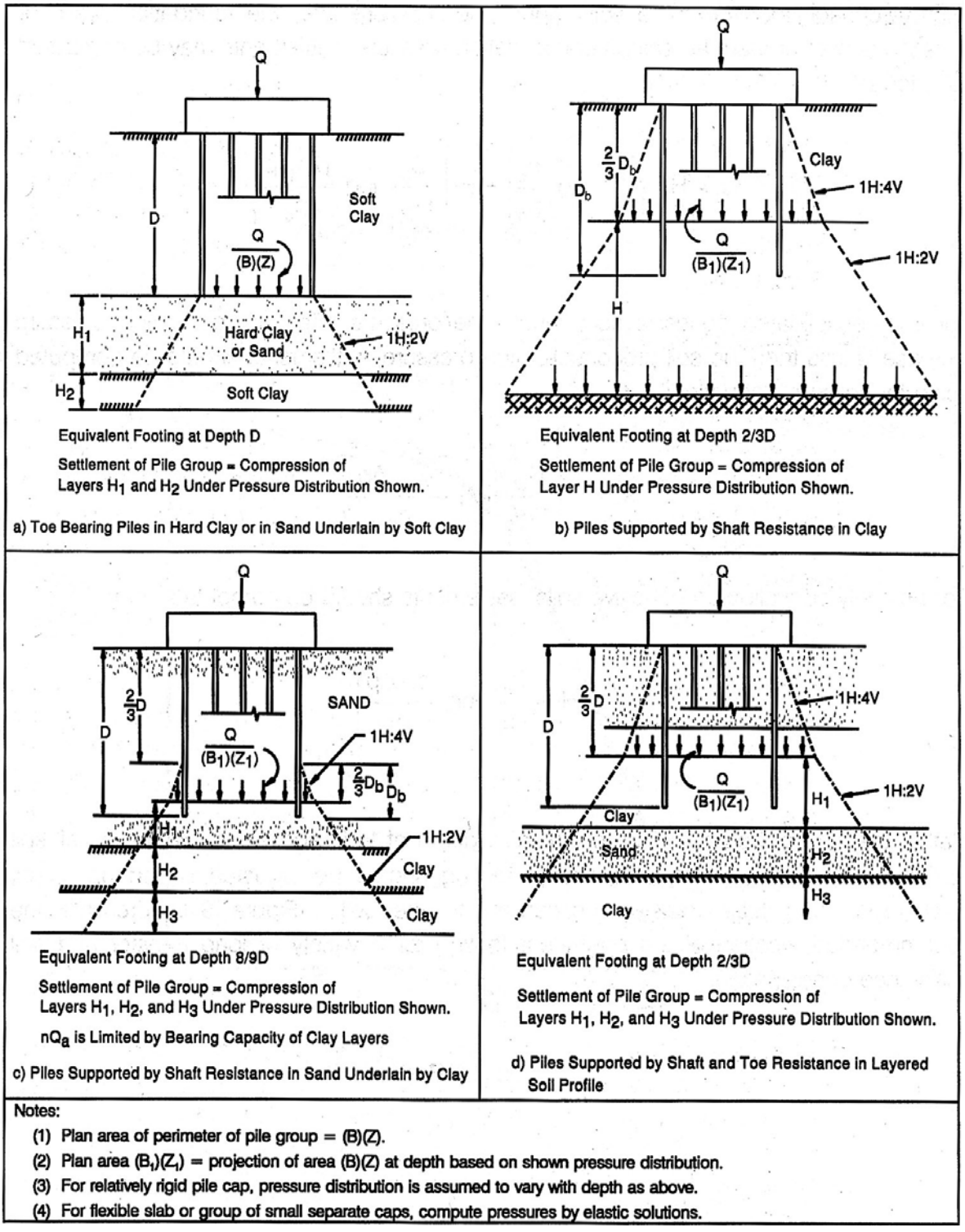

Figure 9-36. Stress distribution below equivalent footing for pile group (FHWA, 2006a).

9.8 DOWNDRAG OR NEGATIVE SHAFT RESISTANCE

When piles are installed through a soil deposit undergoing consolidation, the resulting relative downward movement of the soil around piles induces "**downdrag**" forces on the piles. These "downdrag" force is also called negative shaft resistance. Negative shaft resistance is the reverse of the usual positive shaft resistance developed along the pile surface that allows the soil to support the applied axial load. The downdrag force increases the axial load on the pile and can be especially significant on long piles driven through compressible soils. Therefore, the potential for negative shaft resistance must be considered in pile design. Batter piles should be avoided in soil conditions where relatively large soil settlements are expected because of the additional bending forces imposed on the piles, which can result in pile deformation and damage.

Settlement computations should be performed to determine the amount of settlement the soil surrounding the piles is expected to undergo after the piles are installed. The amount of relative settlement between soil and pile that is necessary to mobilize negative shaft resistance is about 0.4 to 0.5 inches (10 to 12 mm). At that amount of movement, the maximum value of negative shaft resistance is equal to the soil-pile adhesion. The negative shaft resistance can not exceed this value because slip of the soil along the pile shaft occurs at this value. It is particularly important in the design of friction piles to determine the depth at which the pile will be unaffected by negative shaft resistance. Only below that depth can positive shaft resistance provide support to resist vertical loads.

The most common situation where large negative shaft resistance develops occurs when fill is placed over a compressible layer immediately prior to, or shortly after piles are driven. This condition is shown in Figure 9-37(a). Negative shaft resistance can also develop whenever the effective overburden pressure is increased on a compressible layer through which a pile is driven as for example in the case of lowering of the ground water table as illustrated in Figure 9-37(b).

NCHRP (1993) presents the following criteria for identifying when negative shaft resistance may occur. If any one of these criteria is met, negative shaft resistance should be considered in the design. The criteria are:

1. The total settlement of the ground surface will be larger than 4 in (100 mm).

2. The settlement of the ground surface after the piles are driven will be larger than 0.4 in (10 mm).

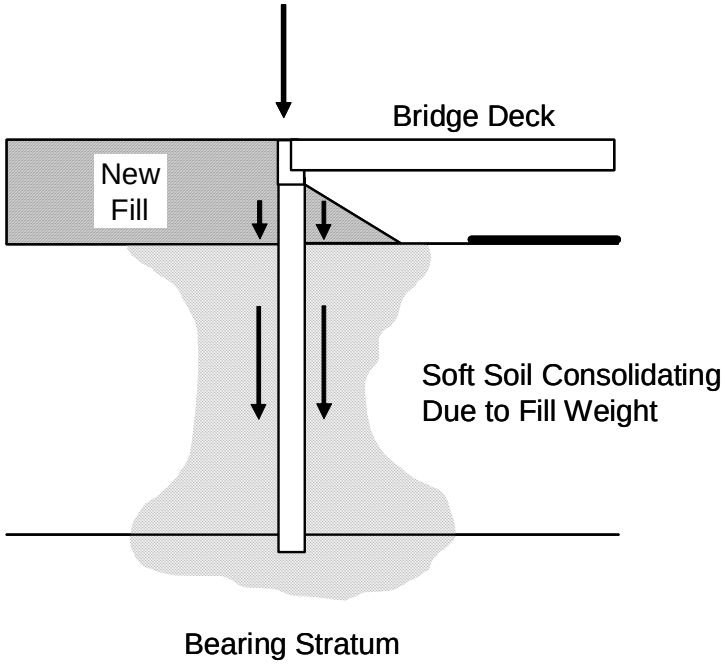

Figure 9-37(a). Common downdrag situation due to fill weight (FHWA, 2006a).

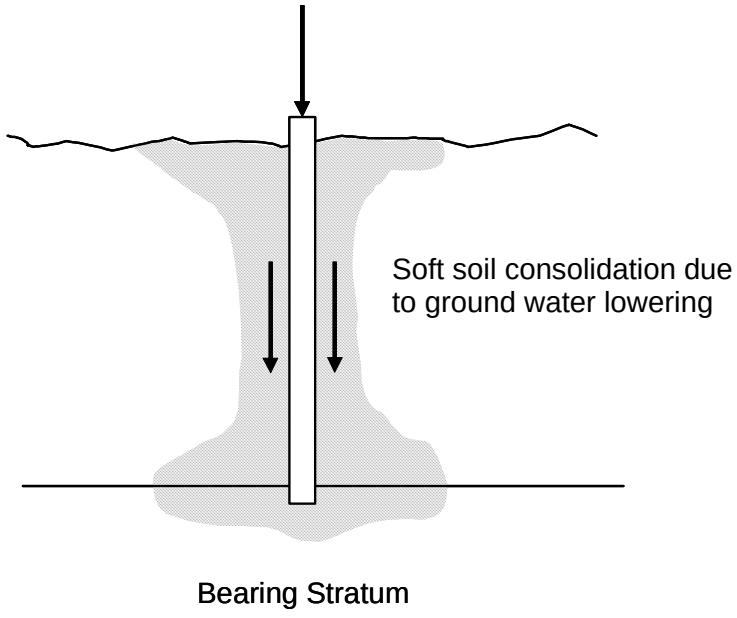

Figure 9-37(b). Common downdrag situation due to ground water lowering (FHWA, 2006a).

3. The height of the embankment to be placed on the ground surface exceeds 6.5 ft (2 m).

4. The thickness of the soft compressible layer is larger than 30 ft (10 m).

5. The water table will be lowered by more than 13 ft (4 m).

6. The piles will be longer than 80 ft (25 m).

For pile groups, the total downdrag load should not be calculated by summation of the downdrag load on each pile in the group. Rather, the downdrag load should be computed based on the perimeter surface area of the group block.

FHWA (2006a) presents several different methods for determining negative shaft resistance. In situations where the negative shaft resistance on piles is relatively large such that a reduction in the pile design load is impractical, negative shaft resistance forces can be handled or reduced by using one or more of the following techniques:

- Reduce soil settlement, e.g. by preloading the soil
- Use lightweight fill material
- Use a friction reducer such as bitumen and plastic wrap. These reducers are prone to being scrapped off during driving and are not considered to be reliable.
- Increase allowable pile-stress
- Prevent direct contact between soil and pile, e.g., pile sleeves

The above options for reducing negative shaft resistance are discussed in FHWA (2006a).

9.9 CONSTRUCTION OF PILE FOUNDATIONS

Construction control of pile operations is a much more difficult proposition than for spread footings. During footing placement an inspector can easily examine a prepared footing area and observe the concrete footing being poured to assure a quality foundation. Piles derive their support below ground. Direct quality control of the finished product is not possible. Therefore, substantial control must be maintained over the peripheral operations leading to the incorporation of the pile into the foundation. In general terms, control is exercised in two areas; the pile material, and the installation equipment. These items are interrelated since changes in one may affect the others. It is mandatory that pile foundation installation be considered during design to insure that the piles shown on the plans can be installed. This section discusses the installation and construction monitoring aspects of driven pile foundations.

9.9.1 Selection of Design Safety Factor Based on Construction Control

The topic of selection of a suitable design safety factor based on construction control was discussed in Section 9.4. It is reiterated that the factor of safety used should be based on the construction control method used for capacity verification. **The factor of safety applied to the design load should increase with the increasing unreliability of the method used for determining ultimate pile capacity during construction.** The recommended factors of safety on the design load for various construction control methods were presented in Table 9-5. The factor of safety for other test methods not included in Table 9-5 should be determined by the individual designer.

9.9.2 Pile Driveability

Greater pile penetration depths are increasingly being required to satisfy performance criteria in special design events such as scour, vessel impact, ice and debris loading, and seismic events. Therefore, the ability of a pile to be driven to the required depth has become increasingly more important and must be evaluated in the design stage. **Pile driveability refers to the ability of a pile to be driven to a desired depth and/or capacity.** All of the previously described static analysis methods are meaningless if the pile cannot be driven to the required design depth without sustaining damage. **The limit of pile driveability is the maximum soil resistance a pile can be driven either without sustaining damage or a refusal driving resistance with a properly sized driving system.**

Primary factors controlling the ultimate geotechnical capacity of a pile are the **pile details** (type and length), **subsurface data**, and the method of **installation**. Table 9-9 highlights these factors

and the items to be included in the plans and specifications that are the design engineer's responsibility. Also included in Table 9-9 are the items to be checked for quality assurance that are the construction engineer's responsibility. Since the pile type, length and method of installation can be specified, it is often erroneously assumed that the pile can be installed as designed to the estimated depth. However, the pile must have sufficient driveability to overcome the soil resistance encountered during driving in order to reach the estimated or specified depth. If a pile section does not have a driveability limit in excess of the soil resistance to be overcome during driving, it will not be driveable to the desired depth. **The failure to evaluate pile driveability is one of the most common deficiencies in driven pile design practice.**

In evaluating the driveability of a pile, the soil disturbance during installation and the time dependent soil strength changes should be considered. Both soil setup and relaxation have been described earlier in this chapter. For economical pile design, the foundation designer must match the soil resistance to be overcome at the time of driving with the pile impedance, the pile material strength, and the pile driving equipment. These factors are discussed in the following section.

9.9.2.1 Factors Affecting Driveability

A pile must satisfy two aspects of driveability. First, the pile must have sufficient stiffness to transmit driving forces large enough to overcome soil resistance. Second, the pile must have sufficient structural strength to withstand the driving forces without damage.

The primary controlling factor on pile driveability is the pile impedance, which is defined as EA/C, where E is the elastic modulus of pile material, A is the cross-sectional area of the pile and C is the wave propagation velocity of pile material. Since E and C are constant for a given type of pile, only increasing the pile cross sectional area, A, will improve the pile driveability. For steel H-piles, the designer can improve pile driveability by increasing the H-pile section without increasing the H-pile size. The driveability of steel pipe piles can be improved by increasing the pipe wall thickness. For open ended pipe piles, an inside-fitting cutting shoe can improve driveability by delaying the formation of a soil plug and thereby reducing the soil resistance to be overcome. Most concrete piles are solid cross sections. Therefore, increasing the pile area to improve driveabilty is usually accompanied by an increase in the soil resistance to driving.

Table 9-9. Responsibilities of design and construction engineers

Item	Design Engineer's Responsibilities	Construction Engineer's Responsibilities
Pile Details	Include in plans and specifications: a. Material and strength: concrete, steel, or timber. b. Cross section: diameter, tapered or straight, and wall thickness. c. Special coatings for corrosion or downdrag. d. Splices, toe protection, etc. e. Estimated pile tip elevation. f. Estimated pile length. g. Pile design load and ultimate capacity. h. Allowable driving stresses.	Quality control testing or certification of materials.
Subsurface Data	Include in plans and specifications: a. Subsurface profile. b. Soil resistance to be overcome to reach estimated length. c. Minimum pile penetration requirements. d. Special notes: boulders, artesian pressure, buried obstructions, time delays for embankment fills, etc.	Report major discrepancies in soil profile to the designer.
Installation	Include in plans and specifications: a. Method of hammer approval. b. Method of determining ultimate pile capacity. c. Compression, tension, and lateral load test requirements (as needed) including specification for tests and the method of interpretation of test results. d. Dynamic testing requirements (as needed). f. Limitations on vibrations, noise, and head room. g. Special notes: spudding, predrilling, jetting, set-up period, etc.	a. Confirm that the hammer and driving system components agree with the contractor's approved submittal. b. Confirm that the hammer is maintained in good working order and the hammer and pile cushions are replaced regularly. c. Determination of the final pile length from driving resistance, estimated lengths and subsurface conditions. d. Pile driving stress control. e. Conduct pile load tests. f. Documentation of field operations. g. Ensure quality control of pile splices, coatings, alignment and driving equipment.

A lesser factor influencing pile driveability is the pile material strength. The influence of pile material strength on driveability is limited, since strength does not alter the pile impedance. However, a pile with a higher pile material strength can tolerate higher driving stresses that may allow a larger pile hammer to be used. Use of larger hammer may allow a slightly higher capacity to be obtained before driving refusal or pile damage occurs.

Other factors that may affect pile driveability include the characteristics of the driving system such as ram weight, stroke, and speed, as well as the actual system performance in the field. The dynamic soil response can also affect pile driveability. Soils may have higher damping characteristics or elasticity than assumed, both of which can reduce pile driveability. These factors are discussed in Section 9.9.3 and 9.9.6.

Even if the pile structural capacity and geotechnical capacity both indicate a high pile capacity could be used, a high pile capacity may still not be obtainable because driving stresses may exceed allowable driving stress limits. A pile cannot be driven to an ultimate static capacity that is as high as the structural capacity of the pile because of the additional dynamic resistance or damping forces generated during pile driving. The allowable static design stresses in pile materials specified by various codes generally represent the static stress levels that can be consistently developed with normal pile driving equipment and methods. Maximum allowable design and driving stresses are presented in Section 9.9.7.

9.9.2.2 Driveability Versus Pile Type

Driveability should be checked during the design stage of all driven piles. It is particularly important for closed end steel pipe piles where the impedance of the steel casing may limit pile driveability. Although the designer may attempt to specify a thin-wall pipe without mandrel in order to save material cost, a thin wall pile may lack the driveability to develop the required ultimate capacity or to achieve the necessary pile penetration depth. Wave equation analyses should be performed in the design stage to select the pile section and wall thickness.

Steel H-piles and open-end pipe piles, prestressed concrete piles, and timber piles are also subject to driveability limitations. This is particularly true as allowable design stresses increase and as special design events such as scour require increased pile penetration depths. The driveability of long prestressed concrete piles can be limited by the pile's tensile strength.

The following sections discuss the various aspects related to pile driveability. First, the pile driving equipment and operation (Section 9.9.3) is introduced followed by the fundamental pile driving formula (Section 9.9.4), basics of the dynamic analysis of pile driving (Section 9.9.5),

use of wave equation methodology to perform dynamic analysis of pile driving (Section 9.9.6), discussion of driving stresses (Section 9.9.7), and some useful guidelines to assess the results of wave equation analysis in terms of pile driveability (Section 9.9.8). General pile construction monitoring considerations are discussed in Section 9.9.10 followed by a brief description of the elements of dynamic pile monitoring in Section 9.9.11.

9.9.3 Pile Driving Equipment and Operation

Proper inspection of pile driving operations requires that the inspector have a basic understanding of pile driving equipment. Estimation of "as driven pile capacity" is usually based on the number of hammer blows needed to advance the pile a given distance. Each hammer blow transmits a given amount of energy to the pile. The total number of blows is the total energy required to move the pile a given distance. This energy can then be related to soil resistance and supporting capacity. However, pile inspection entails more than counting blows of the hammer.

The energy transmitted to the pile by a given hammer can vary greatly depending on the equipment used by the contractor. Energy losses can occur by poor alignment of the driving system, improper or excessive cushion material, improper appurtenances, or a host of other reasons. As the energy losses increase, additional blows are required to move the pile. The manufacturer's rated hammer energy is based on minimal energy losses. Assumptions that the hammer is delivering its rated energy to the pile can prove dangerous if substantial energy is lost in the driving system. Artificially high blow counts can result in acceptance of driven pile lengths, which are shorter than that necessary for the required pile capacity.

Important elements of the driving system include the **leads**, the **hammer cushion**, the **helmet**, and for concrete piles, the **pile cushion**. Typical components of a pile driving system are shown in Figure 9-38. The leads are used to align the hammer and the pile such that every hammer blow is delivered concentrically to the pile system. The helmet holds the top of the pile in proper alignment and prevents rotation of the pile during driving. Typical components of a helmet are shown in Figure 9-39. The hammer and the helmet “ride” in the leads so that hammer - pile alignment is assured.

All impact pile driving equipment, except some gravity hammers should be equipped with a suitable thickness of hammer cushion material. The function of the hammer cushion is to prevent damage to the hammer or pile and insure uniform energy delivery per blow to the pile. Hammer cushions must be made of durable manufactured materials provided in accordance with the hammer manufacturer's guidelines. All wood, wire rope and asbestos hammer cushions are

specifically disallowed and should not be used. The thicker the hammer cushion, the less the amount of energy transferred to the pile. Mandatory use of a durable hammer cushion material, which will retain uniform properties during driving, is necessary to relate blow count to pile capacity accurately. Non-durable materials, which deteriorate during driving, cause erratic energy delivery to the pile and prevent the use of blow counts to determine pile capacity.

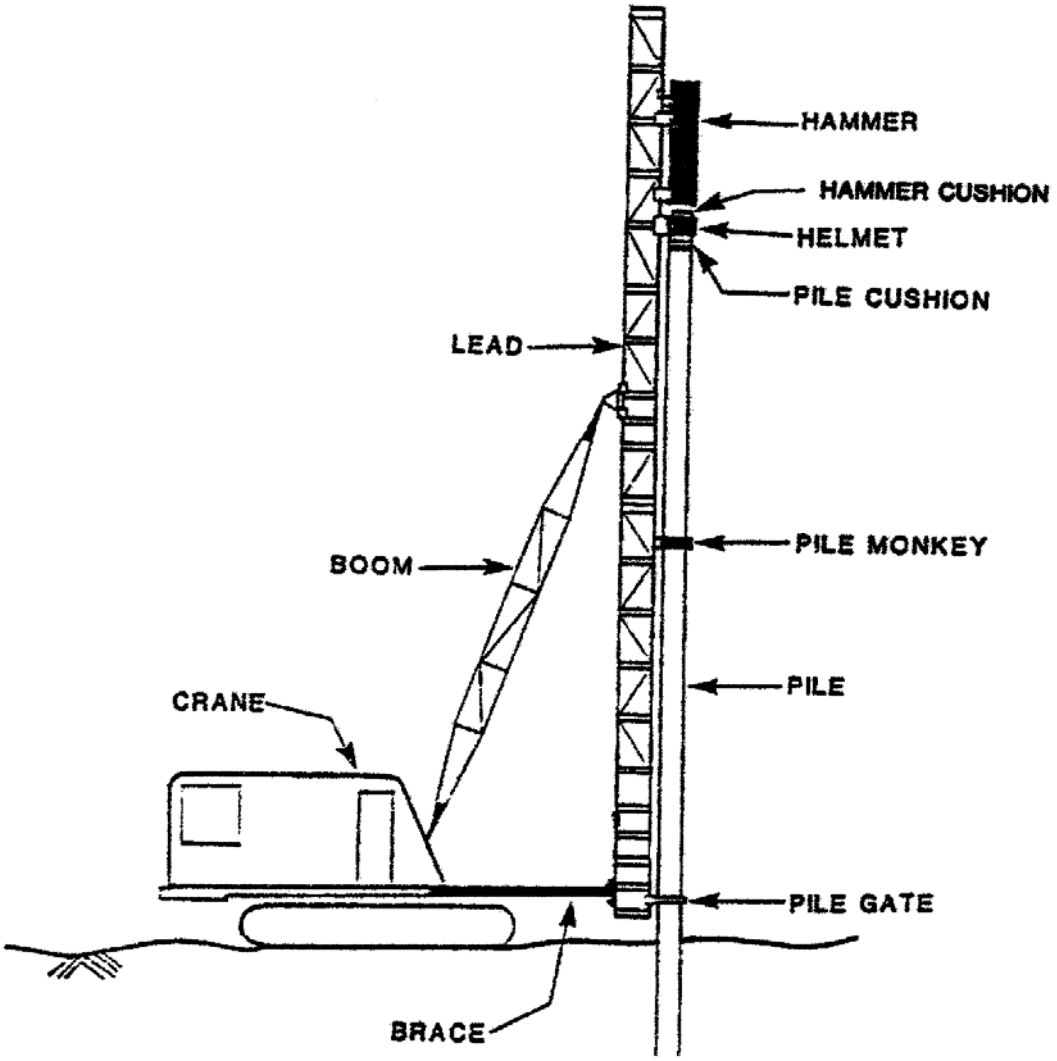

Figure 9-38. Typical components of a pile driving system.

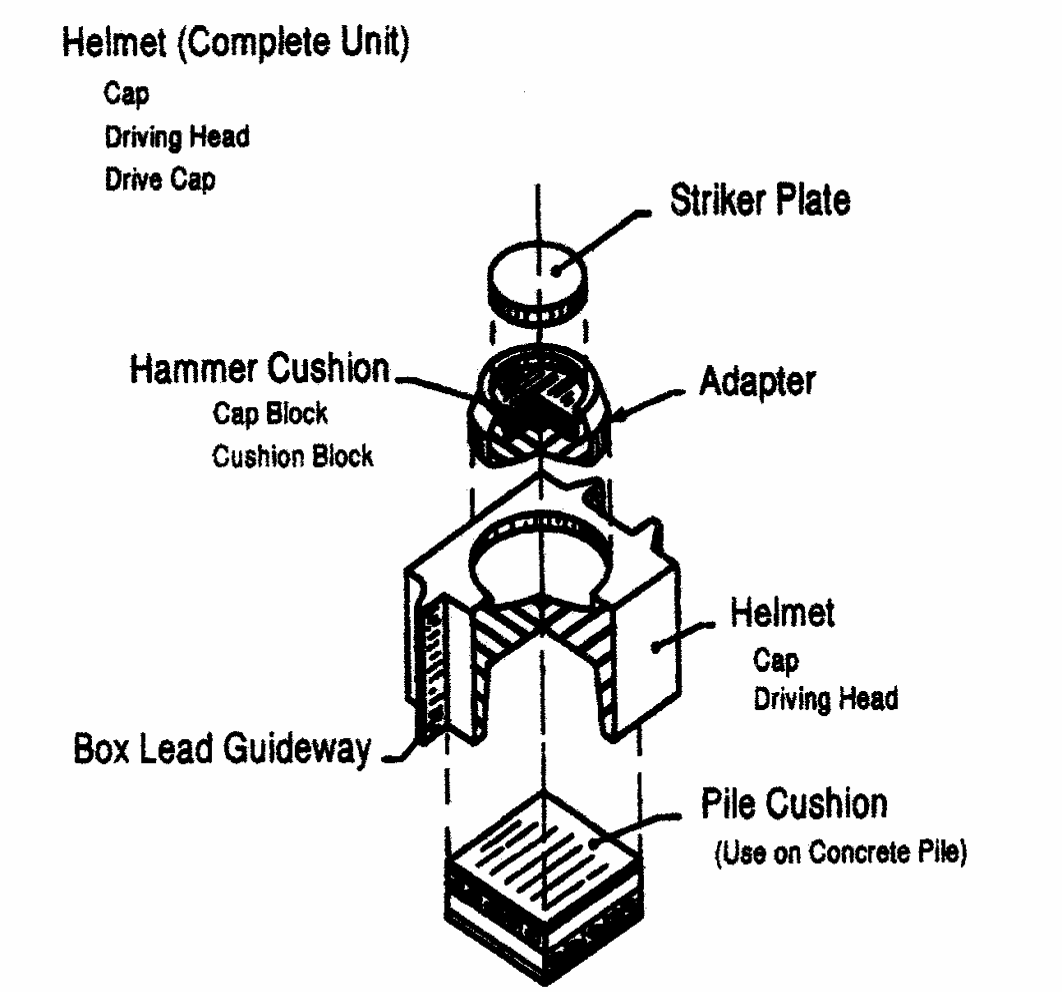

Note: The helmet shown is for nomenclature only. Various sizes and types are available to drive H, pipe, concrete (shown) and timber piles. A system of inserts or adapters is utilized up inside of the helmet to change from size to size and shape to shape.

Figure 9-39. Typical components of a helmet.

The heads of concrete piles must be protected by a pile cushion made of hardwood or plywood. The minimum thickness of pile cushion placed on the pile head should not be less than four inches. A new pile cushion should be provided for each pile.

A non-routine element called a **follower** may be used in the driving system, particularly for piles driven below water. Followers cause substantial and erratic reduction in the hammer energy transmitted to the pile due to the follower is flexibility, poor connection to the pile head, frequent misalignment, etc. Reliable correlation of blow count with pile capacity is impossible when followers are used. Special monitoring with devices such as the Pile Driving Analyzer (PDA) (FHWA, 2006a) should be specified when followers are used.

9.9.4 Dynamic Pile Driving Formulae

In the 1800s, the fundamental pile driving formula was established to relate dynamic driving forces to available pile bearing capacity. The formula was based on a simple energy balance between the kinetic energy of the ram at impact and the resulting work done on the soil, i.e., a distance of pile penetration against a soil resistance. The concept assumed a pure Newtonian impact with no energy loss. The fundamental formula was expressed as follows:

WORK DONE ON SOIL = KINETIC ENERGY INPUT

$$RS = WH = 12\ E_n \qquad 9\text{-}22$$

where: W = weight of the ram in pounds
H = distance of ram fall in feet
R = total soil resistance against the pile (driving capacity) in pounds
S = pile penetration per blow (set) in inches
E_n = driving energy (ft-lbs), which is converted to in-lbs for unit consistency by multiplying by 12.

An inherent difficulty in the pile driving operation is that only a portion of the ram's kinetic energy actually causes penetration of the pile. Studies indicate that typically only 30 to 65 percent of the rated energy is passed through to the pile. Much of the energy is lost in either heat (soil friction, hammer mechanism, pile material, etc.) or strain (elastic compression of the cushion, the pile and the surrounding soil). For example, if the elastic shortening of the pile (ΔL) is RL/AE, where L = the effective length of the pile in inches, A = the cross sectional area of the pile in in^2, and E = modulus of elasticity of the pile material in lbs/in^2, then the average shortening along the length of the pile would be $\Delta L/2$ and the energy lost due to elastic compression of the pile would be $R(\Delta L/2)$ or $R^2L/2AE$. Therefore, if all losses are ignored except those due to elastic compression of the pile, then Equation 9-22 can be re-written as:

$$RS = 12\,E_n - \frac{R^2 L}{2AE} \qquad 9\text{-}23a$$

If the pile is driven through reasonably uniform soil the effective length, L, is the full length of pile penetration. If the pile is driven through relatively firm soil into a weaker substratum, the effective length is generally taken as the length from the head of the pile to the depth of the weak substratum.

If k is defined as RL/2AE then Equation 9-23a can be re-written as:

$$RS = 12\,E_n - Rk \qquad 9\text{-}23b$$

When Equation 9-23b is solved for total soil resistance (R) the result is the Engineering News pile driving formula:

$$R = \frac{12\,E_n}{S + k} \qquad 9\text{-}24$$

The Engineering News (EN) pile driving formula was first published in the *Engineering News* in the year 1888. The EN formula is commonly, but incorrectly termed the ENR formula since the publishers of the *Engineering News* merged with the McGraw-Hill Publishing Company in 1917 to produce the *Engineering News-Record*. The EN formula was developed for wood piles driven by a drop hammer. As expressed by Equation 9-24, the EN formula is for driving resistance. Subsequently, in an attempt to develop a relationship between driving resistance and bearing capacity, the equation was modified to provide the safe load that a pile could withstand to the input energy and set per blow. The basic assumption in the modification of the original EN formula is that the safe working load (P) is one-sixth of the driving resistance. Therefore, the basic EN formula as we know it today is:

$$P = \frac{R}{6} = \frac{2E_n}{S + k} \qquad 9\text{-}25$$

where:
- E_n = driving energy (ft-lbs).
- S = pile penetration per blow (set) in inches.
- k = constant based on hammer type = 0.1 for single acting steam hammer and 1 for drop hammer.

According to Hough (1957), the basic assumption that the safe working load (P) is one-sixth of the driving resistance is not the same as applying a factor of safety of 6 to the ultimate bearing capacity under static load. The real factor of safety for the EN formula may be considerably more or even less than 6 under certain conditions

Most engineers are not aware (1) that the EN formula was originally developed for timber piles, or (2) that the EN formula has a built-in factor of safety of 6. Sowers (1979) states the following about the EN formula:

"The EN formula was derived from observations of the driving of wood piles in sand with free-falling drop hammers. Numerous pile load tests show that the real factor of safety of the formula can be as low as 2/3 and as high as 20. For wood piles driven with free-falling drop hammers and for lightly loaded short piles driven with a steam hammer, the EN formulas give a crude indication of pile capacity. For other conditions they can be very misleading."

In 1988 the Washington State DOT published a study (WSDOT, 1988) based on high quality pile load test data that showed the EN formula to be the least reliable of the 10 dynamic formulae that were analyzed. Subsequent studies by FHWA as part of the Demonstration Project 66 (precursor of the FHWA (2006a) manual) confirmed the unreliability of the EN formula, particularly for higher pile loads where actual safety factors are too frequently less than 1.0.

The WSDOT and FHWA studies resulted in both organizations replacing EN in their specifications with the Gates dynamic formula. However, the Gates dynamic formula, which was originally developed based on correlations with static load test data, is usually restricted to piles that have driving capacities less than 600 kips. The Gates formula, was modified by FHWA for driving capacity as shown below:

$$R_u = 1.75\sqrt{E_r}\log_{10}(10N_b) - 100 \qquad \text{9-26a}$$

where: R_u = the ultimate pile capacity (kips)

E_r = the manufacturer's rated hammer energy (ft-lbs) at the **field observed ram stroke**

N_b = the number of hammer blows per 1 inch at final penetration

The number of hammer blows per foot of pile penetration required to obtain the ultimate pile capacity is calculated as follows:

$$N/ft = 12\ (10^x) \qquad \text{9-26b}$$

where: $x = [(R_u + 100)/(1.75\sqrt{E_r})] - 1$

9.9.5 Dynamic Analysis of Pile Driving

An examination of the pile driving process discloses that the concept of a Newtonian impact does not apply. When viewed in slow motion, the ram does not immediately rebound from the pile after impact. The ram transfers force to the pile head over a finite period of time that depends on the properties of the hammer-pile-soil system. A force pulse is created that travels down the pile in a **wave** shape. The amplitude of the wave will decay due to system damping properties before reaching the pile tip. The force in the wave, which reaches the tip, will "pull" the pile tip into the soil before the wave is reflected back up the pile. After reflection, an amount of permanent "set" of the pile tip will remain. This process is crudely shown in Figure 9-40 for the hammer-pile-soil system.

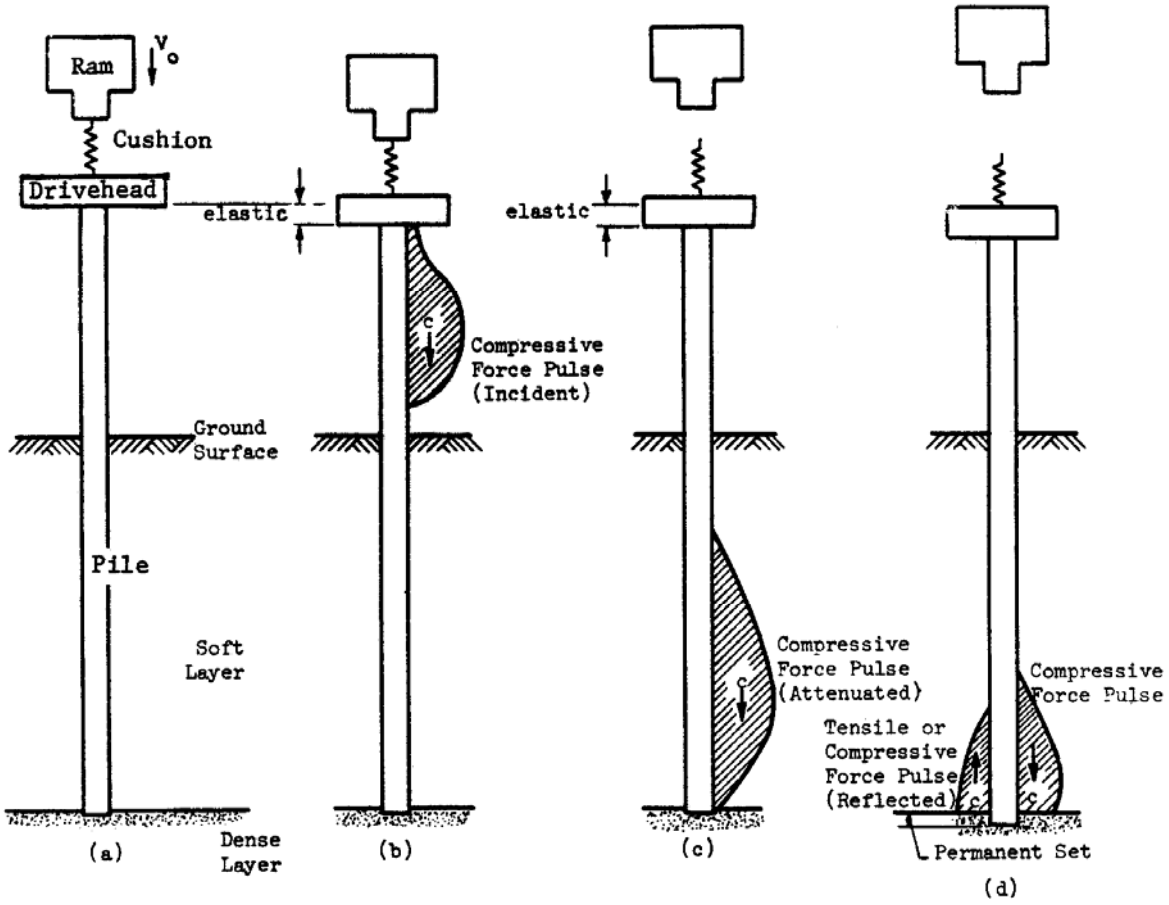

Figure 9-40. Hammer-pile-soil system.

The analysis of the force pulse wave is commonly known as the **wave equation analysis** (WEA). In a WEA a number of variables such as pile length and flexibility are accounted for in addition to the variations in the contractor's driving system and the project soils. Therefore, WEA represents a significant improvement over dynamic formulas. The approach was developed by E.A.L. Smith (1960), and after the rationality of the approach had been recognized, several researchers developed a number of computer programs. For example, the Texas Department of Highways supported research at the Texas Transportation Institute (TTI) in an attempt to determine driving stresses and reduce concrete pile damage by using a realistic analysis method. FHWA sponsored the development of both the TTI program (Hirsch, *et al.,* 1976) and WEAP (Goble and Rausche, 1976). FHWA supported the development of WEAP to obtain analysis results backed by measurements taken on construction piles during installation for a variety of hammer models. WEAP was updated several times under FHWA sponsorship until 1986 (Goble and Rausche, 1986). Later, additional options, improved data files, refined mathematical representations and modern user conveniences were added to this program on a proprietary basis, and the program is now known as GRLWEAP (Pile Dynamics, Inc. 2005). TNOWAVE is a similar program developed in the Netherlands since 1970s and is popular in Europe and elsewhere. Similar computer programs based on the method of characteristics have been developed such as PDPWAVE (Bielefeld and Middendorp, 1992).

The wave equation approach has been subjected to a number of checks and correlation studies. Studies on the performance of WEAP have produced publications demonstrating that program's performance and utility (e.g., Blendy 1979, Soares, *et al.* 1984, Rausche, *et al.*, 2004). In the WEA approach, it is recognized that each element in the hammer-pile-soil system affects the pile penetration and stresses caused in the pile. A few characteristics of each element are discussed below before the WEA methodology is discussed in detail.

1. Hammer

- Pile hammers can be categorized into two main types: impact hammers and vibratory hammers. There are numerous types of impact hammers having variations in the types of power source, configurations, and rated energies.

- Mechanical efficiency determines what percentage of rated energy is transmitted by the ram. Typical values of mechanical efficiency for hammers in good condition are 50% for double or differential acting air hammers, 67% for single acting air/steam hammers, 80% for diesel hammers, and 80 to 95% for hydraulic hammers.

- Force wave shape characteristics are different for different hammer types. The shape affects pile stress and pile penetration.

2. Pile and Appurtenances (Cushions, Helmets, etc.)

- The stiffness of appurtenances such as the hammer cushion is defined by the cross sectional area times the modulus of elasticity divided by the thickness. The stiffness has a major effect on both blow count and stress transfer to the pile. These elements must not degrade during driving as observed blow count will decrease and pile stresses increase.

- As noted in Section 9.9.2.1, pile impedance affects pile driveability. The cross sectional area of the pile does not control pile driveability. As an example, an HP 14x117 has a cross-sectional area of 34.4 in^2 (0.22 m^2) and an impedance of 61.4 k-s/ft (900 kN-s/m). A 12 in square concrete pile has a cross-sectional area of 144 in^2 (0.93 m^2)and an impedance of 57.9 k-s/ft (845 kN-s/m). Hence, the H pile has better driveability even though it has approximately 25% of the cross-sectional area of the concrete pile.

3. Soil

- Soil strength may be permanently or temporarily changed during driving. Piles being driven into soil that contains large percentages of fines may require restrikes to estimate long term capacity due to effects of set-up or relaxation.

- The damping properties of the soil surrounding the pile can have a dramatic effect on the observed blow count. An increase in damping decreases driveability. Damping parameters can be estimated by soil type or from basic index test data. Consideration of the dynamic aspects of the field pile driving operation is necessary so that the driving characteristics can be related to the static pile capacity. Foundation designers should routinely consider the potential for dynamic effects such as set-up and include provisions for field observations such as restrikes. In addition, construction control of pile driving should account for basic dynamic parameters that influence blow count and pile stress. Some of these parameters can be controlled by specification; others require use of a pile wave equation analysis.

9.9.6 Wave Equation Methodology

The wave equation analysis (WEA) is a tool to understand the variable involved in pile driving. In a WEA, the hammer, helmet, and pile are modeled by a series of segments each consisting of a concentrated mass and a weightless spring. A schematic of the wave equation hammer-pile-soil model is presented in Figure 9-41. The hammer and pile segments are approximately 3 ft in length. Spring stiffness and mass values are calculated from the cross sectional area, modulus of elasticity, and specific weight of the corresponding pile section. Hammer and pile cushions are represented by additional springs whose stiffnesses are calculated from area, modulus of elasticity, and thickness of the cushion materials. In addition, coefficients of restitution (COR) are usually specified to model energy losses in cushion materials and in all segments that can separate from their neighboring segments by a certain slack distance. The COR is equal to unity for a perfectly elastic collision that preserves all energy and is equal to zero for a perfectly plastic condition that loses all deformation energy. The usual condition of partially elastic collisions is modeled with an intermediate COR value.

The soil resistance along the embedded portion of the pile and at the pile toe is represented by both static and dynamic components. Therefore, both a static and a dynamic soil resistance force acts on every embedded pile segment. The static soil resistance forces are modeled by elasto-plastic springs and the dynamic soil resistance by dashpots. The displacement at which the soil changes from elastic to plastic behavior is referred to as the soil "**quake**," q. The dynamic soil resistance is proportional to a damping factor, J, times the pile velocity times the assigned static soil resistance. The parameters q and J are shown in lower left hand corner of Figure 9-41. In simple terms, q, is a parameter used in determination of static resistance while J is a parameter used in determination of dynamic resistance.

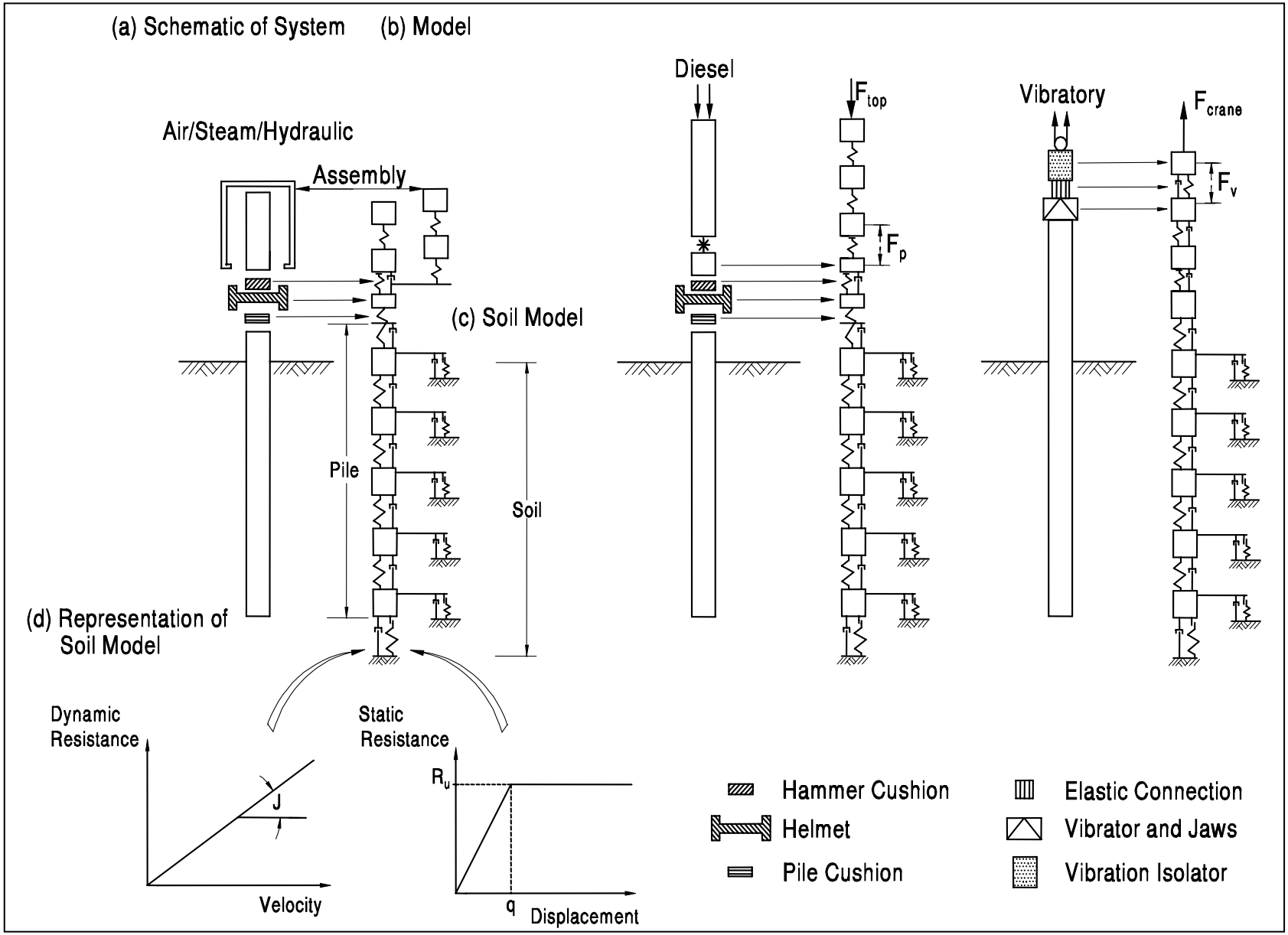

Figure 9-41. Typical Wave Equation models (FHWA 2006a).

9.9.6.1 Input to Wave Equation Analysis

In a typical wave equation analysis, parameters defining the hammer, pile (plus appurtenances), and soil systems are needed. The confidence level that can be assigned to the output is directly related to how well the project-specific input parameters are known. The basic input parameters are discussed below.

- **Hammer Data**: Hammer input properties are usually well known from a manufacturers' database. In a driveability analysis, hammer types are selected based on the soil resistance to be overcome. In construction monitoring analysis the contractor submits the intended driving system for review and approval. If a satisfactory driving system is submitted and approved, then the only major concern in construction is that the hammer is in good working condition as was assumed for the input.

- **Driving System or Appurtenance Data**: The driving system or appurtenance data consists of information on hammer cushion, helmet including striker plate, inserts, adapters, etc. and pile cushion in case of concrete piles. The properties of cushions, for both hammer and pile, are especially critical. Only manufactured materials whose properties remain reasonably constant during driving can be used with confidence. The actual cushion thickness used in the field must be checked and discrepancies reported so that the wave equation analysis can be modified.

- **Pile Data**: Required pile data consists of total length, cross-sectional area, elastic modulus and weight, all as a function of depth. This is the pile profile. ***The wave analysis cannot predict pile length***. This fact is commonly misunderstood by engineers. Pile length is determined by static analysis procedures and then used as input to pile wave analyses. One exception is a "driveability analysis" where pile behavior is assessed at various depths. The cross sectional area of the pile is frequently varied in design analyses to determine which section is both driveable and cost effective. Increasing the pile section has the effect of improving driveability as well as reducing pile stresses.

- **Soil Data**: Soil data input requires both an understanding of site-specific soil properties and the effects of pile driving on those properties. Dynamic properties such as damping and quake are roughly correlated with soil type. These properties are best determined by experienced geotechnical specialist. The driving soil resistance and its distribution are determined from the static analysis. The driving soil resistance may be substantially greater than the design load times the safety factor; particularly for piles in scour situations. Also the dynamic effects of pile driving on soil resistance must be

considered by an experienced geotechnical specialist to determine set-up or relaxation values for ultimate soil resistance. These dynamic effects are frequently overlooked, which can result in large variations between estimated and actual pile lengths.

9.9.6.2 Output Values from Wave Equation Analysis

The results of a wave equation analysis include the predicted blow count, pile stresses, and delivered hammer energy for an assigned driving soil resistance, R_{ult}, and for given hammer, driving system (appurtenance), pile and soil conditions. **Each wave equation analysis is for the specific pile length that was considered in the analysis.** A summary table of the results obtained from a wave equation analysis is shown in Table 9-10. The data shown in Table 9-10 was generated for a specific site where a pile length of 50 ft (15 m) was being analyzed.

Table 9-10
Summary of example results from wave equation analysis

R_{ult} kips	Blow Count BPF	Stroke (EQ) ft	Tensile Stress ksi	Compressive Stress ksi	Transfer Energy ft-kip
35.0	7	3.27	-0.73	1.68	13.6
80.0	16	3.27	-0.32	1.71	13.6
140.0	30	3.27	-0.20	1.73	13.0
160.0	35	3.27	-0.14	1.73	13.0
195.0	49	3.27	-0.00	1.75	12.8
225.0	63	3.27	0.0	1.96	12.7
280.0	119	3.27	0.0	2.34	12.6
350.0	841	3.27	0.0	2.75	12.5
Note that for each driving resistance (R_{ult}), a value of blow count, hammer stroke, tensile stress, compressive stress, and transferred energy has been computed. The data is also commonly shown in graphical form as noted in Figure 9-42.					

9.9.6.3 Pile Wave Equation Analysis Interpretation

The data in Table 9-10, when plotted as shown in Figure 9-42, presents the predicted relationship between pile hammer blow count and other variables for the situation when the pile is embedded 50 ft (15 m) in the ground. The plot, which relates the ultimate capacity to penetration resistance, is known as a **bearing graph**. The data in Table 9-10 is interpreted in the field by comparing them with the measured blow count at a pile penetration of 50 ft (15 m) as follows. When the pile reaches 50 ft (15 m), if the blow count is 49, the driving resistance is 195 kips (867 kN), the stroke is 3.27 ft (0.99 m), the tensile stress is zero ksi, the compressive stress is 1.75 ksi (12,069 kPa), and transferred energy is 12.8 ft-kips (17.3 m-kN). If the blow count had been 63 the driving resistance would have been predicted to be 225 kips (1,000 kN), etc.

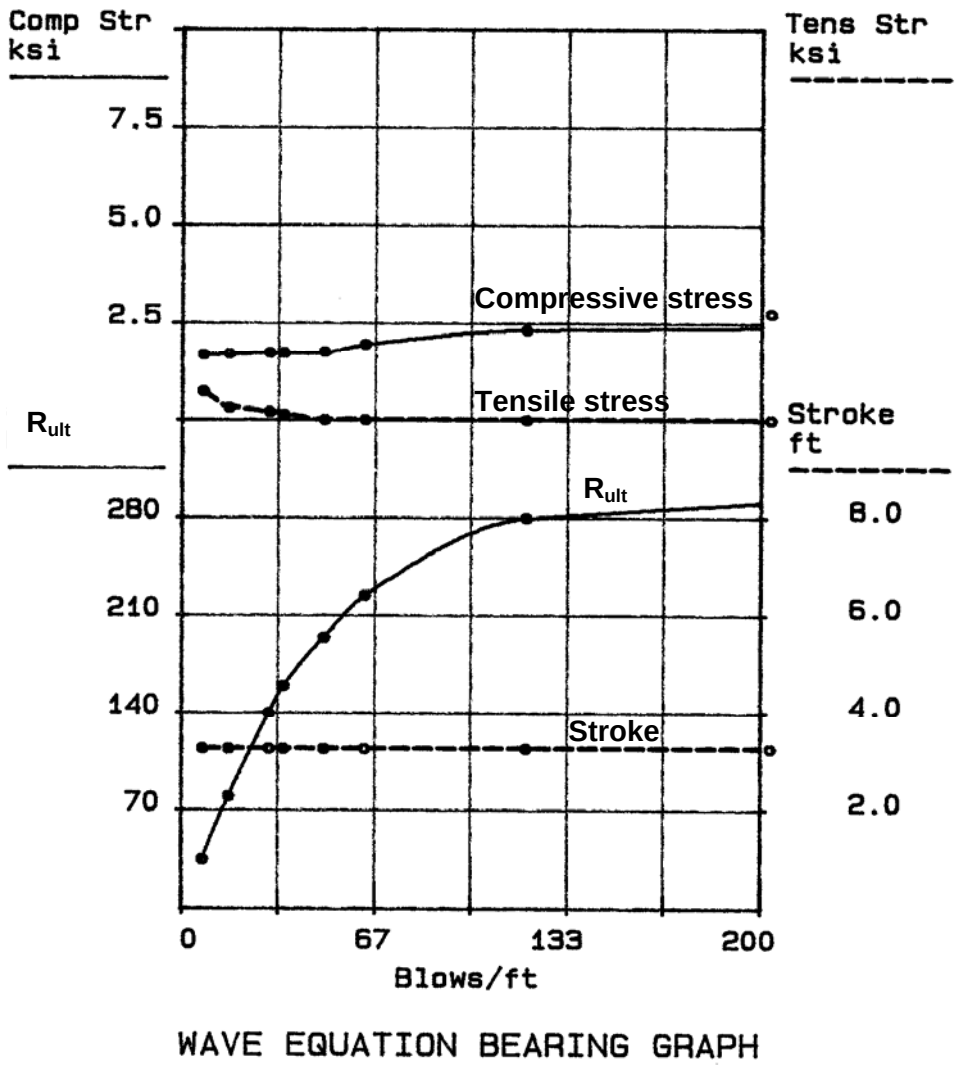

Figure 9-42. Summary of stroke, compressive stress, tensile stress, and driving capacity vs. blow count (blows/ft) for air-steam hammer.

Note that Table 9-10 is an example for an air-steam hammer and the stroke is constant for all blow counts. Diesel hammers operate at different strokes depending on the pile-soil properties. A pile wave summary table for a diesel hammer will display a predicted combination of blow count and stroke that is necessary to achieve the driving capacity. In fact, there are numerous combinations of blow count and stroke that correspond to a particular driving resistance. These combinations may be computed and plotted for a selected driving resistance. A typical plot of diesel hammer stroke versus blow count is shown in Figure 9-43 for a constant resistance of 240 kips (1,067 kN).

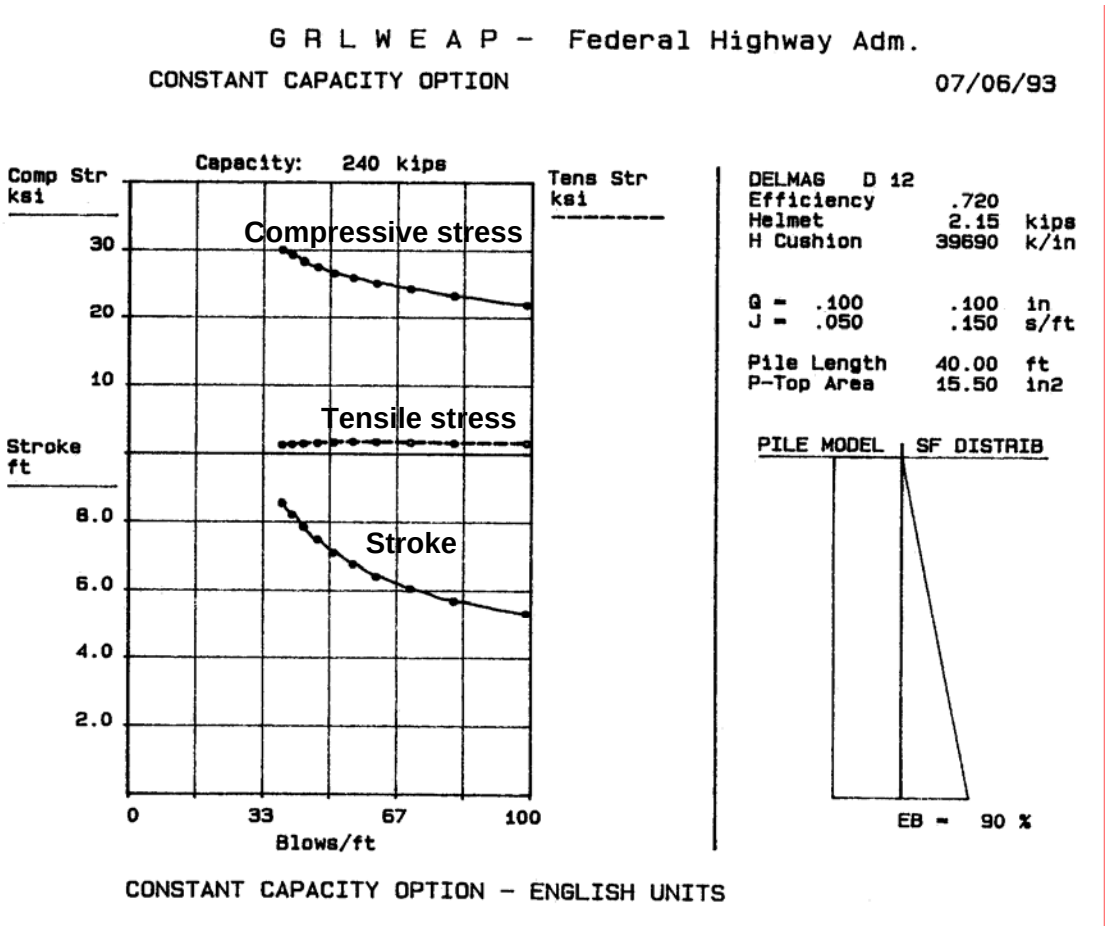

Figure 9-43. Graph of diesel hammer stroke versus blow count for a constant pile capacity.

A wave equation bearing graph is substantially different from a similar graph generated from a dynamic formula. The wave equation bearing graph is associated with a single driving system, hammer stroke, pile type, soil profile, and a particular pile length. If any one of the above items is changed, the bearing graph will also change.

9.9.7 Driving Stresses

In almost all cases, the highest stress levels occur in a pile during driving. High driving stresses are necessary to cause pile penetration. The pile must be stressed to overcome the ultimate soil resistance, plus any dynamic resistance forces, in order to be driven to the design depth and load. The high strain rate and temporary nature of the loading during pile driving allow a substantially higher driving stress limitation than for the static design case. Wave equation analyses can be used for predicting driving stresses prior to installation. During installation, dynamic testing can be used to monitor driving stresses.

The stresses predicted by the wave equation analysis should be compared to safe stress levels. This comparison is usually performed for the tensile and compressive stress shown at the computed driving resistance for the estimated pile length. Table 9-11 presents a summary of design and driving stresses for various types of driven piles.

9.9.8 Guidelines for Assessing Pile Driveability

The last operation in pile design is to insure that the pile can be driven to the estimated length without damage. For this purpose a trial wave equation analysis is done with an appropriately sized hammer. Figure 9-44 can be used to choose a reasonable hammer for wave analysis. In general, the suggested hammer energies in Figure 9-44 are less than the optimum energy necessary to drive the appropriate pile cross section. Judgment should be used in selecting the hammer size. If initial wave equation analysis yield high blow counts and low stresses the hammer size should be increased.

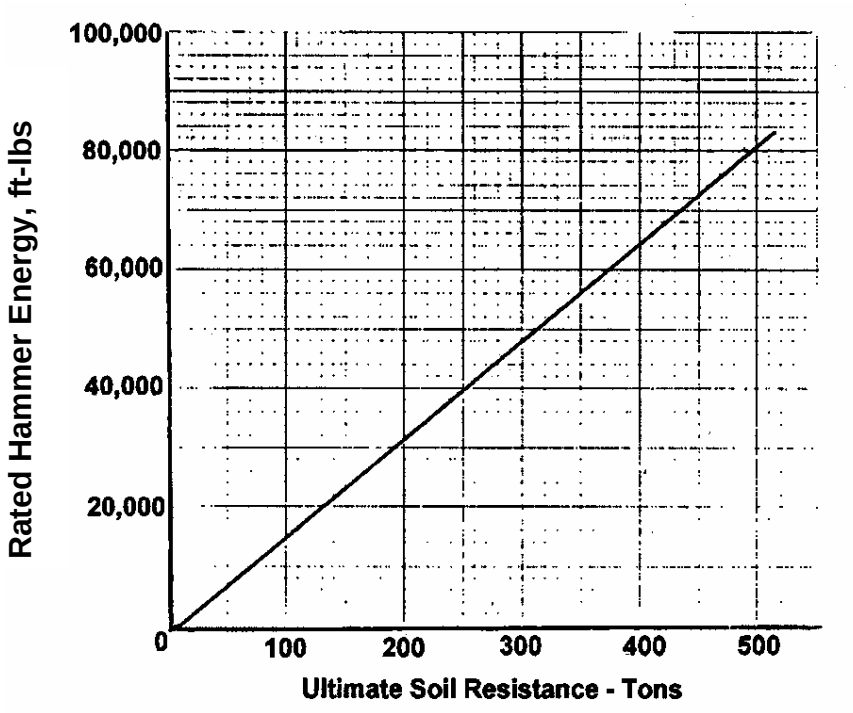

Figure 9-44. Suggested trial hammer energy for wave equation analysis.

During design, a wave equation analysis should be performed to determine if a reasonable range of hammer energies can drive the proposed pile section without exceeding the allowable driving stresses listed in Table 9-11 and a reasonable range of hammer blows, i.e., 30 to 144 bpf for friction piles and higher blows of short duration for end bearing piles. This concept is illustrated numerically by Example 9-4.

Table 9-11. Maximum allowable stresses in pile for top driven piles (after AASHTO, 2002; FHWA, 2006a)

Pile Type	Maximum Allowable Stresses (f_y = yield stress of steel; f'_c = 28-day compressive strength of concrete; f_{pe} = pile prestress)
Steel H-Piles	**Design Stress** 0.25 f_y 0.33 f_y If damage is unlikely, and confirming static and/or dynamic load tests are performed and evaluated by engineer. **Driving Stress** 0.9 f_y
	32.4 ksi (223 MPa) for ASTM A-36 (f_y = 36 ksi; 248 MPa) 45.0 ksi (310 MPa) for ASTM A-572 or A-690, (f_y = 50 ksi; 345 MPa)
Unfilled Steel Pipe Piles	**Design Stress** 0.25 f_y 0.33 f_y If damage is unlikely, and confirming static and/or dynamic load tests are performed and evaluated by engineer. **Driving Stress** 0.9 f_y
	27.0 ksi (186 MPa) for ASTM A-252, Grade 1 (f_y = 30 ksi; 207 MPa) 31.5 ksi (217 MPa) for ASTM A-252, Grade 2 (f_y = 35 ksi; 241 MPa) 40.5 ksi (279 MPa) for ASTM A-252, Grade 3 (f_y = 45 ksi ; 310 MPa)
Concrete filled steel pipe piles	**Design Stress** 0.25 f_y (on steel area) ***plus*** 0.40 f'_c (on concrete area) **Driving Stress** 0.9 f_y
	27.0 ksi (186 MPa) for ASTM A-252, Grade 1 (f_y = 30 ksi; 207 MPa) 31.5 ksi (217 MPa) for ASTM A-252, Grade 2 (f_y = 35 ksi; 241 MPa) 40.5 ksi (279 MPa) for ASTM A-252, Grade 3 (f_y = 45 ksi ; 310 MPa)
Precast Prestressed Concrete Piles	**Design Stress** 0.33 f'_c - 0.27 f_{pe} (on gross concrete area) ; f'_c minimum of 5.0 ksi (34.5 MPa) f_{pe} generally > 0.7 ksi (5 MPa)
	Driving Stress Compression Limit < 0.85 f'_c - f_{pe} (on gross concrete area) Tension Limit (1) < 3 $(f'_c)^{1/2}$ +f_{pe} (on gross concrete area) **US Units*** < 0.25 $(f'_c)^{1/2}$ +f_{pe} (on gross concrete area) **SI Units *** Tension Limit (2) < f_{pe} (on gross concrete area) (1) - Normal Environments ; (2) - Severe Corrosive Environments ***Note:** f'_c and f_{pe} must be in psi and MPa for US and SI equations, respectively.
Conventionally reinforced concrete piles	**Design Stress** 0.33 f'_c (on gross concrete area) ; f'_c minimum of 5.0 ksi (34.5 MPa)
	Driving Stress Compression Limit < 0.85 f'_c ; Tension Limit < 0.70 f_y (of steel reinforcement)
Timber Pile	**Design Stress** 0.8 to 1.2 ksi (5.5 to 8.3 MPa) for pile toe area depending upon species
	Driving Stress Compression Limit < 3 σ_a Tension Limit < 3 σ_a σ_a - AASHTO allowable working stress

Example 9-4: Determine if the 14 inch square concrete pile can be driven to a driving capacity of 225 kips by using the wave equation output summary provided. Assume the concrete compressive strength, f'_c, is 4000 psi and the pile prestress, f_{pe}, is 700 psi.

Wave equation output summary

R_{ult} kips	Blow Count BPF	Stroke (EQ) ft	Tensile Stress ksi	Compressive Stress ksi	Transfer Energy ft-kip
35.0	7	3.27	-0.73	1.68	13.6
80.0	16	3.27	-0.32	1.71	13.6
140.0	30	3.27	-0.20	1.73	13.0
160.0	35	3.27	-0.14	1.73	13.0
195.0	49	3.27	-0.00	1.75	12.8
225.0	63	3.27	0.0	1.96	12.7
280.0	119	3.27	0.0	2.34	12.6
350.0	841	3.27	0.0	2.75	12.5

Solution:

Acceptable driveability depends on achieving the desired driving capacity at hammer blows between 30 and 144 bpf without exceeding the allowable compressive and tensile driving stress.

1. At R_{ult} = 225 kips, blow count = 63 bpf O.K.(between 30 and 144)

2. The allowable driving stresses based on Table 9-11, for prestressed precast concrete piles are calculated as follows:

   - Compressive stress allowed = $0.85\ f'_c - f_{pe} = 0.85\ (4{,}000\ psi) - 700\ psi = 2{,}700\ psi$,
   - Actual maximum compressive stress up to 225 kips from wave equation output summary is 1.96 ksi or 1,960 psi ≤ 2,700 psi allowed value. O.K.
   - Tensile stress allowed = $3\ (f'_c)^{1/2} + f_{pe} = 3\ (4{,}000\ psi)^{1/2} + 700\ psi = 890\ psi$
   - Actual maximum tensile stress up to 225 kips from wave equation output summary is 0.730 ksi or 730 psi ≤ 890 psi allowed value. O.K.

Therefore, the analyzed pile-hammer system can be approved.

9.9.9 Pile Construction Monitoring Considerations

The approval of a contractor's driving equipment is an example of design and construction coordination. It is recommended to use the wave equation analysis to determine if the contractor's equipment is adequate to drive the pile to the estimated length without pile damage. The steps in this procedure are as follows:

1. The pile specifications should include a statement similar to:

   "All pile driving equipment to be furnished by the contractor shall be subject to the approval of the engineer. Prerequisite to such approval, the contractor shall submit the following:

   a. A completed pile and driving equipment data form (Figure 9-45) for each hammer proposed for the project.

   b. A wave equation analysis performed by a professional engineer for each proposed hammer at least to the soil resistance value listed on the plans.

   Contractor notification of acceptance or rejection of the hammer will be made within 14 days of receipt of the data form and wave equation analysis."

   In this case the contractor is charged with performing the wave equation analysis. In some cases, the owner may perform the analysis.

2. The designer should also receive a copy of the data form and the results of wave equation analysis. An independent wave equation analysis should be performed to verify the submitted results and in some cases to establish driving criteria for the piles. The designer should check the results for reasonableness. For example, 30 to 144 blows per foot are considered reasonable for friction piles. Greater blow counts can be permitted for end bearing piles since the duration of high blow counts is short. Then the stresses at that blow count are checked to determine if the values are below the allowable driving stress of the pile material. If these items are satisfied, the equipment can be approved and the information sent to the construction engineer. The results of the wave equation analysis may be transmitted to the field with a recommendation to reject or approve the hammer.

3. The procedure for the changing of approved hammers during the contract is the same.

Contract No.:_____ Structure Name and/or No.:_____

Project: _____ _____

_____ Pile Driving Contractor or Subcontractor:_____

County: _____ _____

(Piles driven by)

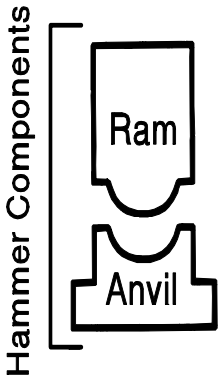

Hammer

Manufacturer:_____ Model No.: _____

Hammer Type: _____ Serial No.: _____

Manufacturers Maximum Rated Energy:____ _____(Joules) (ft-k)

Stroke at Maximum Rated Energy: _____ (meters) (ft)

Range in Operating Energy: _____ to _____ (Joules) (ft-k)

Range in Operating Stroke: _____ to _____ (meters) (ft)

Ram Weight: _____ (kips) (kN)

Modifications: _____

_____

_____

Striker Plate

Weight: _____ (kips) (kN) Diameter: _____(in) (mm)

Thickness: _____ (in) (mm)

Hammer Cushion

	Material #1	Material #2 (for Composite Cushion)
Name:	_____	_____
Area:	_____(in^2) (cm^2)	_____ (in^2) (mm^2)
Thickness/Plate:	_____(in) (mm)	_____ (in) (mm)
No. of Plates:	_____	_____

Total Thickness of Hammer Cushion: _____ (in) (mm)

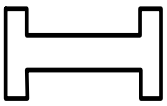

Helmet (Drive Head)

Weight: _____ including inserts (kips) (kN)

Pile Cushion

Material: _____

Area: _____(in^2) (cm^2) Thickness/Sheet: _____(in) (mm)

No. of Sheets: _____

Total Thickness of Pile Cushion: _____ (in) (mm)

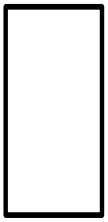

Pile

Pile Type: _____

Wall Thickness: _____(in) (mm) Taper: _____

Cross Sectional Area: _____ (in^2) (mm^2) Weight/ft (m): _____

Ordered Length: _____ (ft) (m)

Design Load: _____ (kips) (kN)

Ultimate Pile Capacity: _____ (kips) (kN)

Description of Splice: _____

_____

Driving Shoe/Closure Plate Description: _____

_____

Submitted By: _____ Date: _____

Telephone No.: _____ Fax No.: _____

Figure 9-45. Pile and driving equipment data form (after FHWA, 2006a).

During production operations, the engineer will check if the necessary blow count is attained at the estimated length shown on the pile driving information form. The resistance is generally acceptable if the blow count is within 10 percent of that expected, or if the expected blow count is achieved within 5 ft (1.5 m) of the estimated length. The construction engineer should be aware that blow counts greater than expected will cause an increase in pile stress. If necessary an upper blow count limit may need to be established to prevent damage.

If either radically different blow counts (greater or less) than those predicted from wave equation analysis or damage are observed during the driving process, the foundation designer should be contacted immediately. The phone number of the foundation designer should be on the information form.

It should be realized that pile driving is not by any means an exact science and actual blow counts and pile lengths may be expected to vary somewhat even in the same footing. The objective of construction monitoring of pile driving is to ensure that the pile is capable of supporting the design load safely. This means that the pile is not damaged and adequate soil resistance is mobilized for support. Both these items can be checked from the wave equation analysis output.

The use of wave equation analysis for construction monitoring provides the engineer with a method to predict the behavior of the driven piles during installation. While this prediction is superior to previous methods of estimating driveability, the optimal method of determining pile driveability is to obtain dynamic measurements during pile installation. Dynamic test methods commonly employ accelerometers and strain gages attached to the pile during driving to measure real time strains and accelerations produced during the driving process. Field computers use these measurements to develop driving variables, which the inspector can use to:

- Monitor hammer and driving system performance,
- Evaluate driving stresses and pile integrity, and,
- Verify pile capacity

Additional details of the dynamic test procedure are discussed in the following section.

9.9.10 Dynamic Pile Monitoring

Dynamic test methods use measurements of strain and acceleration taken near the pile head as a pile is driven or restruck with a pile driving hammer. These dynamic measurements can be used to evaluate the performance of the pile driving system, calculate pile installation stresses, assess pile integrity, and estimate static pile capacity. Dynamic test results can be further evaluated by

using signal matching techniques to determine the relative distribution of soil resistance along the pile, as well as representative dynamic soil properties for use in wave equation analyses. This section provides a brief discussion of the equipment and methods of analysis associated with dynamic measurements.

A typical dynamic monitoring system consists of a minimum of two strain transducers and two accelerometers bolted to diametrically opposite sides of the pile to monitor strain and acceleration and account for nonuniform hammer impacts and pile bending. Because of nonuniform impacts and bending, the use of two diametrically opposite mounted strain transducers is essential for a valid test. The reusable strain transducers and accelerometers are generally attached two to three diameters below the pile head. Almost any driven pile type (concrete, steel pipe, H, Monotube, timber, etc.) can be tested with the pile preparation for each pile type varying slightly.

As the pile is struck by a pile hammer, the strains and accelerations detected by the corresponding gages on the pile are converted into forces and velocities. Typical force and velocity traces generated during dynamic measurements are shown in Figure 9-46. These traces are processed to obtain an estimate of the static pile capacity at the time of testing and for pile design. The additional information obtained and displayed includes compressive and tensile stresses in the pile, transferred energy to the pile, and the force and velocity at the top of the pile throughout the duration of the hammer impact. An experienced operator can use this data to evaluate the performance of the pile driving system and the condition of the pile. The results of the dynamic monitoring are enhanced by the post-testing evaluation in which signal matching is used with computer analysis to verify the correctness of assumed dynamic inputs including damping, quake and load transfer distribution.

ASTM D 4945 contains a detailed description of the equipment requirements and test procedure for dynamic pile load testing.

9.9.10.1 Applications

Dynamic pile monitoring costs much less and requires less time than static pile load testing. Important information can be obtained regarding the behavior of both the pile-soil system and the pile driving system that is not available from a static pile load test. Determination of driving stresses and pile integrity with dynamic test methods has facilitated the use of fewer, higher capacity piles in foundations through better pile installation control Some of the applications of dynamic pile testing are discussed below (FHWA, 2006a).

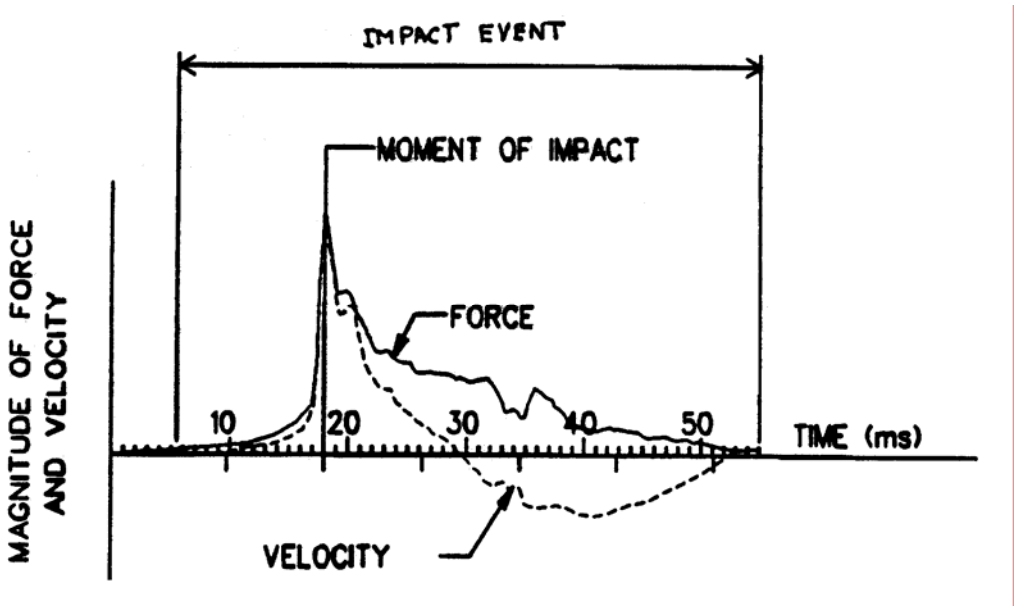

Figure 9-46. Typical force and velocity traces generated during dynamic measurements.

- **Static Pile Capacity**

  a. Evaluation of static pile capacity at the time of testing. Soil setup or relaxation potential can be also assessed by restriking several piles and comparing restrike capacities with end-of-initial driving capacities.

  b. Assessments of static pile capacity versus pile penetration depth can be obtained by testing from the start to the end of driving. This can be helpful in profiling the depth to the bearing stratum and thus the required pile lengths.

  c. Signal matching computer analysis can provide refined estimates of static capacity, assessment of soil resistance distribution, and soil quake and damping parameters for input into a wave equation analysis.

- **Hammer and Driving System Performance**

  a. Calculation of energy transferred to the pile for comparison with the manufacturer's rated energy and wave equation predictions which indicate hammer and drive system performance. Energy transfer can also be used to determine effects of changes in hammer cushion or pile cushion materials on pile driving resistance.

b. Determination of drive system performance under different operating pressures, strokes, or changes in hammer maintenance by comparative testing of hammers, or of a single hammer over an extended period of use.

c. Identification of hammer performance problems, such as preignition problems with diesel hammers or preadmission problems in air/steam hammers.

d. Determination of whether soil behavior or hammer performance is responsible for changes in observed driving resistances.

- **Driving Stresses and Pile Integrity**

a. Calculation of compression and tension driving stresses. In cases with driving stress problems, this information can be helpful when evaluating adjustments to pile installation procedures are being evaluated. Calculated stresses can also be compared to specified driving stress limits.

b. Determination of the extent and location of pile structural damage. With dynamic pile monitoring costly extraction may not be necessary to confirm or quantify damage suspected from driving records.

c. Stress distribution throughout pile by using signal matching computer analysis.

9.9.10.2 Interpretation of Results and Correlation with Static Pile Load Tests

The results of dynamic pile monitoring should be interpreted by an experienced geotechnical specialist who has had the opportunity to observe and evaluate the results from many dynamically test piles and can detect the signs, not always readily apparent, of unusual soil-pile response, pile damage, erratic hammer operation or testing equipment malfunction. It is important that the geotechnical specialist performing the evaluation should have attained an appropriate level of expertise through qualifying examinations by providers of dynamic testing services.

Interpretation of the results of dynamic pile measurements also requires an awareness of the differences in behavior of dynamically and statically loaded piles. Improper correlations of dynamic and static pile loads test may be caused by the following:

- **Incorrectly assumed soil damping, quake and load transfer parameters**. This source of discrepancy can be minimized by performing a post-test computerized analysis to match

measured and computed relationships between force and velocity to determine the most appropriate parameters.

- **Time-related changes in pile capacity**. Depending on soil type and pile characteristics, the capacity of a pile may increase or, less commonly, decrease with time. The principal causes are time-related changes of pore water pressure in cohesive soils and stress relaxation in cohesionless soils. The effects can be assessed by "restriking" the pile at various time intervals after driving and comparing the observed "restrike" capacity to the driving capacity obtained during the initial drive. The pile capacity should be determined during the first few "good" hammer blows during re-strike. When comparing the results of dynamic testing against those of a static pile load test, at least one dynamic test should be performed after completion of static testing.

- **Inadequate pile tip displacement.** Pile tip displacement during dynamic testing may be inadequate to mobilize full end bearing. Frictional resistance between a pile and the surrounding soil is mobilized at a fraction of the pile movement necessary to mobilize full end bearing resistance. A penetration resistance of 10 blows/inch (10 blows/25.4 mm) or higher, may produce insufficient strain in the soil to mobilize full end resistance. This results in an underestimate of the end bearing capacity. For many types of piles, the estimate can be improved by performing a force-velocity match both for the initial drive and for the restrike data. The tip capacity derived from the initial drive is combined with skin resistance from the restrike to obtain the total pile capacity. However, this method may not be applicable for open-ended pipe, H-piles, and precast cylinder piles. In the case of these types of piles, only the structural area of the pile can mobilize the toe bearing during installation. This value of toe bearing may be significantly less than the value that may be experienced in the static load test, since the soil in the static load test will adhere to the pile with time and create a plug.

9.10 CAST-IN-PLACE (CIP) PILES

There are a variety of cast-in-place (CIP) piles as shown in Figure 9-2. In contrast to the driven piles wherein piles manufactured in a factory are driven in the ground, in the case of CIP piles, the load resisting element is constructed in a pre-drilled hole. The load resisting element is often a combination of steel and CIP concrete. As shown previously in Figure 9-2, there are a variety of CIP piles, e.g., drilled shafts, micropiles, auger cast piles, etc.

The design and construction process for CIP piles is shown in Figure 9-47. This process is similar to that for driven piles shown in Figure 9-3 for Blocks 1 to 18. It is in the construction phase where there are major differences between the driven piles and CIP piles. Blocks 19 to 24 are briefly discussed below:

Block 19: Review Contractor's Installation Procedures

The potential that the CIP piles will perform as designed is heavily dependent on the techniques employed by the contractor during construction. For example, soil excavation technique will not be suitable for excavation in IGMs or rocks. The contractor should be required to submit a detailed CIP pile construction procedure that will be reviewed by the geotechnical engineer.

Block 20: Set Preliminary Installation Criteria

Based on the evaluation of the contractor's proposed installation procedures with respect to project installation criteria and any other requirements in the design and specifications, the preliminary approval of the contractor's equipment and procedures can be given. If the contractor's installation procedures are not acceptable, then the process returns to Block 19.

Block 21: Install Test Piles and Evaluate Constructability

Usually, the first CIP pile on a project is considered to be a "test" pile wherein the contractor's proposed equipment and installation procedures are evaluated in the field. Often, where prior experience is not available, the first pile is required to be installed as a sacrificial pile at a location away from the footprint of the production piles. The constructability evaluation of the test pile is critical. Non-destructive (integrity) tests are recommended at this stage to evaluate the quality of the constructed product.

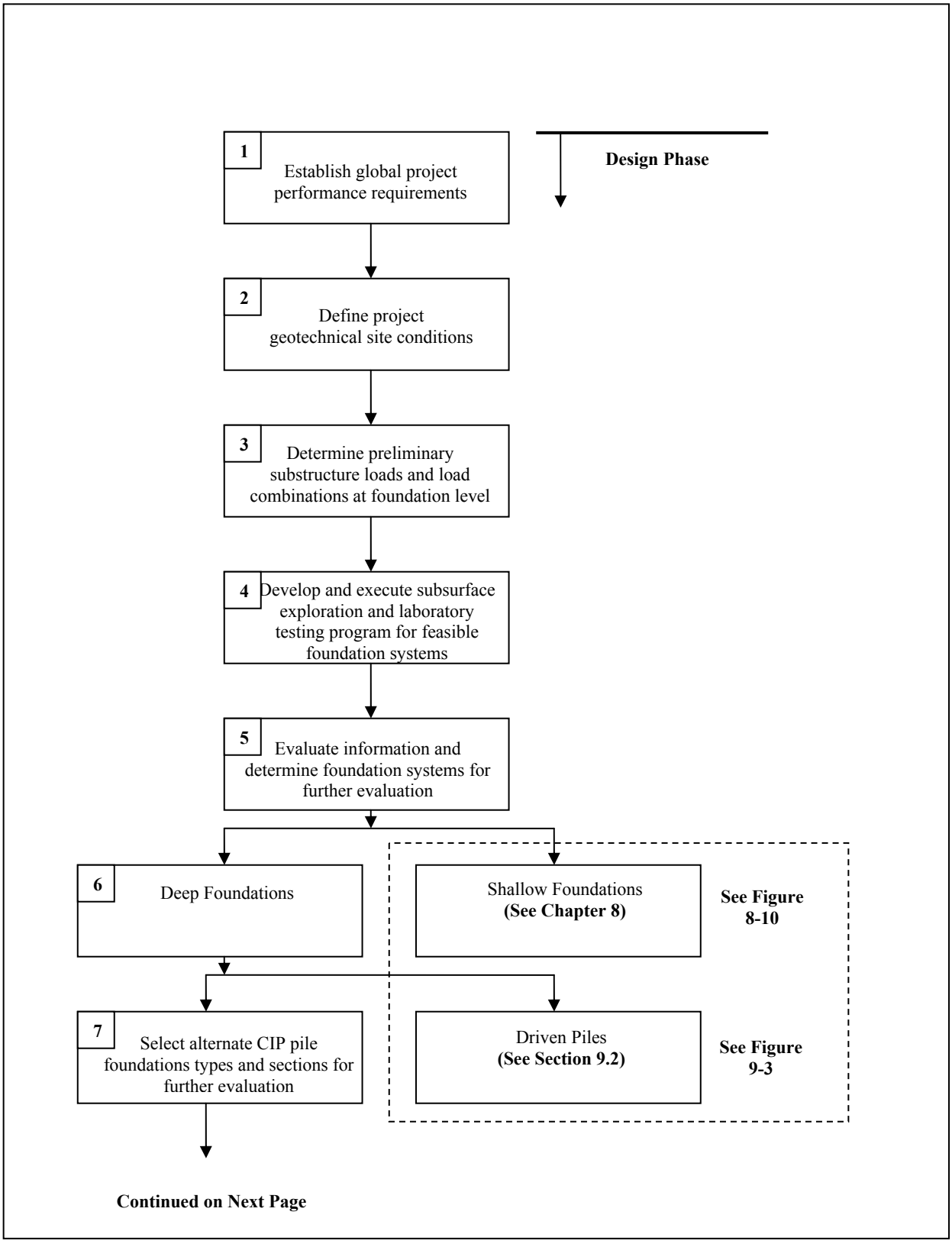

Figure 9-47. Cast-in-Place (CIP) pile design and construction process (modified after FHWA 2006a).

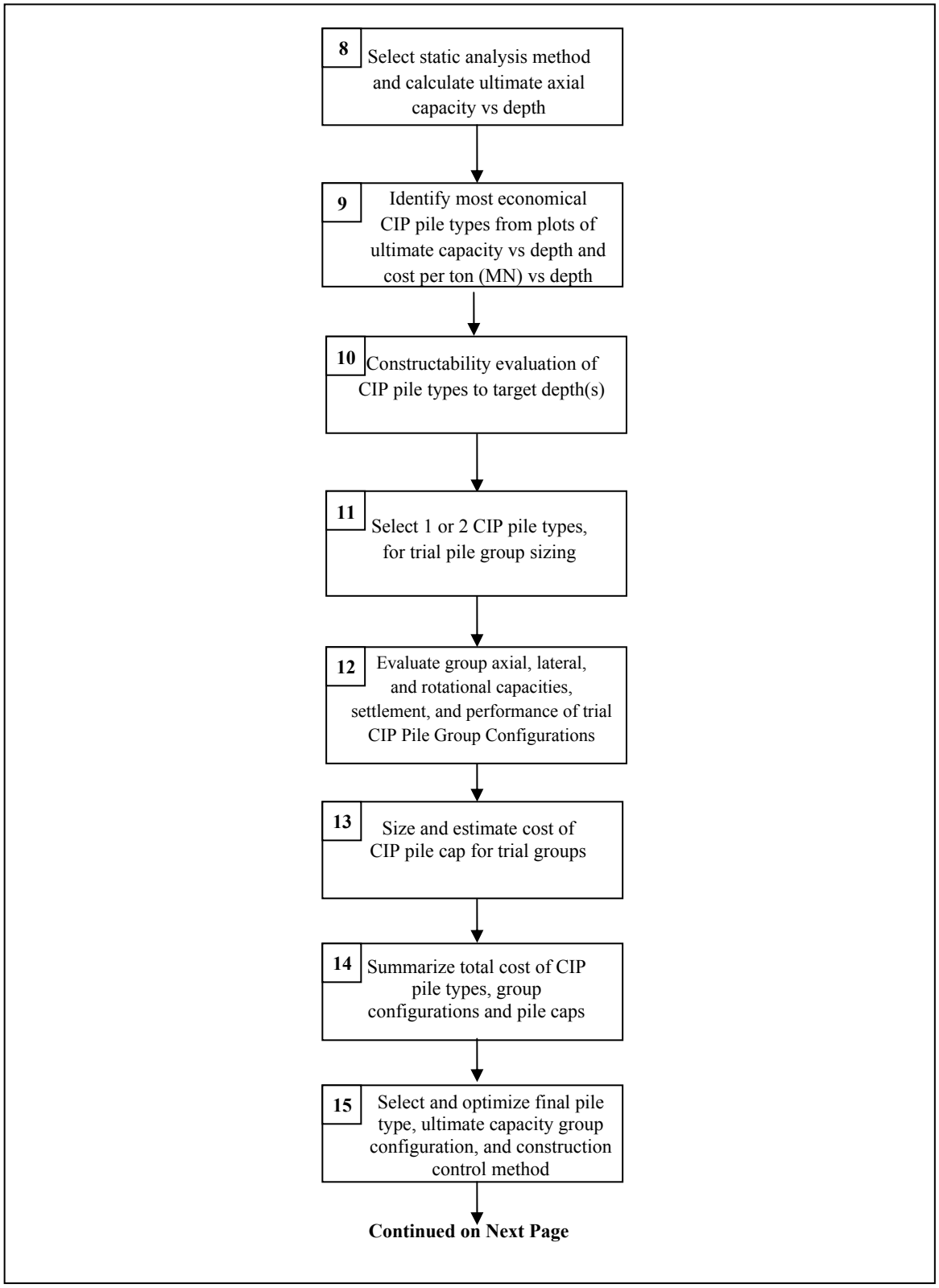

Figure 9-47 (Continued). Cast-in-Place (CIP) pile design and construction process (modified after FHWA 2006a).

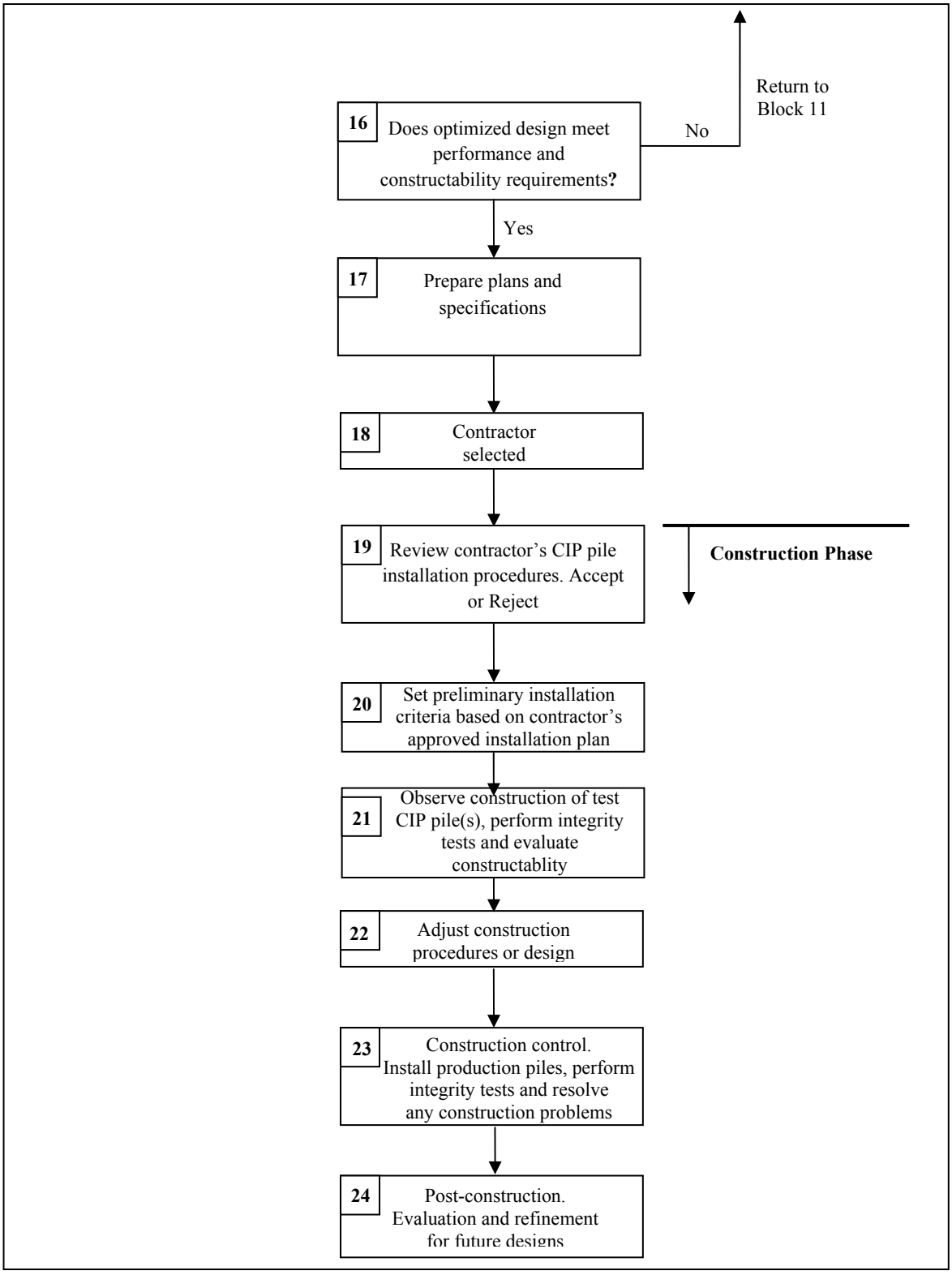

Figure 9-47 (Continued). Cast-in-Place (CIP) pile design and construction process (modified after FHWA 2006a).

Block 22: Adjust Construction Procedures

In this step, an adjustment in the contractor's construction procedures may be required prior to construction of the production piles. If significant adjustments are necessary, then another test pile may be warranted.

Block 23: Construction Control

After the test CIP pile has been successfully constructed, the same construction procedures are applied for the production piles unless different subsurface conditions are encountered that may warrant alternative construction techniques. In this case another test pile may be required. Quality control and assurance procedures including integrity tests are implemented as discussed in Section 9.14. Problems may arise and must be handled in a timely fashion as they occur.

Block 24: Post-Construction Evaluation and Refinement of Design

After completion of the foundation construction, the project should be reviewed and evaluated for its effectiveness in satisfying the project requirements and also its cost effectiveness. The evaluation should be performed from the viewpoint of refining the construction and design procedures as appropriate for future projects.

9.11 DRILLED SHAFTS

A drilled shaft is a form of cast-in-place (CIP) pile. A drilled shaft is a machine- and/or hand-excavated shaft in soil or rock that is filled with concrete and reinforcing steel, with the primary purpose of providing structural support. A drilled shaft is usually circular in cross section and may be belled at the base to provide greater bearing area. A typical drilled shaft is shown in Figure 9-48. Other terminology commonly used to describe a drilled shaft includes: drilled pier, drilled caisson, bored pile and cast-in-drilled hole (CIDH). Rectangular drilled shafts are called barrettes.

Vertical load is resisted by the drilled shaft in base bearing and side friction. Horizontal load is resisted by the shaft in horizontal bearing against the surrounding soil or rock.

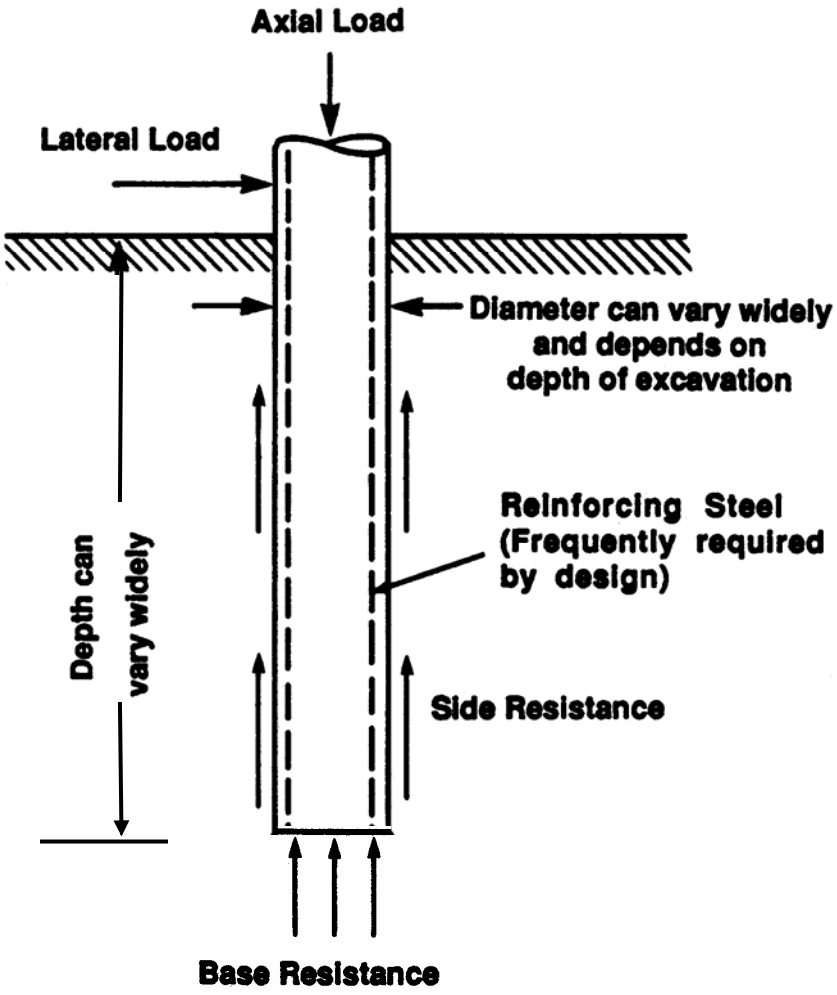

Figure 9-48. A typical drilled shaft and terminology (after FHWA, 1999).

9.11.1 Characteristics of Drilled Shafts

The following special features distinguish drilled shafts from driven pile foundations:

1. The drilled shaft is constructed in a drilled hole, unlike the driven pile.

2. Wet concrete is cast and cures directly against the soil in the borehole. Temporary steel casing may be necessary for stabilization of the open hole and may or may not be extracted.

3. The construction method for drilled shafts is adapted to suit the subsurface conditions.

9.11.2 Advantages of Drilled Shafts

Following are the advantages of drilled shafts.

a. Construction equipment is normally mobile and construction can proceed rapidly.

b. The excavated material and the drilled hole can often be examined to ascertain whether or not the soil conditions at the site agree with the estimated soil profile. For end-bearing situations, the soil beneath the tip of the drilled shaft can be probed for cavities or for weak soil.

c. Changes in geometry of the drilled shaft may be made during the course of the project if the subsurface conditions so dictate.

d. The heave and settlement at the ground surface due to installation will normally be very small.

e. The personnel, equipment, and materials for construction is usually readily available.

f. The noise level from the equipment is less than for some other methods of construction.

g. The drilled shaft is applicable to a wide variety of subsurface conditions. For example, it is possible to drill through a layer of cobbles and into hard rock for many feet. It is also possible to drill through frozen ground.

h. A single drilled shaft can sustain very large loads so that a pile cap may not be needed.

i. Databases that contain documented load-transfer information are available. These databases allow confident designs of drilled shafts to be made in which load-transfer both in end bearing and in side resistance can be considered.

j. The shaft occupies less area than the footing and thus can be built closer to railroads, existing structures and constricted areas.

k. Drilled shafts may be more economical than spread footing construction, especially when the foundation support layer is deeper than 10' below the ground or at water crossings.

9.11.2.1 Special Considerations for Drilled Shafts

a. Construction procedures are critical to the quality of the drilled shaft. Knowledgeable inspection is required.

b. Drilled shafts are not normally used in deep deposits of soft clay or in situations where artesian pressures exist.

c. Static load tests to verify the ultimate capacity of large diameter shafts are very costly.

9.11.3 Subsurface Conditions and Their Effect on Drilled Shafts

Subsurface investigation for drilled shaft designs must include an assessment of the potential methods of shaft construction as well as a determination of soil properties. The standard method for obtaining soil characteristics is similar to pile foundations and involves laboratory testing of undisturbed samples and the use of in situ techniques including the standard penetration test. Constructability is difficult to assess from routine geotechnical investigations. Critical items such as hole caving, dewatering, rock drilling and obstructions can best be examined by drilling a full diameter test shaft hole during the exploration or design phase of the project. These test holes are usually done by local drilled shaft contractors under a short form contract. Prospective bidders should be invited to observe the construction of the test hole. A detailed log should be made of the test hole including items such as type of drilling rig, rate of drilling, type of drill tools and augers used, etc. Such information should be made available for bidders.

Subsurface Conditions Affecting Construction

a. The stability of the subsurface soils against caving or collapse when the excavation is made will determine whether or not a casing is necessary. The dry method of construction can be used only where the soils will not cave or collapse. The casing method must be used if there is danger of caving or collapse.

b. The existence of groundwater at the site must be determined and what rate of flow can be expected into a shaft excavation. This knowledge will permit selection of appropriate slurry type and dosage to support the sides and the bottom of the shaft during drilling and subsequent placement of reinforcing cage and concrete. The groundwater can be regional groundwater or perched water.

c. Any artesian water conditions must be clearly identified in the contract documents. Artesian water flowing could spoil the concrete placement, or cause collapse or

heaving at the excavation. Flowing water can create similar problems during concrete placement as it can leach the cement grout out of the concrete mix. Conventional slurry-assisted drilling alone may not be adequate in cases where artesian pressure is encountered and casing may be required.

d. The presence of cobbles or boulders can cause difficulties in drilling. It is sometimes not easy to extract large pieces of rock, especially with smaller diameter shafts.

e. The presence of existing foundations or structures.

f. The presence of landfill that could contain material that cannot be easily excavated, such as an old car body.

g. The presence of rock may require more sophisticated drilling methods.

h. The presence of a weak stratum just below the base of the drilled shaft. For this situation drilling may have to be extended below the weak stratum.

9.12 ESTIMATING AXIAL CAPACITY OF DRILLED SHAFTS

The procedures for estimation of drilled shaft capacity have improved significantly over the past decade. The major reason for this improvement is a database that has been developed on load transfer in skin friction and in end bearing based on load tests in a broad range of geomaterials. It is now well established that drilled shafts can carry a substantial portion of applied loads in skin friction. As with pile foundations, the ultimate skin friction is mobilized at a relatively small downward movement of the shaft relative to the soil. End bearing resistance is developed in relation to the amount of deflection at the tip.

Separate analyses are required to determine skin friction and end bearing contributions in different soil types and rock. Details of these analyses can be found in FHWA (1999). The basic formulation for drilled shaft capacity in soils and rocks, excerpted from FHWA (1999), is presented herein. The discussions in this manual regarding drilled shaft axial capacity are limited to drilled shafts of uniform cross-section, with vertical alignment, concentric axial loading, and a relatively horizontal ground surface. The reader is referred to FHWA (1999) for procedures to incorporate the effects of enlarged base, group action, and sloping ground.

The ultimate axial capacity (Q_{ult}) of the drilled shaft is determined as follows for compression and uplift loading, respectively:

$$Q_u = Q_s + Q_t - W \quad \text{9-34a}$$

$$Q_u \leq 0.7Q_s + W \quad \text{9-34b}$$

where: Q_u = total ultimate axial capacity of the foundation
Q_s = ultimate skin (side) capacity
Q_t = ultimate tip (base or end) capacity
W = weight of the shaft.

Note that in contra-distinction to the ultimate capacity equation for driven piles (see Equation 9-1), the weight term is included for the drilled shaft since the weight of a shaft is usually much larger than that of a pile. The shaft weight can therefore act as a load in the downward direction or act as a resistance in uplift.

Similar to the driven piles, the **allowable geotechnical soil resistance**, Q_a, is determined as follows:

$$Q_a = \frac{Q_u}{FS} \quad \text{9-35}$$

where FS = factor of safety which typically varies between 2 to 3. If load tests are not performed then the shaft should be designed for a minimum factor of safety of 2.5 (AASHTO, 2002). This minimum recommended factor of safety is based on an assumed normal level of field quality control during shaft construction as per the requirements of FHWA (2002d). If a normal level of field quality control as required by FHWA (2002d) cannot be assured, larger minimum factors of safety such as 3.0 are recommended. If a site-specific load test is performed, consideration may be given to reducing the factor of safety from 2.5 to 2.0.

Shafts in cohesive soils may be designed by total and effective stress methods of analysis, for undrained and drained conditions, respectively. Shafts in cohesionless soils should be designed by effective stress methods of analysis for drained loading conditions. Formulations for both cohesive and cohesionless soils using allowable stress design (ASD) are presented herein based FHWA (1999) and AASHTO (2002). For LRFD based formulations the reader is referred to AASHTO (2004 with 2006 Interims).

9.12.1 Side Resistance in Cohesive Soil

For cylindrical shafts in cohesive soils loaded under undrained loading conditions, the **ultimate side resistance** may be estimated by using the following expression:

$$Q_s = \pi D \sum_{i=1}^{N} \alpha_i s_{ui} \Delta z_i \qquad 9\text{-}36$$

Where, D is the diameter of the shaft and α_i and s_{ui} are the adhesion factor and undrained shear strength, respectively, in a layer Δz_i. The adhesion factor, α, is given as follows.

$$\alpha = 0.55 \qquad \text{for } s_u/p_a \le 1.5 \qquad 9\text{-}37a$$

$$\alpha = 0.55 - 0.1(s_u/p_a - 1.5) \qquad \text{for } 1.5 < s_u/p_a \le 2.5 \qquad 9\text{-}37b$$

where p_a= atmospheric pressure (=1.06 tsf = 2.12 ksf=14.7 psi =101kPa). The units of s_{ui} and p_a should be dimensionally consistent.

The **ultimate unit load transfer in side resistance** at any depth f_{si} is given as follows:

$$f_{si} = \alpha_i \, s_{ui} \qquad 9\text{-}38$$

As illustrated in Figure 9-49, the top and bottom 5-ft of the shaft should not be included in the development of the ultimate skin resistance. Environmental, long-term loading or construction factors may dictate that a depth greater than the top 5-ft should be ignored in estimating Q_s.

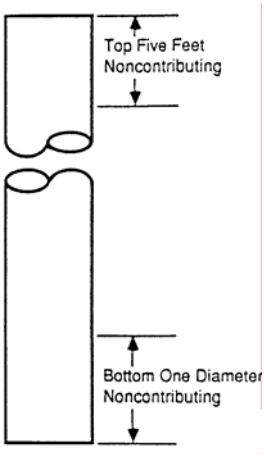

Figure 9-49. Portions of drilled shafts not considered in computing ultimate side resistance (FHWA, 1999).

Effective stress methods for computing Q_s described in Section 9.10.2.3 may be used for the following cases:

- For shafts in cohesive soils under drained loading conditions, and
- In the zones where time-dependent changes in soil shear strength may occur, e.g., swelling of expansive clay or downdrag from a consolidating clay.

9.12.1.1 Mobilization of Side Resistance in Cohesive Soil

Figure 9-50 presents the load-transfer characteristics for side resistance in cohesive soils. The curves presented indicate the proportion of the ultimate side resistance (Q_s) mobilized at various magnitudes of settlement. It can be seen that the full ultimate side resistance is mobilized at displacements of 0.2% to 0.8% of the shaft diameter. Thus, for a 4-ft diameter shaft in cohesive soil, full side resistance will be mobilized at vertical displacements in the range of 1/8" to 3/8" (3 mm to 10 mm).

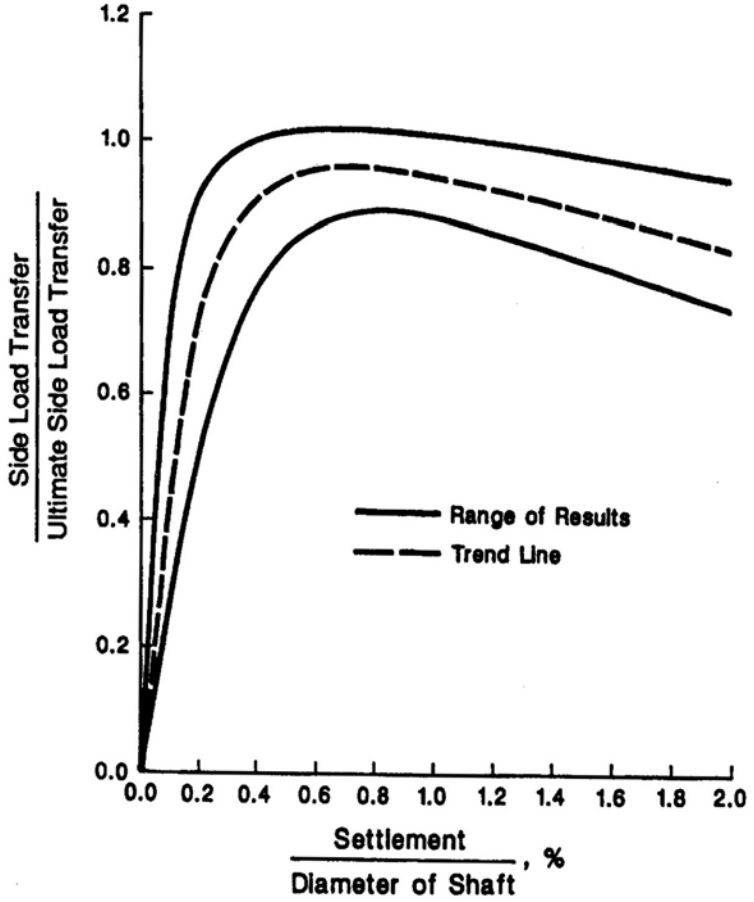

Figure 9-50. Load-transfer in side resistance versus settlement for drilled shafts in cohesive soils (FHWA, 1999).

9.12.2 Tip Resistance in Cohesive Soil

For axially loaded shafts in cohesive soil subjected to undrained loading conditions, the ultimate tip resistance of drilled shafts may be estimated by using the following relationship:

$$Q_t = q_t A_t = N_c s_{ut} A_t \qquad 9\text{-}39$$

Where q_t is the unit tip resistance, N_c is a bearing capacity factor, s_{ut} is the undrained shear strength of the soil at the tip of the shaft and A_t is the tip area of the shaft. Values of the bearing capacity factor, N_c, may be determined by using the following relationship.

$$N_c = 6.0[1+0.2(z/D)]; \quad N_c \leq 9 \qquad 9\text{-}40$$

where z is the depth of the penetration of the shaft and D is the diameter of the shaft. The units of z and D should be consistent.

The limiting value of unit end bearing ($q_t = N_c s_{ut}$) is 80 ksf. The value of 80 ksf is not a theoretical limit but a limit based on the largest measured values. A higher limiting value may be used if it is based on the results of a load test, or previous successful experience in similar soils under similar loading conditions.

The value of s_{ut} should be determined from the results of in-situ and/or laboratory testing of undisturbed samples obtained within a depth of 2.0 diameters below the tip of the shaft. If the soil within 2.0 diameters of the tip has $s_{ut} < 0.5$ ksf, the value of N_c should be multiplied by 0.67.

9.12.2.1 Mobilization of Tip Resistance in Cohesive Soil

Figure 9-51 presents the load-transfer characteristics for tip resistance in cohesive soils. The curves presented indicate the proportion of the ultimate tip resistance (Q_t) mobilized at various magnitudes of settlement. It can be seen that the ultimate tip resistance, Q_t, is fully mobilized at displacements of 2% to 5%. Thus, for a 4-ft diameter shaft in cohesive soil, full tip resistance will be mobilized at vertical displacements in the range of 1" to 2.5" (25 mm to 65 mm). Conversely, if the shaft settles less than these values, then full tip resistance may not be mobilized. For example, if the shaft settles only 1% of the shaft diameter then approximately 60% of the tip resistance will be mobilized as indicated by the trendline shown in Figure 9-51. For smaller tolerable settlements, the mobilized tip resistance will be similarly smaller. If one limits the deformation to between 0.2% and 0.8% to be consistent with full mobilization of side resistance in cohesive soil, then from Figure 9-51, it can be seen that only approximately 10 to 50% of the tip resistance will be available based on the trendline.

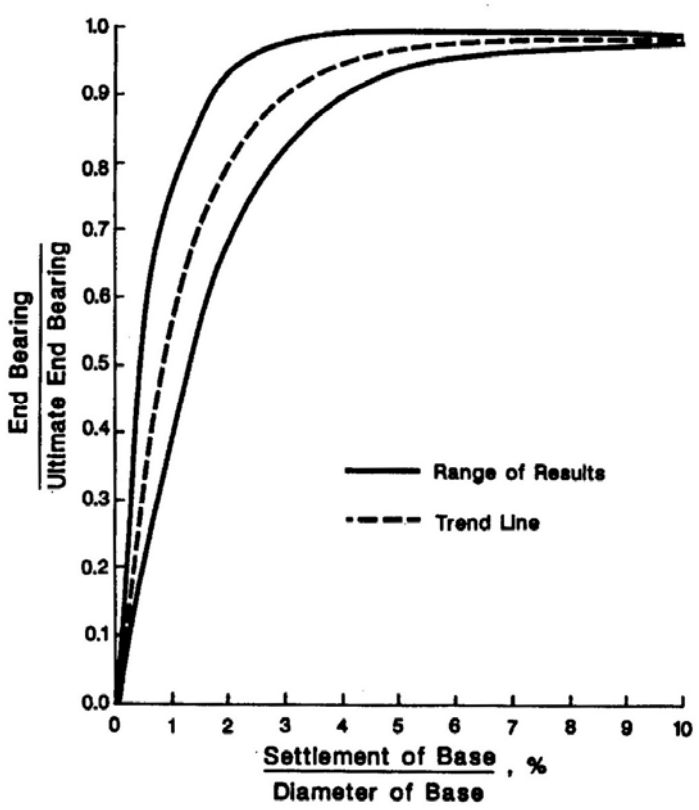

Figure 9-51. Load-transfer in tip resistance versus settlement for drilled shafts in cohesive soils (FHWA, 1999).

The above examples of shaft settlements clearly demonstrate the need to perform detailed settlement analyses by using Figure 9-50 and 9-51 to estimate the shaft resistance based on consistent deformations. For shafts in cohesive soil under drained loading conditions, Q_t, may be estimated by using the procedure described in Section 9.12.3.1 for cohesionless (drained) soils.

9.12.3 Side Resistance in Cohesionless Soil

For cylindrical shafts in cohesionless soil or for effective stress analysis of cylindrical shafts in cohesive soils under drained loading conditions, the ultimate side resistance of axially loaded drilled shafts may be estimated by using the following equation:

$$Q_s = \pi D \sum_{i=1}^{N} \beta_i p_o \Delta z_i \qquad 9\text{-}41$$

where: $\beta_i = 1.5 - 0.135\sqrt{z_i}$ with $1.2 > \beta_i > 0.25$ 9-42

In above equations D is the shaft diameter, N is the number of layers used in the analysis, z_i is the depth in feet to the center of the i^{th} layer and p_o is the effective overburden pressure at the center of the i^{th} layer. The ultimate unit load transfer in side resistance at any depth f_{si} is given as follows:

$$f_{si} = \beta_i \, p_o \qquad 9\text{-}43$$

The limiting value of f_{si} for shafts in cohesionless soils is 4 ksf (191 kPa).

9.12.3.1 Mobilization of Side Resistance in Cohesionless Soil

Figure 9-52 presents the load-transfer characteristics for side resistance in cohesionless soils. The curves presented indicate the proportion of the ultimate side resistance (Q_s) mobilized at various magnitudes of settlement. It can be seen that the full ultimate side resistance, Q_s, is fully mobilized at displacements of 0.1% to 1.0% of the shaft diameter. Thus, for a 4-ft diameter shaft in cohesionless soil, full side resistance will be mobilized at vertical displacements in the range of 0.05" to 0.5" (1.3 to 13 mm).

9.12.4 Tip Resistance in Cohesionless Soil

For axially load drilled shafts in cohesionless soils or for effective stress analysis of axially loaded drilled shafts in cohesive soils, the ultimate tip resistance may be estimated by using the following equation:

$$Q_t = q_t \, A_t \qquad 9\text{-}44$$

The value of q_t may be determined from the results of standard penetration testing using N_{60} blow count readings within a depth of 2B below the tip of the shaft as follows:

$$\text{For } N_{60} \le 75: \quad q_t = 1.2N_{60} \qquad \text{in ksf} \qquad 9\text{-}45a$$

$$\text{For } N_{60} > 75: \quad q_t = 90 \text{ ksf} \qquad 9\text{-}45b$$

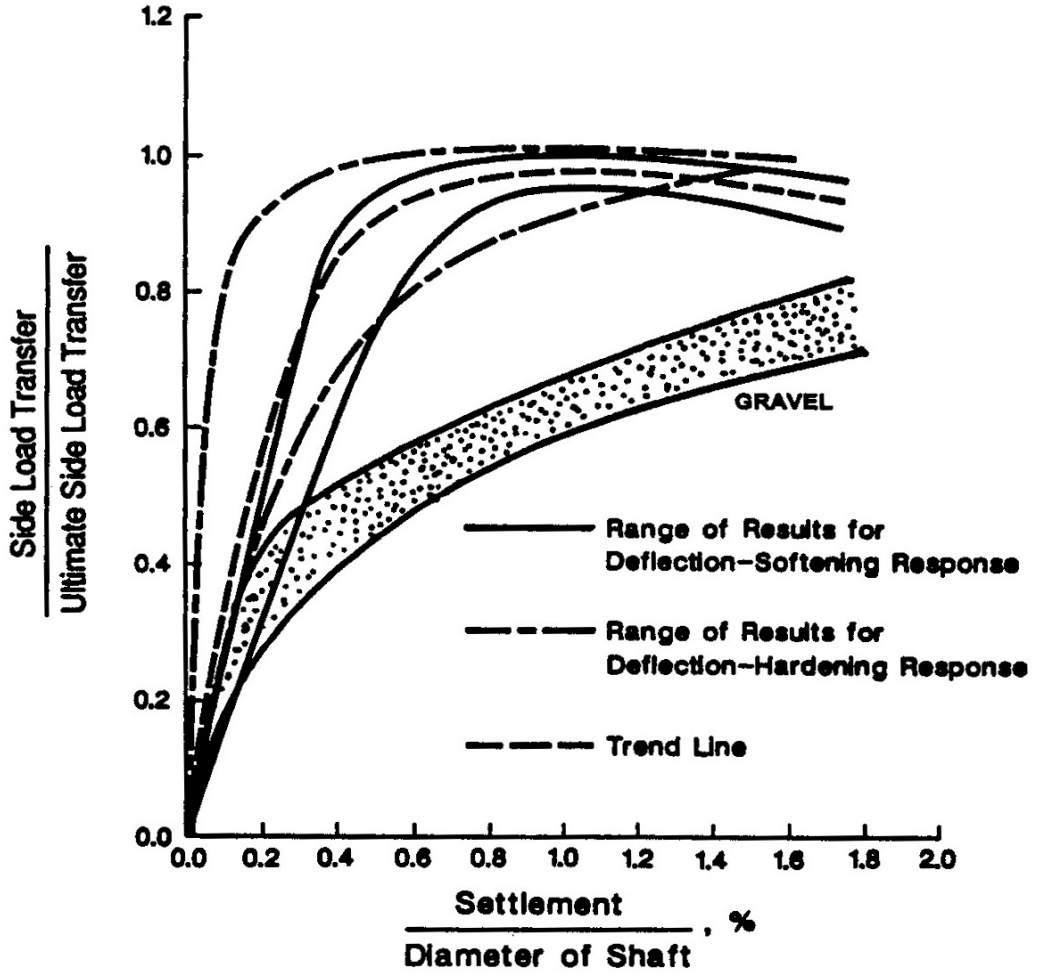

Figure 9-52. Load-transfer in side resistance versus settlement for drilled shafts in cohesionless soils (FHWA, 1999).

9.12.4.1 Mobilization of Tip Resistance in Cohesionless Soil

Figure 9-53 presents the load-transfer characteristics for tip resistance in cohesionless soils. The curves presented indicate the proportion of the ultimate tip resistance (Q_t) mobilized at various magnitudes of settlement. It can be seen that the ultimate tip resistance, Q_t, is fully mobilized at displacements of approximately 5%. Thus, for a 4-ft diameter shaft in cohesive soil, full tip resistance will be mobilized at vertical displacements of approximately 2.4-inches. Conversely, if the shaft settles less than this value, then full tip resistance may not be mobilized. For example if the shaft settles only 1% of the shaft diameter then approximately 30% of the tip resistance will be mobilized as indicated by the trendline shown in Figure 9-53. For smaller settlements, the mobilized tip resistance will be similarly smaller. If one limits the deformation to between

0.1% and 1% to be consistent with full mobilization of side resistance in cohesionless soils, then from Figure 9-53, it can be seen that only approximately 5 to 30% of the tip resistance will be available based on the trendline.

Compared to similar examples for cohesive soils, it can be seen that deformation compatibility is more critical in cohesionless soils due to the relatively large deformation of 5% of shaft diameter that is required to mobilize full tip resistance. This reinforces the need to perform detailed settlement analyses by using Figure 9-52 and 9-53 to estimate the shaft resistance based on consistent deformations.

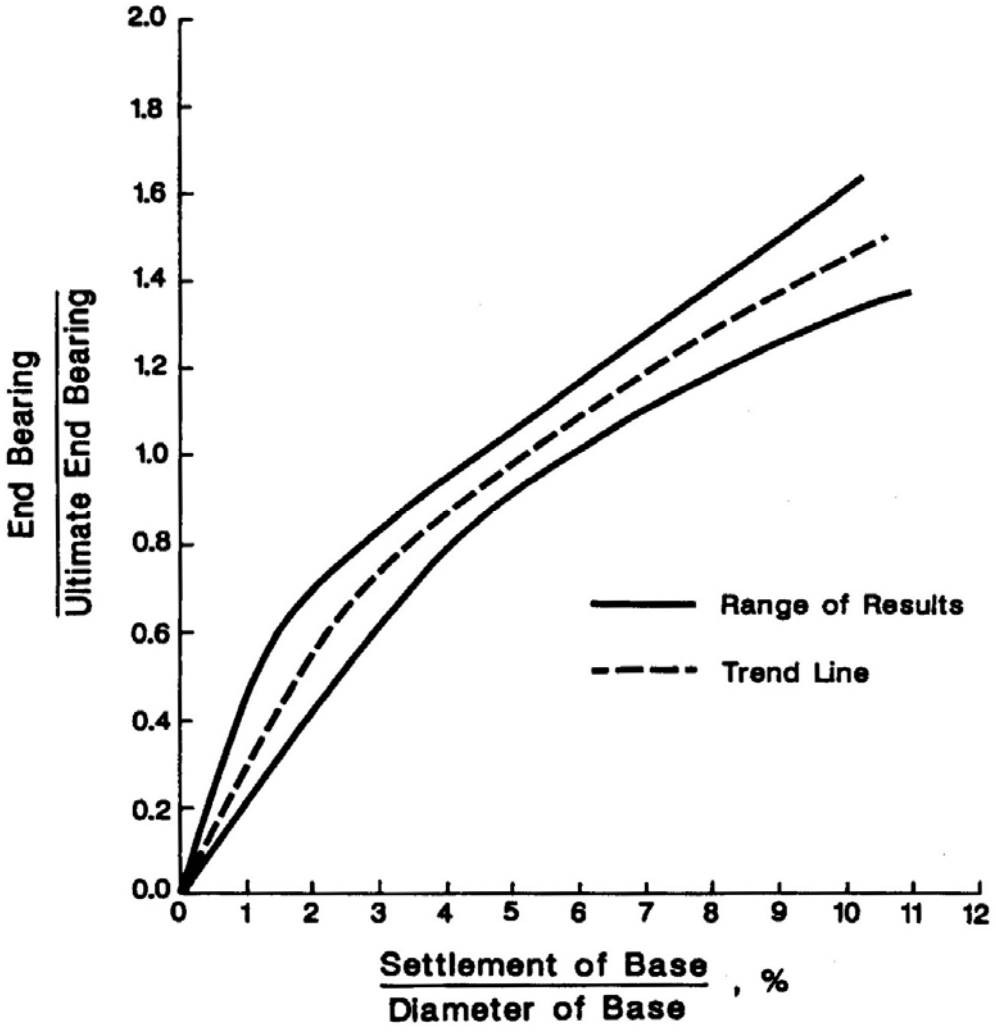

Figure 9-53. Load-transfer in tip resistance versus settlement for drilled shafts in cohesionless soils (FHWA, 1999).

9.12.5 Determination of Axial Shaft Capacity in Layered Soils or Soils with Varying Strength with Depth

The design of shafts in layered soil deposits or soil deposits having variable strength with depth requires evaluation of soil parameters characteristic of the respective layers or depth. The side resistance, Q_s, in such soil deposits may be estimated by dividing the shaft into layers according to soil type and properties, determining Q_s, for each layer, and summing the values for each layer to obtain the total load Q_s. If the soil below the shaft tip is of variable consistency, Q_t, may be estimated using the strength properties of the predominant soil strata within a depth of 2 shaft diameters below the shaft tip. While summing the resistances, particular attention must be paid to deformation compatibility.

For shafts extending through soft compressible layers to firm soil or rock, consideration should be given to the effects of negative skin friction due to the potential consolidation settlement of soils surrounding the shaft. Where the shaft tip would bear on a thin firm soil layer underlain by a softer soil unit, the shaft should be extended through the softer soil unit to eliminate the potential for a punching shear failure into the softer deposit.

9.12.6 Group Action, Group Settlement, Downdrag and Lateral Loads

These topics are similar to those for pile foundations. Their detailed discussion is beyond the scope of this manual. The reader is referred to FHWA (1999) for discussion of these topics.

The concepts regarding axial capacity of drilled shafts in cohesionless or drained cohesive soils are illustrated numerically by Example 9-5. The concepts regarding axial capacity of drilled shafts in layered soils are illustrated numerically by Example 9-6.

Example 9-5: Size a shaft to resist 170 tons of vertical design load in the soil profile shown below. Assume a factor of safety (FS) of 2.5.

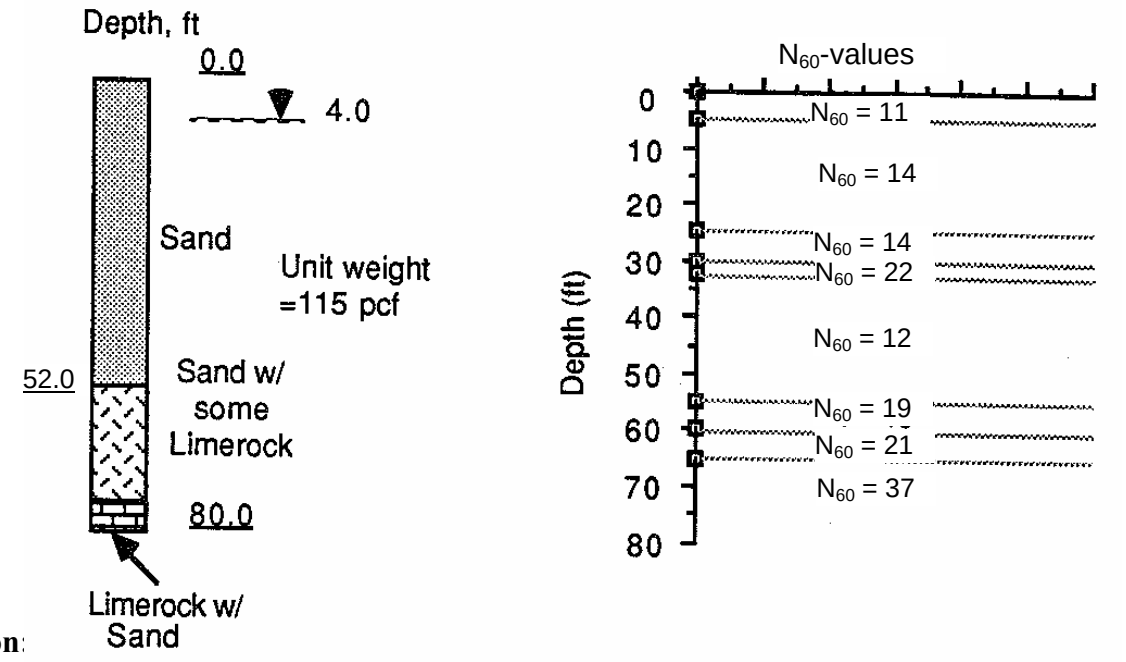

Solution:

The ultimate geotechnical axial load = (FS) (Design Load) = (2.5) (170 tons) = 425 tons. Assume a straight-sided drilled shaft with a diameter of 3-ft and a length of 60-ft. Thus, $\pi(D)$ = 9.42-ft

Use Equation 9-41 to determine ultimate skin resistance, $Q_S = \pi D \sum_{i=1}^{N} \gamma_i' z_i \beta_i \Delta z_i$

Depth Interval, Δz, ft	**Surface Area per depth interval, Δz(π)(D), ft²**	**Average effective vertical (overburden) stress, $p_o=\gamma' z_i$ tsf**	**β** $\beta_i = 1.5 - 0.135\sqrt{z_i}$ with $1.2 > \beta_i > 0.25$	**ΔQ_s Tons**
0 – 4	37.7	0.115	1.20	5.20
4 – 30	245.0	0.572	0.94	131.70
30 – 60	282.7	1.308	0.59	218.20
			Q_S	355.10

Base resistance (N_{60}=21 at 60-ft). Using Equation 9-45a $q_t = 1.2N_{60} = 25.2$ ksf = 12.6 tsf
$A_t = 7.07$ ft² Therefore, $Q_t = (7.07 \text{ ft}^2)(12.6 \text{ tsf}) = 89.1$ tons

Thus, ultimate geotechnical axial resistance, Q_{ult} is given by:

$Q_u = 355.1 + 89.1 = 444.2$ tons ≈ 440 tons > 425 tons Okay.

Example 9-6: Determine the shaft length to resist 150 tons of vertical design load in the mixed (clay on sand) soil profile shown below. Assume a safety factor of 2.5. Assume a total unit weight of 125 pcf for clay and 115 pcf for sand. Water table is at a depth of 17-ft. Assume depth of zone of seasonal moisture change to be 5-ft. Once the shaft is sized for ultimate load, check the deformation under design load of 150 tons.

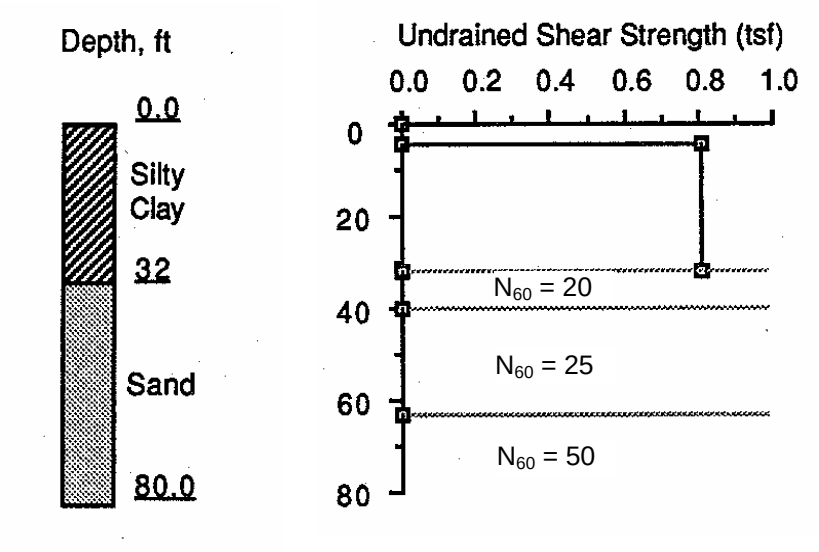

Solution:

For a factor of safety of 2.5, the ultimate axial load is computed to be (2.5)(150 tons) = 375 tons.

For a straight-sided shaft with a diameter of 3.0-ft and a depth of penetration of 50-ft, $\pi(D)$ = 9.42-ft

Use Equation 9-36 and 9-41,

$$Q_s = \pi D \sum_{i=1}^{N} \alpha_i s_{ui} \Delta z_i$$

$$Q_s = \pi D \sum_{i=1}^{N} \gamma_i' z_i \beta_i \Delta z_i$$

Soil	Depth Interval, Δz, ft	Surface Area per depth interval, $\Delta z(\pi)(D)$, ft^2	Shear Strength or Average effective vertical (overburden) stress, tsf	α or β	ΔQ_s Tons
Clay	0 – 5	--	--	0.00	0
Clay	5-32	254.5	0.80 (shear strength)	α = 0.55*	112.0
Sand	32-50	169.6	{(17 ft x 125 pcf) + (32ft -17 ft)(125 pcf-62.4 pcf) +9ft(115 pcf - 62.4 pcf)}/2,000 =3537.4 psf/2,000 = 1.769 tsf	β = 0.64**	192.0
* From Equation 9-37a				**Q_S**	304.0
** From Equation 9-42, $\beta_i = 1.5 - 0.135\sqrt{z_i}$ At mid-depth of sand layer, z_i = 32 ft + (50 ft – 32 ft)/2 = 41 ft At z_i = 41 ft, $\beta_i = 1.5 - 0.135\sqrt{41\,\text{ft}} \approx 0.64$					

Base resistance (N_{60}=25 at 50 ft)

Use Equation 9-45a

$q_t = 1.2N_{60} = 1.2\ (25) = 30$ ksf = 15 tsf

$A_t = 7.07$ ft^2

$Q_t = (7.07\ \text{ft}^2)\ (15.0\ \text{tsf}) = 106$ tons

Total ultimate axial resistance, Q_{ult} is given by:

$Q_u = 304.0 + 106.0 = 416.0$ tons > 375 tons Okay.

<u>Check of settlement under design load (150 tons)</u>

Because most of the load in side resistance and all of the end bearing are derived from sand, Figures 9-52 and 9-53 will be used to estimate settlement. A settlement near the upper bound in both figures will be selected as a conservative estimate.

A settlement of 0.15 percent of the diameter is selected for the average settlement of the sides, or 0.06-inch. That would indicate that about 138 tons is carried in side resistance, and about 12 tons is carried in bearing, assuming that the shaft is essentially incompressible.

Comment: The settlement solution appears to be reasonable.

9.12.7 Estimating Axial Capacity of Shafts in Rocks

Drilled shafts are commonly socketed into rock to limit axial displacements, increase load capacity and/or provide fixity for resistance to lateral loading.

Typically, axial compression load is carried solely by the side resistance on a shaft socketed into rock until a total shaft vertical displacement on the order of 0.4 inches occurs, i.e., elastic compression of the concrete plus downward movement of the shaft under load. At this displacement, the ultimate side resistance in rock, Q_{sr}, is mobilized and slip occurs between the concrete and rock. As a result of this slip, any additional load is transferred to the tip.

The design procedures assume the socket is constructed in reasonably sound rock that is not significantly affected by construction, i.e., the rock does not rapidly degrade upon excavation and/or exposure to air or water, and is cleaned prior to concrete placement, i.e., the rock surface is free of soil and other debris. If the rock is degradable, consideration of special construction procedures, larger socket dimensions, or reduced socket capacities should be considered.

9.12.7.1 Side Resistance in Rocks

For drilled shafts socketed into rock, shaft resistance may be evaluated as follows (Horvath and Kenney, 1979):

$$Q_{sr} = \pi D_r L_r q_{sr} \qquad 9\text{-}46$$

$$q_{sr} = 0.65(\alpha_E)(p_a)\left(\frac{q_u}{p_a}\right)^{0.5} < 0.65(p_a)\left(\frac{f_c'}{p_a}\right)^{0.5} \qquad 9\text{-}47$$

where: D_r = diameter of rock socket (ft)
L_r = length of rock socket (ft)
q_{sr} = unit skin resistance of rock (tsf)
q_u = uniaxial compressive strength of rock (tsf)
p_a = atmospheric pressure =1.06 tsf

α_E = E_M/E_i = reduction factor to account for jointing in rock as provided in Table 5-23 in Chapter 5, where E_M is the elastic modulus of the rock mass and E_i is the elastic modulus of intact rock

f'_c = 28-day compressive strength of concrete (tsf)

Equation 9-46 applies to the case where the side of the rock socket is considered to be smooth or where the rock is drilled using a drilling slurry. Significant additional shaft resistance may be achieved if the borehole is specified to be artificially roughened by grooving. Methods to account for increased shaft resistance due to borehole roughness are provided in FHWA (1999).

Equation 9-46 should be used only for intact rock. When the rock is highly jointed, the calculated q_{sr} should be reduced to arrive at a final value for design. The procedure is as follows:

Step 1. Evaluate the ratio of rock mass modulus to intact rock modulus (i.e., E_m/E_i) by using Table 5-23 in Chapter 5.

Step 2. Evaluate the reduction factor, $\alpha_E = E_M/E_i$, by using Table 5-23.

Step 3. Calculate q_{sr} according to Equation 9-47.

9.12.7.2 Tip Resistance in Rocks

If the rock below the base of the drilled shaft to a depth of 1.0 diameter is either intact or tightly jointed, i.e., there are no compressible materials or gouge-filled seams, and the depth of the socket is greater than 1.5 diameters, then the tip resistance of the rock may be evaluated as follows (FHWA, 1999):

$$Q_{tr} = A_t q_{tr} \qquad 9\text{-}48$$

$$q_{tr} = 2.5\ q_u \qquad 9\text{-}49$$

where: A_t = tip area of rock socket

q_{tr} = unit tip resistance, which is evaluated in terms of q_u, where q_u = unconfined compressive strength of intact rock (tsf)

If the rock below the base of the shaft is jointed and the joints have random orientation, then the reader should refer to the procedures in FHWA (1999).

9.12.8 Estimating Axial Capacity of Shafts in Intermediate GeoMaterials (IGMs)

Intermediate geomaterials (IGMs) are the transitory materials between soils and rocks. IGMs are defined by FHWA (1999) as follows:

- Cohesive IGM – clay shales or mudstones with an undrained shear strength, s_u, of 2.5 to 25 tsf, and
- Cohesionless – granular tills or granular residual soils with N_{60} greater than 50 blows/ft.

For detailed information regarding the estimation of shaft resistances in IGM's, the reader should consult FHWA (1999).

9.13 CONSTRUCTION METHODS FOR DRILLED SHAFTS

There are three basic methods for construction of drilled shafts. These are (a) dry method, (b) wet method and (c) casing method. Each of these methods is briefly presented below.

1. **Dry Method**

   The dry method is applicable to soils above the water table that will not cave or slump when the hole is drilled to its full depth. A soil that meets this specification is a homogeneous stiff clay. The dry method can be employed in some instances with sands above the water table if the sands have some cohesion, or if they will stand for a period of time because of apparent cohesion.

   The dry method can be used for soils below the water table if the soils are low in permeability so that only a small amount of water will seep into the hole during the time the excavation is open.

   The dry method consists of drilling a hole using an auger or bucket drill without casing, cleaning the bottom of the excavation, placing a rebar cage and then filling the hole with concrete. The 4 steps involved in construction of a drilled shaft by the dry method are shown in Figure 9-54.

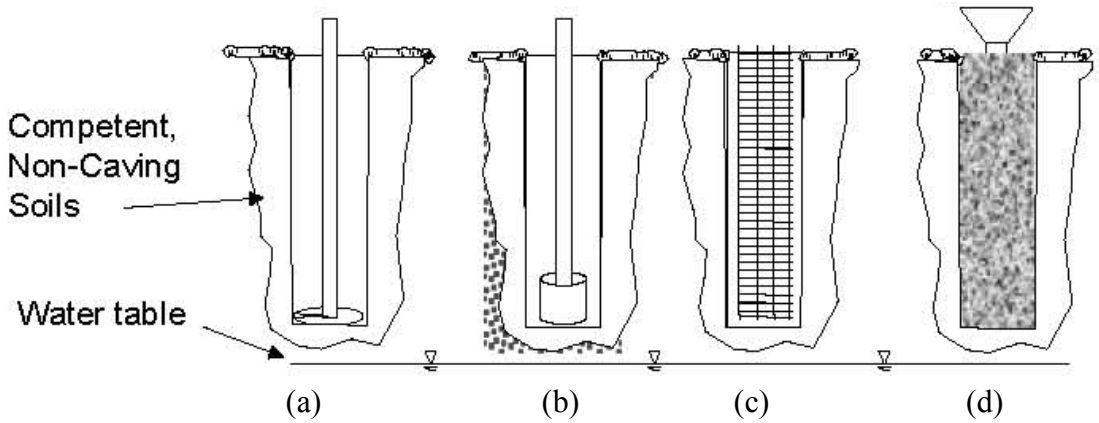

Figure 9-54. Steps in construction of drilled shafts by the dry method (a) drill, (b) clean, (c) position reinforcement cage, and (d) place concrete.

2. **Wet Method**

Bentonite or polymer slurry is introduced into the excavation to prevent caving or deformation of loose or permeable soils. The wet method is commonly used while drilling under the groundwater level. Drilling by use of an auger or clamshell mounted on a kelly bar continues through the slurry. When the desired depth is reached, the excavation is cleaned and the rebar cage is lowered into the slurried hole. Concrete is then tremie-poured into the hole. Slurry is displaced by the heavier concrete and collected at the surface in a sump. The slurry may again be used in another hole. Figure 9-55 shows the 5-step process of shaft construction using wet method.

3. **Casing Method**

The casing method is applicable to sites where soil conditions are such that caving or excessive deformation will occur when a hole is excavated. An example of such a site is a clean sand below the water table. This method employs a cylindrical steel casing inside the excavation to support the caving soil. The excavation is made by driving, vibrating, or pushing a heavy casing to the proposed founding level and by removing the soil from within the casing either continuously as excavation proceeds or in one sequence after the casing has reached the desired depth. Slurry may be required if the excavation is advanced below the ground water table. The excavation is cleaned and the rebar cage is lowered into the excavation. Concrete is then placed, by tremie if the excavation is slurried, and the casing removed. The casing is sometimes permanently left in place. Figure 9-56 shows the 5-step process of shaft construction using the casing method.

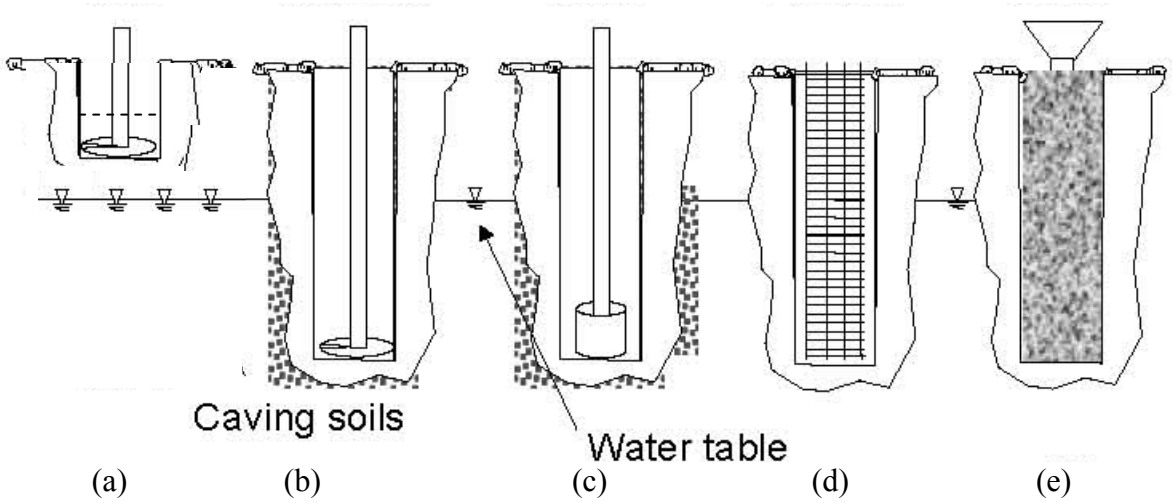

Figure 9-55. Steps in construction of drilled shafts by the wet method (a) start drilling and introduce slurry (bentonite or polymer) in the excavation PRIOR to encountering the known piezometric level, (b) continue drilling with slurry in the excavation, (c) clean the excavation and slurry, (d) position reinforcement cage, and (e) place concrete by tremie.

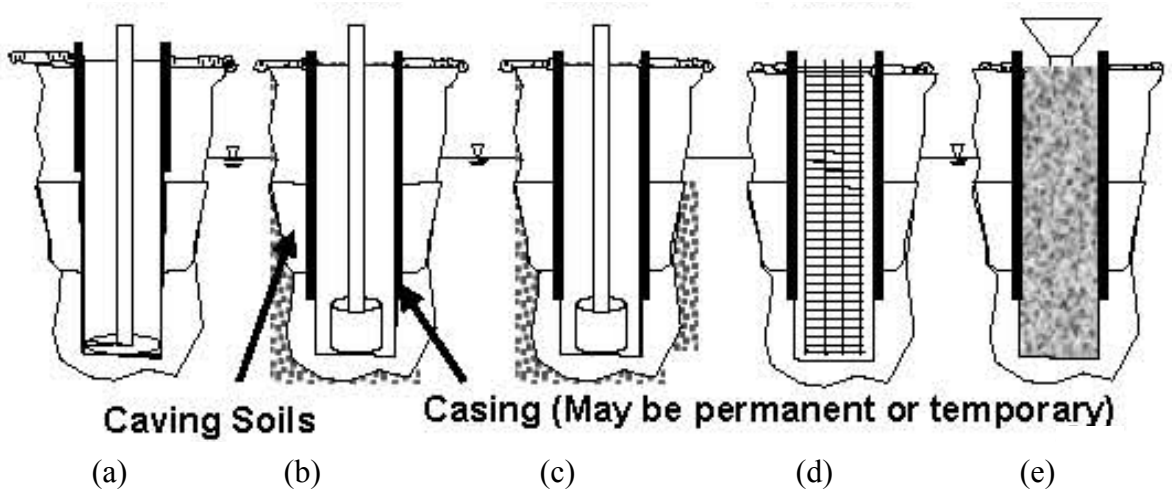

Figure 9-56. Steps in construction of drilled shafts by the casing method (a) start drilling and introduce casing in the excavation PRIOR to encountering the known piezometric level and/or caving soil, (b) advance the casing through the soils prone to caving, (c) clean the excavation, (d) position reinforcement cage, and (e) place concrete and remove the casing if it is temporary.

It is critical that the correct construction method be chosen for a given project. Unlike driven piles, which are assembled under controlled conditions and then driven into the ground, drilled shafts are "manufactured" on-site. Thus, the quality of the constructed drilled shaft will be only as good as the quality of the construction processes. In particular, the side and tip resistances are directly affected by the construction processes. While each of the steps in Figures 9-54 to 9-56 are important, t**he most important step is related to cleaning of the shaft excavation. There are many considerations involved in the proper cleaning of shafts that are beyond the scope of this manual.** Figure 9-57a shows a photograph of a shaft in which the excavation was not cleaned properly, while Figure 9-57b shows a photograph of a shaft where the cleaning was adequate. These photographs clearly illustrate the need for proper cleaning of the shaft excavation. A detailed discussion of the drilled shaft construction and inspection processes including procedures to assure adequate cleaning can be found in FHWA (1999) and FHWA (2002d).

(a)  (b) 

Figure 9-57. Photographs of exhumed shafts (a) shaft where excavation was not adequately cleaned, (b) shaft where excavation was properly cleaned (FHWA, 2002d).

9.14 QUALITY ASSURANCE AND INTEGRITY TESTING OF DRILLED SHAFTS

Unlike piles, which are manufactured in a factory (e.g., steel pipe piles) or a casting yard (e.g., precast concrete piles), drilled shafts are "manufactured" at the site. Anomalies often develop during the construction of drilled shafts as shown in Figure 9-57a. An anomaly is a deviation from an assumed uniform geometry of the shaft and/or from the required physical properties of the shaft. Typical anomalies may include necking or bulbing, "soft bottom" conditions, voids or soil intrusions, poor quality concrete, debonding, lack of concrete cover over the reinforcement steel and honey-combing. Non-destructive test (NDT) methods are used for Quality Assurance (QA) integrity testing of drilled shaft foundations to identify anomalies.

NDT testing techniques can be categorized as external and internal. External NDT techniques are used at the surface of the concrete structure when access to the interior of the concrete is not available. Examples of external NDT techniques include Sonic Echo (SE), Impulse Response (IR) or Ultra-seismic (US). Internal NDT techniques are used when testing equipment can access the interior of a concrete structure through either cast-in-place access tubes or cored access paths, or through cast-in-place equipment within the concrete (e.g., strain gages). **Commonly used internal NDT techniques include standard Cross-hole Sonic Logging (CSL) with zero-offset measurements and Gamma-Gamma Density Logging (GDL)**. Both of these techniques are described below. Other more specialized internal NDT techniques include the Neutron Moisture Logging (NML) and Temperature Logging (TL). All of the NDT methods are discussed in FHWA (2003). Summaries of the methods are given in FHWA (1999), FHWA (2002d) and by Samtani, *et al.* (2005).

9.14.1 The Standard Crosshole Sonic Logging (CSL) Test

In the standard CSL test method, an ultrasonic transmitter or source and receiver probes are first lowered to the bottom of a pair of water-filled pre-installed access tubes as shown in Figure 9-58. It is common industry practice to locate the access tubes inside the reinforcing cage. The two probes are then pulled up simultaneously such that the probes are level with each other, i.e., zero-offset. The travel time of the ultrasonic wave between the tubes is recorded along with the amplitude of the signal as a function of every inch of depth. This test procedure is repeated for all possible paired combination of access tubes along the outer perimeter as well as across the inner diagonal of the shaft as shown in the inset Plan View in Figure 9-58. Typically, one tube per foot diameter of the shaft is installed for CSL tests. Thus, for 6-ft diameter shaft, 6 tubes are used. The minimum number of tubes should be 3.

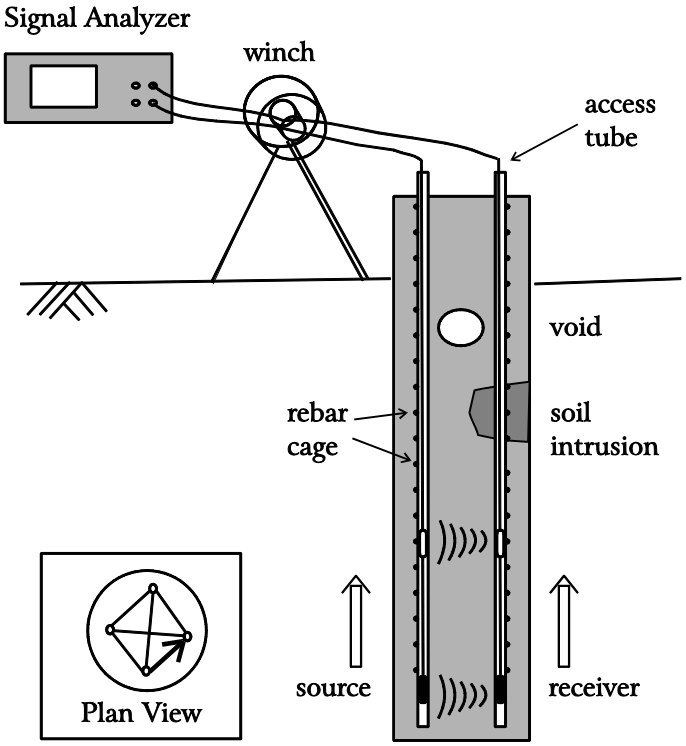

Figure 9-58. Schematic of CSL Test (Samtani, *et al.*, 2005).

The measured travel time, t, between two tubes with a known center to center distance, d, is expressed in terms of velocity as: V =d/t. This computed velocity, V, is compared with the theoretical compressional wave velocity, V_C, in concrete. The theoretical ultrasonic wave velocity in competent concrete with unconfined compressive strength, f_c, in the range from 3,000 to 5,000 psi is approximately 10,000 to 11,500 ft/sec, respectively (Samtani *et al.*, 2005). As a comparison, the sonic velocity in water and air is approximately 5,000 ft/sec and 1,000 ft/sec, respectively. The computed velocity is compared with the theoretical velocity and expressed in terms of velocity reductions, VR = $(1\text{-}V/V_C)(100)\%$. A qualitative rating is assigned to the concrete based on VR, as follows:

VR	Rating
0-10%	Good
10-20%	Questionable
>20%	Poor

The ratings are partially based on the estimated reduction in strength of concrete in anomalous zones. For example, if VR=10% at a given location in a shaft, then the f_c at that location is approximately 65% of the nominal 28-day f'_c value of the concrete in that shaft. Similarly, a concrete with VR=20% implies that f'_c at that location is 40% of the 28-day strength.

With the exception of voids and possibly honeycombs, the locations of poor concrete can be confirmed by checking the signal amplitudes. Weaker concrete absorbs the energy of the sonic wave more than sounder concrete and this phenomenon is reflected in lower signal amplitudes. Thus, if the measurements in the shaft indicate lower velocity and lower signal amplitudes then they typically point to anomalous zones due to soil intrusions or poor quality concrete. An example single plot display format that includes velocity and signal amplitude profiles is shown in Figure 9-59. In this particular case, it can be seen that a soft bottom condition in the shaft is reflected at the very bottom of the profile by a drastic change in both in the velocity and amplitude profiles.

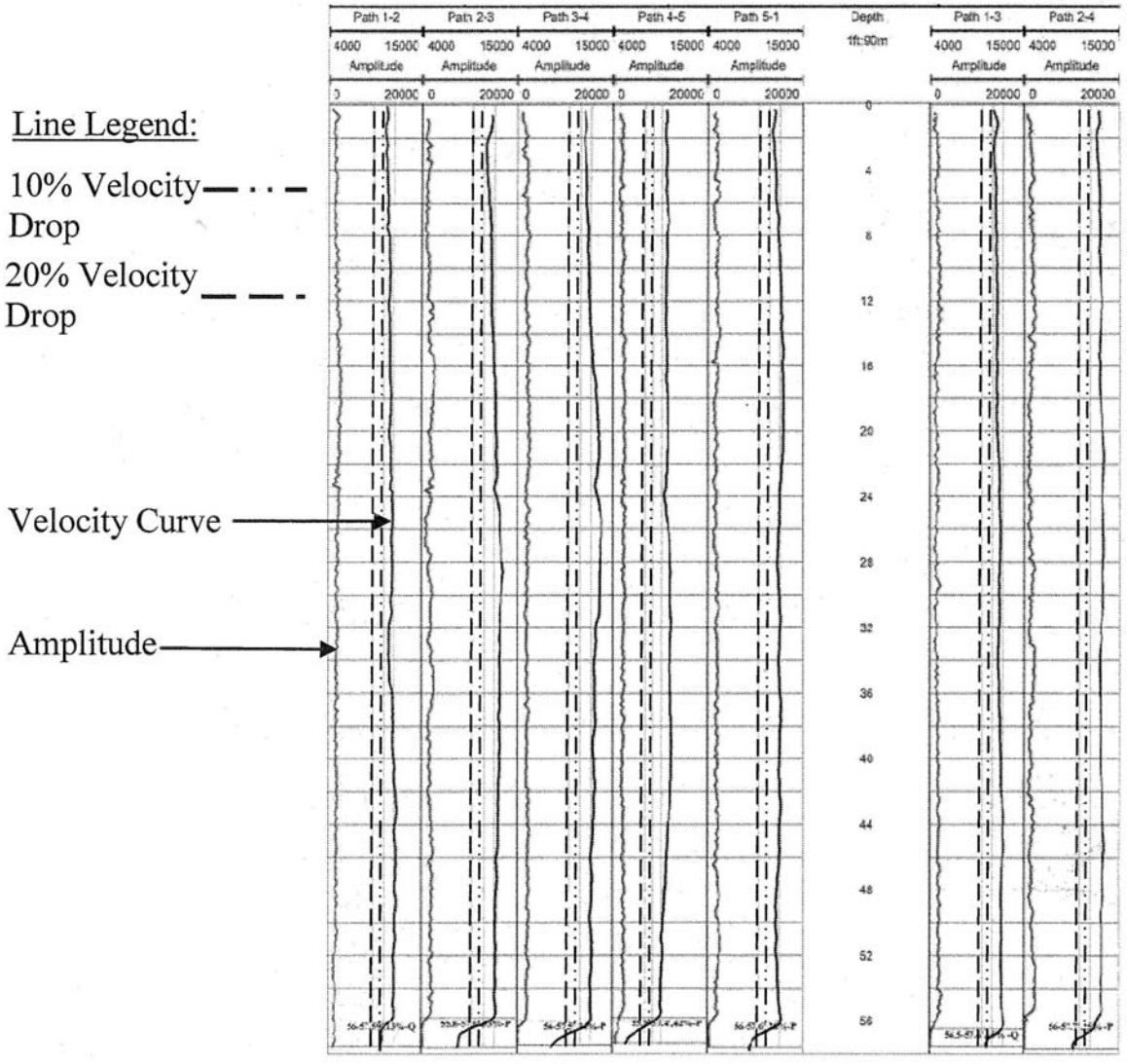

Figure 9-59. Single plot display format for the CSL data for shaft with five tubes (Samtani, *et al.*, 2005).

If the tubes debond from the concrete, i.e., there is a small air gap between the outer surface of the tube and the concrete of the shaft, then the CSL test will record a partial or complete loss of signal depending on the extent of the debonding around the perimeter of the tube at that location. Debonding can occur with Schedule 40 PVC access tubes particularly near the ground surface or above the groundwater table where temperature gradients are generally greater. For Schedule 40 PVC tubes, the debonding may occur within a week after placement of concrete as the concrete sets and tends to shrink away from the tubes. Thus, if Schedule 40 PVC tubes are used, then it is generally recommended to perform the CSL tests within 2 to 3 days after concrete placement. A thicker wall PVC tube, such as a Schedule 80 tube, may help extend this timeframe because it is able to withstand the higher temperature gradients better than a thinner PVC tube. Longer time frames can be achieved by the use of steel tubes that experience minimal to no debonding. Therefore, many owners tend to specify steel tubes to alleviate the debonding problems. However, in doing so, the owners are giving up an advantage of the PVC tubes in that they can serve as access paths to repair the shafts should an anomaly be identified by the CSL test since the PVC tubes can be cut open at any depth by use of a high velocity water jet, commonly known as the "water knife." Use of a water knife is much more difficult, if not impossible, in steel due to the practical limitation of generating a very high water velocity at depth within the access tubes.

Cross-hole Sonic Logging Tomography (CSLT) using multi-offset CSL method is a logical newer extension of the CSL technique and is starting to gain acceptance. The Perimeter Sonic Logging (PSL) is yet another new variation in which zero-offset or multi-offset CSL may be performed in PVC tubes attached to the outside of the reinforcing cage. Samtani, *et al.* (2005) and FHWA (2003) provide summaries of these methods

9.14.2 The Gamma Density Logging (GDL) Test

A typical field setup for the GDL test is shown in Figure 9-60. In this test a weak Cesium-137 (radioactive) source emits gamma rays into the surrounding medium. A small fraction of the gamma ray photons are reflected back to the probe due to Compton scattering. The intensity of the reflected photons is recorded by a NaI scintillation crystal as counts per second (cps). The measured count rate (*cps*) depends on the electron density of the surrounding medium, which is proportional to the mass per unit volume. The instrument is calibrated by placing the probe in an environment of known density in order to convert the measured count rate (cps) into the units of density or unit weight, e.g. lb/ft^3 (pcf).

In the GDL test, the radius of the investigation is largely governed by ½ of the source-detector spacing. Good concrete conditions will result in a near continuous alignment of the data.

Anomalous zones due to soil intrusions, poor concrete or voids are characterized by low density which leads to a high count rate.

A typical GDL log is shown in Figure 9-61. In a GDL log, the measured gamma ray intensity count rate (cps) is presented in terms of unit weight (pcf). In Figure 9-61, the results are plotted in 4 separate sub-plots from the tested access tubes. Each individual sub-plot depicts the GDL results from a 14-inch source-detector separation (corresponding to about 5- to 6-inch radius of investigation) presented in a magnified density scale of 130-180 pcf. Also, in each sub-plot, the mean as well as the minus 2 (-2) and minus three (-3) standard deviation (SD) from mean curves are displayed as vertical guidelines. Depths, in feet, are measured from the top of the shaft and are shown on the vertical axis.

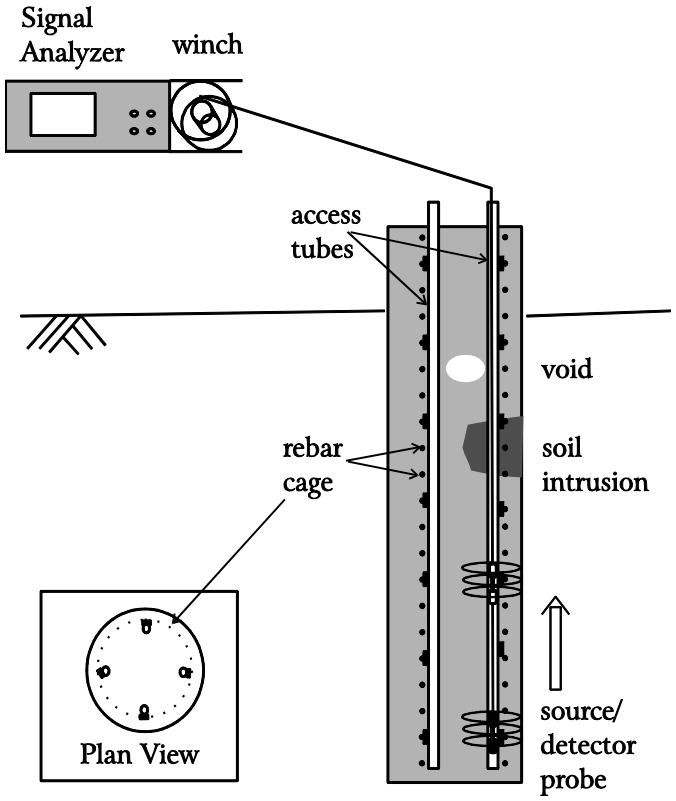

Figure 9-60. Schematic of GDL Test (Samtani, *et al.*, 2005).

The results of GDL tests are used to define "questionable" concrete conditions as a zone with reduction in unit weight between -2SD and -3SD and "poor" concrete conditions as a zone with reduction in unit weight of greater than -3SD from the mean (M). These criteria are based on the observation that a cps data set approximates a standard normal distribution probability function in which 99.73% of the data is within M±3SD. Therefore, when data points are identified

beyond 3SDs, they are considered to represent an anomaly. While these definitions are generally accepted, it is not widely recognized that the computation of M and SD varies during presentation of the results by various testers/agencies. Some testers or agencies define the M and SD with respect to a given tube while others may define these quantities based on all tubes within a shaft, i.e. ignore the variation of steel density and hole geometry, or all tubes from a group of shafts that may form a single overall foundation element for a superstructure. Obviously, the definition of the concrete quality will be different based on the definition of the M and SD. Therefore, the user should be careful with the interpretation of the GDL test data.

Unlike the CSL test, the GDL is not affected much by debonding of the tubes from the concrete. Therefore, a PVC tube is generally used, although steel can also be used with GDL testing. It must be recognized, however, that the thicker or denser the tube material, the lower the measured counts per second (cps) since the tube itself will absorb some of the electrons. Therefore, the user of the data should review the calibration data and check whether the tube type used during calibration is consistent with that used in the actual shaft and the density of the shaft reinforcement.

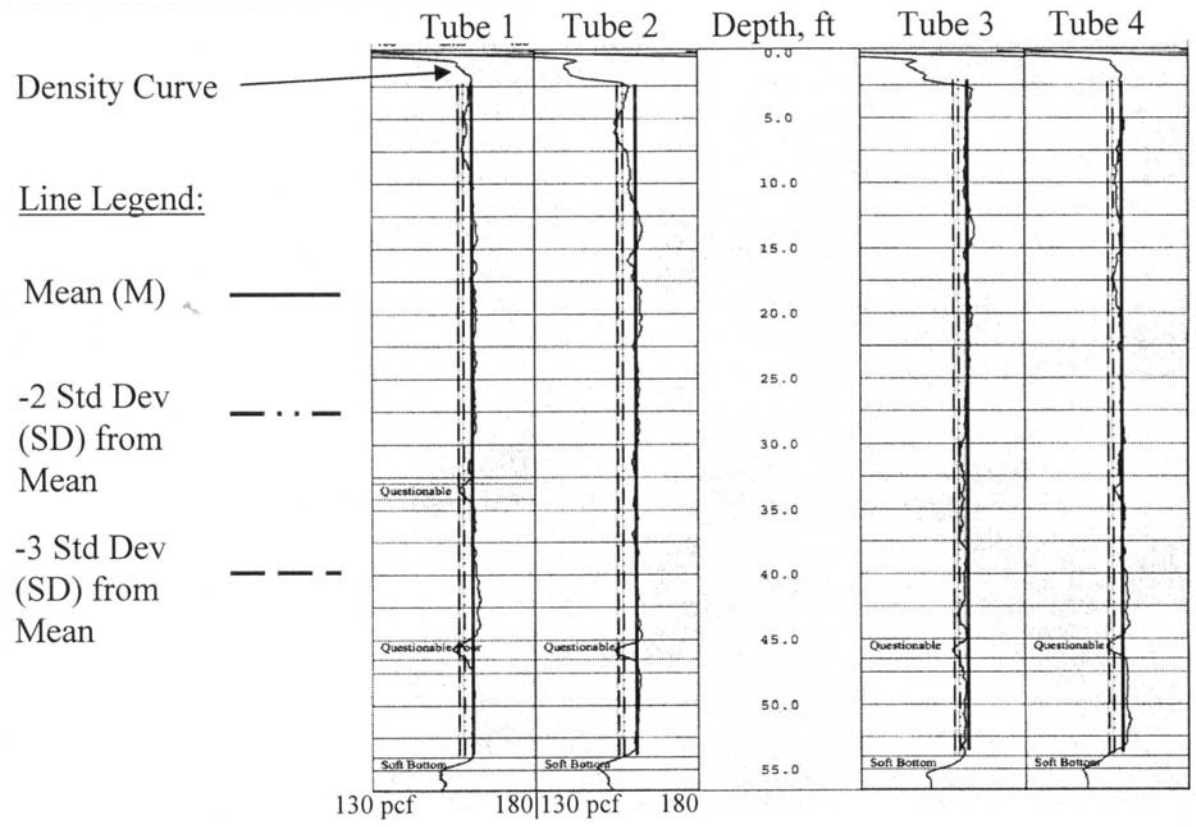

Figure 9-61. Single plot display format for the GDL data for shaft with four tubes (Samtani, *et al.*, 2005).

9.14.3 Selecting the Type of Integrity Test for Quality Assurance

Most agencies use either the CSL or GDL test method to evaluate the structural integrity of a constructed shaft. As shown in Figure 9-58, the CSL test evaluates the area of the shaft between the tubes. Since the tubes are commonly located on the inside of the cage, this means that only the portion of the shaft within the reinforcing cage is evaluated. On the other hand, the GDL test evaluates a portion of the shaft immediately surrounding a tube. In other words, GDL evaluates a zone inside and outside the reinforcing cage as shown in Figure 9-60. Due to the different portions of the shaft evaluated by the CSL and GDL tests, it is recommended that both tests be performed to assure an evaluation of the concrete inside and outside the reinforcing cage.

9.15 STATIC LOAD TESTING OF DEEP FOUNDATIONS

Static load testing of deep foundations is the most accurate method of determining load capacity. Depending upon the size of the project, static load tests may be performed either during the design stage or the construction stage. Conventional load test types include the **axial compression**, **axial tension or lateral load tests**.

The purpose of this section is to provide an overview of static testing and its importance as well as to describe the basic test methods and interpretation techniques. For additional details on load testing for deep foundations, the reader is referred to FHWA (1992c) and ASTM D 1143. It may be noted that ASTM D 1143 was not re-approved in 2006. Therefore, as of the publication date of this manual, there is no accepted ASTM standard for static load tests. However, for the purposes of this manual, the latest ASTM D 1143 prior to 2006 is adequate from the viewpoint of the basic aspects of load testing.

9.15.1 Reasons for Load Testing

1. To minimize risks to the structure by confirming the suitability of the deep foundation to support the design load with an appropriate factor of safety.

2. It is the most positive way for determining the capacity of deep foundations.

3. To develop information for use in the design and/or construction of a deep foundation.

4. Implementation of new static or dynamic analysis methods or procedures.

5. Calibrations of new design procedures such as the Load and Resistance Factor Design (LRFD).

9.15.2 Advantages of Static Load Testing

The advantages of performing static load tests are summarized as follows:

1. A static load test allows a more rational design. Confirmation of pile-soil capacity through static load testing is considerably more reliable than capacity estimates from static capacity analyses and dynamic formulas.

2. An improved knowledge of deep foundation-soil behavior is obtained that may allow a reduction in deep foundations lengths or an increase in the design load, either of which may result in potential savings in foundation costs.

3. With the improved knowledge of deep foundation-soil behavior, a lower factor of safety may be used on the design load. A factor of safety of 2.0 is generally applied to design loads confirmed by load tests as compared to a factor of safety of 3.5 used on design loads in the Modified Gates dynamic formula. Hence, a cost savings potential again exists (Refer to Table 9-5).

4. The ultimate geotechnical capacity determined from load testing allows confirmation that the design load may be adequately supported at the planned foundation penetration depth.

Engineers are sometimes hesitant to recommend a static load test because of cost concerns or potential time delays in design or construction. While the cost of performing a static load test should be weighed against the anticipated benefits, cost alone should not be the determining factor.

Delays to a project in the design or construction stage usually occur when the decision to perform static load tests is added late in the project. Such delays can be minimized by determining early in the project whether a static load test program should be performed. In the construction stage, delays can be minimized by clearly specifying the number and locations of static load tests to be performed as well as the time necessary for the engineer to review the results. In addition, the specifications should state that the static test must be performed prior to ordering pile lengths or commencing production driving. In this way, the test results are available to the design and construction engineer early in the project so that the maximum benefits can be obtained. At the same time the contractor is also aware of the test requirements and analysis duration and can schedule the project accordingly.

9.15.3 When to Load Test

The following criteria, adapted and modified from FHWA (1992c), summarize conditions when pile load testing can be effectively utilized:

1. When substantial cost savings can be realized. This is often the case on large projects involving either friction piles to prove that lengths can be reduced or end bearing piles to prove that the design load can be increased. Testing can also be justified if the savings obtained by using a lower factor of safety equals or exceeds the testing cost.

2. When a safe design load is uncertain due to limitations of an engineer's experience base or due to unusual site or project conditions.

3. When subsurface conditions vary considerably across the project, but can be delineated into zones of similar conditions. Static tests can then be performed in representative areas to delineate foundation variation.

4. When a significantly greater load is contemplated relative to typical design loads and practice.

5. When time dependent changes in deep foundation capacity are anticipated as a result of soil setup or relaxation.

6. Verification of new design or testing methods.

7. When new, unproven deep foundation types and/or pile installation procedures are utilized.

8. When existing deep foundations will be reused to support a new structure with heavier design loads.

9. When a reliable assessment of uplift capacity or lateral behavior is important.

10. When, during construction, the estimated ultimate capacity determined by using dynamic formulas or dynamic analysis methods differs from the estimated capacity at that depth determined by static analysis. For example, H-piles that "run" when driven into loose to medium dense sands and gravels.

11. Calibrations of new design procedures such as the Load and Resistance Factor Design (LRFD).

Experience has also shown that load tests will typically confirm that pile lengths can be reduced at least 15 percent versus the lengths that would be required by the Engineering News (EN) formula on projects where piles are supported predominantly by shaft resistance. This 15 percent pile length reduction was used to establish the following “rule of thumb” formula to compute the total estimated pile length that the project must have to make the load test cost effective based purely on material savings alone.

$$\text{Total estimated pile length in feet on project} \geq \frac{\text{cost of load test}}{(0.15)\,(\text{cost / ft of pile})} \qquad 9\text{-}50$$

The above formula may not be valid for drilled shafts since the EN formula is not applicable.

9.15.4 Effective Use of Load Tests

9.15.4.1 Design Stage

The best information for design of a deep foundation is provided by the results of a load testing program conducted during the design phase. The number of static tests, types of piles/shafts to be tested, method of driving and test load requirements, method of shaft excavation should be selected by the geotechnical and structural engineers responsible for design. A cooperative effort between the two is necessary. The following are the advantages of load testing during the design stage.

a. Allows load testing of several different pile/shaft types and lengths resulting in the design selection of the most economical pile/shaft foundation.

b. Confirm driveability to minimum penetration requirements and suitability of foundation capacity at estimated pile penetration depths.

c. Establishes preliminary driving criteria for production piles.

d. Pile driving information released to bidders should reduce their bid "contingency."

e. Confirm the excavation and excavation support methods for drilled shafts.

e. Reduces potential for claims related to pile driving problems or shaft excavation methods.

f. Allows the results of the load test program to be reflected in the final design and specifications.

9.15.4.2 Construction Stage

Load testing at the start of construction may be the only practical time for testing on smaller projects that can not justify the cost of a design stage program. Construction stage static tests are invaluable to confirm that the design loads are appropriate and that the pile installation procedure

is satisfactory. Driving of test piles and load testing is frequently done to determine the pile order length at the beginning of construction. These results refine the estimated pile lengths shown on the plans and establish minimum pile penetration requirements.

9.15.5 Prerequisites for Load Testing

In order to plan and implement a static load testing program adequately, the following information should be obtained or developed.

1. A detailed subsurface exploration program at the test location. A load test is not a substitute for a subsurface exploration program.

2. Well defined subsurface stratigraphy including engineering properties of soil materials and identification of groundwater conditions.

3. Static pile capacity analyses to select pile type(s) and length(s) as well as to select appropriate location(s) for load test(s).

4. For drilled shafts, caliper-logging to determine the exact dimensions of the shaft excavation. Caliper-logging is required because the actual dimensions of excavations in geomaterials can vary significantly from the diameter of the drilling tool due to a variety of geologic factors or drilling considerations. Calipers are available in either mechanical or electronic configurations. Determination of the exact dimensions of the excavation is the key to proper interpretation of the load test results.

5. For drilled shafts, integrity testing should be performed prior to the load test to determine whether the shaft needs to be structurally repaired so that it has enough structural capacity to sustain the test loads.

9.15.6 Developing a Static Load Test Program

The goal of a static load test program should be clearly established. The type and frequency of tests should be selected to provide the required knowledge for final design purposes or construction verification. A significantly different level of effort and instrumentation is required if the goal of the load test program is simply to confirm the ultimate pile capacity or if detailed load-transfer information is desired for final design. The following items should be considered during the planning stage of the load test program so that the program provides the desired information.

1. The capacity of the loading apparatus (reaction system and jack) should be specified so that the test pile(s) may be loaded to plunging failure. A loading apparatus designed to load a pile to only twice the design load is usually insufficient to obtain plunging failure. Hence, the true factor of safety on the design load cannot be determined, and the full benefit from performing the static test is not realized.

2. Specifications should require use of a load cell and spherical bearing plate as well as dial gages with sufficient travel to allow accurate measurements of load and movement at the pile head. Where possible, deformation measurements should also be made at the pile toe and at intermediate points to allow for an evaluation of shaft and toe bearing resistance.

3. The load test program should be supervised by a person experienced in this field of work.

4. A test pile installation record should be maintained with installation details appropriately noted. Too often, only the hammer model and driving resistance are recorded on a test pile log. Additional items such as hammer stroke (particularly at final driving), fuel setting, accurately determined final set, installation aids used and depths at which they are used, predrilling, driving times, stops for splicing, etc., should be recorded.

5. Use of dynamic monitoring equipment on the load test pile is recommended for estimates of pile capacity at the time of driving, evaluation of drive system performance, calculation of driving stresses, and subsequent refinement of soil parameters for wave equation analysis.

9.15.7 Compression Load Tests

Deep foundations are most often tested in compression, but they can also be tested in tension or for lateral load capacity. Figure 9-62 illustrates the basic mechanism of performing a compression pile load test. This mechanism normally includes the following steps:

1. The pile is loaded incrementally from the pile head according to some predetermined loading sequence, or it can be loaded at a continuous, constant rate.

2. Measurements of load, time, and movement at the pile head and at various points along the pile shaft are recorded during the test.

3. A load movement curve is plotted.

4. The failure load and the movement at the failure load are determined by one of several methods of interpretation.

5. The movement is usually measured only at the pile head. However, the pile can be instrumented to determine movement anywhere along the pile. Telltales (solid rods protected by tubes) shown in Figure 9-62 or strain gages may be used to obtain this information.

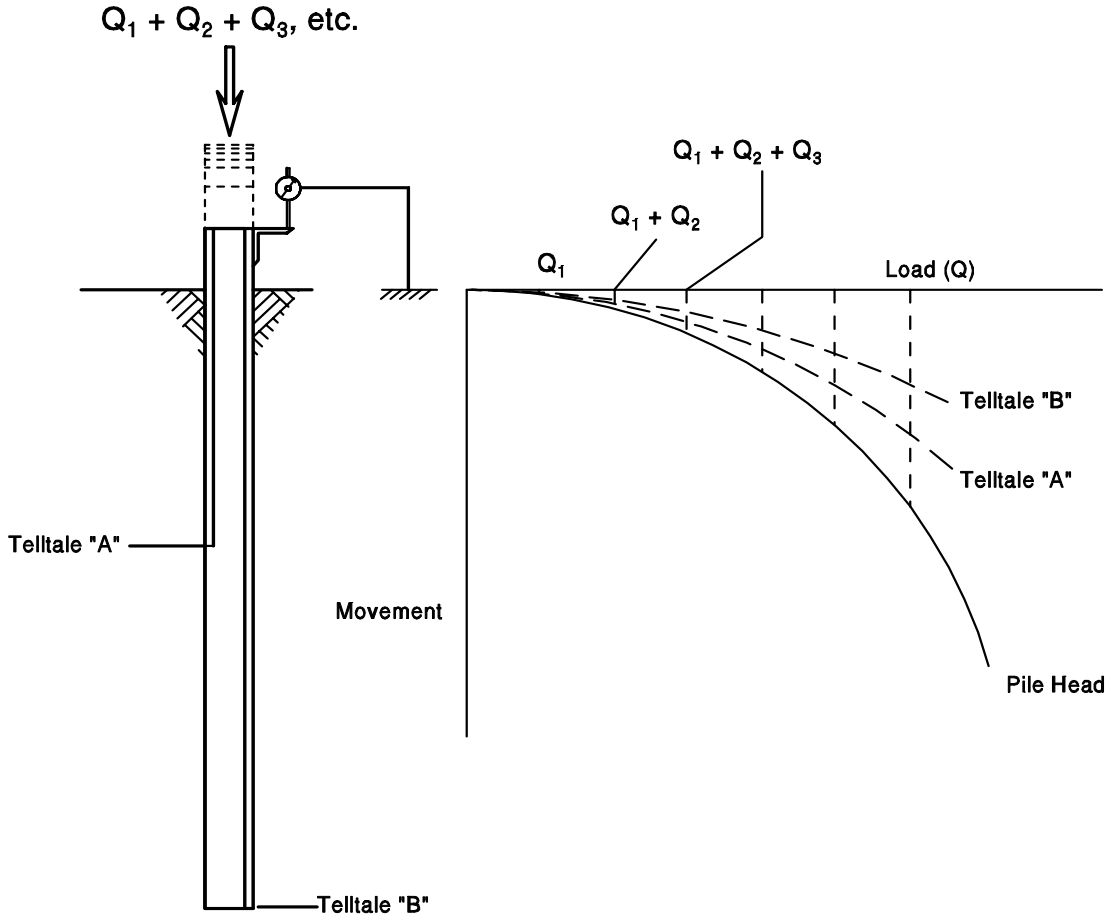

Figure 9-62. Basic mechanism of a compression pile load test (FHWA, 2006a).

9.15.7.1 Compression Test Equipment

ASTM D1143 recommends several alternative systems for (1) applying compressive load to the pile, and (2) measuring movements. Most often, compressive loads are applied by hydraulically jacking against a beam that is anchored by piles or ground anchors, or by jacking against a weighted platform. A schematic of a typical compression load test setup is presented in Figure 9-63. The primary means of measuring the load applied to the pile should be with a calibrated load cell. The jack load should also be recorded from a calibrated pressure gage, such as the Bourdon gage shown in Figure 9-63. To minimize eccentricities in the applied load, a spherical bearing plate should be included in the load application arrangement.

Axial pile or shaft head movements are usually measured by dial gages or LVDT's that measure movement between the pile head and an independently supported reference beam. ASTM requires the dial gages or LVDT's have a minimum of 2 inches (50 mm) of travel and a precision of at least 0.01 inches (0.25 mm). It is preferable to have gages with a minimum travel of 3 inches (75 mm) and with a precision of 0.001 inches (0.025 mm) particularly when testing long piles that may undergo large elastic deformations under load. A minimum of two dial gages or LVDT's mounted equidistant from the center of the pile and diametrically opposite to each other should be used. Two backup systems consisting of a scale, mirror, and wire system should be provided with a scale precision of 0.01 inches (0.25 mm). The backup systems should also be mounted on diametrically opposite pile faces. Both the reference beams and backup wire systems are to be independently supported with a clear distance of not less than 8 ft (2.5 m) between supports and the test pile. A remote backup system consisting of a survey level should also be used in case reference beams or wire systems are disturbed during the test.

ASTM D 1143 specifies that the clear distance between a test pile and reaction piles be at least 5 times the maximum diameter of the reaction pile or test pile, whichever has the greater diameter if not the same pile type, but not less than 7 ft (2 m). If a weighted platform is used, ASTM D 1143 requires the clear distance between the cribbing supporting the weighted platform and the test pile exceed 5 ft (1.5 m).

Photographs of the load application and movement monitoring components are presented in Figures 9-64 and 9-65. A typical compression load test arrangement using reaction piles is presented in Figure 9-66 and a weighted platform arrangement is shown in Figure 9-67. Additional details on load application as well as head load and movement measurements may be found in ASTM D1143 as well as in FHWA (1992c).

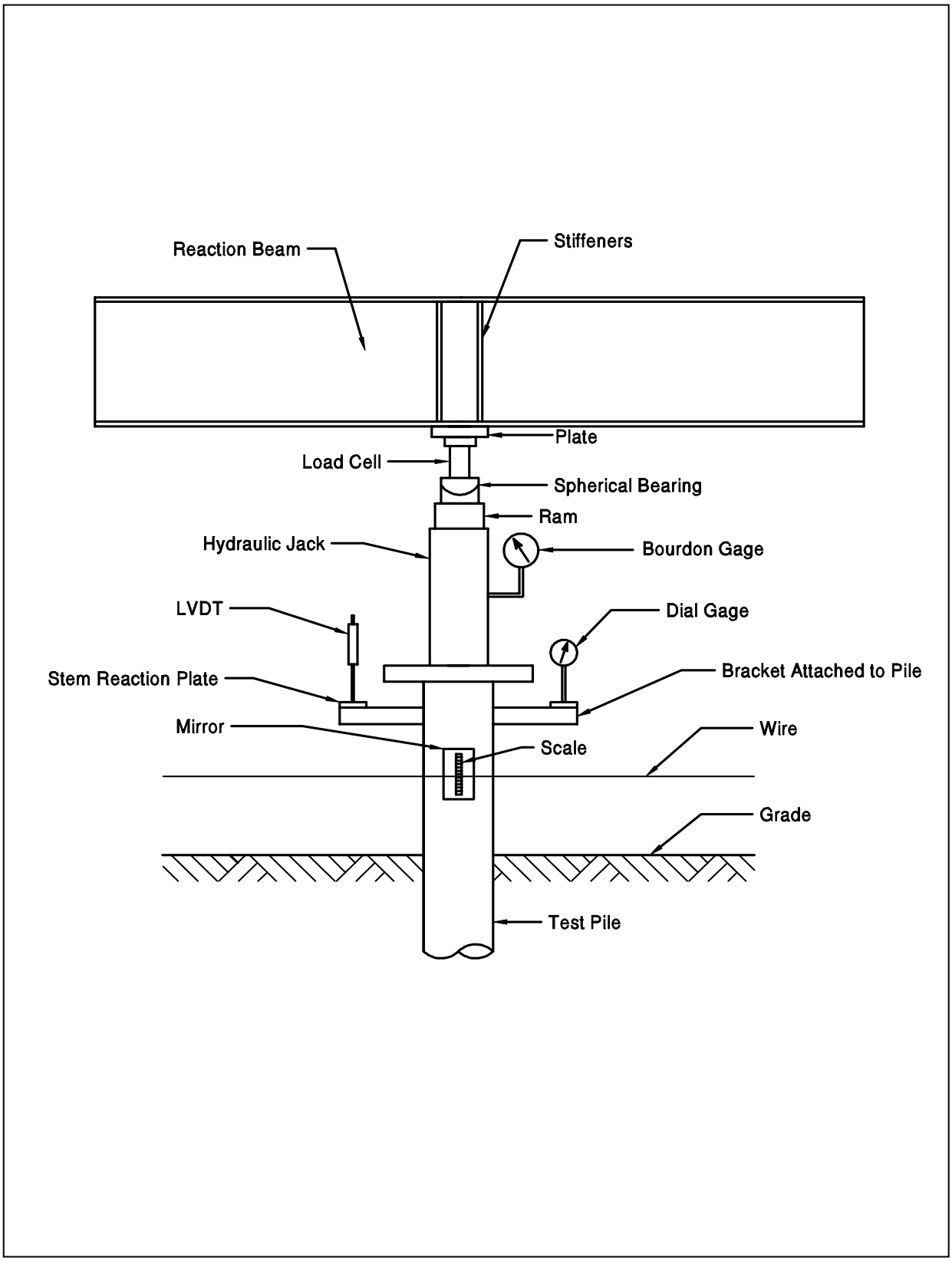

Figure 9-63. Typical arrangement for applying load in an axial compressive test (FHWA, 1992c).

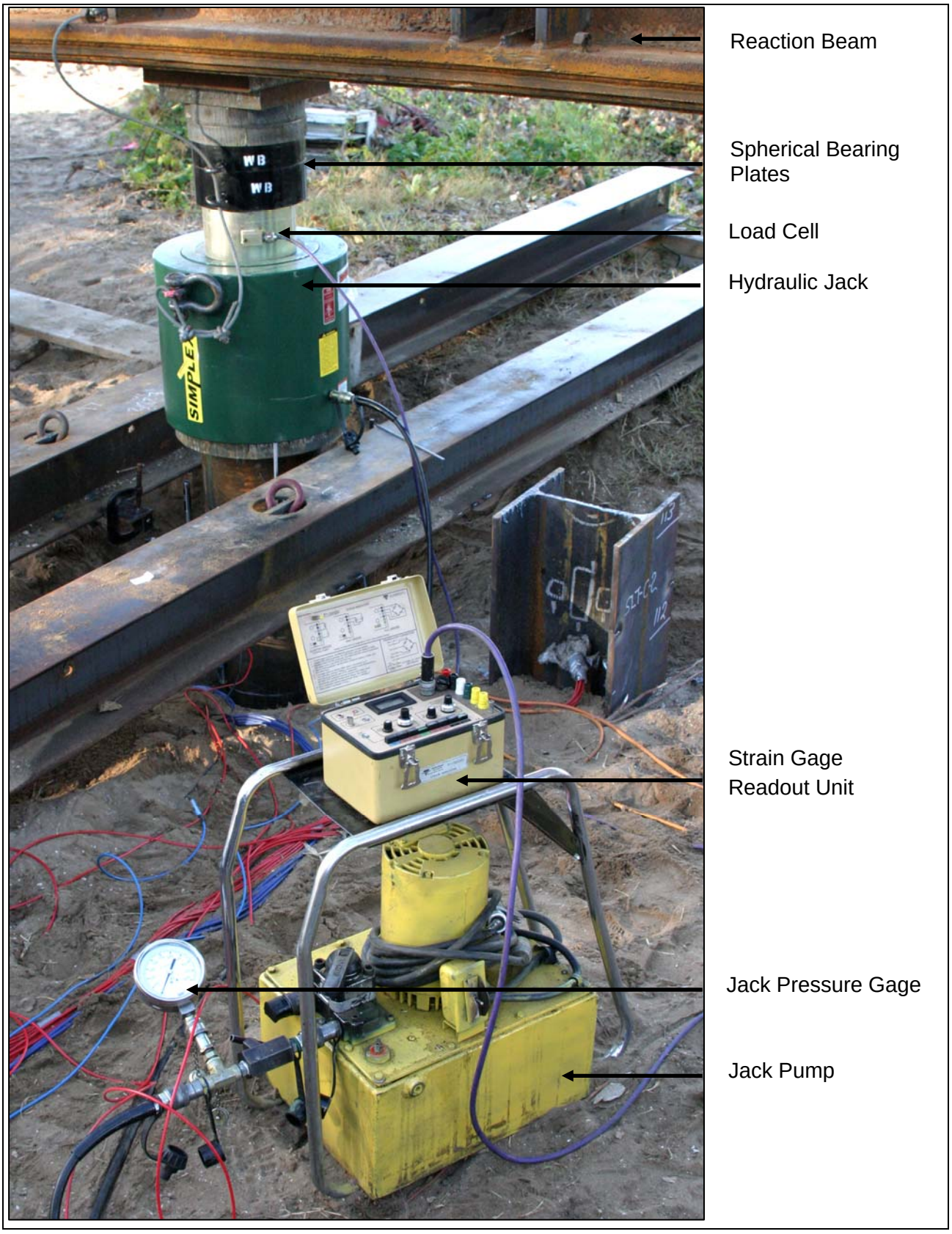

Figure 9-64. Load test load application and monitoring components (FHWA, 2006a).

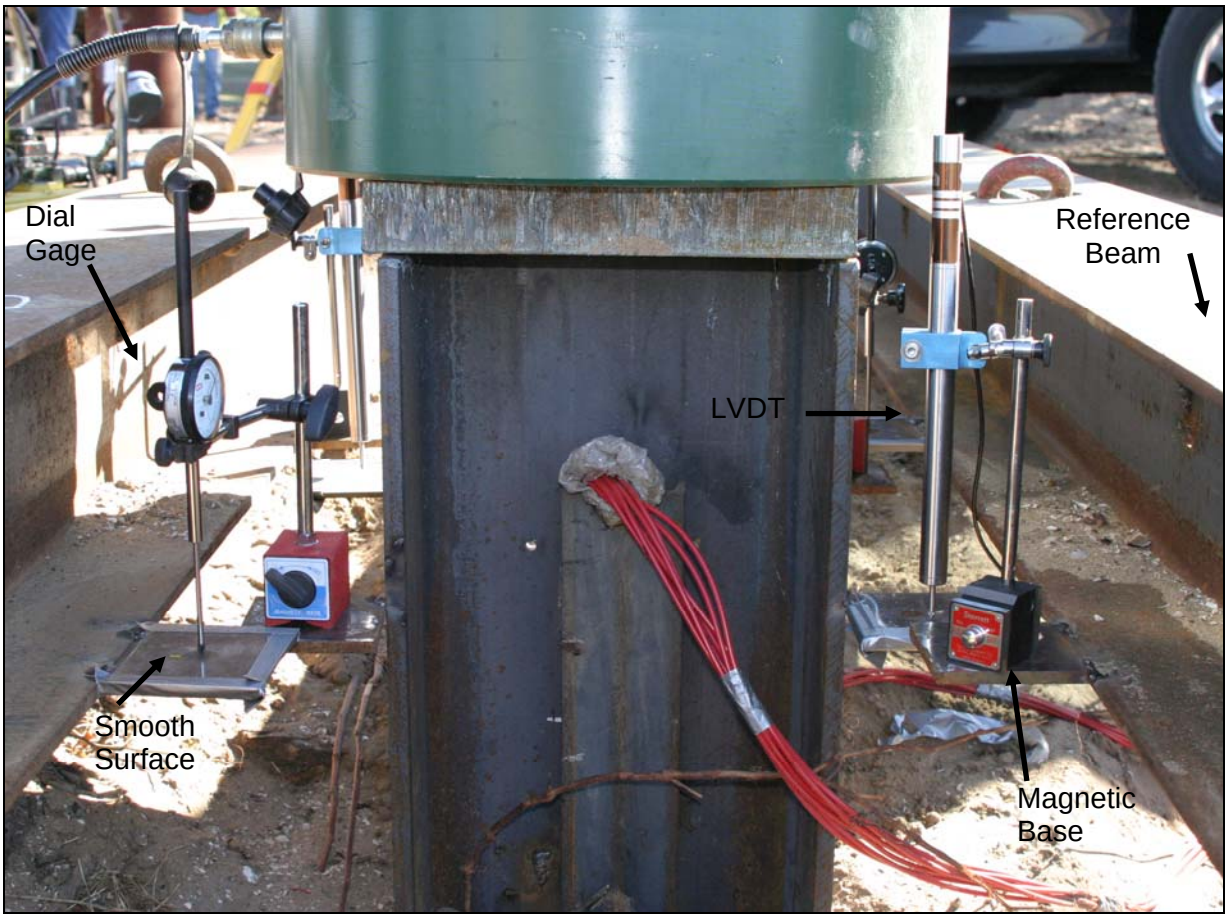

Figure 9-65. Load test movement monitoring components (FHWA, 2006a).

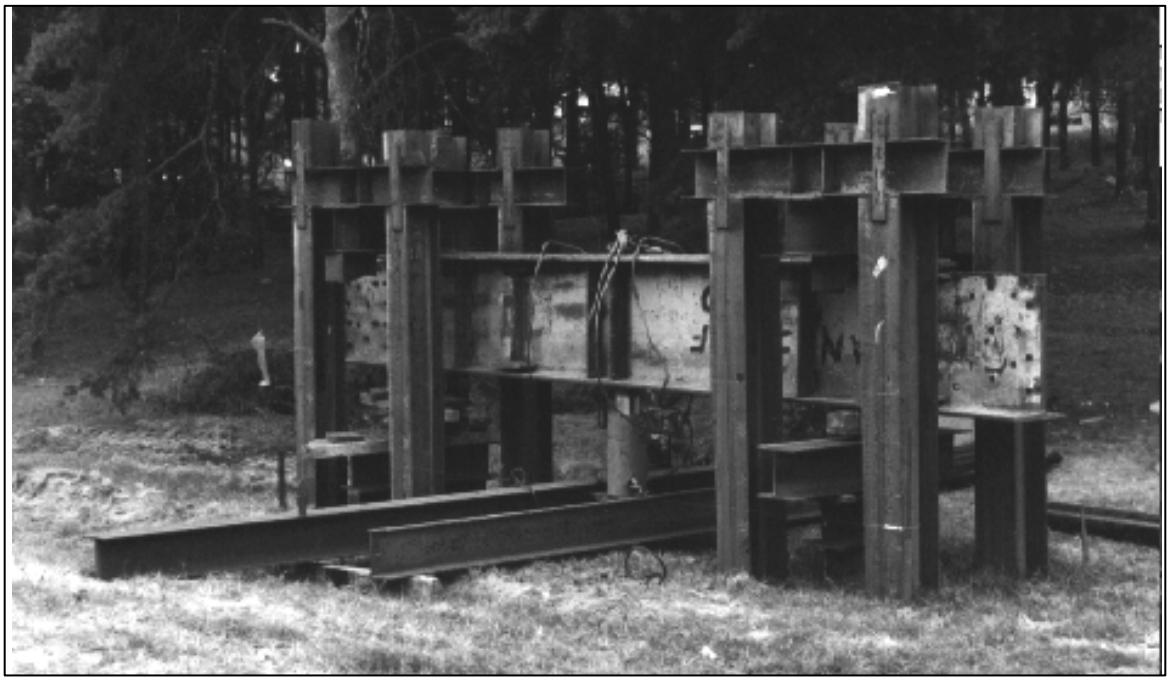

Figure 9-66. Typical compression load test arrangement with reaction piles (FHWA, 2006a).

Figure 9-67. Typical compression load test arrangement using a weighted platform (FHWA, 2006a).

9.15.7.2 Recommended Compression Test Loading Method

It is extremely important that standardized load testing procedures are followed. Several loading procedures are detailed in ASTM D 1143. The quick load test method is recommended. This method replaces traditional methods where each load increment was held for extended periods of time. The quick test method requires that load be applied in increments of 10 to 15% of the pile design load with a constant time interval of 2½ minutes or as otherwise specified between load increments. Readings of time, load, and gross movement are to be recorded immediately before and after the addition of each load increment. This procedure is to continue until continuous jacking is required to maintain the test load or the capacity of the loading apparatus is reached, whichever occurs first. Upon reaching and holding the maximum load for 5 minutes, the pile is unloaded in four equal load decrements, each of which is held for 5 minutes. Readings of time, load, and gross movement are once again recorded immediately after, 2½ minutes after, and 5 minutes after each load reduction, including the zero load.

9.15.7.3 Presentation and Interpretation of Compression Test Results

The results of load tests should be presented in a report conforming to the requirements of ASTM D 1143. A load-movement curve similar to the one shown in Figure 9-68 should be plotted for interpretation of test results.

The literature abounds with different methods of defining the failure load from static load tests. Methods of interpretation based on maximum allowable gross movements, which do not take into account the elastic deformation of the pile shaft, are not recommended. These methods overestimate the allowable capacities of short piles and underestimate the allowable capacities of long piles. Methods that account for elastic deformation and are based on a specified failure criterion provide a better understanding of pile performance and provide more accurate results.

AASHTO (2002) and FHWA (1992c) recommend pile compression test results be evaluated by using an offset limit method as proposed by Davisson (1972). The “double-tangent” is more commonly used for drilled shafts. These methods are shown in Figure 9-68 and are discussed in the following sections.

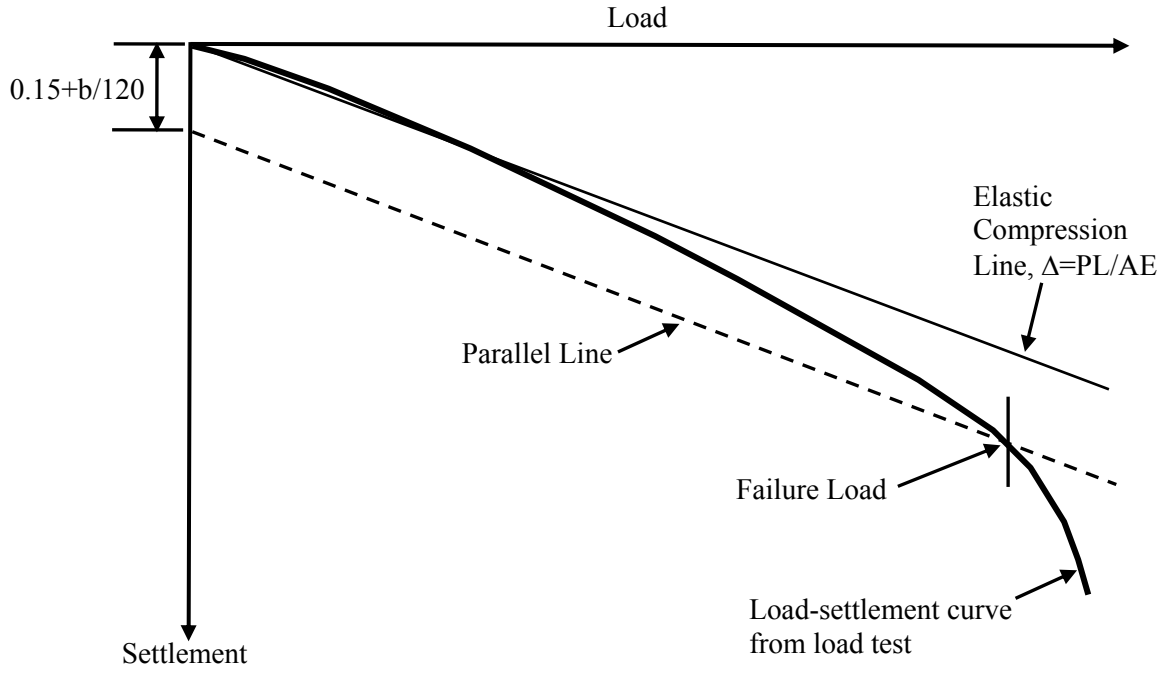

(a)

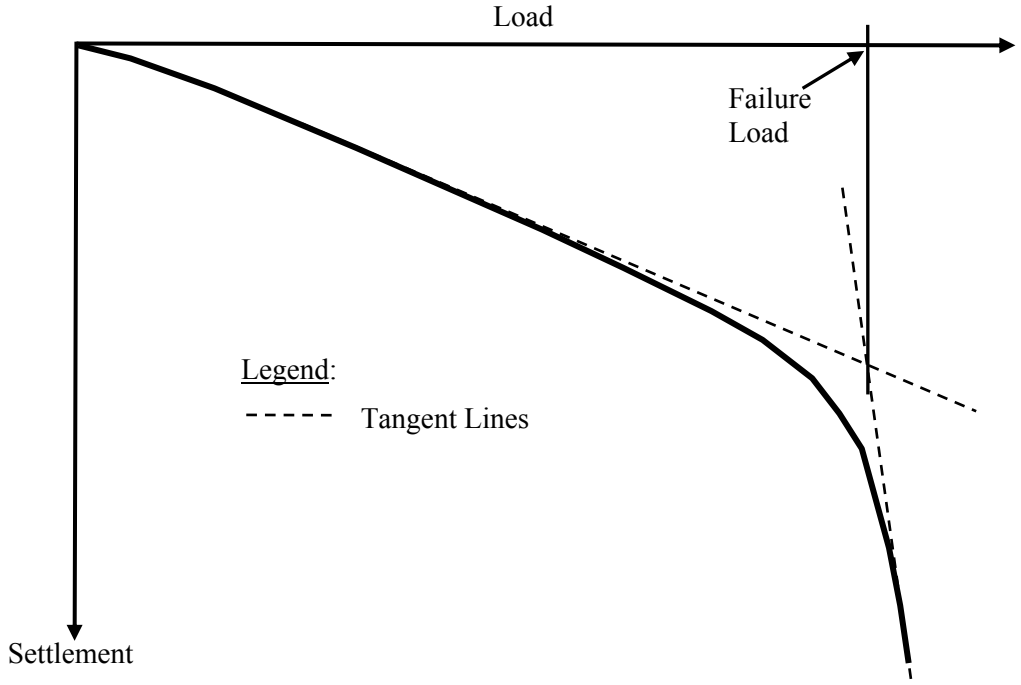

(b)

Figure 9-68. Presentation of typical static pile load-movement results, (a) Davisson's method, (b) Double-tangent method.

9.15.7.4 Plotting the Failure Criteria

Figure 9-68a shows the load-movement curve from a typical pile load test. To facilitate the interpretation of the test results, the scales for the loads and movements are selected so that the line representing the elastic deformation Δ of the pile is inclined at an angle of about 20° from the load axis. The elastic deformation Δ is computed from:

$$\Delta = \frac{QL}{AE} \qquad 9\text{-}51$$

Where: Δ = elastic deformation in inches (mm)
Q = test load in kips (kN)
L = pile length in inches (mm)
A = cross sectional area of the pile in in^2 (m^2)
E = modulus of elasticity of the pile material in ksi (kPa)

9.15.7.5 Determination of the Ultimate (Failure) Load

For pile diameters less than 24 in (610 mm), the ultimate or failure load Q_f of a pile is that load which produces a movement of the pile head equal to:

In US Units

$$s_f = \Delta + \left(0.15 + \frac{b}{120}\right) \qquad 9\text{-}52$$

where: s_f = settlement at failure in inches
b = pile diameter or width in inches
Δ = elastic deformation of total pile length in inches

A failure criterion line parallel to the elastic deformation line is plotted as shown in Figure 9-68a. The point at which the observed load-movement curve intersects the failure criterion is by definition the failure load. If the load-movement curve does not intersect the failure criterion line, the pile has an ultimate capacity in excess of the maximum applied test load.

For pile diameters greater than 24 in (610 mm), additional pile toe movement is necessary to develop the toe resistance. For pile diameters greater than 24 in (610 mm), the failure load can be defined as the load that produces at movement at the pile head equal to:

In US Units

$$s_f = \Delta + \left(\frac{b}{30} \right) \qquad 9\text{-}53$$

For drilled shafts, the failure load is commonly determined based on the "double-tangent" method shown in Figure 9-68b. Alternatively, the failure load is often defined as the test load corresponding to 5% of the shaft diameter because such a movement represents a large movement given that the drilled shafts are often much larger in diameter than driven piles.

9.15.7.6 Determination of the Allowable Geotechnical Load

The allowable geotechnical load is usually determined by dividing the ultimate load, Q_u, by a suitable factor of safety. A factor of safety of 2.0 is recommended by AASHTO (2002) and is often used. However, larger factors of safety may be appropriate under the following conditions:

a. Where soil conditions are highly variable.
b. Where a limited number of load tests are specified.
c. For friction piles in clay, where group settlement may control the allowable load.
d. Where the total movement that can be tolerated by the structure is exceeded.
e. For piles installed by means other than impact driving, such as vibratory driving or jetting.

9.15.7.7 Load Transfer Evaluations

FHWA (1992c) provides a method for evaluation of the soil resistance distribution from telltales embedded in a load test pile. The average load in the pile, Q_{avg}, between two measuring points can be determined as follows:

$$Q_{avg} = A\ E\ \frac{R_1 - R_2}{\Delta L} \qquad 9\text{-}54$$

Where:
- ΔL = length of pile between two measuring points under no load condition
- A = cross sectional area of the pile
- E = modulus of elasticity of the pile
- R_1 = deflection readings at upper of two measuring points
- R_2 = deflection readings at lower of two measuring points

If the R_1 and R_2 readings correspond to the pile head and the pile toe respectively, then an estimate of the shaft and toe resistances may be computed. For a pile with an assumed constant uniform soil resistance distribution, Fellenius (1990) states that an estimate of the toe resistance, R_t, can be computed from the applied pile head load, Q_h by the following equation.

$$R_t = 2Q_{avg} - Q_h \qquad 9\text{-}55$$

The applied pile head load, Q_h, is chosen as close to the failure load as possible. For a pile with an assumed linearly increasing triangular soil resistance distribution, the estimated toe resistance may be calculated by using the following equation:

$$R_t = 3Q_{avg} - 2Q_h \qquad 9\text{-}56$$

The estimated shaft resistance can then be calculated from the applied pile head load minus the toe resistance.

During driving, residual loads can be locked into a pile that does not completely rebound after a hammer blow, i.e., return to a condition of zero stress along its entire length. This mechanism is particularly true for flexible piles, piles with large frictional resistances, and piles with large toe quakes. Load transfer evaluations performed by using telltale measurements described above assume that no residual loads are locked in the pile during driving. Therefore, the load distribution calculated from the above equations would not include residual loads. If measuring points R_1 and R_2 correspond to the pile head and pile toe of a pile that has locked-in residual loads, the calculated average pile load would also include the residual loads. This inclusion of residual loads would result in a lower toe resistance being calculated than actually exists as depicted in Figure 9-69. Additional details on telltale load transfer evaluation, including residual load considerations, may be found in Fellenius (1990).

When detailed load transfer data is desired, telltale measurements alone are insufficient since residual loads cannot be directly accounted for. Dunnicliff (1988) suggests that weldable vibrating wire strain gages be used on steel piles and sister bars with vibrating wire strain gages be embedded in concrete piles for detailed load transfer evaluations. A geotechnical instrumentation specialist should be used to select the appropriate instrumentation to withstand pile handling and installation, to determine the redundancy required in the instrumentation system, to determine the appropriate data acquisition system, and to reduce and report the data acquired from the instrumentation program.

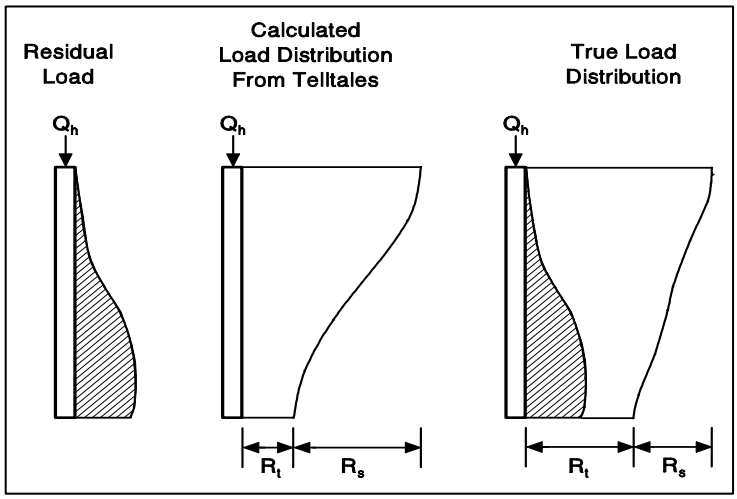

Figure 9-69. Example of residual load effects on load transfer evaluation (FHWA, 2006a).

A sister bar vibrating wire strain gage for embedment in concrete or concrete filled pipe piles is shown in Figure 9-70 and an arc-weldable vibrating wire strain gage attached to a steel H-pile is presented in Figure 9-71. When detailed load-transfer data is desired, a data acquisition system should be used.

Figure 9-70. Sister bar vibrating wire gages for concrete embedment (FHWA, 2006a).

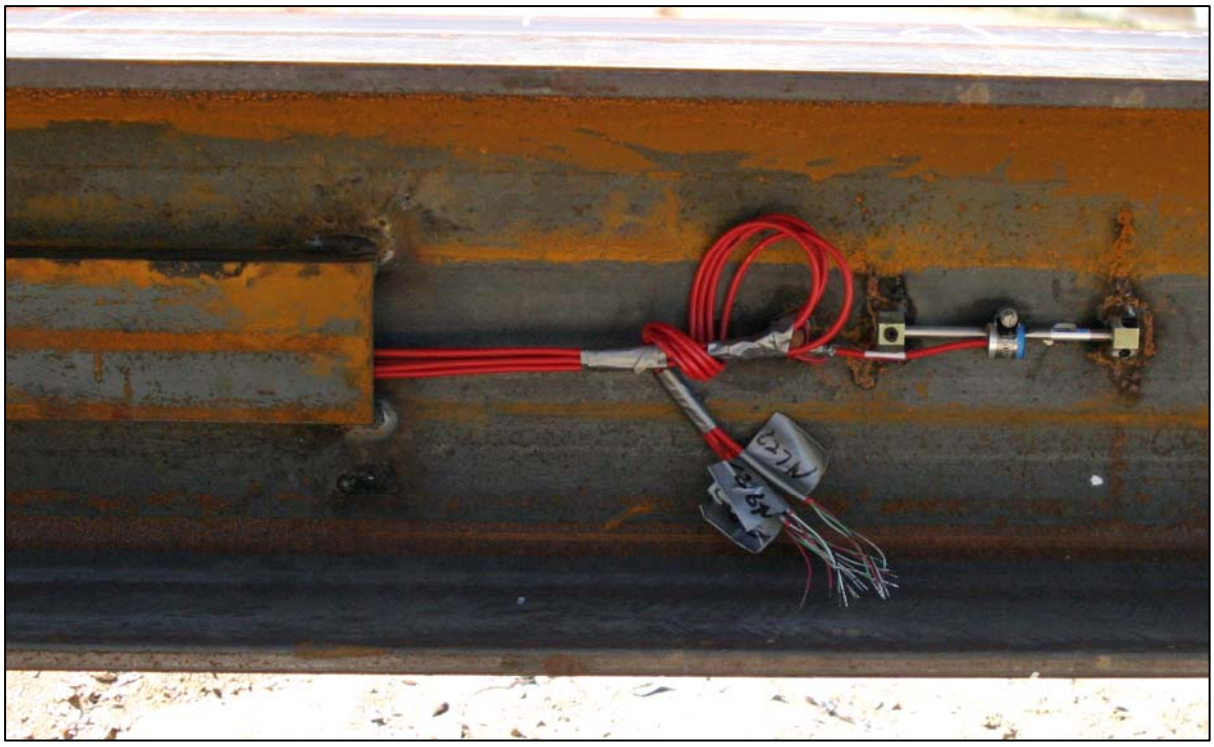

Figure 9-71. Arc-weldable vibrating wire strain gage attached to H-pile. (Note: protective channel cover shown on left) (FHWA, 2006a).

9.15.8 Other Compression Load Tests

Two methods of load testing were introduced in recent years that have been used to varying degrees by highway agencies for testing drilled shafts. These methods are the Osterberg Cell® and the Statnamic® methods, both of which are proprietary methods. Both of these techniques can routinely be used for test loads in range of 10,000 to 15,000 kips. The Osterberg Cell® test can apply loads up to 50,000 kips. Both, driven piles and cast-in-place piles, e.g., drilled shafts, can be tested by these methods. Although the details of each method are beyond the scope of this manual, a brief description follows on each method. Additional details are presented in primary references for this chapter (FHWA, 2006a; FHWA, 1999).

9.15.8.1 The Osterberg Cell® Method

Instead of using a conventional jack, reaction frame and reaction anchor system, the axial loading test can be performed by applying the load with an expendable jack and load cell cast within the test shaft. This jack - load cell is called an Osterberg Cell® after its inventor, Jorj Osterberg and the test in which the Osterberg Cell® is used is commonly known as the O-Cell® test. A schematic of the O-Cell® test in comparison with a static load test with a

reaction frame is shown in Figure 9-72. Figure 9-73 shows some details for the O-Cell® test. Figure 9-74 shows a photograph of an O-cell. Figure 9-75 shows a photograph of an O-Cell® assembly attached to a reinforcing cage just prior to the cage being placed into a drilled shaft excavation.

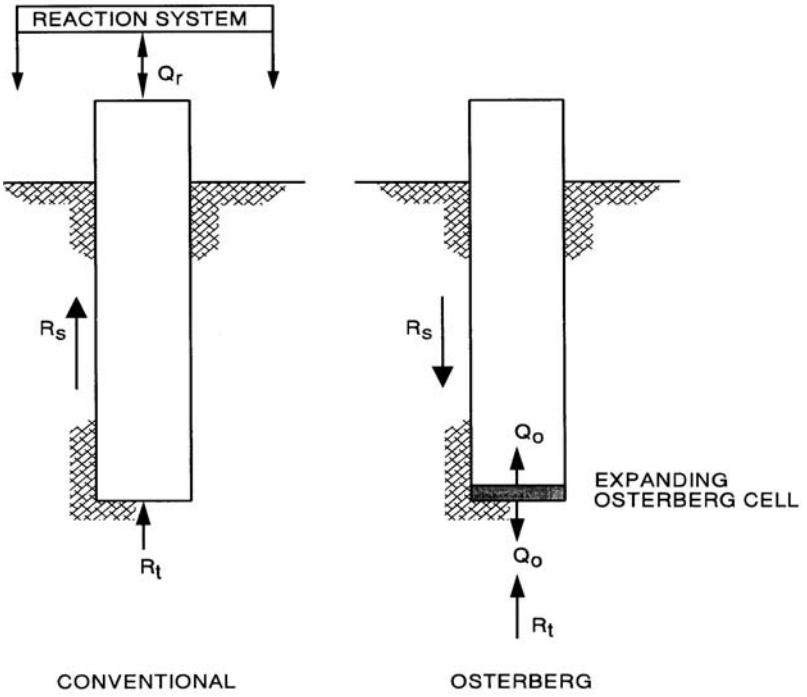

Figure 9-72. Comparison of reaction mechanism between Osterberg Cell® and Static test.

The principle of operation is very simple. The Osterberg Cell® consists essentially of two plates (pistons) of a prescribed diameter between which there is an expandable chamber that can hold pressurized fluid, usually oil or water. The upper and lower plates on the cell can be field welded to steel plates, usually at least 2 in (50 mm) thick, whose diameters are approximately equal to that of the test shaft. The chamber is pressurized by pumping from a reservoir on the ground surface. The unique feature of this device is that the pistons being pressurized have standard diameters that are approximately the full diameter of the cell, which may be up to 32 in (800 mm). Therefore, the pressurized fluid is acting on a very large area, unlike a conventional ram in which the area of the piston is usually small. This characteristic allows the Osterberg Cell® to apply very large loads with relatively low hydraulic pressures. Standard models with a diameter of 32 in (800 mm) are capable of applying loads of up to 3,000 tons (26.7 MN). Smaller sizes are also available from the supplier with consequently smaller capacities. The Osterberg Cell® is manufactured in a variety of sizes for both drilled shaft installations and driven pile installations as shown in Tables 9-12 and 9-13, respectively.

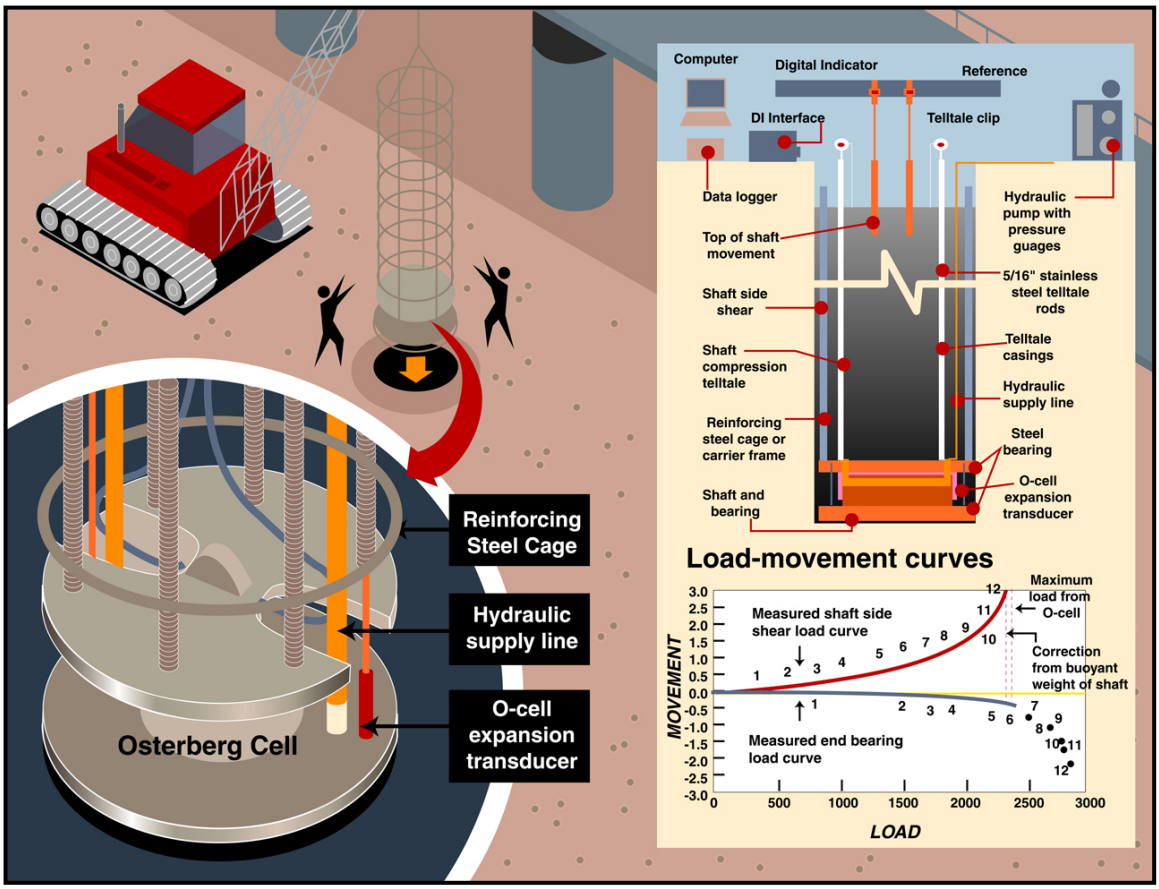

Figure 9-73. Some details of the O-Cell® test (after www.bridgebuildermagazine.com).

Figure 9-74. Photograph of an O-Cell®.

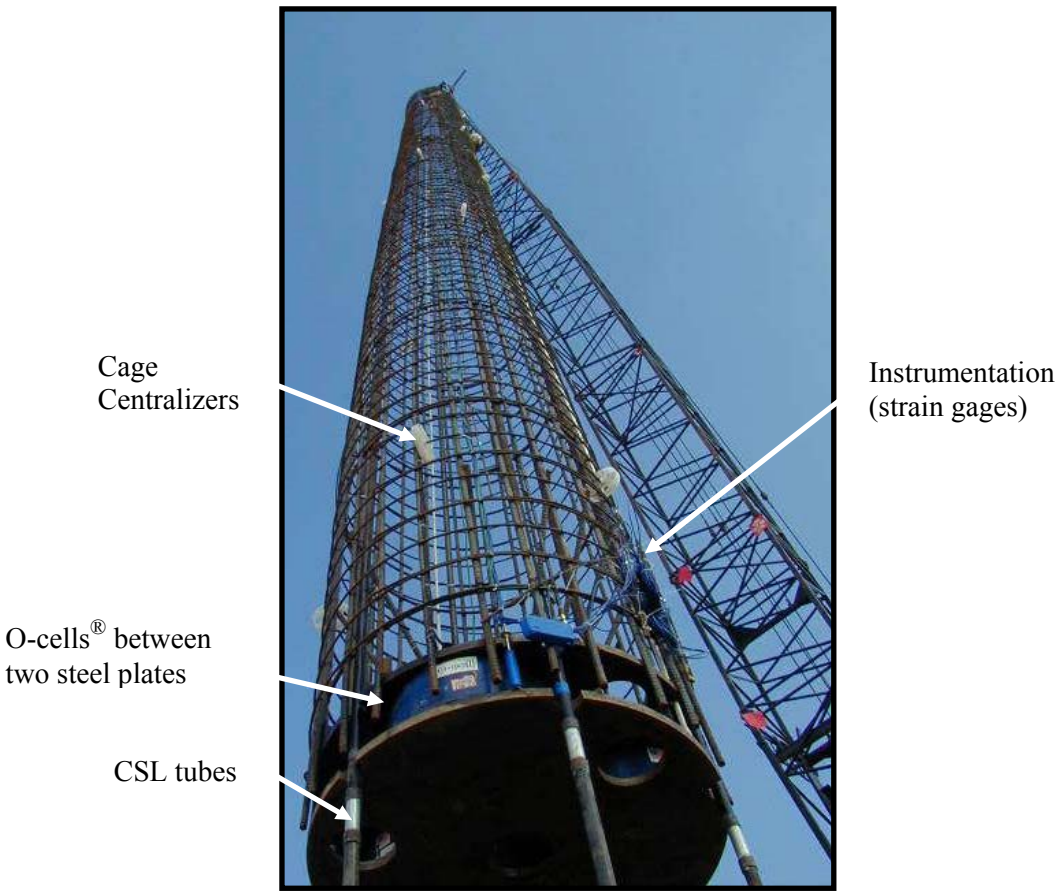

Figure 9-75. O-Cell® assembly attached to a reinforcing cage with other instrumentation.

Table 9-12. Osterberg Cells® for drilled shafts

Size	Diameter Inches	Height Inches	Capacity Tons	Weight Pounds
5	5.25	5.18	75	32
9	9.00	10.75	200	190
13	13.00	11.65	400	300
21	21.25	11.65	1,200	800
26	26.25	11.65	1,800	1,230
34	34.25	12.37	3,000	2,015
Note: 1 in = 25.4 mm; 1 ton = 8.9 kN				

Table 9-13. Osterberg Cells® for driven piles

Size – Inches	Capacity – Tons	Stroke - Inches	Description of Pile
14	200	6	Round-steel pipe
14	300	6	Square-precast Concrete
18	900	8	Round-steel pipe
30	950	9	Square-precast Concrete
Note: 1 in = 25.4 mm; 1 ton = 8.9 kN			

The load being applied to the drilled shaft is usually monitored by measuring the pressure in the fluid being applied by the pump. The Osterberg Cell® will therefore need to be calibrated in a testing machine prior to installation to obtain a relationship between the measured pressure and the load applied by the cell. Ordinarily, a calibration is provided by the supplier. Note that in practice the hydraulic pressure will usually be measured at the ground surface, but the cell is situated at some distance below the ground surface, e.g., about 110 ft (33.5 m) for the Osterberg Cell® assembly shown in Figure 9-75. Therefore, the actual pressure at the level of the cell is the pressure that is measured plus the vertical distance from the pressure gauge to the middle of the cell times the unit weight of the cell fluid. This correction needs to be made before load versus movement is plotted. Movement can be measured at the top of the cell through telltales attached to the top of the cell that are monitored by movement sensors, e. g., dial gauges suspended from stable reference beams on the ground surface. Similarly, movement can be measured at the top of the test shaft by means of movement sensors suspended from stable reference beams. Movement of the bottom plate can be determined by measuring the movement of the top of the Osterberg Cell® with telltales and then measuring the relative movement between the upper and lower ends of the cell by means of sacrificial electronic movement sensors attached between the top and bottom plates.

The O-Cell® test has some limitations in that the total failure load of the foundation element cannot usually be measured; only the failure load of the friction above the cell or the resistance below the cell are measured.

The Osterberg Cell® has been used in a variety of soil and rock conditions. The cell has been used to determine the bond stress in rock sockets and in dense glacial tills. In addition, a variety of strain gage devices have been used in conjunction with the O-Cell® test to develop a distribution of resistance along the foundation element. Such measurements can also be obtained below an Osterberg Cell® installed at the mid-height of a shaft by extending instrumented rebar below the base of the cell.

The cost of a single O-cell® test, including the Osterberg Cell® itself, instrumentation and shaft construction, is often in the range of 50 to 60 per cent of the cost of performing a conventional static load test for situations, such as shafts of small capacity, in which conventional static load tests can be used, although the percentage varies considerably from site to site.

By using multiple Osterberg Cells® in a given shaft, it is possible to mobilize up to 25,000 tons of combined side and base resistance. The O-Cell® test has not been standardized by

AASHTO or ASTM as of 2006. Additional information on the O-Cell® test can be found at www.loadtest.com.

9.15.8.2 The Statnamic® Test Method

The Statnamic® test method is a proprietary method developed by the Berminghammer Foundation Corporation (www.berminghammer.com). A new ASTM draft standard, entitled "Standard Test Method for Piles under Rapid Axial Compressive Load," has been proposed but had not been approved as of 2006.

A Statnamic® loading test also can be performed without the need for an expensive reaction system. An advantage of this type of test relative to the O-Cell® test is that it does not require the loading device to be cast into the shaft. Therefore, the Statnamic® loading test can be performed on a drilled shaft for which a loading test was not originally planned.

The principle of the Statnamic® test is shown in Figure 9-76. Dead weights are placed upon the surface of the test shaft. Beneath the dead weights is a small volume of propellant and a load cell. The propellant is ignited and accelerates the masses upward. As this occurs a reaction force equal to the masses times their acceleration is produced against the head of the shaft, as indicated in Figure 9-76. This force, which increases with time up to one to two hundred milliseconds, causes the shaft to displace downward. As the ignition of the propellant stops, the reaction force rapidly decreases and the shaft rebounds. The displacement of the shaft head is measured by means of a laser beam from a source located some distance away from the test shaft. The laser beam is targeted on the shaft head. The load can be graphed against both time and displacement instantaneously.

For reasons of safety the reaction masses are contained within a metal sheath that is also filled with an energy absorbing material, such as dry gravel, that will cushion the impact of the masses as they fall back upon the head of the drilled shaft. A photograph of a Statnamic® test arrangement, with the gravel-filled sheath surrounding the reaction masses is shown in Figure 9-77 just after igniting the propellant.

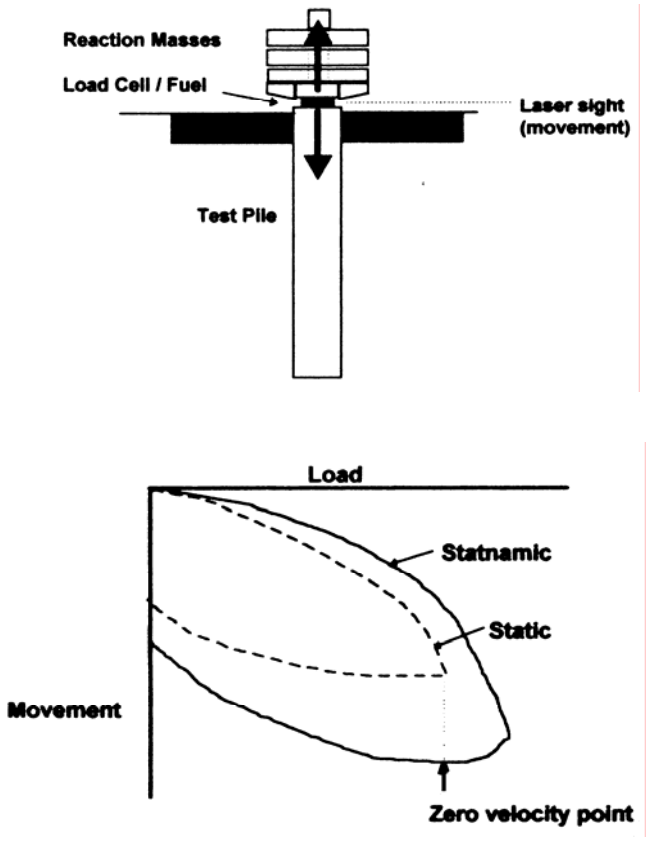

Figure 9-76. Schematic of Statnamic® test

Figure 9-77. Photograph of Statnamic® test arrangement showing masses being accelerated inside gravel-filled sheath.

Since there are dynamic components to the resistance of the drilled shaft, some interpretation of the data is necessary, as illustrated in the bottom part of Figure 9-76. Since the load produced at the head of the shaft by igniting the propellant is applied much more slowly than the load applied by the blow of a pile-driving hammer, it can usually be assumed that the length of the stress wave that is imparted to the drilled shaft is much longer than the length of the shaft itself and that the shaft is therefore penetrating into the soil or rock as a rigid body. It may not be possible to make this simplifying assumption if the test shaft is extremely long. However, if rigid body motion is assumed, the load acting on the head of the shaft can be reasoned to be the sum of (1) the total static soil resistance (base and sides), (2) damping forces produced by the relative velocity between the shaft and the soil/rock, and (3) the mass of the drilled shaft itself times its acceleration. In the Statnamic® test, if the load corresponding to a zero slope on the load-settlement relation measured near the beginning of rebound, as illustrated in Figure 9-76, is selected as the analysis point, then component (2), above, will be zero, since the velocity of the shaft will be zero, and the total static resistance of the drilled shaft, R_T, can be approximated by :

$$R_T = F_{so} - W_s\left(\frac{a_s}{g}\right) \qquad 9\text{-}57$$

where, F_{so} = the force measured by the load cell at the point at which the slope of the rebound curve is zero, identified by the arrow in Figure 9-68

W_s = total weight of the drilled shaft

a_s = acceleration of the drilled shaft corresponding to F_{so}, which can be measured with an accelerometer at the head of the shaft

g = acceleration of gravity.

Note that a_s will not be zero despite the fact that the velocity of the test shaft is momentarily zero at F_{so}. If the test shaft is long, a stress wave analysis may be necessary to obtain an accurate estimate of resistance.

Statnamic® devices have been constructed that are capable of applying head loads of up to approximately 3600 tons (32 MN). The cost of a Statnamic® test will usually be approximately the same as the cost of an O-Cell® test of the same magnitude.

Further technical information on the Statnamic® test method can be found in the *Proceedings of the First International Statnamic Seminar*, Vancouver, British Columbia, 1995. Copies

can be obtained from Berminghammer Foundation Equipment Company, Wellington Street Marine Terminal, Hamilton, Ontario L8L 4Z9, Canada. The reader is also referred to FHWA (2006a) for further information on the load test interpretation.

9.15.9 Limitations of Compression Load Tests

Compression load tests can provide a wealth of information for design and construction of pile foundations and are the most accurate method of determining pile capacity. However, static load test results cannot be used to account for long-term settlement, downdrag from consolidating and settling soils, or to represent pile group action adequately. Other shortcomings of static load tests include cost, the time required to setup and complete a test, and the minimal information obtained on driving stresses or extent of potential pile damage. Static load test results can also be misleading on projects with highly variable soil conditions.

9.15.10 Axial Tension and Lateral Load Tests

Load tests can also be performed such that uplift and lateral loading conditions are simulated. Such load tests are described in FHWA (1999) and FHWA (2006a).

[THIS PAGE INTENTIONALLY BLANK]

CHAPTER 10.0
EARTH RETAINING STRUCTURES

Earth retaining structures or systems are used to hold back earth and maintain a difference in the elevation of the ground surface as shown in Figure 10-1. The retaining wall is designed to withstand the forces exerted by the retained ground or "backfill" and other externally applied loads, and to transmit these forces safely to a foundation and/or to a portion of the restraining elements, if any, located beyond the failure surface.

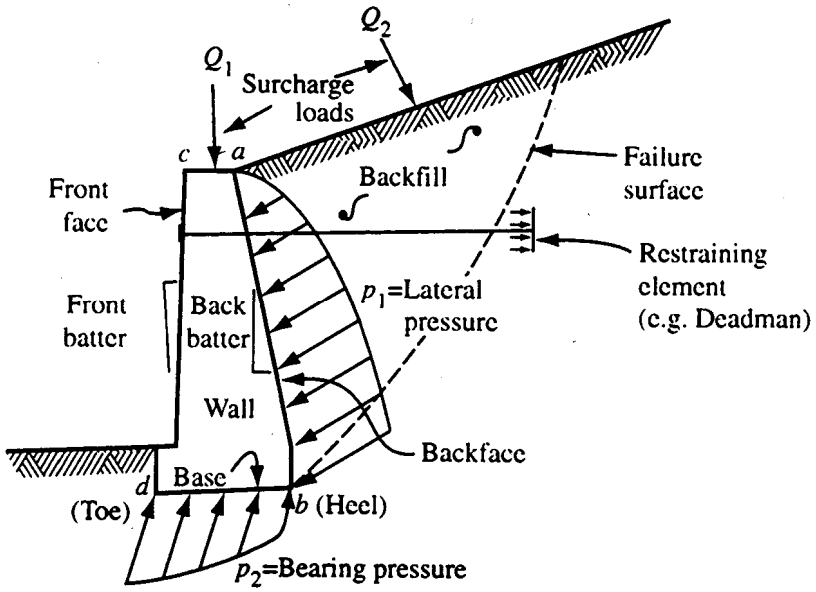

Figure 10-1. Schematic of a retaining wall and common terminology.

In general, the cost of constructing a retaining wall is usually high compared with the cost of forming a new slope. Therefore, the need for a retaining wall should be assessed carefully during preliminary design and an effort should be made to keep the retained height as low as possible.

In highway construction, retaining walls are used along cuts or fills where space is inadequate for construction of cut slopes or embankment slopes. Bridge abutments and foundation walls, which must support earth fills, are also designed as retaining walls.
Typical applications for earth retaining structures in highway construction include:

- new or widened highways in developed areas;
- new or widened highways at mountain or steep slopes;
- grade separation;
- bridge abutments, wing walls and approach embankments;

- culvert walls;
- tunnel portals and approaches;
- flood walls, bulkheads and waterfront structures;
- cofferdams for construction of bridge foundations;
- stabilization of new or existing slopes and protection against rockfalls; and
- groundwater cut-off barriers for excavations or depressed roadways.

Figure 10-2 provides schematic illustrations of several retaining wall systems traditionally used in highway applications. A great number of wall systems have been developed in the past two decades by specialty contractors who have been promoting either a special product or a specialized method of construction, or both. Due to the rapid development of these diversified systems and their many benefits, the design engineer is now faced with the difficult task of having to select the best possible system; design the structure; and ensure its proper construction.

An important breakthrough in the design of earth retaining structures (ERS) that occurred in this era was the recognition that the earth pressure acting on a wall is a function of the type of wall and the amount and distribution of wall movement. Classical earth pressure theories, which were developed by Coulomb (1776) and Rankine (1857), were formalized for use by Caquot and Kerisel (1948) and others. Sophisticated analyses of soil-structure interaction and wall/soil movements began in the 1960s with the development of finite difference and finite element analytical procedures. The simultaneous advancement of geotechnical instrumentation equipment and monitoring procedures made the "observational method" of design (Peck, 1969) popular and cost effective.

Since 1970 there has been a dramatic growth in the number of methods and products for retaining soil. O'Rourke and Jones (1990) describe two trends in particular that have emerged since 1970. First, there has been an increasing use of reinforcing elements, either by incremental burial to create reinforced soils (MSE walls), or by systematic in situ installation to reinforce natural soils or even existing fills (soil nailing); see Figure 10-2b. Mechanically stabilized earth and soil nailing have changed the ways we construct fill or cut walls, respectively, by providing economically attractive alternatives to traditional designs and construction methods. Second, there has been an increasing use of polymeric products to reinforce the soil and control drainage. Rapid developments in polymer manufacturing have supplied a wide array of geosynthetic materials. The use of these products in construction has encouraged a multitude of different earth retention schemes.

The rapid development of these new trends and the increased awareness of the impact of construction on the environment, have led to the emergence of the concept of "earth walls."

In this concept, the soil supports itself or is incorporated into the structure and assumes a major structural or load carrying function. With this concept, structural member requirements of the system are reduced, or eliminated altogether. Examples of recently developed earth walls include the soil-reinforcement systems discussed above, as well as systems involving chemical treatment of the in-situ soil such as jet grouting or deep soil mixing.

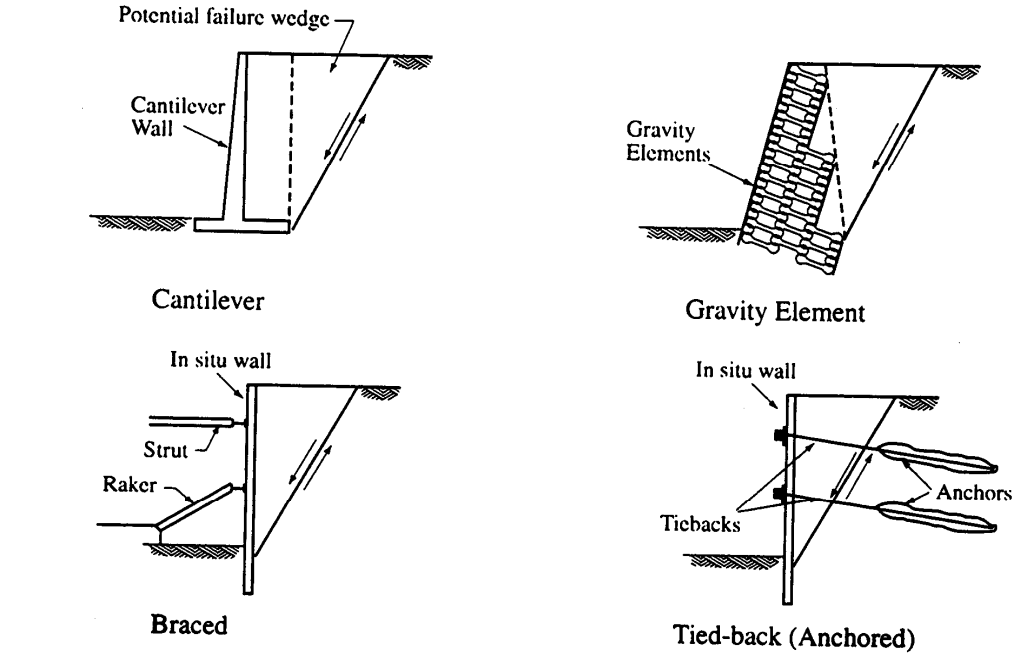

(a) Externally Stabilized Systems

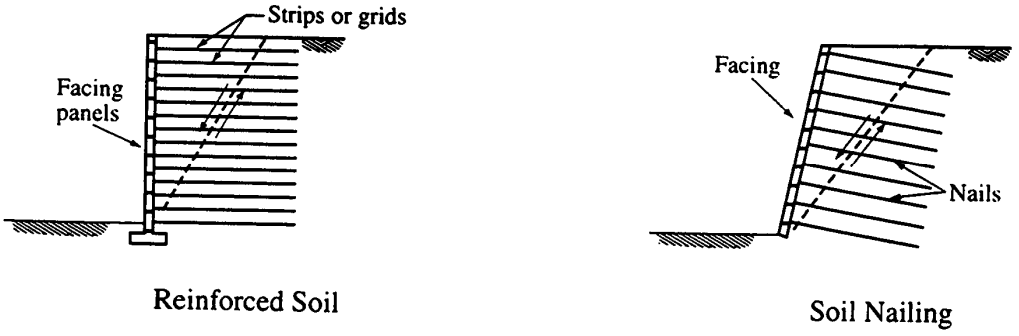

(b) Internally Stabilized Systems

Figure 10-2. Variety of retaining walls (after O'Rourke and Jones, 1990)

10.01 Primary References:

The two primary references for earth retaining structures are:

FHWA (2005b). *Earth Retaining Structures - DRAFT*. Report No. FHWA-SA-05-046, Authors: Tanyu, B.F., Sabatini, P.J. and Berg, R.R., Federal Highway Administration, U.S. Department of Transportation.

AASHTO (2004 with 2006 Interims). *AASHTO LRFD Bridge Design Specifications,* 3rd Edition, American Association of State Highway and Transportation Officials, Washington, D.C.

10.1 CLASSIFICATION OF EARTH RETAINING STRUCTURES

Earth retaining systems may be classified according to:

- load support mechanism, i.e., externally or internally stabilized walls;
- construction method, i.e., fill or cut walls; and
- system rigidity, i.e., rigid or flexible walls.

Every retaining wall can now be classified by using these three factors. For example, a sheet-pile wall would be classified as an **externally-stabilized cut** wall that is relatively **flexible**. A mechanically stabilized earth (MSE) wall is an **internally stabilized fill** wall that is relatively **flexible**. Further description of these classifications is provided subsequently.

10.1.1 Classification by Load Support Mechanism

The stability component of walls can be organized according to two principal categories: externally and internally stabilized systems (O'Rourke and Jones, 1990) as shown in Figure 10-3. An externally stabilized system uses an external structural wall against which stabilizing forces are mobilized. An internally stabilized system involves reinforcements installed within the retained soil mass and extending beyond the potential failure plane. Hybrid systems combine elements of both internally and externally supported walls.

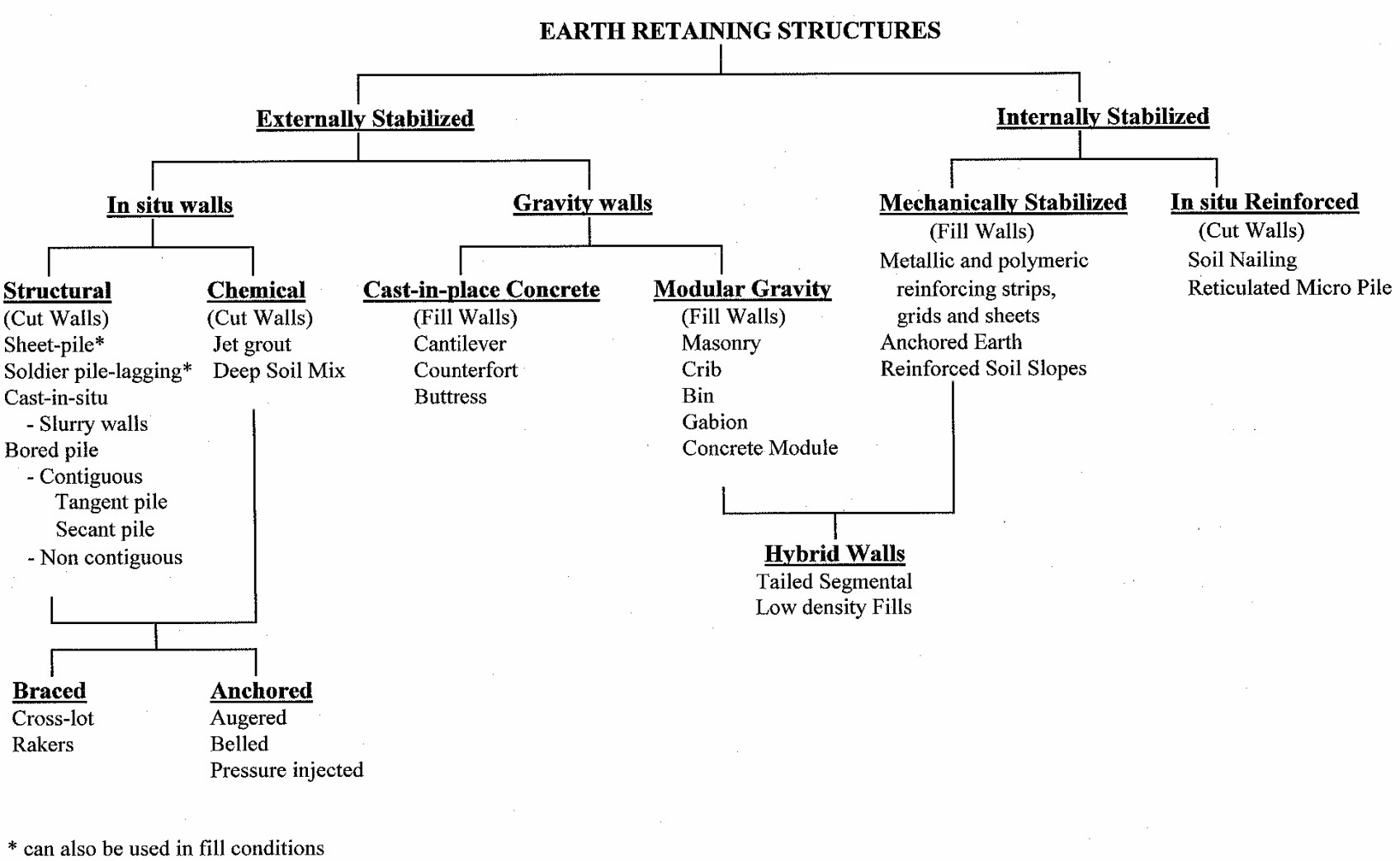

Figure 10-3. Classification of earth retaining systems (after O'Rourke and Jones, 1990).

Virtually all traditional types of walls may be regarded as externally stabilized systems (Refer to Figure 10-2a). Gravity walls, in the form of cantilever structures or gravity elements (e.g., bins, cribs and gabions), support the soil and, through their weight and stiffness, resist sliding, overturning, and shear. Bracing systems, such as cross-lot struts and rakers, provide temporary support for in situ structural and chemically stabilized walls. Ground anchors provide support through their pullout capacity in stable soils outside of the zone of potential failure.

It is in the area of internally stabilized systems that relatively new concepts have been introduced (Refer to Figure 10-2b). Shear transfer to mobilize the tensile capacity of closely spaced reinforcing elements embedded in the retained soil mass has enabled retaining structures to be constructed without an external structural wall element. The shear transfer mechanism allows a composite system of reinforcing elements and soil to serve as the primary structural entity. A facing is required on an internally stabilized system, however, its purpose is to prevent raveling and deterioration rather than to provide primary structural support.

10.1.2 Classification by Construction Method

Earth retaining structures (ERS) can also be classified according to the method required for their construction, i.e., fill construction or cut construction. Fill wall construction refers to a wall system in which the wall is constructed from the base of the wall up to the top, i.e., "bottom-up" construction. Cut wall construction refers to a wall system in which the wall is constructed from the top of the wall down to the base concurrent with excavation operations, i.e., "top-down" construction. The classification of each wall system according to its construction method is also presented in Figure 10-3.

It is important to recognize that the "cut" and "fill" designations refer to how the wall is constructed, not necessarily the nature of the earthwork associated with the project. For example, a prefabricated modular gravity wall, which may be used to retain earth for a major highway cut, is considered a fill wall because its construction is not complete until the backfill has been placed from the "bottom-up" after the excavation for the cut has reached its final grade.

10.1.3 Classification by System Rigidity

The rigidity or flexibility of a wall system is fundamental to the understanding of the development of earth pressures, discussed in Section 10.2. In simple terms, a wall is considered to be rigid if it moves as a unit in rigid body rotation and/or translation and does not experience bending deformations. Most gravity walls can be considered rigid walls. Flexible walls are those that undergo bending deformations in addition to rigid body motion. Such deformations result in a redistribution of lateral pressures from the more flexible to the stiffer portions of the system. Virtually all wall systems, except gravity walls, may be considered to be flexible.

10.1.4 Temporary and Permanent Wall Applications

Permanent wall systems are generally considered to have a service life of 75 to 100 years. However, the ERS listed in Figure 10-3 are technically feasible for both temporary and permanent applications. In most cases, however, certain systems may not be cost-effective for temporary applications. Temporary walls generally have less restrictive requirements on material durability, design factors of safety, performance, and overall appearance than do permanent walls. Also, walls that can be constructed rapidly are often used for temporary applications. For example, MSE walls with segmental, precast facings are not typically used for temporary applications since the cost of the facing components and the select backfill may be more than 50 percent of the total cost of the wall.

The service life of temporary earth support systems is based on the time required to support the ground while the permanent systems are installed. This document has adopted the AASHTO guidance which considers temporary systems to be those that are removed upon completion of the permanent systems. The time period for temporary systems is commonly stated to be 18 to 36 months, but may be shorter or longer based on actual project conditions.

Temporary systems may be divided into "support of excavation" (SOE) temporary systems and "critical" temporary systems. In general the owner will determine which temporary systems are to be designated as critical. That decision is often based on the owner's need to restrict lateral movement of the support system to minimize ground movements behind the support system. In general, specific components or design features for temporary systems may be designed to the same or similar criteria as used for permanent systems. Conversely, SOE systems are commonly designed to less restrictive criteria than permanent systems. The owner commonly assigns the responsibility for design and performance of SOE systems to the contractor. The design of SOE systems is often based more on system stability than on minimizing ground movements.

10.1.5 Wall Selection Considerations

Given the wide variety of retaining walls as shown in Figure 10-3, it is important to select a wall that is most economical for the application being considered. The wall selection process should include consideration of various factors such as (1) ground type, (2) groundwater, (3) construction considerations, (4) speed of construction, (5) right of way, (6) aesthetics, (7) environmental concerns, (8) durability and maintenance, (9) tradition and (10) local contracting practices. A detailed discussion of these wall selection factors is outside the scope of this manual. The reader is referred to FHWA (2005b) where a systematic wall selection process considering these factors is described.

10.2 LATERAL EARTH PRESSURES

Some of the basic concepts of lateral earth and water pressures were discussed in Chapter 2. It is recommended that the reader should review Section 2.9 before proceeding further in this Chapter. Here the principles of lateral earth pressure are explained on the basis of deformation. A total lateral pressure diagram consistent with the assumed deformations is developed for use in assessing the forces acting on the wall from the backfill or retained ground. This section focuses primarily on theoretical earth pressure diagrams, which are most commonly used in the design of rigid gravity structures, nongravity cantilevered walls, MSE walls, and anchored walls with stiff structural facings such as diaphragm walls.

A wall system is designed to resist lateral earth pressures and water pressures that develop behind the wall. Earth pressures develop primarily as a result of loads induced by the weight of the backfill and/or retained in-situ soil, earthquake ground motions, and various surcharge loads. For purposes of earth retaining system design, three different types of lateral earth pressure are usually considered: (1) at-rest earth pressure; (2) active earth pressure; and (3) passive earth pressure. These conditions are shown in Figure 10-4 relative to lateral deformation of the walls. The conditions are defined as follows:

- At-rest earth pressure is defined as the lateral earth pressure that exists in level ground for a condition of no lateral deformation.

- Active earth pressure is developed as the wall moves away from the backfill or the retained soil. This movement results in a decrease in lateral pressure relative to the at-rest condition. A relatively small amount of lateral movement is necessary to reach the active condition.

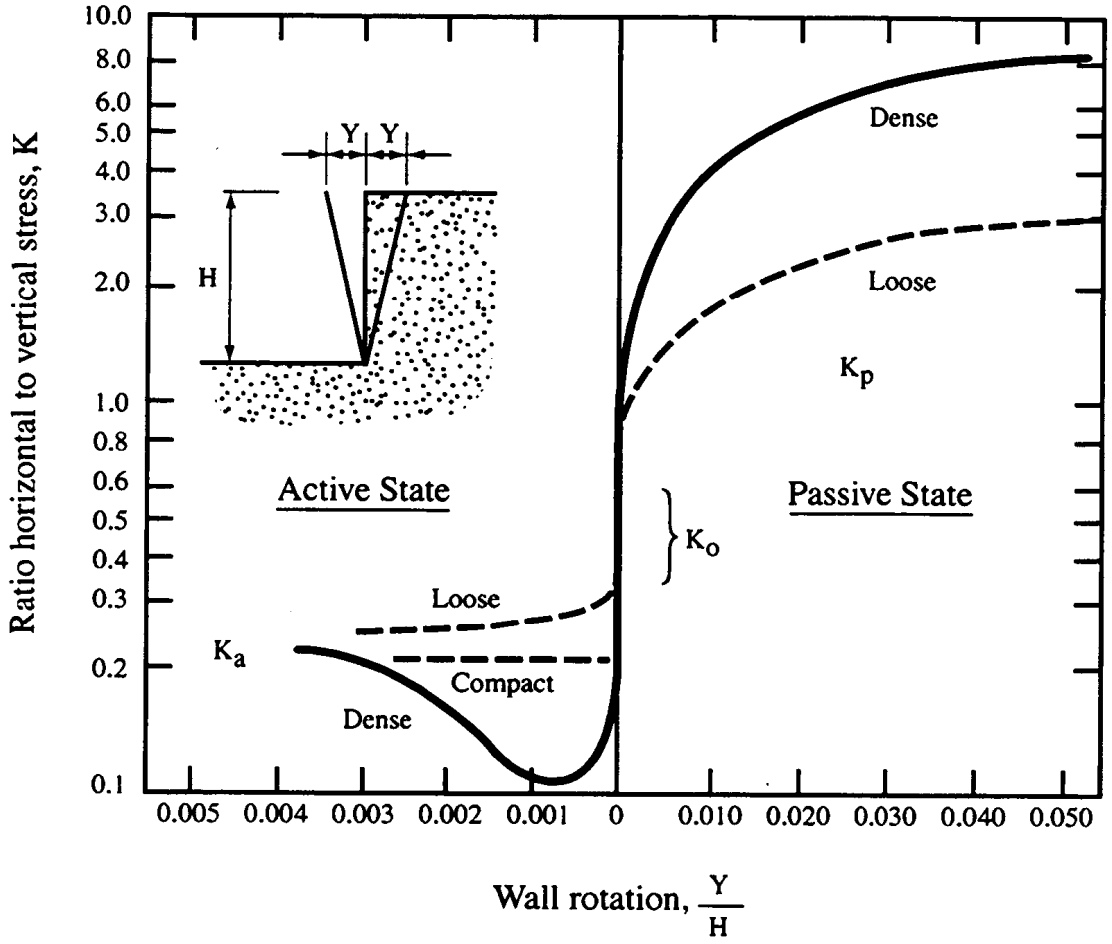

Magnitude of Wall Rotation to Reach Failure

Soil type and condition	Rotation, Y/H	
	Active	Passive
Dense cohesionless	0.001	0.02
Loose cohesionless	0.004	0.06
Stiff cohesive	0.010	0.02
Soft cohesive	0.020	0.04

Figure 10-4. Effect of wall movement on wall pressures (after Canadian Geotechnical Society, 1992).

- Passive earth pressure is developed as the wall moves towards the backfill or the retained soil. This movement results in an increase in lateral pressure relative to the at-rest condition. The movements required to reach the passive condition are approximately ten times greater than those required to develop active earth pressure.

Each of these earth pressure conditions can be expressed in general form by:

$$p_h = Kp_o \qquad 10\text{-}1$$

where p_h is the lateral earth pressure at a given depth behind the wall, p_o, is the vertical stress at the same depth, and K is the earth pressure coefficient that has a value related to the at-rest condition (K_o), active conditions of movement, (K_a), or passive conditions of movement, (K_p).

As shown in Figure 10-4, the magnitudes of these earth pressure coefficients follow the relationship of $K_p > K_o > K_a$. The relationship between the magnitude of retaining wall movement, in this case rotation, Y/H, into or away from the retained material about its toe, and the horizontal pressure exerted by the soil is presented in Figure 10-4, with angular movement along the x axis and the mobilized coefficient of lateral earth pressure on the y axis. Figure 10-4 can also be used to estimate the state of stress for walls with uniform horizontal translation equal to Y. As illustrated in this figure, significantly larger lateral displacements are required to mobilize the passive resistance than those required to develop active pressures. The maximum values of K_a and K_p correspond to fully mobilized pressures that represent active and passive failure conditions, respectively.

When the estimated wall movement is less than the value required to fully mobilize active or passive pressure, the earth pressure coefficient can be adjusted proportionally based on the graphical relationship presented in Figure 10-4.

10.2.1 At-Rest Lateral Earth Pressure

The at-rest earth pressure represents the lateral effective stress that exists in a natural soil in its undisturbed state. For cut walls constructed in near normally consolidated soils, the at-rest earth pressure coefficient, K_o, can be approximated by the equation (Jaky, 1944):

$$K_o = 1 - \sin\phi' \qquad 10\text{-}2$$

where ϕ' is the effective (drained) friction angle of the soil. The magnitude of the at-rest earth pressure coefficient is primarily a function of soil shear strength and degree of

overconsolidation, which, as indicated in Chapter 7, may result from natural geologic processes for retained natural ground or from compaction effects for backfill soils.

In overconsolidated soils, K_o can be estimated as (Schmidt, 1966):

$$K_o = (1 - \sin\phi')(OCR)^{\Omega} \qquad 10\text{-}3$$

where Ω is a dimensionless coefficient, which, for most soils, can be taken as $\sin\phi'$ (Mayne and Kulhawy, 1982) and OCR is the overconsolidation ratio.

Usually, Equations 10-2 and 10-3 for the at-rest earth pressure coefficient are sufficiently accurate for normally to lightly overconsolidated soils provided the overconsolidation ratio has been evaluated from laboratory consolidation testing. For moderately to heavily overconsolidated clays, or where a more accurate assessment is required, laboratory triaxial tests on undisturbed samples and in-situ testing such as pressuremeter testing may be used.

For normally consolidated clay, K_o is typically in the range of 0.55 to 0.65; for sands, the typical range is 0.4 to 0.5. For lightly overconsolidated clays (OCR $\leq$ 4), K_o may reach a value up to 1; for heavily overconsolidated clays (OCR > 4), K_o values may be greater than 2 (Brooker and Ireland, 1965). For heavily overconsolidated soils, values for K_o can be very large. A relatively stiff wall would be required to resist the large forces resulting from the lateral earth pressures in this case. For walls constructed in such soils, consideration should be given to performing pressuremeter tests, which provide a direct measure of lateral pressures in the ground.

In the context of wall designs consisting of steel soldier beams or sheet-pile wall elements, design earth pressures based on at-rest conditions are not typically used since at-rest earth pressures imply that the wall system undergoes no lateral deformation. This condition may be appropriate for heavily preloaded, stiff wall systems, but designing to a requirement of zero wall movement for flexible wall systems is not practical.

10.2.2 Active and Passive Lateral Earth Pressures

As discussed in Chapter 2, in stability analyses active and passive earth pressures are developed as a result of soil displacement within a failure zones developed behind the wall (active) or in front of the wall (passive) assuming that the wall displaces outward. For the purpose of illustration Figure 10-5 shows the two conditions with respect to wall movement relative to the backfill only. In one case the wall moves away from the backfill (active case) in the other case the wall moves into the backfill (passive case) As shown in the figure, the failure zone for both cases is typically bounded by the back face of the wall and a failure surface through the retained soil mass along which the soil has attained limiting equilibrium. In addition to the effect of lateral movements on the values of K_a and K_p shown in Figure 10-4, the magnitude of the active and passive earth pressure coefficients are functions of the soil shear strength, the backfill geometry, i.e., horizontal backfill surface or sloping ground surface above the wall, the orientation of the surface where the wall contacts the backfill or retained soil, i.e., vertical or inclined, and the friction and cohesive forces that develop on this surface as the wall moves relative to the retained ground.

Active and passive earth pressure coefficients based on a plane wedge theory, which considers the effect of wall friction, sloping backfill and sloping wall face, was first proposed by Coulomb (1776) and are shown in Figure 10-5. The pressures calculated by using these coefficients are commonly known as the Coulomb earth pressures. Since Coulomb's method is based on limit equilibrium of a wedge of soil, only the magnitude and direction of the earth pressure is found. Pressure distributions and the location of the resultant are assumed to be triangular.

For simple cases involving vertical walls retaining homogeneous soil with a level ground surface, without friction between the soil and the wall face, and without the presence of groundwater, the formulas for computing the earth pressure coefficients can be simplified considerably by substituting, $\delta = \theta = \beta = 0$ in Coulomb's equations, as shown in Figure 10-5. For such simplified cases, K_a and K_p can be expressed by Equations 10-4 and 10-5, respectively:

$$K_a = \frac{1 - \sin\phi'}{1 + \sin\phi'} = \tan^2(45 - \phi'/2) \qquad 10\text{-}4$$

$$K_p = \frac{1 + \sin\phi'}{1 - \sin\phi'} = \tan^2(45 + \phi'/2) \qquad 10\text{-}5$$

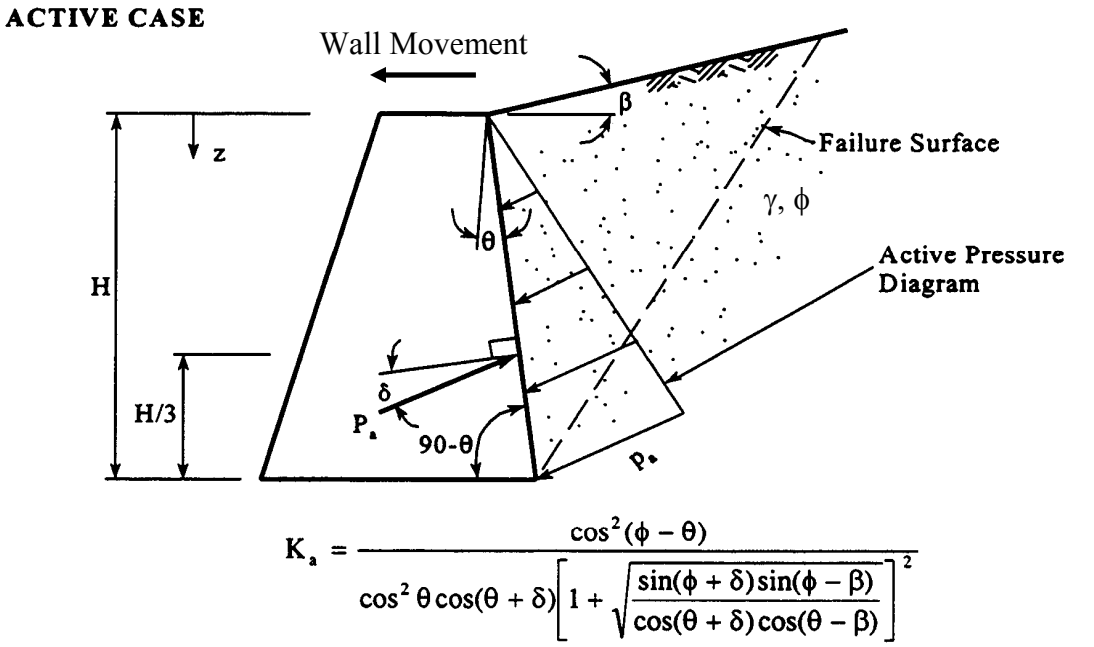

$$K_a = \frac{\cos^2(\phi - \theta)}{\cos^2\theta\cos(\theta + \delta)\left[1 + \sqrt{\frac{\sin(\phi + \delta)\sin(\phi - \beta)}{\cos(\theta + \delta)\cos(\theta - \beta)}}\right]^2}$$

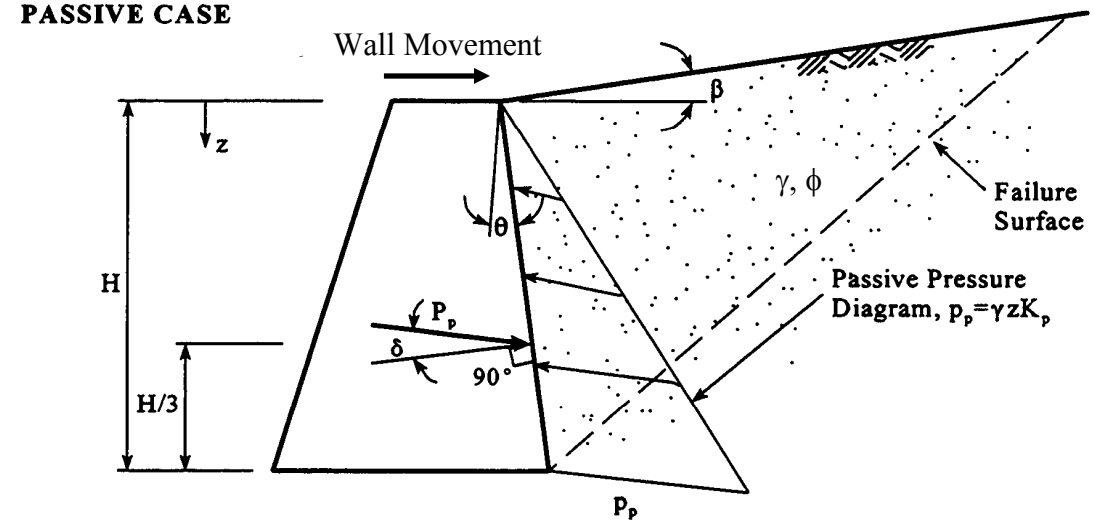

$$K_p = \frac{\cos^2(\theta + \phi)}{\cos^2\theta\cos(\theta - \delta)\left[1 - \sqrt{\frac{\sin(\phi + \delta)\sin(\phi + \beta)}{\cos(\theta - \delta)\cos(\theta - \beta)}}\right]^2}$$

Figure 10-5. Coulomb coefficients K_a and K_p for sloping wall with wall friction and sloping cohesionless backfill (after NAVFAC, 1986b).

These simplified equations were also derived independently by Rankine (1857). Hence, the earth pressures computed by using these equations are commonly known as the Rankine earth pressures.

For a cohesionless soil with a groundwater table, the effective lateral earth pressure acting on the wall at any depth, z, below the surface is a function of the pore water pressure u as follows,

$$p_a' = K_a(\gamma z - u) \tag{10-6}$$

$$p_p' = K_p(\gamma z - u) \tag{10-7}$$

10.2.3 Effect of Cohesion on Lateral Earth Pressures

For a cohesive soil defined by effective stress strength parameters ϕ' and c', the active and passive earth pressure coefficients are:

$$K_a = \tan^2(45 - \phi'/2) - \frac{2c'}{p_o'}\tan^2(45 - \phi'/2) \tag{10-8}$$

$$K_p = \tan^2(45 + \phi'/2) + \frac{2c'}{p_o'}\tan^2(45 + \phi'/2) \tag{10-9}$$

Figure 10-6(a) presents active and passive pressure distributions for cohesionless soils (c' = 0) while Figure 10-6(b) shows similar pressure distributions for c'-ϕ' soils.

For a c'-ϕ' soil with a groundwater table, the effective lateral earth pressure acting on the wall at any depth, z, below the surface is,

$$p_a' = K_a(\gamma z - u) - 2c'\sqrt{K_a} \tag{10-10}$$

$$p_p' = K_p(\gamma z - u) + 2c'\sqrt{K_p} \tag{10-11}$$

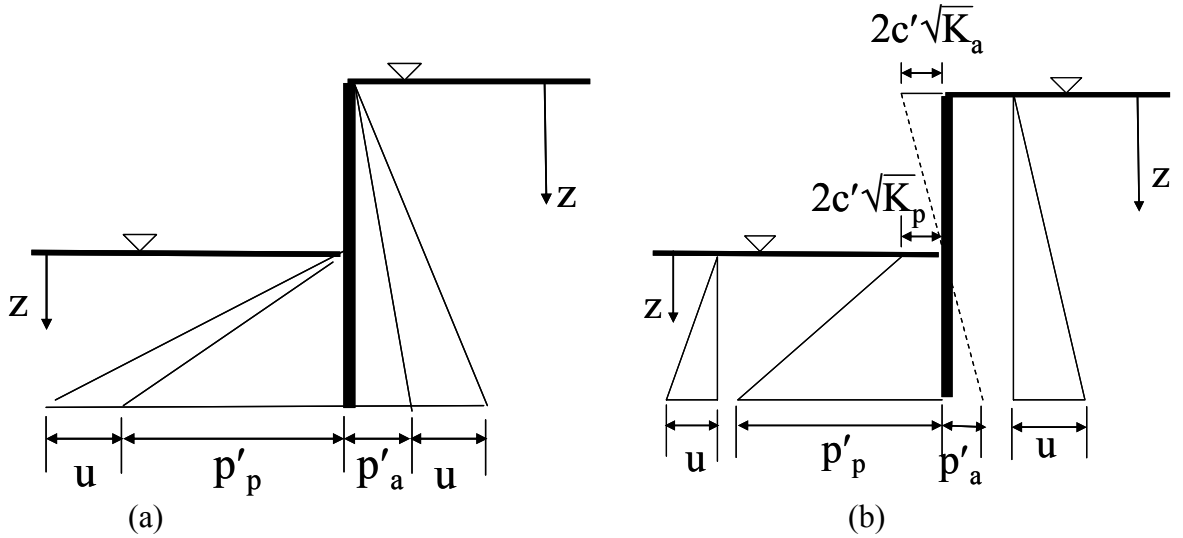

Figure 10-6. (a) Wall pressures for a cohesionless soil, and (b) Wall pressures for soil with a cohesion intercept – with groundwater in both cases (after Padfield and Mair, 1984)

Theoretically, in soils with cohesion, the active earth pressure behind the wall becomes negative from the ground surface to a critical depth z where γz is less than $2c'\sqrt{K_a}$. This critical depth is referred to as the "tension crack." The active earth pressure acting against the wall within the depth of the tension crack is assumed to be zero. Unless positive drainage measures are provided, water infiltration into the tension crack may result in hydrostatic pressure on the retaining structure.

Use of values of c′ for the retained soil, greater than say, 100 psf (5 kPa), results in a significant depth of theoretical negative active earth pressure. Therefore, it is important either to:

- reduce c′ towards the surface, which may be realistic for many clays in view of weathering;
  or
- assume that the effective pressure on the wall at any depth should not be less than 30z psf where z = depth in ft (5z kN/m^2 (z = depth in m).

In all cases where water is present in the soil, full hydrostatic pressure is added to the lateral earth pressure computed by Equations 10-8 to 10-11 to obtain the total lateral pressure that will be experienced by a retaining wall.

10.2.4 Effect of Wall Friction and Wall Adhesion on Lateral Earth Pressures

In practice, walls are not smooth. As indicated previously, wall friction and wall adhesion modify the stress distribution near a wall. Therefore, wall friction, δ, and wall adhesion, c_w, should both be considered as proportions of ϕ', and c' or s_u, respectively. For a rigid wall moving away from the retained soil, the frictional forces exerted by the wall on the soil are in the sense shown in Figure 10-7. The active wedge moves down with respect to the wall, while the passive wedge moves upwards.

An important exception to this mechanism is when the wall acts as a significant load-bearing element, when large vertical loads are applied to the top of the wall, or when an inclined ground anchor is stressed to an appreciable load and the vertical component of the load acts downward. In such cases, the wall has to move down relative to the soil on both sides of the wall in order to mobilize the required skin friction to support the load. Therefore, the friction acts to increase the pressures on both the active and passive sides, because it acts on the soil wedges in a downward direction. This effect, however, is neglected because limiting or failure conditions are considered in calculation of overall stability and the directions in which the frictional forces act should be taken as shown in Figure 10-7.

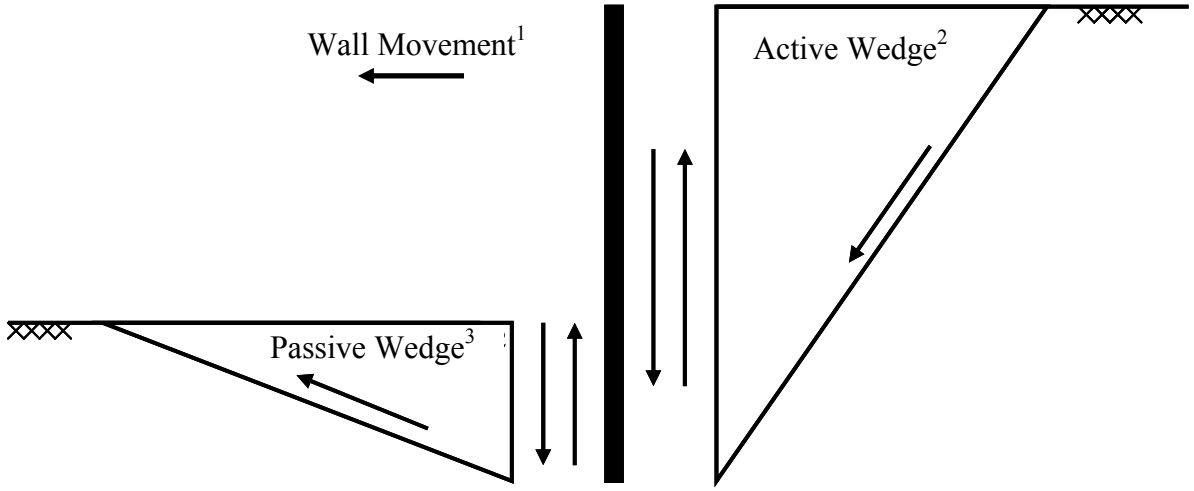

Note: (1) Assume wall moves as a rigid body to the left.
(2) Active wedge moves downward relative to wall
(3) Passive wedge moves upward relative to wall.

Figure 10-7. Wall friction on soil wedges (after Padfield and Mair, 1984)

Wall friction, δ, and wall adhesion, c_w, have an important effect on soil pressures. Equations 10-10 and 10-11 can be written to account for those effects in a more general as follows:

$$p_a' = K_a(\gamma z - u) - K_{ac}c' \qquad 10\text{-}12$$

$$p_p' = K_p(\gamma z - u) + K_{pc}c' \qquad 10\text{-}13$$

where K_a and K_p depend on δ and K_{ac} and K_{pc} depend on δ and c_w, and p_a' and p_p' are the components of effective pressure normal to the wall. Where c' is incorporated into the soil strength characterization, approximate values of K_{ac} and K_{pc} should be calculated from the following expressions:

$$K_{ac} = 2\sqrt{K_a\,(1 + c_w / c')} \qquad 10\text{-}12a$$

$$K_{pc} = 2\sqrt{K_p\,(1 + c_w / c')} \qquad 10\text{-}13a$$

Different values of δ are given by several sources. As shown in Table 10-1, values of δ depend on soil type and the wall material. The maximum wall friction suggested for design is:

Active: $\delta = 2/3\ \phi'$

Passive: $\delta = 1/2\ \phi'$

Where a cohesion intercept is used as part of the characterization of strength in terms of effective stress, a maximum wall adhesion of $c_w = 0.5c'$ could be used, but in view of the inevitable remolding of the clay close to the wall by any construction process, it is recommended that no wall adhesion be allowed in the design.

The values of wall friction provided above and in Table 10-1 are maximum values for design. These values can be adopted in most cases, but the design engineer should consider any circumstances where the values might be affected by the relative movement of the soil and the wall. For example, on the active side, reduced values should be used if there is a tendency for the wall to move downwards, e.g., for load-bearing walls or walls supported by prestressed ground anchors. For walls retaining soft cohesive soils or granular soils that will be subjected to significant vibration, e.g., walls near railway tracks or machine foundations, δ should be assumed to be zero in the design.

Table 10-1
Wall friction and adhesion for dissimilar materials (after NAVFAC, 1986b)

Interface Materials	Friction Factor, tan δ	Friction angle, δ degrees
Mass concrete on the following foundation materials:		
Clean sound rock	0.70	35
Clean gravel, gravel sand mixtures, coarse sand	0.55 to 0.60	29 to 31
Clean fine to medium sand, silty medium to coarse sand, silty or clayey gravel	0.45 to 0.55	24 to 29
Clean fine sand, silty or clayey fine to medium sand	0.35 to 0.45	19 to 24
Fine sandy silt, nonplastic silt	0.30 to 0.35	17 to 19
Very stiff and hard residual or preconsolidated clay	0.40 to 0.50	22 to 26
Medium stiff and stiff clay and silty clay (Masonry on foundation materials has same friction factor)	0.30 to 0.35	17 to 19
Steel sheet piles against the following soils:		
Clean gravel, gravel-sand mixtures, well-graded rock fill with spalls	0.40	22
Clean sand, silty sand-gravel mixtures, single size hard rock fill	0.30	17
Silty sand, gravel or sand mixed with silt or clay	0.25	14
Fine sandy silt, nonplastic silt	0.20	11
Formed concrete or concrete sheet piling against the following soils:		
Clean gravel, gravel-sand mixture, well-graded rock fill with spalls	0.40 to 0.50	22 to 26
Clean sand, silty sand-gravel mixture, single size hard rock fill	0.30 to 0.40	17 to 22
Silty sand, gravel or sand mixed with silt or clay	0.30	17
Fine sandy silt, nonplastic silt	0.25	14
Various structural materials:		
Masonry on masonry, igneous and metamorphic rocks:		
Dressed soft rock on dressed soft rock	0.70	35
Dressed hard rock on dressed soft rock	0.65	33
Dressed hard rock on dressed hard rock	0.55	29
Masonry on wood (cross grain)	0.50	26
Steel on steel at sheet pile interlocks	0.30	17
Interface Materials (Cohesion)	**Adhesion c_a (kPa)**	
Very soft cohesive soil (0 - 12 kPa)	0 - 12	
Soft cohesive soil (12 - 24 kPa)	12 - 24	
Medium stiff cohesive soil (24 - 48 kPa)	24 - 36	
Stiff cohesive soil (48 - 96 kPa)	36 - 45	
Very stiff cohesive soil (96 - 192 kPa)	45 - 62	

The effect of wall friction on the Rankine and Coulomb methods of earth pressure computation is as follows:

1. The Rankine method cannot take account of wall friction. Accordingly, K_a is overestimated slightly and K_p is under-estimated, thereby making the Rankine method conservative for most applications.

2. The Coulomb theory can take account of wall friction, but the results are unreliable for passive earth pressures for wall friction angle values greater than $\phi'/3$ because the failure surface is assumed to be a plane. The failure wedges assumed in the Coulomb analysis take the form of straight lines as shown in Figure 10-8. This may be contrasted with the curved shapes of failure surface observed in model tests. The curvature results from the disturbing influence of wall friction on the stress field near the wall. The error in the Coulomb solutions results in K_a being underestimated slightly and K_p being overestimated very significantly for large values of ϕ'.

If the angle of wall friction δ is small, the failure surface is almost linear. For large values of δ, the failure surface is curved and can be approximated by a log-spiral. The deviation of the curved surface from a planar surface is minor for the active case but significant for the passive case as shown in Figure 10-8. For most applications, the effect of wall friction on active earth pressures is relatively small and is often neglected.

For the passive case, however, large values of δ cause downward tangential shear forces to act on the passive wedge of soil adjacent to the wall, increasing its resistance to upward movement. This increased resistance to upward movement causes a curved failure surface to occur in the soil, as shown in Figure 10-8b. The soil fails on this curved surface of least resistance and not on the Coulomb plane, which would require greater lateral driving force. Hence, passive pressures computed on the basis of the plane wedge theory are always greater than those calculated on the basis of a log-spiral failure surface and may be on the unsafe side since passive earth pressure forces are generally resisting forces in stability analyses.

Based on the above discussions, it is recommended that the log-spiral theory be used for the determination of the passive earth pressure coefficients. Charts for two common wall configurations, sloping wall with level backfill and vertical wall with sloping backfill based on the log-spiral theory are presented in Figures 10-9 and 10-10 (Caquot and Kerisel, 1948; NAVFAC, 1986b). For walls that have a sloping backface and sloping backfill, the passive earth pressure coefficient can be calculated as indicated in Figure 10-5 by using $\delta = \phi'/3$.

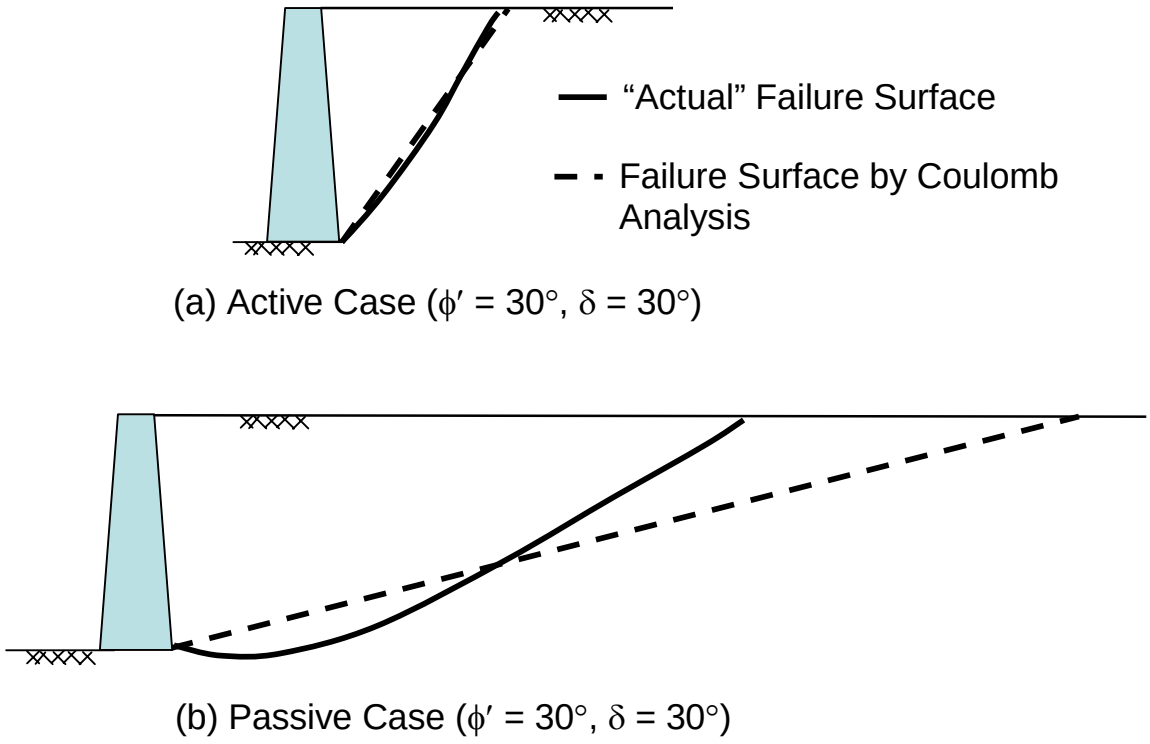

Figure 10-8. Comparison of plane and log-spiral failure surfaces (a) Active case and (b) Passive case (after Sokolovski, 1954) – Note: Depiction of gravity wall is for illustration purpose only.

For the active case, the resultant load predicted by using coefficients based on the plane wedge theory is within 10 percent of that obtained with the more exact log-spiral theory. Hence, for the active case, Coulomb's theory can be used to calculate the earth pressure coefficient (Refer to Figure 10-5).

For some wall types, such as cantilever retaining walls and an MSE walls, the "interface" where the earth pressures are computed is within the retained soils along a vertical plane passing through the heel of the base slab. In such cases, there is soil-to-soil contact and the resultant may be oriented at the angle of mobilized friction. The angle of mobilized friction depends on the factor of safety used for the angle of internal friction. For these cases, it is generally conservative to assume that the earth pressure is parallel to the slope of the backfill.

REDUCTION FACTOR (R) OF K_p FOR VARIOUS RATIOS OF - δ/ϕ								
ϕ	δ/ϕ	-0.7	-0.6	-0.5	-0.4	-0.3	-0.2	-0.1	0.0
10		.978	.962	.946	.929	.912	.898	.881	.864
15		.961	.934	.907	.881	.854	.830	.803	.775
20		.939	.901	.862	.824	.787	.752	.716	.678
25		.912	.860	.808	.759	.711	.666	.620	.574
30		.878	.811	.746	.686	.627	.574	.520	.467
35		.836	.752	.674	.603	.536	.475	.417	.362
40		.783	.682	.592	.512	.439	.375	.316	.262
45		.718	.600	.500	.414	.339	.276	.221	.174

Note: Curves shown are for $\delta/\phi = -1$

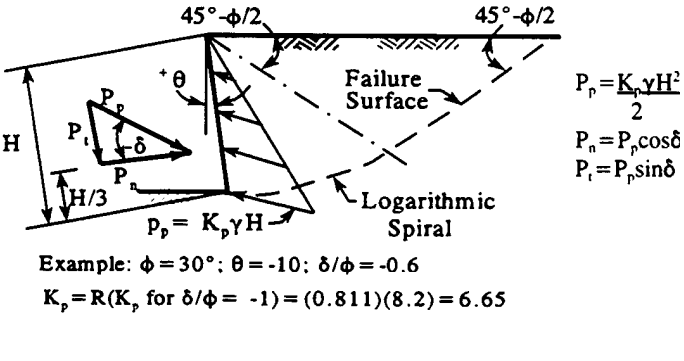

Example: $\phi = 30°$; $\theta = -10$; $\delta/\phi = -0.6$

$K_p = R(K_p \text{ for } \delta/\phi = -1) = (0.811)(8.2) = 6.65$

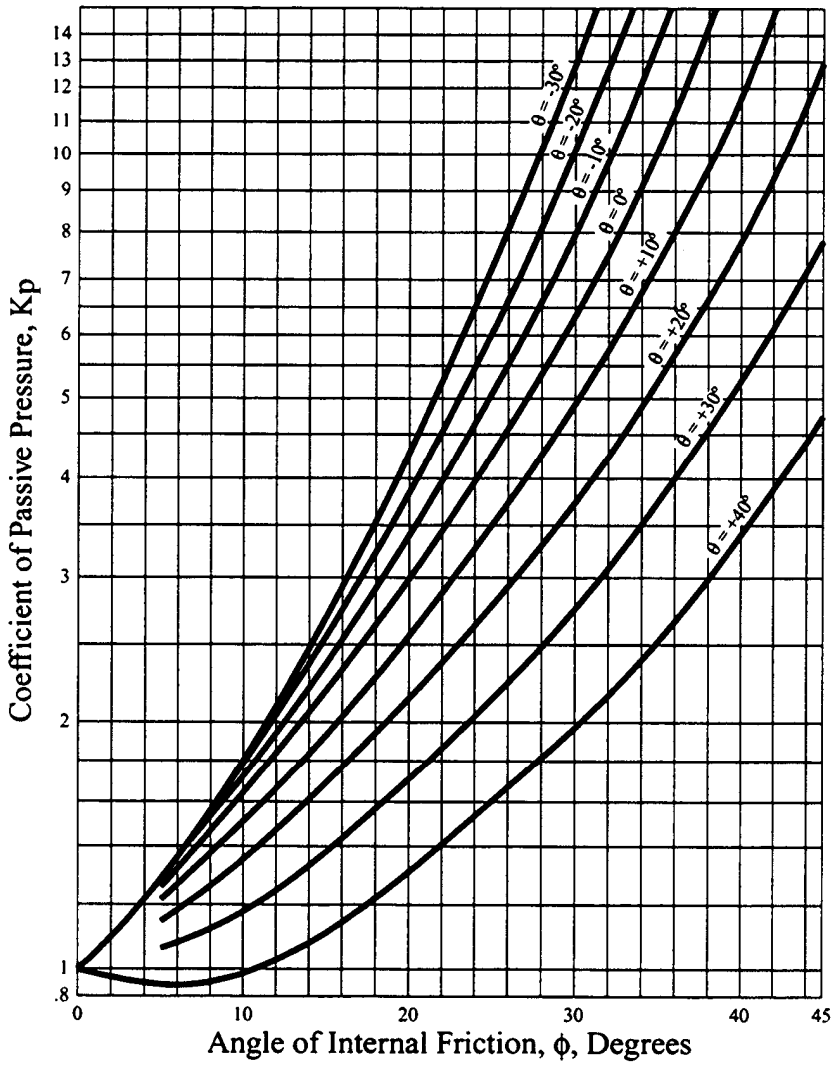

Figure 10-9. Passive coefficients for sloping wall with wall friction and horizontal backfill (Caquot and Kerisel, 1948; NAVFAC, 1986b).

REDUCTION FACTOR (R) OF K_p FOR VARIOUS RATIOS OF - δ/ϕ								
ϕ \ δ/ϕ	-0.7	-0.6	-0.5	-0.4	-0.3	-0.2	-0.1	0.0
10	.978	.962	.946	.929	.912	.898	.881	.864
15	.961	.934	.907	.881	.854	.830	.803	.775
20	.939	.901	.862	.824	.787	.752	.716	.678
25	.912	.860	.808	.759	.711	.666	.620	.574
30	.878	.811	.746	.686	.627	.574	.520	.467
35	.836	.752	.674	.603	.536	.475	.417	.362
40	.783	.682	.592	.512	.439	.375	.316	.262
45	.718	.600	.500	.414	.339	.276	.221	.174

Note: Curves shown are for $\delta/\phi = -1$

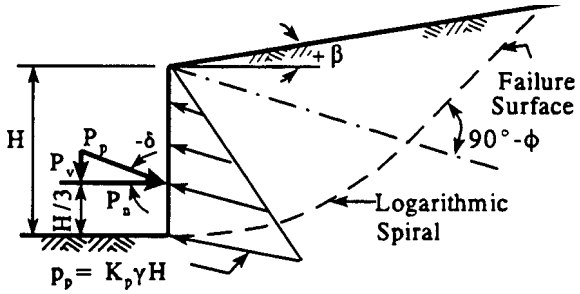

$P_p = K_p \gamma H^2/2$; $P_n = P_p \cos\delta$; $P_v = P_p \sin\delta$

Example: $\phi = 25°$; $\beta/\phi = -0.2$; $\delta/\phi = -0.3$

$K_p = R(K_p \text{ for } \delta/\phi = -1) = (0.711)(3.62) = 2.58$

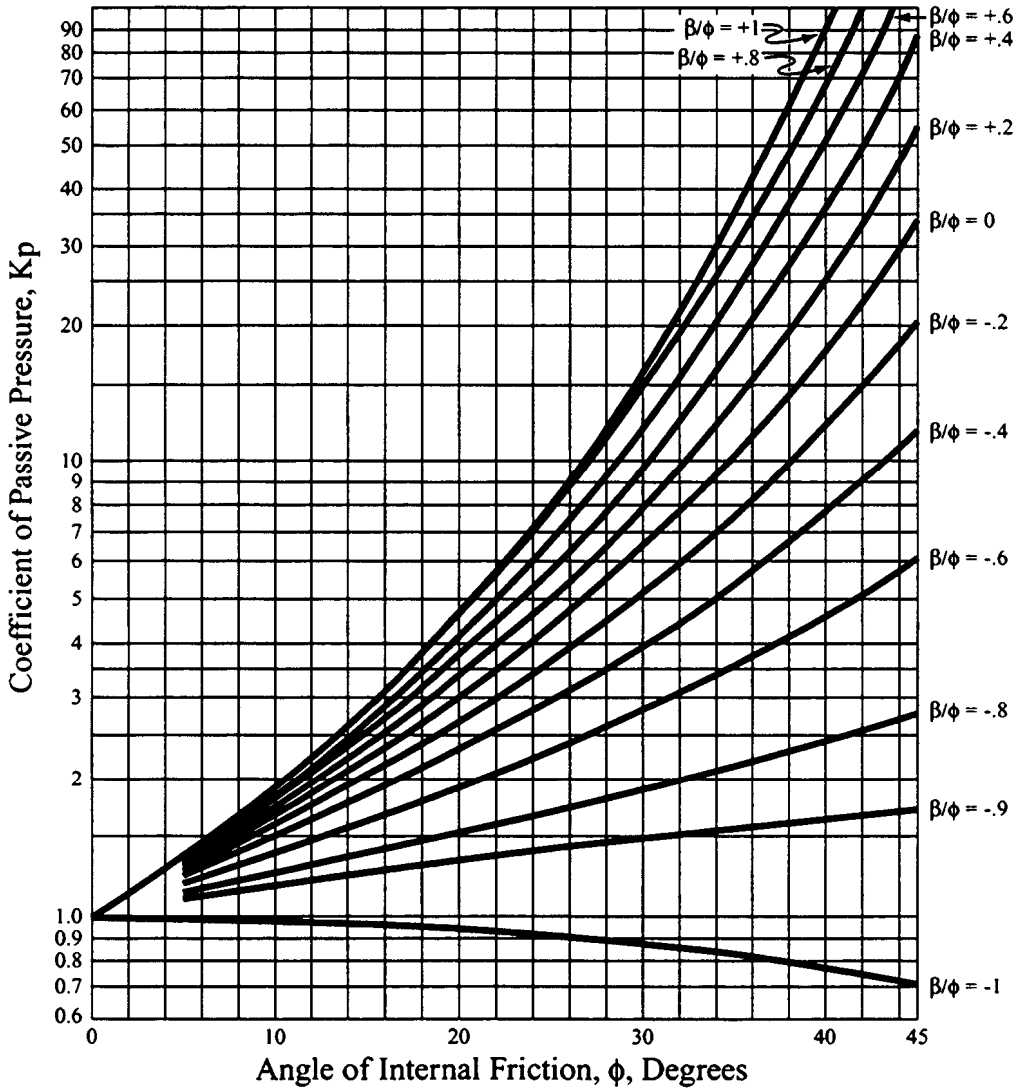

Figure 10-10: Passive coefficients for vertical wall with wall friction and sloping backfill (Caquot and Kerisel, 1948; NAVFAC, 1986b).

10.2.5 Theoretical Lateral Earth Pressures in Stratified Soils

For stratified or non-homogeneous soils, the theoretical earth pressures are assumed to be distributed as shown in Figure 10-11 where the discontinuities in the earth pressure diagram occur at the boundary between soil strata having different unit weights and shear strength parameters. Unless the computed earth pressures vary widely with depth, the total applied lateral force determined from the computed pressure diagram may be redistributed to a corresponding simplified equivalent triangular pressure diagram as indicated in Figure 10-11.

For complex cases such as layered soils, irregular backfill, irregular surcharges, wall friction, and sloping groundwater level, pressures can be determined by graphical solutions. Among the many graphical solutions are Culmann's method (1866) and the Trial Wedge method. These procedures can be found in Bowles (1996) or NAVFAC (1986b). The Trial Wedge method has the advantage of including cohesion as a soil parameter in the analysis.

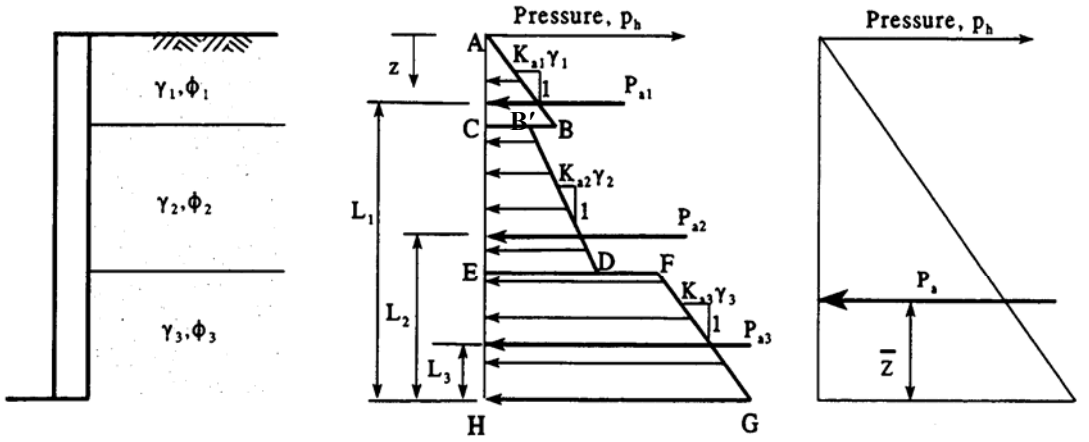

The lateral force is equal to the area of the pressure diagram. Thus,

$$P_{a1} = \text{Area ABC} \qquad P_{a2} = \text{Area CB'DE} \qquad P_{a3} = \text{Area EFGH}$$

Resultant (total) active force per unit length, $P_a = P_{a1} + P_{a2} + P_{a3}$

Location of resultant from base of wall, $\bar{z} = \dfrac{P_{a1}L_1 + P_{a2}L_2 + P_{a3}L_3}{P_a}$

- **Use buoyant unit weight for soils below water table.**
- **Add water pressure as appropriate to obtain total lateral pressure.**
- **The simplified distribution may not be justified for all soil conditions. Use judgment to determine validity of such simplified distributions.**

Figure 10-11. Pressure distribution for stratified soils.

10.2.6 Semi Empirical Lateral Earth Pressure Diagrams

The earth pressure distributions discussed in the previous sections are strictly applicable to rigid wall systems, i.e., walls that translate and/or rotate as a unit and do not experience bending deformations. Most gravity walls can be considered rigid walls.

If a wall system undergoes bending deformations in addition to rigid body motion then such a wall system is considered flexible. Virtually all wall systems, except gravity walls, may be considered to be flexible. The bending deformations result in a redistribution of the lateral pressures from the more flexible to the stiffer portions of the system. Thus, in these walls the final distribution and magnitude of the lateral earth pressure may be considerably different from those used for rigid walls. For example, soldier-pile and lagging walls with multiple levels of support are usually designed by using empirical earth pressure distributions based on observed data. The shape of these empirical earth pressure distributions may vary from rectangular to trapezoidal. The magnitude of the pressures may also vary depending on the soil type.

Other factors that may influence the development of earth pressures are the type of construction, e.g., "bottom-up" or "top-down," the wall support mechanism, e.g., tie-backs, struts, rakers, soil nails, reinforcing elements, single or multiple levels of support, etc., the geometry of the retained soil, e.g., silo pressure, the superimposed or surcharge loads, e.g., strip, line, concentrated, or equipment loads, and the type of analysis, e.g., static or seismic. In addition, for cases of soil reinforced by inclusions such as MSE walls or soil-nailed walls, different types of earth pressure distributions are used to evaluate the internal and external stability of the wall system. The empirical earth pressure distributions are generally related to the basic earth pressure coefficients K_a, K_p and K_o, which, as indicated previously, are a function of the shear strength of the soil.

10.2.7 Lateral Earth Pressures in Cohesive Backfills

Most DOTs involved in the design and procurement of fill wall systems, such as MSE walls, have well-defined backfill material requirements. In general, specifications for wall backfill require high-quality, granular, relatively free-draining backfills. However, in some cases a poorer quality on-site backfill material may be used, especially for temporary systems. These poorer quality backfills are generally more fine-grained and not free-draining. Methods to calculate earth pressures in clayey soils were described previously. In this section cautions are provided regarding the use of fine-grained cohesive backfill soils.

Lateral pressures can be caused by the volume expansion of ice in fine-grained soils such as fine sand, silt and clay. Lateral pressures due to volume expansion of the retained soil may achieve relatively high values that are difficult to predict. Since structures are usually not designed to withstand frost-generated stresses, provisions should be made so that frost-related stresses will not develop behind the structure or be kept to a minimum. The use of one or more of the following measures may be necessary:

- Isolate the backfill from underground sources of water either by providing a permeable drainage system or an impervious barrier;

- Use pervious backfill and provide weep holes in the structure;

- Provide an impervious soil layer near the ground surface, and grade the ground behind the wall to drain surface water away from the wall.

Expansive clays can cause very high lateral pressures on the back of a retaining structure and should therefore be avoided whenever possible. In cases where expansive clays are present behind a wall, swelling pressures should be evaluated based on laboratory tests so that the wall can be designed properly to withstand these swelling pressures, which can be significant Alternatively, one of the following measures can be taken:

- A granular filter material can be provided between the clay backfill and the back of the wall. This material will drain the groundwater away from the expansive soil and, at the same time act as a buffer zone between the expansive soil and the structure.

- The expansive soil can be treated with lime to reduce or even eliminate its swelling potential, if the soil does not contain gypsum. Expansive soils that contain gypsum should not be treated with lime because the combination of the minerals in expansive soils with gypsum and water may lead to the formation of ettringite, which has a much higher swelling potential than the untreated expansive soils.

The following is noted by Duncan, *et al.* (1990) concerning the use of clayey soils as backfill for fill wall applications:

- Clayey backfills generally have lower drained shear strength than cohesionless soils. Low drained shear strength results in: (1) larger lateral earth pressures against the back of the wall; (2) lower frictional resistance along the reinforcement for MSE

walls that employ frictional reinforcement; and (3) lower bearing value for MSE walls that employ passive reinforcement.

- Clayey backfills are more plastic and contain more fines than cohesionless soils. Higher plasticity results in: (1) poor drainage and the potential for the development of water pressures behind the wall; (2) the potential for freezing of retained water and development of ice pressures on the back of the wall; and (3) greater potential for corrosion of metallic reinforcements for MSE walls.

- Clayey backfills have the potential to undergo creep deformations that can lead to higher earth pressures and greater wall face deformations than will occur with soils that do not exhibit significant creep potential. Earth pressures used for design of gravity walls employing clayey backfills should be based on past performance and field experience, as wall design methods do not consider the effects of creep.

Despite these problems, silts and clays may be used as backfill soils provided suitable design procedures are employed, including conservative estimates of lateral earth pressures, and construction control measures are incorporated into the contract documents. When silts and clays are used as backfills, walls may need to be designed for pressures between active and at-rest conditions. For soils that are deemed to have high swell potential, an earth-pressure coefficient as great as 1.0 may be used for design (Canadian Geotechnical Society, 1992). In all cases, water pressures and appropriate surcharge loads also need to be added to these earth pressures.

In general, any permanent fill wall system that incorporates silty or clayey backfills must have an appropriately designed subsurface and surface drainage system to minimize pore pressure build-up and soil saturation. Such wall systems should also include periodic measurements of wall face movements.

10.3 LATERAL PRESSURES DUE TO WATER

In retaining wall design, it is general practice to provide drainage paths, commonly known as "weep holes," through the earth retaining structure, or use other methods to drain groundwater that may otherwise collect behind the structure. The purpose of these drainage features is to prevent the development of water pressure on the structure. Occasionally, however, it may not be feasible or desirable to drain the water from behind the structure. For example, maintenance of existing ground water levels may be desirable to safeguard against potential settlement of adjacent structures or to prevent contaminated groundwater from entering the excavation. In such instances, the earth retaining structure must be designed for both lateral earth pressure and water pressure.

Computation of active lateral earth pressures for the case of a uniform backfill and static groundwater is illustrated in Figure 10-12. In this case, the water pressure represents a hydrostatic condition since there is no seepage or flow of water through the soil. The lateral earth pressure below the water level is based on the effective vertical stress, p'_o, times the active lateral earth pressure coefficient. The lateral pressure due to the water is added to the active lateral earth pressure to obtain the total lateral pressure on the wall. By analogy to lateral earth pressure coefficients, the lateral water pressure coefficient = 1.0. The lateral pressure computations should consider the greatest unbalanced water head anticipated to act on the wall, since this generally results in the largest total lateral load.

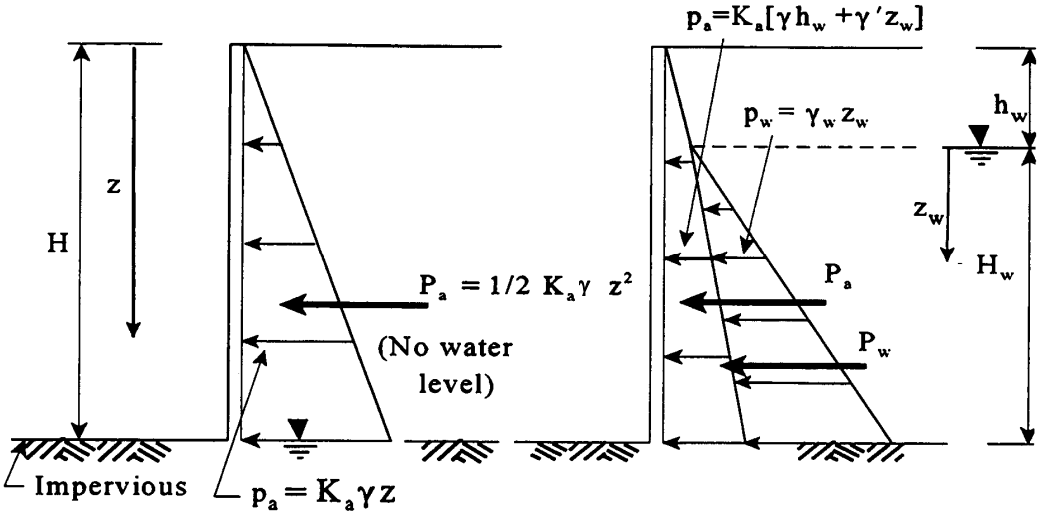

Figure 10-12. Computation of lateral pressures for static groundwater case.

For cases where seepage may occur through or beneath the earth retaining structure, the resulting seepage gradients will result in an increase or reduction in the water pressure depending on the direction of the seepage path. For such cases, flow net procedures can be used to compute the lateral pressure distribution due to water.

The concepts of lateral earth pressures and lateral pressures due to water are illustrated in Example 10-1.

Example 10-1: For the wall configuration shown below, construct the lateral pressure diagram. Assume the face of the wall to be smooth ($\delta = 0$, $c_w = 0$).

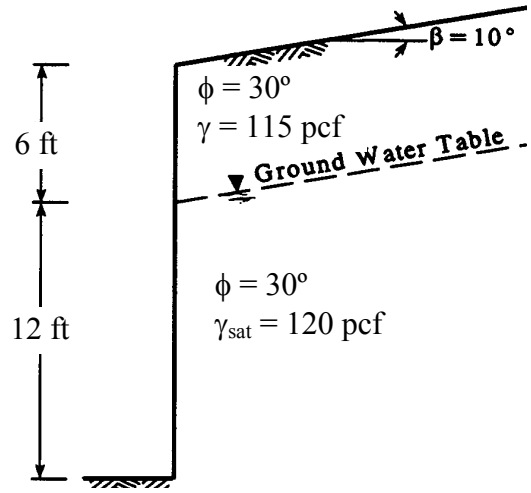

Solution:

Use the Coulomb method (Figure 10-5) for $\phi = 30^o$, $\beta = 10^o$, $\theta = 0$, and $\delta = 0$:

$$K_a = 0.374$$

The pressures at various depths can then be calculated as shown in a tabular format as follows**.** Based on the values in the table, the lateral pressure diagrams due to earth and water can be constructed as shown below. The total lateral pressure diagram is the sum of the two lateral pressure diagrams shown in the figure accompanying this example.

Effective Lateral Earth Pressures, p'_a

z, ft	p_o, psf	$p_a = K_a p_o$, psf
0	0	0
6	(115 pcf) (6 ft) = 690.0 psf	0.374(690.0 psf) = 258.1 psf
18	690 psf +(120 pcf-62.4 pcf)(12 ft) = 1381.2 psf	0.374(1381.2 psf) = 516.6 psf

Hydrostatic Pressure, $u = K_w u_w$

z, ft	z_w, ft	$u_w = z_w \gamma_w$, psf	Lateral water pressures, u psf
0	0	0	= 0
6	0	0	= 0
18	12	12 ft (62.4 pcf) = 748.8 psf	1.0(748.8 psf) = 748.8 psf

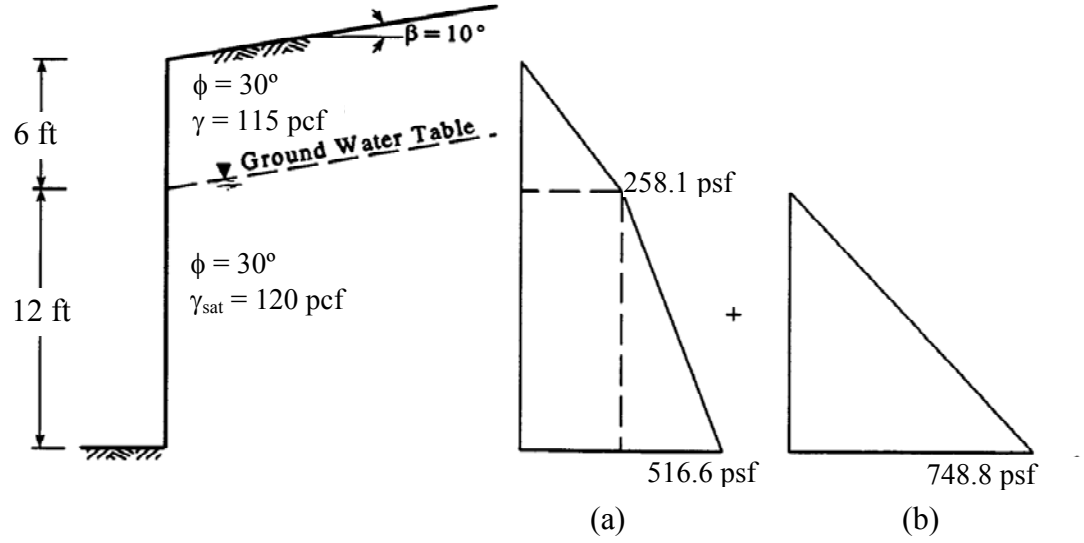

(a) Lateral effective earth pressure diagram and (b) Lateral water pressure diagram.

10.4 LATERAL PRESSURE FROM SURCHARGE LOADS

10.4.1 General

Surcharge loads on the backfill surface near an earth retaining structure also cause lateral pressures on the structure. Typical surcharge loadings may result from railroads, highways, sign/light structures, electric/telecommunications towers, buildings, construction equipment, and material stockpiles.

The loading cases of particular interest in the determination of lateral pressures are:

- uniform surcharge;
- point loads;
- line loads parallel to the wall; and
- strip loads parallel to the wall.

Figure 10-13 shows examples of retaining walls with surcharge loads.

(a)

(b)

Figure 10-13: (a) Retaining wall with uniform surcharge load and (b) Retaining wall with line loads (railway tracks) and point loads (catenary support structure).

10.4.2 Uniform Surcharge Loads

Surcharge loads are vertical loads applied at the ground surface, which are assumed to result in a uniform increase in lateral pressure over the entire height of the wall. The increase in lateral pressure for a uniform surcharge loading can be written as:

$$\Delta p_h = K q_s \qquad 10\text{-}14$$

where: Δp_h is the increase in lateral earth pressure due to the vertical surcharge load, q_s. applied at the ground surface, and K is an appropriate earth pressure coefficient. Examples of surcharge loads for highway wall system applications include: (1) dead load surcharges such as that resulting from the weight of a bridge approach slab or concrete pavement; (2) live load surcharges such as that due to traffic loadings; and (3) surcharges due to equipment or material storage during construction of the wall system.

When traffic is expected to come to within a distance from the wall face equivalent to one-half the wall height, the wall should be designed for a live load surcharge. For temporary walls that are not considered critical, actual surcharge loads may be evaluated and considered in the design instead this prescriptive value. Both temporary and permanent wall designs should account for unusual surcharges such as large material stockpiles. Calculated lateral pressures resulting from these surcharges should be added explicitly to the design lateral earth pressure diagram. Surcharge loads from existing buildings need to be considered if they are within a horizontal distance from the wall equal to the wall height.

10.4.3 Point, Line, and Strip Loads

Point loads, line loads, and strip loads are vertical surface loadings that are applied over limited areas as compared to surcharge loads. As a result, the increase in lateral earth pressure used for wall system design is not constant with depth as is the case for uniform surcharge loadings. These loadings are typically calculated by using equations based on elasticity theory for lateral stress distribution with depth (Figure 10-14). Examples of such loads include heavy cranes (temporary) or walls (permanent). Lateral pressures resulting from these surcharges should be added explicitly to other lateral pressures.

A numerical problem solved by use of Figure 10-14 is presented in Example 10-2.

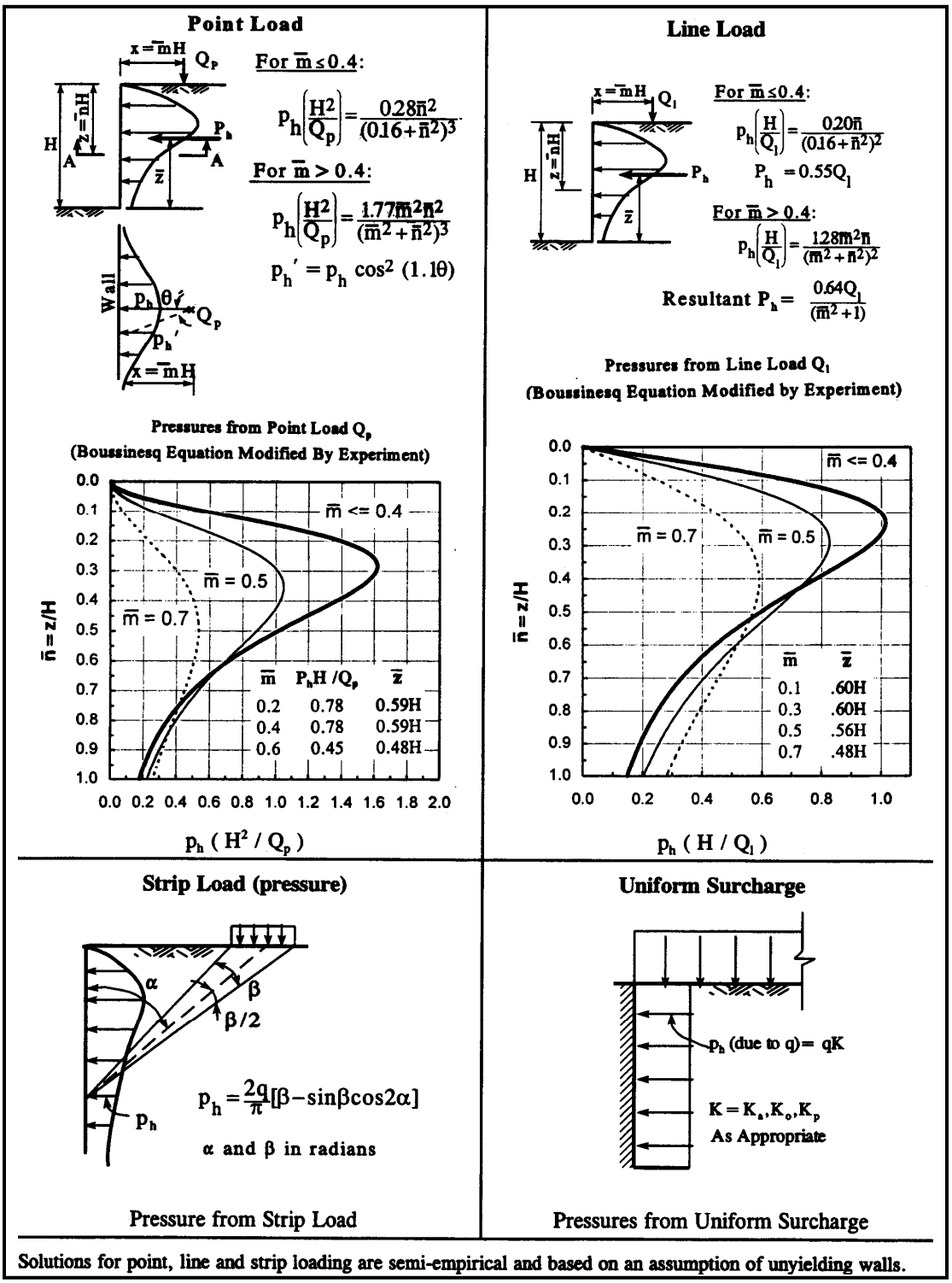

Figure 10-14. Lateral pressure due to surcharge loadings (after USS Steel, 1975)

Example 10-2: Construct the lateral pressure diagram due to a line load of 700 lb/ft located 15 ft behind the top of a 30 ft high unyielding wall shown below.

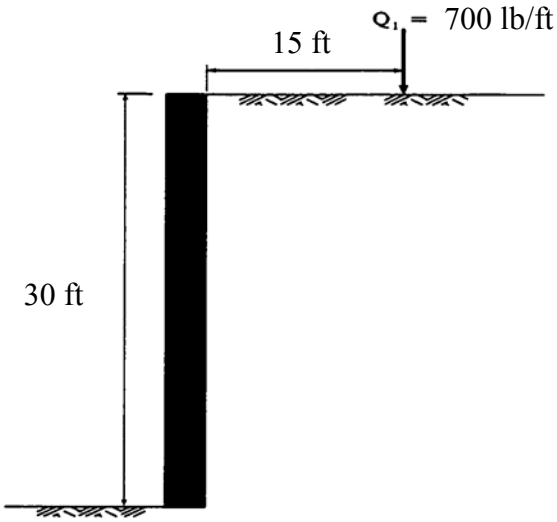

Geometry of the Example Problem 10-2

Solution:

The procedure to calculate the lateral pressures due to a line load is given in Figure 10-14. From this figure the lateral pressure can be found as follows:

$$\overline{m} = \frac{15\,\text{ft}}{30\,\text{ft}} = 0.5 > 0.4$$

For $\overline{m} > 0.4$, the lateral pressure is given by:

$$P_h = 1.28\left(\frac{Q_1}{H}\right)\left[\frac{\overline{m}^2\overline{n}}{\left(\overline{m}^2 + \overline{n}^2\right)^2}\right]$$

For $\overline{m} = 0.5$, Q_l=700 lb/ft and H = 30 ft, the lateral pressure is given by:

$$P_h = 1.28\left(\frac{700\,\text{lb/ft}}{30\,\text{ft}}\right)\left[\frac{0.5^2\overline{n}}{\left(0.5^2 + \overline{n}^2\right)^2}\right] \quad \rightarrow \quad P_h = 29.9\left[\frac{0.25\overline{n}}{\left(0.25 + \overline{n}^2\right)^2}\right]$$

Lateral pressures computed at various depths by using the above formula and the chart for line loads in Figure 10-14 are tabulated below.

Computation of Lateral Earth Pressures Due To Line Load

$\bar{n} = z / H$	Depth below top of wall (ft)	P_h (psf)
0	0	0.00
0.1	3	11.0
0.2	6	17.8
0.3	9	19.4
0.4	12	17.8
0.5	15	14.9
0.6	18	12.0
0.7	21	9.5
0.8	24	7.5
0.9	27	6.0
1.0	30	4.8

The information in the table is used to construct the curve of depth vs. lateral pressure shown below.

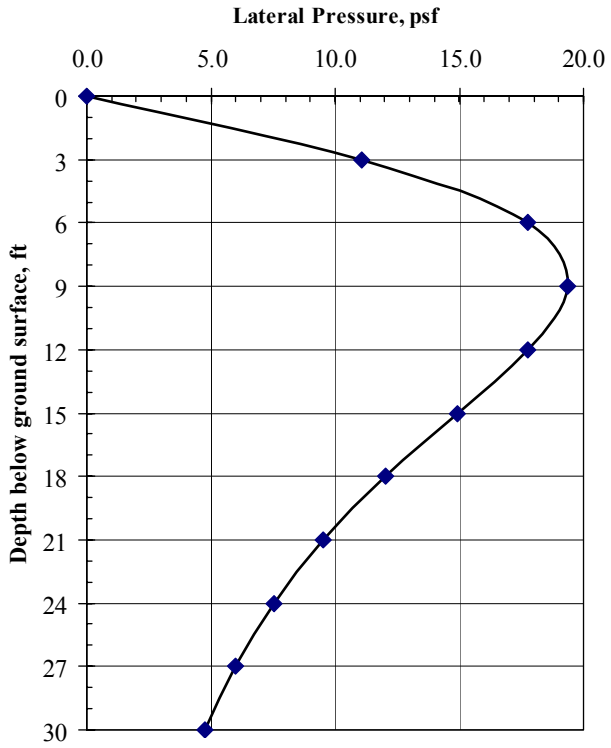

10.5 WALL DESIGN

There are many different types of walls as shown in Figure 10-3. All walls have to be evaluated for stability with respect to different modes of deformation. There are four basic modes of instability from a geotechnical viewpoint. These are (a) sliding, (b) limiting eccentricity or overturning, (c) bearing capacity, and (d) global stability. The four modes of instability are shown in Figure 10-15. Since these modes of instability assume that the wall is intact, the evaluation of these modes is commonly referred to as the "external stability" analysis. All four modes may or may not be applicable to all wall types. Furthermore, depending on the wall type and its load support mechanism (refer to Section 10.1), there may be additional instability modes, such as pullout, tension breakage, bending and shear. The evaluation of these additional modes of instability are commonly referred to as "internal stability" analyses.

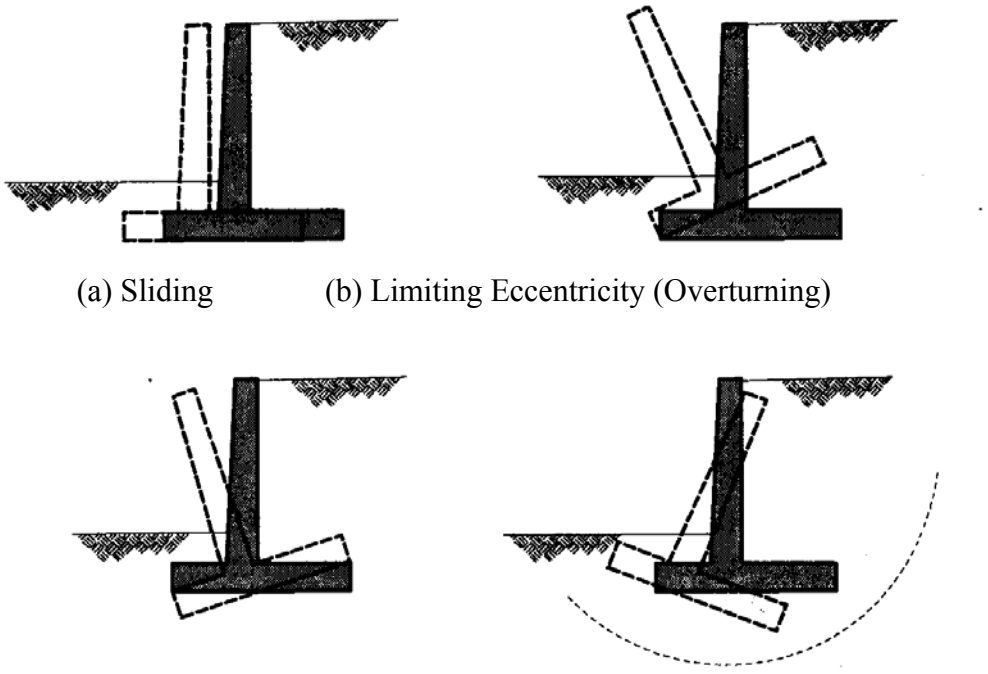

(a) Sliding (b) Limiting Eccentricity (Overturning)

(c) Bearing Capacity (d) Deep-seated (global) Stability

Figure 10-15. Potential failure mechanisms for rigid gravity and semi-gravity walls.

The external stability analysis is best illustrated by using the concept of gravity and semi-gravity walls. Table 10-2 summarizes the major design steps for cast-in-place concrete (CIP) gravity and semi-gravity walls.

Table 10-2
Design steps for gravity and semi-gravity walls

Step 1.	Establish project requirements including all geometry, external loading conditions such as (temporary, permanent, and seismic, performance criteria, and construction constraints.
Step 2.	Evaluate site subsurface conditions and relevant properties of in situ soil and rock and wall backfill.
Step 3.	Evaluate soil and rock parameters for design and establish factors of safety.
Step 4.	Select initial base dimension of wall for evaluation of external stability.
Step 5.	Select lateral earth pressure distribution. Add appropriate water, surcharge, and seismic pressures and develop total lateral pressure diagram for design.
Step 6.	Evaluate bearing capacity.
Step 7.	Evaluate limiting eccentricity (overturning) and sliding.
Step 8.	Check overall stability and revise wall design if necessary.
Step 9.	Estimate maximum lateral wall movement, tilt, and wall settlement. Revise design if necessary.
Step 10.	Design wall drainage systems.

10.5.1 Steps 1, 2, and 3 – Establish Project Requirements, Subsurface Conditions, Design Parameters

It is assumed that Steps 1, 2 and 3 are completed and a CIP wall has been deemed appropriate. Soil and/or rock parameters for design have been established. In general, the required parameters for in situ soil and rock are the same as those required for a spread footing, in particular, foundation shear strength for bearing resistance and compression parameters of the foundation materials to allow for computations of wall settlement. For gravity walls that require deep foundation support, the soil/rock parameters are the same as those required for the design of a driven pile or drilled shaft foundation.

The drainage and shear strength characteristics of the wall backfill soil are assessed as part of Step 3. Guidelines for wall backfill material gradation and drainage behind gravity retaining walls can be found in the AASHTO (2002). Whenever possible, the backfill material should be free draining, nonexpansive, and noncorrosive. All backfill material should be free of organic material. The backfill gradation should follow the guidelines presented in Table 10-3.

Table 10-3
Suggested gradation for backfill for cantilever semi-gravity and gravity retaining walls

Sieve Size	Percent Passing
3 in. (76.2 mm)	100
No. 4 (4.75 mm)	35 – 100
No. 30 (0.6 mm)	20 – 100
No. 200 (0.075 mm)	0 – 15

10.5.2 Step 4 – Select Base Dimension Based on Wall Height

Figure 10-16 shows typical dimensions for a semi-gravity cantilever retaining wall and for a counterfort wall. These dimensions were developed based on a range of backfill properties, geometries, and stable foundation soils and can be used for preliminary design. However, the final external stability calculations should be performed based on the geometry requirements and specific conditions of the project, e.g., limited right-of-way. Similar guidelines exist for other wall types and can be found in FHWA (2005b).

10.5.3 Step 5 – Select Lateral Earth Pressure Distribution

Lateral earth pressures for design of CIP walls are determined by using the procedures presented previously. Generally, Coulomb theory is used to compute earth pressures either directly on the back face of the wall, as is the case with a gravity wall, or on a vertical plane passing through the heel of the base slab, as is the case with a semi-gravity wall. Both of these concepts are illustrated in Figure 10-17.

The procedures described in Figure 10-17 are used to calculate the earth pressure loading for the wall subject to the following considerations:

- Use at-rest earth pressures for walls where rotation and displacement are restrained, e.g., rigid gravity retaining walls resting on rock or batter piles, unyielding walls such as culverts, tunnels and rigid abutment U-walls such as the CIP abutment with integral wingwalls shown in Figure 10-18.

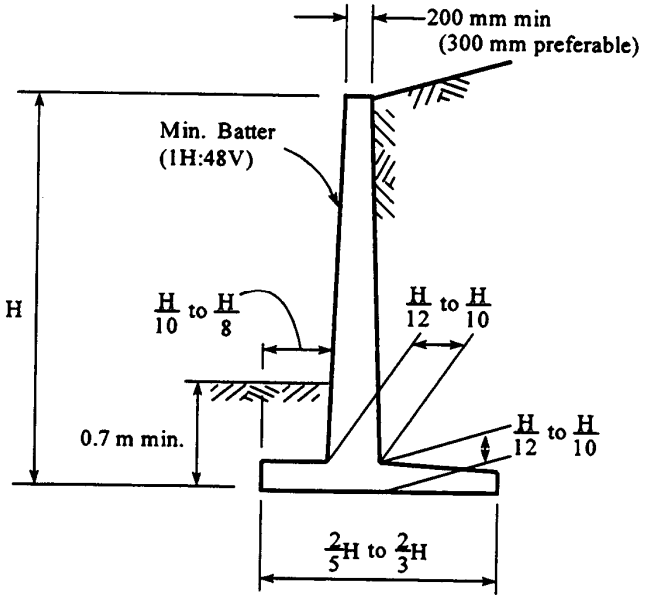

(a)

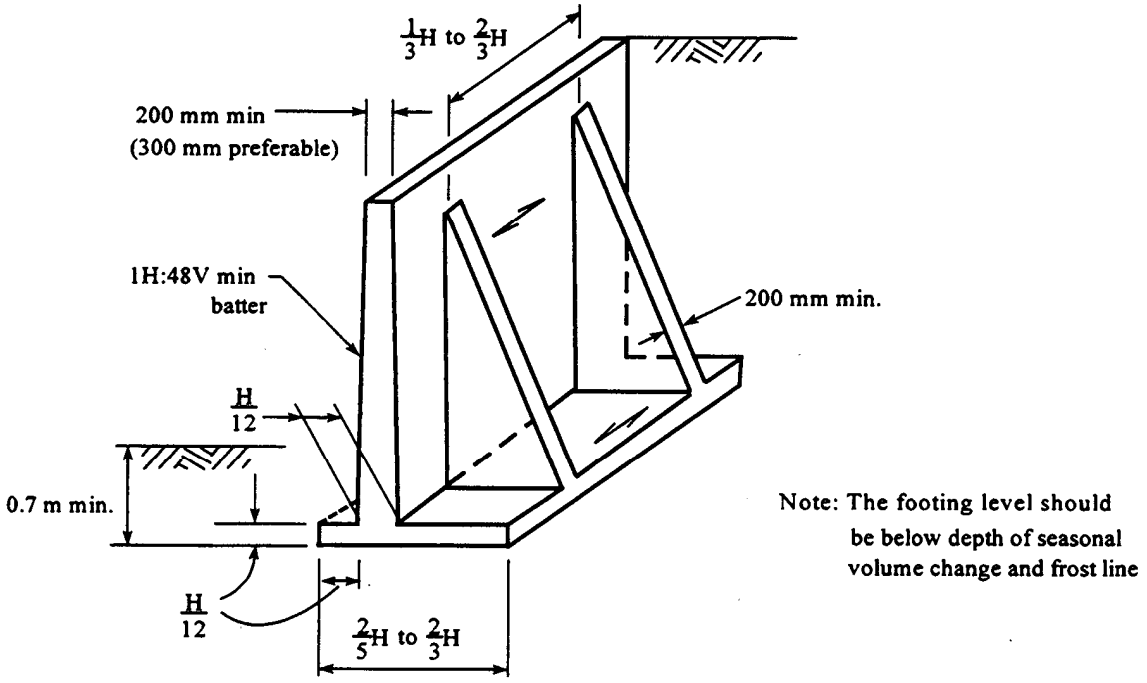

(b)

Figure 10-16. Typical dimensions (a) Cantilever wall, (b) Counterfort wall (Teng, 1962).
[1 m = 3.28 ft; 25.4 mm= 1in]

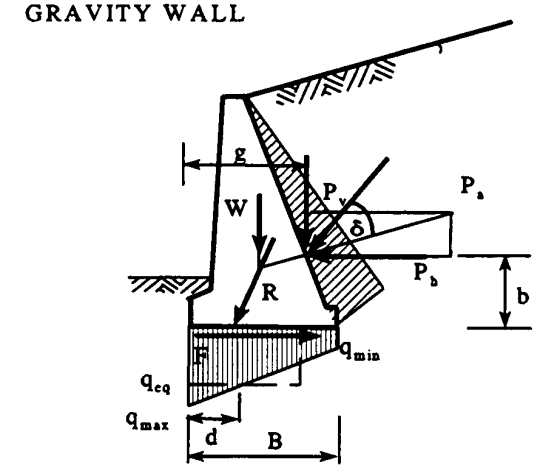

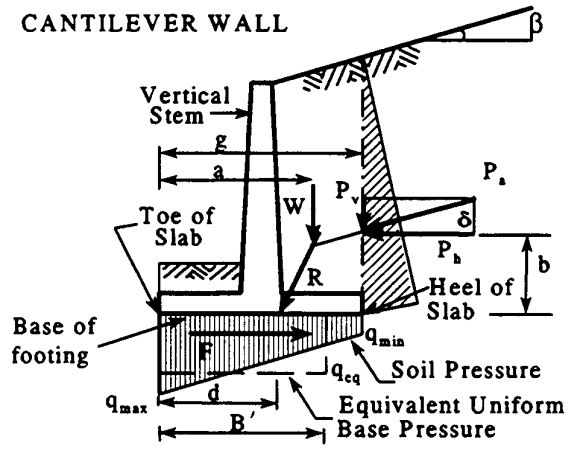

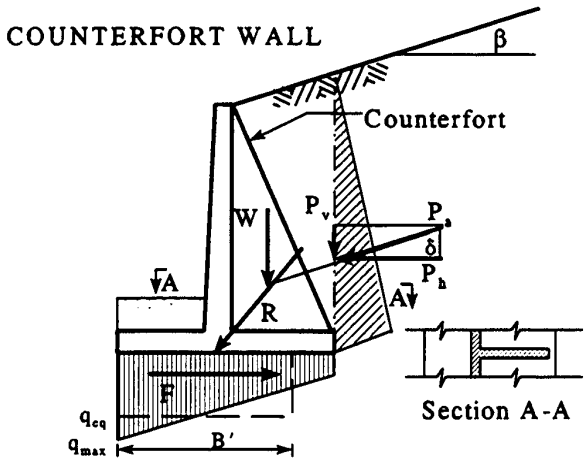

DEFINITIONS

B = width of the base of the footing

$\tan \delta_b$ = friction factor between soil and base (see Table 10-1 for guidance)

W = weight at the base of wall. Includes weight of wall for gravity walls. Includes weight of the soil above footing for cantilever and counterfort walls

c = cohesion of the foundation soil

c_a = adhesion between concrete and soil

δ = angle of wall friction

P_p = passive resistance

LOCATION OF RESULTANT, R

Based on moments about toe (assuming P_p=0)

$$d = \frac{Wa + P_v g - P_h b}{W + P_v}$$

CRITERIA FOR ECCENTRICITY, e

$$e = d - \frac{B}{2} \; ; \; e \le B/6 \text{ for soils; } e \le B/4 \text{ for rocks}$$

FACTOR OF SAFETY AGAINST SLIDING

$$FS_s = \frac{(W + P_v)\tan \delta_b + c_a B}{P_h} \ge 1.5 \, (\min)$$

APPLIED STRESS AT BASE (q_{max}, q_{min}, q_{eq})

$$q_{max} = \frac{(W + P_v)}{B}\left(1 + \frac{6e}{B}\right)$$

$$q_{min} = \frac{(W + P_v)}{B}\left(1 - \frac{6e}{B}\right)$$

Equivalent uniform (Meyerhof) applied stress, q_{eq}, is given as follows:

$$q_{eq} = \frac{(W + P_v)}{B'} \text{ where } B' = B - 2e$$

Use uniform stress, q_{eq}, for soils and settlement analysis; use trapezoidal distribution with q_{max} and q_{min} for rocks and structural analysis

DEEP-SEATED (GLOBAL) STABILITY

Evaluate global stability using guidance in Chapter 6 (Slope Stability)

Figure 10-17. Design criteria for cast-in-place (CIP) Concrete retaining walls (after NAVFAC, 1986b).

Figure 10-18. CIP abutment with integral wingwalls

- Use the average of the at-rest and active earth pressures for CIP semi-gravity walls that are founded on rock or restrained from lateral movements, e.g., by the use of batter piles, and are less than 15 ft (5 m) in height.

- Use active earth pressures for CIP semi-gravity walls founded on rock or restrained from lateral movements that are greater than 15 ft (5 m) in height.

- Use the procedures described previously to compute pressure due to water and lateral earth pressures due to compaction and/or surcharges. Add these pressures to lateral earth pressure due to retained soil.

- Passive resistance in front of the wall should **not** be used in the analyses unless the wall extends well below the depth of frost penetration, scour or other types of disturbance such as a utility trench excavation in front of the wall. Development of the passive earth pressure in the soil in front of the wall requires a relatively large rotation or outward displacement of the wall; accordingly, the passive earth pressure

is neglected for walls with deep foundations and for other cases where the wall is restrained from rotation or displacement.

Figure 10-17 shows general loading diagrams for rigid gravity and semi-gravity walls. Loadings due to earth pressures behind the wall and for resultant vertical pressures at the base of the wall are shown.

If adequate drainage measures are provided, the hydrostatic pressure due to groundwater behind the wall generally need not be considered. However, hydrostatic pressure must be considered for portions of the wall below the level of the weep holes unless a deeper drainage system is provided behind the base of the wall. The wall must be designed for the full hydrostatic pressure when it is necessary to maintain the groundwater level behind the wall.

In addition to the lateral earth pressure, the wall must be designed for lateral pressure due to surcharge loads (see Section 10.4). For stability analyses of CIP gravity walls, the surcharge loads are generally assumed to be applied starting directly behind the top of the wall, unless specific conditions dictate otherwise. For CIP semi-gravity walls, the surcharge loads are generally assumed to be located behind the heel of the wall, and conservatively neglected within the width of the base slab since they contribute to overturning and sliding resistance. However, the surcharge loads within the width of the base slab are considered for the structural design of the wall stem.

10.5.4 Step 6 – Evaluate Bearing Capacity

10.5.4.1 Shallow Foundations

The computed vertical pressure at the base of the wall footing must be checked against the ultimate bearing capacity of the soil. The generalized distribution of the bearing pressure at the wall base is illustrated in Figure 10-17. Note that the bearing pressure at the toe is greater than that at the heel. The magnitude and distribution of these pressures are computed by using the applied loads shown in Figure 10-17. The equivalent uniform bearing pressure, q_{eq}, should be used for evaluating the factor of safety against bearing capacity failure. The procedures for determining the allowable bearing capacity of the foundation soils can be found in Chapter 8 (Spread Foundations) of this manual. Generally, a minimum factor of safety against bearing capacity failure of 3.0 is required for the spread footing foundation.

10.5.4.2 Deep Foundations

CIP walls founded on a deep foundation may be subject to potentially damaging ground and structural displacements at sites underlain by cohesive soils. Such damage may occur if the weight of the backfill material exceeds the bearing capacity of the cohesive subsoils causing plastic displacement of the ground beneath the retaining structure and heave of the ground surface in front of the wall. When the cohesive soil layer is located at or below the base of the wall, the factor of safety against this type of bearing capacity failure can be approximated by the following equation (Peck, *et al.*, 1974):

$$FS = \frac{5c}{(\gamma H + q)} \qquad 10\text{-}15$$

where H is the height of the fill, γ is the unit weight of fill, c is the shear strength of the cohesive soil and q is the uniform surcharge load.

The computed factor of safety should not be less than 2.0 for the embankment loading. Below this value progressive lateral movements of the retaining structure are likely to occur (Peck, *et al.*, 1974). As the factor of safety decreases, the rate of movement will increase until failure occurs at a factor of safety of unity. For CIP walls founded on vertical piles or drilled shafts, this progressive ground movement would be reflected by an outward displacement of the wall. CIP walls founded on battered piles typically experience an outward displacement of the wall base and a backward tilt of the wall face (Figure 10-19).

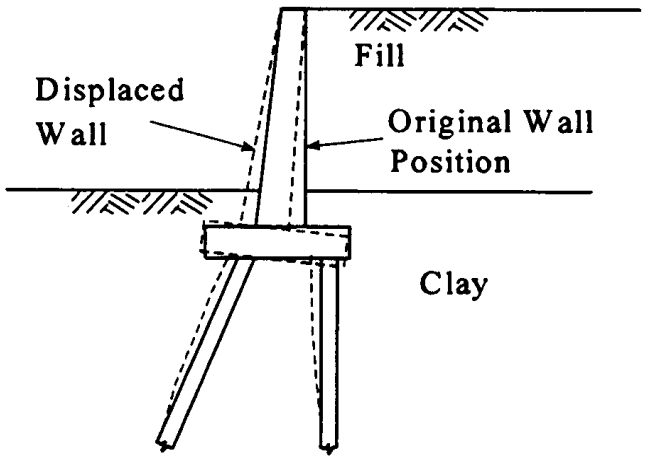

Figure 10-19. Typical Movement of pile-supported cast-in-place (CIP) wall with soft foundation.

10.5.5 Step 7 – Evaluate Overturning and Sliding

Figure 10-17 presents criteria for the design of CIP walls against sliding and eccentricity. The base dimensions of a CIP wall are determined by satisfying the following criteria:

- Sliding: FS ≥ 1.5

  Sliding resistance along the base of the wall is evaluated by using the same procedures as for spread footing design (Refer to Chapter 8.0). Note that any passive resistance provided by soil at the toe of the wall by embedment is ignored due to the potential for the soil to be removed through natural or manmade processes during the service life of the structure. Also, the live load surcharge is not considered as a stabilizing force over the heel of the wall when sliding resistance is being checked.

  If adequate sliding resistance cannot be achieved, design modifications may include: (1) increasing the width of the wall base; (2) using an inclined wall base or battering the wall to decrease the horizontal load; (3) incorporating deep foundation support; (4) constructing a shear key; and (5) embedding the wall base to a sufficient depth so that passive resistance can be relied upon.

  If the wall is supported by rock, granular soils or stiff clay, a key may be installed below the foundation to provide additional resistance to sliding. The method for calculating the contribution of the key to sliding resistance is shown in Figure 10-20.

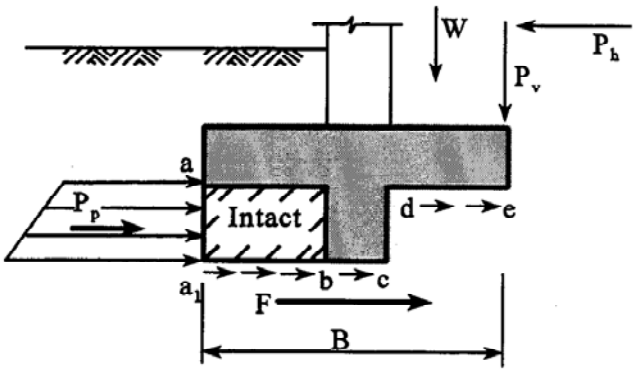

Cohesive Soils:

$$F = (W + P_v)\tan\delta_b + c_a(B - \overline{a_1 b}) + c(\overline{a_1 b}) + P_p$$

Granular Soils:

$$F = (W + P_v)\tan\delta_b + P_p$$

Factor of Safety $FS = F/P_h$

Note: See Figure 10-17 for list of symbol definitions.

Figure 10-20. Resistance against sliding from keyed foundation.

- Eccentricity, e, at base: $\leq$ B/6 in soil
  $\leq$ B/4 in rock

  The eccentricity criterion essentially requires that the safety factor of the wall against overturning is approximately of 2.0 for soils and 1.5 for rocks. If the eccentricity is not within the required limits then it implies inadequate resistance to overturning and consideration should be given to either increasing the width of the wall base or providing a deep foundation.

10.5.6 Step 8 – Evaluate Global Stability

Where retaining walls are underlain by inadequate foundation materials, the overall stability of the soil mass must be checked with respect to the most critical failure surface. As shown in Figure 10-21, both circular and non-circular slip surfaces must be considered. A minimum factor of safety of 1.5 is desirable. If global stability is found to be a problem, deep foundations or the use of lightweight backfill may be considered. Alternatively, measures can be taken to improve the shear strength of the weak soil stratum. Other wall types, such as an anchored soldier pile and lagging wall or tangent or secant pile wall, should also be considered in this case.

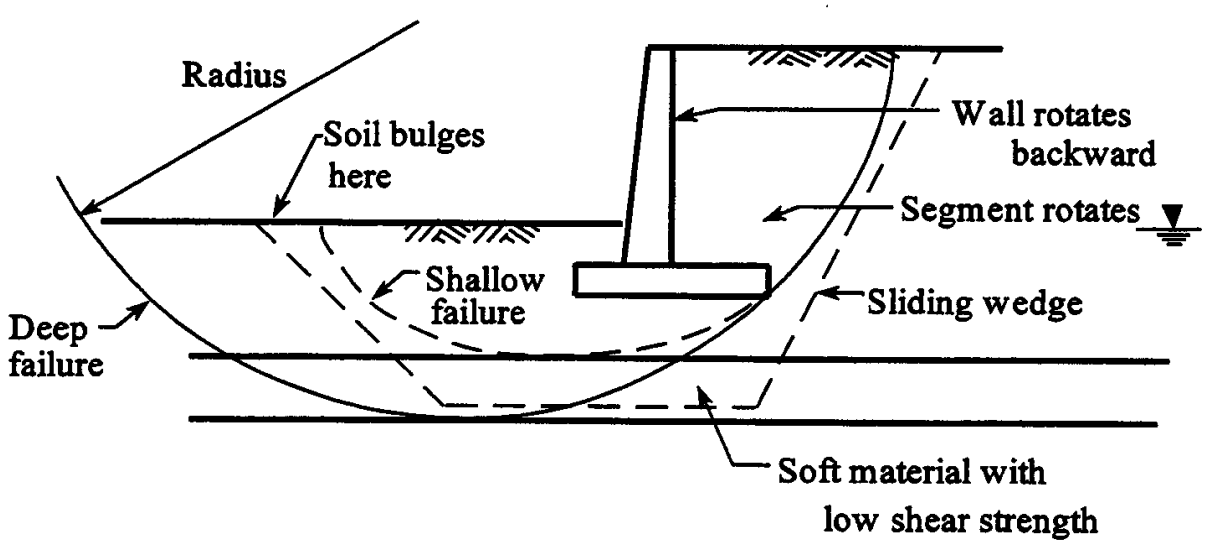

Figure 10-21. Typical modes of global stability (after Bowles, 1996)

10.5.7 Step 9 – Evaluate Settlement and Tilt

Foundation settlement can be computed by the methods discussed in Chapter 8 (Spread Foundations). CIP walls can generally accommodate a differential settlement of up to about 1/500 measured as the ratio of differential settlement of two points along the wall to the horizontal distance between the points. In general, tolerable total settlements of CIP walls are limited to 1 inch as a means to control differential settlement. If the computed settlement and tilt exceed acceptable limits, the wall dimensions can be modified to shift the resultant force closer to the center of the base and thereby reduce the load eccentricity and differential settlement. In some cases, use of lightweight backfill material may solve the problem. The use of deep foundations can also be considered.

Unless CIP walls are provided with a deep foundation, a small amount of wall tilting should be anticipated. It is therefore advisable to provide the face of the wall with a small inward batter to compensate for the forward tilting. Otherwise, a small amount of forward tilting may give the illusion that the wall is unstable.

In cases where the foundation materials are stiffer or firmer at the toe of the base than at the heel, the resulting settlement may cause the wall to rotate backwards towards the retained soil. Such wall movements could substantially increase the lateral pressures on the wall since the wall is now pushing against the soil i.e., generating a passive pressure condition. Such wall movements can be avoided by reproportioning the wall, supporting the wall on a deep foundation, or treating the foundation soils.

10.5.8 Step 10 – Design Wall Drainage Systems

Water can have detrimental effects on earth retaining structures. Subsurface water and surface water can cause damage during and/or after construction of the wall. Control of water is a key component of the design of earth retaining structures.

A subsurface drainage system serves to prevent the accumulation of destabilizing hydrostatic pressures, which may develop as a result of groundwater seepage and/or infiltration of surface water. Subsurface drainage is addressed in Section 10.5.8.1. There may be several soil zones behind an earth retaining structure. Groundwater flow from one zone to another, and then to a drain and outlet feature, should be unimpeded. If impeded, water will backup at the interface of the two adjacent zones thereby increasing hydrostatic pressures and decreasing the stability of the wall structure. Soil filtration and permeability requirements must be met between the two adjacent zones of different soils to prevent impeded flow. Soil

and geotextile filter design and water collection components are discussed in Section 10.5.8.2.

Surface water runoff can destabilize a structure under construction by inundating the backfill. Surface water can also destabilize a completed structure by erosion or by infiltrating into the backfill. Design for surface water runoff is discussed in Section 10.5.8.3.

In most cases, and especially for fill walls, it is preferable to provide backfill drainage rather than design the wall for the large hydrostatic water pressure resulting from a saturated backfill. Saturation of the backfill may result from either a high static water table, from direct and/or indirect rainfall infiltrations, or from other wetting conditions, e.g., ruptured water lines, etc.

10.5.8.1 Subsurface Drainage

Potential sources of subsurface water are surface water infiltration and groundwater as illustrated in Figure 10-22. Groundwater present at an elevation above the base of the wall may have flowed into the backfill from an excavation backcut. Ground water may also be present beneath the bottom of the wall. A groundwater surface beneath a wall may rise into the structure, depending on the hydrogeology of the site. Surface water may infiltrate into the wall backfill from above, or from the front face of the wall for the case of flowing water in front of the structure (after Collin, *et al.*, 2002).

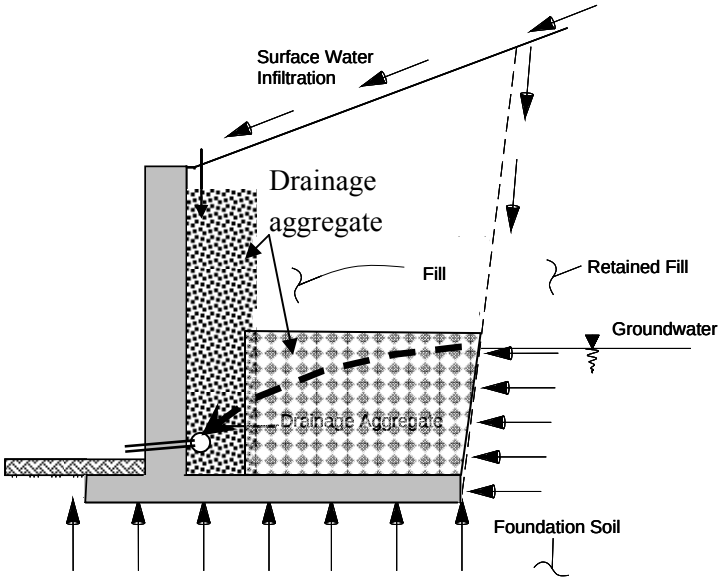

Figure 10-22. Potential sources of subsurface water.

Drainage system design depends on wall type, backfill and/or retained soil type, and groundwater conditions. Drainage system components such as granular soils, prefabricated drainage elements and filters, are usually sized and selected based on local experience, site geometry, and estimated flows, although detailed design is only occasionally performed. Drainage systems may be omitted if the wall is designed to resist full water pressure.

Drainage measures for fill wall systems, such as CIP walls, and cut wall systems typically consist of the use of a free-draining material at the back face of the wall, with "weep holes" and/or longitudinal collector drains along the back face as shown in Figure 10-23. The collector drains may be perforated pipes or gravel drains. This minimum amount of drainage should be sufficient if the wall backfill is relatively free-draining and allows the entire backfill to serve as a drain. It may be costly to fully backfill with free-draining or relatively free-draining material for some project applications therefore, it may be necessary to construct other types of drainage systems.

Fill wall drains may be placed (1) immediately behind the concrete facing or wall stem; (2) between wall backfill and embankment fill; (3) along a backcut; and (4) as a blanket drain beneath the wall. Examples of drains behind a wall stem are shown in Figure 10-24. The drainage system shown in the figure primarily serves to collect surface water that has infiltrated immediately behind the wall and transport it to an outlet. The system may also serve to drain the wall backfill, if the backfill soil is relatively free-draining.

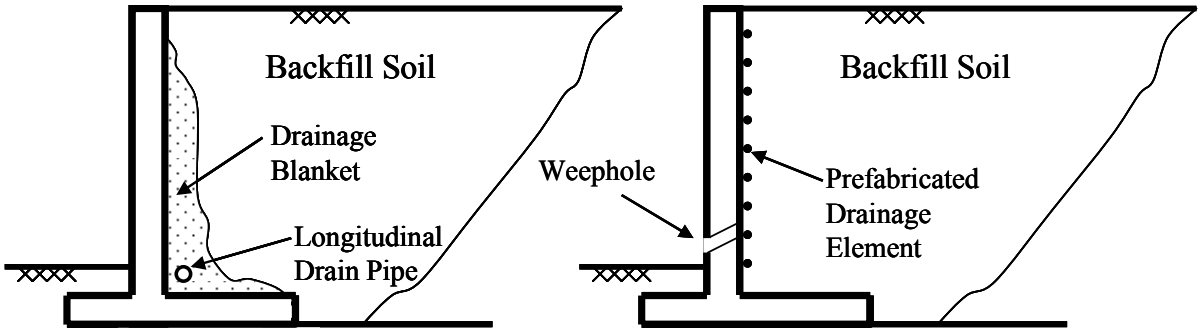

Figure 10-23. Typical retaining wall drainage alternatives.

A drain behind the wall backfill should be used when the backfill is not relatively free-draining. Such a drain may be located as noted in (2) or (3) above, and as illustrated in Figure 10-24. A granular blanket drain with collection pipes and outlets should be used beneath fill wall structures where a high or seasonally high groundwater table exists.

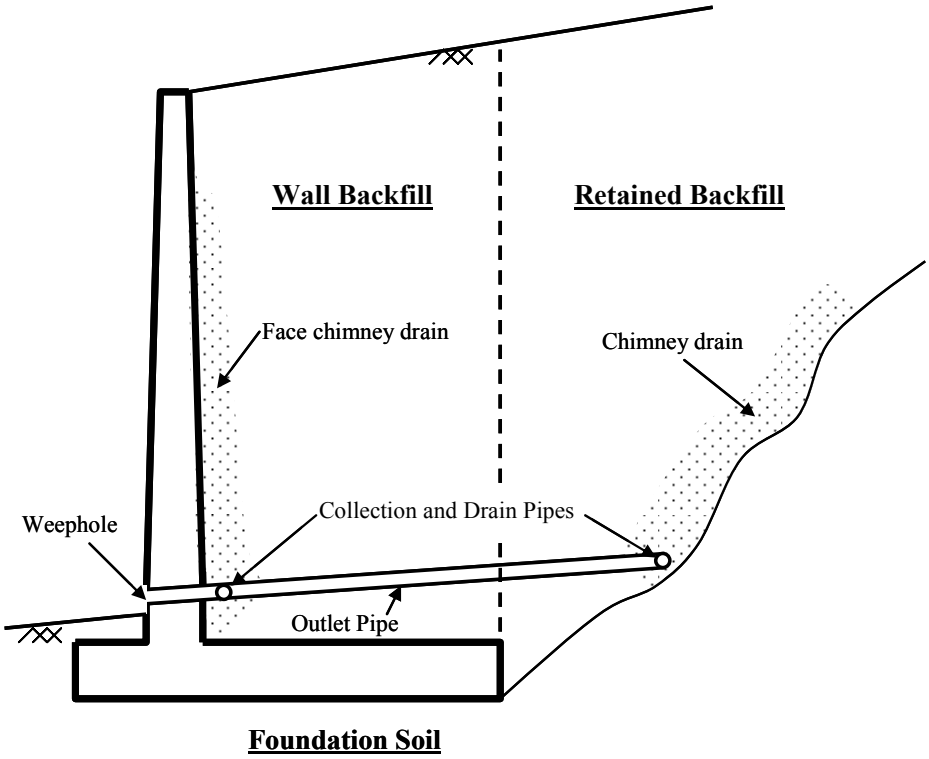

Figure 10-24. Drains behind backfill in cantilever wall in a cut situation.

10.5.8.2 Drainage System Components

Drainage systems for fill walls may include:

- column(s) or zone(s) of free-draining gravel or coarse sand to collect water seepage from the backfill;
- perforated pipe(s) to collect water in the granular column(s) or zone(s);
- conveyance piping;
- outlet(s); and
- filter(s) between backfill soil(s) and granular column(s) or zone(s).

Longitudinal pipes transport collected water to outlet pipes that discharge at appropriate points in front of and/or below the wall. Outlets may be via weep holes through the wall facing that discharge in front of the structure to grade; via conveyance piping to storm sewers as is common in urban applications, or via conveyance piping to a slope beneath the wall structure. Weep holes generally consist of 1½ - 3 in (40 - 75 mm) diameter holes that extend through the wall facing and are closely spaced horizontally along the wall, typically less than 10 ft (3 m) apart. If weep holes are used with a counterfort wall, at least one weep hole

should be located between counterforts. A screen and/or filter are used to prevent soil piping through a weep hole.

The collection and conveyance pipes need to be large enough and sufficiently sloped to effectively drain water by gravity flow from behind the wall while maintaining sufficient pipe flow velocity to prevent sediment buildup in the pipe. Use of 3 to 4 in (75 to 100 mm) diameter pipes is typical and practical. The diameter is usually much greater than that required for theoretical flow capacity. Procedures for the design of pipe perforations, such as holes or slots, is provided in Section 5.2 of Cedergren (1989). Pipe outlets to slope areas beneath wall structures should be detailed similar to pavement drain outlets. If the outlet is to a grass area, it should have a concrete apron, a vertical post marking its location (for maintenance), and a screen to prevent animal ingress.

Filters are required for water flowing between zones of different soils. A filter must prevent piping of the retained soil while providing sufficient permeability for unimpeded flow. The filter may be a soil or a geotextile. A geotextile is not required if the two adjacent soils meet certain soil filtration criteria. An open-graded aggregate will generally not allow the development of a soil filter at its interface with the backfill soil. In this case a geotextile filter will be required.

Geocomposite drains may be used in lieu of clean gravel or coarse sand and a geotextile. A geocomposite, or prefabricated, drain consists of a geotextile filter and a water collection and conveyance core. The cores convey the water and are generally made of plastic waffles, three-dimensional meshes or mats, extruded and fluted plastic sheets, or nets. A wide variety of geocomposites are readily available. However, the filtration and flow properties, detailing requirements, and installation recommendations vary and may be poorly defined for some products.

The flow capacity of geocomposite drains can be determined by using the procedures described in ASTM D 4716. Long-term compressive stresses and eccentric loadings on the geocomposite core should be considered during design and selection. The geotextile of the geocomposite should be designed to meet filter and permeability requirements.

Installation details, such as joining adjacent sections of the geocomposite and connections to outlets, are usually product-specific. Product-specific variances should be considered and addressed in the design, specification, detailing and construction phases of a project. Post installation examination of the drainage core/path with a camera scope should be considered for critical applications.

10.5.8.3 Surface Water Runoff

Surface drainage is an important aspect of ensuring wall performance and must be addressed during design. Appropriate measures to prevent surface water from infiltrating into the wall backfill should be included in the design of all earth retaining structures.

During construction of a fill wall, the backfill surface should be graded away from the wall face at the end of each day of construction to prevent water from ponding behind the wall and saturating the soil. Surface water running onto a partially completed backfill can carry fine-grained soils into the backfill work area and locally contaminate a free-draining granular backfill with fines. If a fine-grained soil is being utilized for the backfill, saturation can cause movements of the partially constructed wall facing.

Finish grading at the top of a wall structure should provide positive drainage away from the wall, when possible, to prevent or minimize infiltration of surface water into the backfill. If the area above the wall is paved, a curb and gutter is typically used to direct the flow away from the wall. Concrete-, asphalt- or vegetation-lined drainage swales may be used where a vegetated finished grade slopes to the wall. Water runoff over the top of a wall where the backfill slopes towards it can lead to erosion and undercutting of the wall and can cause staining of the wall face as soil is carried with the water. Construction of a collection swale close to the wall will help to prevent runoff from going over the top of the wall. Runoff flow will concentrate at grading low points behind the face. Ponding of runoff behind the wall leads to undesirable infiltration of water into the backfill.

Collection and conveyance swales should prevent overtopping of the wall for the design storm event. Extreme events (e.g., heavy rainfalls of short duration) have been known to cause substantial damage to earth retaining structures due to erosion and undercutting, flooding, and/or increased hydrostatic pressures both during and after construction. This is particularly true for sites where surface drainage flows toward the wall structure and where finer-grained backfills are used.

Site drainage features are designed for an assumed or prescribed design storm event, such as, the 25 year storm event. However, extreme events can occur that result in short duration flows, e.g., 1 to 3 hours, that significantly exceed the design capacity of the stormwater management system. When such events occur, site flooding can cause overtopping of the wall, erosion and undercutting, and an increase in hydrostatic forces within and behind the reinforced soil mass.

If surface water flows toward an earth retaining structure, the water is likely to be picked up in a gutter or other collection feature. Such features are often sized based upon the design storm event. The site layout and wall structure should include features for handling flows greater than the design event as is typically done in the design of an overflow spillway for a dam. The wall designer should address potential excess flows and coordinate work with other project designers. Consideration should be given to incorporating details of overflow features, such as a spillway, into the wall design for sites where surface water flows towards the wall structure.

10.6 EXTERNAL STABILITY ANALYSIS OF A CIP CANTILEVER WALL

The following example problem is used to illustrate the procedure for performing an external stability analysis of a CIP cantilever retaining wall.

Example 10-3.

Analyze the CIP cantilever wall shown below for factors of safety against sliding, overturning and bearing capacity failure. The backfill and foundation soils consist of clean, fine to medium sand, and the groundwater table is well below the base of the wall.

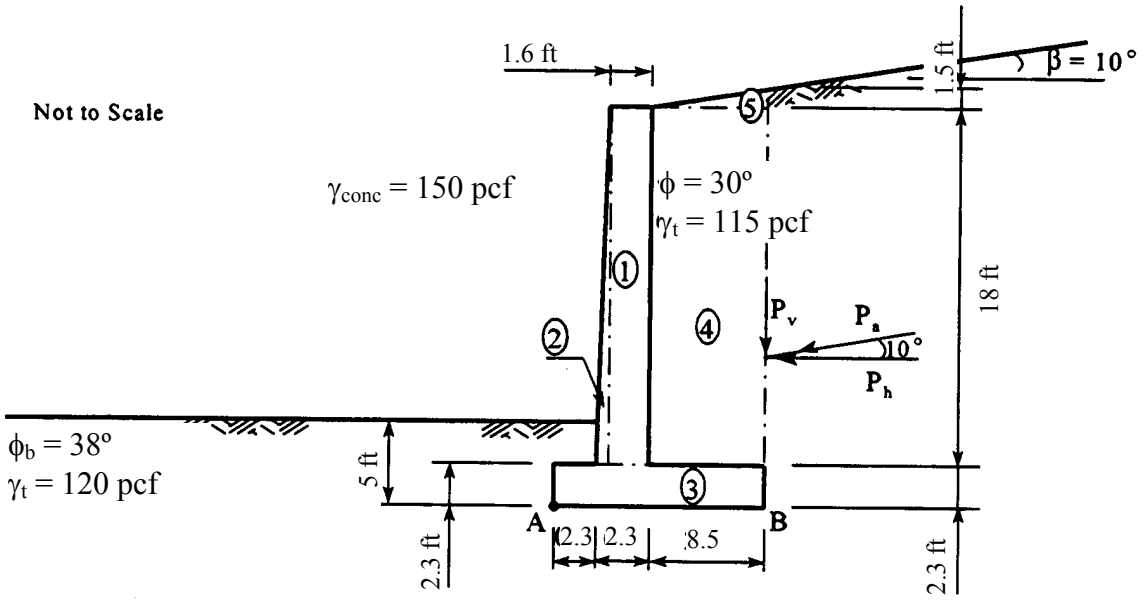

Geometry and parameters for example problem.

Solution

Step 1*:* Determine the total height of soil exerting pressure.

H = thickness of base slab + height of stem + (width of heel slab) tan (backslope angle)

H = 2.3 ft + 18 ft + 8.5 ft (tan 10^o)

= 21.8 ft

Step 2*:* Compute the coefficient of active earth pressure by using the equation of K_a in Figure 10-5 for a vertical backface (θ=0).

$$K_a = \frac{\cos^2 \phi}{\cos\delta\left[1+\sqrt{\frac{\sin(\phi+\delta)\sin(\phi-\beta)}{\cos\delta\cos(-\beta)}}\right]^2}$$

where:

ϕ = internal friction angle of soil = 30^o

β= angle of backfill slope = 10^o

δ= angle of wall friction = β = 10^o

For the example problem:

$$K_a = \frac{\cos^2 30°}{\cos 10°\left[1+\sqrt{\frac{\sin(30°+10°)\sin(30°-10°)}{\cos 10°\cos(-10°)}}\right]^2}$$

$$K_a = 0.35$$

Step 3. Compute the magnitude of the resultant of active pressure, P_a, per foot of wall into the plane of the paper.

$$P_a = \frac{1}{2} K_a \gamma H^2$$

$$= \frac{1}{2}(0.35)(115\,\text{pcf})(21.8\,\text{ft})^2 = 9{,}564.2\,\text{lb/ft}$$

Step 4. Resolve P_a into horizontal and vertical components:

P_h = $P_a \cos \beta$ = (9,564.2 lb/ft) cos 10^o = 9,418.9 lb/ft

P_v = $P_a \sin \beta$ = (9,564.2 lb/ft) sin 10^o = 1,660.8 lb/ft

Moment arm of P_h about point A = (2.3 ft + 18 ft + 1.5 ft)/3 = 21.8/3 = 7.27 ft = b

Moment arm of P_v about point A = 2.3 ft + 2.3 ft + 8.5 ft = 13.1 ft = g

Step 5: Determine weights and sum moments about the toe of the wall (point A).

The weights of various areas and the moments due to the weights shown in the geometry of the example problem are set out in the following table. The unit weight of concrete is assumed to be 150 pcf and the weight of the soil above the footing toe is neglected.

Area	Weight, lb/ft		Moment arm about A, ft		Moment about A, lb.ft/ft	
1	(1.6 ft) (18 ft) (150 pcf)	= 4,320	2.3 ft+0.7 ft+(1.6/2) ft	= 3.80	(4,320 lb) (3.80 ft)	= 16,416.0
2	(0.5) (0.7 ft) (18 ft) (150 pcf)	= 945	2.3 ft+ (2/3) (0.7) ft	= 2.77	(945 lb) (2.77 ft)	= 2,617.7
3	(13.1 ft) (2.3 ft) (150 pcf)	= 4,519.5	13.1/2 ft	= 6.55	(4,519.5 lb) (6.55 ft)	= 29,602.7
4	(8.5 ft) (18 ft) (115 pcf)	= 17,595	2.3 ft+ 2.3 ft+(8.5/2) ft	= 8.85	(17,595 lb) (8.85 ft)	= 155,715.8
5	(0.5) (8.5 ft) (1.5 ft) (115 pcf)	= 733.1	2.3 ft+2.3 ft+(2/3)(8.5) ft	= 10.27	(733.1lb) (10.27 ft)	= 7,528.9
Total	**W = 28,112.6**				**M_w = 211,881.1**	

Step 6*:* Check factor of safety against sliding; neglect passive resistance of embedment depth soil (Refer to Figure 10-20)

$$FS_s = \frac{(W + P_V)\tan\delta_b}{P_h}$$

where:

W = weight of concrete and soil on the base of the wall footing AB

δ_b = friction angle between concrete base and foundation soil

Use $\delta_b = (3/4)\ \phi_b = (3/4)\ (38^o) = 28.5^o$, for friction angle between concrete and clean, fine to medium sand (see NAVFAC, 1986b). This value of δ_b is within the range of values listed in Table 10-1 for clean fine to medium sand.

$$FS_s = \frac{(28{,}112.6\,\text{lb/ft} + 1{,}660.8\,\text{lb/ft})\tan 28.5^\circ}{9{,}418.9\,\text{lb/ft}} = \frac{16{,}165.6\,\text{lb/ft}}{9{,}418.9\,\text{lb/ft}} = 1.72 \qquad \textbf{O.K.}$$

Step 7*:* Check the limiting eccentricity and factor of safety against bearing failure.

(1) Compute the location of resultant at distance d from point A.

$$d = \frac{\sum M_R - \sum M_0}{\sum V}$$

$$d = \frac{M_W - P_h b + P_v g}{W + P_V}$$

$$d = \frac{21{,}1881.1\,\text{lb.ft/ft} + (1{,}660.8\,\text{lb/ft})(13.1\,\text{ft}) - (9{,}418.9\,\text{lb/ft})(7.27\text{ft})}{28{,}112.6\,\text{lb/ft} + 1{,}660.8\,\text{lb/ft}}$$

where: $W + P_V = \Sigma V$

$$d = \frac{16{,}5162.2 \text{ lb.ft/ft}}{29{,}773.4 \text{ lb/ft}} = 5.55 \text{ ft}$$

(2) Compute the eccentricity of the load about the center of base.

$$e = \frac{B}{2} - d = \frac{13.1 \text{ ft}}{2} - 5.55 \text{ ft} = 1.0 \text{ ft}$$

$$e = 1.0 \text{ft} < \frac{B}{6} = \frac{13.1 \text{ ft}}{6} = 2.18 \text{ ft} \quad \text{O.K.}$$

(3) Compute the maximum and minimum pressures under the wall footing.

$$q_{max,min} = \frac{\sum V}{B}\left(1 \pm \frac{6e}{B}\right)$$

$$= \frac{29{,}773.4 \text{ lb/ft}}{13.1 \text{ ft}}\left(1 \pm \frac{6(1.0 \text{ ft})}{13.1 \text{ ft}}\right)$$

$$= 2{,}272.7 \text{ psf (1.46 or 0.54)}$$

i.e., $q_{max} = 3{,}318.1 \text{ psf}$

$q_{min} = 1{,}227.3 \text{ psf}$

(4) Estimate ultimate bearing capacity.

Use the procedures presented in Chapter 8 (Shallow Foundations). Assume that for a footing with eccentric and inclined loading the ultimate bearing capacity computed by the geotechnical specialist is:

q_{ult} =20,000 psf

(5) Check factor of safety against bearing capacity failure.

$$FS_{bc} = \frac{q_{ult}}{q_{max}} = \frac{20{,}000 \text{ psf}}{3{,}318.1 \text{ psf}} = 6.03 > 3.0 \quad \text{O.K.}$$

SUMMARY

Factor of safety against sliding	FS_s	= 1.72
Eccentricity	e	= 1.0 ft < B/6
Factor of safety against bearing failure	FS_{bc}	= 6.03

In addition, the factor of safety against global failure and wall settlement including tilting and lateral squeeze should be evaluated to complete the analysis.

10.7 CONSTRUCTION INSPECTION

FHWA (2005b) discusses construction considerations for many of the walls presented in Figure 10-3. Construction considerations for CIP walls only are presented in this manual. In general, the construction inspection requirements for CIP walls are similar to those for other concrete structures. In some cases, state agencies may have inspector checklists for this type of construction. Table 10-4 provides a summary of typical construction inspection requirements for CIP retaining walls.

Table 10-4
Inspector responsibilities for a typical CIP gravity and semi-gravity wall project

CONTRACTOR SET UP
Review plans and specifications
Review the contractor's schedule
Review test results and certifications for preapproved materials, e.g., cement, coarse and fine aggregate.
Confirm that the contractor's stockpile and staging area are consistent with locations shown on the plans
Discuss anticipated ground conditions and potential problems with the contractor
Review the contractor's survey results against the plans
EXCAVATION
Verify that excavation slopes and/or structural excavation support is consistent with the plans
Confirm that limits of any required excavations are within right-of-way limits shown on plans
Confirm that all unsuitable materials, e.g., sod, snow, frost, topsoil, soft/muddy soil are removed to the limits and depths shown on the plans and that the excavation is backfilled with granular material and properly compacted
Confirm that leveling and proof-rolling of the foundation area is consistent with requirements of the specifications
Confirm that the contractor's excavation operations do not result in significant water ponding
Confirm that existing drainage features, utilities, and other features are protected
Identify areas not shown on the plans where unsuitable material exists and notify the engineer

FOOTING
Approve condition of footing foundation soil/rock before concrete is poured
Confirm reinforcement strength, size, and type consistent with the specifications
Confirm the consistency of the contractor's outline of the footing (footing size and bottom of footing depth) with the plans
Confirm the location and spacing of reinforcing steel consistent with the plans
Confirm water/cement ratio and concrete mix design consistent with the specifications
Record concrete volumes poured for the footing
Confirm appropriate concrete curing times and methods as provided in the specifications
Confirm that concrete is not placed on ice, snow, or otherwise unsuitable ground
Confirm that concrete is being placed in continuous horizontal layers and that the time between successive layers is consistent with the specifications
STEM
Confirm the placement of weep hole inserts (number, elevation, and specific locations) with the plans if weep holes are used,
Confirm that concrete is poured in section lengths consistent with the specifications
Record concrete volumes used to form the stem
Confirm that all wall face depressions, air pockets, gaps, rough spots, etc. are repaired
Confirm that storage of reinforcing bars is consistent with the specifications, e.g.-use of platform or supports.
Perform preliminary check of condition of epoxy-coated reinforcing bars
Confirm that forms are clean and appropriately braced during concrete pour operations
Confirm that all reinforcing bars are held securely in place and are being rigidly supported at the face of forms and in the bottom of wall footings
Confirm that construction joints are being made only at locations shown on the plans or otherwise at locations approved by the engineer
DRAINAGE SYSTEMS AND BACKFILL
Confirm that installation of the drainage system is consistent with the specifications and plans
Confirm that the backfill material being used is approved by the engineer
Confirm that placement of the backfill is performed in lifts consistent with the specifications
Confirm that minimum concrete strength is achieved before backfill is placed and compacted against back of wall
Confirm that the backfill placement method used by the contractor does not cause damage to prefabricated drainage material or drain pipes
Confirm that earth cover over drainage pipes is sufficient to prevent damage from heavy equipment. The minimum cover based on ground pressure from equipment should be provided in the specifications.
Perform required backfill density tests at the frequencies specified, especially for areas that are compacted with lightweight equipment, e.g., areas just behind the wall.
Check that the drainage backfill just behind weep holes is the correct gradation and that it is properly installed
POST INSTALLATION
Verify pay quantities

Note: Throughout the project, check submittals for completeness before transmitting them to the engineer.

[THIS PAGE INTENTIONALLY BLANK]

CHAPTER 11.0
GEOTECHNICAL REPORTS

Upon completion of the subsurface exploration and laboratory testing program, the geotechnical specialist will compile, evaluate, and interpret the data and perform engineering analyses for the design of foundations, cut slopes, embankments, and other required facilities. Additionally, the geotechnical specialist will be responsible for producing a report that presents the subsurface information obtained from the site investigations and provides specific design and construction recommendations. The geotechnical analyses and design procedures to be implemented for the various types of highway facilities are addressed in various other FHWA publications. This chapter provides guidelines and recommendations for developing a geotechnical report.

11.01 Primary References

FHWA (1988). *Checklist and Guidelines for Review of Geotechnical Reports and Preliminary Plans and Specifications.* Report No. FHWA ED-88-053, Federal Highway Administration, U.S. Department of Transportation, Revised 2003.

Geotechnical Engineering Notebook. *FHWA Geotechnical Guidelines GT1–GT16.* http://www.fhwa.dot.gov/engineering/geotech/index.cfm.

11.1 TYPES OF REPORTS

Generally, one or more of three types of reports will be prepared: A geotechnical investigation report; a geotechnical design report and/ or a geoenvironmental report. Several disciplines within an agency may contribute to the development of the geotechnical report. The preparer and the choice of the report depends on the requirements of the highway agency (owner) and the agreement between the geotechnical specialist and the facility designer. The need for multiple types of reports on a single project depends on the project size, phasing and complexity. Regardless, all the typical sections of a report outlined herein must be included. All consultant produced work should be in conformance with the reporting guidelines for the agency.

11.1.1 Geotechnical Investigation Reports

Geotechnical investigation reports present site-specific data and have three major components:

1. **Background Information**: The initial sections of the report summarize the geotechnical specialist's understanding of the facility for which the report is being prepared and the purposes of the subsurface exploration. This section includes information on loads, deformations and additional performance requirements. This section also presents a general description of site conditions, geology and geologic features, drainage, ground cover and accessibility, and any peculiarities of the site that may affect the design and construction.

2. **Work Scope**: The second part of the investigation report documents the scope of the exploration program and the specific procedures used to perform this work. These sections identify the types of exploration methods used; the number, location and depths of borings, exploration pits and in-situ tests; the types and frequency of samples obtained; the dates of subsurface exploration; the subcontractors used to perform the work; the types and number of laboratory tests performed; the testing standards used; and any variations from conventional procedures.

3. **Data Presentation**: This portion of the report, generally contained in appendices with a complementary narrative of explanation, presents the data obtained from the field and laboratory exploration program. The appendices typically include final logs of all borings, exploration pits, and piezometer or well installations, water level readings, data plots from each in-situ bore hole, summary tables and individual data sheets for all laboratory tests performed, rock core photographs, geologic mapping data sheets and summary plots, subsurface profiles developed from the field and laboratory test data, as well as statistical summaries. The geotechnical investigation report often includes copies of existing information such as boring logs or laboratory test data from previous investigations at the project site.

The intent of a geotechnical investigation report is to document the investigation performed and present the data obtained. The report should include a summary of the subsurface and lab data. Interpretations and recommendations on the index and design properties of soil and rock should also be included. The geotechnical investigation report typically does not include detailed design analyses and recommendations, but it should include a narrative that summarizes and provides an interpretation of the subsurface data. The geotechnical

investigation report is sometimes used when the subsurface explorations are subcontracted to a geotechnical consultant, but the data interpretation and design tasks are performed by the owner's or the prime consultant's in-house geotechnical staff. An example Table of Contents for a geotechnical investigation report is presented in Figure 11-1.

11.1.2 Geotechnical Design Reports

A geotechnical design report typically provides an assessment of existing subsurface conditions at a project site, presents, describes and summarizes the procedures and findings of all geotechnical analyses performed, and provides appropriate recommendations for design and construction of foundations, earth retaining structures, embankments, cuts, and other required facilities. Unless a separate geotechnical investigation report was developed previously, the geotechnical design report will also include documentation of any subsurface explorations and laboratory investigations performed and a presentation of the results of those investigations as described in Section 11.1.1. An example Table of Contents for a geotechnical design report is presented in Figure 11-2.

Since the scope, site conditions, and design/construction requirements of each project are unique, the specific contents of a geotechnical design report must be tailored for each project. In order to develop this report, the author must possess detailed knowledge of the facility. In general, however, the geotechnical design report must address all the geotechnical issues that may be anticipated on a project. The report must identify each soil and rock unit of engineering significance, and must provide recommended design parameters for each of these units. To this end, all factual data must be synthesized and analyzed to justify the recommended index and design properties. Groundwater conditions are particularly important for both design and construction and, accordingly, they need to be carefully assessed and described. For every project, the subsurface conditions encountered in the site investigation need to be compared with the geologic setting in order to understand the nature of the deposits better and to predict the degree of variability between exploration locations.

Each geotechnical design issue must be addressed in accordance with the methodology described in the various chapters of this manual. The results of these studies need to be discussed concisely and clearly in the report. Of particular importance is an assessment of the impact of existing subsurface conditions on construction operations, phasing and timing. Properly addressing any construction issues in the report that are related to subsurface conditions can preclude change-of-conditions claims. Examples include but are not limited to:

Figure 11-1. Example Table of Contents for a Geotechnical Investigation Report.

Figure 11-2. Example Table of Contents for a Geotechnical Design Report.

- vertical and lateral limits for recommended excavation and replacement of any unsuitable shallow surface deposits such as peat, muck and top soil;

- excavation and cut requirements, i.e., safe slopes for open excavations or the need for sheeting or shoring;
- anticipated fluctuations of the groundwater table along with the consequences of a high groundwater table on excavations;

- effect of boulders on pile drivability or drilled shaft drilling, and rock hardness on rippability.

Recommendations should be provided for the solution of anticipated problems. The above issues are but a few of those that need to be addressed in a geotechnical design report. To aid engineers with a quantitative review of geotechnical reports, FHWA has prepared review checklists and technical guidelines (FHWA, 2003b). One of the primary purposes of the FHWA guidelines is to provide transportation agencies and consultants with minimum standards/criteria for the geotechnical information that FHWA recommends be included in geotechnical reports as well as plans and specification packages. Technical guidelines for "minimum" site investigation information common to all geotechnical reports for any type of geotechnical feature and basic information and recommendations for specific geotechnical features are provided in the checklists and technical guidelines (FHWA, 2003b). Checklists are presented in the form of a question and answer format for specific geotechnical features such as:

- centerline cuts and embankments;
- embankments over soft ground;
- landslide corrections;
- retaining walls;
- structural foundations such as spread footings, driven piles and drilled shafts;
- borrow material sites.

11.1.3 GeoEnvironmental Reports

When the subsurface exploration indicates the presence of contaminants at the project site, the geotechnical specialist may be requested to prepare a geoenvironmental report in which the findings of the investigation are presented and discussed, and recommendations made for the remediation of the site.

The preparation of such a report usually requires the geotechnical specialist to work with a team of experts, since many aspects of the contamination or the remediation may be beyond his/her expertise. A representative team preparing a geoenvironmental report may be composed of chemists, geologists, hydrogeologists, environmental scientists, toxicologists, air quality and regulatory experts, as well as one or more geotechnical specialists. The report should contain all of the components of the geotechnical investigation report, as discussed above. Additionally, the geoenvironmental report will have a clear and concise discussion of the nature and extent of contamination, the risk factors involved, if applicable, a contaminant transport model, and the source of the contamination , if known, e.g., landfill, industrial waste water line, broken sanitary sewer, above-ground or underground storage tanks, overturned truck or train derailment, etc.

The team may also be required to present solutions to remediate the site. Depending upon the nature and amount of contaminant and its location within the geologic profile and its potential impact on the environment, remediation measures may include removal of the contaminated material, pumping and treatment of the contaminated groundwater, installation of slurry cut-off walls, abandonment of that portion of the right-of-way, deep soil mixing, biorestoration, and electrokinetics. The geoenvironmental report should also address the regulatory issues pertinent to the specific contaminants found and the proposed site remediation methods.

11.2 DATA PRESENTATION

11.2.1 Boring Logs

Boring logs, rock coring, soundings, and exploration logging should be prepared in accordance with the procedures and formats discussed in Chapters 3 through 5. Test boring logs and exploration test pit records can be prepared by using software capable of storing, manipulating, and presenting geotechnical data in simple one-dimensional profiles, or alternatively two-dimensional graphs of the subsurface profiles, or three-dimensional representations. These and other similar software allow for the orderly storage of project data for future reference. The website: http://www.ggsd.com lists over 40 separate software packages available for the preparation of soil boring logs.

Many new software programs offer a menu-based boring log drafting program. The computer-aided drafting tools let users create custom boring log formats that can include graphic logs, monitoring well details, and data plots. Custom designed legends explaining

graphic symbols and containing additional notes can be added to boring logs for greater clarity. These legends can include a library of soil types, sampler and well symbols as well as other nomenclature used on the boring logs. Geological profiles can be generated by the program and may be annotated with text and drawings.

Similarly, the results of various in-situ tests performed by using cones, pressuremeters and vanes, can be presented by the use of available commercial software. Links to many geotechnical software programs may be found at: http://www.usucger.org

Alternatively, it is convenient for the in-situ test data to be reduced directly and simply by using a spreadsheet format such as EXCEL and QUATTRO PRO. In many ways, the spreadsheet is a superior approach as it allows the engineer to tailor the interpretations individually to account for specific geologic settings and local formations. The spreadsheet also permits creativity and uniqueness in the graphical presentation of the results, thereby enhancing the abilities and resources available to the geotechnical personnel. Since soils and rocks are complex materials with enumerable variants and facets, a site-specific tailoring of the interpreted profiles and properties is prudent.

11.2.2 Boring Location Plans

A boring location plan should be provided for reference on a regional or local scale. County or city street maps or USGS topographic quad maps are ideally suited for this purpose. Topographic information at 20 ft (6 m) contour line intervals is now downloadable from the internet (e.g., www.usgs.gov). Topographic maps for the entire United States can also be purchased from commercial suppliers.

The locations of all field tests, sampling, and exploratory studies should be shown clearly on a scaled plan of the specific site under investigation. Preferably, the plan should be a topographic map with well-delineated elevation contours and a properly-established benchmark. The direction of magnetic or true north should be shown. Figure 11-3 shows an example of a boring location plan. The fence baseline defines the line along which a vertical profile of subsurface conditions will be developed based on information from adjacent boring logs. If multiple types of exploratory methods are used, the legend on the site test location plan should clearly show the different types of soundings.

A geographic information system (GIS) can be utilized on the project to locate the test locations with reference to existing facilities on the premises including any and all underground and above-ground utilities, as well as roadways, culverts, buildings, or other

structures. Recent advances have been made in portable measuring devices that utilize global positioning systems (GPS) to permit quick, approximate determinations of coordinates of test locations and installations.

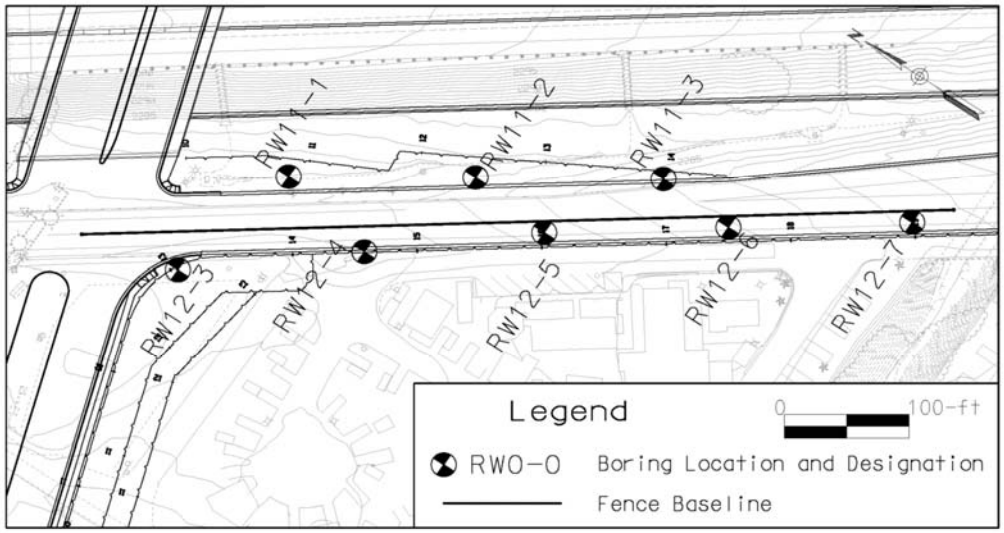

Figure 11-3. Example boring location plan for retaining walls RW-11 and RW-12 retaining an on-ramp to a freeway.

11.2.3 Subsurface Profiles

Geotechnical reports are normally accompanied by the presentation of subsurface profiles developed from the field and laboratory test data. Longitudinal profiles are typically developed along the roadway or bridge alignment, and a limited number of transverse profiles may be included for key locations such as at major bridge foundations, cut slopes or high embankments. Such profiles provide an effective means of summarizing pertinent subsurface information. The subsurface profiles, coupled with judgment and an understanding of the geologic setting, aid the geotechnical specialist in his/her interpretation of subsurface conditions between the investigation sites.

For the development of a two-dimensional subsurface profile, the profile baseline, typically the roadway centerline, needs to be defined on the boring location plan, and the relevant borings projected to this line. Figure 11-4 shows the subsurface profile along the "Fence Baseline" between retaining walls RW-11 and RW-12 shown in Figure 11-3. Judgment should be exercised in the selection of the borings since projection of the borings, even for short distances, may result in a misleading representation of the subsurface conditions in some situations. The subsurface profile should be presented at a scale appropriate to the depth and frequency of the borings and soundings and the overall length of the cross-section. An exaggerated scale of 1(V):10(H) or 1(V):20(H) is typically used.

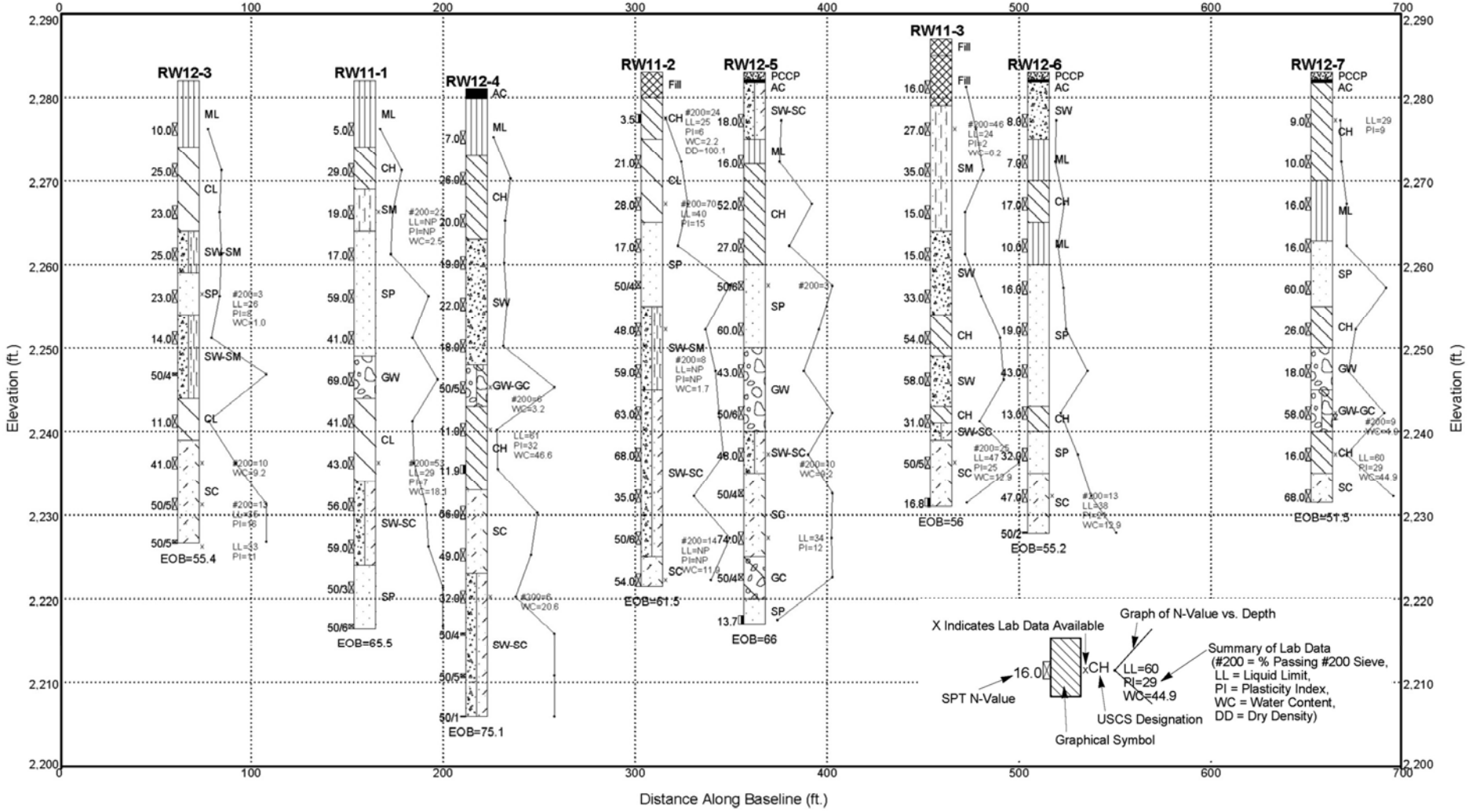

Figure 11-4. Subsurface profile along the baseline between retaining walls RW-11 and RW-12 shown in Figure 11-3.

The subsurface profile can be presented with reasonable accuracy and confidence at the locations of the borings. However, owners and designers generally expect the geotechnical specialist to present a continuous subsurface profile that shows an interpretation of the location, extent and nature of subsurface formations or deposits between borings. At a site where rock or soil profiles vary significantly between boring locations, the value of such presentations become questionable. The geotechnical specialist must be very cautious in presenting such data. Such presentations should include clear and simple caveats explaining that the profiles, as presented, cannot be relied upon fully to represent actual subsurface conditions between investigation locations. Should there be a need to provide more reliable continuous subsurface profiles, the geotechnical specialist should increase the frequency of borings and/or utilize geophysical methods to determine the continuity of subsurface conditions, or lack thereof.

11.3 TYPICAL SPECIAL CONTRACT NOTES

The geotechnical specialist should include in the geotechnical design report any special notes that should be placed in the contract plans or special provisions. The purpose of such special notes is to bring the contractor's and/or project engineer's attention to certain special requirements of the design or construction. Example special notes relating to pile driving, drilled shaft, and embankment construction are as follows:

1. "Difficult driving of piles may be encountered and mechanical equipment may be necessary to remove consolidated material or boulders from the location of piles. This may be accomplished by various types of earth augers, well drilling equipment, or other devices to remove the consolidated material to permit piles to be driven to the desired depth or rated resistance without damage."

2. "If any obstructions to pile driving are encountered ten (10) feet or less from the bottom of the footing, the contractor shall, if so ordered by the engineer, pull the partially driven pile or piles, remove the obstruction, and backfill the hole with approved suitable material, which shall be thoroughly compacted to the satisfaction of the engineer. However, no partially driven pile shall be removed until the engineer is satisfied that the contractor has made every effort to drive the pile through the obstruction. Payment for excavation will be made at the unit price bid for the structure excavation item and for the temporary sheeting under Item_____when sheeting is used. No other extra payment will be made for this work."

3. "The ordered length of pile shall be measured below the cut-off elevation shown on the plans. Any additional lengths of pile or splices above the cut-off elevation necessary to facilitate the contractor's operation shall be at his own expense."

4. "Piles for_____are driven because of possible future scour of the stream bed and shall be driven to the minimum lengths shown on the plans regardless of the resistance to driving. The actual driving resistance is estimated to be____tons."

5. "Piles will be acceptable only when driven to pile driving criteria established by the Chief Bridge Engineer. Prerequisite to establishing these criteria, the contractor shall submit, to the Chief Bridge Engineer, and others as required, Form_____'Pile and Driving Equipment Data'. All information listed on Form _____shall be provided within fourteen (14) days after the award of the contract. Each separate combination of pile and pile driving equipment proposed by the contractor will require the submission of a corresponding Form_____."

6. "Piles for the existing structure shall be removed where they interfere with the pile driving for the new structure."

7. "It shall be the contractor's responsibility to place the cofferdams for_____so that they will not interfere with the driving of batter piles. Pay lines for the cofferdams shall be as shown on the plans."

8. "The general subsurface conditions at the site of this structure are as shown on Drawing No._____."

9. "Pile driving will not be allowed at the abutments until fill settlement is complete. Estimated settlement time is_____months after placement of the_____ foot surcharge."

10. "The bottom of all drilled shafts shall be cleaned with a mechanical cleanout bucket before the concrete is placed in the shaft. A minimum of _____ passes of the cleanout bucket is recommended. For dry shafts, the bottom of the shaft shall be cleaned such that no more than _____ inches of excavated spoil and no more than xxxxx inches of water remain at the bottom of the shaft prior to concreting. If wet (slurry) construction processes are used, then the sand content prior to concreting shall not be greater than _____ % by volume. In the event that wet (slurry) construction processes are used, the Engineer shall be contacted for further criteria."

11. “Temporary surface casing is recommended to aid in alignment of drilled shafts as well as to prevent surface sloughing or raveling and to ensure personnel safety. A minimum _____ ft long temporary surface casing with at least _____ ft stick-up above the ground surface is recommended. The diameter of the surface casing shall not be more than be _____ inches larger than the nominal diameter of the shaft.

12. “Poorly graded sands and gravels were encountered during the design stage investigations. These soils are prone to caving and may cause large fluid losses during slurry-assisted drilled shaft construction. Therefore, localized caving should be anticipated during drilled shaft construction. These local caving zones may be up to _____ ft thick and can occur at various depths.”

13. "The contractor shall coordinate the project construction schedule to allow installation of embankment monitoring instrumentation by the Agency forces." "Instrumentation damaged by the contractor’s personnel shall be repaired or replaced at the contractor's expense. All construction activity in the area of any damaged instrument shall cease until the damage has been corrected."

14. "The contractor's attention is directed to the soil sample gradation test results, which are shown on Drawing No._____. Soil sample gradation test results have been furnished to assist the contractor in determining dewatering procedures, if necessary."

15. "The actual soil resistance to be overcome to reach estimated pile tip elevation is as shown below for each abutment and pier. The contractor shall size his pile driving equipment to install piles to the estimated length without damage."

16. "The south embankment shall be constructed to final grade and a month waiting period observed before pile driving begins. The actual length of the waiting period may be reduced by the Engineer based on an analysis of settlement platform and piezometer data."

11.4 SUBSURFACE INFORMATION MADE AVAILABLE TO BIDDERS

The finished boring logs and/or generalized soil profile should be made available to bidders and included with the contract plans. Other subsurface information, such as soil and rock samples and results of field and laboratory testing, should also be made available for inspection by bidders. The invitation for bids should indicate the type of information available and when and where it may be inspected. The highway agency should have a system for documenting what information each contractor inspects. Such documentation can be of major importance in the event of later claim actions.

The information developed during the subsurface exploration is very useful in the selection of effective construction procedures and for estimating construction costs. Such information is, therefore, of value to knowledgeable contractors bidding on the project. There has been much disagreement among owners and engineers as to what information should be made available to bidders, and how. The legal aspects are conflicting. In general, the owner's best interests are served by releasing pertinent information prior to the bid. Indeed, some courts have opined that failure to reveal information can weaken the owner's position in the event of dispute. On the other hand, some engineers are fearful that the release of information will imply guarantees on their part that the information is fully representative of the actual conditions that will be encountered.

One of the best surveys of the problem was prepared by Standing Subcommittee No. 4 of the U.S. National Committee on Tunneling Technology. The Subcommittee was composed of engineers and attorneys having experience dealing with owners, engineering firms, and contracting organizations.

The following is excerpted from their recommendations:

> "In sum, all subsurface data obtained for a project, professional interpretations thereof, and the design considerations based on these data and interpretations should be included in the bidding documents or otherwise made readily available to prospective contractors. Fact and opinion should be clearly separated.
>
> The bidder should be entitled to rely on the basic subsurface data, with no obligation to conduct his own subsurface survey.

It is considered, however, that specific disclaimers of responsibility for accuracy are appropriate, with respect to the following categories:

- Information obtained by others, perhaps at other times and for other purposes, which is being furnished prospective bidders in order to comply with the legal obligation to make full disclosure of all available data.

- Interpretations and opinions drawn from basic subsurface data, because equally competent professionals may reasonably draw different interpretations from the same basic data."

Additional information on this topic is included in *Geotechnical Guideline No. 15 – Geotechnical Differing Site Conditions* of FHWA's Geotechnical Engineering Notebook.

11.5 LIMITATIONS (DISCLAIMERS)

Soil and rock exploration and testing have inherent uncertainties. Thus users of the data who are unfamiliar with the variability of natural and manmade deposits should be informed in the report of the limitations inherent in the extrapolation of the limited subsurface information obtained from the site investigation. This notification often takes the form of "Disclaimer" clauses. The validity that courts give disclaimer clauses varies from state to state. However, the courts generally give much more validity to "specific" versus "general" disclaimer clauses. "General" disclaimer clauses are the types that say, in effect - subsurface information was gathered for use in design. However, the contractor should not rely on this information in preparing his bid. It is no big surprise, therefore, that judges give little validity to such general disclaimer clauses since common sense dictates that if the subsurface information is good enough to base the design on, then the contractor should be able to place some reliance on the information in preparing his bid. Dr. Ralph Peck, a noted geotechnical specialist, put it succinctly when asked his opinion concerning general disclaimer of subsurface information on a recent large Interstate project. He stated, "If the state or engineers it has engaged to develop the contract documents have accepted certain information as the basis for those documents, that information should not be disclaimed."

As mentioned previously, the courts have generally upheld the use of "specific" disclaimer clauses. The use of specific disclaimer clauses is strongly recommended over the use of general disclaimer clauses. An example of a specific disclaimer would be a statement such

as – “the boring logs are representative of the conditions at the location where the boring was made but conditions may vary between borings.”

The following are examples of good "specific" disclaimer clauses used by one highway agency. These disclaimer clauses are placed on the interpreted soil profile that is included in the contract plans:

General Notes

1. The explorations were made between ____and _____ by _____.

2. General soil and rock (where encountered) strata descriptions and indicated boundaries are based on an engineering interpretation of all available subsurface information by the *Agency Name* and may not necessarily reflect the actual variation in subsurface conditions between borings and samples. Data and field interpretation of conditions encountered in individual borings are shown on the subsurface exploration logs.

3. The observed water levels and/or conditions indicated on the subsurface profiles are as recorded at the time of exploration. These water levels and/or conditions may vary considerably, with time, according to the prevailing climate, rainfall or other factors and are otherwise dependent on the duration of and methods used in the explorations program.

4. Sound engineering judgment was exercised in preparing the subsurface information presented hereon. This information was prepared and is intended for State design and estimate purposes. Its presentation on the plans or elsewhere is for the purpose of providing intended users with access to the same information available to the State. This interpretation of subsurface information is presented in good faith and is not intended as a substitute for personal investigation, independent interpretations or judgment of the contractor.

5. All structural details shown hereon are for illustrative purposes only and may not be indicative of the final design conditions shown in the contract plans.

6. Footing elevations shown are as indicated at the time of this drawing's preparation.

Other examples of site-specific disclaimers are as follows:

- "The boring logs for BAF-1 through BAF-4 are representative of the conditions at the location where each boring was made, but conditions may vary between borings."

- "Although boulders in large quantities were not encountered on this site, in the borings that are numbered BAF-1 through BAF-4, previous projects in this area have found large quantities of boulders. Therefore, the contractor should be expected to encounter substantial boulder quantities in excavations. The contractor should include any perceived extra costs for boulder removal in this area in his bid price for Item xxx."

The reader is referred to a document entitled *"Important Information About Your Geotechnical Engineering Report,"* which is published by ASFE, The Association of Engineering Firms Practicing In The Geosciences (www.asfe.org). This document presents suggestions for writing a geotechnical report and observations to help reduce the geotechnical-related delays, cost overruns and other costly headaches that can occur during a construction project.

[THIS PAGE INTENTIONALLY BLANK]

CHAPTER 12.0
REFERENCES

AASHTO (1988). *Manual on Subsurface Investigations.* American Association of State Highway and Transportation Officials, Washington, D.C.

AASHTO (1994). *AASHTO LRFD Bridge Design Specifications,* 1st Edition. American Association of State Highway and Transportation Officials, Washington, D.C.

AASHTO (1996). *Standard Specifications for Highway Bridges.* American Association of State Highway and Transportation Officials, Washington, D.C.

AASHTO (2002). *Standard Specifications for Highway Bridges.* American Association of State Highway and Transportation Officials, Washington, D.C.

AASHTO (2004 with 2006 Interims). *AASHTO LRFD Bridge Design Specifications.* 3rd Edition, American Association of State Highway and Transportation Officials, Washington, D.C.

AASHTO (2006). *Standard Specifications for Transportation Materials and Methods of Sampling and Testing, Parts I and II.* American Association of State Highway and Transportation Officials, Washington, DC.

ACI (1956). *Building Code Requirements for Reinforced Concrete, ACI 318-56.* American Concrete Institute, Detroit, MI.

ACI (1963). *Building Code Requirements for Reinforced Concrete, ACI 318-63.* American Concrete Institute, Detroit, MI.

ACI (1968). *Building Code Requirements for Reinforced Concrete, ACI 318-68.* American Concrete Institute, Detroit, MI.

ACI (2002). *Building Code Requirements for Structural Concrete, ACI 318-02.* American Concrete Institute, Detroit, MI.

API-RP-2A (1993). *Recommended Practice for Planning, Designing and Constructing Fixed Offshore Platforms - Load and Resistance Factor* Design. American Petroluem Institute – Recommended Practices.

ASCE (1993). *Unsaturated Soils*, Editors: Houston, S. L. and Wray, W. K., Geotechnical Special Publication No. 39, American Society of Civil Engineers, Reston, VA.

ASCE (1994). *Predicted and Measured Behavior of Five Spread Footings on Sand*. Editors: Briaud, J-L, and Gibbens, R. M. Geotechnical Special Publication No. 41, American Society of Civil Engineers (co-sponsored by the Federal Highway Administration).

ASCE (1997). *Unsaturated Soil Engineering Practice*, Editors: Houston, S. L. and Fredlund, D. G., Geotechnical Special Publication No. 68, American Society of Civil Engineers, New York, NY.

ASTM (1988). *Vane Shear Strength Testing in Soils: Field and Laboratory Studies.* American Society for Testing and Materials, Committee D-18 on Soil and Rock For Engineering Purposes, Philadelphia, PA.

ASTM (2006). *Annual Book of ASTM Standards – Sections 4.02, 4.08, 4.09 and 4.13.* ASTM International, West Conshohocken, PA.

Atterberg, A. (1911). "Über die Physikalische Bodenuntersuchung und über die Plastizität der Tone." *Internationale Mitteilungen Für Bodenkunde*, 1, 10-43.

Bielefeld, M.W. and Middendorp, P. (1992). Improved Pile Driving Prediction for Impact and Vibratory Hammers, Proceedings of the 4th International Conference on the Application of Stresswave Theory to Piles, The Hague, A.A. Balkema Publishers.

Bieniawski, Z. T. (1989). *Engineering Rock Mass Classification*. John Wiley & Sons, NY.

Bishop, A. W. (1955). “The Use of the Slip Circle in the Stability Analysis of Slopes.” *Geotechnique*, Vol. 5 (1), 7-17.

Blendy, M.M. (1979). Rational Approach to Pile Foundations. Symposium on Deep Foundations, ASCE National Convention.

Boussinesq, J. (1885). *Application des potentiels à l'étude de l'équilibre et du mouvement des solides élastiques: principalement au calcul des déformations et des pressions que produisent, dans ces solides, des efforts quelconques exercés sur une petite partie de leur surface ou de leur intérieur : mémoire suivi de notes étendues sur divers points de physique, mathematique et d'analyse.* Gauthier-Villars, Paris.

Bowles, J. E. (1979). *Physical and Geotechnical Properties of Soils.* McGraw-Hill, New York.

Bowles, J. E. (1996). *Foundation Analysis and Design.* 5th Edition, McGraw-Hill, New York.

Brooker, E. W., and Ireland, H. O. (1965). "Earth Pressures at Rest Related to Stress History." *Canadian Geotechnical Journal,* Vol II, No. 1, 1-15.

Burmister, D. M. (1970). "Suggested Methods for Identification of Soils." *Special Procedures for Testing Soil and Rock for Engineering Purposes,* American Society for Testing and Materials, Committee D-18 on Soil and Rock for Engineering Purposes, Philadelphia, PA, 311-323.

Campanella, R. G. (1994). "Field Methods for Dynamic Geotechnical Testing: An Overview of Capabilities and Needs." *Dynamic Geotechnical Testing II,* Special Technical Publication No. 1213, American Society for Testing and Materials, Philadelphia, PA, 3-23.

Canadian Geotechnical Society. (1992). *Canadian Foundation Engineering Manual.* 3rd, Canadian Geotechnical Society, Richmond, B.C.

Caquot, A., and Kerisel, F. (1948). *Tables for the Calculation of Passive Pressure, Active Pressure and Bearing Capacity of Foundations.* Gautier-Villars, Paris.

Carter, M., and Bentley, S. P. (1991). *Correlations of Soil Properties.* Pentech Press Limited, London, U.K.

Casagrande, A. (1936). "The Determination of the Preconsolidation Load and its Practical Significance." *Discussion 34, Proceedings of the First International Conference on Soil Mechanics and Foundation Engineering,* (III), 60-64.

Casagrande, A., and Fadum, R. E. (1940). "Notes on Soil Testing for Engineering Purposes." *Publication 268,* Graduate School of Engineering, Harvard University, Cambridge, MA.

Casagrande, A. (1959). "Discussion of Requirements for the Practice of Applied Soil Mechanics." *Proceedings of the First Panamerican Conference on Soil Mechanics and Foundation Engineering,* Vol III, 1029-1037.

Cedergren, H. R. (1989). *Seepage, Drainage, and Flow Nets.* 3rd Edition, John Wiley & Sons, New York.

Cernica, J. N. (1982). *Geotechnical Engineering.* CBS College Publishing, Holt, Rinehart and Winston, New York.

Chen, W., and McCarron, W. O. (1991). "Bearing Capacity of Shallow Foundations." *Foundation Engineering Handbook,* 2nd, Van Nostrand Reinhold, New York, 144-165.

Clarke, B. G. (1995). *Pressuremeters in Geotechnical Design.* Blackie Academic & Professional, London.

Collin, J. G., Berg, R. R., and Meyers, M. (2002). "Segmental Retaining Wall Drainage Manual." National Concrete Masonry Association, Herdon, Va.

Cornell, C. A. (1969). "Probability-Based Structural Code." *American Concrete Institute Journal,* 66(12), 974-985.

Coulomb, C. A. (1776). *Essai sur une application des règles de maximis & minimis à quelques problèmes de statique, relatifs à l'architecture.* De l'Imprimerie Royale, Paris.

Culmann, K. (1866). *Die Graphische Statik.* Meyer & Zeller, Zürich.

Daniel, C. R., Howie, J. A., and Sy, A. (2003). "A Method for Correlating Large Penetration Test (LPT) to Standard Penetration Test (SPT) Blow Counts." *Canadian Geotechnical Journal,* 40(1), 66-77.

D'Appolonia, D. J., D'Appolonia, E. E., and Brissette, R. F. (1968). "Settlement of Spread Footings on Sand." American Society of Civil Engineers, *Journal of the Soil Mechanics and Foundations Division,* 94 (SM3), 735-760.

D'Appolonia, D. J., D'Appolonia, E. E., and Brissette, R. F. (1970). Closure to discussions on "Settlement of Spread Footings on Sand." American Society of Civil Engineers, *Journal of the Soil Mechanics and Foundations Division,* 96 (SM2), 754-761.

Das, B. M. (1990). *Principles of Geotechnical Engineering.* 2nd Edition, PWS-Kent Pub. Co, Boston, MA.

Davisson, M.T. (1972). “High Capacity Piles.” *Proceedings, Soil Mechanics Lecture Series on Innovations in Foundation Construction*. American Society of Civil Engineers, Illinois Section, Chicago, 81-112.

Day, R. W. (1999). *Geotechnical and Foundation Engineering: Design and Construction.* McGraw-Hill, NY.

Deere, D. U. (1963). "Technical Description of Rock Cores for Engineering Purposes." *Felsmechanik Und Ingenieurgeologie,* 1(1), 16-22.

Deere, D. U., and Deere, D. W. (1989). "Rock Quality Designation (RQD) After Twenty Years." Report No. DACW39-86-M-4273, U.S. Army Corps of Engineers, Washington, D.C.

Deere, D. U., and Patton, F. D. (1971). "Slope Stability in Residual Soils." *Proceedings 4th Panamerican Conference on Soil Mechanics and Foundation Engineering, June 1971,* San Juan, PR, 87-170.

Duncan, J. M. (2000). "Factors of Safety and Reliability in Geotechnical Engineering." American Society of Civil Engineers, *Journal of Geotechnical and Geoenvironmental Engineering,* 126(4), 307-316.

Duncan, J. M., and Buchignani, A. L. (1976). *An Engineering Manual for Settlement Studies.* University of California, Department of Civil Engineering, Berkeley, CA.

Duncan, J. M., Clough, G. W., and Ebeling, R. M. (1990). "Behavior and Design of Gravity Earth Retaining Structures." American Society of Civil Engineers, *Geotechnical Special Publication No. 25,* 251-277.

Duncan, J. M., and Tan, C. K. (1991). "Engineering Manual for Estimating Tolerable Movements of Bridges." *Manuals for the Design of Bridge Foundations: Shallow Foundations, Driven Piles, Retaining Walls and Abutments, Drilled Shafts, Estimating Tolerable Movements, Load Factor Design Specifications, and Commentary.,* NCHRP Report No. 343, Transportation Research Board, National Research Council, Washington, D.C., 219-225.

Duncan, J. M., and Wright, S. G. (2005). *Soil Strength and Slope Stability*. John Wiley & Sons, New York.

Dunnicliff, J. (1988). *Geotechnical Instrumentation for Monitoring Field Performance*. John Wiley & Sons, NY.

Ellingwood, B., Galambos, T. V., MacGregor, J. G., and Cornell, C. A. (1980). *Development of a Probability Based Load Criterion for American National Standard A-58: Building Code Requirements for Minimum Design Loads in Buildings and Other Structures.* U.S. Department of Commerce, National Bureau of Standards, Washington, D.C.

Fellenius, B. H. (1990). *Guidelines for the Interpretation and Analysis of the Static Loading Test.* Deep Foundation Institute, Sparta, NJ.

Fellenius, B. H. (1991). *Guidelines for Static Pile Design: Unified Design of Piles and Pile Groups Considering Capacity, Settlement, and Negative Skin Friction.* Deep Foundations Institute, Sparta, NJ.

Fellenius, B.H., Riker, R.E., O'Brien, A.J. and Tracy, G.R. (1989). "Dynamic and Static Testing in a Soil Exhibiting Set-up." American Society of Civil Engineers, *Journal of Geotechnical Engineering,* Vol. 115, No. 7, 984-1001.

Fellenius, W. (1936). "Calculation of the Stability of Earth Dams." *Proceedings of the Second Congress of Large Dams,* Vol. 4, 445-463.

FHWA (1978). *Design and Construction of Compacted Shale Embankments.* Report No. FHWA RD-78-141, Authors: Strohm, W. E., Bragg, G. H., Zeigler, T. W., Federal Highway Administration, U.S. Department of Transportation.

FHWA (1982). *Performance of Highway Bridge Abutments on Spread Footings on Compacted Fill.* Report No. FHWA RD-81-184, Author: DiMillio, A. F., Federal Highway Administration, U.S. Department of Transportation.

FHWA (1984). *Handbook on Piles and Drilled Shafts under Lateral Load.* Report No. FHWA IP-84-11, Federal Highway Administration, U.S. Department of Transportation.

FHWA (1985). *Tolerable Movement Criteria for Highway Bridges.* Report No. FHWA RD-85-107, Authors: Moulton, L. K., GangaRao, H. V. S., Halvorsen, G. T., Federal Highway Administration, U.S. Department of Transportation.

FHWA (1986). *Prefabricated Vertical Drains – Vol. I, Engineering Guidelines*. Report No. FHWA/RD-86/168, Authors: Rixner, J. J., Kraemer, S. R., and Smith, A. D., Federal Highway Administration, U.S. Department of Transportation.

FHWA (1987). *Spread Footings for Highway Bridges.* Report No. FHWA RD-86-185, Author: Gifford, D. G., Kraemer, S. R., Wheeler, J. R., McKown, A. F., Federal Highway Administration, U.S. Department of Transportation.

FHWA (1988). *Checklist and Guidelines for Review of Geotechnical Reports and Preliminary Plans and Specifications.* Report No. FHWA ED-88-053, Federal Highway Administration, U.S. Department of Transportation, Revised 2003.

FHWA (1989a). *Geotechnical Differing Site Conditions.* Geotechnical Engineering Notebook GT-15, Federal Highway Administration, U.S. Department of Transportation.

FHWA (1989b). *The Pressuremeter Test for Highway Applications.* Report No. FHWA IP-89-008, Authors: Briaud, J., Federal Highway Administration, U.S. Department of Transportation.

FHWA (1992a). *The Cone Penetrometer Test*. Report No. FHWA NHI-91-043, Authors: Riaund J-L and Miran J., Federal Highway Administration, U.S. Department of Transportation.

FHWA (1992b). *The Flat Dilatometer Test.* Report No. FHWA SA-91-044, Authors: Riaund, J. L., and Miran, J., Federal Highway Administration, U.S. Department of Transformation.

FHWA (1992c). *Static Testing of Deep Foundations.* Report No. FHWA SA-91-042, Author: Kyfor, Z. G., Federal Highway Administration, U.S. Department of Transportation.

FHWA (1996). *Determination of Pile Driveability and Capacity from Penetration Tests.* FHWA Contract No. DTFH61-91-C-00047, Authors: Rausche, F., Thendean, G., Abou-matar, H., Likins, G. and Goble, G., Federal Highway Administration, U.S. Department of Transportation.

FHWA (1997). *Subsurface Investigations: Training Course in Geotechnical and Foundation Engineering.* Report No. FHWA HI-97-021, Authors: Arman, A., Samtani, N. C., and Castelli, R. J., Federal Highway Administration, U.S. Department of Transportation.

FHWA (1998a). *Rock Slopes: Reference Manual.* Report No. FHWA HI-99-007, Authors: Wyllie, D. and Mah, C., Federal Highway Administration, U.S. Department of Transportation.

FHWA (1998b). *DRIVEN 1.0: A Microsoft Windows ™ Based Program For Determining Ultimate Vertical Static Pile Capacity*. Report No. FHWA SA-98-074, Authors: Mathias, D., and Cribbs, M., Federal Highway Administration, U.S. Department of Transportation.

FHWA (1999). *Drilled Shafts: Construction Procedures and Design Methods.* Report No. FHWA IF-99-025, Authors: O'Neill, M. W., Reese, L. C., Federal Highway Administration, U.S. Department of Transportation.

FHWA (2001a). *Soil Slope and Embankment Design Reference Manual.* Report No. FHWA NHI-01-026, Authors: Collin, J. G., Hung, J. C., Lee, W. S., Munfakh, G., Federal Highway Administration, U.S. Department of Transportation.

FHWA (2001b). *Mechanically Stabilized Earth Walls and Reinforced Soil Slopes: Design and Construction Guidelines.* Report No. FHWA NHI-00-043, Authors: Elias, V., Ryan B., Federal Highway Administration, National Highway Institute, U.S. Department of Transportation.

FHWA (2001c). *Evaluating Scour at Bridges.* Hydraulic Engineering Circular No. 18, Authors: Richardson, E. V. and Davis, S. R., Federal Highway Administration, U.S. Department of Transportation.

FHWA (2002a). *Geotechnical Engineering Circular 5 (GEC5) - Evaluation of Soil and Rock Properties*. Report No FHWA-IF-02-034. Authors: Sabatini, P.J, Bachus, R.C, Mayne, P.W., Schneider, J.A., Zettler, T.E., Federal Highway Administration, U.S. Department of Transportation.

FHWA (2002b). *Subsurface Investigations (Geotechnical Site Characterization)*. Report No. FHWA NHI-01-031, Authors: Mayne, P. W., Christopher, B. R., and DeJong, J., Federal Highway Administration, U.S. Department of Transportation.

FHWA (2002c). *Geotechnical Engineering Circular 6, Shallow Foundations.* Report No. FHWA-SA-02-054, Author: Kimmerling, R.E. 2002, Federal Highway Administration, U.S. Department of Transportation.

FHWA (2002d). *Drilled Shaft Inspector's Qualification Course.* Report No. FHWA NHI-03-018, Authors: Willams, R., Burnett, D., and Savidge, J., Federal Highway Administration, U.S. Department of Transportation.

FHWA (2003). *Application of Geophysical Methods to Highway Related Problems.* Contract No. DTFH68-02-P-00083, Authors: Wightman, W. E., Jalinoos, F., Sirles, P., and Hanna, K., Federal Highway Administration, U.S. Department of Transportation.

FHWA (2005a). "Micropile Design and Construction," Report No. FHWA NHI-05-039, Authors: Sabatini, P.J., Tanyu, B., Armour., P., Groneck, P., and Keeley, J., National Highway Institute, Federal Highway Administration, U.S. Department of Transportation.

FHWA (2005b). *Earth Retaining Structures - DRAFT*. Report No. FHWA-SA-05-046, Authors: Tanyu, B.F., Sabatini, P.J. and Berg, R.R., Federal Highway Administration, U.S. Department of Transportation.

FHWA (2006a). *Design and Construction of Driven Pile Foundations - Vol. I and II*, Report No. FHWA-NHI-05-042 and FHWA-NHI-05-043, Authors: Hannigan, P.J., G.G. Goble, G. Thendean, G.E. Likins and F. Rausche., Federal Highway Administration, U.S. Department of Transportation.

FHWA (2006b). *Ground Improvement Methods*, FHWA NHI-06-019 (Vol. I) and FHWA NHI-06-020 (Vol. II) Authors: Elias, V., Welsh, J., Warren, J., Lukas, R., Collin, J.G. and Berg, R.R., Federal Highway Administration, U.S. Department of Transportation.

FHWA (2006c) *Geotechnical Engineering Circular No. 8, Continuous Flight Auger Piles*, Authors: Brown, D. and Dapp, S., Federal Highway Administration, U.S. Department of Transportation. (unpublished).

FoSSA (2003). ADAMA Engineering (www.GeoPrograms.com), Newark, DE.

Fredlund, D. G., and Rahardjo, H. (1993). *Soil Mechanics for Unsaturated Soils*. John Wiley & Sons, NY.

Geotechnical Engineering Notebook. *FHWA Geotechnical Guidelines GT1 –GT16.* http://www.fhwa.dot.gov/engineering/geotech/index.cfm.

Glossop, R. (1968). "The Rise of Geotechnology and its Influence on Engineering Practice." Eighth Rankine Lecture, *Geotechnique*, Vol. 18 (2), 107-150.

Goble, G. G. and Rausche, F. (1976). *Wave Equation Analysis of Pile Driving – WEAP Program*. Vol. I-IV, Federal Highway Administration, U.S. Department of Transportation.

Goodman, R. E. (1989). *Introduction to Rock Mechanics.* 2nd Edition, John Wiley & Sons, NY.

Goodman, R. E. (1993). *Engineering Geology: Rock in Engineering Construction.* John Wiley & Sons, NY.

Hansen, J. B., and Inan, S. (1970). *A Revised and Extended Formula for Bearing Capacity*. Bulletin No. 28, Danish Geotechnical Institute, Copenhagen.

Hazen, A. (1911). Discussion of "Dams on Sand Foundations." By A. C. Koenig, *Transactions*, ASCE, Vol. 73, 199-203.

Hirsch, T.J., Carr, L. and Lowery, L.L. (1976). Pile Driving Analysis. TTI Program, U.S. Department of Transportation, Federal Highway Administration, Offices of Research and Development, IP-76-13, Washington, D.C., Volumes I-IV.

Holloway, D.M. and Beddard, D.L. (1995). "Dynamic Testing Results Indicator Pile Test Program - I-880." *Proceedings of the 20th Annual Members Conference of the Deep Foundations Institute.*

Holtz, R. D., and Kovacs, W. D. (1981). *An Introduction to Geotechnical Engineering.* Prentice-Hall, Englewood Cliffs, N.J.

Holtz, W. C., and Hilf, J. W. (1961). "Settlement of Soil Foundations Due to Saturation." *Proceedings of the 5th International Conference on Soil Mechanics and Foundation Engineering*, Paris, France, 673-679.

Horvath, R. G., and Kenney, T. C. (1979). "Shaft Resistance of Rock-Socketed Drilled Piers." *Proceedings of the Symposium on Deep Foundations,* American Society of Civil Engineers, Atlanta, GA, 182-214.

Hough, B. K. (1957). *Basic Soils Engineering.* 2nd Edition, The Ronald Press Company, New York, NY.

Hough, B. K. (1959). "Compressibility as Basis for Soil Bearing Value." American Society of Civil Engineers, *Journal of the Soil Mechanics and Foundations Division,* 85(SM4, Part 1), 11-39.

Hussein, M.H., Likins, G.E. and Hannigan, P.J. (1993). "Pile Evaluation by Dynamic Testing During Restrike." *Eleventh Southeast Asian Geotechnical Conference, Singapore.*

Hvorslev, M. J. (1948). *Subsurface Exploration and Sampling of Soils for Civil Engineering Purposes.* U.S. Army Corps of Engineers, Waterways Experiment Station, Vicksburg, MS.

Ingles, O. G. (1962). "Bonding Forces in Soils, Part 3: A Theory of Tensile Strength for Stabilised and Naturally Coherent Soils." *Proceedings of the First Conference of the Australian Road Research Board,* Victoria, Australia, 1025-1047.

ISRM. (1981). *Suggested Methods for the Quantitative Description of Discontinuities in Rock Masses.* International Society for Rock Mechanics, Committee on Field Tests, No. 4, Pergamon Press, UK.

Jaky, J. (1944). "The Coefficient of Earth Pressure at Rest." *Journal of the Society of Hungarian Architects and Engineers,* Vol. 78, No. 22, 355-358.

Janbu, N. (1954). "Applications of Composite Slip Surfaces for Stability Analysis." *Proceedings of the European Conference on the Stability of Earth Slopes,* Stockholm, Vol. 3, 39-43.

Janbu, N. (1968). *Stability Analysis of Slopes with Dimensionless Parameters.* Harvard University, Cambridge, MA.

Jumikis, A. R. (1962). *Soil Mechanics.* D. Van Nostrand Company, Princeton, N.J.

Komurka, V. E., Wagner, A. B., and Edil, T. (2003). *Estimating Soil/Pile Set-Up.* Wisconsin Highway Research Program, Madison, WI.

Krebs, R. D., and Walker, R. D. (1971). *Highway Materials.* McGraw-Hill, NY.

Kulhawy, F. H., and Mayne, P. W. (1990). *Manual on Estimating Soil Properties for Foundation Design.* Report EL-6800, Electric Power Research Institute, Palo Alto, CA.

Kulhawy, F.H. (1983). *Transmission Line Structure Foundations for Uplift and Compression Loading*, Report No. EL-2870, Electric Power Research Institute.

Kulicki, J. M. (1998). *Development of Comprehensive Bridge Specifications and Commentary.* NCHRP Research Results Digest 198, Transportation Research Board, National Research Council, Washington, D.C.

Lambe, P. C. (1996). "Residual Soils." *Landslides Investigation and Mitigation,* Special Report No. 247, Transportation Research Board, National Research Council, Washington, D.C., 507-524.

Lambe, T. W., and Whitman, R. V. (1979). *Soil Mechanics: SI Version.* John Wiley & Sons, NY.

Lee, K. L., and Singh, A. (1971). "Compaction of Granular Soils." *Proceedings of the 9th Annual Engineering Geology and Soils Engineering Symposium*, Idaho Department of Highways, Boise, ID, 161-174.

Leshchinsky, D. and Perry, E. B. (1987). "A Design Procedure for Geotextile-Reinforced Walls." *Proceedings Geosynthetics '87 Conference.*, IFAI, Industrial Fabric Association International, New Orleans, 95-107.

Lunne, T., Robertson, P. K., and Powell, J. J. M. (1997). *Cone Penetration Testing in Geotechnical Practice.* E & FN Spon, New York, NY.

Mayne, P. W., and Kulhawy, F. H. (1982). "K_o-OCR Relationships in Soil." American Society of Civil Engineers, *Journal of the Geotechnical Engineering Division*, 108(GT6), 851-872.

Meyerhof, G. G. (1953). "The Bearing Capacity of Foundations under Eccentric and Inclined Loads." *Proceedings of the 3rd International Conference of Soil Mechanics and Foundation Engineering, Volume I* Zurich, 440-445.

Meyerhof, G. G. (1957). "The Ultimate Bearing Capacity of Foundations on Slopes." *Proceedings of the 4th International Conference of Soil Mechanics and Foundation Engineering*, London, Paris, 384-386.

Meyerhof, G. G. (1976). "Bearing Capacity and Settlement of Pile Foundations." American Society of Civil Engineers, *Journal of Geotechnical Engineering*, 102(No. GT3), 197-228.

Mitchell, J. K. (1976). *Fundamentals of Soil Behavior.* John Wiley & Sons, NY.

Murthy, V. N. S. (1989). *Soil Mechanics and Foundation Enigineering.* Vol I - Soil Mechanics, 3rd Edition, Sai Kripa Technical Consultants, Bangalore.

NAVFAC (1986a). *Design Manual 7.01 - Soil Mechanics.* Department of the Navy, Naval Facilities Engineering Command, Alexandria, VA.

NAVFAC (1986b). *Design Manual 7.02 - Foundation and Earth Structures.* Department of the Navy, Naval Facilities Engineering Command, Alexandria, VA.

NCHRP (1983). *Shallow Foundations for Highway Structures*. NCHRP Report 107, Author: Wahls, H. E., Transportation Research Board, National Research Council, Washington, D.C.

NCHRP (1989). *Treatment of Problem Foundations for Highway Embankments*. NCHRP Report 147, Author: Holtz, R. D., Transportation Research Board, National Research Council, Washington, D.C.

NCHRP (1990). *Design and Construction of Bridge Approaches*. NCHRP Report 159, Author: Wahls, H. E., Transportation Research Board, National Research Council, Washington, D.C.

NCHRP (1991). *Manuals for the Design of Bridge Foundations : Shallow Foundations, Driven Piles, Retaining Walls and Abutments, Drilled Shafts, Estimating Tolerable Movements, Load Factor Design Specifications, and Commentary*. NCHRP Report 343, Authors: Barker, R.M., J.M. Duncan, K.B. Rojiani, P.S.K. Ooi, C.K. Tan and S.G. Kim, Transportation Research Board, National Research Council, Washington, D.C.

NCHRP (1993). *Downdrag on Bitumen-Coated Piles*. NCHRP Report 24-5, Author: Briaud, J-L and Tucker, L. M., Transportation Research Board, National Research Council, Washington, D.C.

NCHRP (1997). *Settlement of Bridge Approaches (The Bump at the End of the Bridge)*. NCHRP Report 234, Authors: Briaud, J-L, James, R. W., and Hoffman S. B., Transportation Research Board, National Research Council, Washington, D.C.

Nicu, N. D., Antes, D. R., and Kessler, R. S. (1971). "Field Measurements on Instrumented Piles Under an Overpass Abutment." *Highway Research Record No. 354 - Bridges and Bridge Foundations*, Discussion by Seymour-Jones, Highway Research Board, National Research Council, Washington, D.C., 90-102.

Nordlund, R. L. (1979). "Point Bearing and Shaft Friction of Piles in Sand." *5th Annual Fundamentals of Deep Foundation Design*.

Nordlund, R. L. (1963). "Bearing Capacity of Piles in Cohesionless Soils." American Society of Civil Engineers, *Journal of the Soil Mechanics and Foundations Division*, 89(SM3), 1-35.

NYSDOT. "Pressure Coefficients Beneath the End of a Fill." Drawing SM 1330, New York State Department of Transportation, Albany, NY.

O'Neill, M. W. (1983). "Group Action in Offshore Piles." *Proceedings of the Conference on Geotechnical Practice in Offshore Engineering*, American Society of Civil Engineers, University of Texas at Austin, Austin, TX., 25-64.

O'Neill, M. W., and Raines, R. D. (1991). "Load Transfer for Pipe Piles in Highly Pressured Dense Sand." American Society of Civil Engineers, *Journal of Geotechnical Engineering*, 117(8), 1208-1226.

O'Rourke, T. D., and Jones, C. J. F. P. (1990). "Overview of Earth Retention Systems: 1970-1990." *Proceedings of Conference on Design and Performance of Earth Retaining Structures*, American Society of Civl Engineers, New York, NY, 22-51.

Padfield, C. J., and Mair, R. J. (1984). *Design of Retaining Walls Embedded in Stiff Clay*. Report No. 104, Construction Industry Research and Information Association, London, England.

Paikowsky, S. G., and Whitman, R. V. (1990). "Effects of Plugging on Pile Performance and Design." *Canadian Geotechnical Journal,* 27(4), 429-440.

Peck, R. B. (1969). "Advantages and Limitations of the Observational Method in Applied Soil Mechanics." *Geotechnique,* Vol. 19 (2), 171-187.

Peck, R. B., Hanson, W. E., and Thornburn, T. H. (1974). *Foundation Engineering.* 2nd Edition, John Wiley & Sons, NY.

Perloff, W. H., and Baron, W. (1976). *Soil Mechanics: Principles and Applications.* John Wiley & Sons, NY.

Pile Dynamics, Inc. (2005). GRLWEAP Procedures and Models, Version 2005. 4535 Renaissance Parkway, Cleveland, OH.

Poulos, H. G., and Davis, E. H. (1974). *Elastic Solutions for Soil and Rock Mechanics.* John Wiley & Sons, NY.

Powers, J. P. (1992). *Construction Dewatering: New Methods and Applications.* 2nd, John Wiley & Sons, NY.

Raines, R. D., Ugaz, O. G., and O'Neill, M. W. (1992). "Driving Characteristics of Open-Toe Piles in Dense Sand." American Society of Civil Engineers, *Journal of Geotechnical Engineering,* 118 (No. 1), 72-88.

Rankine, W. J. M. (1857). "On the Stability of Loose Earth." *Proceedings of the Royal Society of London,* London, 185-187.

Rausche, F., Liang, L., Allin, R., and Rancman, D. (2004). "Applications and Correlations of the Wave Equation Analysis Program GRLWEAP." *Proceedings of the 7th International Conference on the Application of Stresswave Theory to Piles,* Petaling Jaya, Selangor, Malaysia, 2004.

Reese, L. C., Isenhower, W. M., and Wang, S-T. (2006). *Analysis and Design of Shallow and Deep Foundations.* John Wiley & Sons, NY.

ReSSA (2001). ADAMA Engineering (www.GeoPrograms.com), Newark, DE.

Roberts, F.L., Kandhal, P.S., Brown, E.R., Lee, D.Y., and Kennedy, T.W. (1996). *Hot Mix Asphalt Materials, Mixture Design, and Construction*. National Asphalt Pavement Association Education Foundation. Lanham, MD.

Robertson, P. K., Campanella, R. G., Gillespie, D., and Greig, J. (1986). "Use of Piezomenter Cone Data." *Geotechnical Special Publication No. 6, Use of In-Situ Tests in Geotechnical Engineering,* American Society of Civil Engineers, New York, N.Y., 1263-1280.

Robertson, P. K., and Campanella, R. G. (1983). "Interpretation of Cone Penetration Tests." *Canadian Geotechnical Journal*, 20(4), 718-754.

Samtani, N.C., Jalinoos, F., and Poland, D. M. (2005). "Integrity Testing of Drilled Shafts – Existing and New Techniques." *Proceedings of the GEO^3 Conference,* ADSC, Dallas, TX.

Schmertmann, G. R., Chouery-Curtis, V. E., Johnson, R. D., and Bonaparte, R. (1987). "Design Charts for Geogrid-Reinforced Soil Slopes." *Proceedings Geosynthetics '87 Conference.*, IFAI, Industrial Fabric Association International, New Orleans, 108-120.

Schmertmann, J. H. (1955). "The Undisturbed Consolidation Behavior of Clay." *Transactions,* ASCE, Vol. 120, 1201-1233.

Schmertmann, J. H., Hartman, J. P., and Brown, P. R. (1978). "Improved Strain Influence Factor Diagrams." American Society of Civil Engineers, *Journal of the Geotechnical Engineering Division,* 104 (No. GT8), 1131-1135.

Schmidt, B. (1966). "Discussion of, Earth Pressure At-Rest Related to Stress History." *Canadian Geotechnical Journal,* 3(4), 239-242.

Schroeder, W. L. (1980). *Soils in Construction.* 2nd Edition, John Wiley & Sons, NY.

Seed, H. B., Woodward, R. J., and Lundgren, R. (1962). "Prediction of Swelling Potential for Compacted Clays." American Society of Civil Engineers, *Journal of the Soil Mechanics and Foundations Division,* 88(SM3, Part 1), 53-87.

Silvestri, V. (1983). "Bearing Capacity of Dykes and Fills Founded on Soft Soils of Limited Thickness." *Canadian Geotechnical Journal,* 20(3), 428-436.

Skempton, A. W. (1953). "The Collodial Activity of Clays." *Proceedings 3rd International Conference on Soil Mechanics and Foundation Engineering,* 57-61.

Skempton, A. W. (1957). "Discussion on the Planning and Design of the New Hong Kong Airport." *Proceedings of the Institution of Civil Engineering,* 7(3), 305-307

Skempton, A. W. (1986). "Standard Penetration Test Procedures and the Effects in Sands of Overburden Pressure, Relative Density, Particle Size, Ageing, and Overconsolidation." *Geotechnique*, Vol. 3(1), 30-53.

SLOPE/W (2004). Geo-SLOPE/W International Ltd., Calgary, Alberta, Canada.

Smith, E.A.L. (1960). "Pile Driving Analysis by the Wave Equation." American Society of Civil Engineers, *Journal of the Soil Mechanics and Foundations Division*, 86(4), 35-61.

Stevens, R.F. (1988). "The Effect of a Soil Plug on Pile Driveability in Clay." *Proceedings of the Third International Conference on the Application of Stress Wave Theory to Piles*, B.H. Fellenius, Editor, BiTech Publishers, Vancouver, 861-868.

Soares, M., de Mello, J. and de Matos, S. (1984). "Pile Driveability Studies, Pile Driving Measurements." *Proceedings of the Second International Conference on the Application of Stress-Wave Theory to Piles*, Stockholm, 64-71.

Sokolovski, V. V. (1954). *Statics of Soil Media.* Translated from Russian by D. H. Jones and A. N. Schoefield, Butterworths, London.

Sowers, G. F. (1979). *Introductory Soil Mechanics and Foundations: Geotechnical Engineering.* 4th Edition, Macmillan, New York, NY.

Spencer, E. (1967). "A Method of Analysis of Embankments assuming Parallel Interslice Forces." *Geotechnique*, Vol. 17 (1), 11-26.

Taylor, D. W. (1948). *Fundamentals of Soil Mechanics.* John Wiley & Sons, New York, NY.

Teng, W. (1962). *Foundation Design*. Prentice-Hall, Inc., Englewood Cliffs, NJ.

Terzaghi, K. (1943). *Theoretical Soil Mechanics.* John Wiley & Sons, New York, NY.

Terzaghi, K., and Peck, R. (1967). *Soil Mechanics in Engineering Practice.* 2nd Edition, John Wiley & Sons, New York, NY.

Terzaghi, K., Peck, R. B., and Mesri, G. (1996). *Soil Mechanics in Engineering Practice.* 3rd Edition, John Wiley & Sons, New York, NY.

Thompson, C. D., and Thompson, D. E. (1985). "Real and Apparent Relaxation of Driven Piles." American Society of Civil Engineers, *Journal of Geotechnical Engineering,* 111(2), 225-237.

Thorburn, S. H. (1966). "Large Diameter Piles Founded in Bedrock." *Proceedings, Symposium on Large Bored Piles* (Institute for Civil Engineering, London), 95-103.

Tomlinson, M. J. (1994). *Pile Design and Construction Practice.* 4th Edition, E & FN Spon, New York, NY.

Tomlinson, M. J. (1980). *Foundation Design and Construction.* 4th Edition, Pitman, Boston, MA.

Tomlinson, M. J. (1995). *Foundation Design and Construction.* 6th Edition, Pitman, Boston, MA.

Tschebotarioff, G.P. (1951). *Soil Mechanics, Foundations and Earth Structures*, McGraw-Hill, New York.

USACE (1994). *Settlement Analysis.* US Army Corps of Engineers, Washington, D.C.

USBR (1960). *Design of Small Dams.* U.S. Bureau of Reclamation, Washington, D.C.

USDA (1993). *Soil Survey Manual.* U.S. Department of Agriculture, Washington, D.C.

USS Steel (1975). *USS Steel Sheet Piling Design Manual.* USS Steel, Pittsburg, PA.

Utah DOT – Pavement Design and Management Manual (2005).

Vaughan, P. R., Maccarini, M., and Mokhtar, S. M. (1988). "Indexing the Engineering Properties of Residual Soil." *Quarterly Journal of Engineering Geology & Hydrogeology,* 21(1), 69-84.

Vesic, A. S. (1977). *Design of Pile Foundations.* NCHRP Report 42, Transportation Research Board, National Research Council, Washington, D.C.

Vesic, A. S. (1975). "Bearing Capacity of Shallow Foundations." *Foundation Engineering Handbook*, 2nd, Van Nostrand Reinhold, New York, NY, 121-147.

Westergaard, H. M. (1938). *A Problem of Elasticity Suggested by a Problem in Soil Mechanics: Soft Material Reinforced by Numerous Strong Horizontal Sheets.* Harvard University, Cambridge, MA.

Winterkorn, H. F., and Fang, H. (1975). *Foundation Engineering Handbook.* 2nd Edition, Van Nostrand Reinhold, New York, NY.

Woodward, R. J., Gardner, W. S., and Greer, D. M. (1972). *Drilled Pier Foundations*. McGraw-Hill, NY.

Wright, S. G., Arcement, B., and Benson, C. H. (2003). "Comparison of Maximum Density of Cohesionless Soils Determined Using Vibratory and Impact Compaction Methods." *Soil and Rock America 2003, Proceeding of the 12th Panamercian Conference on Soil Mechanics and Geotechnical Engineering*, Cambridge, MA, 1709-1715.

WSDOT (1988). Comparison of Methods for Estimating Pile Capacity. Report No. WA-RD 163.1, Authors: Fragasny, R. J., Higgins, J. D., and Argo, D. E., Washington State Department of Transportation, Olympia.

Wyllie, D. C. (1999). *Foundations on Rock.* 2nd Edition, E & FN Spon, New York, NY.

[THIS PAGE INTENTIONALLY BLANK]

APPENDIX A

APPLE FREEWAY PROJECT

[THIS PAGE INTENTIONALLY BLANK]

APPENDIX A
APPLE FREEWAY PROJECT
GENERAL NOTES

This appendix presents the geotechnical engineering considerations and calculations for a fictitious bridge project from conception to completion in a serialized illustrative workshop design problem. The appendix is divided into several sections. Each section corresponds to a specific phase in the design and construction monitoring process. The section numbering system is as follows:

A.#

where A denotes appendix designation and # denotes the section number in the manual. Thus, Section A.2 relates to the second section in the appendix. Within each section, the numbering system for pages, figures, tables, etc. is in accordance with the following format:

A.# - *

where # denotes the section number in the appendix and * denotes the page number, figure number and so on in that section. Thus, for example, "Figure A.2-4" refers to the fourth figure in the second section, and "A.2-4" at the bottom of the page refers to the fourth page in the second section.

As an aid to following the design process, a summary of relevant concepts and/or procedures is presented at the beginning of each section with cross reference to the appropriate chapter(s) in the text of the manual. Equations used in the computations are also cross referenced to the equation number listed in the text of the manual.

To simplify hand calculations, the unit weight of water, γ_w, of 60 pcf has been used in some of the calculations. In actual calculations for any given project, the user should use the more common value of $\gamma_w = 62.4$ pcf unless higher values are justified, e.g., in brackish water.

SECTION A.1
INTRODUCTION AND SCOPE OF WORK

A.1-1 RELEVANT CONCEPTS AND PROCEDURES

- Description of the project.
- Development of a scope of work

A.1-2 DESCRIPTION OF THE PROJECT

Figure A.1-1 shows the layout of a two-span bridge that carries Interstate 0 (I-0) over the Apple Freeway, which is a divided freeway. The center pier of the I-0 bridge will be in the median between the northbound (NB) and southbound (SB) freeway. The approaches to the bridge will be constructed on embankment fills. The fills will have an end-slope spilling through the abutment locations at a grade of 2H:1V (H: Horizontal, V: Vertical) as shown in Figure A.1-1.

A.1-3 SCOPE OF WORK

The scope of the work includes the following:

- Setup and perform the field investigations. The field investigations should include SPTs in drilled holes and CPTs to obtain continuous stratigraphic profiles. Develop idealized subsurface profile based on visual description of soils and information from CPT sounding profiles.
- Setup and perform laboratory investigations including consolidation and strength tests.
- Perform slope stability analyses for the 2H:1V end-slopes. Evaluate the end-slopes for both circular and block failure mechanisms.
- Perform immediate and consolidation settlement analyses and lateral squeeze computations for embankment fills. If warranted, perform ground improvement as necessary to mitigate large long-term settlements. Evaluate two alternatives (a) surcharging and (b) surcharging with wick-drains.
- Evaluate and analyze spread shallow foundations at both abutment and pier locations. Determine the allowable bearing capacity, anticipated settlement and settlement rates.
- Evaluate and analyze driven pile foundations at both abutments and pier locations. Evaluate driving resistance for pile foundation alternative. Estimate the possible abutment lateral movement due to lateral squeeze of soils.
- Perform wave equation analyses for pile foundations as part of construction monitoring and QA/QC.
- Prepare a memorandum report summarizing the above work.

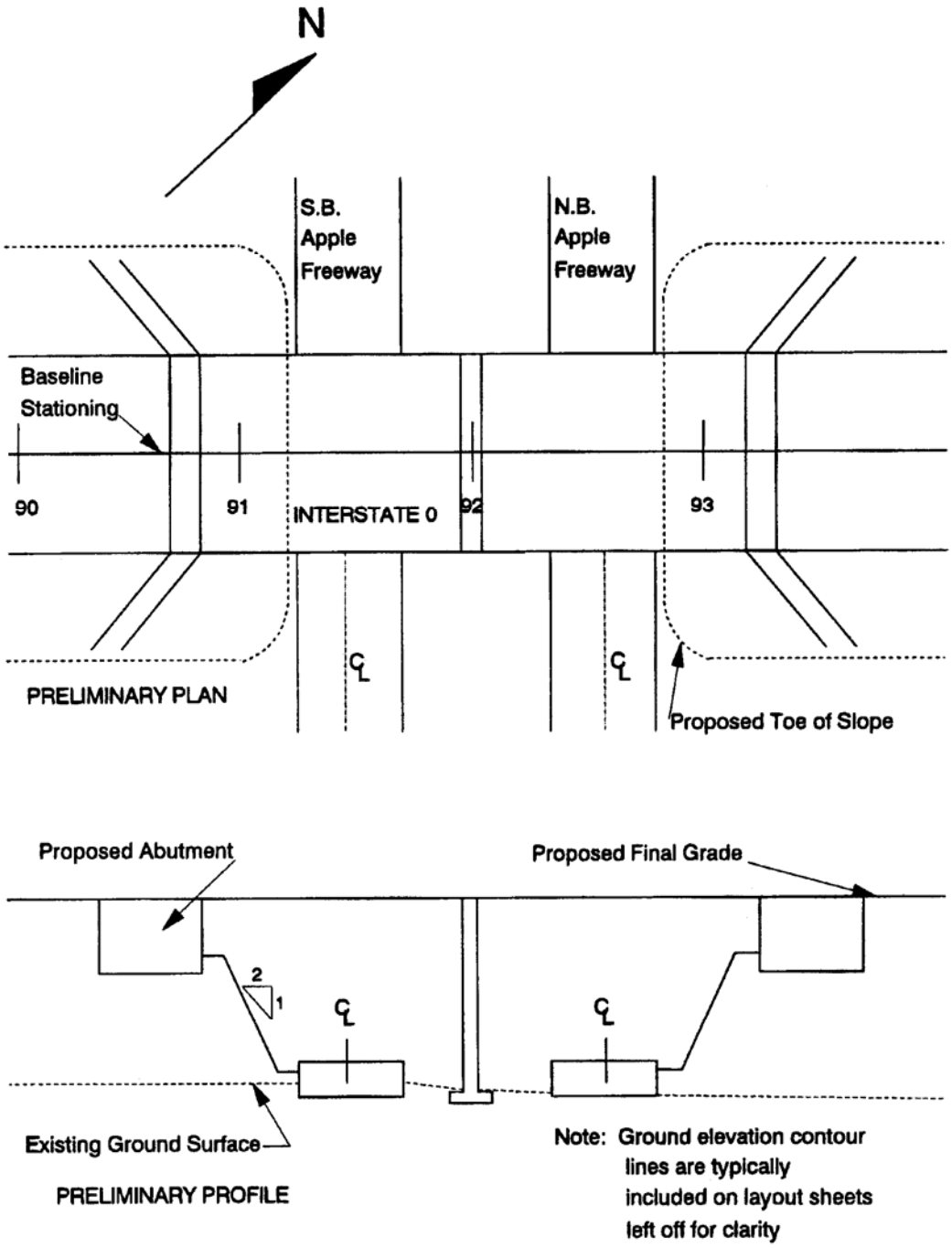

Figure A.1-1. Apple Freeway plan and section.

[THIS PAGE INTENTIONALLY BLANK]

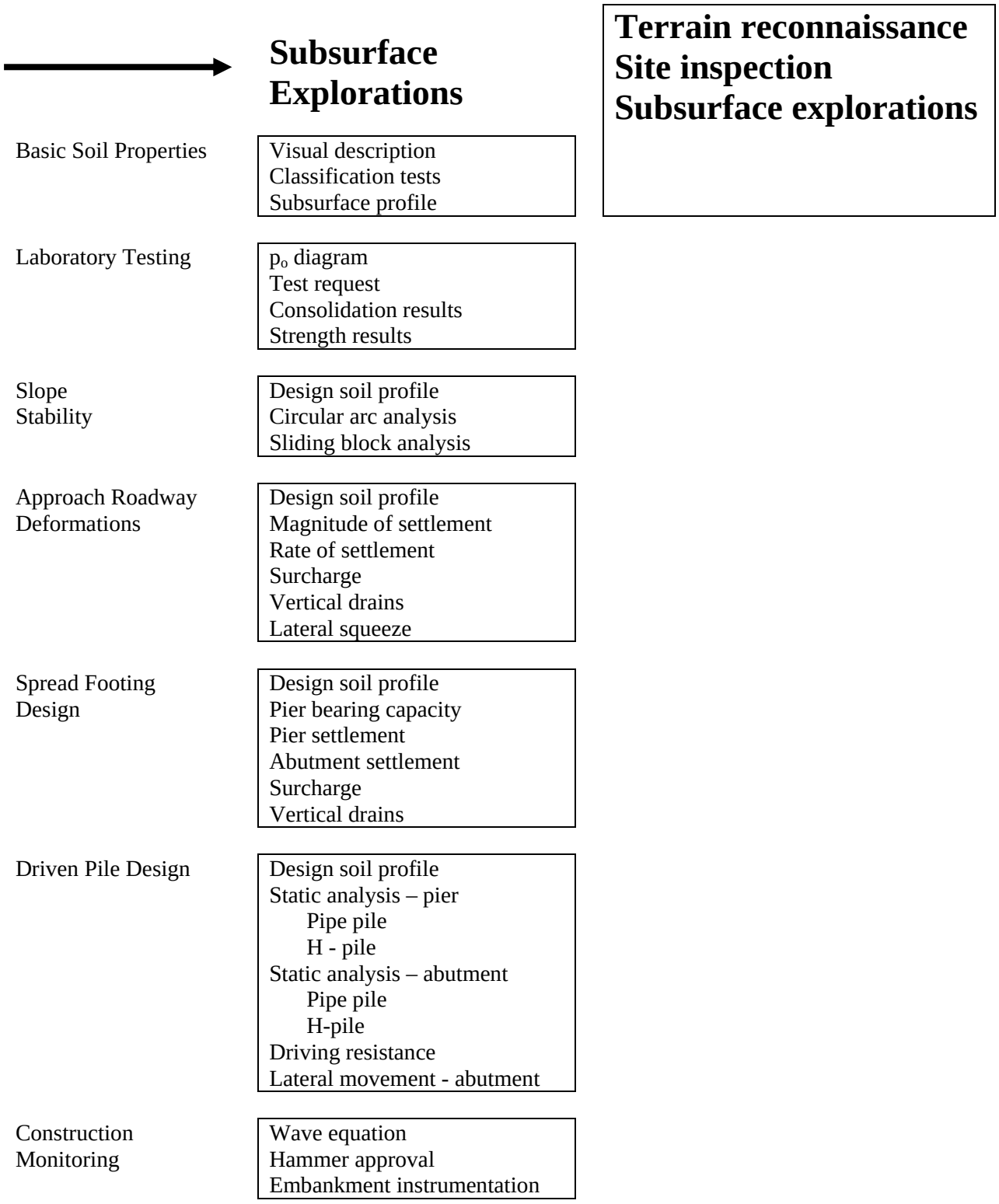

Figure A.2-1. Overview of the geotechnical work to be performed.

SECTION A.2
SUBSURFACE EXPLORATIONS

A.2-1 RELEVANT CONCEPTS AND PROCEDURES (Refer to Figure A.2-1)

- Terrain reconnaissance and site inspection – Chapter 3
- Preparation of a field exploration program – Chapter 3
- Subsurface borings for SPT sampling – Chapter 3
- Subsurface soundings for CPT logging – Chapter 3

A.2-2 DETAILED PROCEDURES

Given: Examination of USGS topo and geology maps and USDA soil map showed structure to be located in a delta landform. Field inspection showed wet area with cattails in vicinity of east abutment.

Required: Plan subsurface exploration program and prepare boring request.

Solution Procedure:

Step 1: **Prepare terrain reconnaissance and site inspection**

- Locate structure on USGS topo map or other maps available from local agencies that show greater surface detail to obtain preliminary estimates of boring locations and site access by drilling equipment.
- Visit the site to verify conditions.

Step 2: **Prepare preliminary field exploration program (see Figure A.2-2)**

- Identify types of subsurface borings and establish location of each.
- Specify borings with disturbed SPT sampling (DH BAF) at each abutment and intermediate support
- Specify CPT soundings (CPT BAF) immediately next to the drill hole in which the SPTs were performed.
- Specify hand auger holes (EA) in wet area within east approach fill limits

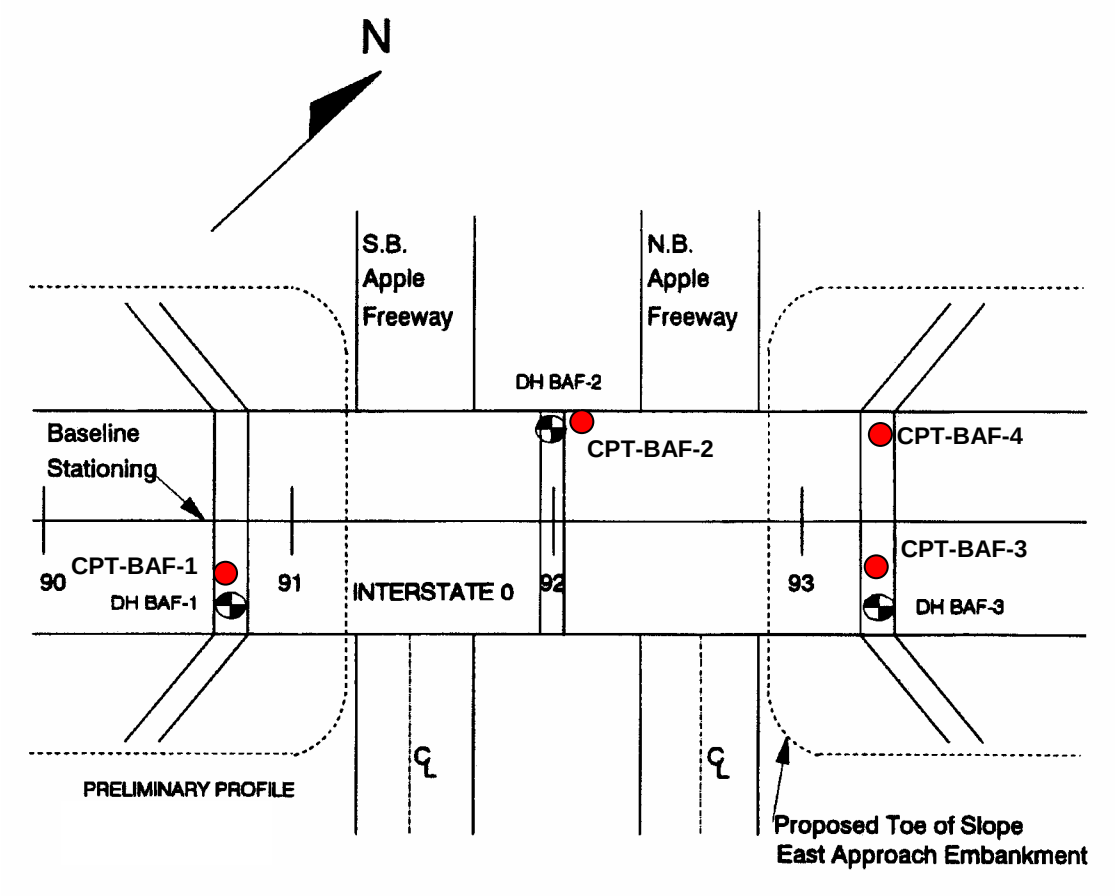

Figure A.2-2. Proposed site exploration – Preliminary.

Step 3: Establish criteria for determining boring depth

- SPT holes to depth where the minimum average SPT-N equals 20 for 20-ft depth or 10-ft into bedrock, whichever depth is less.
- Based on the observations from terrain reconnaissance, use a 20-ton CPT rig which should be sufficient to explore the soft and/or organic soils
- Hand auger holes to a maximum depth of 10-ft or at least 3-ft below bottom of unstable soils (soft and/or organic soils), whichever depth is less.

Step 4: Establish sampling criteria

- East and west abutments: disturbed SPT every 5-ft.
- Pier footing: continuous SPT samples to depth of 15-ft, then 5-ft intervals since spread footings may be considered
- Wet area: obtain representative samples from each auger hole.

- CPTs: perform with a piezocone to permit pore water pressure measurements

Step 5: Identify and address other important considerations.

- Since area is a delta landform, granular deposits overlying clay may be encountered. If so, an undisturbed drill hole (UDH) will be required. The location, depth, and sampling details will be selected based on the results of the three SPT boring. Notify the drillers of possibility of UDH and field vane shear so necessary equipment can be taken to site.
- Long-term water level reading should be taken in one hole.
- Obtain all required right-of-way (ROW) and entry permits. Consult with state and local departments of environmental quality for any environmental permits if required.
- Arrange for traffic control on Apple Freeway

Step 6: Prepare preliminary field exploration request (see Figure A.2-3).

Step 7: Perform field exploration and prepare final field exploration layout (see Figure A.2-4)

- Perform three (3) SPT drill hole (DH) borings (DH BAF-1, DH BAF-2, DH BAF-3)
- Perform four (4) CPT probes (CPT BAF-1, CPT BAF-2, CPT BAF-3 and CPT BAF-4)
- Perform one (1) undisturbed drill hole (UDH) borings (UDH BAF-4)
- Perform nine (9) hand-augured holes (EA1 to EA9) on a rectangular grid pattern at the east abutment site
- Logs of borings, CPT soundings and hand-augured holes are included herein.

SUBSURFACE EXPLORATION REQUEST

August 1, 2006

Subject: Request for Subsurface Exploration
Interstate Structure over the Apple Freeway

From: Foundation Engineer

To: Regional Office

In accordance with project authorization from the Chief Engineer dated January 16, 2006, a subsurface exploration program has been prepared for the subject structure. We request that your office advance a 2½ - inch diameter cased drill hole and a CPT sounding at each of the following locations:

Hole No.	Baseline Station	Offset (ft)
DH-BAF-1	90 + 77	50' Rt
DH-BAF-2	92 + 00	50' Lt
DH-BAF-3	93 + 27	50' Rt

The locations may be field adjusted along the footing line shown on the attached drawing if necessary.

Each boring shall extend to a depth where the blow count per foot on the sample spoon exceeds 20 for a 20-feet depth. If rock is encountered above this depth, 10 feet of rock core shall be cored and extracted. Spoon samples shall be taken at intervals of 5-feet except for the top 15-feet of BAF-2 where continuous spoon samples are required. On completion of BAF-2 a perforated plastic pipe shall be inserted before extracting the casing to permit long-term water level observation. It is anticipated that soft clay soils may be encountered at this site. If so, an additional 4-inch diameter cased hole (UDH) may be required to extract undisturbed tube samples and/or perform in situ vane shear tests. Before the drill crew demobilizes, the driller should telephone the results of the first three SPT borings to the project engineer, Mr. Richard Cheney at 202-555-0355. At that time, a decision on the details of the UDH will be issued.

The CPT soundings shall be performed by using CPTu equipment that includes a piezocone to permit continuous pore water pressure measurements. The CPT truck should provide a minimum reaction of 20 tons. A CPT sounding shall be performed in the immediate vicinity of each of the drilled holes.

A wet area of potentially unstable soil (soft and/or organic soils) exists in the area of the proposed east approach embankment. Please define the depth of this deposit beneath the limits of the east approach embankment back to Baseline station 93 + 50 with hand auger exploration. Perform at least 9 hand auger holes in that area on a rectangular grid pattern and show the locations on the final exploration layout plan.

The present schedule for structure design requires that all samples and subsurface logs be received in the main office by November 1, 2006.

Attachment: Proposed preliminary site exploration plan (Figure A.2-2).

Figure A.2-3. Typical preliminary exploration request.

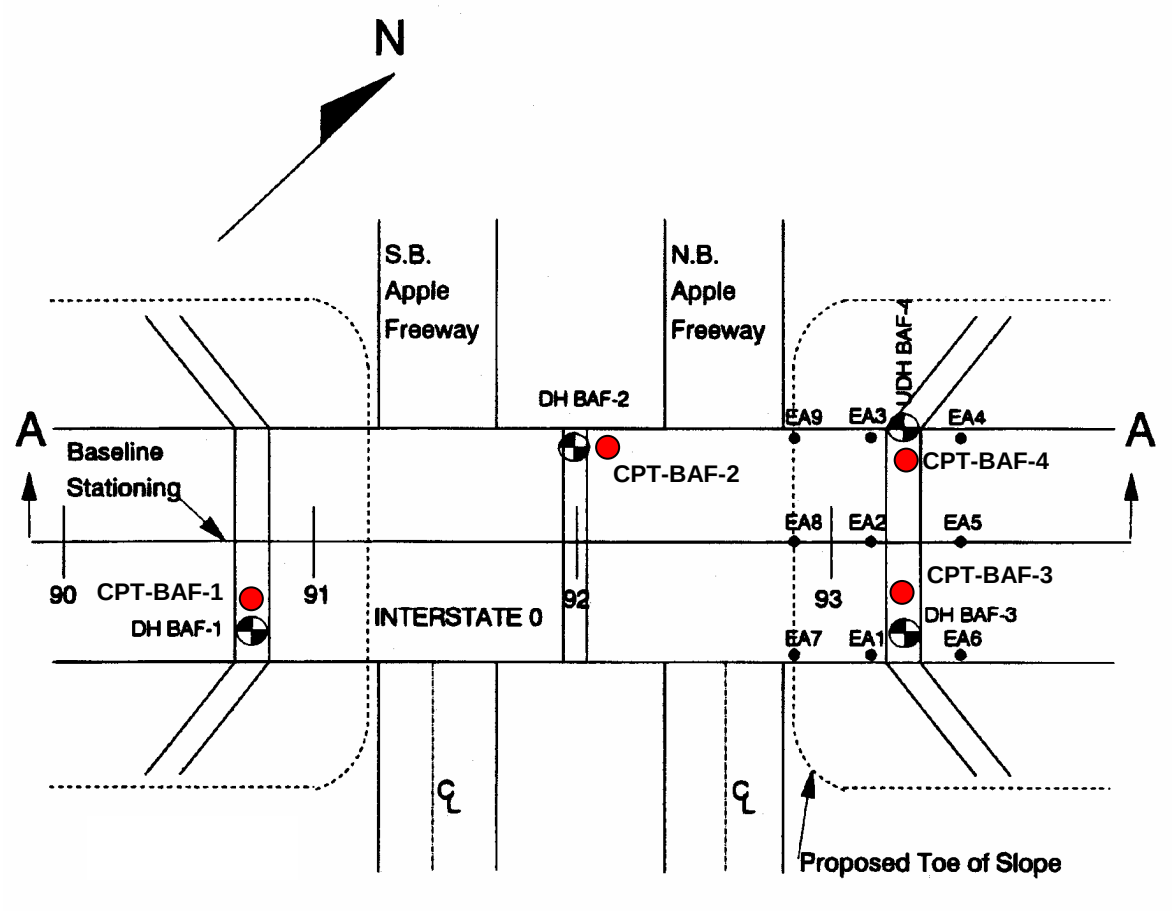

Figure A.2-4. Final field exploration layout.

A.2-3 SUMMARY OF THE SITE EXPLORATION PHASE FOR THE APPLE FREEWAY DESIGN PROBLEM

1. Terrain Reconnaissance

    - Delta landform - possible clay deposit buried

2. Site Inspection

    - Unsuitable soils near east approach embankment
    - Easy access for drilling equipment and CPT rig.

3. Subsurface Borings

    - Hand auger holes define limits and depth of unsuitable organic deposit.
    - SPT drill holes show sand over clay over gravel and rock.
    - CPT soundings indicate that the clay layer may have thin silt seams in it (this would possibly help in reducing consolidation time)
    - Undisturbed samples and vane shear tests taken in clay.

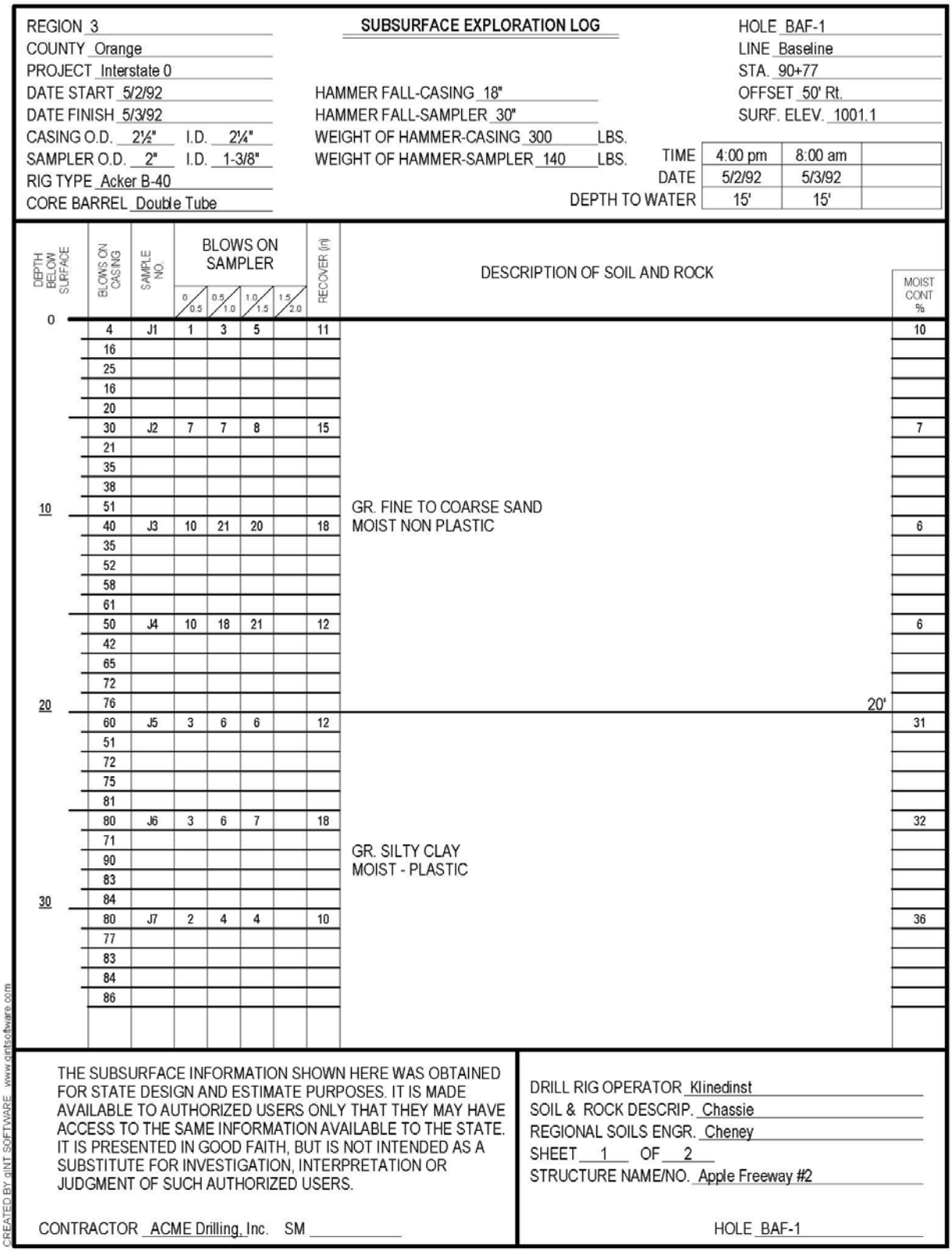

SUBSURFACE EXPLORATION LOG

REGION 3
COUNTY Orange
PROJECT Interstate 0
DATE START 5/2/92
DATE FINISH 5/3/92
CASING O.D. 2½" I.D. 2¼"
SAMPLER O.D. 2" I.D. 1-3/8"
RIG TYPE Acker B-40
CORE BARREL Double Tube

HAMMER FALL-CASING 18"
HAMMER FALL-SAMPLER 30"
WEIGHT OF HAMMER-CASING 300 LBS.
WEIGHT OF HAMMER-SAMPLER 140 LBS.

HOLE BAF-1
LINE Baseline
STA. 90+77
OFFSET 50' Rt.
SURF. ELEV. 1001.1

TIME	4:00 pm	8:00 am	
DATE	5/2/92	5/3/92	
DEPTH TO WATER	15'	15'	

DEPTH BELOW SURFACE	BLOWS ON CASING	SAMPLE NO.	BLOWS ON SAMPLER 0/0.5	0.5/1.0	1.0/1.5	1.5/2.0	RECOVER (in)	DESCRIPTION OF SOIL AND ROCK	MOIST CONT %
0	4	J1	1	3	5		11		10
	16								
	25								
	16								
	20								
	30	J2	7	7	8		15		7
	21								
	35								
	38								
10	51							GR. FINE TO COARSE SAND	
	40	J3	10	21	20		18	MOIST NON PLASTIC	6
	35								
	52								
	58								
	61								
	50	J4	10	18	21		12		6
	42								
	65								
	72								
20	76							20'	
	60	J5	3	6	6		12		31
	51								
	72								
	75								
	81								
	80	J6	3	6	7		18		32
	71								
	90							GR. SILTY CLAY	
	83							MOIST - PLASTIC	
30	84								
	80	J7	2	4	4		10		36
	77								
	83								
	84								
	86								

THE SUBSURFACE INFORMATION SHOWN HERE WAS OBTAINED FOR STATE DESIGN AND ESTIMATE PURPOSES. IT IS MADE AVAILABLE TO AUTHORIZED USERS ONLY THAT THEY MAY HAVE ACCESS TO THE SAME INFORMATION AVAILABLE TO THE STATE. IT IS PRESENTED IN GOOD FAITH, BUT IS NOT INTENDED AS A SUBSTITUTE FOR INVESTIGATION, INTERPRETATION OR JUDGMENT OF SUCH AUTHORIZED USERS.

CONTRACTOR ACME Drilling, Inc. SM

DRILL RIG OPERATOR Klinedinst
SOIL & ROCK DESCRIP. Chassie
REGIONAL SOILS ENGR. Cheney
SHEET 1 OF 2
STRUCTURE NAME/NO. Apple Freeway #2

HOLE BAF-1

CREATED BY gINT SOFTWARE www.gintsoftware.com

Figure A.2-5. Field log for boring DH BAF-1 (0-35 ft).

REGION 3
COUNTY Orange
PROJECT Interstate 0
DATE START 5/2/92
DATE FINISH 5/3/92
CASING O.D. 2½" I.D. 2¼"
SAMPLER O.D. 2" I.D. 1-3/8"
RIG TYPE Acker B-40
CORE BARREL Double Tube

SUBSURFACE EXPLORATION LOG

HAMMER FALL-CASING 18"
HAMMER FALL-SAMPLER 30"
WEIGHT OF HAMMER-CASING 300 LBS.
WEIGHT OF HAMMER-SAMPLER 140 LBS.

HOLE BAF-1
LINE Baseline
STA. 90+77
OFFSET 50' Rt.
SURF. ELEV. 1001.1

TIME	4:00 pm	8:00 am
DATE	5/2/92	5/3/92
DEPTH TO WATER	15'	15'

DEPTH BELOW SURFACE	BLOWS ON CASING	SAMPLE NO.	BLOWS ON SAMPLER 0/0.5	0.5/1.0	1.0/1.5	1.5/2.0	RECOVER (in)	DESCRIPTION OF SOIL AND ROCK	MOIST CONT %
	80	J8	2	3	3		9		38
	76							GR. SILTY CLAY	
	85							MOIST - PLASTIC	
	87								
40	89							40'	
	81		3	3	50				
	120								
	140								
	156								
	180							GR SANDY GRAVEL	
	160		35	50				MOIST - NON PLASTIC	
	195								
	200								
	210								
50	230							TOP OF ROCK 50'	
							55	HARD UNWEATHERED BASALT	
								Run 1 50 - 55'	
								RQD = 70%	
								55'	
							56	HARD UNWEATHERED BASALT	
								Run 2 55 - 60'	
								RQD = 80%	
60								60'	
								END OF BORING 60'	
70									

THE SUBSURFACE INFORMATION SHOWN HERE WAS OBTAINED FOR STATE DESIGN AND ESTIMATE PURPOSES. IT IS MADE AVAILABLE TO AUTHORIZED USERS ONLY THAT THEY MAY HAVE ACCESS TO THE SAME INFORMATION AVAILABLE TO THE STATE. IT IS PRESENTED IN GOOD FAITH, BUT IS NOT INTENDED AS A SUBSTITUTE FOR INVESTIGATION, INTERPRETATION OR JUDGMENT OF SUCH AUTHORIZED USERS.

CONTRACTOR ACME Drilling, Inc. SM

DRILL RIG OPERATOR Klinedinst
SOIL & ROCK DESCRIP. Chassie
REGIONAL SOILS ENGR. Cheney
SHEET 2 OF 2
STRUCTURE NAME/NO. Apple Freeway #2

HOLE BAF-1

Figure A.2-5 (Continued). Field log for boring DH BAF-1 (35-60 ft).

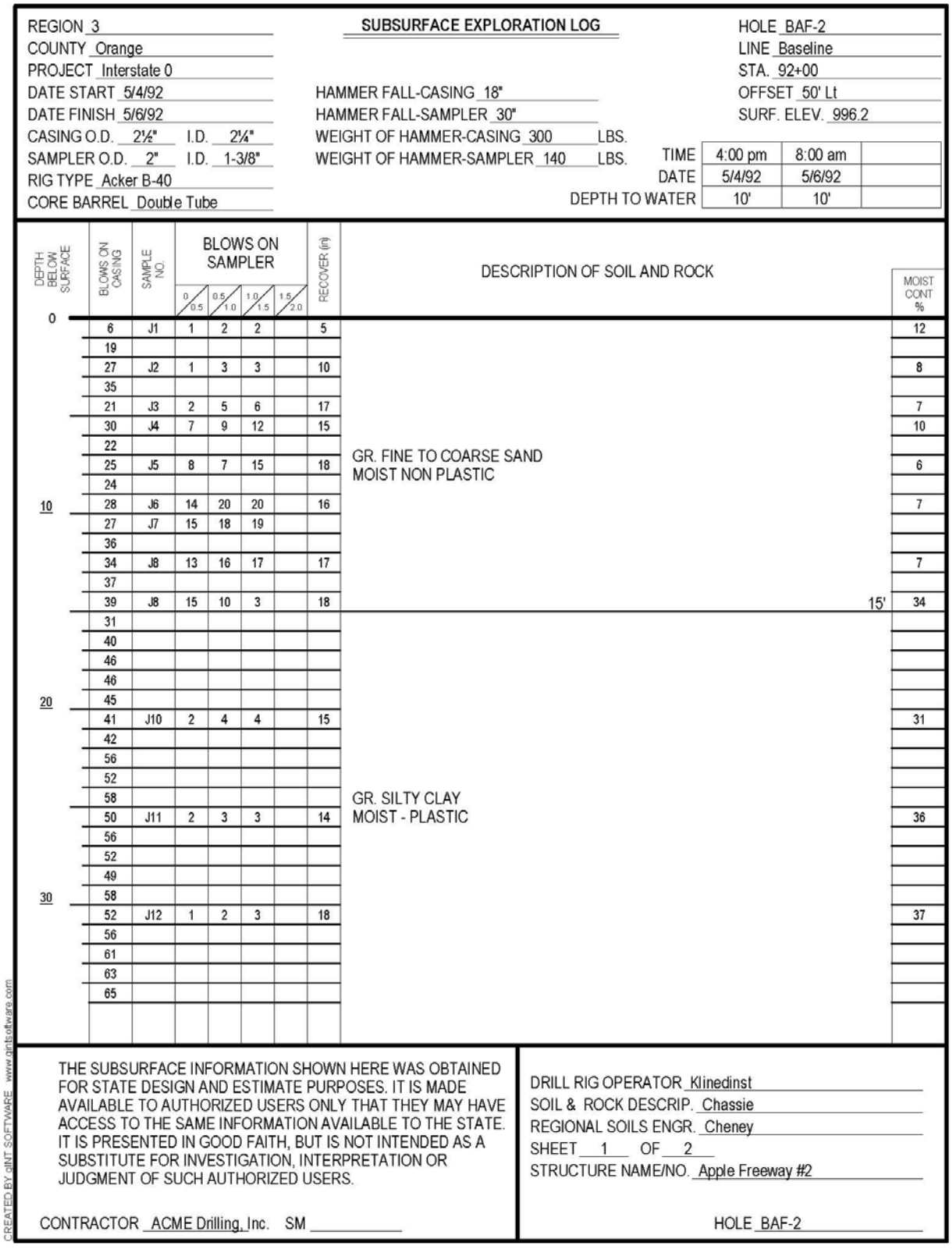

SUBSURFACE EXPLORATION LOG

REGION 3
COUNTY Orange
PROJECT Interstate 0
DATE START 5/4/92
DATE FINISH 5/6/92
CASING O.D. 2½" I.D. 2¼"
SAMPLER O.D. 2" I.D. 1-3/8"
RIG TYPE Acker B-40
CORE BARREL Double Tube

HAMMER FALL-CASING 18"
HAMMER FALL-SAMPLER 30"
WEIGHT OF HAMMER-CASING 300 LBS.
WEIGHT OF HAMMER-SAMPLER 140 LBS.

HOLE BAF-2
LINE Baseline
STA. 92+00
OFFSET 50' Lt
SURF. ELEV. 996.2

TIME	4:00 pm	8:00 am
DATE	5/4/92	5/6/92
DEPTH TO WATER	10'	10'

DEPTH BELOW SURFACE	BLOWS ON CASING	SAMPLE NO.	BLOWS ON SAMPLER 0/0.5	0.5/1.0	1.0/1.5	1.5/2.0	RECOVER (in)	DESCRIPTION OF SOIL AND ROCK	MOIST CONT %
0	6	J1	1	2	2		5		12
	19								
	27	J2	1	3	3		10		8
	35								
	21	J3	2	5	6		17		7
	30	J4	7	9	12		15		10
	22								
	25	J5	8	7	15		18	GR. FINE TO COARSE SAND MOIST NON PLASTIC	6
	24								
10	28	J6	14	20	20		16		7
	27	J7	15	18	19				
	36								
	34	J8	13	16	17		17		7
	37								
	39	J8	15	10	3		18	15'	34
	31								
	40								
	46								
	46								
20	45								
	41	J10	2	4	4		15		31
	42								
	56								
	52								
	58							GR. SILTY CLAY MOIST - PLASTIC	
	50	J11	2	3	3		14		36
	56								
	52								
	49								
30	58								
	52	J12	1	2	3		18		37
	56								
	61								
	63								
	65								

THE SUBSURFACE INFORMATION SHOWN HERE WAS OBTAINED FOR STATE DESIGN AND ESTIMATE PURPOSES. IT IS MADE AVAILABLE TO AUTHORIZED USERS ONLY THAT THEY MAY HAVE ACCESS TO THE SAME INFORMATION AVAILABLE TO THE STATE. IT IS PRESENTED IN GOOD FAITH, BUT IS NOT INTENDED AS A SUBSTITUTE FOR INVESTIGATION, INTERPRETATION OR JUDGMENT OF SUCH AUTHORIZED USERS.

CONTRACTOR ACME Drilling, Inc. SM

DRILL RIG OPERATOR Klinedinst
SOIL & ROCK DESCRIP. Chassie
REGIONAL SOILS ENGR. Cheney
SHEET 1 OF 2
STRUCTURE NAME/NO. Apple Freeway #2

HOLE BAF-2

CREATED BY gINT SOFTWARE www.gintsoftware.com

Figure A.2-6. Field log for boring DH BAF-2 (0-35 ft).

REGION 3
COUNTY Orange
PROJECT Interstate 0
DATE START 5/4/92
DATE FINISH 5/6/92
CASING O.D. 2½" I.D. 2¼"
SAMPLER O.D. 2" I.D. 1-3/8"
RIG TYPE Acker B-40
CORE BARREL Double Tube

SUBSURFACE EXPLORATION LOG

HAMMER FALL-CASING 18"
HAMMER FALL-SAMPLER 30"
WEIGHT OF HAMMER-CASING 300 LBS.
WEIGHT OF HAMMER-SAMPLER 140 LBS.

HOLE BAF-2
LINE Baseline
STA. 92+00
OFFSET 50' Lt
SURF. ELEV. 996.2

TIME	4:00 pm	8:00 am	
DATE	5/4/92	5/6/92	
DEPTH TO WATER	10'	10'	

DEPTH BELOW SURFACE	BLOWS ON CASING	SAMPLE NO.	BLOWS ON SAMPLER 0/0.5	0.5/1.0	1.0/1.5	1.5/2.0	RECOVER (in)	DESCRIPTION OF SOIL AND ROCK	MOIST CONT %
	62	J13	1	2	4		16	GR. SILTY CLAY	34
	63							MOIST - PLASTIC	
	72								
	71							39'	
40	89								
	75		30	20	35				
	81								
	104								
	120							GR SANDY GRAVEL	
	140							MOIST - NON PLASTIC	
	110							(Cored Boulder 42.5' to 45' recovered 12"-7 pieces: used boulder buster)	
	136								
	166								
	191								
50	482							TOP OF ROCK 50'	
								HARD UNWEATHERED BASALT	
								Run 1 50 - 55'	
								RQD = 80%	
								55'	
								HARD UNWEATHERED BASALT	
								Run 2 55 - 60'	
60								RQD = 75%	
								60'	
								END OF BORING 60'	
70									

THE SUBSURFACE INFORMATION SHOWN HERE WAS OBTAINED FOR STATE DESIGN AND ESTIMATE PURPOSES. IT IS MADE AVAILABLE TO AUTHORIZED USERS ONLY THAT THEY MAY HAVE ACCESS TO THE SAME INFORMATION AVAILABLE TO THE STATE. IT IS PRESENTED IN GOOD FAITH, BUT IS NOT INTENDED AS A SUBSTITUTE FOR INVESTIGATION, INTERPRETATION OR JUDGMENT OF SUCH AUTHORIZED USERS.

CONTRACTOR ACME Drilling, Inc. SM

DRILL RIG OPERATOR Klinedinst
SOIL & ROCK DESCRIP. Chassie
REGIONAL SOILS ENGR. Cheney
SHEET 2 OF 2
STRUCTURE NAME/NO. Apple Freeway #2

HOLE BAF-2

Figure A.2-6 (Continued). Field log for boring DH BAF-2 (35-60 ft).

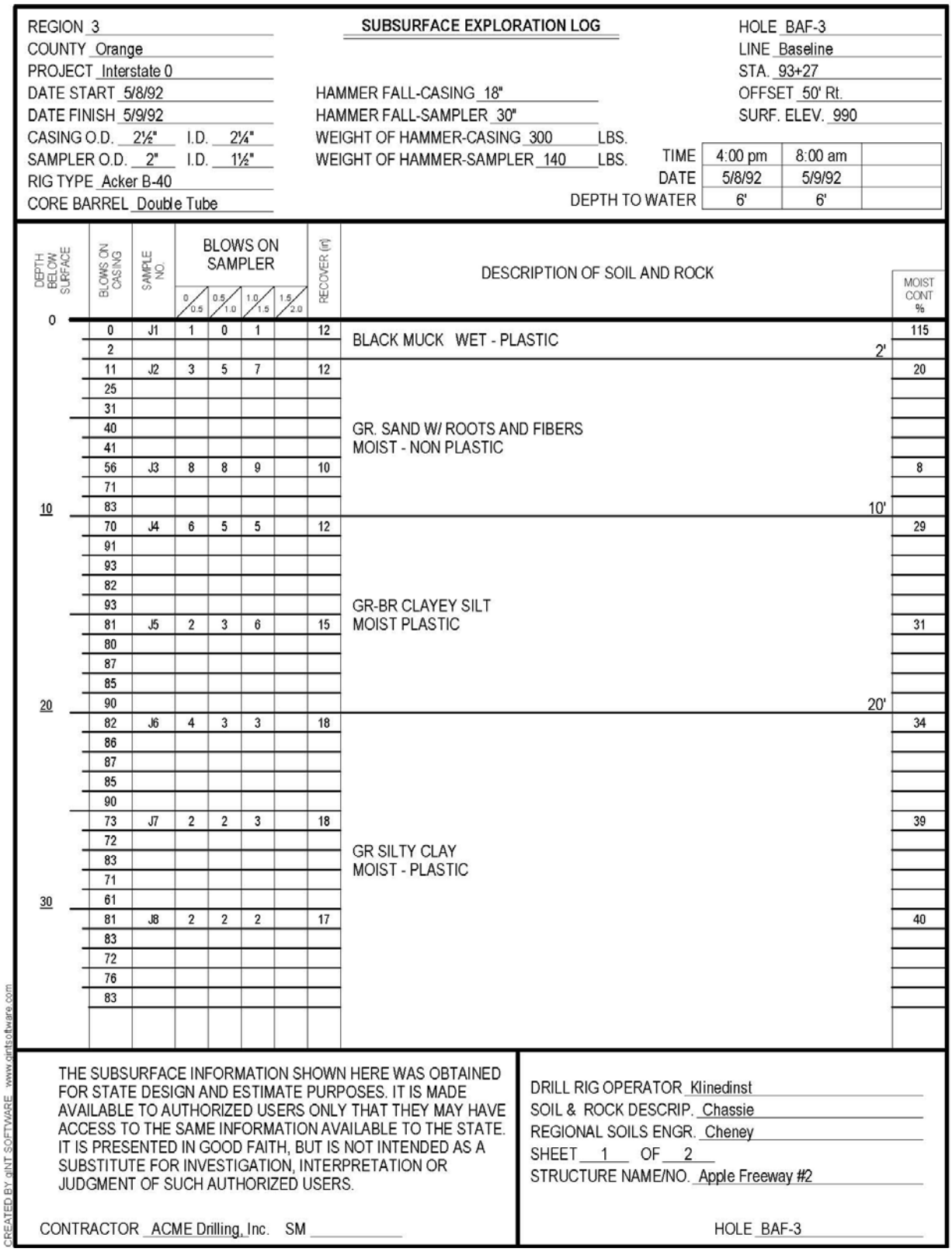

REGION 3
COUNTY Orange
PROJECT Interstate 0
DATE START 5/8/92
DATE FINISH 5/9/92
CASING O.D. 2½" I.D. 2¼"
SAMPLER O.D. 2" I.D. 1½"
RIG TYPE Acker B-40
CORE BARREL Double Tube

SUBSURFACE EXPLORATION LOG

HAMMER FALL-CASING 18"
HAMMER FALL-SAMPLER 30"
WEIGHT OF HAMMER-CASING 300 LBS.
WEIGHT OF HAMMER-SAMPLER 140 LBS.

HOLE BAF-3
LINE Baseline
STA. 93+27
OFFSET 50' Rt.
SURF. ELEV. 990

TIME	4:00 pm	8:00 am	
DATE	5/8/92	5/9/92	
DEPTH TO WATER	6'	6'	

DEPTH BELOW SURFACE	BLOWS ON CASING	SAMPLE NO.	BLOWS ON SAMPLER 0/0.5	0.5/1.0	1.0/1.5	1.5/2.0	RECOVER (in)	DESCRIPTION OF SOIL AND ROCK	MOIST CONT %
0	0	J1	1	0	1		12	BLACK MUCK WET - PLASTIC	115
	2							2'	
	11	J2	3	5	7		12		20
	25								
	31								
	40							GR. SAND W/ ROOTS AND FIBERS	
	41							MOIST - NON PLASTIC	
	56	J3	8	8	9		10		8
	71								
10	83							10'	
	70	J4	6	5	5		12		29
	91								
	93								
	82								
	93							GR-BR CLAYEY SILT	
	81	J5	2	3	6		15	MOIST PLASTIC	31
	80								
	87								
	85								
20	90							20'	
	82	J6	4	3	3		18		34
	86								
	87								
	85								
	90								
	73	J7	2	2	3		18		39
	72								
	83							GR SILTY CLAY	
	71							MOIST - PLASTIC	
30	61								
	81	J8	2	2	2		17		40
	83								
	72								
	76								
	83								

THE SUBSURFACE INFORMATION SHOWN HERE WAS OBTAINED FOR STATE DESIGN AND ESTIMATE PURPOSES. IT IS MADE AVAILABLE TO AUTHORIZED USERS ONLY THAT THEY MAY HAVE ACCESS TO THE SAME INFORMATION AVAILABLE TO THE STATE. IT IS PRESENTED IN GOOD FAITH, BUT IS NOT INTENDED AS A SUBSTITUTE FOR INVESTIGATION, INTERPRETATION OR JUDGMENT OF SUCH AUTHORIZED USERS.

CONTRACTOR ACME Drilling, Inc. SM

DRILL RIG OPERATOR Klinedinst
SOIL & ROCK DESCRIP. Chassie
REGIONAL SOILS ENGR. Cheney
SHEET 1 OF 2
STRUCTURE NAME/NO. Apple Freeway #2

HOLE BAF-3

CREATED BY gINT SOFTWARE www.gintsoftware.com

Figure A.2-7. Field log for boring DH BAF-3 (0-35 ft).

REGION 3
COUNTY Orange
PROJECT Interstate 0
DATE START 5/8/92
DATE FINISH 5/9/92
CASING O.D. 2½" I.D. 2¼"
SAMPLER O.D. 2" I.D. 1½"
RIG TYPE Acker B-40
CORE BARREL Double Tube

SUBSURFACE EXPLORATION LOG

HAMMER FALL-CASING 18"
HAMMER FALL-SAMPLER 30"
WEIGHT OF HAMMER-CASING 300 LBS.
WEIGHT OF HAMMER-SAMPLER 140 LBS.

HOLE BAF-3
LINE Baseline
STA. 93+27
OFFSET 50' Rt.
SURF. ELEV. 990

TIME	4:00 pm	8:00 am
DATE	5/8/92	5/9/92
DEPTH TO WATER	6'	6'

DEPTH BELOW SURFACE	BLOWS ON CASING	SAMPLE NO.	BLOWS ON SAMPLER 0/0.5	0.5/1.0	1.0/1.5	1.5/2.0	RECOVER (in)	DESCRIPTION OF SOIL AND ROCK	MOIST CONT %
	71	J9	2	3	2		14		36
	79								
	86								
	83							GR SILTY CLAY	
	85							MOIST - PLASTIC	
40	82	J10	3	4	3		15		35
	81								
	93								
	91								
	96							45'	
	121	J11	20	21	35		13		10
	450								
	391								
	220								
50	230								
	200	J12	15	36	40		12	GR. SILTY GRAVEL	5
	370							MOIST - NON PLASTIC	
	400							52' to 53' CORED BOULDER	
	410							RECOVERY 3"	
	380							MANY FRAGMENTS	
		J13	40	60	80		15		7
60									
		J14	100			Refusal		TOP OF ROCK 60.5'	
								HARD UNWEATEHRED BASALT	
								Run 1 60.5 - 65'	
								RQD = 70%	
								65'	
								HARD UNWEATEHRED BASALT	
								Run 2 65 - 70.5'	
								RQD = 95%	
								69'	
70									
								END OF BORING 69'	

THE SUBSURFACE INFORMATION SHOWN HERE WAS OBTAINED FOR STATE DESIGN AND ESTIMATE PURPOSES. IT IS MADE AVAILABLE TO AUTHORIZED USERS ONLY THAT THEY MAY HAVE ACCESS TO THE SAME INFORMATION AVAILABLE TO THE STATE. IT IS PRESENTED IN GOOD FAITH, BUT IS NOT INTENDED AS A SUBSTITUTE FOR INVESTIGATION, INTERPRETATION OR JUDGMENT OF SUCH AUTHORIZED USERS.

CONTRACTOR ACME Drilling, Inc. SM

DRILL RIG OPERATOR Klinedinst
SOIL & ROCK DESCRIP. Chassie
REGIONAL SOILS ENGR. Cheney
SHEET 2 OF 2
STRUCTURE NAME/NO. Apple Freeway #2

HOLE BAF-3

Figure A.2-7 (Continued). Field log for boring DH BAF-3 (35-69 ft).

REGION 3
COUNTY Orange
PROJECT Interstate 0
DATE START 5/10/92
DATE FINISH 5/12/92
CASING O.D. 4" I.D. 3½"
SAMPLER O.D. 2" I.D. 1-3/8"
RIG TYPE Acker B-40
CORE BARREL Double Tube

SUBSURFACE EXPLORATION LOG

HAMMER FALL-CASING 18"
HAMMER FALL-SAMPLER 30"
WEIGHT OF HAMMER-CASING 300 LBS.
WEIGHT OF HAMMER-SAMPLER 140 LBS.

HOLE BAF-4
LINE Baseline
STA. 93+27
OFFSET 50' Lt
SURF. ELEV. 991

TIME	4:00 pm	8:00 am	3:00 pm
DATE	5/10/92	5/12/92	5/20/93
DEPTH TO WATER	6'	6'	Dry

DEPTH BELOW SURFACE	BLOWS ON CASING	SAMPLE NO.	BLOWS ON SAMPLER 0/0.5	0.5/1.0	1.0/1.5	1.5/2.0	RECOVER (in)	DESCRIPTION OF SOIL AND ROCK	MOIST CONT %
0	0	J1	1	1	1		12	BLACK ORGANIC SILT WET - PLASTIC	120
	2								
	11							3'	
	25								
	31								
	40	J2	4	8	9		12	GR. SAND MOIST - NON PLASTIC	12
	41								
	56								
	71								
10	83							10'	
	70	T3						(10' - 12' PUSHED TUBE)	33
	91								
	93								
	82		Vane					(13' VANE SHEAR TEST)	
	93								
	81	T4						(15' - 17' PUSHED TUBE)	35
	80								
	87								
	85		Vane					(18' VANE SHEAR TEST)	
20	90								
	82	T5						(20' - 22' PUSHED TUBE)	31
	86								
	87							GR. CLAYEY SILT MOIST - PLASTIC	
	85		Vane					(23' VANE SHEAR TEST)	
	75								
	73	T6						(25' - 27' PUSHED TUBE)	36
	72								
	83								
	71	T						(28' - ' PUSHED TUBE)	
30	61								
	81	T7						(30' - 32' PUSHED TUBE)	38
	83								
	72								
	76								
	83								

THE SUBSURFACE INFORMATION SHOWN HERE WAS OBTAINED FOR STATE DESIGN AND ESTIMATE PURPOSES. IT IS MADE AVAILABLE TO AUTHORIZED USERS ONLY THAT THEY MAY HAVE ACCESS TO THE SAME INFORMATION AVAILABLE TO THE STATE. IT IS PRESENTED IN GOOD FAITH, BUT IS NOT INTENDED AS A SUBSTITUTE FOR INVESTIGATION, INTERPRETATION OR JUDGMENT OF SUCH AUTHORIZED USERS.

CONTRACTOR ACME Drilling, Inc. SM

DRILL RIG OPERATOR Klinedinst
SOIL & ROCK DESCRIP. Chassie
REGIONAL SOILS ENGR. Cheney
SHEET 1 OF 2
STRUCTURE NAME/NO. Apple Freeway #2

HOLE BAF-4

Figure A.2-8. Field log for boring DH BAF-4 (0-35 ft).

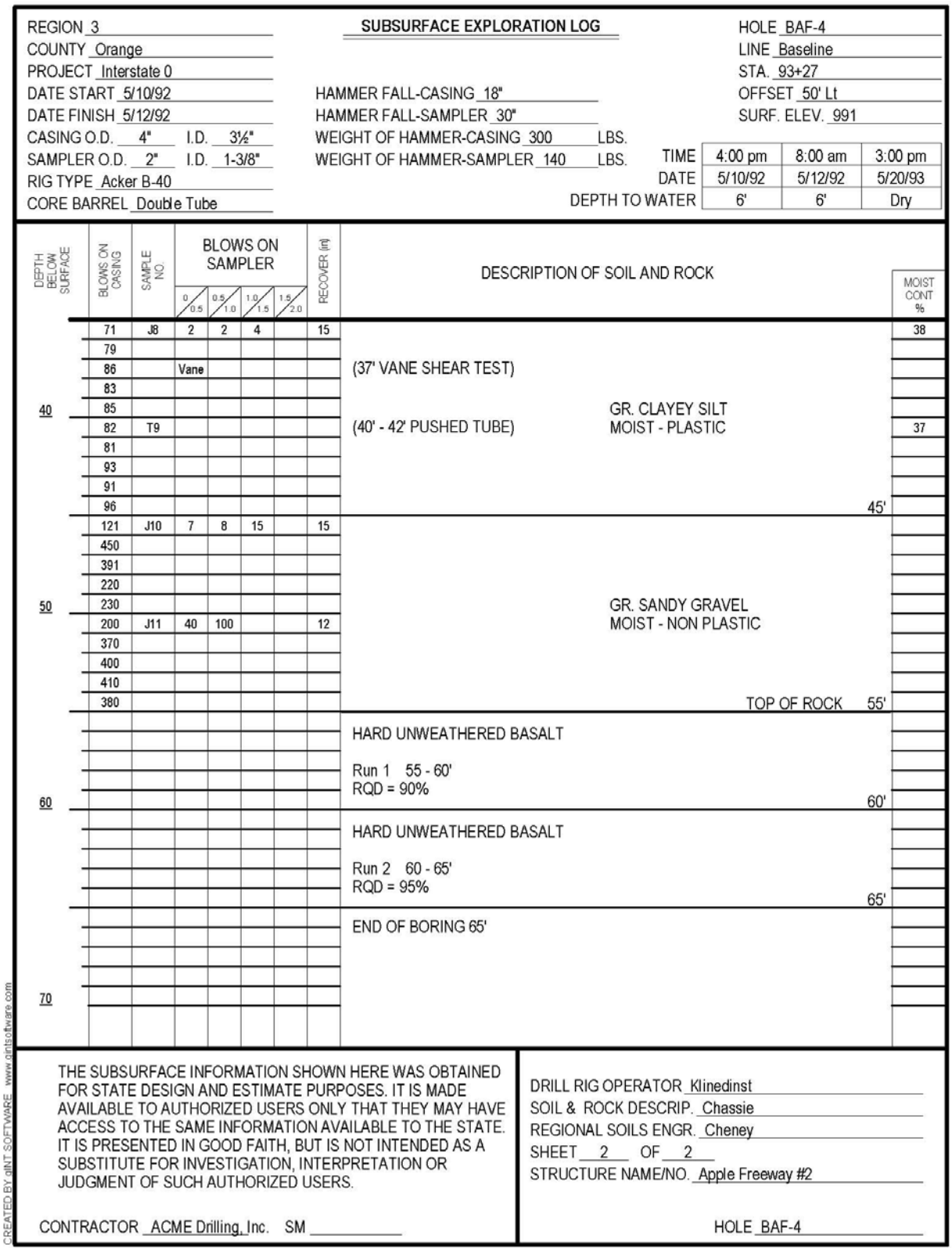

REGION 3
COUNTY Orange
PROJECT Interstate 0
DATE START 5/10/92
DATE FINISH 5/12/92
CASING O.D. 4" I.D. 3½"
SAMPLER O.D. 2" I.D. 1-3/8"
RIG TYPE Acker B-40
CORE BARREL Double Tube

SUBSURFACE EXPLORATION LOG

HAMMER FALL-CASING 18"
HAMMER FALL-SAMPLER 30"
WEIGHT OF HAMMER-CASING 300 LBS.
WEIGHT OF HAMMER-SAMPLER 140 LBS.

HOLE BAF-4
LINE Baseline
STA. 93+27
OFFSET 50' Lt
SURF. ELEV. 991

TIME	4:00 pm	8:00 am	3:00 pm
DATE	5/10/92	5/12/92	5/20/93
DEPTH TO WATER	6'	6'	Dry

DEPTH BELOW SURFACE	BLOWS ON CASING	SAMPLE NO.	BLOWS ON SAMPLER 0/0.5	0.5/1.0	1.0/1.5	1.5/2.0	RECOVER (in)	DESCRIPTION OF SOIL AND ROCK	MOIST CONT %
	71	J8	2	2	4		15		38
	79								
	86		Vane					(37' VANE SHEAR TEST)	
	83								
40	85							GR. CLAYEY SILT	
	82	T9						(40' - 42' PUSHED TUBE) MOIST - PLASTIC	37
	81								
	93								
	91								
	96							45'	
	121	J10	7	8	15		15		
	450								
	391								
	220								
50	230							GR. SANDY GRAVEL	
	200	J11	40	100			12	MOIST - NON PLASTIC	
	370								
	400								
	410								
	380							TOP OF ROCK 55'	
								HARD UNWEATHERED BASALT	
								Run 1 55 - 60' RQD = 90%	
60								60'	
								HARD UNWEATHERED BASALT	
								Run 2 60 - 65' RQD = 95%	
								65'	
								END OF BORING 65'	
70									

THE SUBSURFACE INFORMATION SHOWN HERE WAS OBTAINED FOR STATE DESIGN AND ESTIMATE PURPOSES. IT IS MADE AVAILABLE TO AUTHORIZED USERS ONLY THAT THEY MAY HAVE ACCESS TO THE SAME INFORMATION AVAILABLE TO THE STATE. IT IS PRESENTED IN GOOD FAITH, BUT IS NOT INTENDED AS A SUBSTITUTE FOR INVESTIGATION, INTERPRETATION OR JUDGMENT OF SUCH AUTHORIZED USERS.

CONTRACTOR ACME Drilling, Inc. SM

DRILL RIG OPERATOR Klinedinst
SOIL & ROCK DESCRIP. Chassie
REGIONAL SOILS ENGR. Cheney
SHEET 2 OF 2
STRUCTURE NAME/NO. Apple Freeway #2

HOLE BAF-4

CREATED BY gINT SOFTWARE www.gintsoftware.com

Figure A.2-8 (Continued). Field log for boring DH BAF-4 (35-65 ft).

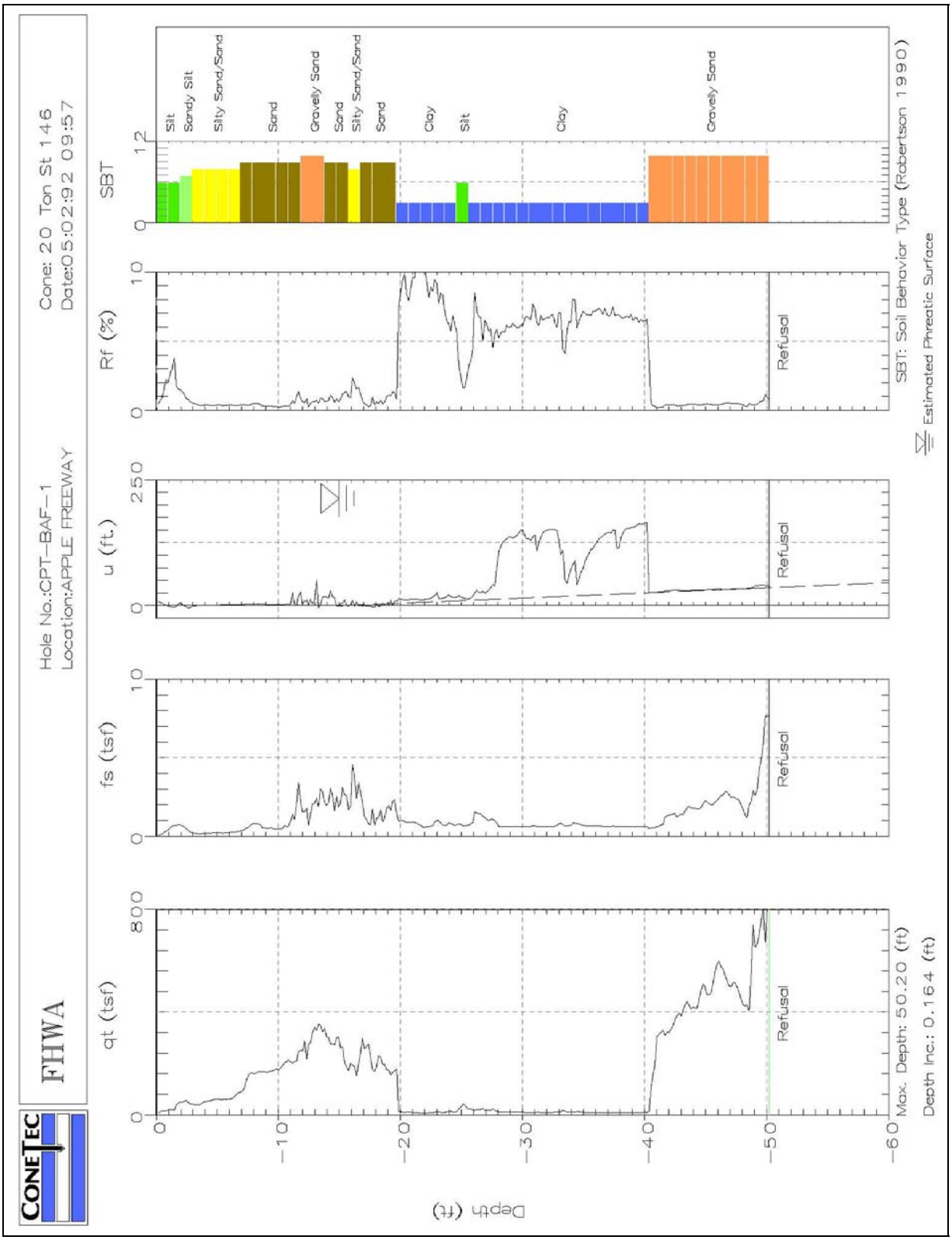

Figure A.2-9. CPT sounding from CPT-BAF-1 in vicinity of DH BAF-1.

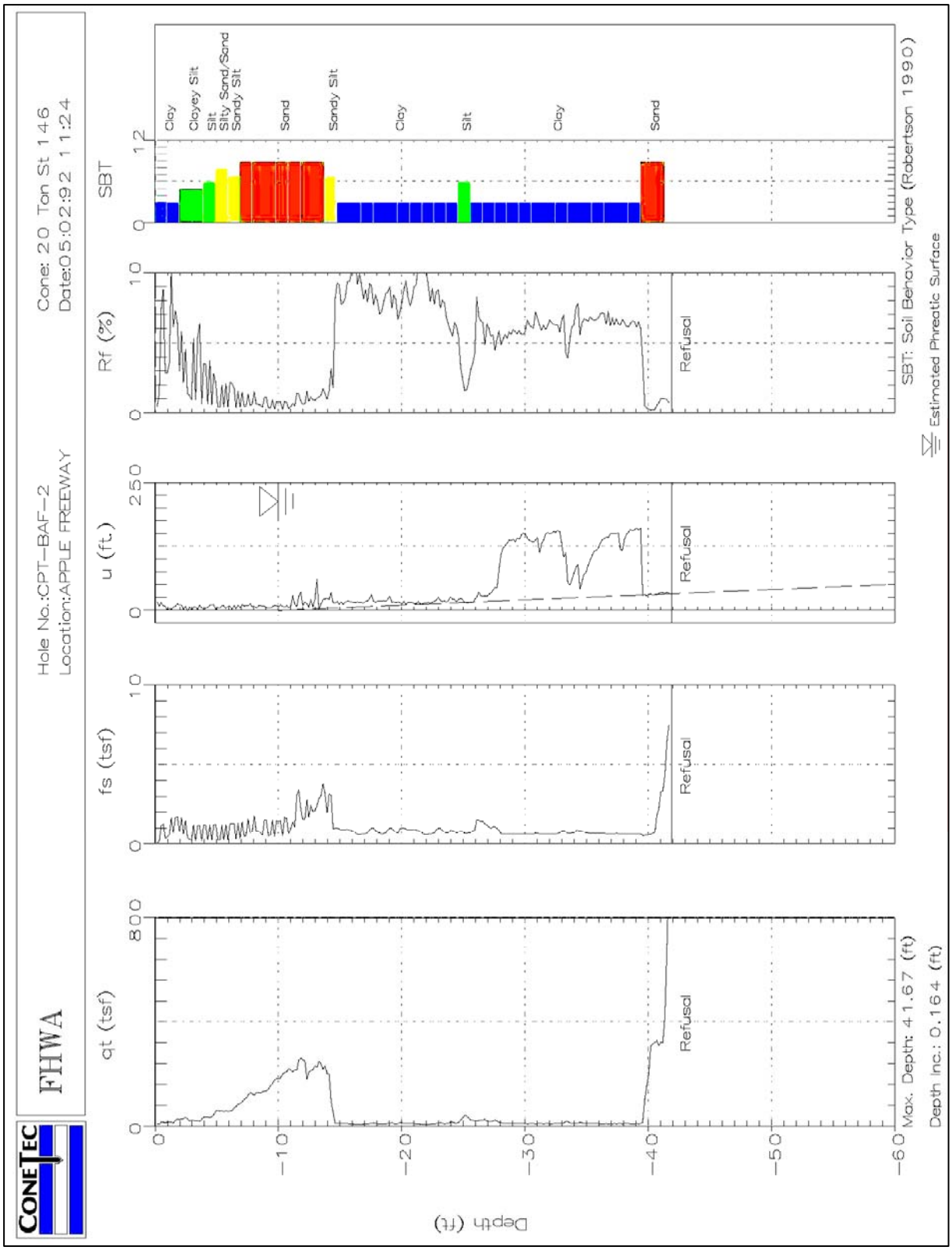

Figure A.2-10. CPT sounding from CPT-BAF-2 in vicinity of DH BAF-2.

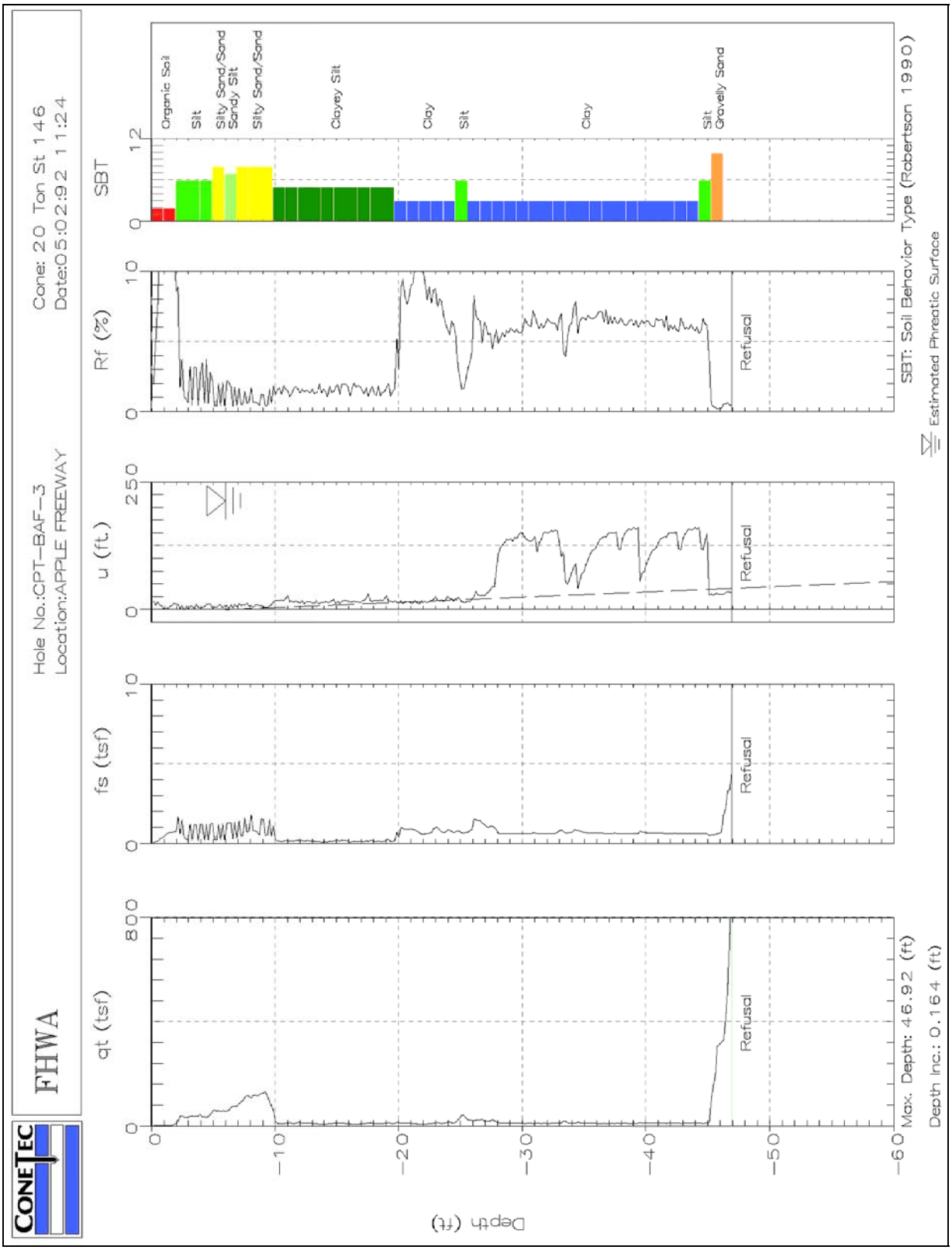

Figure A.2-11. CPT sounding from CPT-BAF-3 in vicinity of DH BAF-3.

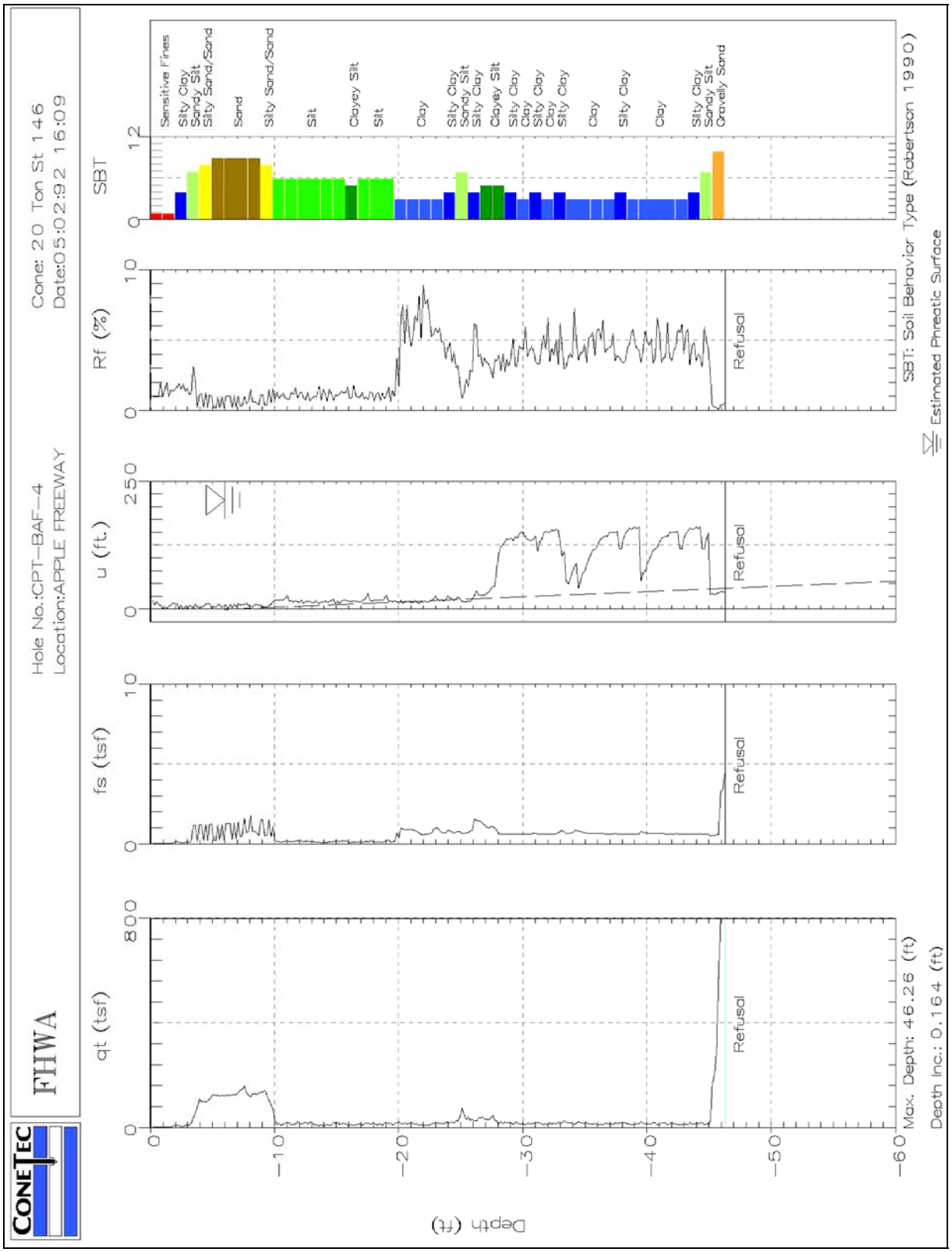

Figure A.2-12. CPT sounding from CPT-BAF-4 in vicinity of UDH BAF-4.

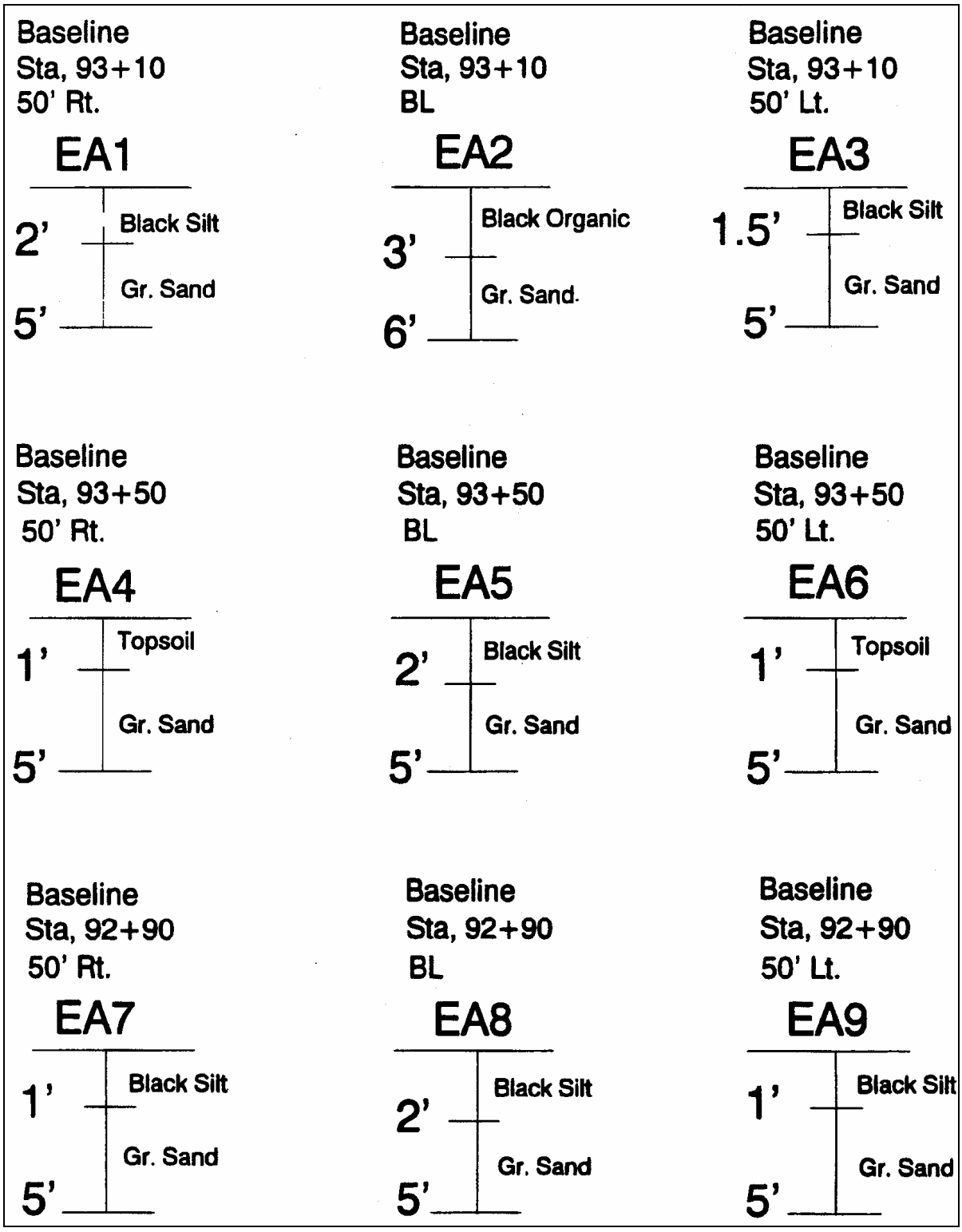

Figure A.2-13. Hand Auger Hole Logs - East Abutment Area.

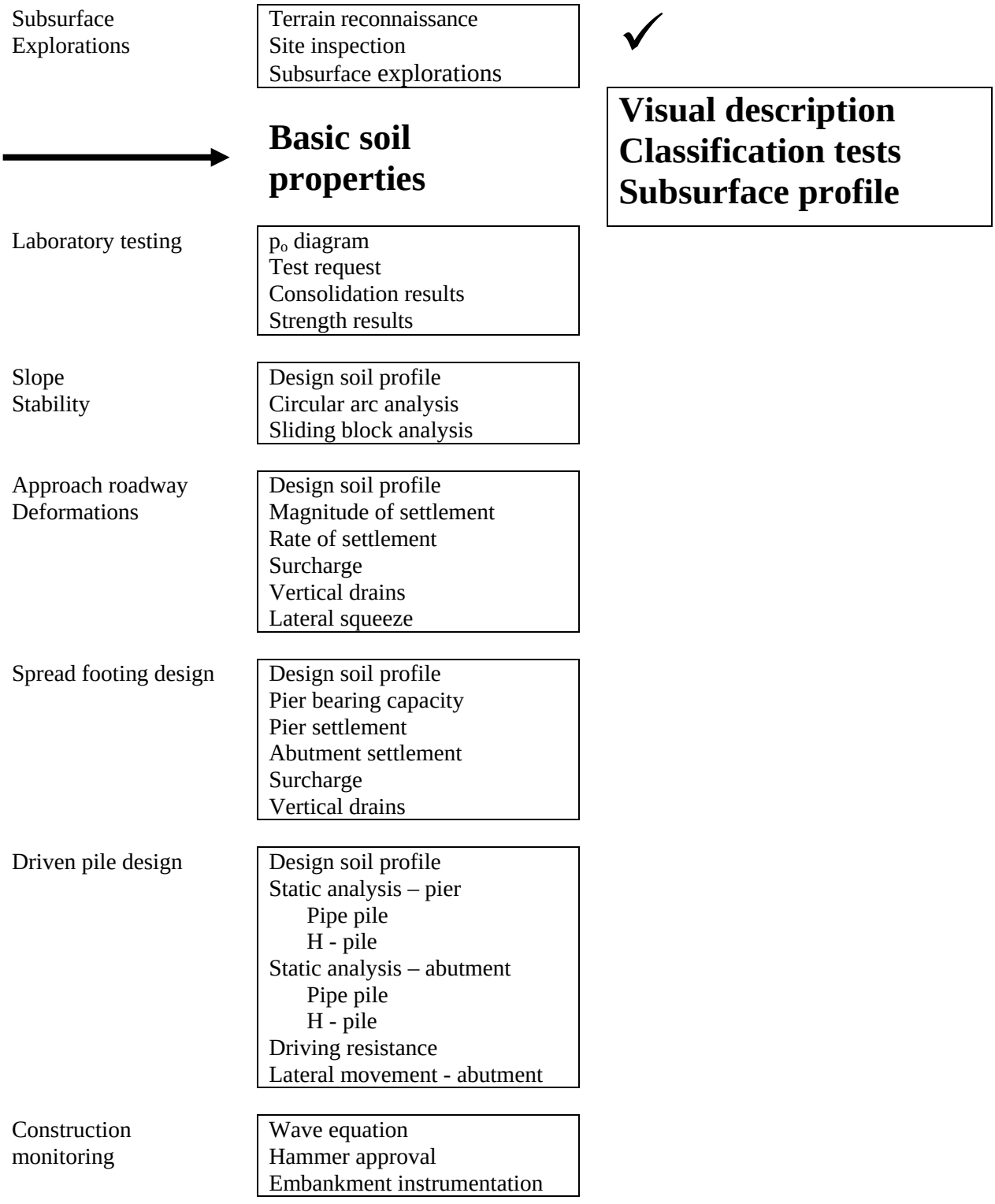

Figure A.3-1. Overview of the geotechnical work to be performed.

SECTION A.3
BASIC SOIL PROPERTIES

A.3-1 RELEVANT CONCEPTS AND PROCEDURES (Refer to Figure A.3-1)

- Visual description of soils – Chapter 4.1
- Classification tests – Chapter 4.2
- Engineering characteristics of main soil types – Chapter 4.3
- Idealized soil profile – Chapter 4.7

In this section the process of estimating the engineering characteristics of the main soil types based on visual descriptions (logs) and classification tests (field and laboratory) is illustrated. The boring logs, CPT soundings and laboratory moisture content test data presented in Appendix A.2-1 are used to illustrate how an idealized soil profile is established for analysis and design. Note that the idealized profile is not suitable for bidding purposes

A.3-2 DETAILED PROCEDURES

Given: Boring logs with SPT-N, logs of CPT soundings, and laboratory moisture content test data.

Required: Develop a preliminary idealized soil profile for analysis and design.

Solution Procedure:

Step 1: **Locate the borings in plan (Refer to Figure A.3-2).**

- Distinguish between SPT borings (target symbols), CPT soundings (large solid circles), and hand-auger borings (small solid circles).
- Use appropriate designations to identify each probe (Refer to Section A.2-2 – Step 2).

Step 2: **Show corresponding elevation view of borings, soundings and auger holes (Refer to Figure A.3-3).**

- Plot the variation of field SPT-N values and laboratory moisture content test data with depth.
- SPT values are boxed and designated by the symbol “N”.
- Corresponding moisture contents are listed to the right of the SPT-N values and are designated by the symbol “W.”
- Make sure the designation used to identify each probe is consistent with

that shown in Figure A.3-2.

- Plot the observed water levels in the borings and the date observed.

Step 3: **Develop a preliminary idealized soil profile by interpolating between borings to identify zones where soils may have similar characteristics.**

- Use SPT-N values and visual descriptions made by field personnel as the initial criteria for distinguishing between different types of soil.
- Include soil descriptions on the elevation drawings.
- Perform a preliminary classification of the soils according to the Unified Soil Classification System (USCS) or some other system commonly used in region. The preliminary classification according to visual-manual procedures (ASTM D2488) will be verified or changed based on the results of the laboratory testing phase of the geotechnical investigation. In lieu of the soil descriptions, USCS symbols may be included on the profile.
- Show the idealized profile on the elevation drawing in terms of zones, with the top and bottom of each zone clearly marked in each boring. The lines between borings are solely for the purpose of the design and should not be shown on bid documents since such well-defined boundaries may not exist in reality.
- Compare the preliminary idealized soil profile with CPT soundings and adjust as necessary.

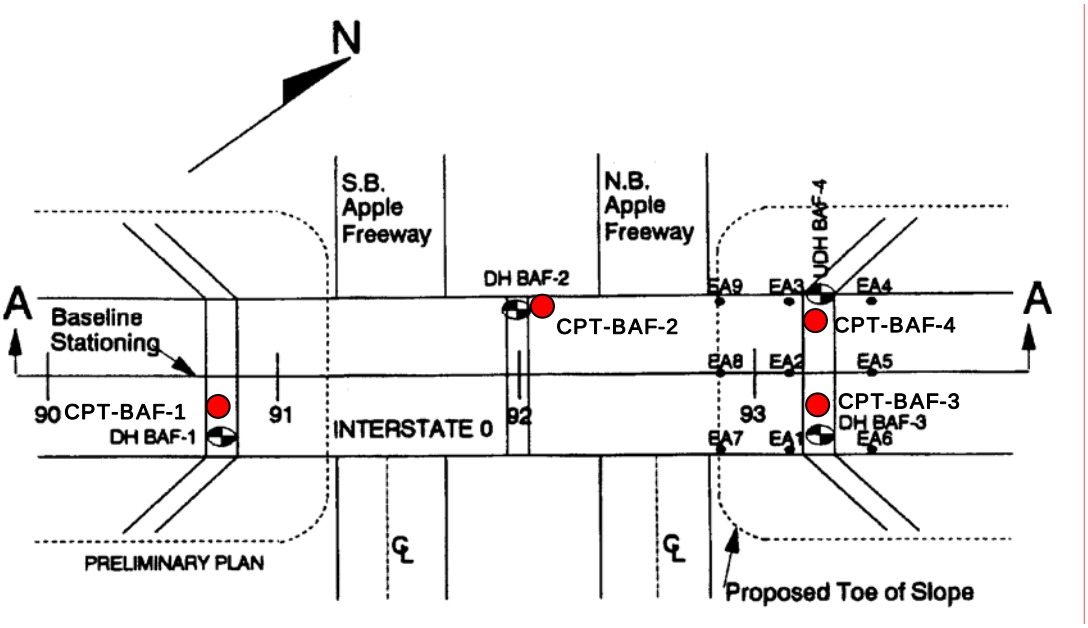

Figure A.3-2. Location Plan – SPT Borings, CPT Soundings and Hand-Auger Holes.

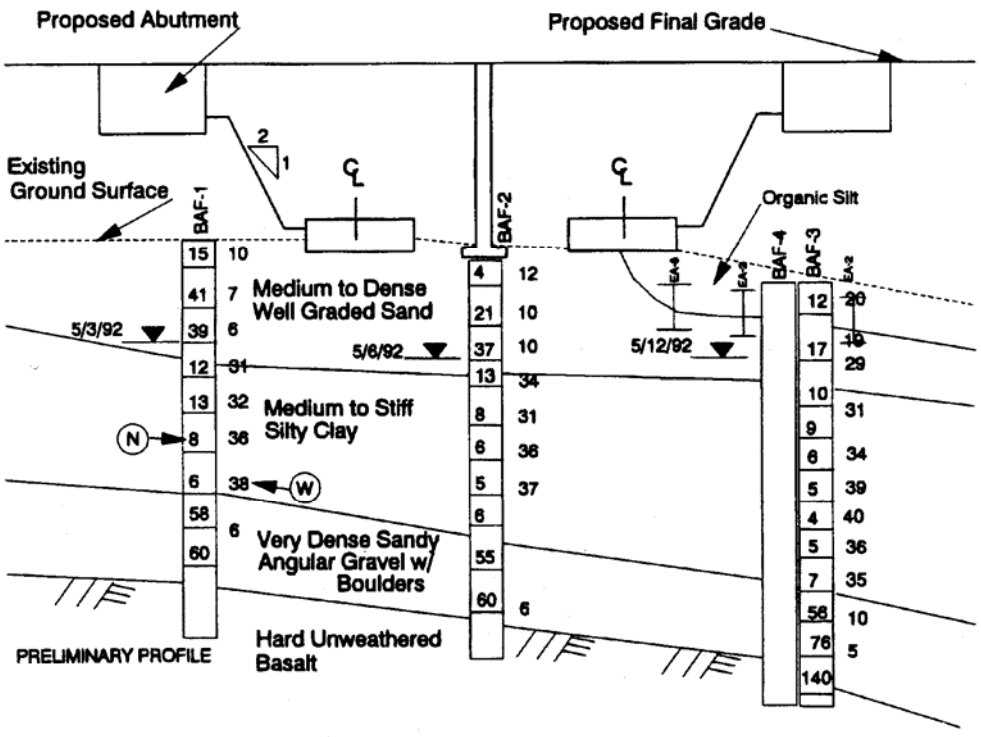

Figure A.3-3. Designer's interpretation of preliminary idealized soil profile through Section A-A.

A.3-3 SUMMARY OF SOIL CHARACTERISTICS FROM RESULTS OF FIELD INVESTIGATIONS AND THEIR USE IN DEVELOPING AN IDEALIZED SOIL PROFILE

1. Boring location (plan and elevation) prepared by designer

    - SPT-N and depth to ground water table are shown on longitudinal and transverse sections cut through selected boring locations shown on plan.

2. Visual description of materials encountered during drilling performed by field personnel

    - Predominant soil types are sand, silty clay and sandy gravel.
    - Rock

3. Visual-manual procedures used by field personnel to classify soils

    - Preliminary classifications are sand (SW), silty clay (CL), and sandy gravel (GW) according to the Unified Soil Classification System

4. Moisture content determined in the laboratory.

    - Values of moisture content are shown on the sections next to SPT-N values.

5. Preliminary idealized soil profile developed based on information shown on the sections.

    - Subsurface variation of soil layers and ground water estimated between borings.
    - Idealized profile expressed in terms of zones with boundaries shown at boring locations only.
    - Profile may differ in transverse and longitudinal directions.
    - Preliminary profile compared to CPT soundings to refine characteristics of soils identified. For example, CPT soundings indicate that the silty clay layer may contain distinct seams of silt. The presence of such seams may help to reduce consolidation time.

[THIS PAGE INTENTIONALLY BLANK]

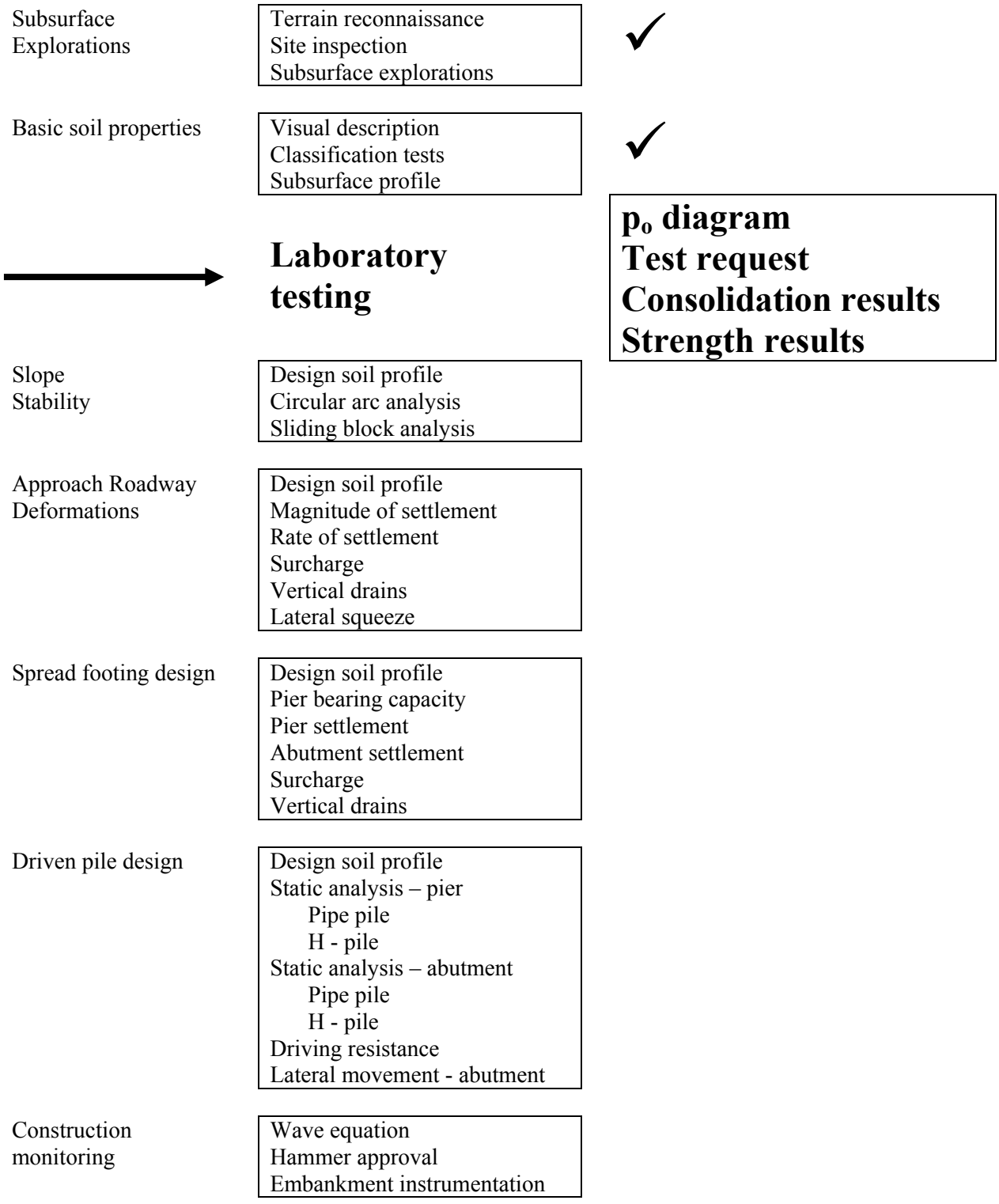

Figure A.4-1. Status of geotechnical work.

SECTION A.4
LABORATORY TESTING

A.4-1 RELEVANT CONCEPTS AND PROCEDURES (Refer to Figure A.4-1)

- Construction of the p_o diagram – Example 2-1.
- Preparation of a soil mechanics laboratory test request.
- Presentation of typical consolidation test results – Chapter 5.4.
- Presentation of typical strength test results – Chapter 5.5.

In this section the construction of a p_o diagram based on the Apple Freeway soil profile is demonstrated. A laboratory test request for consolidation and strength tests is presented. The numerical results of such tests are included in tabular form at the end of the chapter. The results are also presented in graphical form to show the variation of maximum past effective stress (p_c) and undrained shear strength (s_u) with depth.

A.4-2 DETAILED PROCEDURES

Given: Preliminary idealized soil profile as determined in Section A.3 and total (γ_t) and dry (γ_d) unit weights of soils in the profile as determined from laboratory tests (Refer to Chapter 2)

Required:

- Construct the p_o diagram (Refer to Figure A.4-2). The p_o diagram represents the variation of the effective geostatic vertical stress (p_o) with depth. Typically, the variation of the total geostatic vertical stress (p_t) with depth is also shown on the p_o diagram to illustrate the effect of the groundwater table on the effective stress distribution. The difference between the two curves is the hydrostatic pore water pressure (p_w) (Refer to Chapter 2)
- Prepare laboratory test request for consolidation and strength testing (Refer to Figure A.4-3).
- Superimpose on the p_o diagram a plot of the maximum past effective stress (p_c) as determined from the results of consolidation tests (Refer to Figure A.4-4 and Table A.4-3).
- Prepare a plot of undrained shear strength (s_u) with depth based on the results of vane shear tests, unconsolidated -undrained (UU) and consolidated-undrained (CU) triaxial tests (Refer to Figure A.4-5 and Table A.4-4)

Solution:

Step 1: Construct the p_o diagram at boring UDH BAF – 4.

- UDH BAF – 4 is the boring where the samples for strength and consolidation tests were obtained.
- Table A.4-1 shows the unit weights of the soils in the idealized profile as determined in the laboratory.
- The computations for p_o, p_t, and p_w at soil layer and ground water table boundaries are shown in Table A.4-2. (Refer to Chapter 2 and Example 2-1)

Step 2: Based on the effective geostatic vertical pressure (p_o) at each depth specify test parameter for consolidation and strength tests.

- Specify loads, test duration and loading pattern for consolidation tests (Refer to Figure A.4-3)
- Specify confining pressure for UU tests corresponding to total in situ geostatic vertical stress at the depth from which each sample was retrieved (Refer to Figure A.4-3)
- Specify three consolidation pressures for each CU test starting with p_o at the depth from which each sample was retrieved (Refer to Figure A.4-3).

Step 3: Use the results laboratory tests to determine design parameters.

- From consolidation test results determine the maximum past effective stress (p_c), the compression index (C_c), the recompression index (C_r) and the coefficient of consolidation (c_v) for samples retrieved at various depths (Refer to Table A.4-3).
- Plot the values of maximum past effective stress (p_c) as estimated from the results of the consolidation tests on the p_o diagram to determine the stress history of the compressible layer (Refer to Figure A.4-4). Since the OCR (p_c/p_o) >1, the soil is overconsolidated (Refer to Chapter 5.4)
- From UU tests determine the undrained shear strength (s_u) directly as one-half the undrained shear strength (Refer to Table A.4-4).
- From CU tests determine the undrained shear strength (s_u) as one-half the undrained shear strength for each sample consolidated under a confining pressure equal to p_o at the depth from it was retrieved (Refer to Table A.4-4).
- From vane shear tests determine the undrained shear strength directly as one-half the measured undrained shear strength for both undisturbed and

remolded conditions (Refer to Table A.4-4).

- Plot the results of the vane shear tests (V), UU tests (U) and CU tests (C) versus depth in the clay layer (Refer to Figure A.4-5). Select 1,100 psf as the design value since it is (a) close to the middle of the consolidating clay layer and (b) it is a lower bound value.

A.4-3 Summary of Laboratory Testing and Illustration of the Use of Laboratory Test Results to Obtain Values for Geotechnical Design Parameters

1. Construct p_o diagram
   - Show increase of total and effective vertical geostatic pressures with depth
   - Show effect of groundwater table and hydrostatic pore water pressure

2. Prepare soil mechanics laboratory test request
   - Assign consolidation test pressures and load times.
   - Assign confining pressures for UU strength test to simulate variation of total geostatic pressures with depth.
   - Assign range of consolidation pressures for CU test performed on samples retrieved from various depths to simulate effective stresses states ranging from initial value to final value due to the embankment.

3. Consolidation test results
   - Determine compression and recompression indices, maximum past effective stress, overconsolidation ratio (OCR), and coefficient of consolidation at various depths within the silty clay deposit.

4. Strength test results
   - Determine variation of undrained shear strength with depth (confining pressure) from results of vane shear tests.
   - Determine variation of undrained shear strength with depth (confining pressure) from results of UU tests.
   - Determine variation of undrained shear strength with depth (confining pressure) from results of CU tests.
   - Compare differences of undrained shear strength obtained from the three tests and select a design value based on anticipated loading conditions.

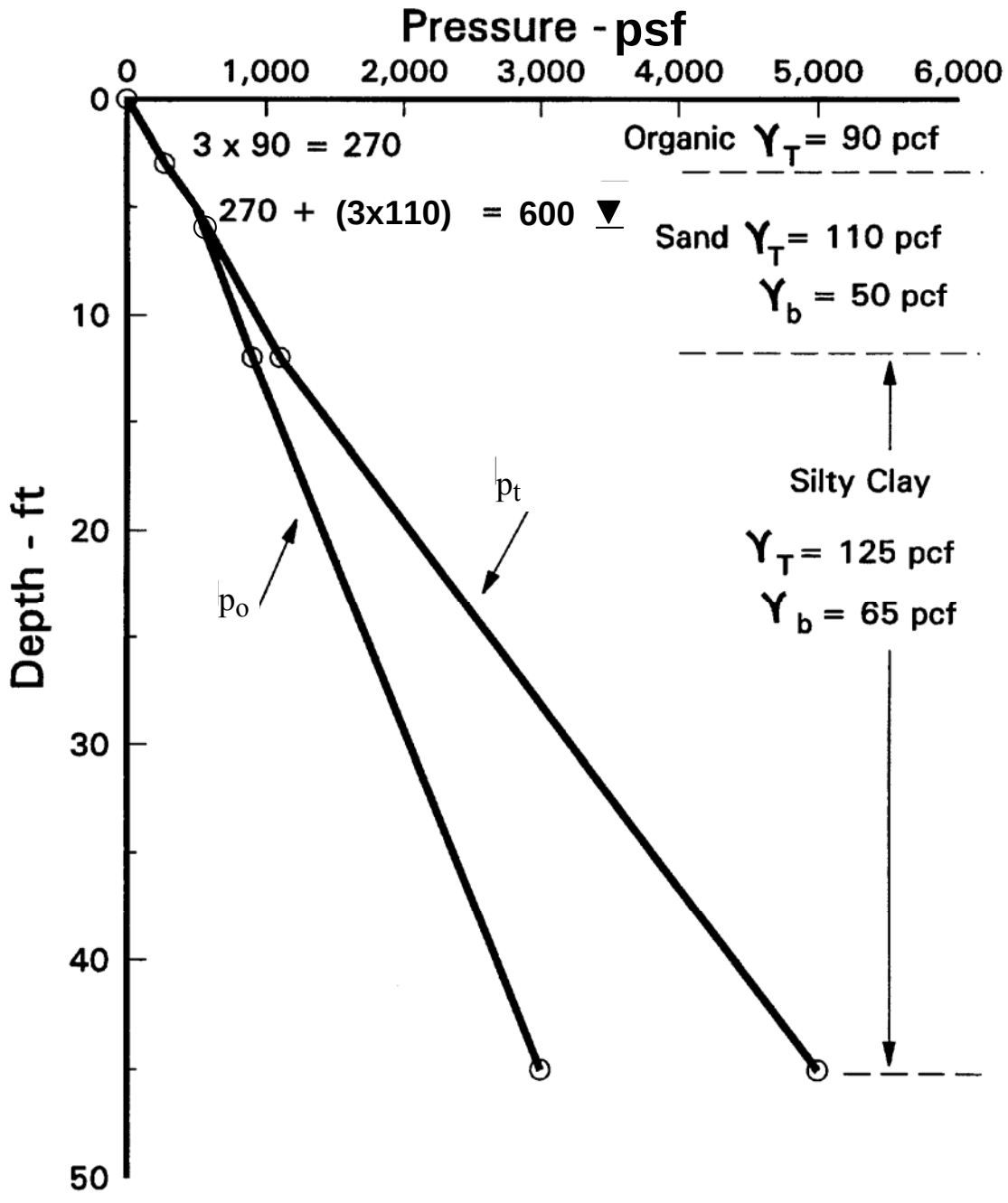

Figure A.4-2. The p_o diagram for boring UDH BAF – 4
(Note: Ground water was encountered at a depth of 6 ft in UDH BAF-4).

SOIL MECHANICS LABORATORY TEST REQUEST

PROJECT I-10 APPLE FREEWAY — PROJ. NO. 23127 — HOLE NO. BAE-4
DATE 6-3-82 REQUEST BY _____ APPROVED BY _____ — STATION _____ OFFSET 50'LT
ORIGINAL REQUEST ☒ SUPPLEMENTAL REQUEST ☐

CONSOLIDATION TESTS					STRENGTH TESTS												SPECIAL AND ADDITIONAL TESTS**		
								TYPE OF TEST AND CONSOLIDATION PRESSURE											
SAMPLE NUMBER	MACHINE CAPACITY	LOAD BY FOR LOAD	LOAD TIME	RECYCLE	STATUS*	SAMPLE NUMBER	SAMPLE DIAM. 1.4" / D_{TUBE}	U	UU*	CONF. PRESS (PSI)	CU	CONS. PRESS (PSI) 1	2	3	STATUS*	% ORG.	% INERT	
T3	32K	500	3 hr.	Yes		T4		Full	✓	12									
T4		1000		Yes		T4	✓				✓	8	21	36					
T5				No		T5		Full	✓	17									
T6				Yes		T5	✓				✓	10	24	38					
T7				No		T6		Full	✓	21									
T9			↓	No		T6	✓				✓	12	26	40					
						T7		Full	✓	26									
						T7	✓				✓	15	29	43					
						T9		Full	✓	33									
						T9	✓				✓	19	33	47					
									*			*							
									Proof			Proof							

ADDITIONAL REQUESTS: CONSOLIDATION TESTS - SPECIFIC GRAVITY ON ALL TESTS
STRENGTH TESTS - ATTERBURG LIMITS AND HYDROMETER ON ALL TESTS

* CHECK MARK WHEN TEST IS PUT IN PROGRESS ✓ ; CIRCLE WHEN COMPLETED (✓) ; CROSS HATCH WHEN COMPUTED ⊗
** TO SUPPLEMENT ROUTINE CLASSIFICATION TESTS ON CONSOLIDATION AND STRENGTH TEST SAMPLES.

Figure A.4-3. Laboratory test request.

Table A.4-1
Unit weights of soils in idealized profile (Boring UDH BAF-4)
(Assume unit weight of water = 60 pcf)

Soil stratum	Inclusive Depth (ft.)	Total unit weight (γ_t) pcf	Saturated unit weight (γ_{sat}) pcf	Buoyant unit weight (γ_b) pcf
Organics	0 - 3	90	-	-
Sand	3 - 10	110	110	50
Silty clay	10 - 45	125	125	65

Table A.4-2
Computations for construction of p_o diagram (Boring UDH BAF-4)
(The ground water table [GWT] is located at a depth of 6-ft below the surface)

Depth (ft) to a boundary	Total (p_t) geostatic vertical pressure (psf)	Effective (p_o) geostatic vertical pressure (psf)	Hydrostatic (p_w) pore water pressure (psf)
3	3-ft x 90 pcf = 270 psf	3-ft x 90 pcf = 270 psf	$p_t - p_o = 0$ (above GWT)
6	270 psf + 3 ft x 110 pcf = 600 psf	270 psf + 3 ft x 110 pcf = 600 psf	$p_t - p_o = 0$ (at GWT)
10	600 psf + 4 ft x 110 pcf = 1,040 psf	600 psf + 4 ft x 50 pcf = 800 psf	1,040 psf – 800 psf = 240 psf or 4 ft x 60 pcf = 240 psf
45	1,040 psf + 35 ft x 125 pcf = 5,415 psf	800 psf + 35-ft x 65 pcf = 3,075 psf	5,415 psf – 3,075 psf = 2,340 psf or 39-ft x 60 pcf = 2,340 psf

Table A.4-3
Consolidation test results summary (Boring UDH BAF-4)

Depth, ft	Tube No.	w %	p_o, psf	e_o	p_c, psf	C_r	C_c	c_v ft^2/day
11	T3	33	800	0.91	6,500	0.033	0.35	0.6
16	T4	35	1150	0.89	6,000	0.031	0.32	0.4
21	T5	31	1450	0.96	4,800	0.040	0.36	0.8
26	T6	36	1790	1.01	4,200	0.035	0.34	0.6
31	T7	38	2130	0.98	3,400	0.037	0.34	0.8
40	T9	37	2720	1.02	3,800	0.032	0.35	0.4

Table A.4-4
Shear strength test results summary (Boring UDH BAF-4)

Undrained Shear Strength – psf						
Depth, ft	**Tube No.**	**w %**	**s_u from UU tests (U)**	**s_u @ p_o from CU tests (C)**	**s_u from vane shear tests (V)**	
					Undisturbed	**Remolded**
13		34			1,150	550
16	T4	34	1,050	1,150		
18		36			1,100	600
21	T5	35	950	1,250		
23		38			1,050	500
26	T6	39	975	1,200		
28		37			1,125	550
31	T7	40	1,000	1,250		
37		35			1,250	600
40	T9	38	800	1,300		

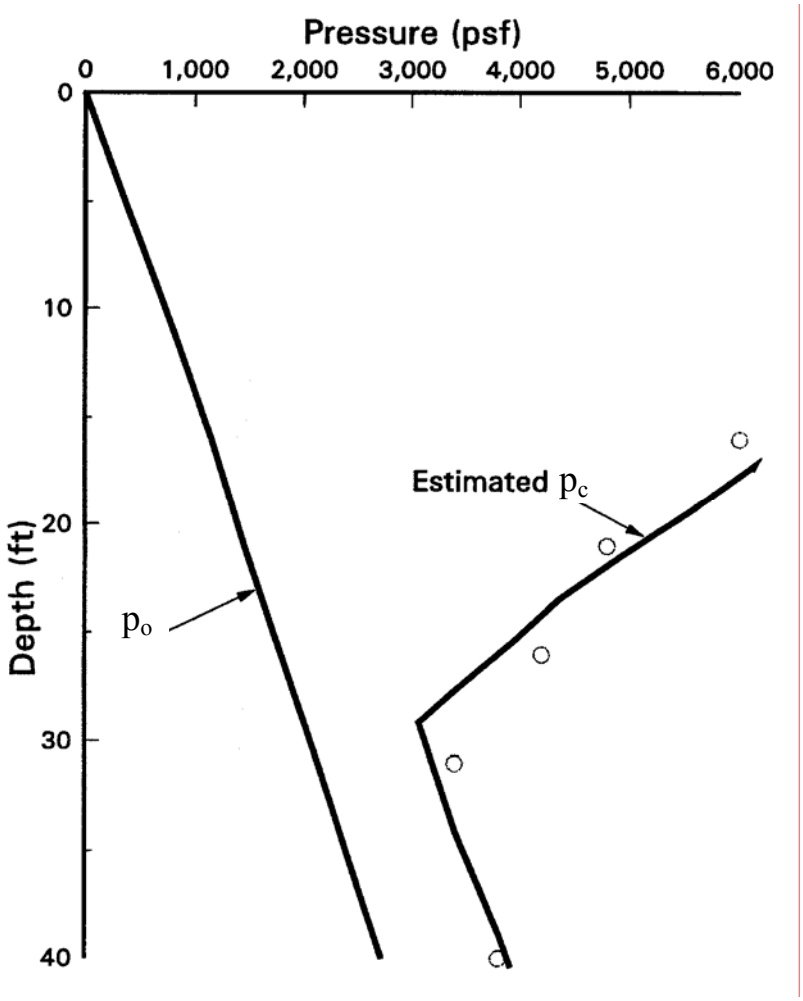

Figure A.4-4. Plot of estimated preconsolidation pressure, p_c, on a p_o plot.

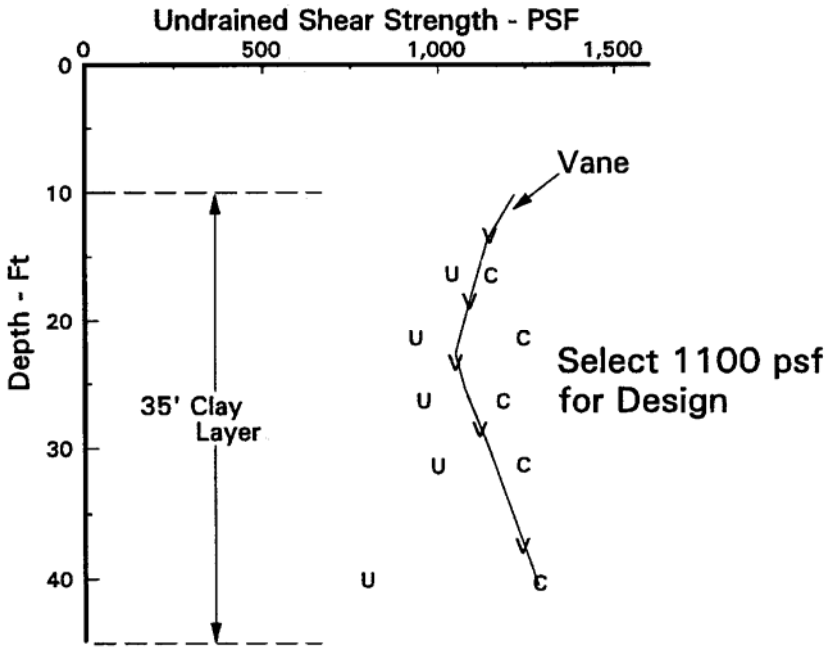

Figure A.4-5. Plot of variation of undrained shear strength with depth determined by various test methods (U = UU Test, C = CU Test, V = Undisturbed Vane Shear Test).

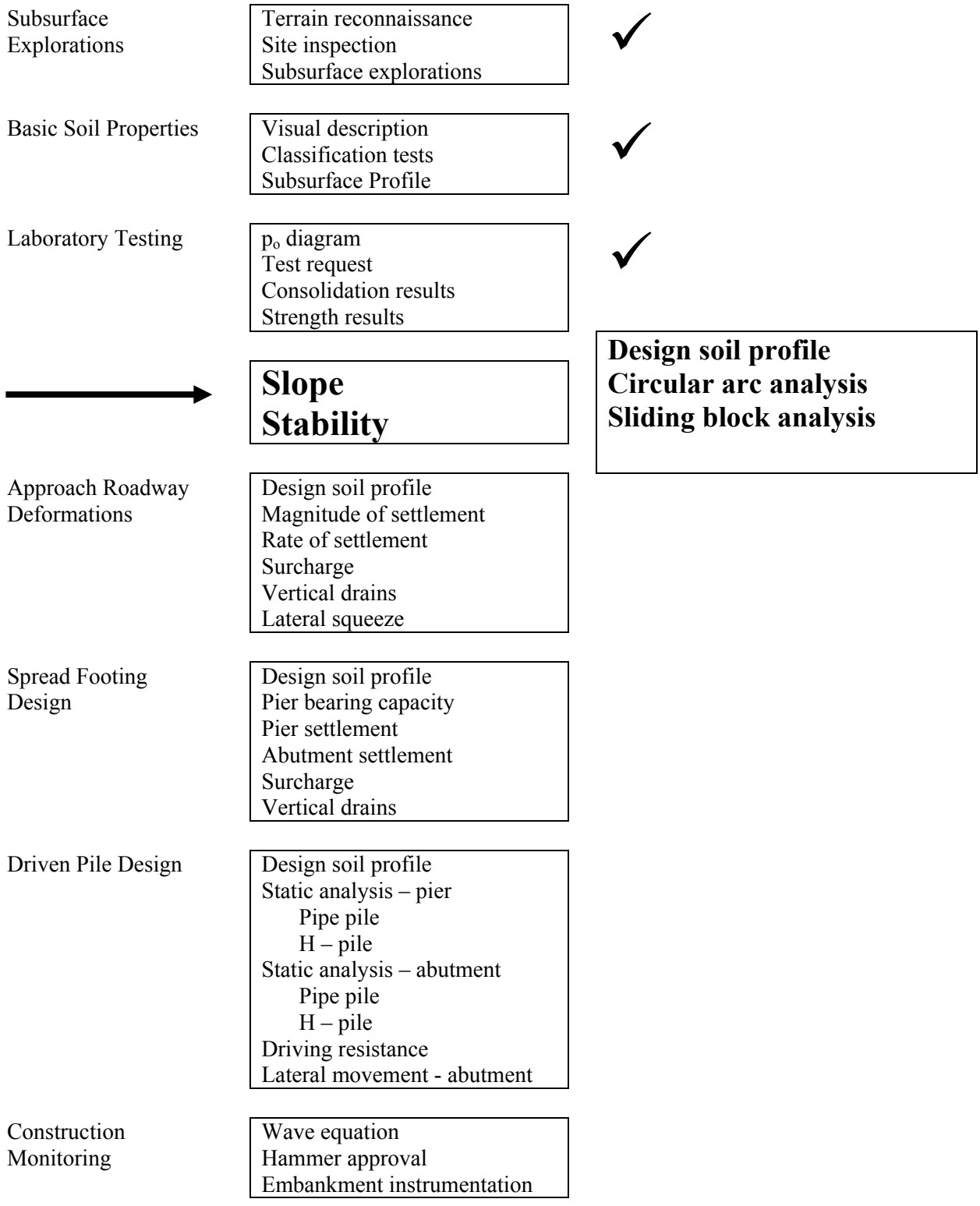

Figure A.5-1. Status of geotechnical work.

SECTION A.5
SLOPE STABILITY

A.5-1 RELEVANT CONCEPTS AND PROCEDURES (Refer to Figure A.5-1)

- Design factor of safety (FS) - Chapter 6.2.
- Ordinary Method of Slices – hand solution - Chapter 6.4.3.
- Bishop's Method – computer solution - Chapter 6.4.4; Table 6-1.
- Sliding (Rankine) Block Method – hand solution - Chapter 6.7.

In this section the analysis and design of an embankment with respect to global stability considerations are illustrated. The Ordinary Method of Slices is used to perform a stability analysis of the I-0 embankment. The results of hand calculations are compared to the results of computer-generated solutions based on the Ordinary Method of Slices and Bishop's Simplified Method. A sliding block analysis is performed and the possibility of lateral squeeze is examined.

A.5-2 DETAILED PROCEDURES

Given: The proposed embankment geometry as shown in Figure A.5-2 and the embankment and foundation soil properties at the east approach as provided in Table A.5-1. Assume that the shallow (≈ 3′) surface layer of organic material shown in the idealized soil profile (Figure A.4-2) has been removed and replaced with select material having the same properties as the embankment fill.

Required:

- Perform hand calculations based on the Ordinary Method of Slices to compute the minimum factor of safety of the I-0 approach embankment at the east abutment.
- Compare the minimum factor of safety obtained from the hand calculations with the minimum factors of safety obtained from computer analyses based on the Ordinary Method of Slices and Bishop's Method.
- Perform hand calculations based on the sliding (Rankine) block method to compute the minimum factor of safety of the I-0 approach embankment at the east abutment and compare the result with the results obtained from the two circular arc type failure analyses. Determine critical failure mode.
- Perform hand calculations to assess the potential for lateral squeeze of the embankment foundation soils at this location.

Table A.5-1
Geotechnical engineering properties of embankment and foundation soils
East Abutment - (Boring BAF-4)

Soil Type	Cohesion (c) - psf	Friction angle (ϕ')	γ_t (pcf)	γ_{sat} (pcf)	γ_b (pcf)
Embankment fill	**0**	**40°**	**130**		
Sand	**0**	**36°**	**110**	**110**	**50**
Silty clay	**1,100**	**0**	**125**	**125**	**65**
Gravel	**0**	**43°**	**130**	**130**	**70**

Solution:

Step 1: As illustrated in Figure A.5-2, construct an idealized design profile to scale including the embankment and accounting for the assumption listed above.

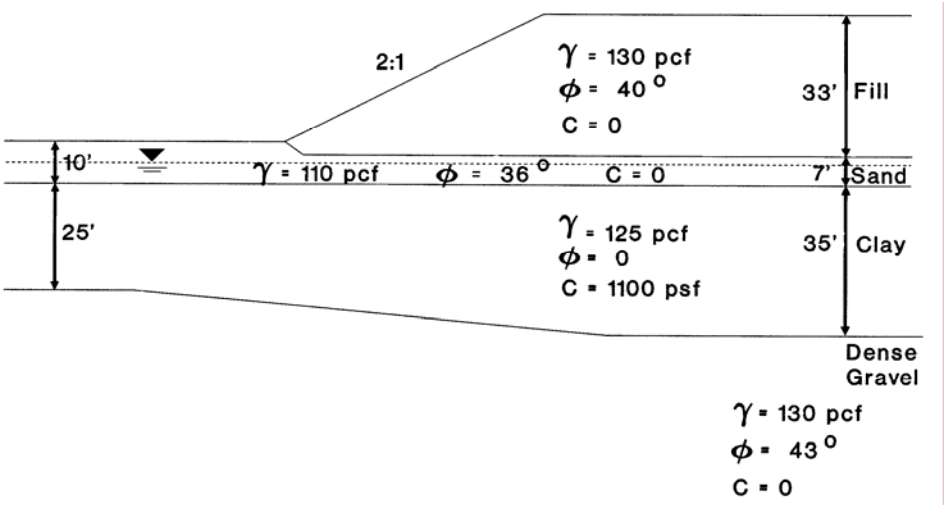

Figure A.5-2. Idealized design soil profile – East Abutment.

Step 2: Compute the FS against circular arc failure by a hand solution based on the Ordinary Method of Slices.

- Chose a trial failure circle, i.e., select a center (Point O) of a circle having radius (R) that will subtend a failure arc through the soils shown in Figure A.5-3. Depending upon the soil profile, the critical circle may be "deep seated", i.e., be tangent to a relatively strong stratum underlying a much weaker layer, or it may be a "toe circle", i.e., the arc passes through the toe of the slope when the soil profile is virtually homogeneous.

- For a complete hand solution many trail failure circles must be chosen to determine the minimum factor of safety. The circles typically cover a range of center points and radii.

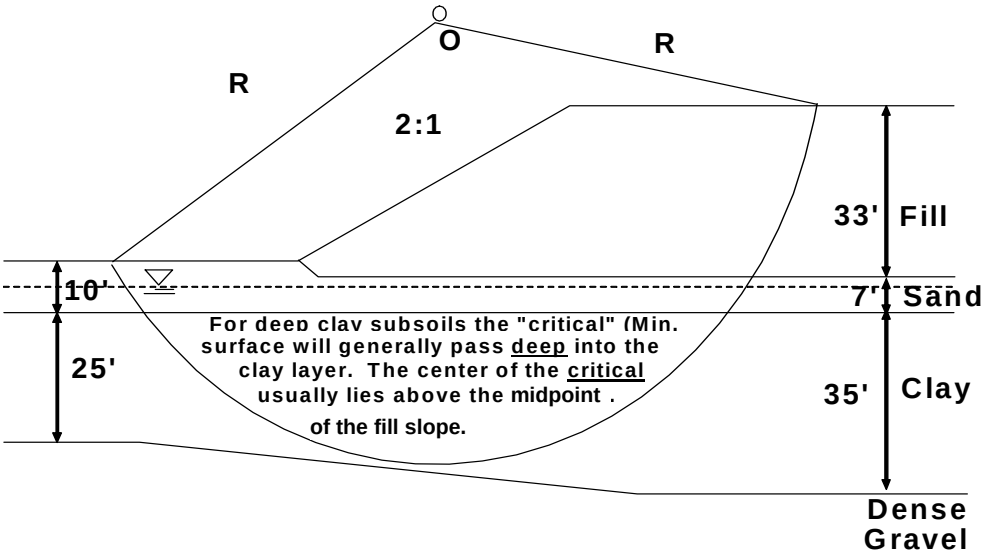

Figure A.5-3. Trial failure circle – Embankment fill - East Abutment.

- For the purpose of illustrating the hand procedure here and for comparison with the computer solution later on, the coordinates of the Point O chosen in this example correspond to the coordinates for the circle yielding the minimum factor of safety as determined by the computer solution based on Bishop's Method.

- Depending upon the geometry of the cross section and the number of soil layers intersected by the failure arc, divide the soil mass above the arc of the failure circle into at least 10 and no more than 20 vertical slices For this example there are 16 slices selected as shown in Figure A.5-4.

- As shown in Figure A.5-5, determine the α – angles for each vertical slice, where α = the angle, as measured at Point O, between a vertical line through Point O and the radius that intersects the middle of the failure arc segment for a given slice.

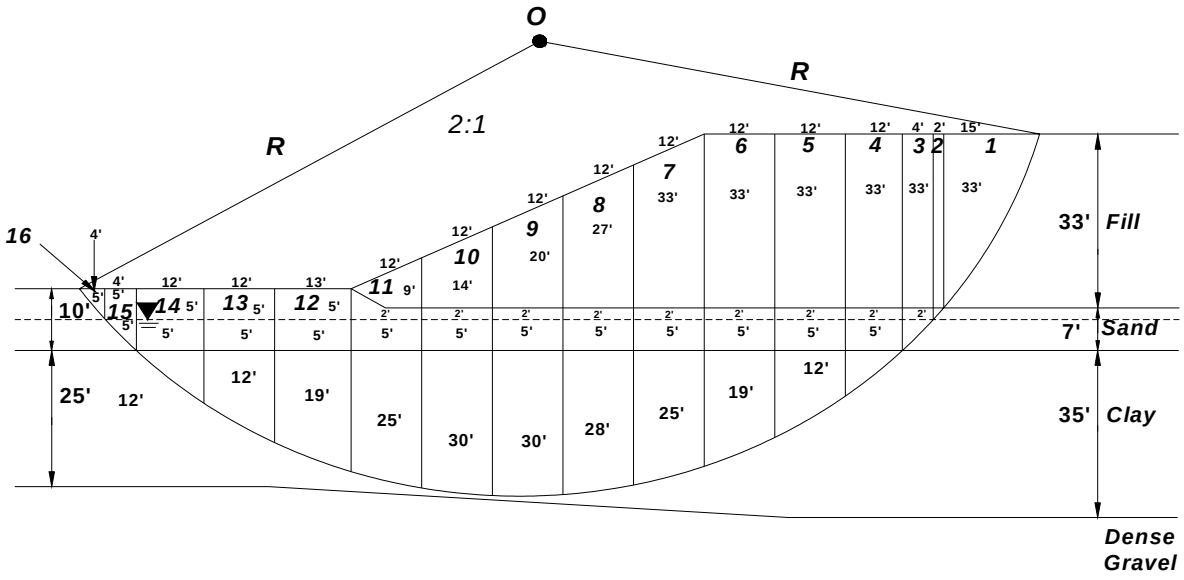

Figure A.5-4. Vertical slices above assumed failure arc – East Abutment.
(Not-to-scale)

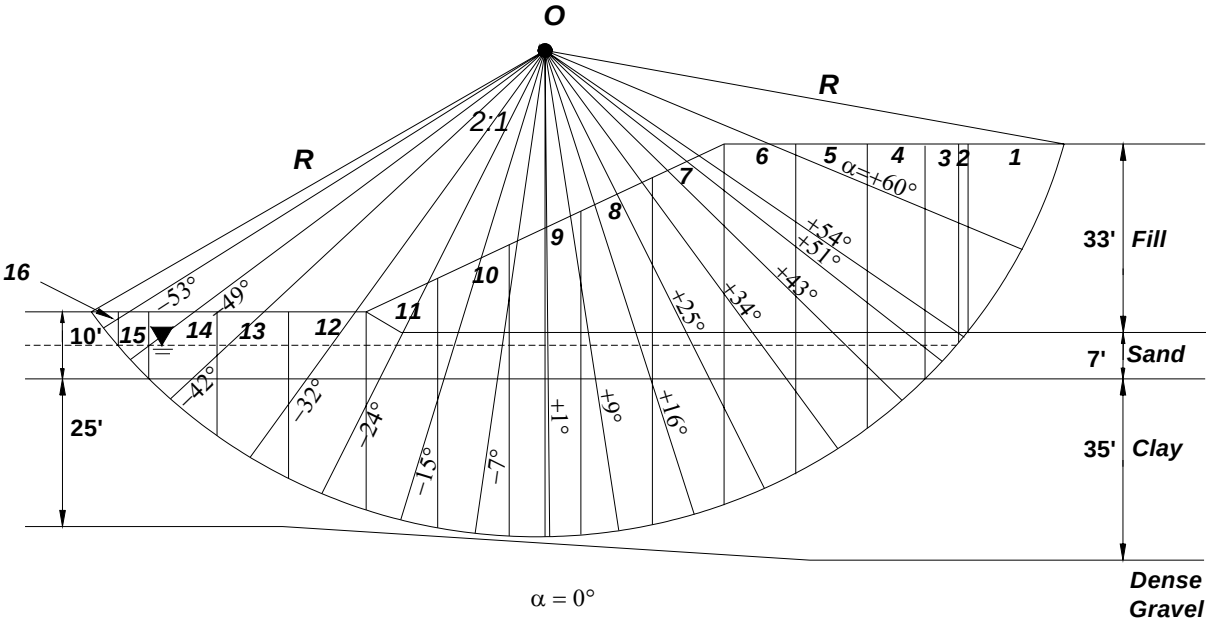

Figure A.5-5. Determination of α – Angles corresponding to each vertical slice above assumed failure arc – East Abutment.
(Not-to-scale)

- Once the geometry and α – angle for each vertical slice have been determined, compute the resisting and driving forces for all slices by use of the following procedure as illustrated for Slice 7. Figure A.5-6 shows the geometry of the slice and the relevant soil properties. (Refer to equations 6-14 to 6-20).

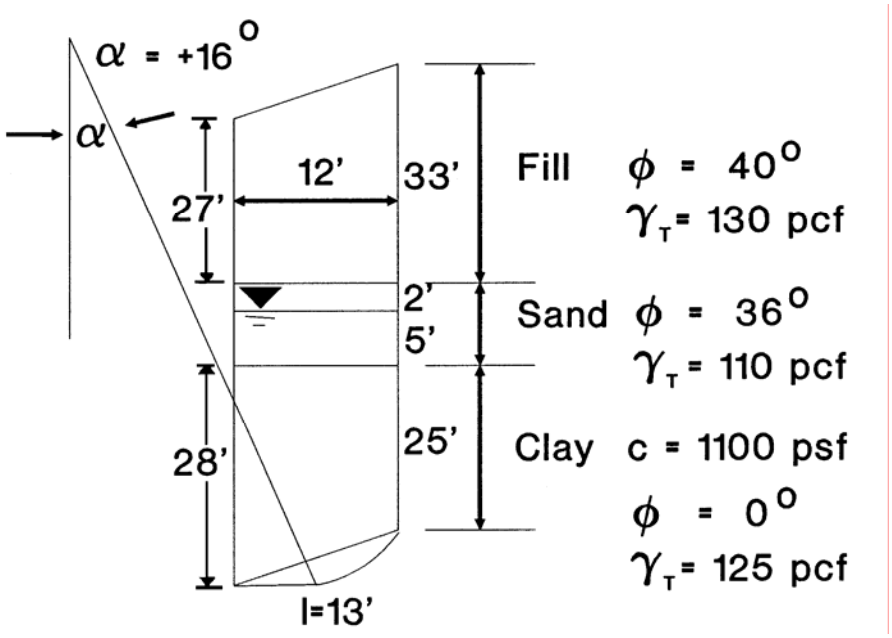

Figure A.5-6. Geometry and relevant soil properties for slice 7 (Not-to-scale).

- Calculate the total weight of the slice for a unit thickness into the plane of the paper by summing the contributions of the various soil strata lying above the failure arc.

$$W_T = (1\,\text{ft})(12\,\text{ft})\left(\frac{27\,\text{ft}+33\,\text{ft}}{2}\right)(130\,\text{pcf}) + (1\,\text{ft})(12\,\text{ft})(7\,\text{ft})\,(110\,\text{pcf}) +$$
$$(1\,\text{ft})(12\,\text{ft})\left(\frac{28\,\text{ft}+25\,\text{ft}}{2}\right)(125\,\text{pcf}) = 95{,}790\,\text{lbs}$$

- Calculate the tangential driving force, which is the component of the weight of the slice acting perpendicular to the radius (R).

$$T = W_T \sin\alpha = 95{,}790 \text{ lbs } (\sin 16°) = 26{,}403 \text{ lbs}$$

- Calculate the shearing resistance along the length of arc subtended by the failure surface. Use the length of the chord (l) to approximate the arc length. In general, the shearing resistance consists of a frictional component and a cohesion component. For a unit thickness into the plane of the paper, the frictional component is given by: $N' \tan\phi = (W_T \cos\alpha - ul) \tan\phi$, where u = the average

pore water pressure acting along the chord length, l (Refer to Eq. 6-18). The cohesion component is given by cl where c = the cohesion for drained conditions and the undrained shear strength (s_u) for undrained conditions. Since undrained conditions are usually critical, the undrained shear strength (s_u) is generally used in the calculation.

Since the bottom of Slice 7 is in clay where $\phi = 0$, N tan $\phi = 0$. Therefore, the total shearing resistance for a unit thickness into the plane of the paper is given by the cohesion component as follows:

$$c\,l = (1{,}100 \text{ psf})(13 \text{ ft})(1 \text{ ft}) = 14{,}300 \text{ lbs}$$

Therefore for Slice 7:
Driving Force = T = 26,403 lbs
Resisting Force =c l = 14,300 lbs

- Slice 7 was used to illustrate the case where the failure surface passed through a purely cohesive material below the ground water table. Slice 15 is used to illustrate the procedure when the failure surface passes through a purely frictional material below the ground water table. Figure A.5-7 shows the geometry of Slice 15 and the relevant soil properties.

  - As before, calculate the total weight of the slice for a unit thickness into the plane of the paper

$$W_T = (1\,\text{ft})(4\,\text{ft})\left(\frac{10\,\text{ft} + 5\,\text{ft}}{2}\right)(110\,\text{pcf}) = 3{,}300\,\text{lbs}$$

  - As before, calculate the tangential driving force

$$T = W_T \sin \alpha = 3{,}300 \text{ lbs } (\sin(-49°)) = -\,2{,}491 \text{ lbs}$$

Note: T is negative for this slice since the weight tends to RESIST sliding.

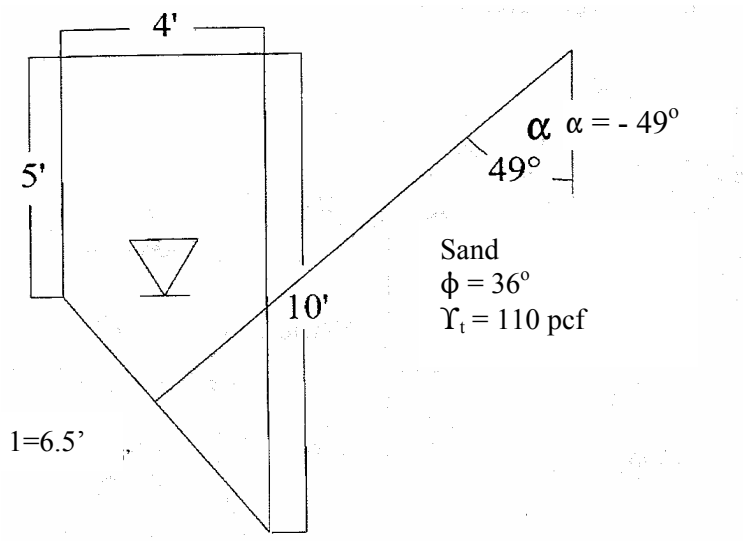

Figure A.5-7. Geometry and relevant soil properties for slice 15 (Not-to-scale).

- As before, calculate the shearing resistance along the length of arc subtended by the failure surface. Use the length of the chord (l) to approximate the arc length.

  Since the bottom of Slice 15 is in sand where c = 0, cl = 0. Therefore, the total shearing resistance for a unit thickness into the plane of the paper is given by the frictional component based on $\phi = 36°$ as follows:

  $N = W_t \cos \alpha - ul$
  $N = (3{,}300 \text{ lbs})(\cos (-49°)) – (1 \text{ ft})(5 \text{ ft}/2)\ (6.5 \text{ ft})\ (60 \text{ pcf})$
  $N = 2{,}165 \text{ lbs} – 975 \text{ lbs} = 1{,}190 \text{ lbs}$
  $N \tan \phi = 1{,}190 \text{ lbs} (\tan 36°) = 865 \text{ lbs}$

  Therefore, for Slice 15:
  Driving Force = T = -2,491 lbs
  Resisting Force = 865 lbs

- Follow the procedures described above to calculate weights for each slice. For ease in computation use the tabular format illustrated in Table A.5-2.

Table A.5-2
Tabular form for computing total weights of slices for a unit thickness into the plane of the paper

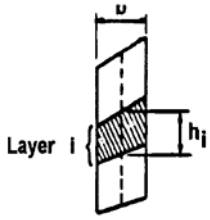

γ_i = unit weight of layer i
h_i = height of layer at center of slice
W_i = partial weight = b h_i γ_i
ΣW_i = total weight of slice W_T

Slice No.	B (ft)	h_I (ft)	γ_i (pcf)	W_i (lbs/ft)	$\sum W_i = W_T$ (lbs)
1	15	33/2	130	32,175	32,175
2	2	33	130	8,580	
		2/2	110	220	8,800
3	4	33	130	17,160	
		(7+2)/2	110	1,980	19,140
4	12	33	130	51,480	
		7	110	9,240	
		12/2	125	9,000	69,720
5	12	33	130	51,480	
		7	110	9,240	
		(19+12)/2	125	23,250	83,970
6	12	33	130	51,480	
		7	110	9,240	
		(19+25)/2	125	33,000	93,720
7	12	(27+33)/2	130	46,800	
		7	110	9,240	
		(25+28)/2	125	39,750	95,790
8	12	(20+27)/2	130	36,660	
		7	110	9,240	
		(30+28)/2	125	43,500	89,400
9	12	(14+20)/2	130	26,520	
		7	110	9,240	
		30	125	45,000	80,760
10	12	(9+14)/2	130	17,940	
		7	110	9,240	
		(28+30)/2	125	43,500	70,680
11	12	(9+3)/2	130	9,360	
		7	110	9,240	
		(25+28)/2	125	39,750	58,350
12	13	10	110	14,300	
		(19+25)/2	125	35,750	50,050
13	12	10	110	13,200	
		(12+19)/2	125	23,250	36,450
14	12	10	110	13,200	
		12/2	125	9,000	22,200
15	4	(5+10)/2	110	3,300	3,300
16	4	5/2	110	1,100	1,100

- Follow the computational procedures described above and record the relevant soil and geometric properties and the calculated values of driving and resisting forces for each slice in a table. For ease in computation of the global factor of safety, use the tabular format illustrated in Table A.5-3.

- Calculate the global factor of safety by using the equations shown in Table A.5-3.

- Summarize the results of the Ordinary Method of Slices based on hand calculations by showing the critical failure circle and its associated minimum factor of safety graphically (Refer to Figure A.5-8).

Step 3: Compute the FS against circular arc failure by computer solutions based on the Ordinary Method of Slices and the Bishop Simplified Method.

- Summarize the results of the Ordinary Method of Slices (OMS) and Bishop's Simplified Method based on a computer solution by showing the critical failure circle and its associated minimum factor of safety graphically (Refer to Figure A.5-9). Note that for the purpose of illustrating the difference between the FS for the two computer solutions, the coordinates of Point O and the radius of the failure arc, R, for the Ordinary Method of Slices computer solution correspond to those of the circle yielding the minimum factor of safety as determined by the computer solution based on Bishop's Method. As noted previously, the same geometry was used for the Ordinary Method of Slices solution by hand calculations.

- Figure A.5-10 illustrates the search routine used by the computer program to obtain the minimum FS. Contours of equal FS are shown with the minimum FS being the point at the center of the contours. The contours represent the results of many computer runs in which the center and radius of the failure circle were varied in a systematic way until the minimum FS was reached. The efficiency of the computer solution over the hand solution in terms of time and accuracy is obvious.

Table A.5-3
Tabular form for computing factor of safety by Ordinary Method of Slices

Slice No.	W_T (from Table A.5-2) (lbs)	l (ft)	α (deg)	c (psf)	ϕ (deg)	u (psf)	ul (lbs)	$W_T\cos\alpha$ (lbs)	$N' = W_T\cos\alpha - ul$ (lbs)	$N'\tan\phi$ (lbs)	cl (lbs)	$T = W_T\sin\alpha$ (lbs)
1	32,175	36	60	0	40	0	0	16,088	16,088	13,499	0	27,864
2	8,800	3	54	0	36	0	0	5,173	5,173	3,758	0	7,119
3	19,140	7	51	0	36	150	1,050	12,045	10,995	7,988	0	14,875
4	69,720	17	43	1,100	0	-	-	-	-	0	18,700	47,549
5	83,970	15	34	1,100	0	-	-	-	-	0	16,500	46,955
6	93,720	15	25	1,100	0	-	-	-	-	0	16,500	39,608
7	95,790	13	16	1,100	0	-	-	-	-	0	14,300	26,403
8	89,400	13	9	1,100	0	-	-	-	-	0	14,300	13,985
9	80,760	12	1	1,100	0	-	-	-	-	0	13,200	1,409
10	70,680	12	-7	1,100	0	-	-	-	-	0	13,200	-8,614
11	58,350	13	-15	1,100	0	-	-	-	-	0	14,300	-15,102
12	50,050	14	-24	1,100	0	-	-	-	-	0	15,400	-20,357
13	36,450	14	-32	1,100	0	-	-	-	-	0	15,400	-19,316
14	22,200	16	-42	1,100	0	-	-	-	-	0	17,600	-14,855
15	3,300	6.5	-49	0	36	150	975	2,165	1,190	865	0	-2,491
16	1,100	6.5	-53	0	36	0	0	662	662	481	0	-878
									Σ	26,591	169,400	144,154

$$FS = \frac{\Sigma\,(W_T\cos\alpha - ul)\tan\phi + \Sigma\,cl}{\Sigma\,W_T\sin\alpha} = \frac{\Sigma\,N'\tan\phi + \Sigma\,cl}{\Sigma\,W_T\sin\alpha} = \frac{26{,}591\ \text{lbs} + 169{,}400\ \text{lbs}}{144{,}154\ \text{lbs}} = 1.36$$

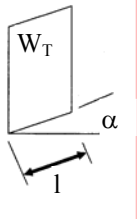

Legend: Refer to Figure 6-10 for definition of various slice quantities

- W_T = Total weight of Slice (soil + water)
- l = Base length of the slice
- c = Cohesion at base of slice
- ϕ = angle of internal friction
- u = pore water pressure at base of slice

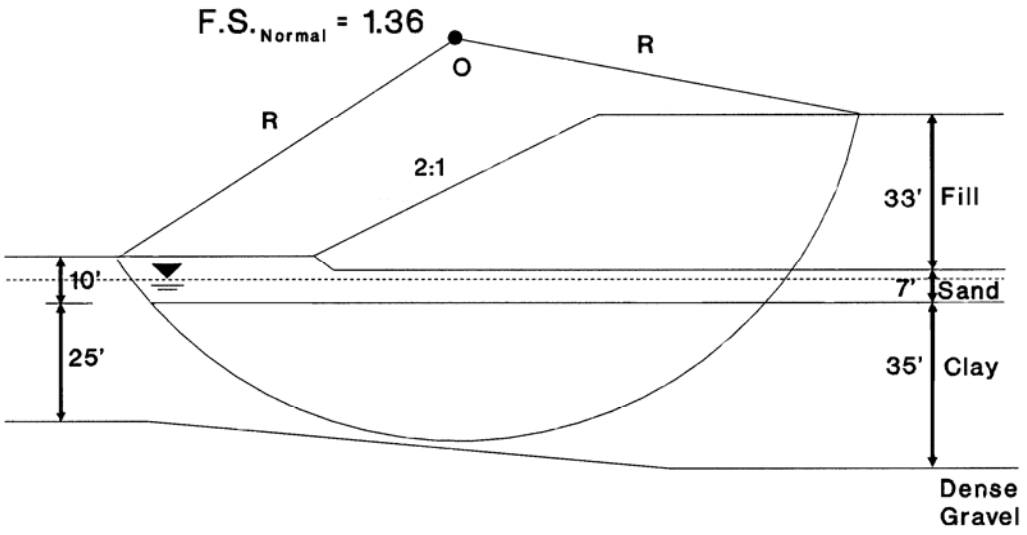

Figure A.5-8. Graphical representation of solution for minimum Factor of Safety by Ordinary Method of Slices/Hand computation – East Abutment.

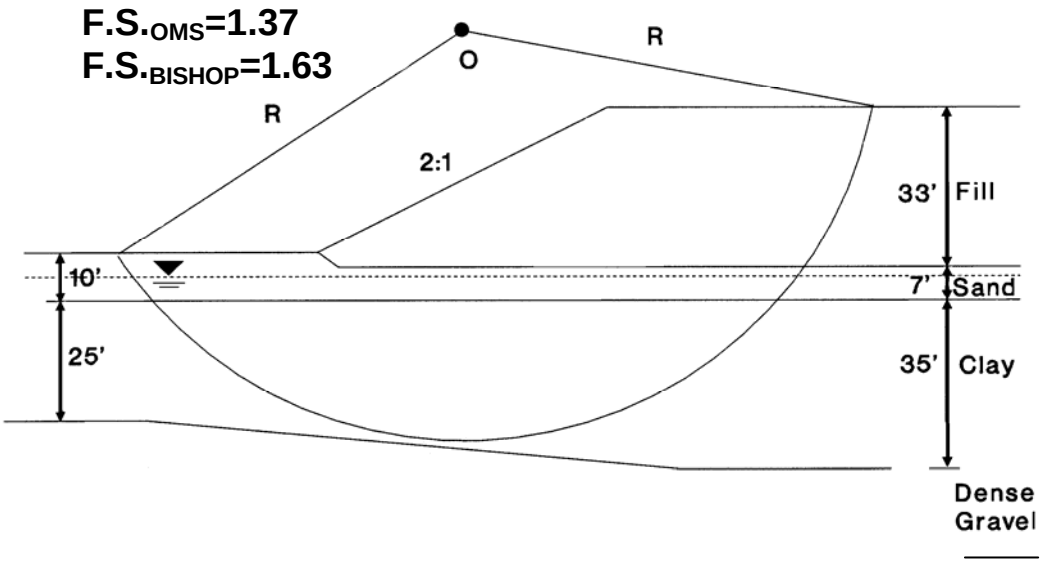

Figure A.5-9. Graphical representation of solution for minimum Factor of Safety by Ordinary Method of Slices (OMS)/Computer solution and Bishop's Method – East Abutment.

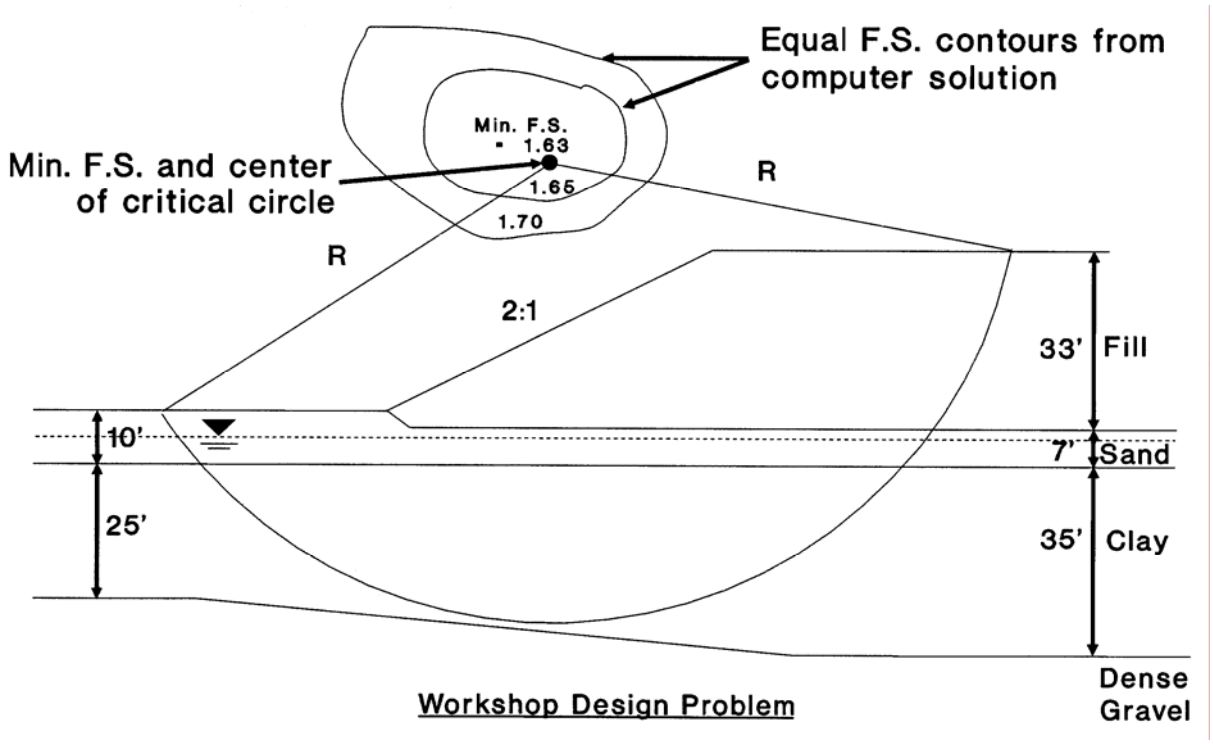

Figure A.5-10
Illustration of search routine used by computer program to develop contours of equal FS that converge on the point of minimum FS and center of critical circle.

Step 4: Compare the FS against circular arc failure computed by each of the three methods and select a design FS.

F.S. = 1.36 - Ordinary Method of Slices: Hand Solution
F.S. = 1.37 - Ordinary Method of Slices: Computer Solution
F.S. = 1.63 - Bishop's Simplified Method: Computer Solution

Use a minimum factor of safety for design F.S. (Bishop) = 1.63

Step 5: Calculate FS against a Sliding Block Type Failure by Using Rankine Wedges and Sliding Block Analysis

- Choose a trial block type failure surface along the top of clay layer as shown in Figure A.5-11.

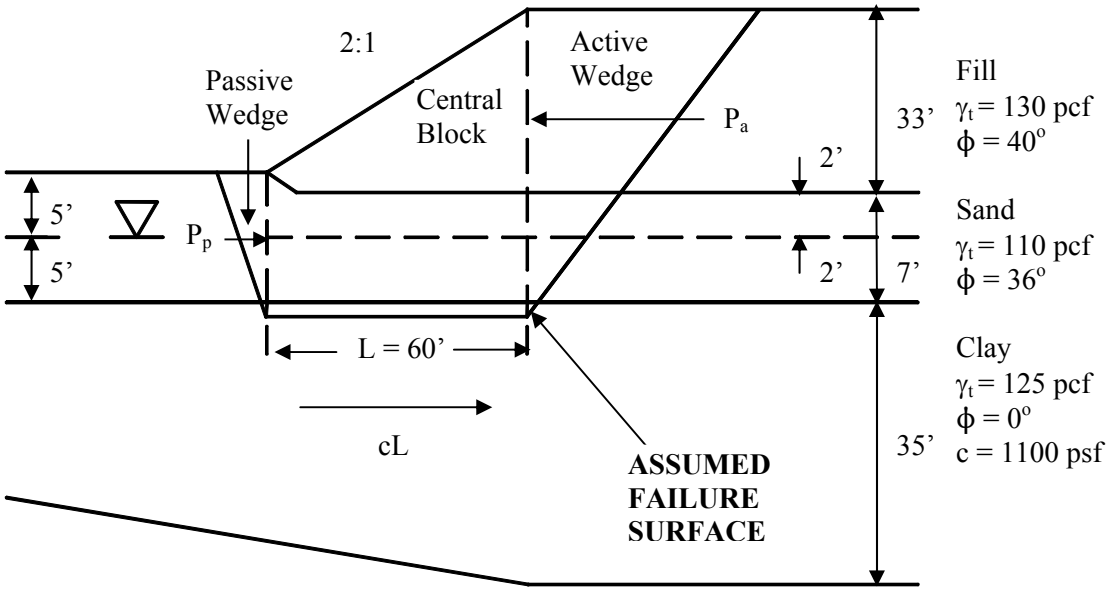

Figure A.5-11. Trial failure surface consisting of Active and Passive Rankine wedges and central sliding block.

- Calculate active Rankine coefficient of lateral earth pressure (K_a)
  - For fill (Soil Layer 1)
    $K_{a1}=\tan^2(45° - 40°/2) = \tan^2(25°) = 0.22$
  - For sand (Soil Layer 2)
    $K_{a2}=\tan^2(45° - 36°/2) = \tan^2(27°) = 0.26$

- Calculate active lateral earth pressure (p_a) (Units of kips are used to facilitate use of less digits in the calculations: 1 kip = 1,000 lbs; kip is abbreviated as k)
  - At base of fill (Soil Layer 1)
    $p_{a1} = \gamma_1 h_1 Ka_1 = (0.130 \text{ kcf})(33 \text{ ft})(0.22) = 0.94 \text{ ksf}$
  - At top of sand layer (Soil Layer 2)
    p_{a2} (top of sand) $= \gamma_1 h_1 K_{a2} = (0.130 \text{ kcf})(33 \text{ ft})(0.26) = 1.11 \text{ ksf}$
  - At depth of 2 ft below top of sand layer (i.e. at water table elevation)
    $p_{a3} = 1.11 \text{ ksf} + (0.110 \text{ kcf})(2 \text{ ft})(0.26) = 1.17 \text{ ksf}$
  - At base of sand layer
    $p_{a4} = 1.17 \text{ ksf} + (0.050 \text{ kcf*})(5 \text{ ft})(0.26) = 1.24 \text{ ksf}$
    (*buoyant unit weight below water table)

- Calculate active Rankine force (P_a) for a unit thickness into the plane of the paper and plot force and active lateral earth pressure diagram as shown in Figure A.5-12
  - $P_a = (0.94 \text{ ksf})(33 \text{ ft})(1/2)(1 \text{ ft}) + ((1.11 \text{ ksf} + 1.17 \text{ ksf})/2)(2 \text{ ft})(1 \text{ ft}) + ((1.17 \text{ ksf} + 1.24 \text{ ksf})/2)(5 \text{ ft})(1 \text{ ft}) = 15.5 \text{ kips} + 2.3 \text{ k} + 6 \text{ k} \approx 24 \text{ k}$

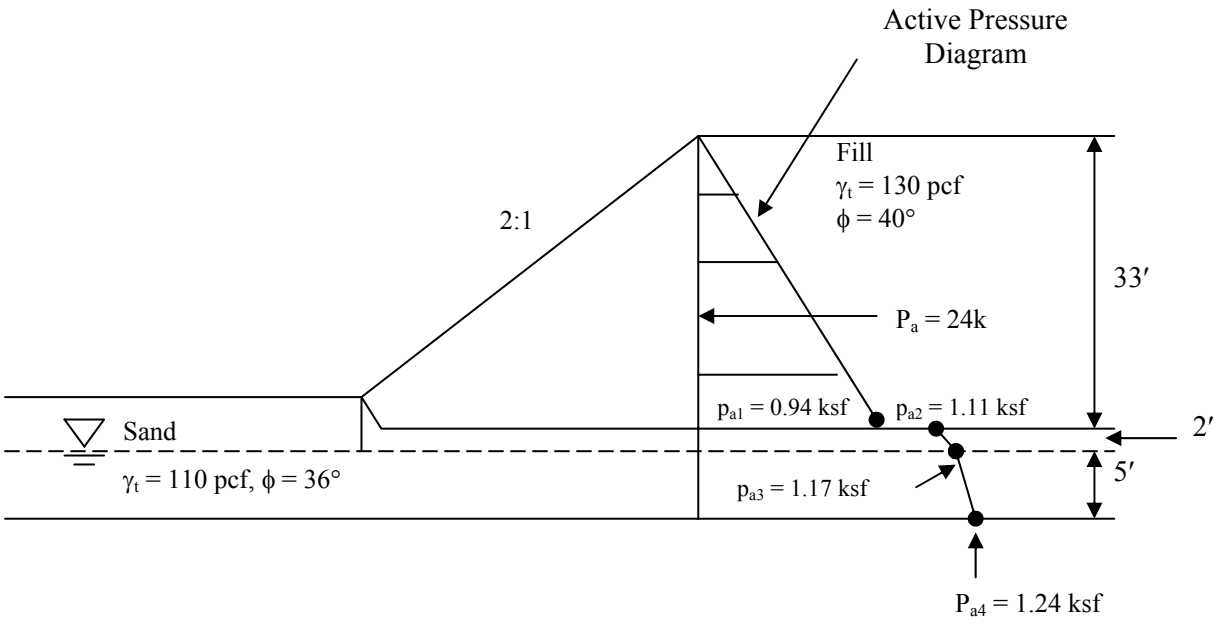

Figure A.5-12
Active earth pressure diagram and resultant active Rankine force

- Calculate passive Rankine coefficient of lateral earth pressure (K_p)
  - For sand
    $K_p = \tan^2 (45° + 36°/2) = \tan^2 (63°) = 3.85$

- Calculate passive lateral earth pressure (p_p)
  - At 5-ft below top of sand layer (i.e. at water table elevation)
    $p_{p1} = (0.110 \text{ kcf})(5 \text{ ft})(3.85) = 2.1 \text{ ksf}$
  - At base of sand layer
    $p_{p2} = 2.1 \text{ ksf} + (0.050 \text{ kcf*})(5 \text{ ft})(3.85) = 3.1 \text{ ksf}$
    (*buoyant unit weight below water table)

- Calculate passive Rankine force (P_p) for a unit thickness into the plane of the paper and plot force and passive lateral earth pressure diagram as shown in Figure A.5-13
  - $P_p = (2.1 \text{ ksf})(5 \text{ ft})(1/2)(1 \text{ ft}) + ((2.1 \text{ ksf}+3.1 \text{ ksf})/2)(5 \text{ ft})(1 \text{ ft}) = 5.3 \text{ k} + 13 \text{ k}$
    $\approx 18 \text{ k}$

- Calculate the resisting force of the central block for assumed failure plane along the top of the clay layer and the plot the force system as shown on Figure A.5-14.
  - $c = 1{,}100 \text{ psf} = 1.1 \text{ ksf}$
  - $L = 60 \text{ ft}$
  - $cL = (1.1 \text{ ksf})(60 \text{ ft})(1 \text{ ft}) = 66^k$

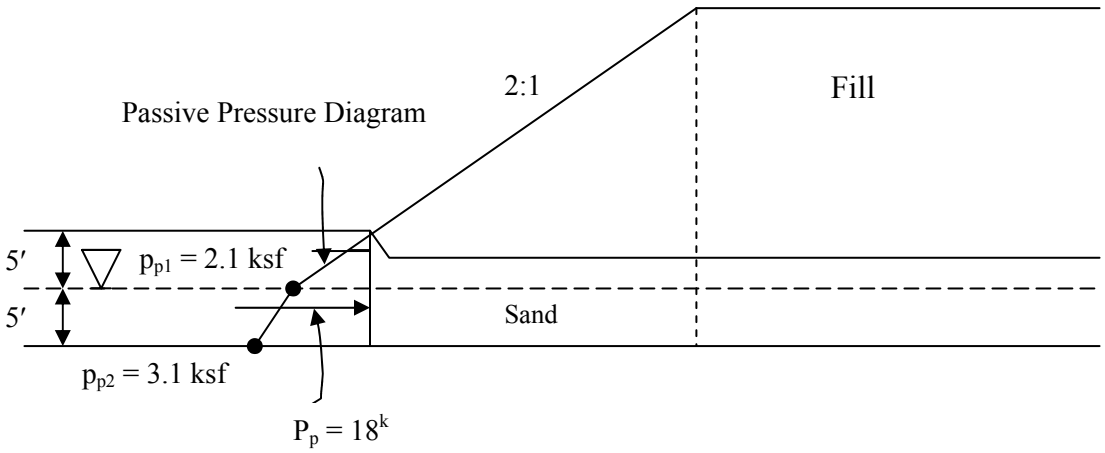

Figure A.5-13. Passive earth pressure diagram and resultant passive Rankine force.

- Calculate the FS against sliding failure

$$F.S. = \frac{\text{Horizontal Resisting Forces}}{\text{Horizontal Driving Forces}} = \frac{P_p + CL}{P_A}$$

$$= \frac{18^K + 66^K}{24^K} = \frac{84^K}{24^K} = 3.5$$

- Compare FS against sliding failure (3.5) vs. minimum FS against circular arc failure (1.63).
- Conclusion: circular arc failure is more critical and governs the design.

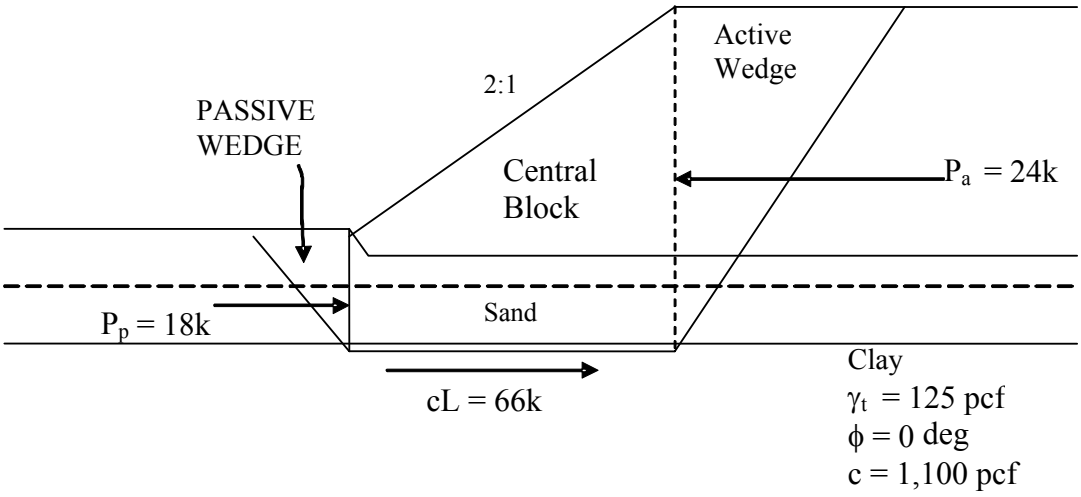

Figure A.5-14. Force system acting on central block.

A.5-3 SUMMARY OF THE APPROACH USED TO DETERMINE EMBANKMENT STABLITY FOR THE APPLE FREEWAY DESIGN PROBLEM

1. Construct an idealized design profile to scale.
    - Use idealized soil profile from Boring UDH BAF-4
    - Include 33-ft high embankment at east abutment.
    - Estimate geotechnical properties of soil layers from results of field and laboratory tests.

2. Perform hand calculations to determine FS against circular arc failure by using the Ordinary Method of Slices.
    - For illustration use center and radius of circle from computer solution that provided minimum FS by Bishop Simplified Method
    - Divide the soil mass above the arc of the failure circle into at least 10 and no more than 20 vertical slices.
    - Set up a table to aid in the performance of the calculations.
    - Fill the table with soil properties and geometric data for each slice.
    - Illustrate calculations performed for Slice 7 – arc segment in clay.
    - Illustrate calculations performed for Slice 15 – arc segment in sand.
    - Calculate the FS for the assumed center and radius.

3. Compute the FS against a circular arc failure by using computer solutions based on the Ordinary Method of Slices and the Bishop Simplified Method.

4. Compare the FS against a circular arc failure computed by each of the three methods and select the minimum FS.
    - Note that only the computer solution by Bishop's Modified Method provides a minimum FS against circular arc failure. The values obtained from the Ordinary Method of Slices hand calculations and computer solution may not be the minima for that method since the center and radius of the circle used here to illustrate the method are those that provided the minimum FS by Bishop Simplified Method computer solution.

5. Calculate the FS against a sliding block type failure by using Rankine wedges and sliding block analysis.
    1. Calculate the active and passive coefficients of lateral earth pressure for each soil layer by using Rankine equations.

2. Calculate the active and passive lateral earth pressure distributions taking into account changes in soil layering and the presence of ground water.
3. Calculate the active (driving) and passive (resisting) forces due to the Rankine wedges.
4. Assume that sliding occurs along the top of the clay layer and calculate the resisting force of the central block.
5. Calculate the FS against a sliding block type failure and compare it to the minimum FS against a circular arc failure. Select the lower of the two as the design FS.

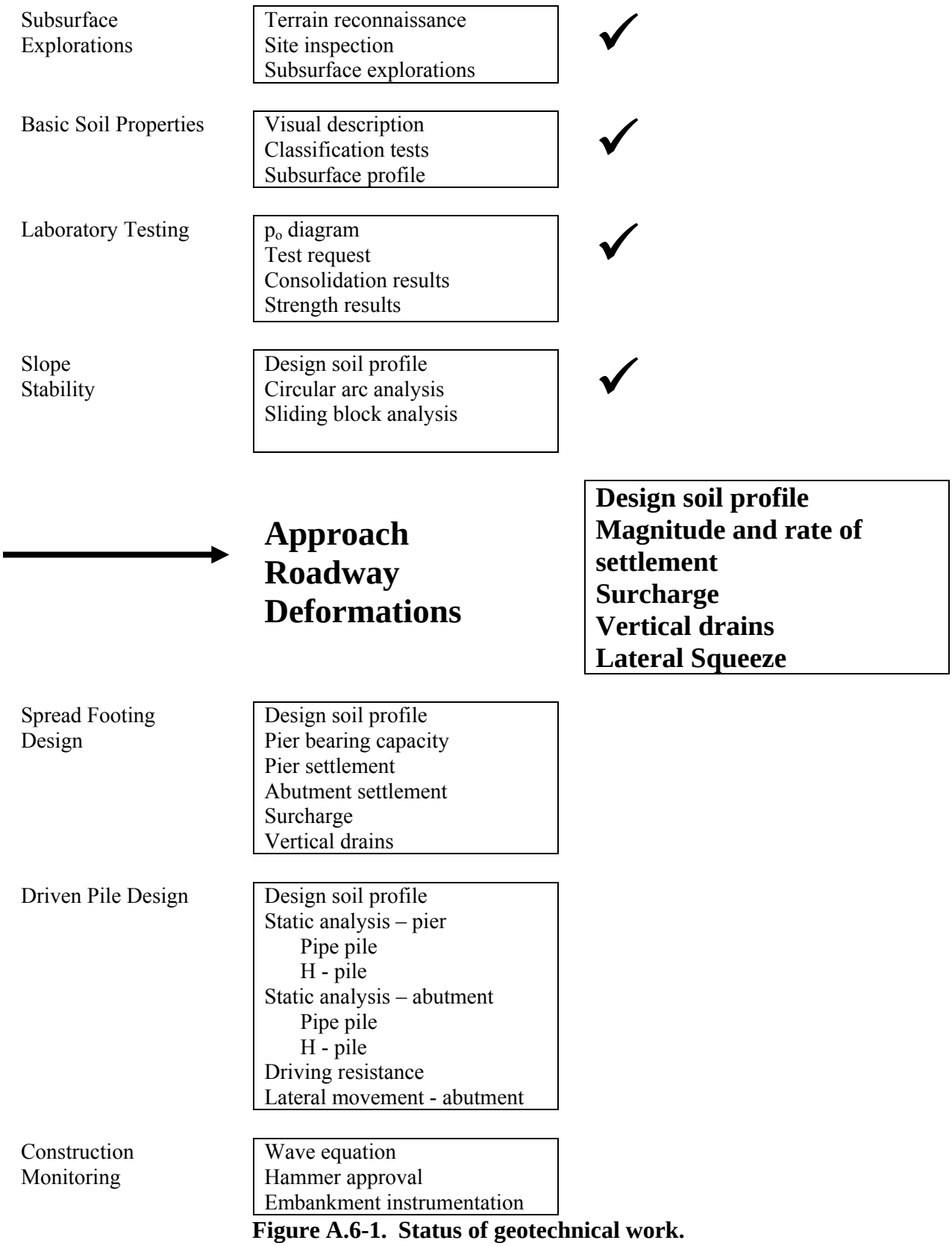

Figure A.6-1. Status of geotechnical work.

SECTION A.6
APPROACH ROADWAY DEFORMATIONS

A.6-1 RELEVANT CONCEPTS AND PROCEDURES (Refer to Figure A.6-1)

- General procedure to determine pressure distribution with depth due to approach embankment; Chapter 7.3
- Immediate settlement – computation of magnitude; Chapter 7.4.
- Consolidation settlement – computation of magnitude; Chapter 7.5.
- Consolidation settlement – computation of time rate; Chapter 7.5.3.
- Treatment by surcharging to accelerate consolidation settlement and reduce time; Chapter 7.7
- Treatment by Wick Drains without surcharge to accelerate consolidation settlement and reduce time; Chapter 7.7
- Estimating horizontal movement due to lateral squeeze of embankment foundation soils; Chapter 7.6

In this section the computation of the magnitude of immediate settlement of a sand layer and the magnitudes and rates of consolidation settlement of an organic layer and a clay layer due to the construction of an embankment fill are illustrated. The options of surcharging and vertical drains with and without surcharge are also examined as a means of treatment to accelerate consolidation settlement and reduce time.

A.6-2 DETAILED PROCEDURES

Given:

- The subsurface profile and soil properties shown in Figure A.6-2 for the east abutment embankment of the Apple Freeway Bridge.
- The consolidation test results presented in Table A.6-1.
- Assume that N-values in the profile are N_{60} values.

Required:

- Perform hand calculations to compute the pressure distribution with depth due to the embankment fill.
- Perform hand calculations to compute the magnitude of the anticipated consolidation settlement due to the embankment fill.
- Perform hand calculations to compute the time required for the settlement to occur without treatment by surcharging or vertical drains and plot the time vs. settlement

curve.

- Evaluate the stability of the 30 ft embankment fill with the addition of 10 ft of surcharge treatment.
- Examine the effect of treatment by surcharging on settlement and time (including cost analysis).
- Examine the effect of treatment by vertical wick drains without surcharge on settlement and time (including cost analysis).
- Estimate the amount of horizontal deformation due to lateral squeeze of the embankment foundation soils

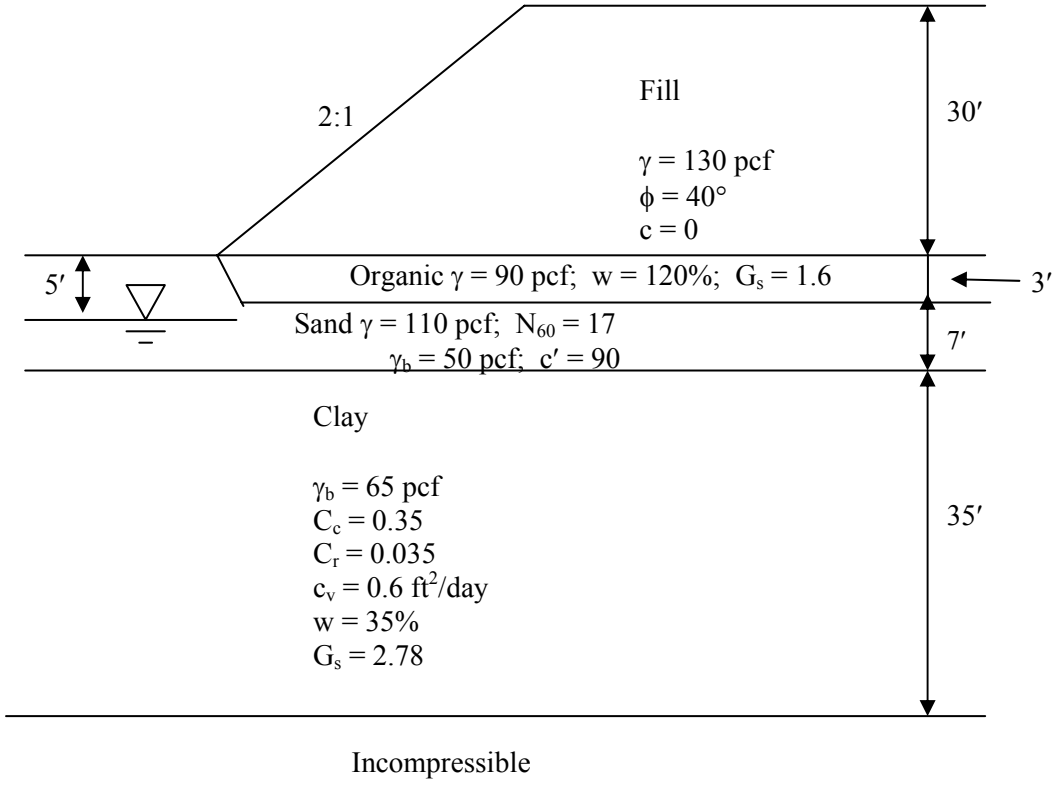

Figure A.6-2. Design subsurface profile and soil properties at east embankment location.

A.6-3 SOLUTION TO DETERMINE THE MAGNITUDE OF AND TIME FOR THE ANTICIPATED SETTLEMENT DUE TO THE EMBANKMENT FILL

Step 1: Obtain soil consolidation characteristics (from laboratory tests).

Table A.6-1
Consolidation test results summary (Hole BAF-4)

Depth	Tube	p_c (psf)	C_c	C_r	c_v (ft^2/day)
11	T3	6,500	0.35	0.033	0.6
16	T4	6,000	0.32	0.031	0.4
21	T5	4,800	0.36	0.040	0.8
26	T6	4,200	0.34	0.035	0.6
31	T7	3,400	0.34	0.037	0.8
40	T9	3,800	0.35	0.032	0.4
e_o (average) = 0.97					

Step 2: Plot overburden pressure (Figure A.4-2) and preconsolidation pressure (Table A.6-1) with Depth as shown in Figure A.6-3.

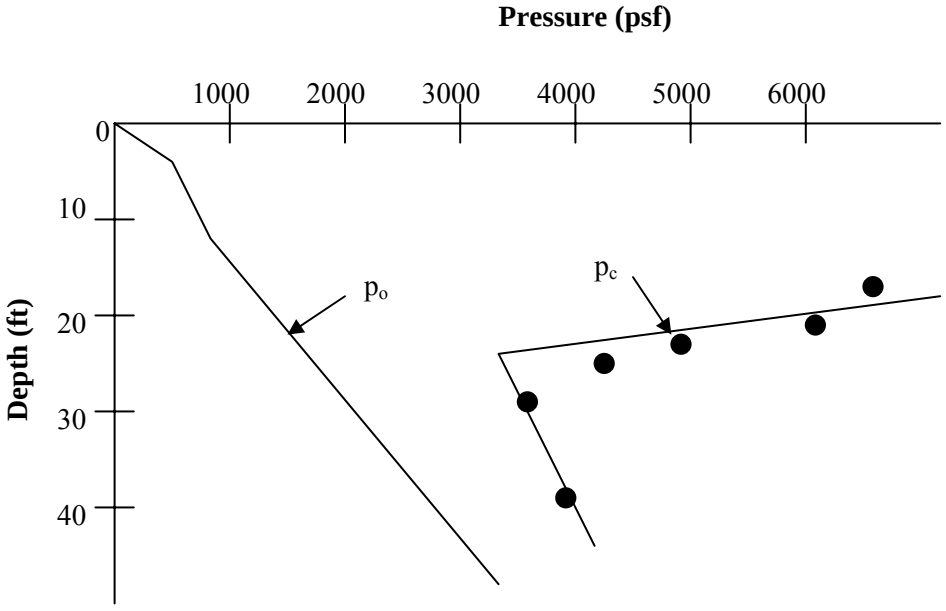

Figure A.6-3. Variation of overburden pressure and preconsolidation pressure with depth.

Step 3: Determine the distribution of pressure increase with depth due to the embankment pressure (p_f) at end of construction:

- Obtain embankment geometry. Use the same geometry (plan and section) from Example 7-1 in Chapter 7.
- Embankment top width = 100 ft
- Side and end slopes = 1V on 2H
- Top of end slope from toe = 60 ft
- Embankment height = 30 ft
- Embankment load (at longitudinal centerline) = $H_{emb} \times \gamma_{emb}$ = 30 ft × 130 pcf = 3,900 psf
- Use Figure A.6-4 to obtain pressure coefficient K (left ordinate) for b= $\left(\frac{100\,\text{ft}}{2}+\frac{60\,\text{ft}}{2}\right)$ = 80 ft and a distance from midpoint of end slope = 0.375b.
- Abutment center located 30 ft from midpoint of end slope → $\frac{30\,\text{ft}}{80\,\text{ft}}(\text{b}) = 0.375\text{b}$
- Use a series of charts corresponding to different depths expressed as a percentage of b_f (right ordinate) to obtain a distribution of pressure coefficients with depth.
- Compute pressure change Δp = K × embankment load at various depths expressed as a percentage of b_f. The results of these computations are presented in Table A.6-2.

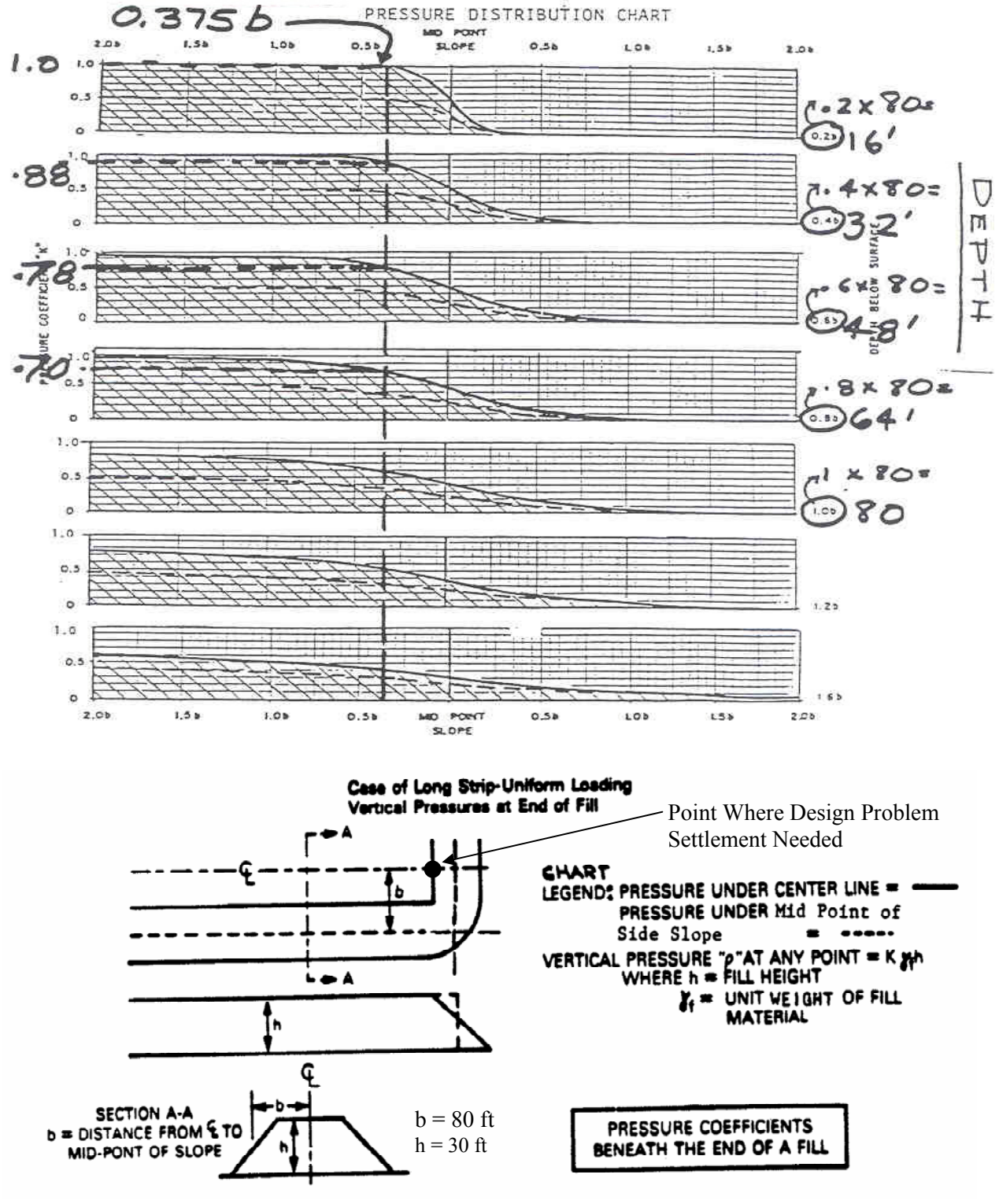

Figure A.6-4. Pressure distribution chart used to estimate the change in pressure at depths below the end of an embankment fill.

Table A.6-2
Summary of pressure increments at various depths due to embankment fill

Depth (ft)	"K" - from Figure A.6-4	Δp = "K" × 3,900 psf Distributed pressure (psf)
0.2 b_f = 16 ft	1.00	3,900
0.4 b_f = 32 ft	0.88	3,432
0.6 b_f = 48 ft	0.78	3,042
0.8 b_f = 64 ft	0.70	2,730
1.0 b_f = 80 ft	0.60	2,340

Step 4: **Calculate the final pressure ($p_f = p_o + \Delta p$) at various depths and plot the overburden pressure (p_o), preconsolidation pressure (p_c), and p_f with depth as shown in Figure A.6-5**

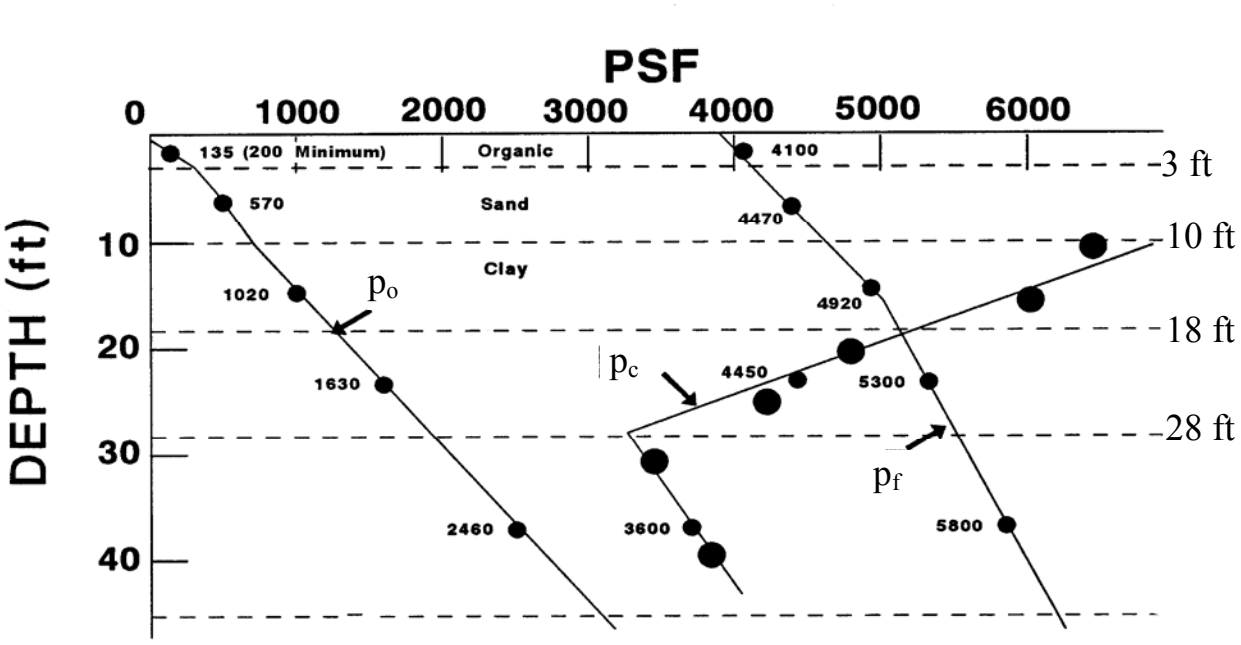

Figure A.6-5. Variation of overburden pressure (p_o), preconsolidation pressure (p_c) and final pressure due to embankment (p_f) with depth.

In settlement analyses, use pressures measured at the center of a layer or a partial layer. Thick layers should be subdivided (i.e., if a layer is 20 ft thick compute settlement in 10 ft increments) unless the slope of p_o, p_c, or p_f are slowly converging straight lines. Dashed horizontal lines in Figure A.6-5 show the increments selected here for analysis.

Step 5: Compute settlement in each layer (or partial layer).

- ***Layer 1 – Organic (0 ft to 3 ft)*** – use equation for consolidation settlement (Refer to Chapter 7.5). As indicated in the logs of Borings BAF-3 and BAF-4 where this material was encountered, no tube samples were obtained for consolidation testing. Therefore, the stress history of the layer cannot be determined from test results. However, based on the description of the material given in the boring logs and from experience with surface and near-surface organic soils, the organic layer is assumed to be normally consolidated for the computation presented here as shown in the sketch of the generic consolidation curve below. As is generally the case with these soils in practice, for the Apple Freeway Bridge the organic layer will be removed and replaced with compacted select material before the embankment fill is constructed. Settlement of 3-ft of compacted select material is considered to be negligible. The situation presented here illustrates the importance of sampling and testing all soils that have the potential to cause problems during and after construction.

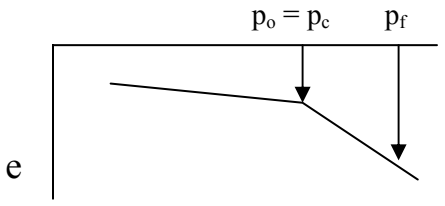

$$\Delta H = H \frac{C_c}{1 + e_o} \log \frac{p_f}{p_o}$$

H = 3 ft – 0 ft = 3 ft

The mid-thickness depth of the Organic Layer is $\frac{3\,\text{ft}}{2} = 1.5\,\text{ft}$

$C_c = 0.0115\,w = 0.0115\ (120) = 1.38$ - (Refer to Table 5-5 of Chapter 5)

From Figure 5-9 of Chapter 5, $C_c \approx 1.0$

Therefore use C_c (average) = 1.2

$$e_0 = \frac{w \times G_s}{\%Sat.} = \frac{120 \times 1.6}{100} = 1.9$$

$$\Delta H = 3\,\text{ft}\left(\frac{1.2}{1+1.9}\right)\log\frac{4{,}100\,\text{psf}}{200\,\text{psf}\ *} \qquad * \text{Remember } (p_o \geq 200\text{psf})$$

$$\Delta H = 1.63\,\text{ft} = 19.54\,\text{in}$$

This enormous amount of settlement corresponds to more than 50% of the original thickness of the organic layer, which is one of the reasons why such materials, when located at or close to the surface, should be removed and replaced with compacted select material.

- ***Layer 2 – Sand (3 ft to 10 ft)*** – use equation for immediate settlement (Refer to Chapter 7.4).

$$\Delta H = H\frac{1}{C'}\log\frac{p_f}{p_o}$$

H = 10 ft - 3 ft = 7 ft

The mid-thickness depth of the Sand Layer is $3\,\text{ft} + \frac{7\,\text{ft}}{2} = 6.5\,\text{ft}$

To find C′ use N_{60} = 17 (Refer to Boring BAF–3 at depth = 7 ft)

$$\frac{N1_{60}}{N_{60}} = 2 \;@\; p_o = 500\,\text{psf}$$ (Refer to Eq. 3-3 in Chapter 3)

Therefore $N1_{60}$ = 34

C′ = 90 (Refer to Figure 7-7 in Chapter 7 – interpolate between silty sand & fine to coarse sand)

$$\Delta H = (7\,\text{ft})\left(\frac{1}{90}\right)\log\frac{4470\,\text{psf}}{570\,\text{psf}}$$

$$\Delta H = 0.069\,\text{ft} = 0.83\,\text{in}$$

- ***Layer 3 – Clay – Sub-layer 1 (10 ft to 18 ft)*** – use equation for consolidation settlement (Refer to Chapter 7.5). As shown in Figure A.6-5, the clay layer is over-consolidated since $p_c > p_o$ and remains so during application of the entire load increment within this depth range as shown in the sketch of the generic

consolidation curve below, i.e., $p_f < p_c$. (Refer to Chapter 7.5.2)

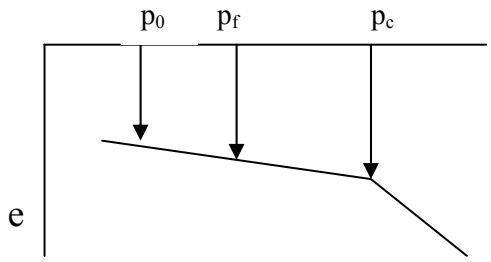

$$\Delta H = H \frac{C_c}{1 + e_o} \log \frac{p_f}{p_o}$$

$H = 18\text{ ft} - 10\text{ ft} = 8\text{ ft}$

The mid-thickness depth of Clay Sub-layer 1 is $10\,\text{ft} + \frac{8\,\text{ft}}{2} = 14\,\text{ft}$

From consolidation test data:
C_r (average) = 0.035
e_o (average) = 0.97

$$\Delta H = (8\,\text{ft})\left(\frac{0.035}{1 + 0.97}\right) \log \frac{4{,}920\,\text{psf}}{1{,}020\,\text{psf}}$$

$$\Delta H = 0.097\,\text{ft} = 1.17\,\text{in}$$

- ***Layer 3 – Clay - Sub-layer 2 (18 ft to 28 ft)*** - use equation for consolidation settlement (Refer to Chapter 7.5). The thickness of this sub-layer of the clay stratum was chosen because of the sharp break in the slope of the p_c vs. depth curve at 28-ft (Refer to Figure A.6-5). As shown in Figure A.6-5, the clay layer is over-consolidated within this depth range since $p_c > p_o$, but at the mid-depth the load increment causes $p_f > p_c$. Therefore the settlement for this sub-layer must be calculated in two steps as shown in the following sketch of the generic consolidation curve, one step for the pressure increment from p_o to p_c for which C_r applies, and the other for the pressure increment from p_c to p_f for which C_c applies. (Refer to Chapter 7.5)

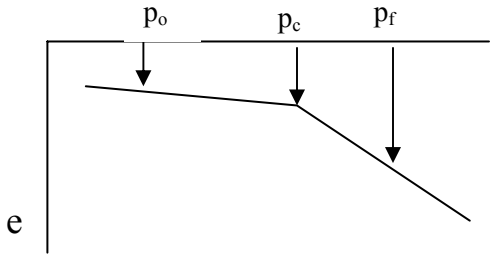

$$\Delta H = H\frac{C_r}{1+e_o}\log\frac{p_c}{p_o} + H\frac{C_c}{1+e_o}\log\frac{p_f}{p_c}$$

$H = 28\text{ ft} - 18\text{ ft} = 10\text{ ft}$

Mid-thickness depth of Clay Sub-layer 2 is at $18\text{ ft} + \frac{10\text{ ft}}{2} = 23\text{ ft}$

From consolidation test data:

C_r (avg.) = 0.035
C_c (avg.) = 0.35
e_o (avg.) = 0.97

$$\Delta H = (10\text{ ft})\left(\frac{0.035}{1+0.97}\right)\log\frac{4{,}450\text{ psf}}{1{,}630\text{ psf}} + 10\text{ ft}\left(\frac{0.35}{1+0.97}\right)\log\frac{5{,}300\text{ psf}}{4{,}450\text{ psf}}$$

$$\Delta H = 0.077\text{ ft} + 0.135\text{ ft} = 0.93\text{ in} + 1.62\text{ in} = 2.55\text{ in}$$

- ***Layer 3 – Clay - Sub-layer 3 (28 ft to 45 ft)*** - use equation for consolidation settlement (Refer to Chapter 7.5). The thickness of this sub-layer of the clay stratum represents the depth from the sharp beak in the p_c vs. depth curve at 28-ft to the bottom of the clay stratum (Refer to Figure A.6-5). As shown in Figure A.6-5, the clay layer is over-consolidated within this depth range since $p_c > p_o$, but at the mid-depth the load increment causes $p_f > p_c$. Therefore the settlement for this sub-layer, as was the case for Sub-layer 2, must be calculated in two steps as shown in the following sketch of the generic consolidation curve, step one for the pressure increment from p_o to p_c for which C_r applies, and the other for the pressure increment from p_c to p_f for which C_c applies. (Refer to Chapter 7.5)

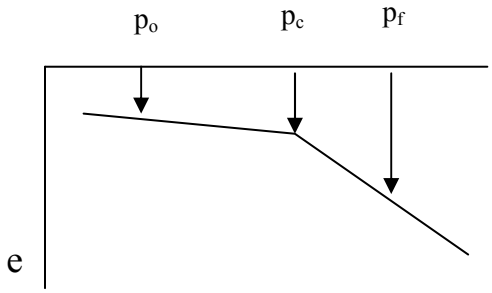

$$\Delta H = H\frac{C_r}{1+e_o}\log\frac{p_c}{p_o} + H\frac{C_c}{1+e_o}\log\frac{p_f}{p_c}$$

H = 45 ft – 28 ft = 17 ft

The mid-thickness depth of Clay Sub-layer 3 is $28\text{ ft} + \frac{17\text{ ft}}{2} = 36.5\text{ ft}$

From consolidation test data:

C_r (average) = 0.035
C_c (average) = 0.35
e_o (average) = 0.97

$$\Delta H = (17\text{ ft})\left(\frac{0.035}{1+0.97}\right)\log\frac{3{,}600\text{ psf}}{2{,}460\text{ psf}} + (17\text{ ft})\left(\frac{0.35}{1+0.97}\right)\log\frac{5{,}800\text{ psf}}{3{,}600\text{ psf}}$$

$$\Delta H = 0.050\text{ ft} + 0.63\text{ ft} = 0.60\text{ in} + 7.51\text{ in} = 8.11\text{ in}$$

Table A.6-3
Summary of layer and sub-layer settlements due to embankment fill and computation of total settlement

Layer	Settlement (in)
Layer 1 – Organic (0 ft to 3 ft) - replaced with compacted select material	≈ 0
Layer 2 – Sand (3 ft to 10 ft)	0.83 in
Layer 3 – Clay (10 ft to 45 ft)	
Sub-layer 1 - (10 ft to 18 ft)	1.17 in
Sub-layer 2 - (18 ft to 28 ft)	2.55 in
Sub-layer 3 - (28 ft to 45 ft)	8.11 in
ΔH_{Total}	12.66 in

Step 6: Compute Time for Settlement to Occur in Clay (Layer 3)

- Layer 1 – Select backfill material no settlement expected.
- Layer 2 – 0.83 inch settlement occurs immediately in sand.
- Layer 3 – ΔH_{Total} (Layer 3) = 1.17 in + 2.55 in + 8.11 in = 11.83 in

Time required for a specified percentage of total settlement to occur is computed from: $t = \frac{T_v \, H_d^2}{c_v}$ where:

H_d = longest drainage path (ft) = ½ thickness of clay layer since permeable layers exist above and below. Therefore, for the clay layer

$$H_d = \frac{35\,\text{ft}}{2} = 17.5\,\text{ft}$$

$c_v = 0.6\ \text{ft}^2/\text{day}$

T_v = time factor corresponding to a specified average percent consolidation (U) - (Refer to Table 7-4 in Chapter 7 or calculate by using Equation 7-8 in the Chapter 7)

Table A.6-4 provides a convenient template for performing computations to obtain settlement vs. time values for arbitrarily chosen values of average percent consolidation.

Table A.6-4
Template to compute values of consolidation settlement (ΔH) in clay layer at various times (t) after application of embankment load

Average % Consol. (U)	ΔH (in) = (U)(ΔH_{Total} (Layer 3)	Time Factor (T) From Table 7-4	$\frac{H_d^2}{c_v}$	t (days)
20	2.4	0.031	510.4	16
50	5.9	0.197	↓	101
70	8.3	0.403	↓	206
90	10.6	0.848	↓	432

The time-settlement plot can now be constructed for all soil layers. Remember to include 0.83 inch sand settlement, which occurs immediately as load is applied. Therefore ΔH_{Total} = 12.66 in

Step 7: Plot Settlement vs. Time Curve – (include ΔH Sand = 0.83 in)

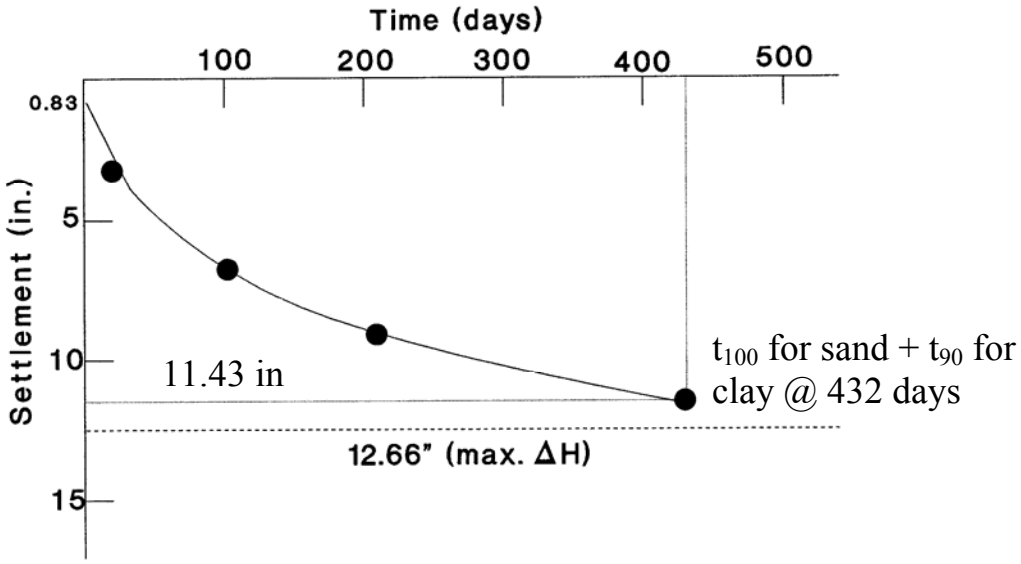

Figure A.6-6. Settlement vs. Time after construction of 30-ft embankment fill.

The designer must insure that 90% consolidation is achieved before construction of the abutment foundation begins. If the waiting period is too long, as it is in this case for the Apple Freeway (432 days ≈ 14 months), the choices of treatment are:

1. Surcharge.
2. Vertical drains

It should be noted that the decision on the choice of treatments will be made before construction of the embankment fill begins. That decision will influence the construction procedure, e.g., if surcharging is chosen, the surcharge will be placed as part of the embankment fill and removed afterward.

A.6-4 CONSIDERATION OF SURCHARGE OPTION TO ACCELERATE CONSOLIDATION SETTLEMENT AND REDUCE TIME REQUIRED FOR SETTLEMENT DUE TO THE EMBANKMENT FILL

Assume:

- 10-ft high compacted surcharged (γ = 130 pcf). Therefore, the total change in pressure (Δp_{total}) at the surface is now due to the embankment fill (Δp_{fill}) plus the surcharge (Δp_s) = (30-ft)(130 pcf) + (10-ft)(130 pcf) = 5,200 psf.
- The pressure increase at various depths below the surface is calculated as before, but with the value of the change in pressure at the surface = 5,200 psf. Since the dimensions of the embankment, except for the height, are the same as before, the values of "K" are unchanged. The results of these computations are presented in

Table A.6-5.

- Additional immediate settlement of sand due to the surcharge is negligible.
- e_o remains 0.97 although the actual value is less due to compression under the previous load.

Step 1: Obtain pressure increase with depth (use previous "K" value)

Table A.6-5
Pressure increments at various depths due to embankment fill + surcharge

Depth (ft)	″K″ - from Figure A.6-4	Δp_{total} = ″K″ × 5,200 psf Distributed pressure (psf)
0.2b = 16 ft	1.00	5,200
0.4b = 32 ft	0.88	4,580
0.6b = 48 ft	0.78	4,060

Step 2: Calculate the new final pressure ($p_f + p_s = p_o + \Delta p_{total}$) at various depths and plot the overburden pressure (p_o), preconsolidation pressure (p_c), and the new final pressure due to the embankment plus the surcharge ($p_f + p_s$) with depth.

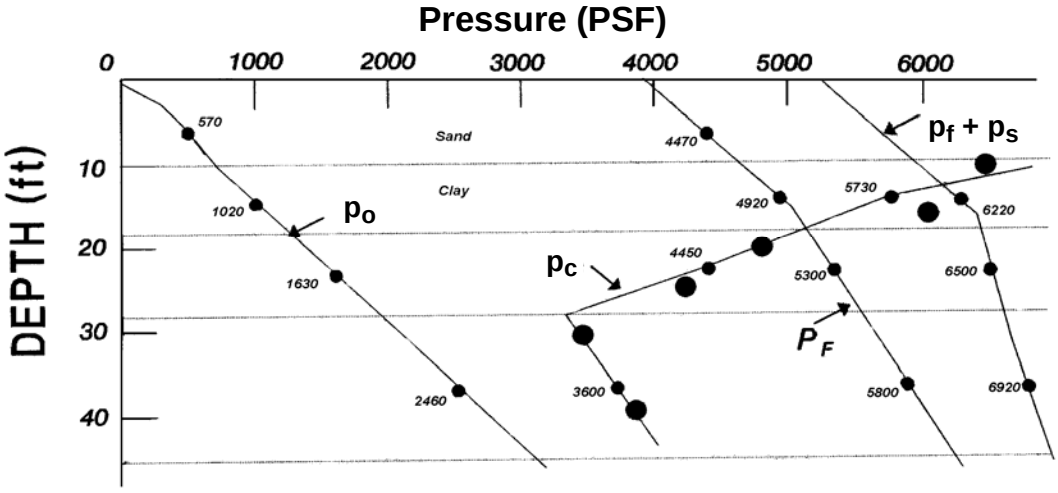

Figure A.6-7. Variation of overburden pressure (p_o), preconsolidation pressure (p_c) and final pressure due to embankment + surcharge ($p_f + p_s$) with depth.

Step 3: Compute Settlement in Layer 3

The Layer 1 organics were replaced by compacted select fill, therefore any settlement of this layer will be negligible even with the 10 ft surcharge. As indicated previously, additional settlement of Layer 2 due to an additional 10 ft of surcharge fill will also be negligible. Therefore, Layer 3 is the only layer that will settle more than originally calculated due to the additional 10 ft of surcharge. As was done originally, subdivide Layer 3 into three partial layers or sub-layers for computational purposes.

- ***Layer 3 – Clay – Sub-layer 1 (10 ft to 18 ft)*** – use equation for consolidation settlement (Refer to Chapter 7.5). As shown in Figure A.6-5, the clay layer is over-consolidated since $p_c > p_o$, but at the mid-depth the load increment due to the additional 10 ft of surcharge causes $p_f + p_s > p_c$. Therefore the settlement for this sub-layer must now be calculated in two steps as shown in the following sketch of the generic consolidation curve, one step for the pressure increment from p_o to p_c for which C_r applies, and the other for the pressure increment from p_c to $(p_f + p_s)$ for which C_c applies. (Refer to Chapter 7.5)

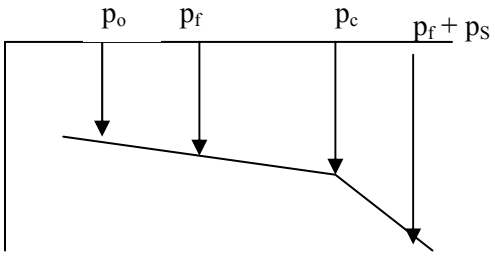

$$\Delta H = H\frac{C_r}{1+e_o}\log\frac{p_c}{p_o} + H\frac{C_c}{1+e_o}\log\frac{p_f+p_s}{p_c}$$

$$\Delta H = (8\,\text{ft})\left(\frac{0.035}{1+0.97}\right)\log\frac{5{,}730\,\text{psf}}{1{,}020\,\text{psf}} + (8\,\text{ft})\left(\frac{0.35}{1+0.97}\right)\log\frac{6{,}220\,\text{psf}}{5{,}730\,\text{psf}}$$

$$\Delta H = 0.11\,\text{ft} + 0.05\,\text{ft} = 0.16\,\text{ft}$$

$$\Delta H = 1.32\,\text{in} + 0.61\,\text{in} = 1.93\,\text{in}$$

- ***Layer 3 – Clay - Sub-layer 2 (18 ft to 28 ft)*** - use equation for consolidation settlement (Refer to Chapter 7.5). The thickness of this sub-layer of the clay stratum was chosen because of the sharp break in the slope of p_c vs depth curve at 28-ft (Refer to Figure A.6-5). As shown in Figure A.6-5, the clay layer is over-consolidated within this depth range since $p_c > p_o$, but at the mid-depth the load increment including the 10-ft surcharge causes $p_f + p_s > p_c$. Therefore the settlement for this sub-layer must be calculated in two steps as shown in the following sketch of the generic consolidation curve, one step for the pressure increment from p_o to p_c for which C_r applies, and the other for the pressure increment from p_c to $(p_f + p_s)$ for which C_c applies. (Refer to Chapter 7.5)

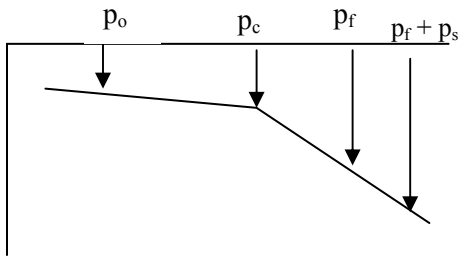

$$\Delta H = H\frac{C_r}{1+e_o}\log\frac{p_c}{p_o} + H\frac{C_c}{1+e_o}\log\frac{p_f + p_s}{p_c}$$

$$\Delta H = (10\,\text{ft})\left(\frac{0.035}{1+0.97}\right)\log\frac{4{,}450\,\text{psf}}{1{,}630\,\text{psf}} + 10\,\text{ft}\left(\frac{0.35}{1+0.97}\right)\log\frac{6{,}500\,\text{psf}}{4{,}450\,\text{psf}}$$

$$\Delta H = 0.08\,\text{ft} + 0.29\,\text{ft} = 0.37\,\text{ft}$$

$$\Delta H = 0.93\,\text{in} + 3.51\,\text{in} = 4.44\,\text{in}$$

- ***Layer 3 – Clay - Sub-layer 3 (28 ft to 45 ft)*** - use equation for consolidation settlement (Refer to Chapter 7.5). The thickness of this sub-layer represents the depth from the sharp break in the p_c vs. depth curve at 28-ft to the bottom of the clay stratum (Refer to Figure A.6-5). As shown in Figure A.6-5, the clay layer is over-consolidated within this depth range since $p_c > p_o$, but at the mid-depth the load increment including the 10-ft surcharge causes $p_f + p_s > p_c$. Therefore the settlement for this sub-layer, must also be calculated in two steps as shown in the following sketch of the generic consolidation curve, step one for the pressure increment from p_o to p_c for which C_r applies, and the other for the pressure increment from p_c to $(p_f + p_s)$ for which C_c applies. (Refer to Chapter 7.5).

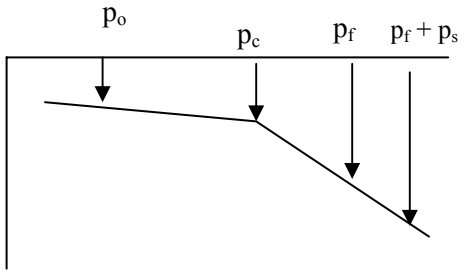

$$\Delta H = H\frac{C_r}{1+e_o}\log\frac{p_c}{p_o} + H\frac{C_c}{1+e_o}\log\frac{p_f + p_s}{p_c}$$

$$\Delta H = (17\,\text{ft})\left(\frac{0.035}{1+0.97}\right)\log\frac{3{,}600\,\text{psf}}{2{,}460\,\text{psf}} + (17\,\text{ft})\left(\frac{0.35}{1+0.97}\right)\log\frac{6{,}920\,\text{psf}}{3{,}600\,\text{psf}}$$

$$\Delta H = 0.05\,\text{ft} + 0.86\,\text{ft} = 0.91\,\text{ft}$$

$$\Delta H = 0.60\,\text{in} + 10.32\,\text{in} = 10.89\,\text{in}$$

Table A.6-6
Summary of sub-layer settlements in clay due to embankment fill + surcharge and computation of total settlement of clay - Layer 3

Layer	Embankment Only	Embankment + Surcharge	Surcharge
10 ft to 18 ft	1.17 in	1.93 in	0.76 in
18 ft to 28 ft	2.55 in	4.44 in	1.89 in
28 ft to 45 ft	8.11 in	10.89 in	2.78 in
Total ΔH =	11.83 in	17.26 in	5.43 in

Step 4: Obtain Time-Settlement Relationship: $t = \dfrac{T_v\, H_d^2}{c_v}$

Table A.6-7
Template to compute values of consolidation settlement (ΔH) in clay layer at various times (t) after application of embankment and surcharge loads

Average % Consol. (U)	ΔH (in) = (U)(ΔH_{Total} - Layer 3)	Time Factor (T) From Table 6-3	$\frac{H_d^2}{c_v}$	t (days)
20	3.5 in	0.031	510.4	16
50	8.6 in	0.197	↓	101
70	12.1 in	0.403	↓	206
90	15.5 in	0.848	↓	432

Step 5: Plot Settlement vs. Time Curve – (include ΔH Sand = 0.83 in)

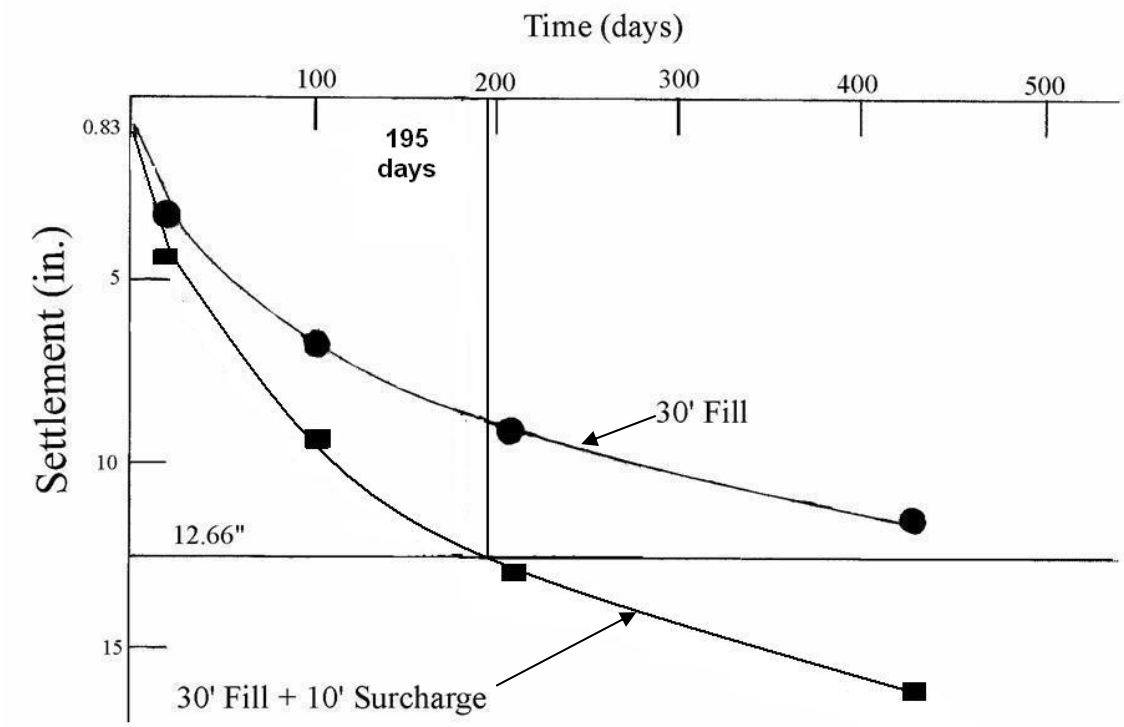

Figure A.6-8. Settlement vs. Time after construction of 30 ft embankment fill with and without surcharge.

Step 6: Determine time of waiting period with surcharge to obtain equivalent settlement to that of proposed embankment.

Enter the settlement vs. time plot for 30 ft fill with 10 ft surcharge with 12.66 inches (total [immediate + consolidation] settlement expected for 30 ft fill). Extend the line across to the "30' Fill + 10' Surcharge" curve and read the waiting period time in days on the time axis, i.e. 195 days or 6.5 months.

Step 7: Recommend instrumentation for monitoring settlement and pore water pressures – (Table A.6-8)

Table A.6-8
Recommend instrumentation for monitoring settlement and excess pore water pressures at East Abutment

Instrument	Station	Depth Below Ground
Settlement plate	90 + 00	At ground surface
Settlement plate	93 + 50	At ground surface
Settlement plate	96 + 50	At ground surface
Piezometers	93 + 50	20 ft, 28 ft, 36 ft
Piezometers	96 + 50	20 ft, 28 ft, 36 ft

Step 8: Recheck stability of 30 ft fill with 10 ft surcharge – Refer to procedure in Section A.5

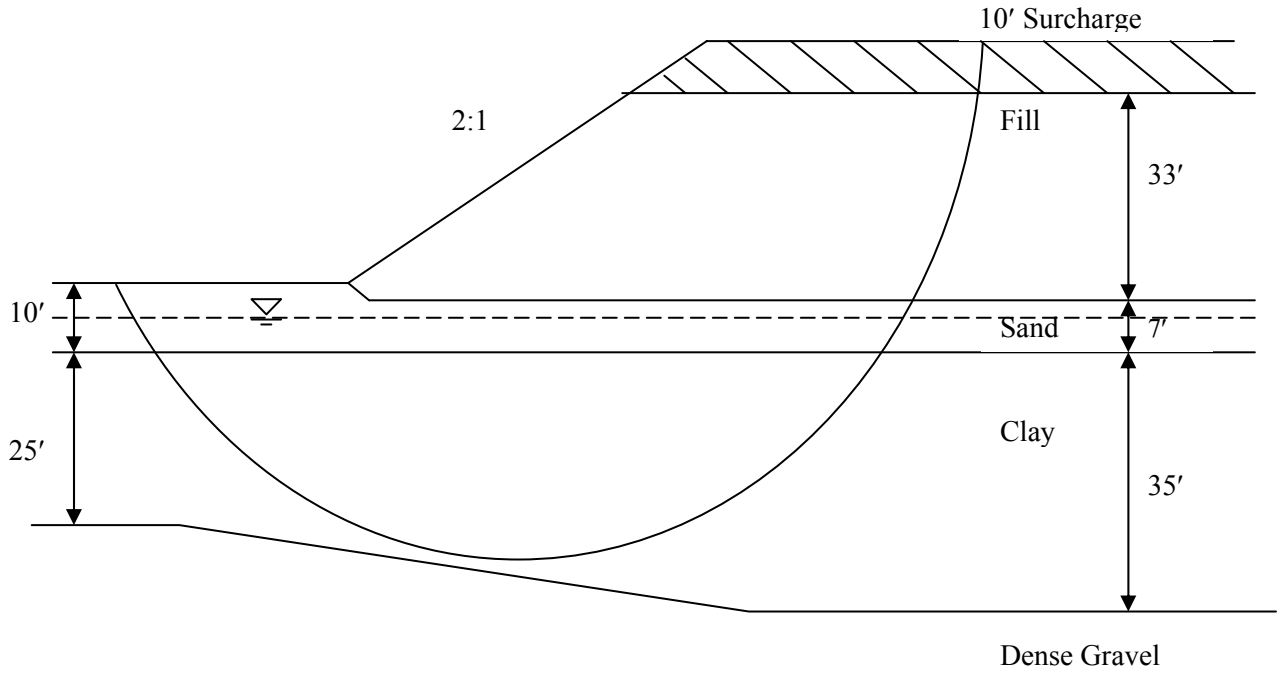

Figure A.6-9. Trial failure circle – embankment fill + surcharge - East Abutment.

Safety Factor with surcharge = 1.33.
Safety Factor without surcharge = 1.63.
Conclusion: the safety factor in both cases is greater than 1.30, which is minimum recommended for bridge approach stability for the temporary case of surcharge.

Step 9: Prepare cost estimate for surcharge

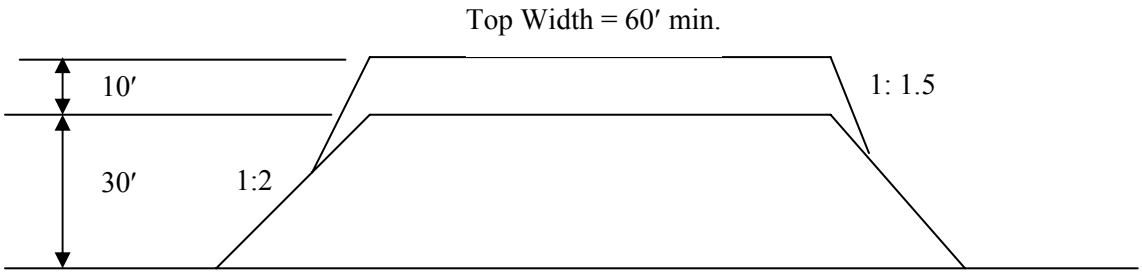

Figure A.6-10. Idealized cross section of embankment fill + surcharge.

- Assume 500 linear feet behind top of end slope to be surcharged at each approach, therefore total length of surcharge = 1,000 feet.
- Assume average width of surcharge = 80 feet including side slopes.
- Calculate surcharge quantity (V_{sur}) as:

$$80\,\text{ft} \times 10\,\text{ft} \times \frac{1{,}000\,\text{ft}}{27\,\text{ft}^3/\text{yd}^3} = 29{,}630\,\text{yd}^3$$

- Unit cost to place and remove surcharge = \$4.00 /yd^3, therefore total cost is as follows:
  Total cost = 29,630 yd^3 × \$4.00 /yd^3 ≈ \$120,000
  [THIS IS AN EXAMPLE. ALWAYS CHECK THE LOCAL UNIT PRICES]

A.6-5 CONSIDERATION OF WICK DRAIN OPTION (NO SURCHARGE) TO ACCELERATE CONSOLIDATION SETTLEMENT AND REDUCE TIME REQUIRED FOR SETTLEMENT DUE TO THE EMBANKMENT FILL

Step 1: Choose reasonable spacing of wick drains – assume equivalent wick drain diameter of 0.5 ft and try 7.5-ft center to center triangular spacing.

- Recent designs for wick drains have used equivalent diameters of 0.5 ft, i.e., $d_w = 0.5$ ft
- For triangular spacing:
  $d_e = 1.05 \times s = 1.05 \times 7.5$ ft = 7.875 ft
  $\eta = d_e/d_w = 7.875$ ft / 0.5 ft = 15.75 ft ≈ 16 ft

Step 2: Compute settlement-time-relationship

- $c_v = c_r = 0.6$ ft^2/day

- Arbitrarily select a reasonable range of values of time (days) and calculate the corresponding time factors for vertical (T_v) and radial (T_r) drainage as follows:

  $T_r = t\, c_h/d_e^2 = t$ (days) 0.6 ft^2/day/(7.875 ft)^2
  $T_v = t\, c_v/H_d^2 = t$ (days) 0.6 ft^2/day/(17.5 ft)^2

  $H_d = ½\, H = 17.5$ ft (Refer to previous calculation for vertical drainage only)

- Calculate the values of average percent consolidation (U_v) corresponding to the calculated values of time factor (T_v) by:

  $U_v = (4\ T_v / \pi)^{1/2}$

- Estimate the values of average percent consolidation (U_r) corresponding to the calculated values of time factor (T_r) for $\eta = 16$ from the curves in Figure 4 in FHWA (1986).

- Calculate average percent consolidation for combined drainage (U_c) by:

  $U_c = 1 - [(1 - U_r)(1 - U_v)]$

  where U_r and U_v are in decimals.

- Calculate values of consolidation settlement ΔH (inches) in clay Layer 3 due to combined vertical and radial drainage corresponding to the arbitrarily assumed values of time –use template shown in Table A.6-10 to aid in the calculation.

Table A.6-10
Template to compute values of consolidation settlement (ΔH) in clay -Layer 3 at various times (t) after application of embankment load (wick drains with no surcharge) due to combined vertical and radial drainage

Time after loading t (days)	Time factor- T_v	Average % Consolidation U_v	Time factor- T_r	Average % Consolidation U_r	Combined Average % Consolidation U_c%	Layer 3 ΔH (in)
10	0.020	16	0.097	34	44	5.2
20	0.039	22	0.193	57	66	7.8
30	0.059	27	0.290	71	79	9.3
40	0.078	32	0.387	81	87	10.3
50	0.098	35	0.484	85	90	10.6
60	0.118	39	0.580	92	95	11.2
70	0.137	42	0.677	94	97	11.4
80	0.157	45	0.774	97	98	11.6
90	01.76	47	0.871	99	99	11.8

Step 3: Plot settlement-time-curve for wick drains – Refer to Figure A.6-11.

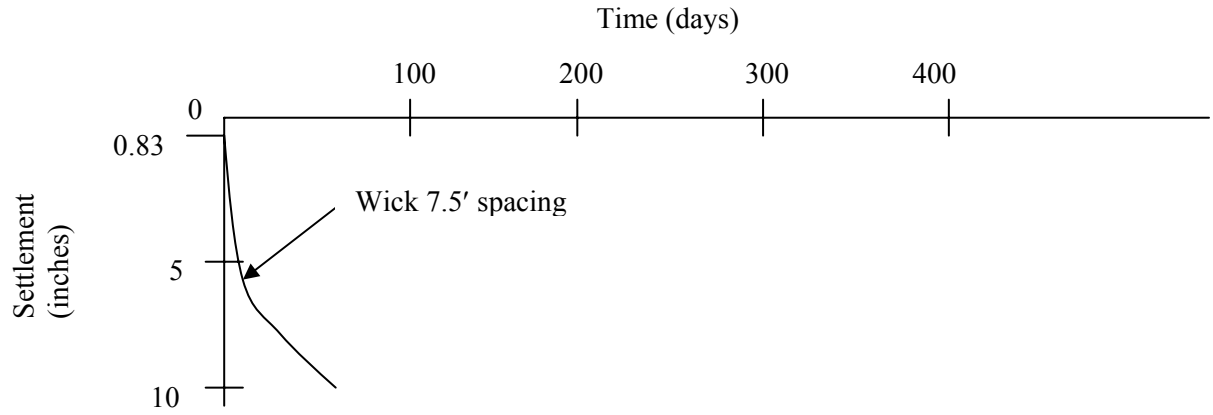

Figure A.6-11. Time versus settlement after completion of embankment fill for wick drain treatment without surcharge.

Step 4: Prepare cost estimate for wick drains

- Assume:
  1. 500 linear feet of drains at both approaches, therefore total length = 1,000 linear feet.
  2. Width of drain treatment midslope to midslope = 160 linear ft
  3. Length of each drain = 45 ft
  4. Unit cost per wick drain: $1.00/ft (**THE USER SHOULD CALL THE LOCAL CONTRACTORS FOR LATEST COSTS**)

- Consider Wick Drains - 7.5 ft center to center.
  Treated area/drain = 0.866 S^2 = 0.866(7.5 ft)^2 = 49 ft^2/drain
  No. of drains = (160 ft)(1,000 ft)/49 ft^2/drain = 3,265 drains
  Linear feet of drain = (3,265 drains) 45 ft/drain = 146,925 ft
  Cost = (146,925 ft)($1.00/ft) + $25,000 (Mobilization) = $172,000

Step 5: Prepare settlement–time curves for (a) 30-ft embankment fill, (b) 30-ft embankment fill with 10-ft surcharge (c) 30-ft fill embankment with vertical drains (wick) without surcharge (Refer to Figure A.6-12)

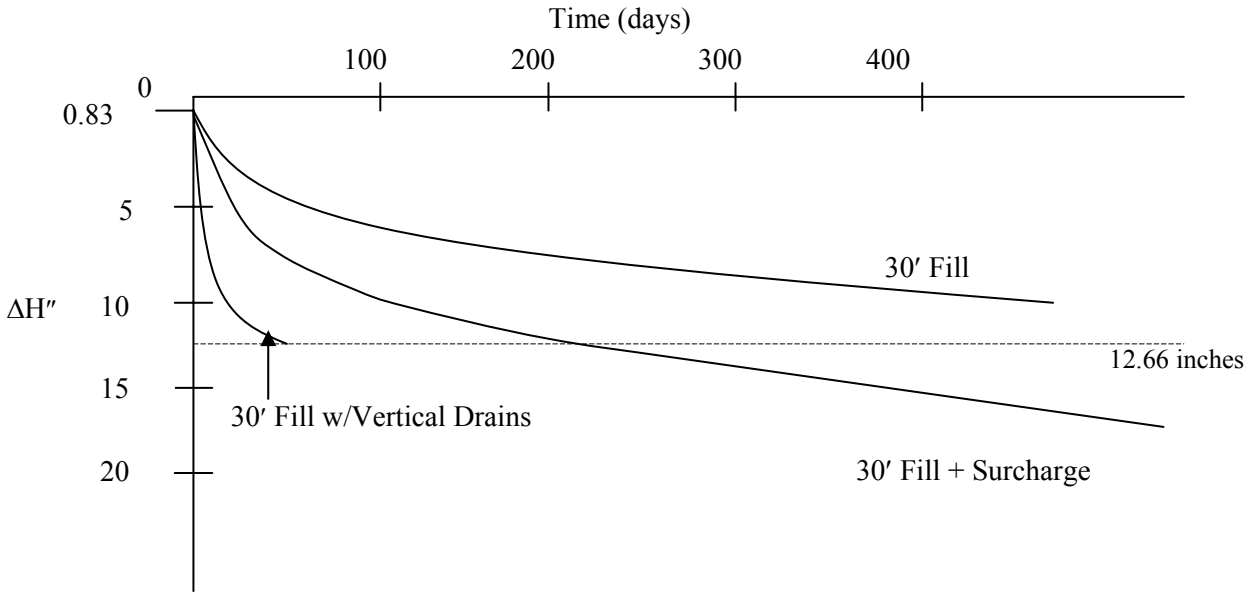

Figure A.6-12. Summary of time-settlement curves for baseline case (30-ft embankment fill) and various treatment options.

Step 6: Prepare table showing summary of results for base-line case (embankment fill only) and various treatment options in terms of waiting period and extra costs of treatment. Refer to Table A.6-12

Table A.6-12
Summary of results for base-line case (embankment fill only) and various treatment options

Treatment	Time for at Least 90% Consolidation (Months)	Extra Cost
Fill only	14	Base line
Fill with 10-ft of surcharge	6.5	$120,000
Fill with Wick Drains	2	$172,000

A.6-6 CHECK FOR LATERAL SQUEEZE OF CLAY

Step 1 Determine whether or not lateral squeeze will occur.

Lateral squeeze causes pile supported abutments to rotate into embankment or spread footing abutments to move laterally. Lateral squeeze occurs if (see Chapter 7.6):

$\gamma_{fill} H_{fill} > 3 \times$ cohesion

For East Abutment:

$\gamma_{fill} H_{fill} = 130$ pcf x 30 ft > 3 x 1,100 psf

3,900 psf > 3,300 psf, therefore:

- lateral squeeze may occur.
- consider waiting period to dissipate settlement of fill.
- do not construct abutments until settlement dissipates, i.e. until the average percent consolidation (U) ≥ 90%.

Step 2 Estimate amount of horizontal movement of abutment due to lateral squeeze of clay - Layer 3.

Assume baseline case – 30-ft embankment fill only

Rule of thumb:

Horizontal Movement = 0.25 ΔH of embankment (in clay)
= 0.25 × 11.83 in
Horizontal Movement = 3 in

Recommend no spread footing construction or pile driving until settlement is at least 90% complete, i.e., at time = t_{90}.

A.6-7 SUMMARY OF THE APPROACH ROADWAY STABILITY – FOR DETAILS REFER TO SECTION A.5-4 OF PREVIOUS PROBLEM

1. Develop a design soil profile
   - Soil layer unit weights and strength estimated.

2. Circular Arc Analysis
   - Approach embankment safety factor 1.63 against circular failure.

3. Sliding and Block Analysis
   - Approach embankment safety factor 3.5 against sliding failure.

4. Lateral Squeeze
   - Possible abutment rotation problem.

A.6-8 SUMMARY OF EMBANKMENT SETTLEMENT ANALYSES AT EAST ABUTMENT

1. Construct an idealized design profile to scale.
   - Use idealized soil profile from Boring UDH BAF-4
   - Include 30-ft high embankment at east abutment (assume 3 ft organic layer at the surface is replaced by compacted select material).
   - Estimate consolidation properties of clay layer from results of field and laboratory tests.

2. Determine overburden pressure (p_o), change in pressure due to embankment fill (Δp), and maximum past pressure (p_c) , all as a function of depth.
   - Plot pressure distributions with depth and determine stress history of impacted layers.

3. Calculate settlement of each layer impacted by 30-ft embankment fill
   - Compacted select fill (Layer 1 organic replacement material) - negligible settlement
   - Sand (Layer 2) - 0.8 inches of immediate settlement
   - Clay (Layer 1) - 11.83 inches of consolidation settlement.
   - Total of 12.6 inches of settlement predicted.

4. Calculate time required for 90% of primary consolidation to occur and plot settlement vs. time curve including immediate settlement of sand layer.
    - t_{90} = 432 days. (organic material replaced)

5. Consider surcharge option to accelerate consolidation settlement and reduce time required for settlement due to the embankment fill.
    - Calculate the new final pressure due to the embankment plus the surcharge (p_f + p_s) and plot values of (p_f + p_s), the overburden pressure (p_o), and the preconsolidation pressure (p_c) with depth.
    - Calculate settlement in Layer 3.
    - Calculate and plot settlement-time relationship.
    - Determine waiting time with 10-ft of surcharge to obtain settlement equivalent to that of proposed embankment.
    - t_{90} = 432 days. (organic material replaced)
    - Recheck stability of 30 ft fill with 10 ft surcharge – FS = 1.33.
    - Prepare cost estimate for surcharge - cost = $120,000.

6. Consideration of vertical drain option (wick drains - no surcharge) to accelerate consolidation settlement and reduce time required for settlement due to the embankment fill.
    - Choose reasonable spacing of drains.
    - Calculate and plot settlement-time-curve for combined vertical and radial drainage.
    - Determine waiting times to obtain settlement equivalent that of proposed embankment.
    - $t_{90} \approx 50$ days for wick drains (organic material replaced).
    - Prepare cost estimate for vertical drains - cost = $172,000 (wick drains).

[THIS PAGE INTENTIONALLY BLANK]

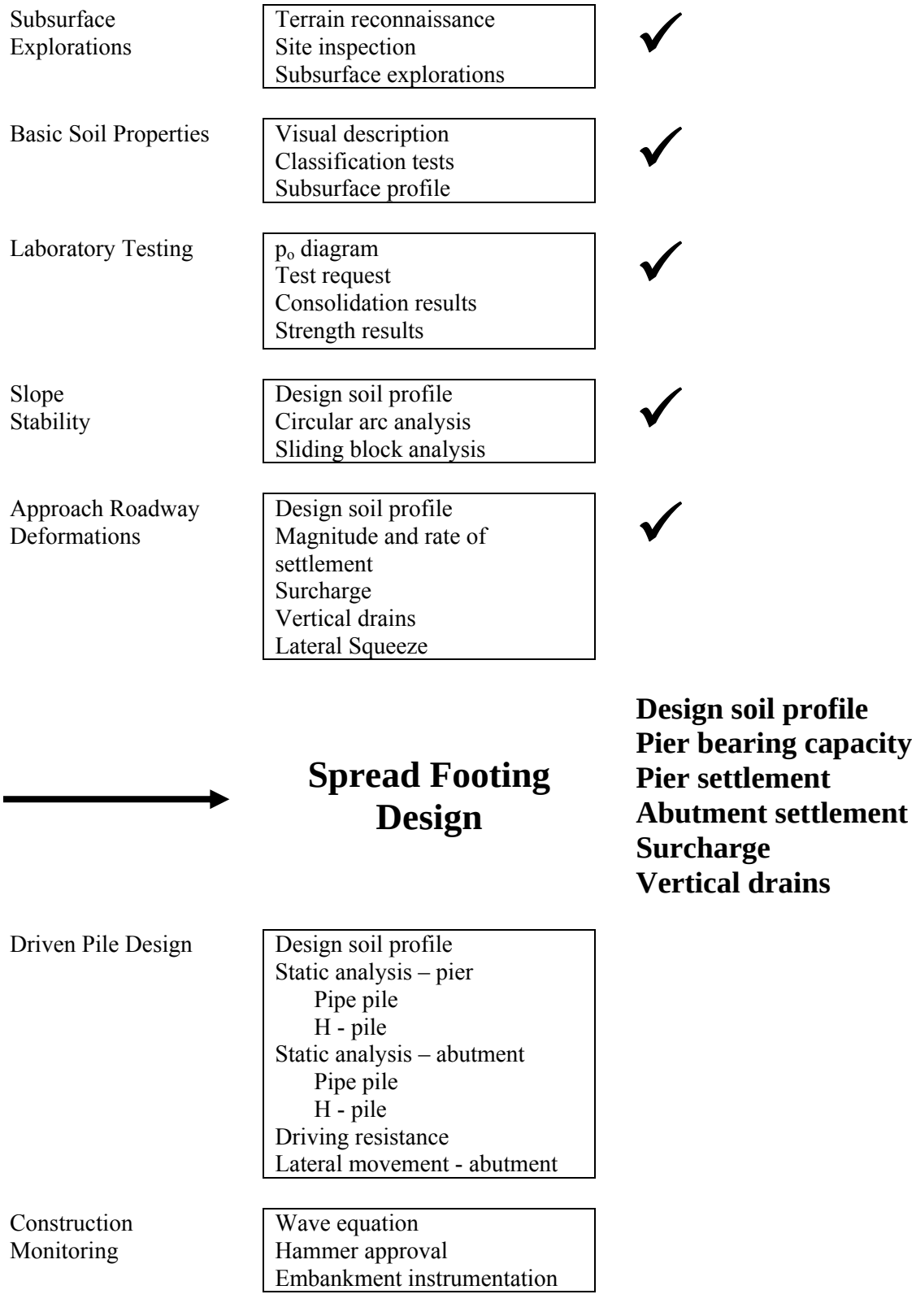

Figure A.7-1. Status of geotechnical work.

SECTION A.7
GEOTECHNICAL DESIGN OF SPREAD FOOTING

A.7-1 RELEVANT CONCEPTS AND PROCEDURES (Refer to Figure A.7-1)

- General procedure to calculate ultimate bearing capacity of a rectangular footing in a layered subsurface profile; Chapter 8
- Procedure based on 2:1 geometric attenuation of applied pressure with depth to determine pressure distribution with depth due to rectangular footing; Chapter 2.
- Immediate and consolidation settlement of rectangular footing – computation of magnitude; Chapter 7 and Chapter 8
- Consolidation settlement - rectangular footing – computation of time rate; Chapter 7.
- Effect of pre-construction treatment by surcharging or vertical drains on consolidation settlement of rectangular footing; Chapter 7.

In this section the geotechnical design process for spread footings for the pier and abutment foundations is illustrated. The computation procedures for the evaluation of ultimate bearing capacity are presented. The assessment of allowable bearing capacity is discussed with the context of settlement criteria. Settlement analysis for both immediate and consolidation settlement are performed to illustrate the effect of footing geometry on the magnitude of those settlements. The effect of pre-treatment by surcharging or vertical drains on both the magnitude of settlement and time required for full consolidation settlement is illustrated.

A.7-2 DETAILED PROCEDURES

Given:

- The footing geometry and subsurface conditions shown in Figure A.7-2 for the center pier of the Apple Freeway Bridge.
- The results of Standard Penetration tests (SPT-N blow counts) performed in Boring BAF – 2 as shown in Figure A.7-2.
- The footing geometry and subsurface conditions shown in Figure A.6-2 for the east embankment of the Apple Freeway Bridge.
- Values of relevant soil as provided in the previous example (Refer to Section A.6)

Required:

- Compute the ultimate bearing capacity of a rectangular footing at the pier location and apply an appropriate factor of safety to obtain the allowable bearing pressure.
- Compute the pressure transmitted to the underlying clay layer by the footing and compare that pressure to the allowable clay bearing capacity.
- Compute the magnitudes of the anticipated immediate and consolidation settlement due to the rectangular footing at the pier location.
- Compute the ultimate bearing capacity of a rectangular footing founded within the embankment at the East Abutment and apply an appropriate factor of safety to obtain the allowable bearing pressure
- Compute the magnitudes of the anticipated immediate and consolidation settlement due to the rectangular footing founded within the embankment at the East Abutment. Taking into account pretreatment by wick drains (Refer to Section A.6-5).
- Compute the time required for the settlement of the footing to occur. Take into account pretreatment by wick drains and continuing consolidation due to the embankment fill.
- Plot settlement-time curves for both the pier and embankment footings.

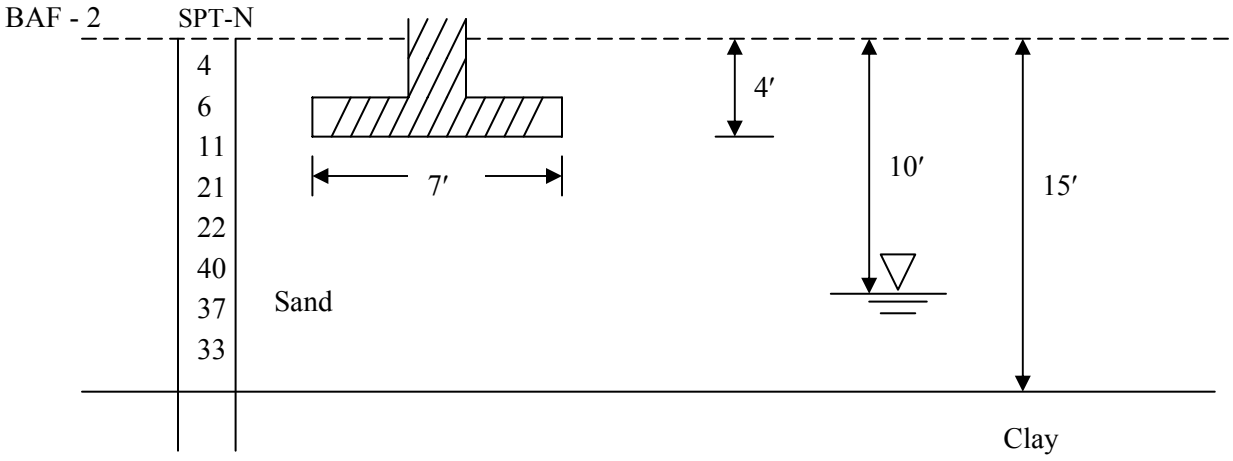

Figure A7-2. Footing geometry and subsurface conditions for center pier of the Apple Freeway Bridge including SPT-N blow counts from Boring BAF-2.

A.7-3 COMPUTE ULTIMATE AND ALLOWABLE BEARING CAPACITY OF PIER FOOTING

- **Define geometry of the problem.**
  - Footing embedment below final grade (D_f) = 4 feet.
  - Footing width (B_f) = 1/3 pier height = 7 feet
  - Footing length (L_f) = 100 feet
  - Depth to ground water below base of footing (D_w) = 6 feet.

- **Identify characteristics of geometry that are relevant to solution.**
  - L_f / B_f = 100 ft / 7 ft > 10, therefore consider the footing to be continuous.
  - If ($D_w < 1.5B_f + D_f$), the effect of ground water table must be considered. Check: 6 ft < 1.5 (7 ft), therefore ground water table must be considered.
  - Use SPT-N values to estimate internal friction angle (ϕ) of the sand.

Step 1: Find average corrected SPT-N blow count ($N1_{60}$) below footing (Refer to Section 3-7 of text) and estimate internal friction angle (ϕ) of soil.

Table A-7.1
Determination of SPT-N values corrected for hammer energy and depth

Depth (ft)	p_o (psf)	p_o (tsf)	N (bpf)	Hammer Efficiency (E_f)	E_f / 60	N_{60} (bpf)	C_N	$N1_{60}$ (bpf)
5	550	0.275	11	65	1.083	12	1.43	17
7	770	0.385	21	65	1.083	23	1.32	30
8	880	0.440	22	65	1.083	24	1.28	31
10	1100	0.550	40	65	1.083	43	1.20	52
12	1195	0.598	37	65	1.083	40	1.17	47
14	1290	0.645	33	65	1.083	36	1.15	41
						Average corrected blow count =		36

- For average corrected blow count assume internal friction angle of sand $\phi \approx 36^o$ (Refer to Table 8-3 in Chapter 8)

Step 2: Determine ultimate capacity (q_{ult}).

- Equation 8-6 in the text can be re-written as follows since cohesion = 0.

$$q_{ult} = c \cancel{N_c}^{0} s_c b_c + q N_q C_{Wq} s_q b_q d_q + 0.5 \gamma B_f N_\gamma C_{W\gamma} s_\gamma b_\gamma$$

- By using the appropriate equations in Table 8-4 of the text the shape factors are:
  $s_q = 1.05$
  $s_\gamma = 0.97$
- Since the base of the footing is horizontal, the base inclination factors b_q and b_γ both = 1.0
- The surcharge parameter $q = \gamma_t D_f = 110$ pcf (4 ft) = 440 psf
- By using the Table 8-5 in the text, the groundwater correction factors are:
  $C_{Wq} = 1.0$ (i.e., the groundwater level is below the base of the footing)
  $C_{W\gamma} = 0.786$ (i.e., the groundwater level is within $1.5B_f$ of the bottom of the footing.)
- From Table 8-6 in the text, the depth correction factor for $D_f / B_f = 4$ ft / 7 ft = 0.57 is estimated as:
  $d_q \approx 1.15$
- The bearing capacity factors for $\phi = 36^o$ are estimated from Table 8-1 in the text as:
  $N_q = 37.8$
  $N_\gamma = 56.3$

Therefore, the ultimate bearing capacity of the pier footing in sand is calculated as:

q_{ult} = (440 psf)(37.8)(1.0)(1.05)(1.0)(1.15) + 0.5(110 pcf)(7 ft)(56.3)(0.786)(0.97)(1.0)
q_{ult} = 20,083 psf + 16,526 psf = 36,609 psf

Step 3: Determine allowable bearing capacity (use FS = 3)

$$q_{all} = \frac{36{,}609\ \text{psf}}{3} = 12{,}203\ \text{psf} = 6.1\ \text{tsf} \approx 6\ \text{tsf}$$

A7-4 CHECK PRESSURE TRANSMITTED TO CLAY LAYER AND COMPARE IT TO THE ALLOWABLE BEARING CAPACITY OF THE CLAY

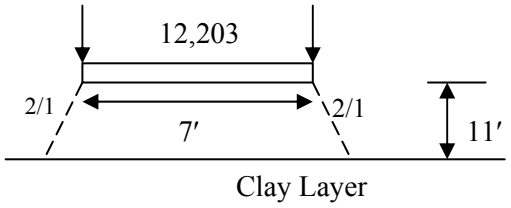

Step 1 Determine pressure on clay layer (Refer to Section A.6-3 of text)

- Footing pressure transmitted to clay surface (p_{clay}) = $\left(\frac{7\,\text{ft}}{7\,\text{ft}+11\,\text{ft}}\right)(12{,}203\,\text{psf}) = 4{,}746$ psf

Step 2 Check bearing capacity of virtual footing on top of clay layer

For the virtual (transferred) footing:

- Footing embedment below final grade (D_{tf}) = 4 ft + 11 ft = 15 ft
- Footing width (B_{tf}) = 7 ft +11 ft = 18 ft
- Footing length (L_{tf}) = 100 ft + 11 ft = 111 ft
- Ground water is 5 ft above the base of virtual footing

Equation 8-6 in the text can be re-written as follows for a purely cohesive soil ($\phi = 0$) for which $N_\gamma = 0$.

$$q_{ult\ clay} = c\ N_c\ s_c\ b_c + q\ N_q\ C_{Wq}\ s_q\ b_q\ d_q + 0.5\ \gamma\ B_{tf}\ \overset{0}{\nearrow} N_\gamma\ C_{W\gamma}\ s_\gamma\ b_\gamma$$

- By using the appropriate equations in Table 8-4 of the text the shape factors are:
  $s_q = 1.00$
  $s_c = 1.03$
- Since the base of the footing is horizontal, the base inclination factors b_q and b_γ both = 1.0
- The surcharge parameter q = 110 pcf (10 ft) + 50 pcf(5 ft) = 1,350 psf
- By Table 8-5 in the text, the groundwater correction factors are:
  $C_{Wq} = 0.5$ (i.e., the groundwater level is at or above the footing base).
- From Table 8-6 in the text, the depth correction factor for D_{tf} / B_{tf} = 15 ft/ 18 ft = 0.83 is estimated as:
  $d_q \approx 1.18$
- The bearing capacity factors for $\phi = 0^o$ are estimated from Table 8-1 in the text as:
  $N_q = 1.0$
  $N_c = 5.14$

Therefore, the ultimate bearing capacity of the virtual footing on clay is calculated as:

$q_{ult.clay}$ = (1,100 psf)(5.14)(1.03)(1.0) + (1,350) psf(1.0)(0.83)(1.0)(1.0)(1.18) =
$q_{ult.clay}$ = 5,824 psf + 1,322 psf = 7,146 psf

Step 3: Determine allowable bearing capacity of virtual footing on clay (use FS = 3)

$$q_{all\ clay} = \frac{7{,}146\,psf}{3} = 2{,}382\,psf$$

Since $q_{all\ clay} < p_{clay}$, the actual footing pressure needs to be reduced since $q_{all\ clay}$ controls bearing capacity of pier footing founded on the layered system.

Step 4: Transfer $q_{all\ clay}$ up to the base of the pier footing to determine the limiting allowable bearing capacity $q_{all\ max}$ of the pier footing founded on sand.

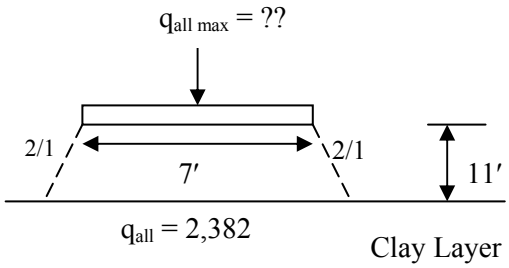

$$q_{all\ max} = q_{all\ clay}\left(\frac{7\,ft + 11\,ft}{7\,ft}\right)$$

$$q_{all\ max} = 2{,}382\ psf\left(\frac{18\,ft}{7\,ft}\right) = 6{,}125\,psf$$

$$q_{all\ max} \approx 6{,}125\ psf \approx 3.1\ tsf$$

- Check with bridge designer to see if 3.1 tsf is a realistic pressure.
- Designer estimates a maximum un-factored structural load of 2,200 tons, and a minimum footing width of 7 ft
- The estimated maximum footing pressure (q_{fts})= $\frac{2{,}200\,tons}{7\,ft \times 100\,ft}$ = 3.14 tsf
- Since the estimated maximum footing pressure is virtually identical to the estimate allowable bearing capacity, the footing size is acceptable for the load and use applied pressure (q) = 3 tsf for settlement analysis.

A7-5 CALCULATE SETTLEMENT OF PIER FOOTING FOUNDED WITHIN A TWO-LAYER SYSTEM

Step 1: Find pressure distribution by 2 on 1 construction (Refer to Chapter A.6-3 of text for procedure and Table A.7-2 below for results)

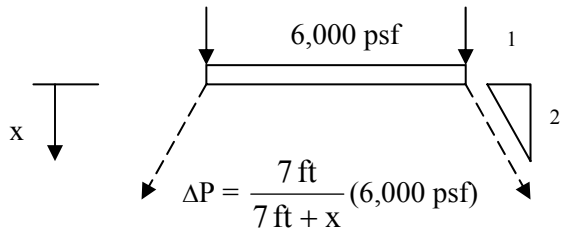

Table A.7-2
Computation of pressure change at various depths due to pressure applied by footing

Depth x (feet)	$k = \frac{7\text{ ft}}{7\text{ ft} + x}$	$\Delta p = k$ (6,000 psf) (psf)
3.5	0.67	4,000
7	0.50	3,000
10.5	0.40	2,400
14	0.33	2,000
21	0.25	1,500
28	0.20	1,200
35	0.17	1,000

Step 2: Calculate the final pressure ($p_f = p_o + \Delta p$) at various depths and plot the overburden pressure (p_o), preconsolidation pressure (p_c), and p_f with depth as shown in Figure A.7-3

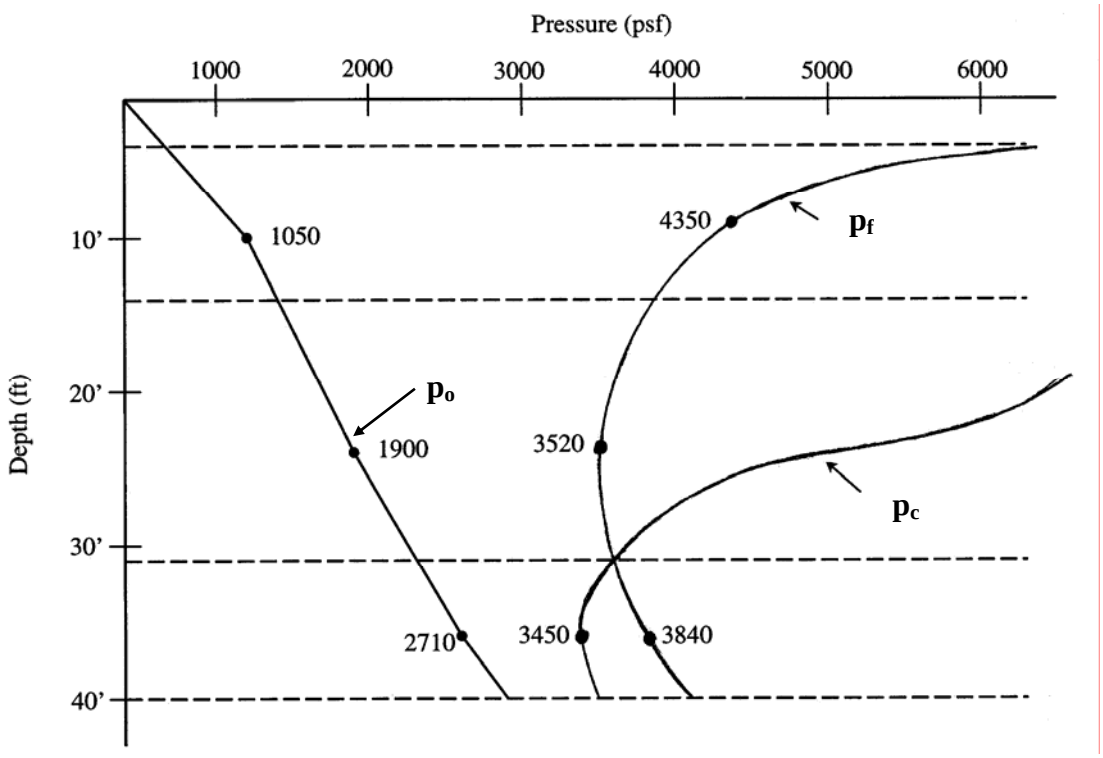

Figure A.7-3. Variation of overburden pressure (p_o), preconsolidation pressure (p_c) and final pressure due to pier footing (p_f) with depth.

Step 3: Calculate immediate settlement of the pier due to compression of the sand layer from 4 ft to 15 ft

Settlement computation by Hough's Method

- Thickness of sand layer beneath pier footing = 15 ft - 4 ft = 11 ft
- Calculate immediate settlement (Refer to Chapter 7.4.1 in text)

$$\Delta H = H \frac{1}{C'} \log \frac{p_f}{p_o}$$

- For ($N1_{60}$) average = 36, C′ = 90 (Refer to Figure 7-7 of text –use curve for "well-graded fine to medium silty sand").
- Calculate settlement for p_o = 1,050 psf and p_f = 4,350 psf.

$$\Delta H = 11\,\text{ft}\left(\frac{1}{90}\right)\log\frac{4{,}350\,\text{psf}}{1{,}050\,\text{psf}}\left(\frac{12\,\text{in}}{\text{ft}}\right)$$

$$\Delta H = 0.90\ \text{in}$$

Settlement Computation by Schmertmann's method (Chapter 8.5 in the text)

- Begin by drawing the strain influence diagram. The L_f/B_f ratio for the footing is: 100 ft/7 ft = 14.3

  Determine the value of the strain influence factor at the base of the footing, I_{ZB}, as follows:

  $I_{ZB} = 0.2$ for plane strain case $\quad (L_f/B_f \geq 10)$

- Determine the maximum depth of influence, D_I, as follows:

  $D_I = 4B_f$ for $L_f/B_f > 10$
  $D_I = 4 \times 7 \text{ ft} = 28 \text{ ft}$

- Determine the depth to the peak strain influence factor, D_{IP}, as follows:

  $D_{IP} = B_f$ for $L_f/B_f > 10$
  $D_{IP} = 7 \text{ ft}$

- Determine the value of the maximum strain influence factor, I_{ZP}, as follows:

$$I_{ZP} = 0.5 + 0.1\left(\frac{\Delta p}{p_{op}}\right)^{0.5}$$

$$\Delta p = 6{,}000\,\text{psf} - 4\,\text{ft}\,(110\,\text{pcf}) = 5{,}560\,\text{psf} = 5.56\,\text{ksf}$$

$$p_{op} = 10\,\text{ft}\,(110\,\text{pcf}) + 1\text{ft}(110\text{pcf} - 62.4\text{pcf}) = 1{,}147.6\,\text{psf} = 1.15\,\text{ksf}$$

$$I_{ZP} = 0.5 + 0.1\sqrt{\frac{5{,}560\text{psf}}{1{,}147.6\text{psf}}} = 0.72$$

- Draw the I_Z vs. depth diagram as shown below. The hatched portions show portions of the strain influence diagram within the sand layer and the clay layer. The immediate settlement will occur only in the sand layer. Therefore, the portion of the strain influence diagram in the clay layer will not be considered in the computation of the immediate settlement.

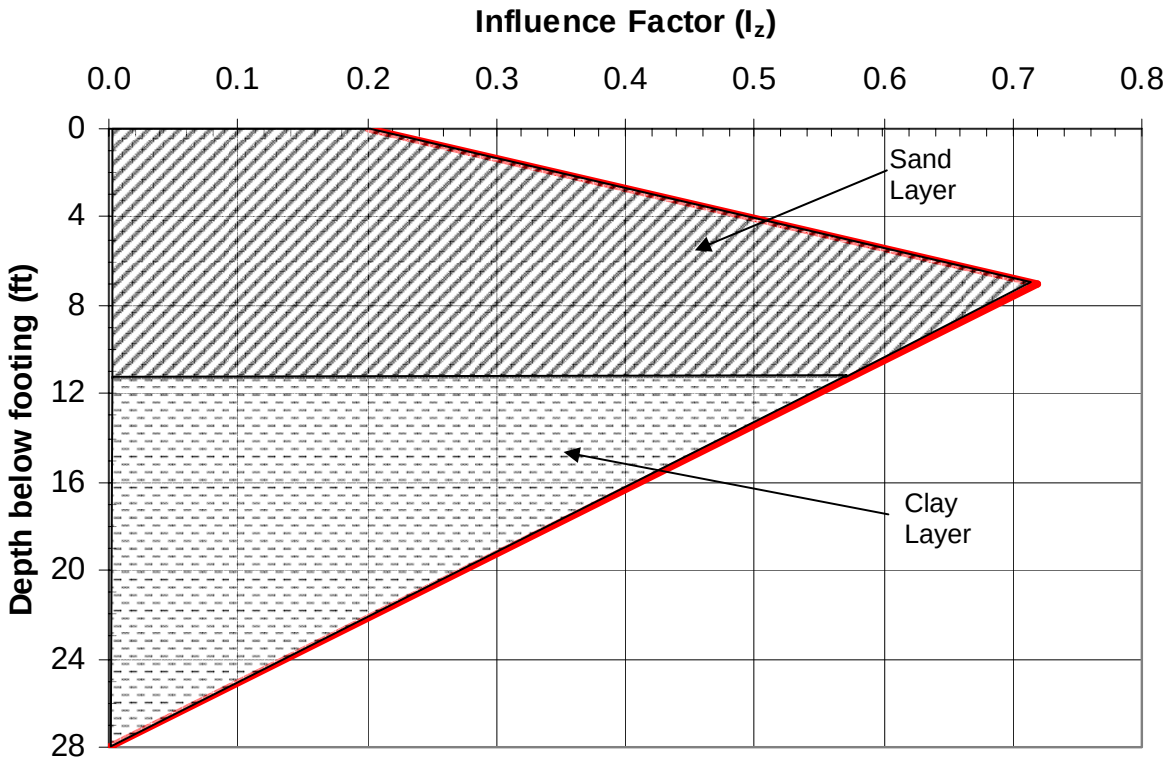

- Determine value of elastic modulus E_s from Table 5-16 in Chapter 5.

  For "clean fine to medium sands with slightly silty sands" $E_s = 7N1_{60}$ tsf. Since the elastic modulus E_s is based on correlations with $N1_{60}$-values obtained from Table 5-16, calculate the X multiplication factor as follows:

  $X = 1.75$ for $L_f/B_f \geq 10$
  Thus, XEs = 1.75 (7) (36) = 441 tsf.

- Divide the sand layer into convenient sublayers using the guidelines in Chapter 8.5.1.2. Using those guidelines, the sand layer below the footing is divided into 1 ft and 2 ft sublayers. Using the sublayers determine the settlement by setting up a table as follows:

Layer	H_c (inches)	$N1_{60}$	E_s (tsf)	XE_s (tsf)	Z_1 (ft)	I_Z at Z_i	$H_i = \frac{I_Z}{XE_s} H_c$ (in/tsf)
1	12	36	252	441	0.5	0.237	0.00645
2	24	36	252	441	2.0	0.349	0.01897
3	12	36	252	441	3.5	0.460	0.01252
4	24	36	252	441	5.0	0.571	0.03110
5	24	36	252	441	7.0	0.720	0.03918
6	24	36	252	441	9.0	0.651	0.03543
7	12	36	252	441	10.5	0.600	0.01633
						ΣH_i=	**0.15998**

- Determine embedment factor (C_1) and creep factor (C_2) as follows:

  a) Embedment factor

  $$C_1 = 1 - 0.5\left(\frac{p_o}{\Delta p}\right) = 1 - 0.5\left(\frac{4\,\text{ft} \times 110\,\text{pcf}}{5{,}560\,\text{psf}}\right) = 0.960$$

  b) Creep Factor

  $$C_2 = 1 + 0.2\log_{10}\left(\frac{t(\text{years})}{0.1}\right)$$

  For end of construction t(yrs) = 0.1 yr (1.2 months)

  $$C_2 = 1 + 0.2\log_{10}\left(\frac{0.1}{0.1}\right) = 1.0$$

- Determine the settlement at end of construction as follows:

  $$S_i = C_1 C_2 \Delta p \sum H_i$$

  $$S_i = (0.960)(1.0)\left(\frac{5{,}560\text{psf}}{2{,}000\,\text{psf}/\text{tsf}}\right)\left(0.15998\,\frac{\text{in}}{\text{tsf}}\right)$$

  $$S_i = 0.43\,\text{inches}$$

Note: The settlement computed by Hough's method was 0.90 inches which is approximately 2 times more than that computed above by Schmertmann's method. This difference is similar to that found by FHWA (1987) and discussed in Chapter 8.5.1 in the text.

Step 4: Calculate settlement of the pier due to consolidation of the clay layer. Use equation for consolidation settlement (Refer to Chapter 7.5) and consider two sublayers; sublayer 1 from 15 ft to 32 ft and sublayer 2 from 32 ft to 40 ft

- Thickness of clay Sub-layer 1 = 32 ft - 15 ft = 17 ft

  - As shown in Figure A.7-3, the clay in Sub-layer 1 is over-consolidated since $p_o < p_c$ and the load increment results in p_f which is also less than p_c within this depth range. Therefore, calculate settlement for the pressure increment from p_o = 1,900 psf to p_f = 3,520 psf and use the recompression index C_r.

$$\Delta H = H \frac{C_r}{1 + e_o} \log \frac{p_f}{p_o}$$

$$\Delta H = 17\,\text{ft} \frac{0.035}{1 + 0.97} \log \frac{3{,}520\,\text{psf}}{1{,}900\,\text{psf}} \left(\frac{12\,\text{in}}{\text{ft}} \right)$$

$$\Delta H = 0.97\ \text{in}$$

- Thickness of clay Sub-layer 2 = 40 ft - 32 ft = 8 ft

  - As shown in Figure A.7-3, the clay in Sub-layer 2 is over-consolidated within this depth range since $p_c > p_o$, but at the mid-depth the load increment causes $p_f > p_c$. Therefore the settlement for this sub-layer must be calculated in two steps, one step for the pressure increment from p_o to p_c for which C_r applies, and the other for the pressure increment from p_c to p_f for which C_c applies. (Refer to Chapter 7.5.2)

  - Calculate settlement of clay Sub-layer 2 for the pressure increment from p_o = 2,710 psf to p_c = 3,450 psf.

$$\Delta H = H \frac{C_r}{1 + e_o} \log \frac{p_c}{p_o}$$

$$\Delta H = 8\,\text{ft} \frac{0.035}{1 + 0.97} \log \frac{3{,}450\,\text{psf}}{2{,}710\,\text{psf}} \left(\frac{12\,\text{in}}{\text{ft}} \right)$$

$$\Delta H = 0.18\ \text{in}$$

- Calculate settlement of clay Sub-layer 2 for the pressure increment from p_c = 3,450 psf to p_f = 3,840 psf.

$$\Delta H = H \frac{C_c}{1 + e_o} \log \frac{p_f}{p_c}$$

$$\Delta H = 8\,\text{ft} \frac{0.35}{1 + 0.97} \log \frac{3{,}840\,\text{psf}}{3{,}450\,\text{psf}} \left(\frac{12\,\text{in}}{\text{ft}} \right)$$

$$\Delta H = 0.80\ \text{in}$$

Step 5: Summarize settlement contributions from sand and clay layers (Refer to Table A.7-3)

Table A.7-3
Summary of settlement of pier footing

Layer	Settlement (in)
Sand (4 ft to 15 ft)	0.90 in
Clay – Sub-layer 1 (15 ft to 32 ft)	0.97 in
Clay – Sub-layer 2 (32 ft to 40 ft)	0.98 in
Total settlement =	2.85 in
Total settlement of clay layer =	1.95 in

Step 6: Compute time for settlement due to pier footing to occur in clay layer

- **Obtain time for various percentages of settlement as shown in Table A.7-4 by using Table 7-4 in Chapter 7.5.3.1 in the text and the following equations**

- H_d = ½ H = ½ (40 ft – 15 ft) =12.5 ft
- c_v = 0.6 ft^2/day
- $(H_d)^2/c_v$ = $(12.5\ ft)^2$ / (0.6 ft^2/day) = 260 days
- For time (t) use Equation 7-8 of text

$$t = \frac{T H_d^2}{c_v}$$

Table A.7-4 provides a convenient template for performing computations to obtain settlement vs. time values for arbitrarily chosen values of average percent consolidation.

Table A.7-4
Template to compute values of consolidation settlement (ΔH) in clay layer at various times (t) after application of pier footing load (refer to section A.6)

Average % Consol. (U)	ΔH (in) = (U)(ΔH_{Total} Clay Layer)	Time Factor (T) (from Table 7-4 in text)	$\frac{H_d^2}{c_v}$	t (days)
20	0.39	0.031	260	8
50	0.98	0.197	↓	51
70	1.37	0.403	↓	104
90	1.76	0.848	↓	220

Step 7: Plot settlement-time curve for the pier including immediate settlement of sand as shown in Figure A.7-4.

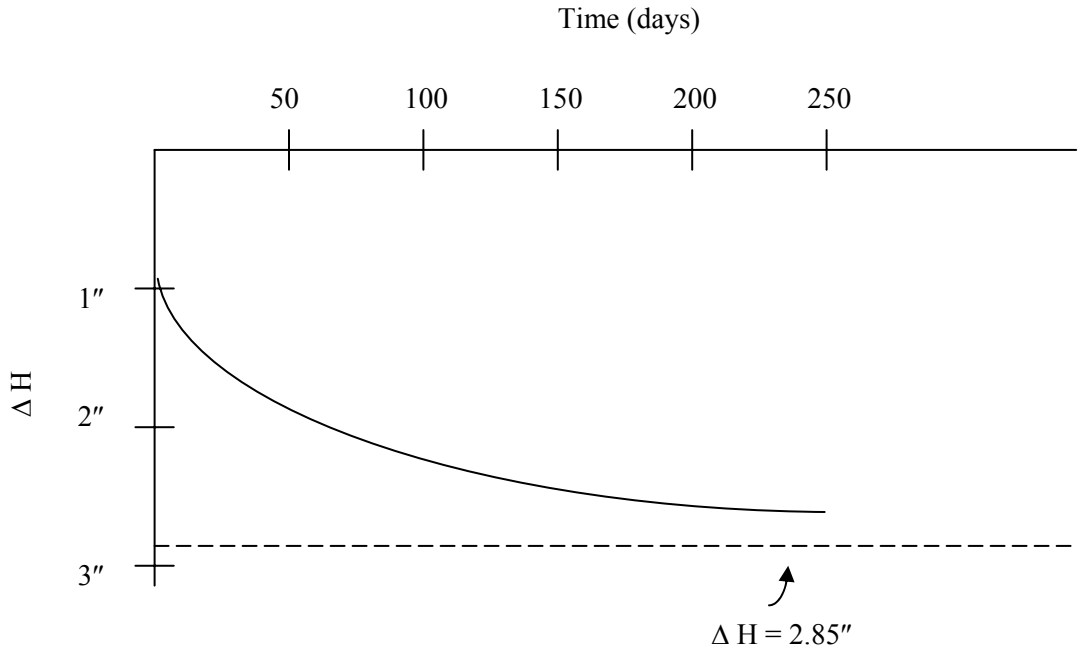

Figure A.7-4. Settlement-time curve for pier including immediate settlement of sand.

A.7-6 CALCULATE SETTLEMENT OF EAST ABUTMENT FOOTING FOUNDED WITHIN A TWO-LAYER SYSTEM

- **Define geometry of the problem and state relevant assumptions.**
  - Footing embedment below final grade of embankment fill (D_f) = 10 ft
  - Footing width (B_f) = 1/3 pier height = 7 ft
  - Footing length (L_f) = 100 ft
  - Depth to ground water below base of footing (D_w) = 25 ft
  - Internal consolidation of embankment fill under its own weight is negligible.
  - Organic layer is excavated and replaced with 3-feet of compacted select fill.

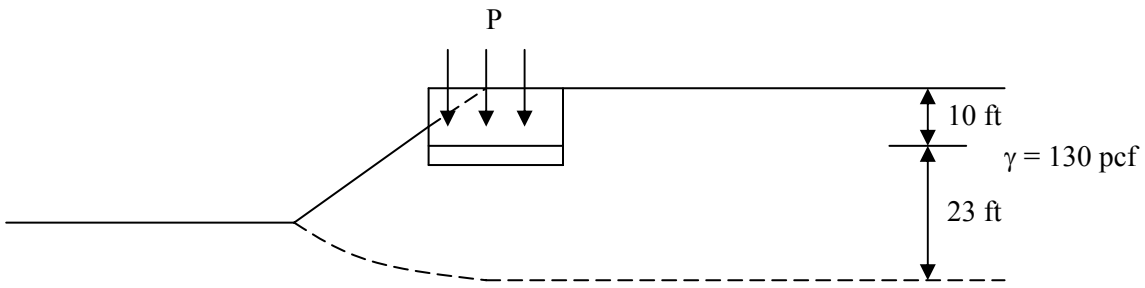

Figure A.7-5. Footing geometry for embankment footing.

Step 1: Determine net footing pressure at footing embedment depth due to soil removal for footing excavation.

- p = the net pressure applied at the footing level. Assume that the abutment will be constructed after the embankment fill is in place.
- p = 6,300 psf – (10 ft)130 pcf) = 5,000 psf

Step 2: Calculate change in pressure due to embankment footing by 2:1 construction. Consider layer mid-depths corresponding to those considered in calculation of p_o and p_f in Section 6 for embankment settlement. (Refer to Figure A.6-5 Refer to Table A.7-5 below for results)

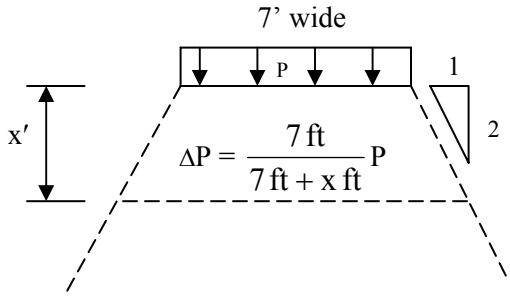

- $p_{abut} = p_f + \Delta p_{abut}$ where
  $p_f = p_o$ + change in pressure due to embankment load (Refer to Table A.6-2)

Table A.7-5
Computation of pressure change due to pressure applied by abutment footing and p_{abut} at various depths the embankment

Layer	Thickness (feet)	Depth x from top of sand to layer mid-point (ft)	Depth z to midpoint (feet)	$k = \frac{7\,ft}{7\,ft + x}$	Δp_{abut} = k (5,000 psf) (psf)	p_f (psf)	p_{abut} (psf)
Sand	7	3.5	26.5	0.21	1,050	4,470	5,520
Clay Sub-layer 1	8	11.0	34.0	0.17	850	4,920	5,770
Clay Sub layer 2	27	28.5	51.5	0.12	600	5,650	6,250

Step 3: Plot the pressure distributions with depth of the overburden pressure (p_o), preconsolidation pressure (p_c), final pressure due to embankment fill only (p_f), and the final pressure due to embankment fill plus abutment footing (p_{abut}) as shown in Figure A.7-6

Step 4: Calculate immediate settlement of the abutment footing due to compression of the sand layer (3 ft to 10 ft).

- Thickness of sand layer beneath pier footing = 10 ft - 3 ft = 7 ft
- Calculate immediate settlement (Refer to Chapter 7)

$$\Delta H = H\frac{1}{C'}\log\frac{p_{abut}}{p_f}$$

$$\Delta H = 7\,ft\left(\frac{1}{90}\right)\log\frac{5{,}520\,psf}{4{,}470\,psf}$$

$$\Delta H = 0.0071\ ft \sim 0.09\ in$$

Note: Schmertmann's method can also be used. This was demonstrated earlier.

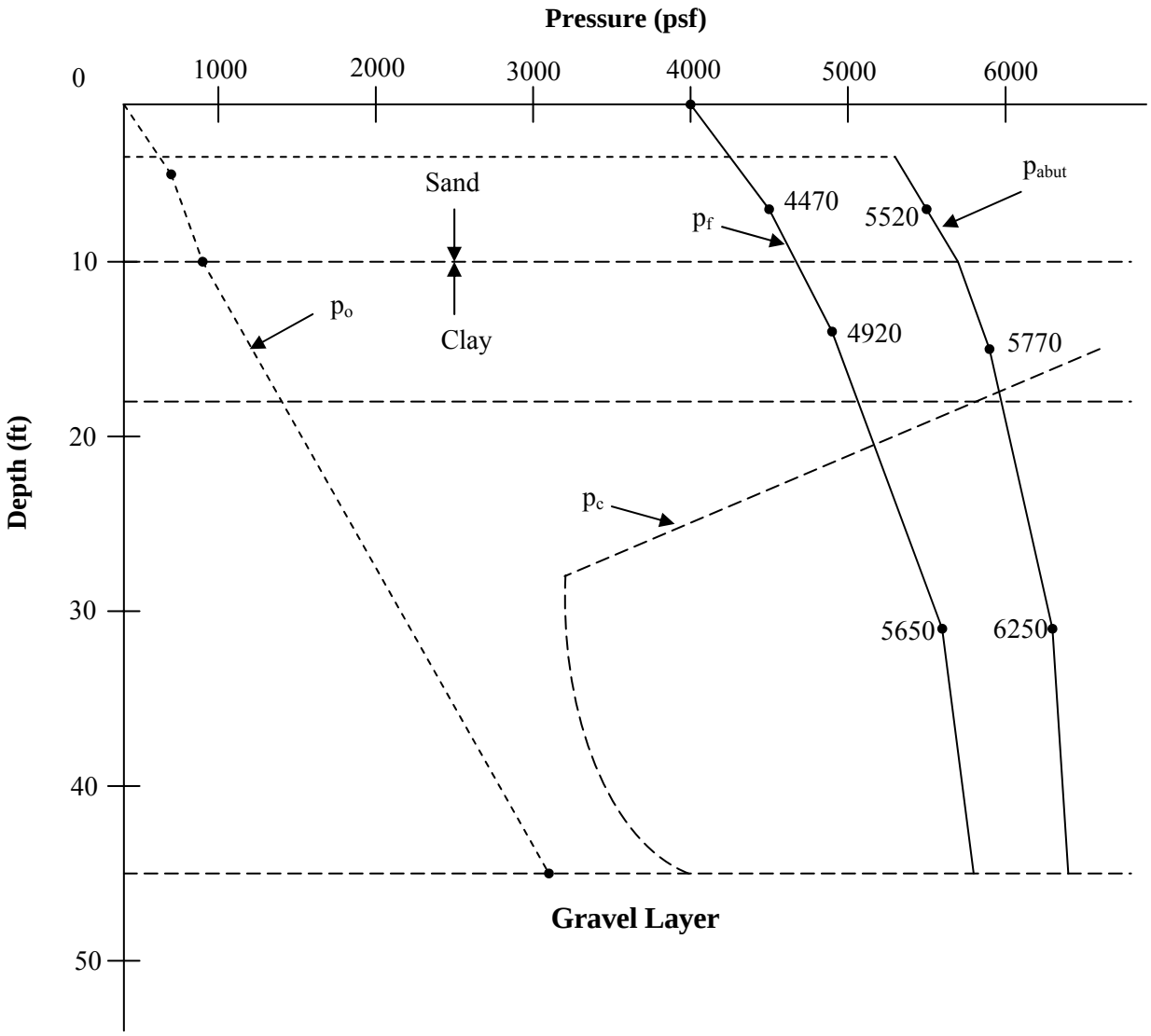

Figure A.7-6. Pressure distributions with depth at East Abutment for the overburden pressure (p_o), preconsolidation pressure (p_c), final pressure due to embankment fill only (p_f), and the final pressure due to embankment fill plus abutment footing (p_{abut}).

Step 5: Calculate settlement of the abutment footing due to consolidation of the clay layer. Use equation for consolidation settlement (Refer to Chapter 7.5) and consider two partial layers, Sub-layer 1 from 10 ft to 18 ft and Sub-layer 2 from 18 ft to 45 ft.

- Thickness of clay Sub-layer 1 = 18 ft - 10 ft = 8 ft

  - As shown in Figure A.7-6, the clay in Sub-layer 1 was over-consolidated prior to the construction of the embankment fill since $p_o < p_c$ and remained so during and after consolidation under the embankment fill since p_f is also $< p_c$. Figure A.7-6 further shows that Sub-layer 1 will continue to be over-consolidated during and after consolidation under the abutment footing, i.e., p_{abut} is also $< p_c$ within this depth range. Therefore, calculate settlement due to the abutment footing for the pressure increment from p_f = 4,920 psf to p_{abut} = 5,770 psf and use the recompression index C_r= 0.035.

$$\Delta H = H \frac{C_r}{1 + e_o} \log \frac{p_{abut}}{p_f}$$

$$\Delta H = 8\,\text{ft} \frac{0.035}{1 + 0.97} \log \frac{5{,}770\,\text{psf}}{4{,}920\,\text{psf}}$$

$\Delta H = 0.0098$ ft ~ 0.12 in

- Thickness of clay Sub-layer 2 = 45 ft - 18 ft = 27 ft

  - As shown in Figure A.7-6, the clay in Sub-layer 2 was also over-consolidated prior to the construction of the embankment fill since $p_o < p_c$. However, during consolidation under the embankment fill, the pressure increment at every depth in Sub-layer 2 caused the final pressure p_f to become $> p_c$. It was for this reason that the total consolidation settlement for this Sub-layer under the embankment fill had to be calculated by the use of a two-step procedure. In the first step the settlement was calculated as the pressure increased from p_o to p_c; in the second step the settlement was calculated as the pressure increased from p_c to p_f. As described in Step 5 of Section A.6-3, C_r was used in the first step and C_c in the second. Therefore, unless the abutment footing is built after 100% consolidation of the clay layer under the embankment load has occurred, the clay will be under-consolidated at the time of construction of the footing, i.e., settlement due to the abutment footing will be accompanied by continued settlement due to the embankment. Therefore, calculate settlement due to the abutment footing for the

pressure increment from p_f = 5,650 psf to p_{abut} = 6,250 psf and use the compression index $C_c = 0.35$.

$$\Delta H = H \frac{C_c}{1 + e_o} \log \frac{p_{abut}}{p_f}$$

$$\Delta H = 27\,\text{ft} \frac{0.35}{1 + 0.97} \log \frac{6{,}250\,\text{psf}}{5{,}650\,\text{psf}}$$

$\Delta H = 0.21$ ft ~ 2.50 in

Step 6: Summarize contributions to settlement under abutment footing loads from sand and clay layers (Refer to Table A-7.6)

Table A.7-6
Summary of settlement of pier footing

Layer	Settlement (in)
Sand (3 ft to 10 ft)	0.09 in
Clay – Sub-layer 1 (10 ft to 17 ft)	0.12 in
Clay – Sub-layer 2 (17 ft to 45 ft)	2.50 in
Total settlement due to abutment footing=	2.71 in
Total settlement of clay layer due to abutment footing=	2.62 in

Step 7: Compute Time for Settlement Due to Abutment Footing to Occur in Clay Layer

- **Obtain time for various percentages of settlement as shown in Table A.7-4 by using Table 7-4 in Chapter 7.5.3.1 in the text and the following equations**

- $H_d = ½\ H = ½\ (45\ \text{ft} - 10\ \text{ft}) = 17.5$ ft
- $c_v = 0.6\ \text{ft}^2/\text{day}$
- $(H_d)^2/c_v = (17.5\ \text{ft})^2 / (0.6\ \text{ft}^2/\text{day}) = 510$ days
- For time (t) use Equation 7-8 of text

$$t = \frac{T H_d^2}{c_v}$$

Table A.7-7 provides a convenient template for performing computations to obtain settlement vs. time values for arbitrarily chosen values of average percent consolidation.

Table A.7-7
Template to compute values of consolidation settlement (ΔH) in clay layer at various times (t) after application of abutment footing load (refer to section A.6)

Average % Consol. (U)	ΔH (in) = (U)(ΔH_{Total} Clay Layer)	Time Factor (T)	$\frac{H_d^2}{c_v}$	t (days)
20	0.52	0.031	510	16
50	1.31	0.197	↓	100
70	1.83	0.403	↓	206
90	2.36	0.848	↓	432

Step 9: Plot settlement-time curve for the pier including immediate settlement of sand as shown in Figure A.7-7.

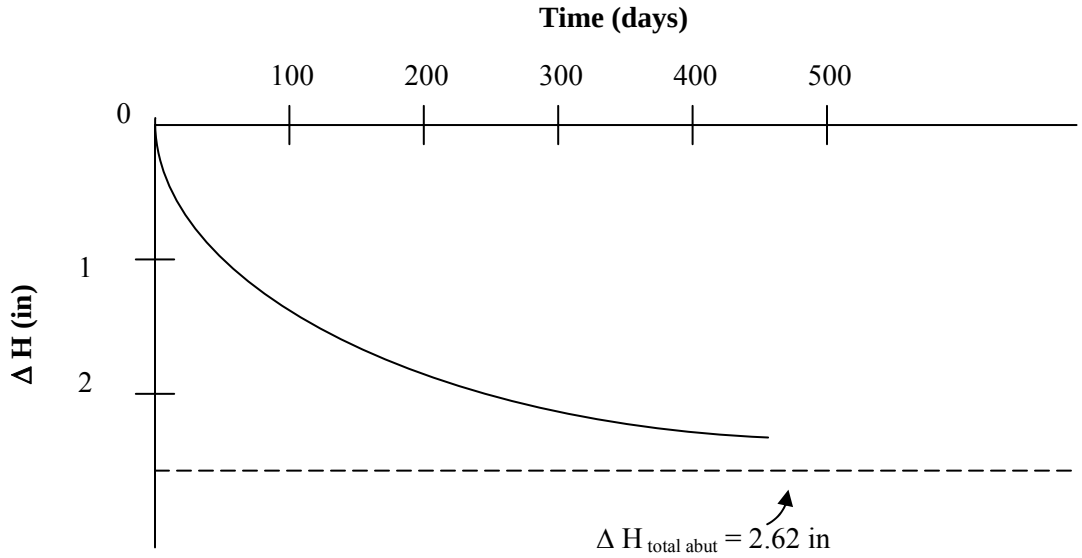

Figure A.7-7. Settlement-Time curve for abutment footing.

A.7-7 EVALUATE THE EFFECT OF PRE-TREATMENT ON THE SETTLEMENT OF EAST ABUTMENT FOOTING

- As indicated in Step 6 of Section A.7-6 above, the settlement due to the abutment footing will occur while the settlement remaining due to embankment load continues. Therefore the actual settlement of is the sum of these two components of settlement. For example, if the abutment footing were built immediately after placement of the embankment fill (t = 0) without pre-treatment by surcharging and/or vertical drains, the total consolidation settlement of the abutment footing would be:

$$\Delta H_{\text{total (emb + abut)}} = \Delta H_{\text{total emb}} + \Delta H_{\text{total abut}} = 12.66 \text{ in} + 2.62 \text{ in} = 15.28 \text{ in}$$

- However, pretreatment by surcharges and/or vertical drains can be used to accelerate consolidation of the clay layer under the embankment load so that when the abutment footing is built at a later time, e.g., at a time when the t_{90} for the embankment fill without treatment is reached, the total settlement due to the abutment footing ($\Delta H_{\text{total (emb + abut)}}$) will be only slightly larger than the settlement due to the abutment footing alone ($\Delta H_{\text{total abut}}$).

- For the case of pre-treatment by wick drains, Figure A.7-8 shows that the t_{90} settlement of 11.43 inches due to the 30 ft of embankment fill without treatment is reached after approximately 50 days. If the abutment footing is constructed at that time, only about 1.23 inches of settlement due to the embankment alone remains. Therefore, the abutment footing will undergo a total settlement of 1.23 in + 2.62 in = 3.85 in as compared to 15.28 in it would have undergone had the pre-treatment not been used and the abutment footing built immediately after construction of the embankment.

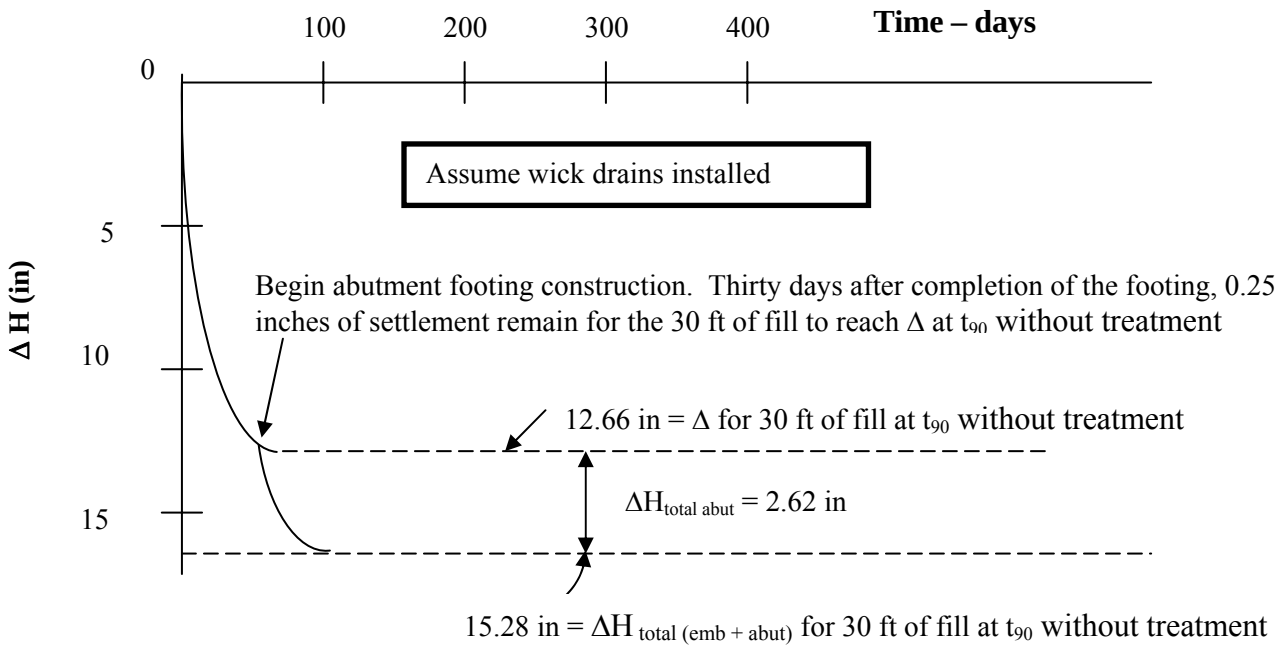

Figure A.7-8. Settlement –Time curve for abutment footing built 6 months after completion of embankment fill with vertical drain pre-treatment.

- For the case of pre-treatment by 10 ft of surcharge, Figure A.7-9 shows that the t_{90} settlement of 13.7 inches due to 30 ft of embankment fill plus surcharge is reached after approximately 240 days.

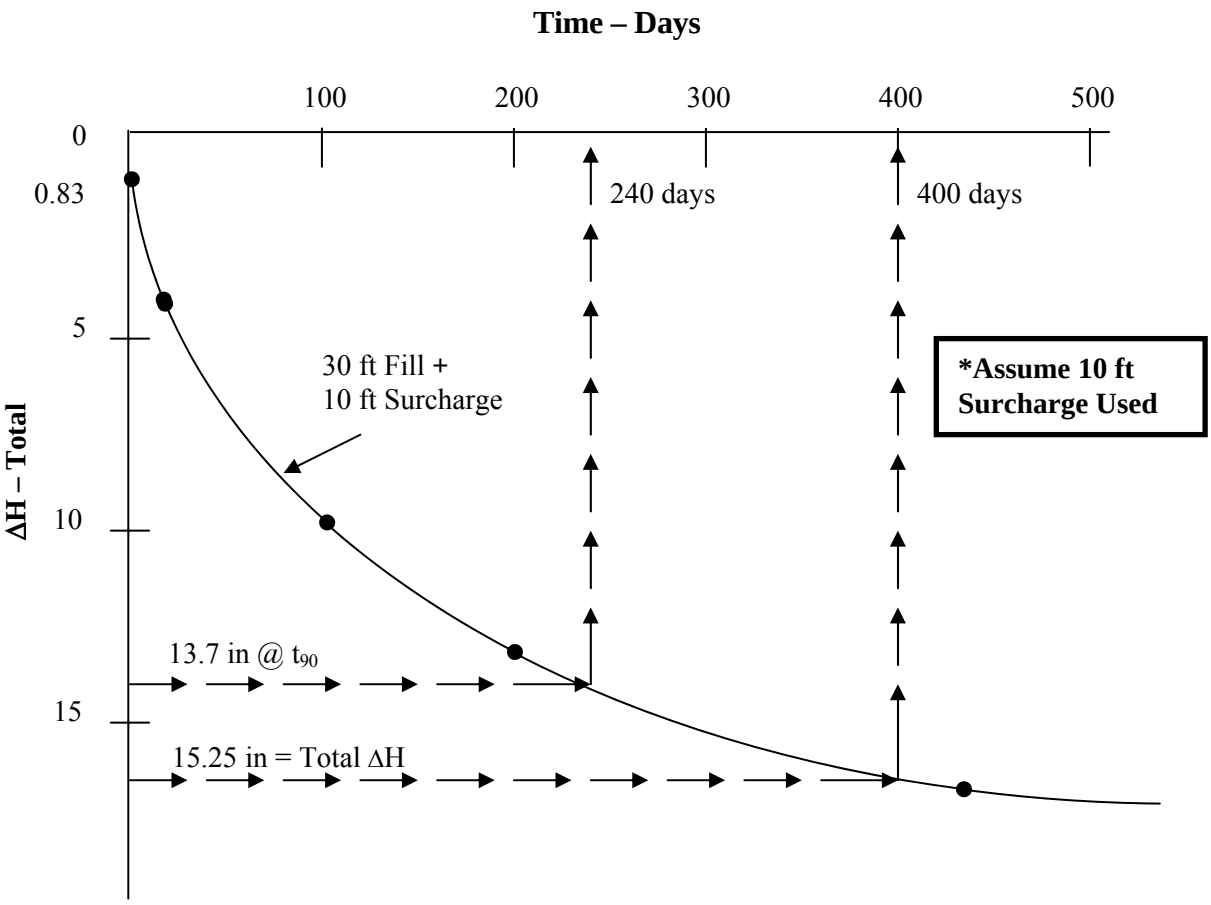

Figure A.7-9. Settlement –Time curve for 30 ft of embankment fill plus 10 ft surcharge.

* Surcharge must be left in place for 13 months to dissipate all embankment and abutment ΔH

Summary of the Spread Footing Design Phase for Apple Freeway Design Problem

- Design Soil Profile

  Strength and consolidation values selected for all soil layers. Footing elevation and width chosen.

- Pier Bearing Capacity

  $Q_{allowable}$ = 3 tsf

- Pier Settlement

  Settlement = 2.67 in, t_{90} = 220 days.

- Abutment Settlement

  Settlement = 2.7 in, t_{90} = 432 days.

- Vertical Drains

  t_{90} = 60 days - could reduce settlement to 0.25 in after abutment constructed and loaded.

- Surcharge

  10 ft surcharge: t_{90} = 240 days
  before abutment constructed.

A.7-7 SUMMARY OF GEOTECHNICAL DESIGN OF PIER AND ABUTMENT SPREAD FOOTINGS

1. Construct idealized design profile with footing geometry shown.
   - Use logs of appropriate borings
   - Include 30 ft high embankment at East abutment (assume 3 ft organic layer at the surface is replaced by compacted select material).
   - Estimate consolidation properties of clay layer at each location from results of field and laboratory tests.
   - Estimate internal friction angle of sand from SPT-N corrected blow counts ($\phi \approx 36^{o}$)

2. Determine overburden pressure at each location, change in pressure due to pier footing, change in pressure due to embankment fill at East abutment, change in pressure due to abutment footing, and maximum past pressure at each location, all as a function of depth.

   - Plot pressure distributions with depth and determine stress history of impacted layers at each location.

3. Calculate ultimate and allowable bearing capacity of pier footing

   - Footing width = 7 ft
   - Footing length = 100 ft
   - Depth of embedment = 4 ft
   - q_{ult} = 33,000 psf
   - q_{all} = 11,000 psf

4. Check pressure transmitted to clay layer and compare it to the allowable bearing capacity of the clay

    - $q_{all\ max} \approx 3.1$ tsf– use 3 tsf for settlement analysis

5. Calculate settlement of pier footing founded within a two-layer system and plot settlement time relationship

    - Sand (4–15 ft) = 0.91 in
    - Clay (15–32 ft) = 0.97 in
    - Clay (32-40 ft) = 0.98 in
    - Total settlement = 2.85 in due to clay plus sand
    - Total settlement = 1.95 in due to clay alone
    - t_{90} = 220 days

6. Calculate settlement of East abutment footing founded within the embankment and underlain by a two-layer system. Plot settlement time relationship
    - Sand (3-10 ft) = 0.09 in
    - Clay (10-17 ft) = 0.12 in
    - Clay (17-45 ft) = 2.50 in
    - Total settlement = 2.71 in - footing due to clay plus sand
    - Total settlement = 2.62 in - footing due to clay alone
    - Total settlement = 15.28 in - footing plus embankment due to clay plus sand
    - t_{90} = 433 days for embankment alone without pre-treatment

7. Evaluate the effect of pre-treatment on the settlement-time relationship of the East abutment footing and embankment fill.

    - t_{90} = 60 days for embankment alone pre- treated with vertical drains.
    - Total settlement = 0.25 in remaining due to embankment.
    - Abutment footing constructed at this time.
    - Total settlement = 0.25 in + 2.60 in = 2.85 in – footing plus embankment due to clay alone after abutment footing constructed and loaded.

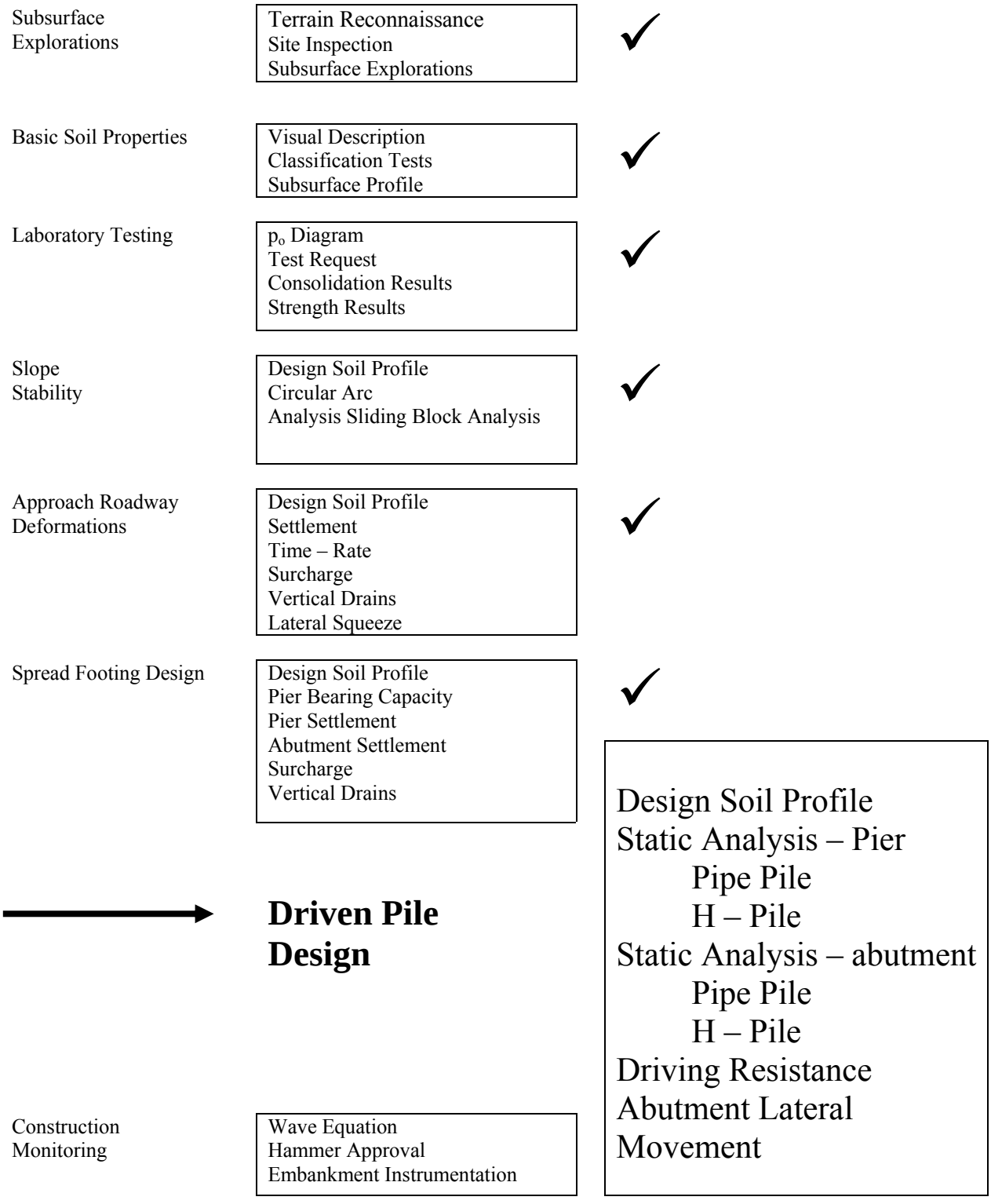

Figure A.8-1. Status of geotechnical work.

SECTION A.8
DRIVEN PILE DESIGN

A.8-1 RELEVANT CONCEPTS AND PROCEDURES (Refer to Figure A.8-1)

- Refer to Chapter 9 for driven pile design

In this Section, the Apple Freeway is used to illustrate the pile design for support of the pier and abutment. **Although drilled shafts may also be a feasible deep foundation design alternate for this structure, only driven piles are discussed herein because they involve a lot more detail in design and construction.** The computation process for static analysis to determine pile capacity by Nordlund Method is presented along with the computation of pile driving resistance.

Given: **The subsurface profile and soil properties shown below.**

Required: **Determine the allowable pile capacity using static analysis.**

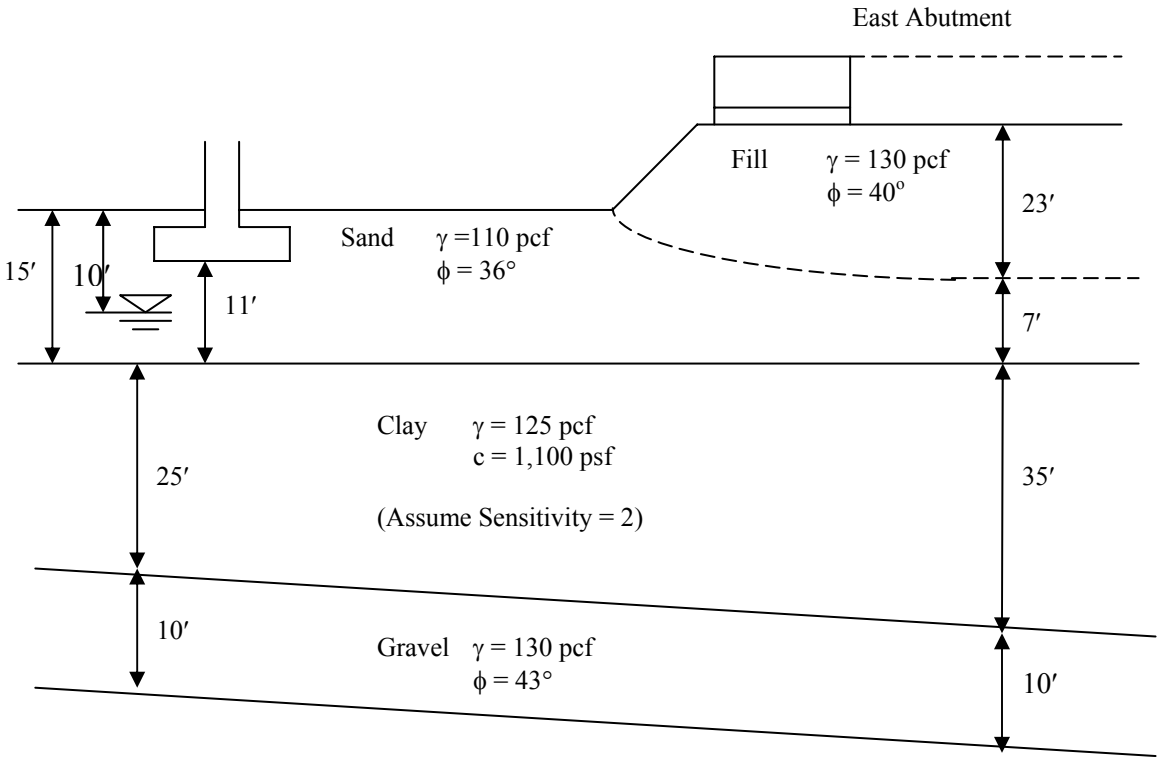

A.8-2 CONSIDERATION FOR PILE TYPE SELECTION

- Spread footings would be feasible at both the pier and abutment except for settlements due to consolidation of the clay deposit. To eliminate these settlements any pile type selected must achieve capacity below the bottom of the clay deposit.
- End bearing will provide most of the ultimate resistance at either the pier or abutment location due to the minimal thickness of the gravel layer.
- The maximum estimated design structural load of 2,200 tons can be supported by either the gravel or the rock layer. However pile driveability appears to be an issue in design.
- Required loads, end bearing support, and difficult driving concerns would favor a straight-sided steel pile over either a timber or concrete or tapered pile.
- Static analyses will be used to determine if a displacement pile with an end plate or a non-displacement pile will provide the best choice for both bearing and driveability. The designer selected a 12 inch diameter closed end pipe pile and a 12 inch H-pile for alternate evaluation at this site. The project's structural engineer usually designs the pipe pile for a 70-ton design load and the H-pile for a 120-ton design load.

Step 1: Plot p_o diagram.

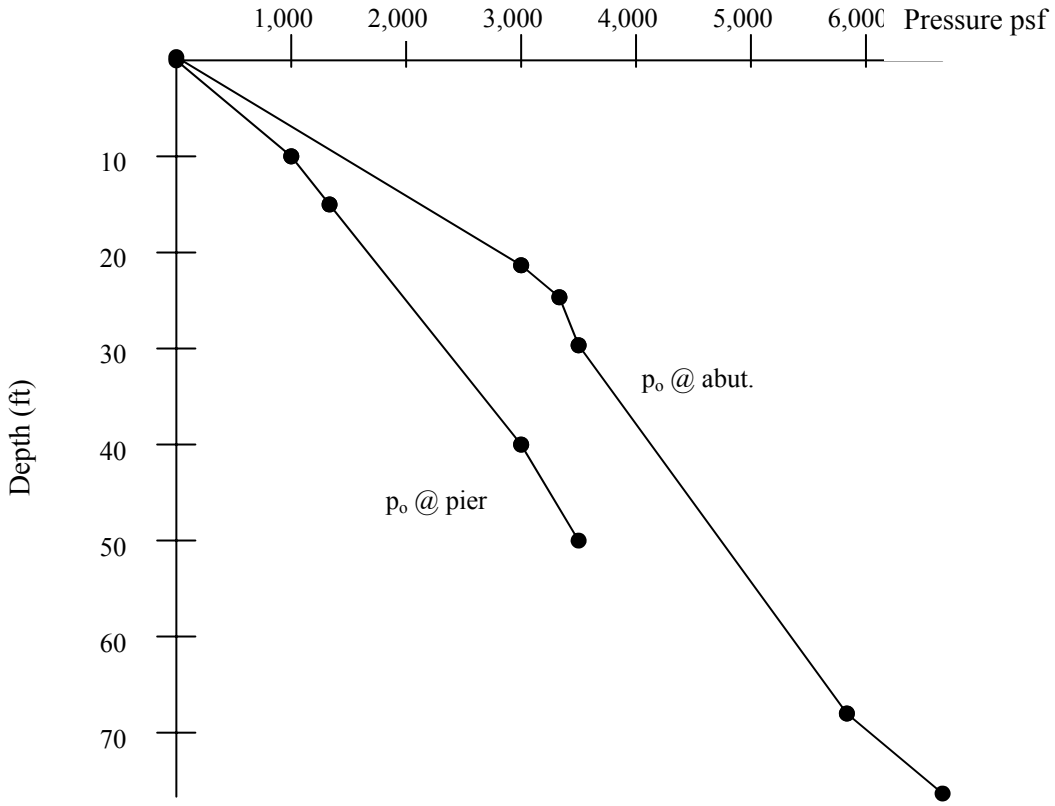

A.8-3 STATIC PILE ANALYSIS – PIER

A. <u>For 12 inch diameter pipe pile (closed end, 70 ton design)</u>

Step 2A: Compute shaft resistance.

- Sand Layer (4 ft – 15 ft - Use Nordlund Method – Chapter 9.5.1.1)

  D = 15 ft – 4 ft = 11 ft

  $$V = \frac{\text{pile vol.}}{\text{foot}}$$
  $$= \frac{\pi d^2}{4} = 0.785\,\text{ft}^3/\text{ft}$$

  $\delta/\phi = 0.6$ (for closed end pipe pile from Figure 9-7 in Chapter 9)

  $\delta = (0.6)(36°) = 21.6°$

  $K_\delta = 1.92$ (for $\phi = 36°$ from Table 9-6(a) in Chapter 9)

  Correction Factor, $C_F = 0.75$ (from Figure 9-12 in Chapter 9)

  $C_d = \pi\, d = \pi\,(1\text{ ft}) = 3.14$ ft

  p_d Avg. @ $\frac{4\text{ ft} + 15\text{ ft}}{2} = 9.5$ ft is 1,050 psf

  $R_{s\,(sand)} = K_\delta\,(C_F)(p_d)(C_d)(\sin\delta)D$ (Equation 9-6 in Chapter 9)
  $= (1.92)(0.75)(1{,}050\text{ psf})(3.14\text{ ft})(\sin 21.6°)(11\text{ ft})$
  $R_{s\,(sand)} = 19{,}225$ lbs = 9.6 tons

- Clay Layer (15 ft – 40 ft)

  $R_{s(clay)} = c_a C_d D$

  c_a (Adhesion) ≅ 1,100 psf (assume adhesion ≈ cohesion, i.e., $\alpha \approx 1.0$)

  $R_{s(clay)} = 1{,}100$ psf (3.14 ft) 25 ft = 86,350 lbs = 43.1 tons

- *Gravel Layer (Try 4 ft Embedment i.e.. 40 ft – 44 ft)

  *Remember to reduce ϕ of 43° to maximum 36° value for hard, angular gravel skin friction.

$R_s = (K_\delta)(C_F)(p_d)(C_d)(\sin \delta)D$

$\delta/\phi = 0.6$

$\delta = (0.6)(36°) = 21.6°$

$K_\delta = 1.92$ (for $\phi = 36°$ from Table 9-6(a) in Chapter 9)

$C_F = 0.7$ (from Figure 9-12 in Chapter 9)

$p_o = 3{,}200$ psf

$R_{s(gravel)} = (1.92)(0.7)(3{,}200 \text{ psf})(3.14 \text{ ft})(\sin 21.6°)4 \text{ ft}$

$R_{s(gravel)} = 19{,}885$ lbs $= 9.9$ tons

Step 3A: Compute toe resistance.

- Gravel Layer

For $\phi = 43°$, $\alpha \approx 0.75$ from Figure 9-13(a) in Chapter 9
For $\phi = 43°$, $N'_q = 300$ from Figure 9-13(b) in Chapter 9

a. $R_t = A_p \alpha_t p_t N'_q$ (p_t max.) (Equation 9-7a in Chapter 9)
$= (0.785 \text{ ft}^2)(0.75)(3{,}000 \text{ psf})(300)$
$R_t = 529{,}875$ lbs $= 265$ tons

b. $R_t(\text{max}) = q_L \times A_p$ (Equation 9-7b in Chapter 9)
$= (680 \text{ ksf})(0.785 \text{ ft}^2)$ (q_L=680 ksf for $\phi = 43°$ from Figure 9-14 in Chapter 9)

$R_t(\text{max}) = 533.8$ kips $= 267$ tons

$\therefore R_t = 265$ tons

It is obvious that any embedment in gravel layer will produce capacities > 200 tons. Therefore, estimate pile length to top of gravel.

Step 4A: Determine soil resistance to driving SRD for 70 ton load with SF = 2.

$$\text{SRD} = R_{s(\text{sand})} + \frac{R_{s(\text{clay})}}{\text{sensitivity}} + (70 \text{ tons} \times 2)$$

$$= 9.6\,\text{tons} + \frac{43.1\,\text{tons}}{2} + 140\,\text{tons}$$ (note sensitivity = 2 is given in problem statement)

SRD = 171. 1 tons

B. <u>For 12 inch H-Pile* (120 ton design load)</u>
<u>*Assume HP 12x84 pile section</u>

Step 2B: Compute Shaft Resistance

(References to Figures and Tables are as in Step 2A above)

Sand Layer (4 ft - 15 ft)

$$V = \frac{24.6}{144} = 0.17\,\text{ft}^3/\text{ft}$$

$$\delta/\phi = 0.80$$

$\delta = (0.80)(36°) = 28.8°$

$K_\delta = 1.30$

$C_F = 0.92$

$C_d = 4$ ft

p_d Avg. @ $\frac{4\,\text{ft} + 15\,\text{ft}}{2} = 9.5$ ft is 1,050 psf

$R_{s\,(sand)} = (1.30)(0.92)(1{,}050\ \text{psf})(4\ \text{ft})(\sin 28.8^o)\ (11\ \text{ft})$
$R_{s\,(sand)} = 26{,}619\ \text{lbs} \approx 13.0\ \text{tons}$

Clay Layer (15 ft - 40 ft)

$R_{s(clay)} = c_a C_d D$

c_a (Adhesion) ≅ 1,100 psf (assume adhesion ≈ cohesion, i.e., $\alpha \approx 1.0$)

$R_{s(clay)} = 1{,}100$ psf (4 ft) 25 ft = 110,000 lbs = 55 tons

- *Gravel Layer (Try 4 ft Embedment, ie. 40 ft – 44 ft)

  *Use $\phi_{Max} = 36°$

  $q_s = (K_\delta)(C_F)(P_0)(C_d)(\text{Sin } \delta)D$

  $V = \frac{24.6}{144} = 0.17\ {}^{CF}/_{Ft.}$

  ${}^{\delta}/_{\phi} = 0.80$

  $\delta = (0.80)(36°) = 28.8°$

  $K_\delta = 1.30$

  $C_F = 0.92$

  $C_d = 4$ ft

  $p_d = 3{,}200$ psf

  $R_{s(gravel)} = (1.30)(0.92)(3{,}200 \text{ psf})\ (4 \text{ ft})(\sin 28.8°)\ (4 \text{ ft})$

  $R_{s(gravel)} = 29{,}500 \text{ lbs} \approx 14.7 \text{ tons}$

Step 3B: **Compute toe resistance** (Use $\phi = 43°$) at 44 ft

(References to Figures and Tables are as in Step 3A above)

- Gravel Layer

  For $\phi = 43º$, $\alpha_t \approx 0.75$ from Figure 9-13(a) in Chapter 9
  For $\phi = 43º$, $N'_q = 300$ from Figure 9-13(b) in Chapter 9

  c. $R_t = A_p\, \alpha_t\, p_t\, N'_q$ (p_t max.) (Equation 9-7a in Chapter 9)

  $$= \frac{24.6 \text{ in}^2}{144\ {}^{\text{in}^2}/_{\text{ft}^2}}(0.75)(3{,}000 \text{ psf})(300)$$

  $R_t = 115{,}313 \text{ lbs} \approx 57.7 \text{ tons}$

d. $R_t(\max) = q_L \times A_p$ (Equation 9-7b in Chapter 9)

$$= (680\text{ksf})\frac{24.6\text{in}^2}{144\text{in}^2/\text{ft}^2}$$

(q_L=680 ksf for $\phi = 43°$ from Figure 9-14 in Chapter 9)

$R_t(\max) = 116.2$ kips = 58.1 tons > 57.7 tons

$\therefore R_t = 57.7$ tons

- Total useable soil capacity below clay is = 14.7 tons + 57.7 tons = 72.4 tons
- Total Required capacity is 240 Tons
- Extending pile to 50 ft only increases R_s to 37 tons

Conclusion: Pile must bear on rock to develop 240 tons capacity below clay layer. Therefore estimate pile length to rock.

Step 4B: Determine soil resistance to driving SRD for 120 ton load with SF = 2.

$$\text{SRD} = R_{s(\text{sand})} + \frac{R_{s(\text{clay})}}{\text{sensitivity}} + (120\text{ tons} \times 2)$$

$$= 13.0\text{ tons} + \frac{55\text{ tons}}{2} + 240\text{ tons}$$

(note sensitivity = 2 is given in problem statement)

SRD = 280.5 tons

* Composed of 37 tons skin friction in the gravel and 203 tons in end bearing on rock.

STATIC PILE ANALYSIS - ABUTMENT @ STA 93 + 50

A. For 12 inch Diameter Pipe Pile

Step 2A & 3A: Based on computation at the pier, the pipe pile will develop the 140 ton ultimate load at the top of the gravel layer, ie. an estimated length of 65 ft. However the driving resistance will increase.

Step 4A: Compute driving resistance.

- Fill (Use $\phi_{max} = 36°$)

$q_s = (K_\delta)(C_F)(p_o)(C_d)(\sin \delta)\, C_d\, D$

$V = 0.785\ ft^3/ft.$

$\delta/\phi = 0.6$ (for closed end pipe pile from Figure 9-7 in Chapter 9)

$\delta = (0.6)(36°) = 21.6°$

$K_\delta = 1.92$ (for $\phi = 36º$ from Table 9-6(a) in Chapter 9)

Correction Factor, $C_F = 0.75$ (from Figure 9-12 in Chapter 9)

$C_d = \pi\, d = \pi\, (1\ ft) = 3.14\ ft$

$p_d = 1{,}650\ psf$

$R_{s\,(fill)} = K_\delta\,(C_F)(p_d)(C_d)(\sin \delta)D$ (Equation 9-6 in Chapter 9)
$= (1.92)(0.75)(1{,}650\ psf)(3.14\ ft)(\sin 21.6º)(23\ ft)$
$R_{s\,(fill)} = 63{,}168\ lbs \approx 31.6\ tons$

- Sand

$R_{s(sand)} = (1.92)(0.75)(3{,}330\ psf)(3.14\ ft))(\sin 21.6°)\ (7\ ft)$
$R_{s(sand)} = 38{,}800\ lbs \approx 19.4\ tons$

- Clay

$$R_{s(clay)} = \frac{c_a C_d D}{\text{sensitivity}}$$

$$R_{s(clay)} = \frac{(1{,}100\,psf)(3.14)(1\,ft)(35\,ft)}{2} = 60{,}445\,lbs \approx 30.2\ tons$$

Soil Resistance to driving, SRD @ top of gravel= 31.6 tons + 19.4 tons +30.2 tons + 140 tons = 221.2 tons

Step 5A: Check driving resistance in embankment.

Assume pile tip embedded 23 ft

$R_{s(fill)}$ = 31.6 tons (from Step 4A)

$R_t = A_p \alpha_t p_{d \text{ at } 23'} N'q$
$= (0.785 \text{ ft}^2)\ (0.74)\ (2{,}990 \text{ psf})\ 170$

R_t = 147.6 tons < R_t (max) = 200 (0.785) = 157 tons

SRD(fill) = 31.6 tons + 147.6 tons = 179.2 tons

To overcome this SRD, pre-augering may be required through the fill

B. 12 inch H – Pile (120 ton design) – assume HP 12×84 section

Steps 2B & 2C: Estimate length to rock i.e., 75 ft, as pier computation showed H-pile must bear on rock to achieve designed ultimate capacity.

Step 4B: Compute driving resistance.

- Fill

V = 0.17 CF/Ft.

$\delta / \phi = 0.80$

$\delta = (0.80)(36°) = 28.8°$
(ϕ_{max})

K_δ = 1.30

C_F = 0.92

$R_{s(fill)} = (1.30)(0.92)(1{,}495 \text{ psf})(4 \text{ ft})(\sin 28.8°)(23 \text{ ft})$
$R_{s(fill)}$ = 79,247 lbs ≈ 39.6 tons

- Sand

$R_{s(sand)} = (1.30)(0.92)(3{,}303 \text{ psf})(4 \text{ ft})(\sin 28.8°)(7 \text{ ft})$

$R_{s(sand)}$ = 53,287 lbs ≈ 26.6 tons

- Clay

$$R_{s(clay)} = \frac{c_a C_d D}{\text{sensitivity}}$$

$$R_{s(clay)} = \frac{(1{,}100\ \text{psf})(4\ \text{ft})(35\ \text{ft})}{2} = 77{,}000\ \text{lbs} = 38.5\ \text{tons}$$

- Gravel

$R_{s(gravel)}$ = (1.30)(0.92)(5,600 psf)(4 ft)(sin 28.8°)(10 ft)
$R_{s(gravel)}$ = 129,063 lbs ≈ 64.5 tons

Total $R_s = R_{s(fill)} + R_{s(sand)} + R_{s(clay)} = R_{s(gravel)}$

Total R_s = 39.6 tons + 26.6 tons + 38.5 tons + 64.5 tons

Total R_s = 169.2 tons = 338.4 kips

SRD = 39.6 tons + 26.6 tons + 38.5 tons + [64.5 $\underbrace{\text{tons} + 175.5\ \text{tons}}_{240\ \text{tons}}$]

SRD = 344.7 tons = 689.4 kips

$\therefore$ (Total R_s)/SRD = 338.4 kips / 689.4 kips = 0.49 or 49%

Step 5B: Check H – Pile driving resistance in embankment

Assume pile tip embedded 23 ft

$R_{s(fill)}$ = 39.6 tons (from Step 4B)

$R_t = A_p \alpha_t p_{d\ at\ 23'} N'q$

$$R_t = \frac{24.6\ \text{in}^2}{144\ \text{in}^2/\text{ft}^2}(0.74)(2{,}990\ \text{psf})170$$

R_t = 64,257 lbs ≈ 32.1 tons < q_{lim} = (200)(0.17)=34 tons > 32.1 tons (use 32.1 tons)

SRD (fill) = 39.6 tons + 32.1 tons = 71.7 tons

To overcome this SRD, pre-augering may be required through the fill

Summary of the Pile Design Phase for the Apple Freeway Design Problem

- Design Soil Profile

  Strength value selected for all layers.

- Static Analysis - Pier

  12 inch closed end pipe pile - 70 ton – 36 ft length required
  12 inch HP 12x84 - 120 ton – 46 ft length required.

- Static Analysis Abutment

  12 inch closed end pipe pile- 70 ton – 65 ft length required
  12 inch HP 12 x 84- 120 ton – 75 ft length required.

- Soil Driving Resistance

  Driving Resistances computed for both pipe and H-piles to permit design check of pile section overstress.

  Pipe pile will require pre-augering through embankment.

- Abutment Lateral Movement

  From Step 2 in Section A.6-6, 3 inch possible horizontal movement even with a pile foundation unless recommended waiting period observed prior to pile driving.

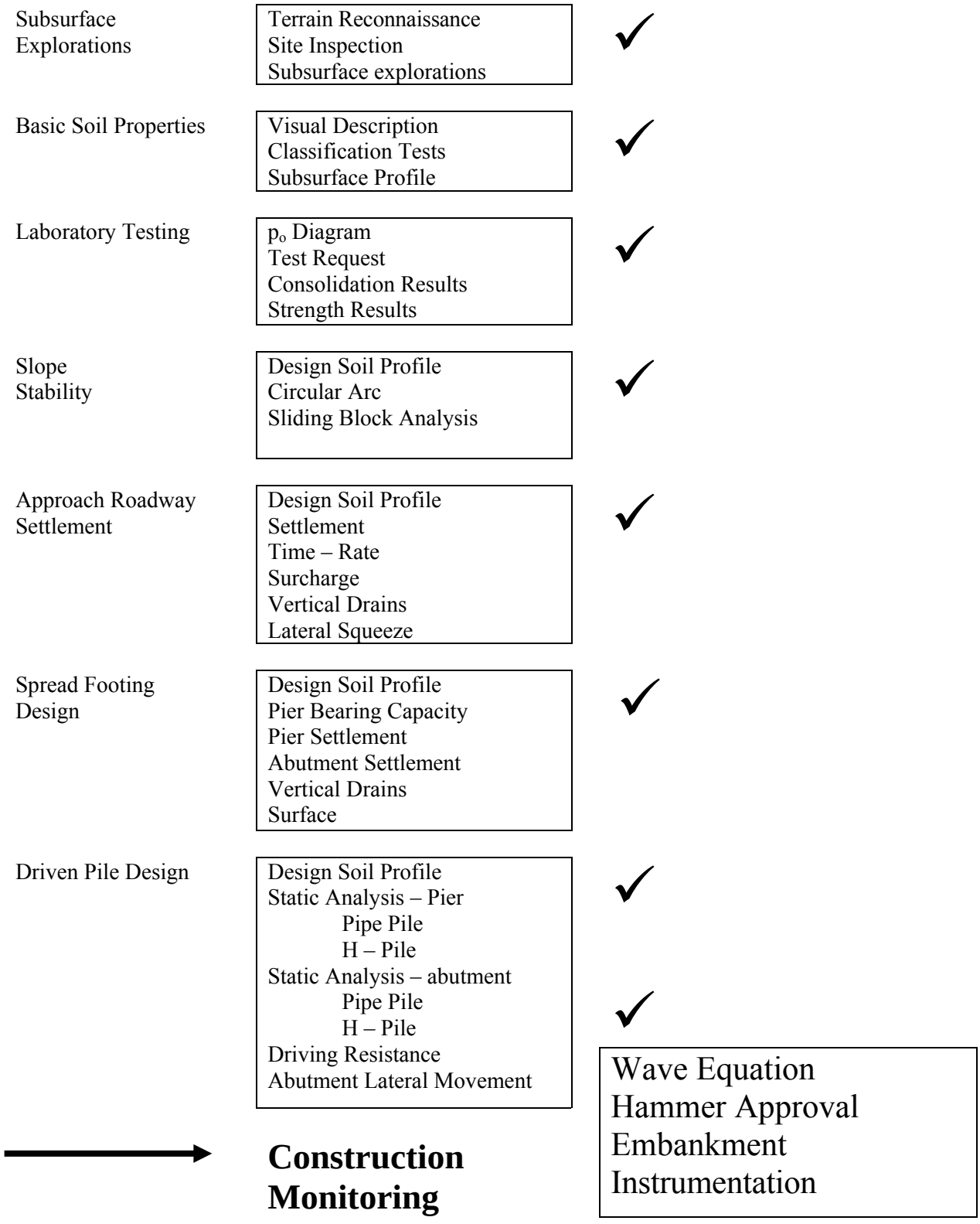

Figure A.9-1. Status of geotechnical work.

SECTION A.9
CONSTRUCTION MONITORING OF DRIVEN PILES

In this Section the Apple Freeway Design Example is use to illustrate the wave equation analysis using a wave equation analysis program. The use of wave equation analysis for pile driveability analysis, checking suitability of contractors driving system, and determining pile driving criteria is addressed. A commonly used wave equation analysis program is the GRLWEAP. Other similar products such as TNOWave are also available as noted in Chapter 9. Herein, the program GRLWEAP will be used for the example problem. The use of GRLWEAP does not constitute an endorsement of the product by FHWA.

Given: Using the soil profile and pile driving resistance previously computed (Section A.8)

Required: Complete wave equation analyses using the GRLWEAP program for the following:

- Driveability of the proposed design pile section
- Acceptance of contractors driving system
- Production pile driving criteria

Solution:

Driveability of Proposed Design Pile Section

Proposed pile section is a HP 12 × 84. The maximum driving resistance determined from static analyses is at the east abutment where the total driving resistance including embankment penetration is 689.4 kips. Perform wave equation analysis for the proposed pile section using the maximum driving resistances.

Step 1: Prepare Wave Equation Input:

1. Select hammer (IHAMR)

   - Hammer size selected from Figure 9-44 in Chapter 9 using maximum driving resistance of 689.4 kips (345 tons). Minimum hammer energy = 57,000 ft-lbs.

   - Using GRLWEAP help screen, scan hammer library for hammers with sufficient energies. Select Delmag 30 – 13 hammer which has slightly more energy than required (66,000 ft-lbs) to insure efficient driving.

2. Select uniform or non-uniform pile cross-section along the entire pile (NCROSS)

   Select non-uniform option (1) because pile point will be used. Pile cross-section described on input screen NCROSS =1 as shown on "page 7" of the GRLINP input printoutogram.

3. Select percent pile skin friction (IPERC)

   - From static analysis, (skin friction resistance/total driving resistance) = (338/689)(100) = 49%.

4. Select skin friction distribution (ITYS)

   - Use the actual skin friction distribution determined in the static analysis ultimate driving resistance computation (ITYS = 0). An analysis using the actual skin friction distribution is more realistic and accurate. From static analyses (see next page).

5. Select helmet and hammer cushion information (helmet weight, hammer cushion area, elastic modulus and thickness).

   - Using GRLWEAP help screen, scan hammer library for Delmag Hammers using the proposed pile section.

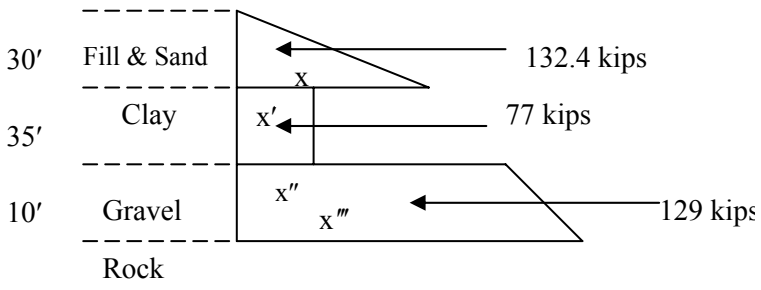

$$x = \frac{132.4}{30} \times 2 = 8.83$$

$$x' = \frac{77}{35} = 2.2$$

$$x'' = \frac{5{,}250}{5{,}600}\left(\frac{129}{10}\right) = 12.08$$

$$x''' = \frac{5{,}950}{5{,}600}\left(\frac{129}{10}\right) = 13.72$$

6. Select Pile Top Information (length, x-section area, elastic modulus, specific weight, coefficient of restitution).

   - Using GRLWEAP help screen, obtain the x-sectional area and weight for the proposed HP12×84.

7. Select soil parameters (quake and damping).

   - Using GRLWEAP help screen, select appropriate soil parameters.

8. Select ultimate driving capacities to be analyzed.

   - Input a range of ultimate driving capacities around and including the maximum soil driving resistance (SRD) calculated from static analyses (689.4 kips). A range of capacities highlights trends within the graphical plots.

GRLINP Input Screens for HP 12×84 Driven through the Embankment Material – Ultimate Resistance 689.4 kips.

```
Title:  APPLE FREEWAY H-PILE @ ABUTMENT                          Page:    1

ANALYSIS OPTIONS
     IOUT       IJJ      IHAMR      IOSTR      IFUEL      IPEL
        .         .         13.         .          .         .

ANALYSIS OPTIONS
        N      ISPL     NCROSS     IBEDAM     IPERCS     ISMITH     DMPEXP
        .         .         1.         .         49.         .         .0

ANALYSIS OPTIONS
     ITYS       IPHI      IRSAO       ITER      IDAHA      IMAXT
        .         .          .          .          .          .

HELMET AND HAMMER CUSHION INFORMATION
   Helmet          ┌──────────────────── Hammer Cushion ────────────────────┐
   Weight          Area    ElasMod Thickness    C.O.R.   RoundOut Stiffness
     2.15        283.50      280.0     2.000      .800      .0100         .0
```

```
Title:  APPLE FREEWAY H-PILE @ ABUT FULL EMBEDMT                 Page:    2

PILE CUSHION INFORMATION
          Elastic                                  Round
     Area Modulus Thickness     C.o.R.      Out  Stiffness
      .00      .0      .000       .500    .0100         .0

PILE TOP INFORMATION
    Total      X-Sectn Elastic   Specific                    Round  D.O.A.1   D.O.A.2
   Length       Area   Modulus    Weight     C.o.R.          Out   Slck P2  Stiff P2
    75.00      24.60   30000.0    492.00      .850         .0100       .00        .00

HAMMER OVERRIDE VALUES
                          Reaction  ComDelay   Comb Exp   Stroke
   Stroke     Effcy  Pressure   Weight   Ign Vol    Coeff   Conv Crit
      .00      .000         .0     .000      .000      .00       .00

SOIL PARAMETERS
   ┌─── Quake ──┐   ┌── Damping ──┐   ┌──────────── Toe No. 2 ────────────┐
     Skin     Toe     Skin     Toe     Quake   Damping  Fraction     Depth
     .100     .100     .050     .150     .000      .000      .000       .00
```

```
Title:  APPLE FREEWAY H-PILE @ ABUTMENT                          Page:    3

ULTIMATE CAPACITIES
Give up to 10 Capacities (5 on first line)
   350.00    550.00    631.80    689.40    740.00

ULTIMATE CAPACITIES (Continued)
(5 on the second line)
      .00       .00       .00       .00       .00
```

CONTINUE GRLINP INPUT SCREENS FOR HP12x84 (689.4 kips).

Title: APPLE FREEWAY H-PILE @ ABUTMENT Page: 7

NCROSS=1: NON-UNIFORM PROFILE, 1ST PILE ** PILE LENGTH: 75.00

Depth	Area	Elastic Modulus	Specific Weight
.00	24.60	30000.0	492.00
74.60	24.60	30000.0	492.00
74.60	42.50	30000.0	492.00
75.00	42.50	30000.0	492.00

75500 PILE POINT (12" H)
AREA = 42.5 in^2
HEIGHT = 4.8 in

Title: APPLE FREEWAY H-PILE @ ABUTMENT Page: 8

ITYS=-1, 0: SKIN FRICTION DISTRIBUTION, 1ST PILE ** PILE LENGTH: 75.00

Depth	Relative Distribn
.00	.000
30.00	8.830
30.00	2.200
65.00	2.200
65.00	12.080
75.00	13.720

SUMMARY OF GRLWEAP RESULTS FOR HP12X84 (DELMAG 30-13)

Rut (kips)	Bl Ct (bpf)	Stroke (ft) down	Stroke (ft) up	min Str (ksi)	max Str (ksi)	ENTHRU (kip-ft)	Bl Rt (b/min)
350.0	32.9	6.83	6.70	.00(	29.09(	25.9	45.3
550.0	79.6	7.38	7.32	.00(	31.53(	26.3	43.5
631.8	114.8	7.66	7.44	.00(	32.67(	26.9	42.9
689.4	170.6	7.51	7.47	.00(	32.46(	26.3	43.1
740.0	256.7	7.44	7.49	.00(	32.19(	25.9	43.2

G R L W E A P - Federal Highway Adm.

APPLE FREEWAY H-PILE @ ABUTMENT 05/10/93

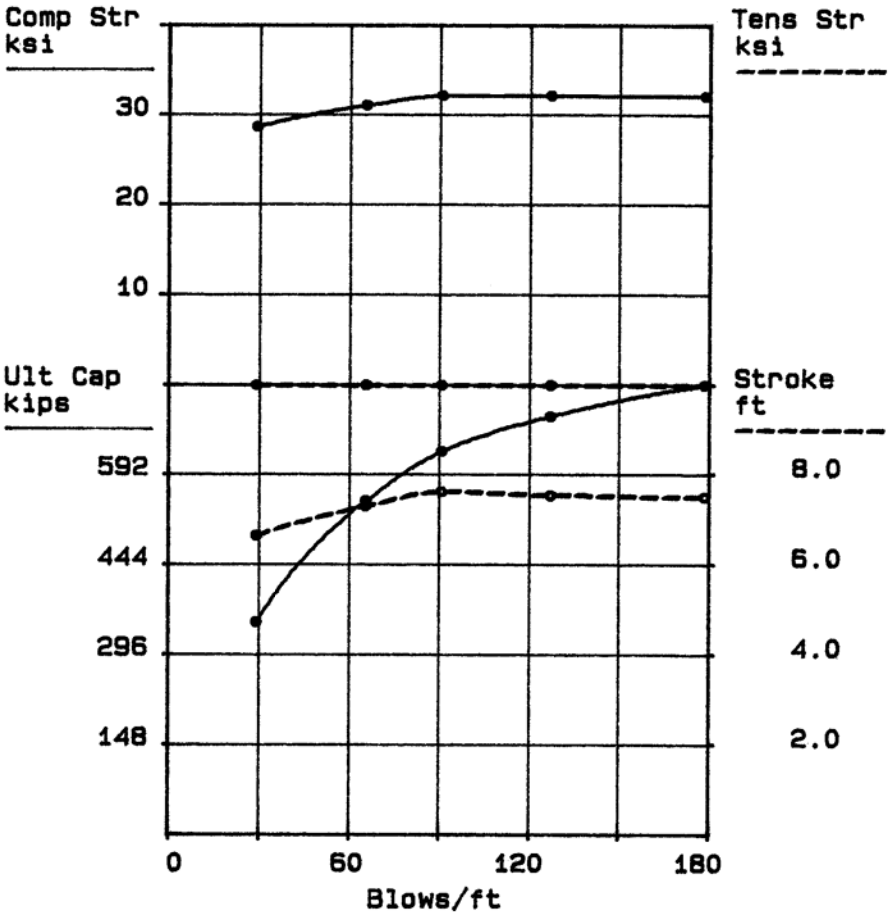

DELMAG D 30-13		
Efficiency	.720	
Helmet	2.15	kips
H Cushion	39690	k/in
Q = .100	.100	in
J = .050	.100	s/ft
Pile Length	75.00	ft
P-Top Area	24.60	in2

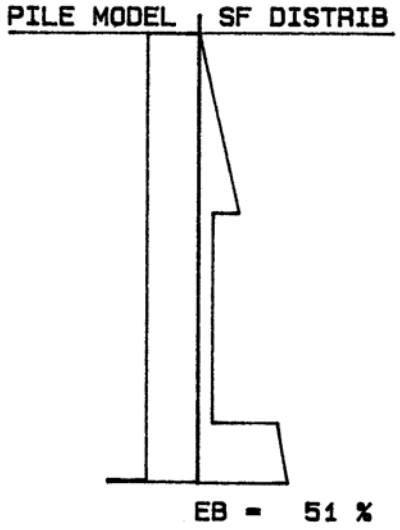

APPLE FREEWAY - HP12x84 DRIVEN THROUGH EMBANKMENT MATERIAL

SUMMARY OF DRIVEABILITY ANALYSES FOR HP12X84

Pile section is adequate for the hardest driving conditions encountered at the east abutment. Driving stresses are below the maximum allowable driving stress of 32.4 ksi. Stresses are insensitive to the blow count and therefore, the pile won't be damaged when seated into the rock.

HP12X84 pile section is acceptable ✓

ACCEPTANCE OF CONTRACTORS DRIVING SYSTEM

Contractor has submitted a ICE 70-S driving system. The pile and driving equipment data sheet is shown below.

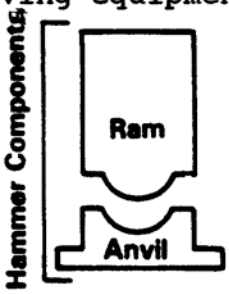

Hammer

Manufacturer: ICE Model: 70S
Type: OED Serial No.: 123
Rated Energy: 79,000 lb-ft at 10 ft Length of Stroke
Modifications: _____

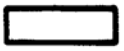

Hammer Cushion

Material: Micarta
Thickness 2in Area: 398 in²
Modulus of Elasticity – E 280,000 psi (P.S.I.)
Coefficient of Restitution-e 0.8

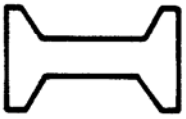

Drive Head

Helmet
Bonnet
Anvil Block
Pile Cap

– Weight: 2.44 kips

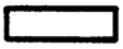

Pile Cushion

Cushion Material: N/A
Thickness: _____ Area: _____
Modulus of Elasticity – E _____ (P.S.I.)
Coefficient of Restitution _____

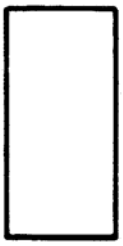

Pile

Pile Type: HP12X84
Length (In-Leads) – 75'
Weight/ft. 498 lbs/ft³
Wall Thickness: _____ Taper: No
Cross Sectional Area 24.6 in² in²
Design Pile Capacity: 120 (Tons)
Description of Splice: _____
Tip Treatment Description: _____

Driving Resistance: 280.5 tons @ Pier
344.7 tons @ Embankments

Perform wave equation analysis for the submitted driving system.

- Modify hammer data in the GRLWEAP input file previously used to analyze the HP 12×84 pile section. Use the submitted driving system data, and the GRLWEAP driveability option.

GRLINP Input Screens for GRLWEAP Driveability option. Screens not Shown Below are Unchanged from the Pile Section Analysis.

```
Title:  FULL EMBEDMT - DRIVABILITY OPTION                        Page:    1

ANALYSIS OPTIONS
     IOUT       IJJ      IHAMR      IOSTR      IFUEL       IPEL
   -100.          .       129.          .          .          .

ANALYSIS OPTIONS
        N      ISPL     NCROSS     IBEDAM     IPERCS     ISMITH     DMPEXP
        .         .         1.          .          .          .         .0

ANALYSIS OPTIONS
     ITYS       IPHI      IRSAO       ITER      IDAHA      IMAXT
        .          .          .          .          .          .

HELMET AND HAMMER CUSHION INFORMATION
   Helmet      ┌──────────────── Hammer Cushion ─────────────────────┐
   Weight       Area    ElasMod Thickness    C.O.R.  RoundOut Stiffness
     2.44     398.00      280.0      2.000      .800      .0100         .0
```

Continue GRLINP Input Screens for GRLWEAP Driveability Options Analysis of Ice 70S Driving System.

```
Title:  FULL EMBEDMT - DRIVABILITY OPTION                        Page:    3

IPERCS = 0:  Friction Loss/Gain Factors
Give up to 10 Friction Loss/Gain Factors (5 on first line)
      .90       1.00       1.10        .00        .00

IPERCS = 0:  Friction Loss/Gain Factors
(5 on the second line)
      .00        .00        .00        .00        .00
```

Title: FULL EMBEDMT - DRIVABILITY OPTION Page: 6

IPERCS=0: DEPTHS & DRIVING SYSTEMS MODIFICATIONS ** PILE LENGTH: 75.00

Analysis Depth	Stroke	IFUEL	Efficiency	Stiffn. Factor	Cushion CoR
20.00	.00	.0	.00	.00	.00
30.00	.00	.0	.00	.00	.00
45.00	.00	.0	.00	.00	.00
65.00	.00	.0	.00	.00	.00
74.00	.00	.0	.00	.00	.00
74.50	.00	.0	.00	.00	.00
74.88	.00	.0	.00	.00	.00
75.00	.00	.0	.00	.00	.00
.00	.00	.0	.00	.00	.00

Title: FULL EMBEDMT - DRIVABILITY OPTION Page: 8

IPERCS = 0: SOIL PARAMETERS VS DEPTH ** PILE LENGTH: 75.00

Depth	Skin Friction	End Bearing	Skin Quake	Toe Quake	Skin Damping	Toe Damping	Sens.
.00	.000	5.000	.100	.100	.050	.150	.000
30.00	8.830	58.000	.100	.100	.050	.150	.000
30.00	2.200	5.000	.100	.100	.200	.150	.000
65.00	2.200	5.000	.100	.100	.200	.150	.000
65.00	12.080	96.000	.100	.100	.050	.150	.000
75.00	13.720	351.000	.100	.100	.050	.150	.000

SUMMARY RESULTS OVER DEPTH FOR ICE 70S HAMMER

FRICTION LOSS/GAIN FACTOR: .900

Depth (ft)	Rut (kips)	Frictn (kips)	End Bg (kips)	Bl Ct (bpf)	max Str (ksi)	min Str (ksi)	Bl Rte (b/min)	ENTHRU (kip-ft)
20.0	83.7	48.4	35.3	4.1	15.493	.000	45.4	34.8
30.0	170.1	114.4	55.7	8.5	25.056	-.032	40.8	35.0
45.0	148.1	143.3	4.8	7.2	23.653	-4.327	41.7	33.6
65.0	189.3	184.5	4.9	10.9	27.935	-7.017	39.9	31.3
74.0	***384.7***	***289.6***	***95.1***	***31.3***	***31.664***	***-.150***	***37.2***	***29.3***
74.5	***390.8***	***295.7***	***95.1***	***31.6***	***31.888***	***-.148***	***37.1***	***29.7***
74.9	***395.5***	***300.4***	***95.1***	***32.1***	***31.942***	***-.154***	***37.1***	***29.7***
75.0	***651.9***	***302.9***	***349.0***	***128.3***	***31.664***	***.000***	***36.8***	***30.0***

Total Driving Time 15.72 min; Total No. of Blows 631

FRICTION LOSS/GAIN FACTOR: 1.000

Depth (ft)	Rut (kips)	Frictn (kips)	End Bg (kips)	Bl Ct (bpf)	max Str (ksi)	min Str (ksi)	Bl Rte (b/min)	ENTHRU (kip-ft)
20.0	89.6	54.1	35.5	4.3	15.098	.000	45.3	34.0
30.0	183.3	127.5	55.8	9.7	24.582	-.135	40.9	32.0
45.0	164.6	159.8	4.8	8.4	24.303	-4.221	41.2	32.5
65.0	210.3	205.4	4.9	12.8	28.075	-6.177	39.5	30.2
74.0	*417.1*	*322.0*	*95.1*	*35.1*	*32.602*	*-.115*	*37.0*	*29.5*
74.5	*423.9*	*328.8*	*95.2*	*36.1*	*32.693*	*-.069*	*37.0*	*29.4*
74.9	*429.1*	*334.0*	*95.2*	*36.8*	*32.740*	*-.052*	*37.0*	*29.4*
75.0	*685.8*	*336.7*	*349.1*	*158.6*	*32.103*	*.000*	*37.3*	*29.6*

Total Driving Time 18.08 min; Total No. of Blows 720

FRICTION LOSS/GAIN FACTOR: 1.100

Depth (ft)	Rut (kips)	Frictn (kips)	End Bg (kips)	Bl Ct (bpf)	max Str (ksi)	min Str (ksi)	Bl Rte (b/min)	ENTHRU (kip-ft)
20.0	95.5	59.8	35.7	4.5	16.319	.000	44.9	34.6
30.0	196.6	140.6	56.0	10.2	25.761	-.978	40.6	32.9
45.0	181.2	176.3	4.8	9.3	26.005	-4.863	40.7	32.7
65.0	231.2	226.3	4.9	14.3	29.119	-5.837	39.0	30.6
74.0	*449.6*	*354.4*	*95.2*	*40.4*	*33.106*	*-.338*	*37.4*	*29.2*
74.5	*457.1*	*361.9*	*95.2*	*41.6*	*33.171*	*-.348*	*37.4*	*29.2*
74.9	*462.8*	*367.6*	*95.2*	*42.5*	*33.191*	*-.350*	*37.4*	*29.1*
75.0	*719.6*	*370.5*	*349.2*	*204.9*	*32.518*	*-.066*	*37.3*	*29.2*

Total Driving Time 20.19 min; Total No. of Blows 799

GRLWEAP Output – plot

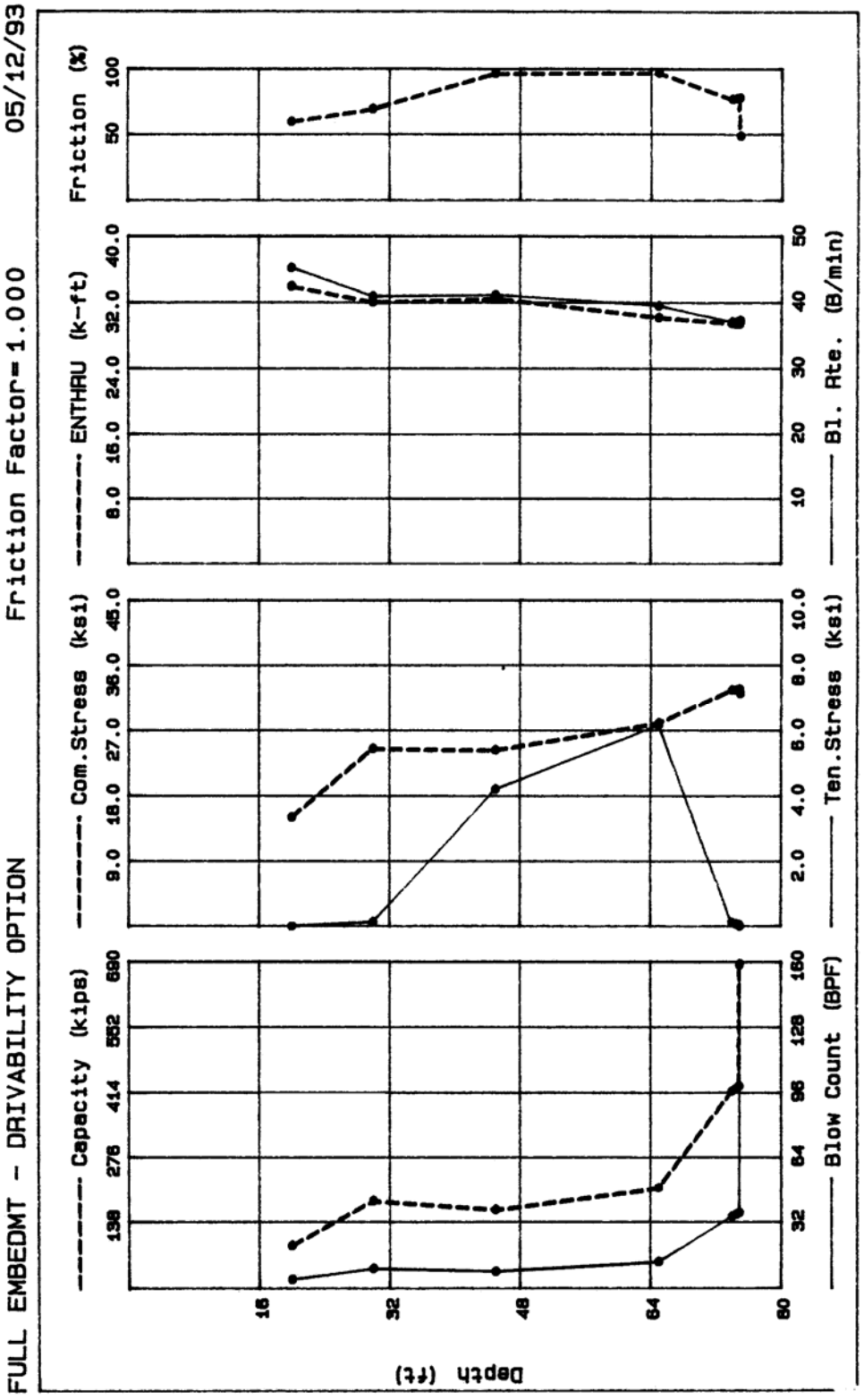

SUMMARY OF DRIVEABILITY ANALYSES FOR ICE 70S

Driving Stresses: 32.7 ≈ 32.4 ksi ✓OKAY

Driving stresses vary between 31.66 ksi (0.9 friction reduction) to 33.19 ksi (1.1 friction reduction), well below the yield strength of 36 ksi. Since, the maximum stresses occur when the pile has penetrated the rock and is at near refusal conditions, the piles should be capable of being seated into the rock without damage.

Blow Count: 159 bpf ≈ 144 bpf ✓ OKAY

The blow count is approximately 35 bpf at just above the rock line, and near refusal 150 - 220 bpf in the rock layer. Therefore, the hammer should (if operating properly) penetrate quickly through the embankment and into the rock.

HAMMER APPROVED ✓

PRODUCTION PILE DRIVING CRITERIA FOR ICE 70S DRIVING SYSTEM

Drive HP12x84 pile through the embankment material and into the rock. Pile driving shall be terminated when the combination of stroke and blow count indicates a driving capacity of 690 kips. If pre-augering is used the driving capacity of 650 kips should be attained.

Stroke Vs. Blow Count Plot

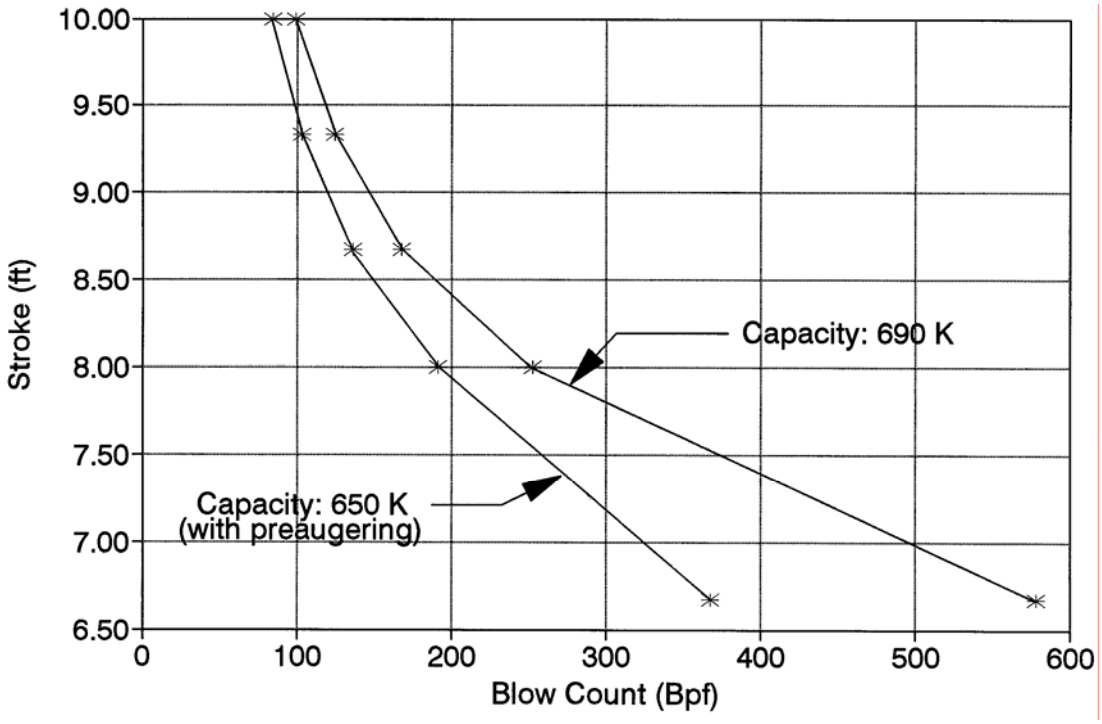

CONSTRUCTION CONTROL

- Pile Driveability

  Driveability of HP 12 x 84 pile

  Section verified for most difficult driving condition.

- Driveability versus Depth

  Driveability of HP 12 x 84 computed for full 75 feet depth.

  Pile installation time expected to vary between 16 and 20 minutes (no pre- augering).

SECTION A.10
GEOTECHNICAL DESIGN SUMMARY REPORT

A typical example of a Geotechnical Design Summary Report is presented in the following section with reference to the Apple Freeway Design Example. The report illustrates the inclusion of various items discussed in the preceding sections of this chapter and summarize the pertinent results and conclusions obtained from the various analysis/design stages in the preceding chapters.

WORKSHOP DESIGN PROBLEM - GEOTECHNICAL DESIGN SUMMARY REPORT

December 15, 2006
Geotechnical Design Summary Report

To: Mr. A. J. Jones
Chief Engineer

From: Mr. A. B. Smith
Chief Foundation Engineer

Subject: Interstate 0 Structure over the Apple Freeway

The Geotechnical Section has completed an analysis of the foundation conditions at the site of the subject structure. Our analysis is based on the following information:

1. A 1-inch equals 20 feet plan and profile prepared by the Bridge Division and received in this office October 1, 2006.

2. An interpretation of the boring logs and analysis of soil samples from three drill holes numbered BAF-1 thru 3, nine auger holes numbered EA-1 thru 9, one drill hole numbered BAF-4 from which undisturbed samples were taken, and four Cone Penetration Test (CPT) soundings numbered CPT BAF-1 through 4.

3. Laboratory testing on undisturbed samples from BAF-4.

Subsurface Conditions:

The general subsurface conditions are shown on Drawing No. 5 GS 331.

Foundation Recommendations:

1. Elevation Assumptions

   The foundation recommendations are based on the following bottom of footing elevations:

West Abutment	1011
Pier	992
East Abutment	1012

Changes to footing elevations may affect the foundation recommendations and should be discussed with this office.

2. Embankment Construction

A. Unsuitable Subexcavation

An approximate 1 to 3-foot thick organic layer exists between approximate stations 92+70 to 94+00 in the area of the east approach embankment. This organic layer should be removed and replaced with granular embankment material in accordance with Bridge Design Data Sheet 80-1.

B. Embankment Material and Placement

The approach embankment shall be constructed of materials placed in accordance with Bridge Design Data Sheet 80-1.

C. Embankment Settlement

An estimated 12 inches of fill settlement will occur due to consolidation of the 35-foot thick clay layer underlying the proposed 30-foot high east approach embankment. Estimated settlement time for 90 percent primary settlement is 14 months. Settlement time can be reduced to, (1) 6 months by use of a 10-foot surcharge fill or (2) 2 months with wick drains at 7.5 foot center to center spacing. Estimated cost for each of these treatments is:

Treatment	**Estimated Settlement Time**	**Estimated Extra Cost**
Fill only	14 months	$ ---
Fill w/10 foot surcharge	6 months	120, 000
Fill w/wick drains	2 months	172,000

It is understood the construction schedule will not allow a 14-month waiting period but will allow up to an 8-month waiting period, therefore, the 10-foot surcharge treatment is recommended as the most cost-effective method to reduce settlement time. The surcharge should be placed full height for a length of 500 feet back of the bridge ends on both the east and west approach and sloped at 1 vertical to 1.5 horizontal down to the embankment grade.

D. Embankment Stability

The estimated immediate end of construction factor of safety for the proposed 30' high east approach embankment is 1.63. The estimated immediate end-of-construction factor of safety for the proposed 30-foot fill plus 10 foot temporary surcharge is 1.33. Both factors of safety are adequate and no special approach embankment treatment is necessary. Long-term factor of safety will increase as consolidation of the foundation soils occur. The factor of safety for the west approach embankment will be higher as the fill height is 10' less. An analysis of highway borings confirms that no stability problems will occur due to the 500' extension of the surcharge.

E. Embankment Monitoring

Fill settlement is recommended to be monitored with settlement plates and piezometers. Settlement plates should be installed at existing ground elevation at centerline stations 90+00, 93 + 50, and 96 + 50. Piezometers to monitor excess pore pressure buildup and dissipation in the clay subsoil are recommended at centerline stations 93 + 50 and 96 + 50. A total of three piezometers should be installed at each location - one each at 20, 28, and 36 foot depths. Instrumentation will be installed by State forces.

3. Abutment Foundation

A. Spread Footings

The abutments may be supported on spread footings placed on compacted select material with a maximum allowable bearing capacity of 3 tons per square foot assuming a footing width of 7 feett is used. Changes to the footing width affect both bearing capacity and settlement and should be discussed with this office. The total settlement of the east and west abutments respectively will be 2.6 and 1.9

inches which occurs over respective time periods of 14 months and 7 months. About 60 percent of the settlement will occur in 2 months after structure construction. This settlement may be reduced by extending the surcharge period. For 90 percent consolidation the surcharge should remain in place a total of 8 months; 2 months longer than required for embankment considerations. If vertical drains are installed during embankment construction, these drains will reduce the time for abutment settlement such that only ¼" will remain 30 days after all abutment loads have been placed

B. Piles

Two pile types were analyzed at the abutment; a displacement pile (12" diameter closed end pipe) and a non-displacement pile (HP 12 x 84 pile). Displacement type piles are not recommended due to their inability to be driven through the fill and the uncertainty of obtaining penetration in the dense gravel stratum. Non-displacement H-piles are recommended. However, to insure that the pile can be driven to rock without damage, the section should not be less than a HP 12 x 84 pile. A HP 12 x 84 pile driven to rock may be designed for a maximum load of 120 tons. Tip reinforcement, such as APF 75500, should be used to prevent tip damage by boulders in the gravel stratum and to insure penetration to rock. Estimated pile lengths are 60 feet at the west abutment and 75 feet at the east abutment.

At the abutments, negative skin friction may be expected if the piles are installed before fill settlement is complete. In addition lateral squeeze of the clay subsoil will occur as the clay consolidates. Therefore, to prevent increased vertical downdrag pile loads, bending of abutment piles and rotation of the abutment toward the fill, the abutment piling should not be installed until embankment settlement is complete.

The actual driving resistance estimated to develop the design load for the H-pile at the estimated length is 345 tons at the east abutment and 290 tons at the west abutment. The contractor should size his equipment to achieve this resistance without damaging the pile.

4. Pier Foundation

A. Spread Footings

The pier may be supported on spread footings placed 4 feet below ground on natural undisturbed soil and designed for a maximum allowable bearing capacity of 3 tons per square foot assuming a footing width of 7' is used. Changes in footing width should be discussed with this office. Approximately 2.8 inches of settlement is expected at this location over about 7 months with 1 inch occurring immediately and 2 inches occurring in less than 2 months. If a spread footing foundation is chosen, consideration should be given to increasing the structure clearance over the Apple Freeway to account for these settlements. Settlement along the footing axes will be uniform. However a short term differential settlement of 1.5" can be expected between the abutment and pier footings if spread footings are used.

B. Piles

A 12" diameter closed end pipe pile and a HP 12 x 84 pile were analyzed at the pier. The closed end pipe may be designed for 70 tons with a safety factor of 2 if driven into the dense gravel layer. The estimated length is 36 feet. However a minimum wall thickness of 0.375 inches should be used to prevent overstress during driving. A driving resistance of 170 tons is estimated to reach the estimated length. A conical reinforced point should be used to prevent tip damage due to boulders. The cost per ton on a per foot basis equals $11.

A HP 12 x 84 pile may be designed for 120 tons with a safety factor of 2 if driven to rock. The estimated length is 46 feet. A driving resistance of 280 tons is estimated to obtain design resistance at the estimated length. A reinforced tip similar to APF 75500 should be used to prevent tip damage due to boulders. The cost per ton on a per foot basis equals $8.

We recommend that H-piles be chosen if piles are used because of cost advantages and installation advantages.

5. Special Notes

The following special notes are recommended to be included in the contract documents.

1. The general subsurface conditions at this site are shown on Drawing No. 5 GS 331.

2. A 6-month waiting period will be imposed between completion of the 10-foot surcharge on the east embankment. The actual length of the waiting period may be reduced by the Engineer based on an analysis of settlement platform and piezometer readings.

3. The contractor shall coordinate his construction schedule to allow installation of instrumentation by State forces.

4. Instrumentation damaged by contractor personnel shall be repaired or replaced at the contractor's expense. All construction activity in the area of any damaged instrument shall cease until the damage has been corrected.

If piles are used the additional special notes should be provided.

5. Pile driving will not be allowed at the abutments until fill settlement is complete. Estimated maximum settlement time is 6 months after placement of the 10-foot surcharge. This time may be reduced based on interpretation by the State of settlement plate readings.

6. Piles will be acceptable only when driven to pile driving criteria established by the Deputy Chief Engineer (Structures). Prerequisite to establishing these criteria, the contractor shall submit, to the Deputy Chief Engineer (Structures) and others as required, Form entitled, "Pile and Driving Equipment Data." All information listed on the Form shall be provided within 14 days after the award of the contract. Each separate combination of pile and pile driving equipment proposed by the contractor will require the submission of a corresponding Form.

The actual driving resistance to install the 12 x 84 H-piles to the estimated lengths shown on the plans is estimated to be 280 tons at the pier, 345 tons at the east abutment and 290 tons at the west abutment. The contractor's equipment shall be capable of overcoming these resistances without inflicting pile damage.

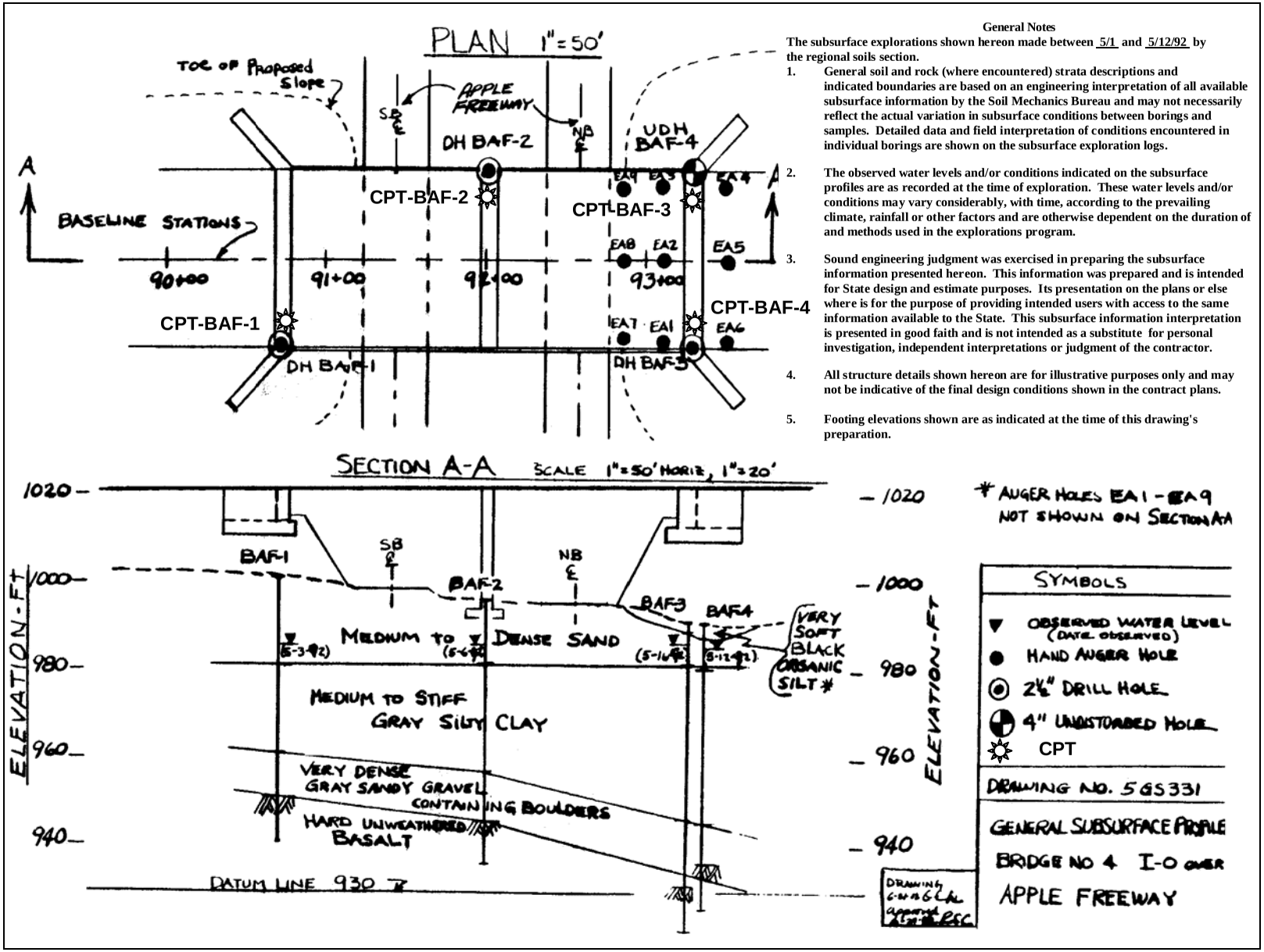

General Notes

The subsurface explorations shown hereon made between 5/1 and 5/12/92 by the regional soils section.

1. **General soil and rock (where encountered) strata descriptions and indicated boundaries are based on an engineering interpretation of all available subsurface information by the Soil Mechanics Bureau and may not necessarily reflect the actual variation in subsurface conditions between borings and samples. Detailed data and field interpretation of conditions encountered in individual borings are shown on the subsurface exploration logs.**

2. **The observed water levels and/or conditions indicated on the subsurface profiles are as recorded at the time of exploration. These water levels and/or conditions may vary considerably, with time, according to the prevailing climate, rainfall or other factors and are otherwise dependent on the duration of and methods used in the explorations program.**

3. **Sound engineering judgment was exercised in preparing the subsurface information presented hereon. This information was prepared and is intended for State design and estimate purposes. Its presentation on the plans or else where is for the purpose of providing intended users with access to the same information available to the State. This subsurface information interpretation is presented in good faith and is not intended as a substitute for personal investigation, independent interpretations or judgment of the contractor.**

4. **All structure details shown hereon are for illustrative purposes only and may not be indicative of the final design conditions shown in the contract plans.**

5. **Footing elevations shown are as indicated at the time of this drawing's preparation.**

APPENDIX B

MOHR'S CIRCLE AND ITS APPLICATIONS IN GEOTECHNICAL ENGINEERING

[THIS PAGE INTENTIONALLY BLANK]

APPENDIX B
MOHR'S CIRCLE AND ITS APPLICATIONS IN GEOTECHNICAL ENGINEERING

The relationship between the normal and shear stress acting on any plane within a solid mass (continuum) may be represented graphically by an extremely useful device known as *Mohr's Circle for Stress*. It is named after the German engineer Otto Mohr who devised it in 1882.

B.1 BASIC CONVENTIONS FOR PLOTTING A MOHR'S CIRCLE

The basic conventions for plotting a Mohr's circle are as follows:

1. The *normal* stresses (σ) are plotted on the abscissa. In conventional solid mechanics, *tensile* stresses are considered positive (plotted to the right of the origin) and *compressive* stresses are considered negative (plotted to the left of the origin).

2. The *shear* stresses (τ) are plotted on the ordinate. In both conventional solid mechanics and soil mechanics, positive shear stresses are plotted above the origin while negative shear stresses are plotted below the origin. This sign convention for plotting the shear stresses should not be confused with the sign convention for the shear stresses themselves. Although sign conventions for the shear stresses themselves vary from one text to another, in general positive shear causes clockwise rotation of the stress element and negative shear causes counterclockwise rotation of the stress element (as discussed in Section B.2).

3. Positive angles on the circle are measured in the counterclockwise sense; negative angles are obtained in the clockwise sense. An angle of 2θ on the circle corresponds to an angle of θ on the element, where θ is defined as the angle between any two planes within the soil element (as discussed in Section B.2).

B.2 MOHR'S CIRCLE CONSTRUCTION FOR GENERAL STRESS CONDITIONS

Figure B-1(a) shows a solid element subjected to a normal stress (σ) and a shear stress (τ) on each of its four planes. The element can be considered to consist of a set of two mutually perpendicular planes – one horizontal, e.g., Plane Q, the other vertical, e.g., Plane P. Table B-1 presents a summary of the stresses acting on the four planes shown in Figure B-1(a) and their directions (sign) according to the conventions discussed in Section B.1.

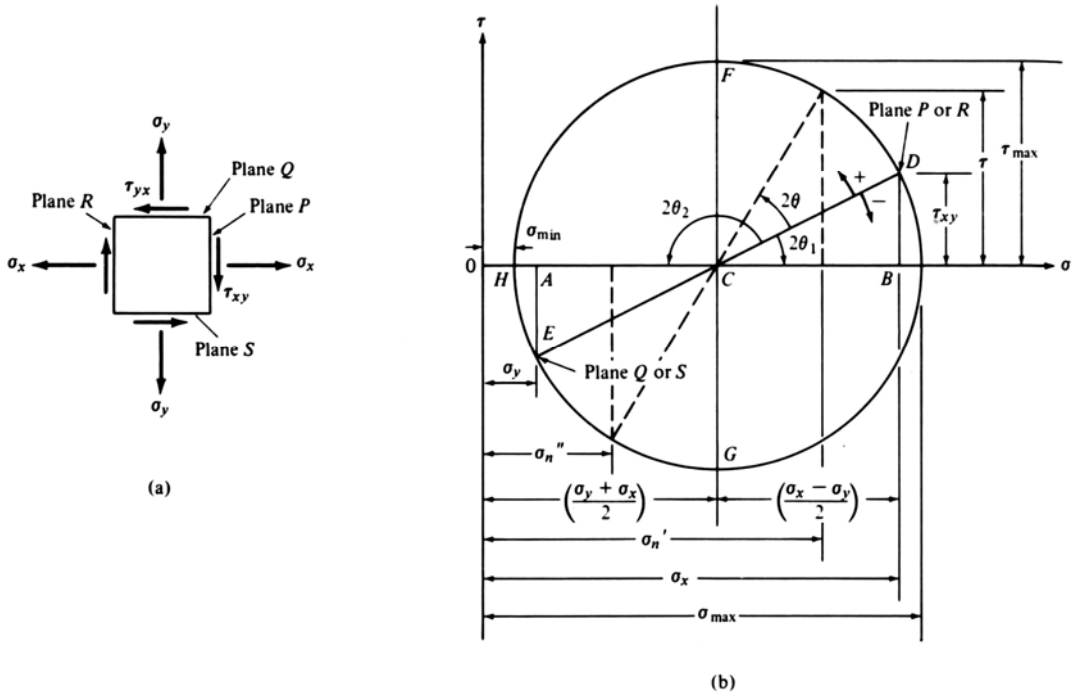

Figure B-1. Mohr's circle for general stress conditions (Cernica, 1982).

Table B-1
Summary of stresses acting on the four planes shown in Figure B-1(a)

Plane	Normal Stress	Sign	Shear Stress	Sign
P	σ_x	+	τ_{xy}	+
Q	σ_y	+	τ_{yx}	-
R	σ_x	+	τ_{yx}	+
S	σ_y	+	τ_{xy}	-

Note: In this table and Figure B-1, the sign convention is according to that commonly used in solid mechanics, i.e., tensile (normal) stresses are considered positive and are plotted to the right of the origin. In soil mechanics it is customary to indicate *compressive* stresses as positive because soil cannot sustain tensile stresses since it has virtually no strength in tension. The use of the soil mechanics convention will be illustrated in Sections B.3 and B.4.

The following convention is used for the subscripts in Figure B-1:

- For normal stresses, the subscript denotes the orientation of the stress with respect to an x-y coordinate system centered on the element where x is the horizontal axis and y is the vertical axis. Thus σ_y acts in the vertical direction on planes Q and S, both of which are horizontal planes. Since the element is in static equilibrium, the normal stresses acting on the two horizontal planes must be equal. The same logic applies to σ_x, which acts horizontally on vertical planes R and P.

- For shear stress, there are two letters in the subscript. The first letter refers to the subscript of the normal stress acting on the same plane as the shear stress. The second letter refers to the direction in which the shear stress itself is acting. Thus, τ_{yx} acts on Plane Q where the normal stress is σ_y and it acts horizontally (x-direction). Since τ_{yx} causes counterclockwise rotation of the element, it is considered to be negative as per the sign convention discussed previously. Although it is not shown on the figure, the shear stress acting on Plane S is also τ_{yx} and it also causes counterclockwise rotation of the element. Since moment equilibrium must exist for the element to be in static equilibrium, $\tau_{xy} = \tau_{yx}$ but the signs must be opposite. This can be verified by reference to Table B-1, which was derived from Figure B-1(a).

For the purpose of illustration, assume $\sigma_x > \sigma_y > 0$ The Mohr circle for the stress element shown in Figure B-1(a) is then plotted as follows (Recall that Mohr's circle is plotted on shear stress (τ) vs. normal stress (σ) coordinates where (τ) is the ordinate and (σ) is the abscissa.):

1. Find the planes having the larger normal stress and determine its sign. In this case, σ_x acts on planes P and R and its sign is positive (tension). Determine the magnitude and sign of the shear stress acting on those planes; τ_{xy} is of known magnitude and it causes clockwise rotation of the element, therefore it is positive. Refer to Table B.1 for confirmation. The normal and shear stresses on plane P (or R) represent a point on the τ-σ axis shown in Figure B-1(b).

2. Plot the normal and shear stress values on plane P (or R) at the coordinate point D shown in Figure B-1(b). The reason the stresses on these two planes plot at the same point is that one plane is oriented 180-degrees from the other on the stress element, i.e., refer to Figure B-1(a) and rotate vertical plane P and its normal and shear stresses by 180-degrees to obtain vertical Plane R that has the same magnitude and direction

(sign) of normal and shear stresses as plane P. Since an angle between two planes on the stress element (θ) plots as twice the angle on the Mohr's circle (2θ), point D represents the stress conditions on both planes P and R since 2θ = 360-degrees. The same holds true for the stress conditions on planes S and Q. Note that the point plots in the first quadrant since both σ_x and τ_{xy} are positive as per the sign convention discussed previously.

3. Find the planes perpendicular to planes P and R; those are planes Q and S. The lesser normal stress, σ_y, acts on those planes and it too is positive (tension). Determine the magnitude and sign of the shear stress acting on those planes; τ_{yx} is of known magnitude and it causes counterclockwise rotation of the element, therefore it is negative. Refer to Table B-1 for confirmation. The normal and shear stresses on plane Q (or S) represent a point on the τ-σ axis shown in Figure B-1(b).

4. As in Step 2, plot the normal and shear stress values on plane Q (or S) at the coordinate point E shown in Figure B-1(b). The reason that both planes plot at the same point was explained previously in #2. Note that the point plots in the fourth quadrant since both σ_x is positive but and τ_{yx} is negative as per the sign convention discussed previously.

5. The line ED represents the diameter of the Mohr's circle. The center of the circle lies on the σ axis at point C, which is simply the average value of the normal stresses σ_x and σ_y. Use the center of the circle and the diameter to draw the full circle.

A number of important stress conditions can be determined once the full Mohr's circle is drawn. For example, the values of the major and minor principal stresses can be read directly from the circle. By definition, **the major and minor principal stresses are normal stresses that occur on planes where the shear stress equals zero.** The major principal stress is shown as σ_{max} and the minor principal stress as σ_{min} (point H) on Figure B-1(b). In soil mechanics, the major and minor principal stresses are called σ_1 and σ_3, respectively.

Also, **the magnitude of the maximum shear stress (τ_{max}), which is equal to the radius of the circle**, can be read directly from the circle at points F (or G) on Figure B-1(b). Alternatively, the radius of the circle can be calculated from triangle ACE shown in the figure. The orientation of the maximum shear stress with respect to the original plane can either be measured directly on the Mohr's circle or easily calculated with the help of trigonometry.

In general, the normal and shear stresses on any plane oriented at an angle θ from a plane of known stress conditions (2θ on the Mohr's circle), e.g., planes P, Q, R, S, can either be read directly from the Mohr's circle or easily calculated with the help of trigonometry.

B.3 BASIC RELATIONSHIPS DERIVED FROM THE MOHR'S CIRCLE

Figure B-2 shows a simplified version of Figure B-1(b). A number of basic relationships between stresses can be obtained from a Mohr's circle. The following relationships can be observed directly from Figure B-2:

1. As indicated previously, **the maximum shear stress (τ_{max}) is equal to the radius of the circle**. Furthermore, since τ_{max} is oriented at + or – 90º (2θ) from a principle stress on the Mohr's circle, the maximum shear stress in the stress element acts on planes that make an angle (θ) of + or – 45º with the principal stress planes.

2. For the stress conditions (σ, τ) at a point S on the circle, which correspond to the stress conditions on some plane in the soil element, the resultant stress (0S) has a magnitude of $\sqrt{\sigma^2 + \tau^2}$ as shown in Figure B-2. Furthermore, the angle of obliquity (α) of the resultant is equal to $\tan^{-1}$ (τ/σ). **The angle of obliquity is the angle formed between the σ-axis and the line drawn from the point on the σ-axis where τ = 0 to any point on the Mohr's circle.**

3. **The maximum angle of obliquity (α_f) is constructed by passing a line through the origin that is also tangent to the Mohr circle**, such as line 0T in Figure B-2. The normal and shear stresses that correspond to point T on the circle represent the stresses on the plane of maximum obliquity. Note that the shear stress on this plane is less than τ_{max} and that slippage occurs at the point of maximum obliquity and not at the angle where τ_{max} occurs. Therefore α_f assumes the more prominent position regarding slip failure.

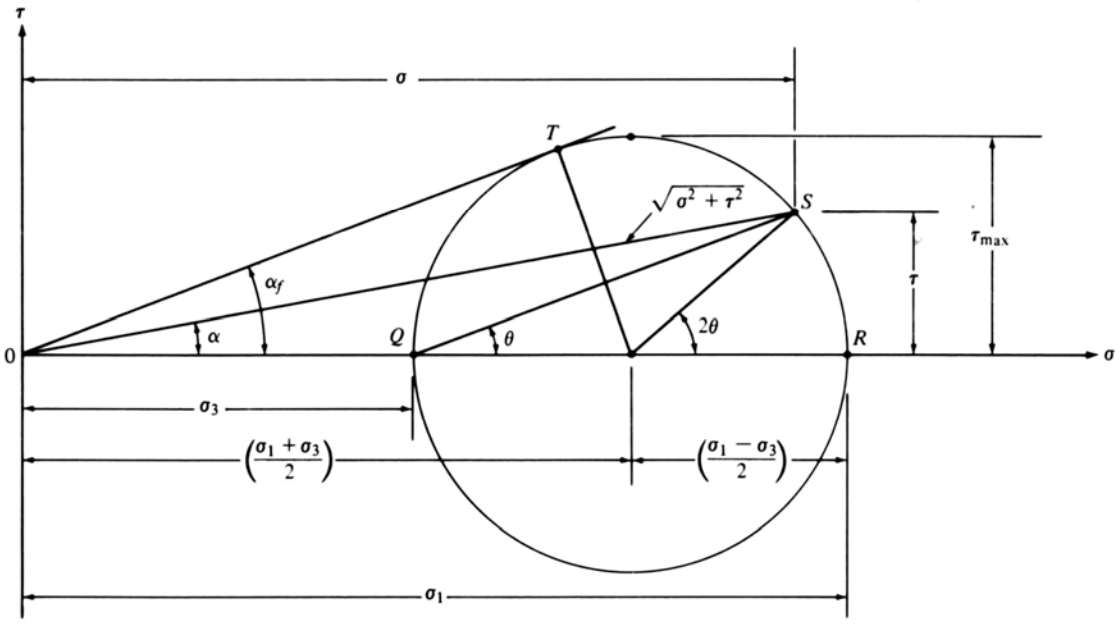

Figure B-2. Simplified version of Figure B-1(b) showing some basic relationships and characteristics of the Mohr's Circle (Cernica, 1982).

B.4 MOHR'S THEORY OF FAILURE – APPLICATION TO SOILS

The following concise description of Mohr's theory of failure is provided by Cernica (1982).

"The shear strength of soil is generally regarded as the resistance to deformation by continuous shear displacement of soil particles along surfaces or rupture. That is, the shear strength of the soil is not regarded solely in terms of its ability to resist peak stresses, but it must be viewed in the context of deformation which may govern its performance. In that light, therefore, shear failure is necessarily viewed as the state of deformation when the functional performance of the soil mass is impaired.

There are a number of different theories as to the nature and extent of the state of stress and deformation at the time of failure. Failure of a soil mass, particularly cohesionless soil which develops its strength primarily from solid frictional resistance between and interlocking of grains, appears to be best explained by Mohr's rupture theory. According to Mohr's theory, the shear stress in the plane of slip reaches, at the limit a maximum value which depends on the normal stress acting in the same planes and the properties of the material. This represents the combination of normal

and shear stresses which results in a maximum angle of obliquity α_f." (see Figure B-2)."

The combination of normal and shear stresses that results in the line inclined at the maximum angle of obliquity α_f represents the stress conditions on the failure plane within the soil mass. **The Mohr's circle corresponding to failure conditions is called the "Mohr failure circle" and the straight line inclined at the maximum angle of obliquity α_f is called the "Mohr failure envelope."** The combination of stresses at any other point on the Mohr's circle defined by an obliquity angle smaller than α_f represents stress conditions on a plane where failure has not occurred even though the soil mass has failed. Thus, for example, failure does not occur on the plane where the shear stress equals τ_{max}.

In reality, the relationship between normal stress and shear stress in soils is usually non-linear, as shown in Figure B-3(a). In addition, depending upon the type of soil and the conditions of loading, a soil might exhibit shear strength when the normal stress = 0, as is also illustrated in Figure B-3(a). Fortunately, the curvature of the Mohr failure envelope is relatively small for most practical problems where the stress range of interest is fairly narrow. Thus, it is mathematically convenient to represent the Mohr envelope by a straight line, sloped at an angle ϕ, that intersects the τ-axis at a value of shear stress = c. This is shown in Figure B-3(b) where ϕ represents the internal friction angle of the soil and c represents its "cohesion." The cohesion and friction angle are called the shear strength parameters of the soils.

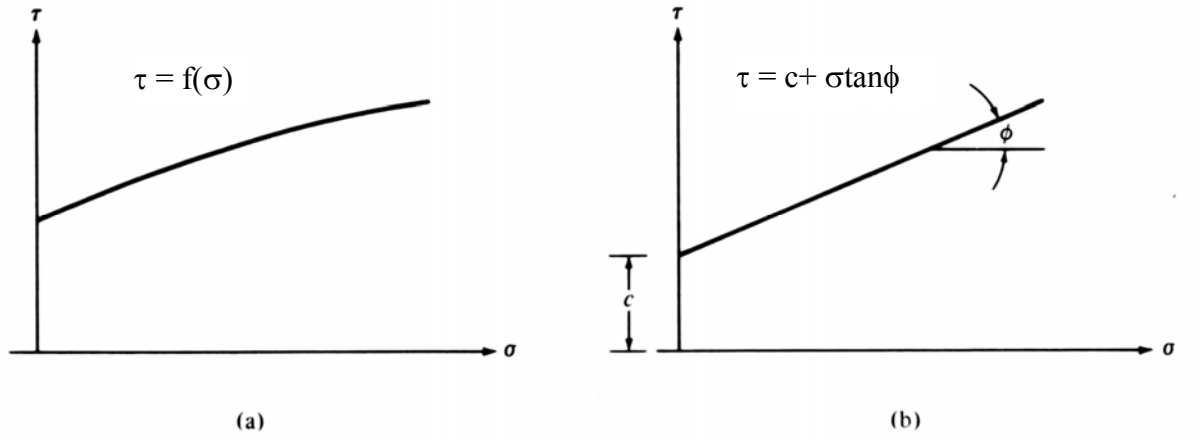

Figure B-3. Shear strength according to Mohr (a) and Coulomb (b) (Cernica, 1982).

The linear approximation was first proposed by Coulomb in 1776 in connection with his investigations of retaining walls. Therefore, the linear approximation to the Mohr failure envelope is called the "Mohr-Coulomb failure envelope" and constitutes the Mohr-Coulomb failure criterion. As shown in Figure B-3(b), the Mohr-Coulomb failure criterion can be expressed as:

$$\tau = c + \sigma \tan \phi \qquad \text{B-2a}$$

Equation B-2a is a general expression of the Mohr-Coulomb failure criterion that is applicable to all soils and conditions of loading. It can be easily modified to account of those cases. For example:

- For cohesionless soils (c = 0)

$$\tau = \sigma \tan \phi \qquad \text{B-2b}$$

- For purely cohesive soils ($\phi = 0$)

$$\tau = c \qquad \text{B-2c}$$

- For use with effective stress parameters ($c = c'$, $\phi = \phi'$)

$$\tau' = c' + \sigma' \tan \phi' \qquad \text{B-2d}$$

Since many applications of soil mechanics to problems in practice involve knowledge of the principal stresses in the soil (e.g. lateral earth pressure theory and use of triaxial test results for slope stability analyses), it is useful to express the Mohr Coulomb failure criterion in terms of principal stresses rather than in the formats used in Equations B-2a to B-2d. Figure B-4 shows the Mohr coulomb strength envelope for one Mohr circle at failure. The principal stresses contain a subscript "f" to indicate that they are the principal stress acting at failure on the stress element shown in the insert.

The following relationships can be derived from Figure B-4.

$$\sin \phi = \frac{R}{D} \qquad \text{B-3a}$$

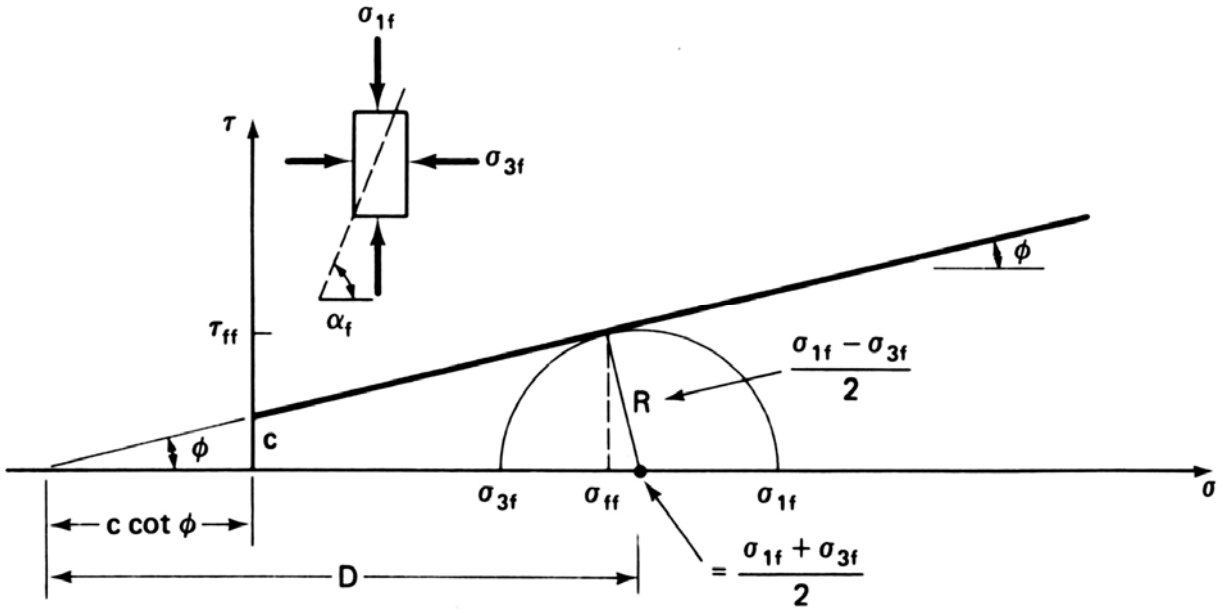

Figure B-4. Mohr coulomb failure envelope with one Mohr failure circle (Holtz and Kovacs, 1981).

Substitution of the stresses corresponding to R and D into Eq. B-3a yields:

$$\sin\phi = \frac{\frac{\sigma_{1f} - \sigma_{3f}}{2}}{\frac{\sigma_{1f} + \sigma_{3f}}{2} + c\cot\phi} \qquad \text{B-3b}$$

Rearrangement of terms in Eq. B-3b and substitution of trigonometric identities yields:

$$(\sigma_{1f} - \sigma_{3f}) = (\sigma_{1f} + \sigma_{3f})\sin\phi + 2c\cos\phi \qquad \text{B-3c}$$

Solving Eq. B-3c for σ_{1f} yields:

$$\sigma_{1f} = \sigma_{3f}\left[\frac{(1+\sin\phi)}{(1-\sin\phi)}\right] + \left[\frac{2c\cos\phi}{(1-\sin\phi)}\right] \qquad \text{B-3d}$$

Substitution of the identity $\cos\phi = (1 - \sin^2\phi)^{1/2}$ into Eq. B-3d yields:

$$\sigma_{1f} = \sigma_{3f}\left[\frac{(1+\sin\phi)}{(1-\sin\phi)}\right] + \left[\frac{2c\sqrt{(1+\sin\phi)}}{\sqrt{(1-\sin\phi)}}\right] \qquad \text{B-3e}$$

Equation B-3e represents the general relationship between the major (σ_1) and minor (σ_3) principal stresses in terms of the soil strength parameters c and ϕ.

For cohesionless soils (c = 0), Eq. B-3e reduces to:

$$\frac{\sigma_{1f}}{\sigma_{3f}} = \frac{(1+\sin\phi)}{(1-\sin\phi)} \qquad \text{B-3f}$$

The reciprocal of Eq. B-3f yields:

$$\frac{\sigma_{3f}}{\sigma_{13f}} = \frac{(1-\sin\phi)}{(1+\sin\phi)} \qquad \text{B-3g}$$

By the use of trigonometric identities Eq. B-3f can be re-written as:

$$\frac{\sigma_{1f}}{\sigma_{3f}} = \tan^2\left(45° + \frac{\phi}{2}\right) \qquad \text{B-3h}$$

Similarly, Eq. B-3g can be re-written as:

$$\frac{\sigma_{3f}}{\sigma_{1f}} = \tan^2\left(45° - \frac{\phi}{2}\right) \qquad \text{B-3h}$$

Equation B-3h gives the coefficient of passive earth pressure, K_p, while Equation B-3i gives the coefficient of active earth pressure, K_a that were introduced in Chapter 2. Many concepts in geotechnical engineering can be similarly explained by used of Mohr's circle. The most common use of Mohr's circle is for interpretation of the results of shear strength tests discussed in Chapter 5. For use of Mohr's circle in interpretation of shear strength tests, the reader is referred to well-known text books such as Holtz and Kovacs (1981) and Lambe and Whitman (1979).

APPENDIX C

LOAD AND RESISTANCE FACTOR DESIGN (LRFD)

[THIS PAGE INTENTIONALLY BLANK]

APPENDIX C
LOAD AND RESISTANCE FACTOR DESIGN (LRFD)

C.1 INTRODUCTION

In 1994, the AASHTO Subcommittee on Bridges adopted a Bridge Design Specification based on the use of the Load and Resistance Factor (LRFD) method (AASHTO, 1994). The geotechnical parts of the new specification had been developed by an NCHRP Research Project (NCHRP, 1991). The most recent version of the LRFD specifications is the 2004 version of AASHTO. Most states are now in the process of implementing the LRFD specifications.

The geotechnical portion of the LRFD specification has proven to be one of the most difficult to implement. This includes shallow and deep foundations, and earth retaining systems. In fact, the Section 10 of the LRFD specification, was significantly updated in 2006 Interims. In this Appendix, basic concepts of LRFD will be presented including a brief discussion on comparison of LRFD with allowable stress design (ASD) approach. The purpose here is to provide the necessary basis for preparing the geotechnical specialist to use this new method. The material presented in this Appendix has been adapted from similar material included in the FHWA (2006a) manual on driven pile foundations.

C.1.1 Primary References

The primary references for this Appendix are as follows:

AASHTO (2002). *Standard Specifications for Highway* Bridges. 17th Edition, American Association of State Highway and Transportation Officials, Washington, D.C.

AASHTO (2004 with 2006 Interims). *AASHTO LRFD Bridge Design Specifications,* 3rd Edition, American Association of State Highway and Transportation Officials, Washington, D.C.

C.2 CONCEPTS OF ASD AND LRFD

To understand and appreciate LRFD approach, it is necessary to first briefly summarize the fundamental basis for allowable stress design (ASD) and then to review the history of the development of the LRFD and its early implementation.

Allowable Stress Design (ASD) evolved from the development of methods of structural analysis during the nineteenth century. Prior to these developments, structures were designed based entirely on experience and of rules-of-thumb. The methods of structural analyses were developed based on the assumption that the structure behaved elastically and that they produced a rational evaluation of structural behavior that satisfied both equilibrium and compatibility. But, the analyses only explained structural behavior. It was desirable that a rational design approach be developed and it was logical to limit the calculated stresses in a structure to some fraction of the structural material strength. Gradually, structural loads appropriate for design were defined and then codified. So, if member stresses could be calculated it was logical to limit those stresses and values of allowable stresses were gradually accepted based on the experience that the structure did not fail. These limiting stress values became known "**design stresses**" or "**allowable stresses**." For instance, the allowable stresses in steel beams in bending have been limited to between about 0.4 and 0.66 times the steel yield strength.

But, linear elastic behavior is not universally observed in all structural elements. For example, the failure strength of a column is related the slenderness ratio of the member and methods are available to confidently calculate the failure load. Similar considerations affect the design of other structural elements. The approach that came to be used in some applications during the development of ASD was to apply a "**factor of safety**" to the calculated ultimate member capacity.

Once the structural analysis was performed based on linear elastic theory and an appropriate factor of safety, the forces at the foundation element were obtained. At this stage, it was realized that the foundation element is embedded in geomaterials (i.e., soils and rocks) which are inherently inelastic and use of linear elastic theory will not represent the strength of a soil structure. Therefore, to account for inherent uncertainties in the characterization of geomaterials, the use of the concept of factor of safety was extended to geomaterials as well and has become universal in geotechnical design. Rather than use of two factors of safety, one for structural analysis and one for geotechnical analysis, a single combined factor of safety was applied to account for all uncertainties and this was commonly applied in the geotechnical analysis.

The combined factors of safety were selected so that failures were very unlikely, based on experience, but the magnitudes of the factors of safety were based only on experience. The geotechnical engineer should understand that he/she does not "own" all of the factor of safety. It must be adequate to deal with the variability of the loads and the inadequacy of the analysis in addition to the strength variability.

Until 1956, the analysis of a concrete section subject to bending was performed assuming that the compression stress in the concrete was linearly distributed on the cross section with the further assumption that concrete could carry no tension. Designs were limited by placing limits on the calculated stress in both the concrete in compression and in the steel in both tension and compression (if compression steel was present). In other words, the element strength was treated as if the materials were elastic and, to perform the analysis, the steel was then "transformed" into concrete based on the relative moduli of the two materials. The result of these assumptions produced quite conservative results, particularly if compression reinforcement was present as is always the case with columns. The time dependent deformation of concrete subjected to compression causes its effective modulus to be time dependent. Extensive research was performed in the first half of the twentieth century to understand what the actual stress distribution was and how it could be used in design.

These fundamental probIems with the use of ASD caused the American Concrete Institute (ACI) in 1956 to adopt a new edition of their Building Code for the design of concrete structures and in that code an Appendix was included that used a **strength design** approach (ACI 1956) to replace the allowable stress method described above. The ultimate strength of the element in bending was calculated using a prescribed, nonlinear concrete stress distribution on the section at failure. The computational procedure was quite simple and the result was element strength not stress. The Appendix of ACI 318-56 achieved little use.

The ACI Committee that prepared this method then took another major step. Instead of selecting a factor of safety for particular failure modes they broke the factor of safety into parts. They realized that the limiting value of ultimate load should depend on the variability of the particular load types. So they specified different "**load factors**" for the various types of loads and, indirectly, they applied an additional multiplier to provide structural safety for the strength variability of member types and failure modes.

ACI 318-63, adopted in 1963, made extensive changes from the 1956 Code and the result had the form that we now know as LRFD (ACI 1963).

$$\Sigma\gamma_{ij}\, Q_{ij} \leq \phi_k\, R_{nk} \qquad \text{C-1}$$

Where, γ is the **load factor**, Q is the **load effect** (this refers the element load calculated from the applied loads by a linear elastic structural analysis.) The subscripts i and j refer to the load condition (dead, live, wind, etc.) and the load combination, respectively. φ is the **resistance factor** for a given **limit state** (failure mode), R_{nk} is the **nominal resistance** in the k^{th} limit state. The term nominal resistance was adopted to define the element strength determined by some specified method. (**It should be noted that in the AASHTO LRFD Code the term nominal resistance is used instead of nominal strength.**) The summation on the left side of Equation (1) is known as the **factored load**. A generally used name for the right side of the expression has not been accepted. The term **factored resistance** will be used here.

The version of Equation (1) used in the AASHTO LRFD Design Specification is somewhat different. It has the following form:

$$\Sigma\eta\gamma_{ij}\, Q_{ij} \leq \phi_k\, R_{nk} \qquad \text{C-2}$$

where η is a factor related to the ductility, redundancy and operational importance.

When ACI 318-63 was adopted, the load and resistance factors were generated based on judgment followed by extensive comparative designs. By 1965, the designers of concrete structures in the private sector had almost universally adopted the ACI LRFD Code. There were a few minor changes in the load factors in the next edition of the Code in 1968 (ACI 1968) and the ASD section was dropped completely. The ACI LRFD Building Code was then essentially unchanged until 2002 (ACI 2002) when extensive changes were made primarily to the load and resistance factors. During this entire development period the design method was known as "**Ultimate Strength Design**."

The LRFD procedure adopted by ACI 318-63 was applicable to structural concrete elements for buildings only. It did not apply to the geotechnical aspects of foundation design. This produced a considerable anomaly for reinforced concrete building designers. For example, in the design process the geotechnical engineer recommended an allowable bearing pressure for a spread footing. The structural designer then had to size the footing using allowable loads – and that implied the use of a different set of loads - but perform the structural design of the reinforced concrete footing with factored loads.

Driven pile cap design was even more absurd. The geotechnical engineer selected an ultimate pile capacity based on subsurface conditions. Most of the methods that are used to establish pile capacity produce ultimate capacity. As discussed in Chapter 9, those methods include wave equation analysis, dynamic testing or static load testing. The one exception is

the use of a dynamic formula and most formulas usually give allowable loads. The Gates Formula is an exception in that it produces a predicted ultimate load. The geotechnical engineer then selected a factor of safety to arrive at an allowable load. Again, the structural engineer had to use allowable loads to do the pile group selection and layout but then use factored loads to design the pile cap. Private sector designers have been dealing with this inconsistency for forty years.

In 1969, Cornell published a paper in the ACI Journal (Cornell, 1969) showing that the load and resistance factors could be determined rationally using a probabilistic analysis. As input to that analysis the variability of both the loads and the resistance was required. The National Bureau of Standards (NBS) completed a research project to collect the necessary information for buildings and they generated the associated factors (Ellingwood, *et al.*, 1980). At that time the only LRFD Design Code in use was the ACI Code and the NBS factors were quite different than those contained in the ACI Code. These differences continued until 2002.

Today, LRFD design specifications are available for both steel and concrete buildings. Beginning with the 2002 ACI Building Code the load factors for both steel and concrete structures became the same. All concrete buildings are designed using LRFD but in the case of steel buildings the implementation of LRFD is not complete and an ASD design specification is still available and widely used for steel structures.

C.3 CALIBRATION OF PROBABILITY BASED LRFD

The original work of Cornell (1969) produced a major research effort to develop a probabilistic approach to structural design based on the load and resistance factor concept. The fundamental concept held that, since neither the loads nor the resistance are deterministic, it is appropriate to treat both load and resistance as random variables and to develop an approach to the design of structures based on probability theory. The concept is illustrated in Figure C-1 where **probability density functions** (PDFs) are shown for both the load effect, Q, and the resistance, R. The area under the resistance curve between a and b represents the probability of the resistance being between a and b. The region where the two curves overlap represents cases of "**failure**." Probability-based design is founded on the concept that the design be selected so that the probability of failure is equal to, or less than, some prescribed value. The limiting failure probability was originally established from laboratory test data on structural elements.

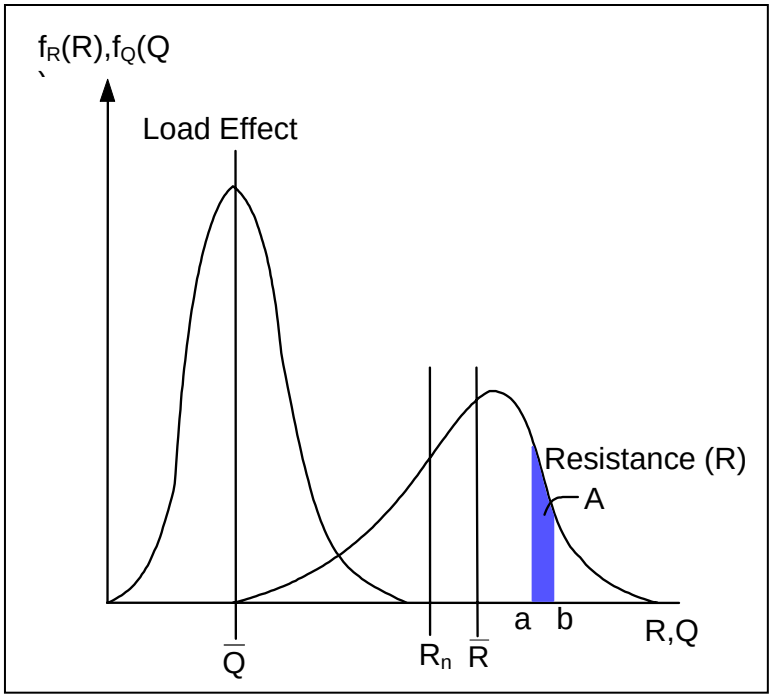

Figure C-1. Example of Probability Density Functions for both Load and Resistance.

The load effect in Figure C-1 has been shown much narrower than the resistance for illustrative purposes, indicating that, in this case, the load has less variability than the resistance. The variability is defined by the standard deviation of the distribution. (The standard deviations are not shown in Figure C-1.) In Figure C-1, the mean values are denoted by $\overline{Q}$ and $\overline{R}$. The **nominal resistance, R_n** is not necessarily the same as the **mean resistance** as illustrated in Figure C-1, but is the resistance that would be determined by the specified analysis method.

If distributions are available for both the load effect and the resistance, then the probability of failure can be determined. One approach that has been used is to consider the combined probability density function for R-Q and this is illustrated in Figure C-2. **Failure is defined when R-Q is less that zero and the region is shaded in Figure C-2.** The probability of failure is the area of the shaded portion under the curve. The basis for design is to require that the mean of that distribution, $\overline{R-Q}$, be greater than the value of R-Q = 0. The distance of that mean above zero is taken as a multiple, β, of the standard deviation of the distribution. β is known as the **safety index** or **reliability index**. There are other approaches to establishing a measure of safety. A more detailed discussion of probabilistic code calibration has been presented by Kulicki (1998).

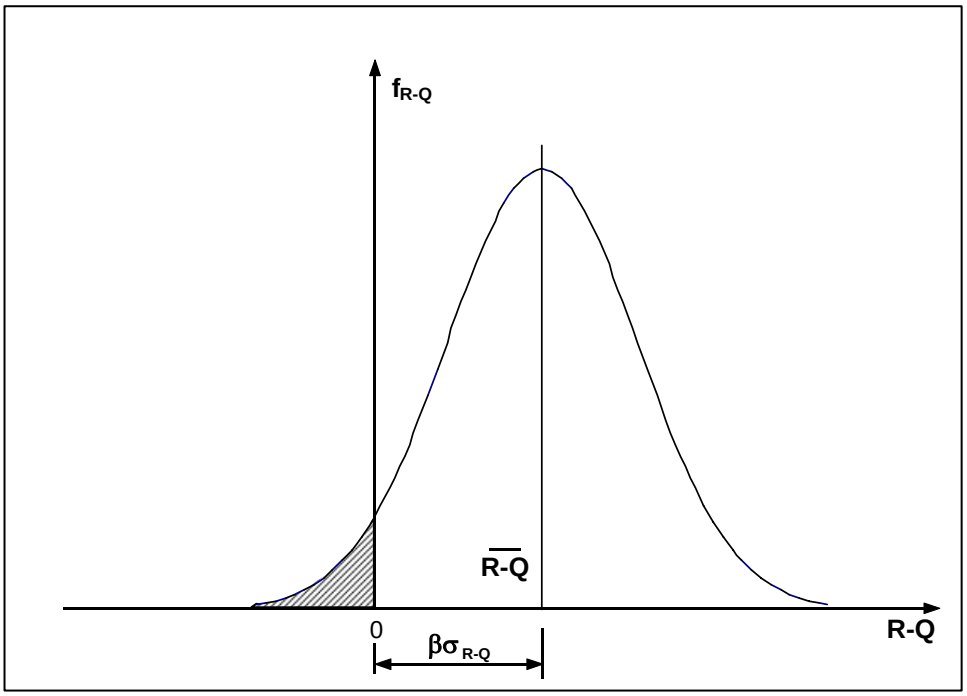

Figure C-2. Probability Density Function for R-Q.

Existing structures that have performed satisfactorily have been analyzed to determine safety indices and from these analyses recommended values have been determined. Then, with knowledge of the load and the strength variabilities it is possible to select load and resistance factors to produce the required safety index. Structural engineers have established load factors for the various load types in the AASHTO Bridge Code and most of these values are probably not subject to change today. So the geotechnical resistance factors must be selected to achieve the required appropriate safety index.

Geotechnical strength measurement is very difficult to describe statistically due to the lack of standardized procedures for material characterization of soils. But, load and resistance factors can be calibrated based on a direct comparison with existing design practice. Load factors have been selected for the AASHTO LRFD Bridge Code so resistance factors can be directly determined to produce designs similar to those obtained in current ASD practice. For example, the AASHTO Strength I case is considered since it is commonly critical in design. The equality condition is used to obtain a unique and limiting expression. The expression can be stated in a simplified fashion as

$$\gamma_D Q_D + \gamma_L Q_L = \phi_k R_{nk} \qquad \text{C-3}$$

where the subscript D refers to dead load and L refers to live load. Values are available for the dead and live load factors for Strength I in the AASHTO LRFD Bridge Code and Equation C-3 becomes

$$1.25\ Q_D + 1.75\ Q_L = \phi_k\ R_{nk} \qquad \text{C-4}$$

The equivalent ASD relationship can be stated

$$(Q_D + Q_L)\ FS = R_{nk} \qquad \text{C-5}$$

where FS is the ASD factor of safety. For the equality condition, R_{nk} can be eliminated from Equations C-4 and C-5 and this results in a single relationship for ϕ_k, in terms of FS and the Q_L/Q_D ratio.

$$\phi_k = \frac{FS(1 + Q_L / Q_D)}{(1.25 + 1.75 Q_L / Q_D)} \qquad \text{C-6}$$

Figure C-3 shows resistance factors for various factors of safety as a function of Q_L/Q_D ratio for the AASHTO LRFD Code. From Equation C-6 and Figure C-2, the importance of live-dead load ratio becomes clear. For short span bridges the live load may be much larger than the dead load while for very long spans structures the live loads can be almost inconsequential. Regardless of the source of resistance factors they must be checked against existing ASD practice. For example, if the probability analysis produced smaller resistance factors than the equivalent ASD factors of safety this would imply an unnecessary increase in conservatism in the design.

The factor η in Equation C-2 has been ignored in the above discussion. The primary concern with η in foundation design comes when only a very few deep foundation elements are used so that the foundation is non-redundant. While it is not so clear how redundancy can be determined since it is to some degree controlled by the superstructure geometry it can be critical and must be evaluated. Certainly a single deep foundation element will be non-redundant. Of course, most driven pile foundations will have enough piles to be redundant.

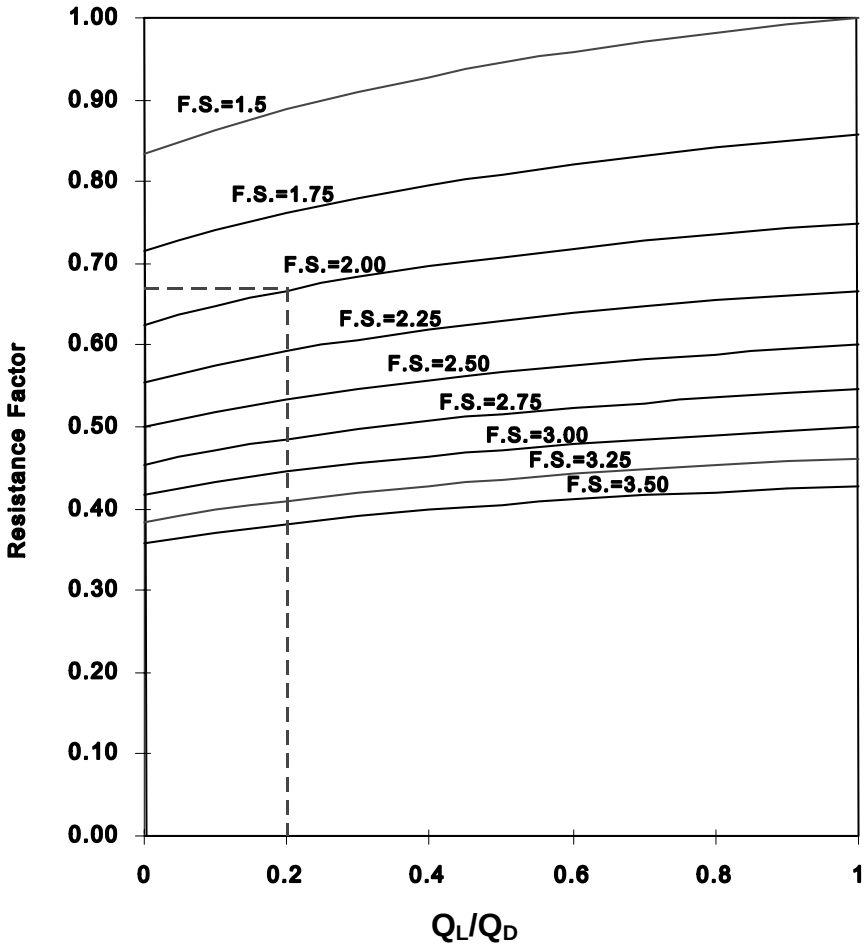

Figure C-3. Resistance factor as a function of Q_L/Q_D for various factors of safety for the AASHTO LRFD Bridge Code.

C.4 LRFD DETAILS

The issue of the verification of the safety safety of an LRFD-based design is now discussed. The question that will be considered is, "Does the structural element (pile) have adequate axial strength." To answer this question it is best to consider some details. First, consider the determination of the loads that would be used in bridge design. There are five strength limit states, two extreme event limit states, four serviceability limit states and one fatigue limit state given in Table 3.4.1-1 of the AASHTO LRFD Bridge Code (AASHTO 2004 with 2006 Interims). Here only the strength limit states will be considered for illustration purposes. The factored loads for those five cases are as shown in Table C-1. These load combinations have been somewhat simplified for this discussion.

Table C-1

Strength Limit State	Load Combination
I	$\gamma_p D + 1.75\ L + 1.0\ WA + 1.0\ FR$
II	$\gamma_p D + 1.35\ L + 1.0\ WA + 1.0\ FR$
III	$\gamma_p D + 1.0\ WA + 1.4\ WS + 1.0\ FR$
IV	$\gamma_p\ D + 1.0\ WA + 1.0\ FR$ (but for dead load due to structural components only 1.5 D)
V	$\gamma_p D + 1.35\ L + 1.0\ WA + 0.4\ WS + 1.0\ WL + 1.0\ FR$

Notations:

γ_p – load factor for the various types of dead load. For the superstructure dead load γ_p is 1.25, but other values are specified for other types of dead load.

D – dead load.

L – live load

WA – water and stream load

FR – friction load

WS – wind load on the structure

WL – wind load on the live load

Since the load combinations have been somewhat simplified, the reader is encouraged to review Section 3 of the AASHTO LRFD Bridge Design Specifications (AASHTO 2004 with 2006 Interims). Probably geotechnical engineers that are responsible for foundation design will not be required to determine the factored loads, but a general understanding of those loads provides a better understanding of the entire design process. While the above loads and load combinations have differences from that of previous AASHTO Specifications the general structure of the loads is unchanged. Since there may be several different sets of loads (for instance, maximum and minimum) for each of the strength limit states the final set of factored loads will usually be larger than the five given above and sometimes much larger, particularly if extreme event conditions must be considered.

At this stage of the foundation design process, the factored loads will have been determined by the structural designer and with the exception of the downdrag case it is unlikely that these loads or load combinations will change in future AASHTO Codes. Therefore, the left side of Equation C-2 has now been determined.

The right side of Equation C-2 is of greater concern for the geotechnical foundation designer who must determine values of ϕ_k, the **resistance factor**, and R_{nk}, the **nominal strength**. Values for φ_k must be defined by code. It has often been implied that resistance factors may be determined in the design process using a probability analysis. This is not realistic and

certainly not necessary for deep foundation design. At the present, the resistance factors are prescribed in AASHTO (2004 with 2006 Interims) and are not always unique. The reader is referred to Sections 10 and 11 of AASHTO 2006 Interims for selection of appropriate resistance factors and methods to determine the nominal strength, R_{nk}.

C.5 THE DESIGN PROCESS

The design process for LRFD will now be reviewed. The flow chart for LRFD-based design is given in Figure C-4. In Blocks 1 to 5, project requirements must be determined and the subsurface must be explored and evaluated to obtain the necessary geotechnical design quantities. In Blocks 6 and 7, an appropriate foundation type is selected. For illustration purposes herein, a driven pile type is selected. Then in Block 8 the factored loads are determined. After determining whether the pile is driven in soil or to rock (see Blocks 9 or 11), the designer selects the resistance factor in Blocks 10 or 12 based on the capacity verification procedure and the quality control method that has been selected. In the ASD method, a factor of safety is selected based on the information in Table 4.5.6.2.1A of AASHTO (2002). The resistance factor for LRFD is given in the Tables 10.5.5.2.3-1, 10.5.5.2.3-2 of AASHTO (2004 with 2006 Interims). Selection of the proper value for resistance factor from the LRFD Specification will not be discussed here.

The rest of the flow chart is similar to the one for ASD. It can be seen that there is little difference in the design process for LRFD composed to ASD.

C.6 A SIMPLE EXAMPLE

A very simple numerical design example will be solved to illustrate the differences between ASD and LRFD. Only strength will be considered since those limitations are the only ones that are different for the two methods. The soil is a medium dense sand with an adjusted $N1_{60}$-value of 20 and a friction angle of 33 degrees. The site has some variability and in terms of low, medium and high variability, the site can be characterized as having medium variability. In this trial design, a closed end steel pile having a length of 66 ft (20 m) and a cross section 14 in x 5/16 in (356 mm x 8 mm) has been selected and a geotechnical analysis indicates a nominal axial resistance of 330 kips (1470 kN). The working load on the foundation will be taken as 500 kips (2,225 kN) dead load and 800 kips (3,560 kN) live load including impact. Assume one (1) static load test will be performed.

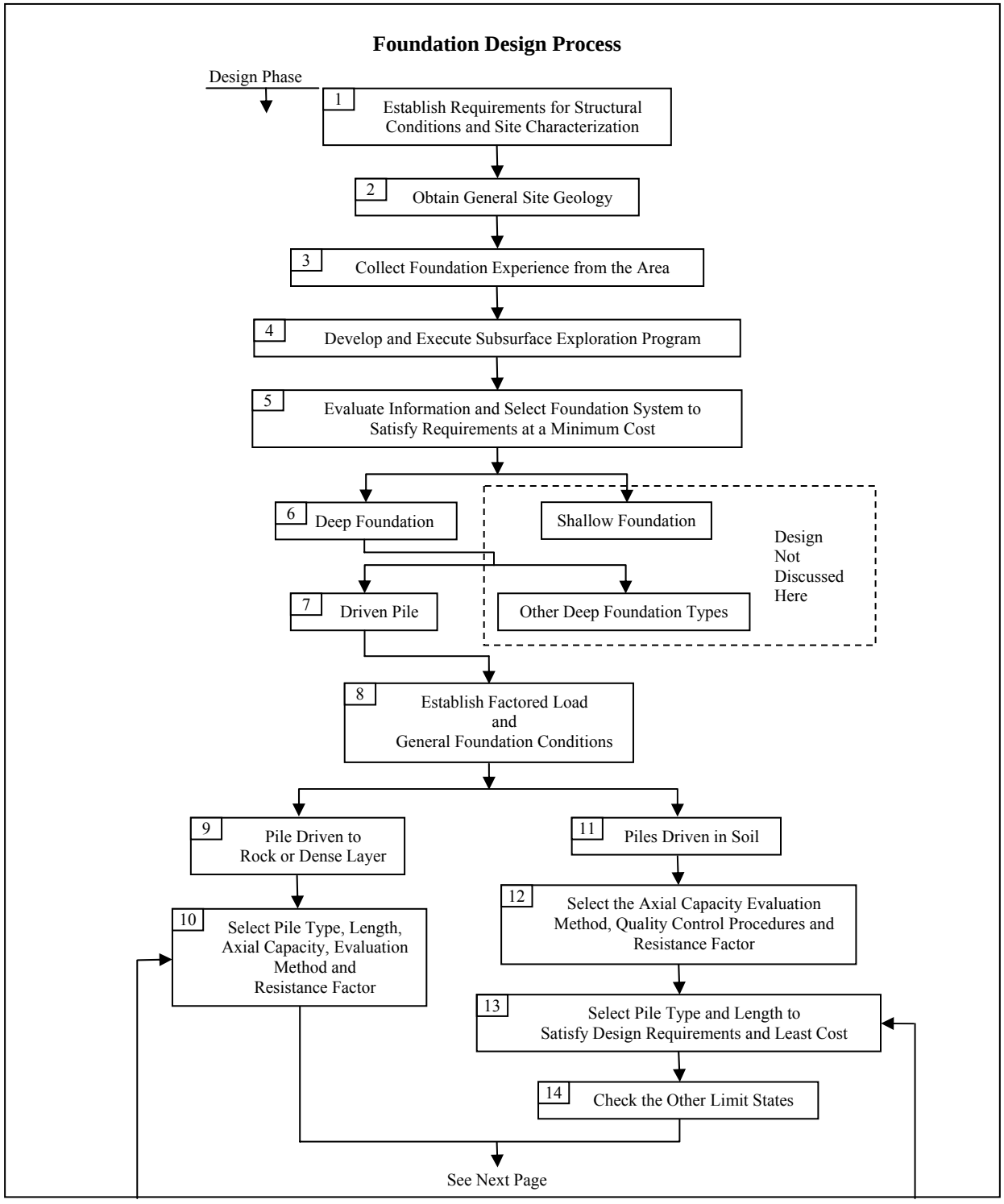

Figure C-4. Driven pile design and construction process by LRFD (FHWA, 2006a).

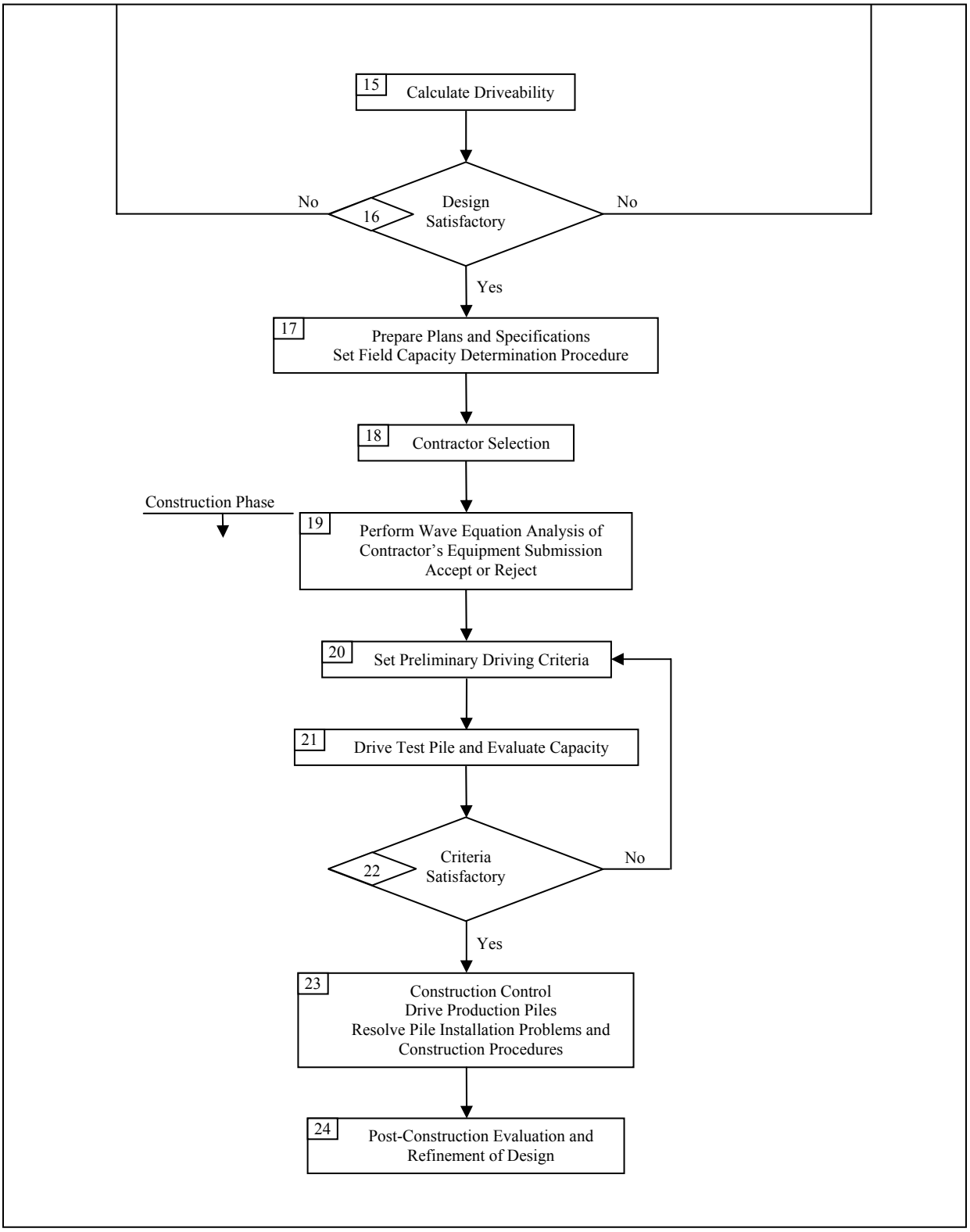

Figure C-4. Driven pile design and construction process by LRFD (FHWA, 2006a) (Continued).

C.6.1 ASD

According to Table 3.22.1A of AASHTO (2002) for the service load Case I, the design load is

500 kips + 800 kips = 1,300 kips (5,785 kN)

First, assume that a static load test will be used in addition to a drivability analysis by wave equation with subsurface exploration and static analysis to verify the driving criteria. Therefore, the factor of safety specified in Table 4.5.6.2A of AASHTO (2002) is 2.0 and the required nominal axial resistance is 2,600 kips (11,570 kN). Now if the pile nominal resistance is 330 kips (1,470 kN), then the total required number of piles will be

2,600 kips/330 kips = 7.8 piles, say 8 piles

If dynamic measurement and analysis is used the specified factor of safety is 2.25 per AASHTO (2002), giving a required ultimate axial resistance of 1,300 kips x 2.25 = 2,925 kips (13,016 kN). In this case the required number of piles will be

2,925 kips/330 kips = 8.9 piles, say 9 piles

C.6.2 LRFD

First, determine the factored load. In this very simple example, only Strength I of Table 3.4.1-1 of the AASHTO LRFD Bridge Code (AASHTO 2004 with 2006 Interims) will be considered.

1.25 x 500 + 1.75 x 800 = 2,025 kips (9,007 kN)

As per Table 10.5.5.2.3-2 of AASHTO (2004 with 2006 Interims), the specified resistance factor to be used for the case of one (1) on a site with medium variability is 0.70. Based on this resistance factor, the required nominal resistance is as follows:

2,025 kips / 0.70 = 2,893 kips (12,868 kN)

The required number of piles is

2,892 kips / 330 kips = 8.8 piles, say 9.0 piles

C.6.3 Comments

This very simple example illustrates the difference between ASD and LRFD. Of course, only one failure mode limit state was considered. In a real design problem, several load combinations would be included, the loads would include overturning loads and all aspects of the problem would be much more complex. This simple example illustrates the difference between ASD and LRFD clearly and simply. No conclusions should be made regarding the fact that the LRFD design for this simple example was virtually the same as the ASD design. For other load combination, the design may be different. (In the latter case, Strength IV load combination would become critical and fewer piles would be required.)

[THIS PAGE INTENTIONALLY BLANK]

APPENDIX D

USE OF THE COMPUTER PROGRAM ReSSA

[THIS PAGE INTENTIONALLY BLANK]

APPENDIX D
USE OF THE COMPUTER PROGRAM ReSSA

D.1 INTRODUCTION

The computer program Reinforced Slope Stability Analysis (ReSSA), version 2.0 was developed by ADAMA Engineering, Inc. (ADAMA), Newark, Delaware under contract to FHWA. The following description of the program is provided by ADAMA:

> *"ReSSA(2.0) is an interactive program for analyzing rotational and translational stability of slopes. It was developed to allow for convenient integration of horizontally placed reinforcement, thus also enabling the analysis of mechanically stabilized earth slopes. The sole purpose of the ReSSA software is to assist experienced engineers in the analysis of reinforced and unreinforced earth slopes."*

ReSSA(1.0), the first released version, is a user-friendly, Windows-based program that is provided free-of-charge (but in a limited number of licenses) to each state DOT for use on reinforced and slope stability analysis applications. ReSSA(2.0) has additional features that were added in response to users comments. For rotational (i.e., circular) failure modes, the program addresses moment equilibrium utilizing the Modified Bishop method of analysis. For translational (i.e., sliding) failure modes, the program addresses moment and force equilibrium utilizing the Spencer's method of analysis. For reinforced soil slopes (RSS) in fill, the program incorporates the AASHTO/FHWA method of analysis (FHWA, 2001b). In these regards, it is recognized that ReSSA is not a comprehensive slope stability software package because it does not deal with general-shape slip surface. This limitation notwithstanding, ReSSA is an extremely powerful design and analysis software package that can address complex subsurface stratigraphic conditions and slope configurations. Given the potential application of ReSSA to DOT projects and to provide an introduction to the course participants regarding the utility of computer programs that have been developed to address slope stability problems, a summary of the use and capabilities of ReSSA is provided herein as part of the Soils and Foundations course.

This appendix was prepared to provide a narrative summary of some of the specific features of ReSSA, as most of these capabilities are also included in other readily available commercial computer programs that are used for assessing slope stability. It is recognized that this document is provided in lieu of a hands-on demonstration of the program capabilities as part of the course. The instructor is available to demonstrate ReSSA if there is interest among individual participants. It is important to note, however, that this summary

was never intended to serve as or replace the Users Manual and the supporting technical documentation provided with the ReSSA program by ADAMA.

The remainder of this appendix is organized to provide several screen shots from ReSSA and will demonstrate the use of the program to assess the calculated factor of safety of a 30 ft deep cut slope in a uniform deposit of clay. This problem was originally presented in the Reference Manual in Chapter 6 and was explicitly selected because the solution (i.e., the calculated factors of safety) was presented as an example problem in the Reference Manual to demonstrate the use of chart solutions.

D.2 PREPARING FOR INPUT TO THE COMPUTER PROGRAM

Before any slope stability analysis can be performed using a computer, it is essential that the user/designer prepare a hand sketch using an "unexaggerated" x-y scale (i.e., the same scale in the x and y directions). This sketch should show the geometry of slope, the subsurface stratigraphy, and the location of the water table. It will be necessary to assign coordinates to the various points on this sketch so that information regarding the geometry can be input to the computer. Remember that the computer will only solve the problem that the user asks it to solve, so the user needs to be sure that the geometry developed in the hand sketch matches the geometry presented on the computer screen. Once the hand sketch is developed, it is possible to now enter the information into the computer. This initial step of developing a hand sketch is absolutely essential, particularly for complex subsurface conditions. If the subsurface conditions change across the actual project site, it is necessary to develop multiple cross-sections for analysis so that the most critical cross-section can be identified and reported.

D.3 WORKING WITH ReSSA

When ReSSA is executed, an introductory screen is provided, identifying the copyright information. This is followed by a screen that flashes the ReSSA startup screen (Figure D-1). Most important here is the "File" button on the taskbar. From here the user can start a new analysis or retrieve a previous project; this latter capability of being able to retrieve previous problems is one of the biggest advantages of computer programs. For our example, the Example 6-1 in Chapter 6 will be launched from this menu. What follows next is the Main Menu for ReSSA (Figure D-2), where the user will sequentially develop the problem and perform the stability analysis.

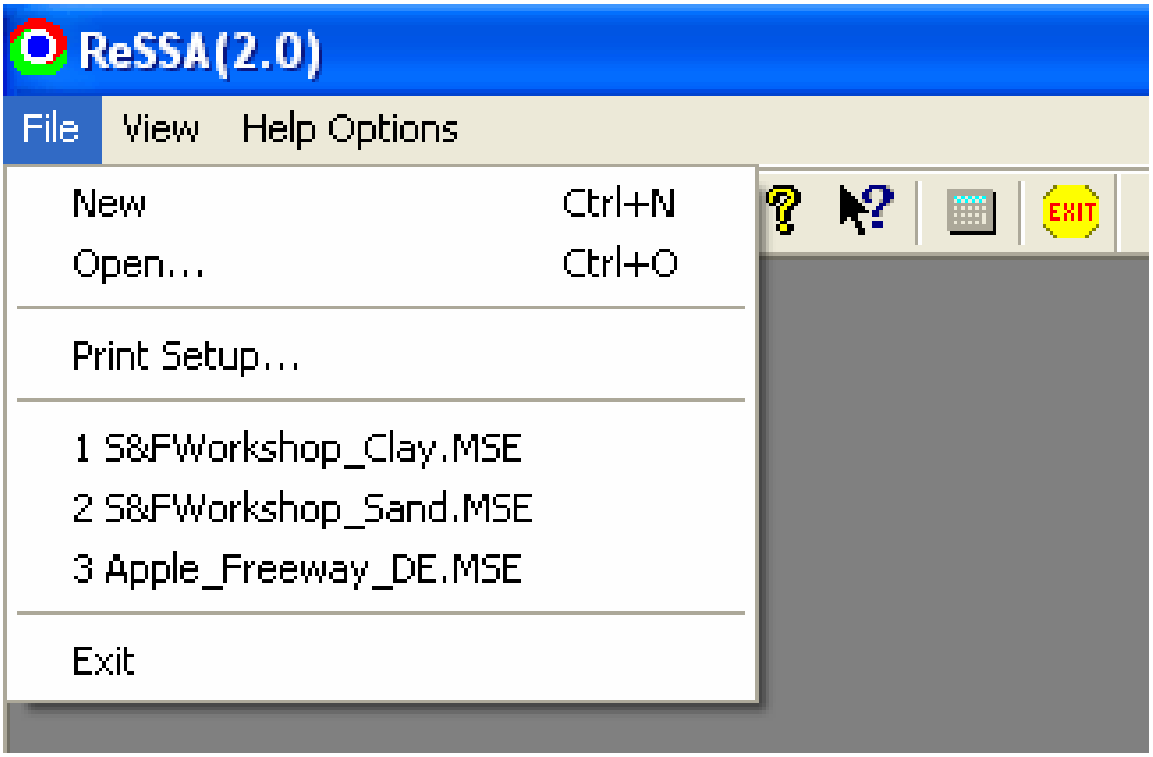

Figure D-1. ReSSA startup screen.

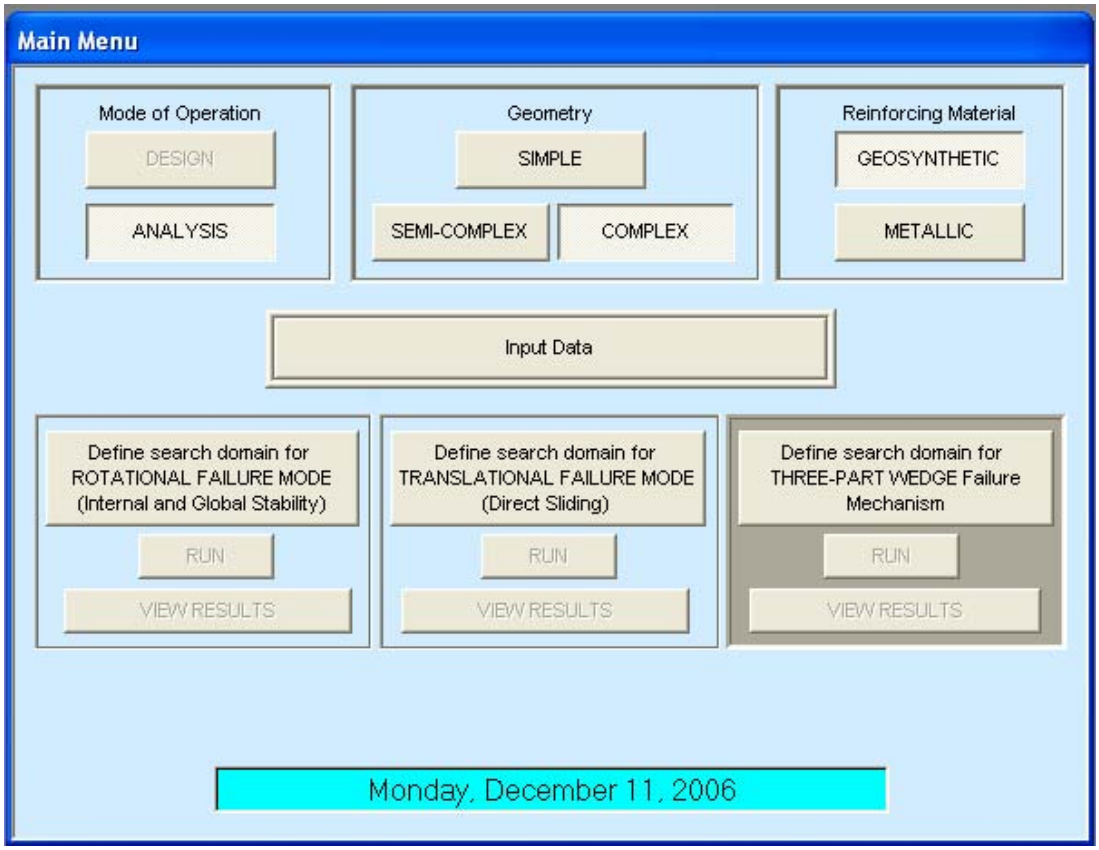

Figure D-2. ReSSA main menu.

In ReSSA, the user has the following options:

- **Mode of Operation**: User selects whether a "design" or "analysis" will be performed. For slope stability, we select "analysis." For MSE slopes, the user can either use the "design" or "analysis" mode. In "design" mode, ReSSA determines the length of the reinforcement based on target factors of safety; this option is limited to simple slopes and should be used only as a first step. The user can switch from "design" to "analysis" and find the actual factors of safety corresponding to the computer generated reinforcement layout or any other layout specified by the user.

- **Geometry**: User can select several different inputs modes in ReSSA. In general, the "simple" and "semi-complex" modes are used when performing parametric analyses to assess relative sensitivity of parameter (i.e., slope angle, strength, etc.) selection. For the vast majority of slope stability analyses, it is recommended (and often required) to select the "complex" method of data entry.

- **Reinforcement**: ReSSA can perform an MSE slope analysis using either geosynthetic or metallic reinforcement. For unreinforced slope stability calculations, no reinforcement is used. At this step, the user selects one of the two reinforcement types and will later have the opportunity to overwrite this selection. This select/overwrite requirement is simply a procedural detail in ReSSA.

The next step is the select the "Input Data" tab (Figure D-3), where the user has the opportunity to set up the slope stability analysis project and essentially convert the handwritten slope geometry to an electronic record. Importantly, if a previous version of the project is selected, it is possible to change select parameters from the previous selection and then proceed with analysis. Data are input using the following screens:

- **Units**: User selects whether the input data are provided in English or SI units. It is important to recognize the specific units that are used and to be consistent throughout the analysis.

- **General Information**: This screen (Figure D-4) allows user to input information about the specific analysis and can help distinguish between various computer runs.

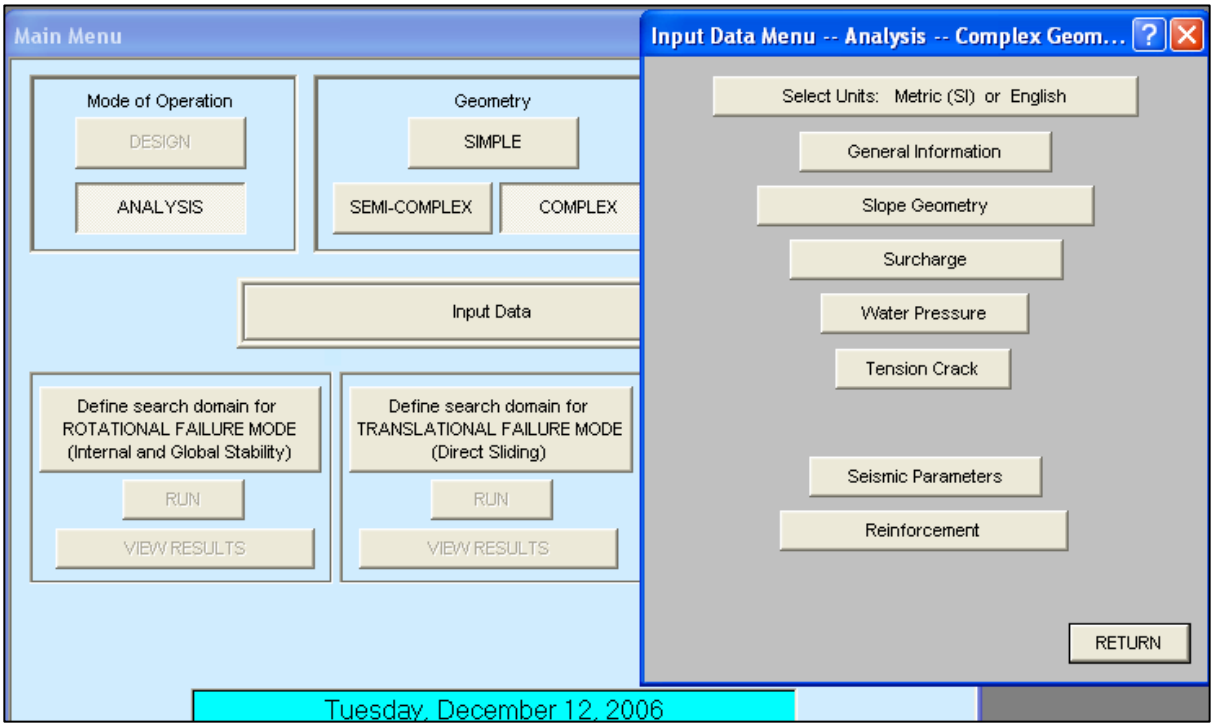

Figure D-3. Data input screen from main menu.

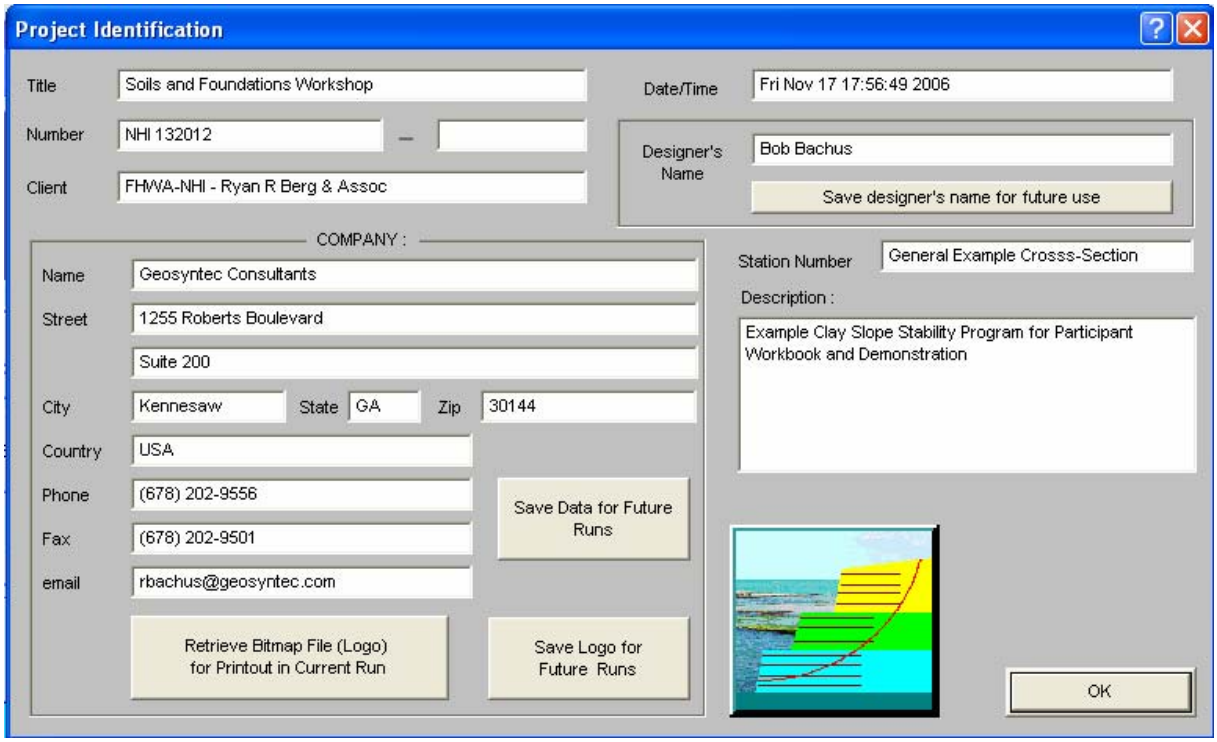

Figure D-4. General information screen.

- **Slope Geometry**: When the user selects the "Slope Geometry" tab, they are given the opportunity select the technique used to input the slope and subsurface geometry (Figure D-5). ReSSA also provides a "tip" to help the user in the data input process. Other computer programs have similar nuances that were incorporated by the developer to facilitate data input. The user next selects the number of input soil layers that will be used and then the "Define Geometry of Layers" tab. For the selected problem, Figure D-6 shows an example of the slope and subsurface profile that was previously input. The following information is presented on this figure:
    - Layer Number: For each layer, commencing at the ground surface, the user defines the geometry of the layer and the properties of the soils beneath the layer. When the geometry of a layer is entered, the user selects the next layer and repeats the geometry/properties data input. Once the geometry for the entire problem is entered, the user can return to these tabs and rapidly assess and modify any of the information.
    - Unit Weight: The total unit weight of the soil within the selected layer.
    - Friction Angle: The angle of internal friction for the soils within the selected layer.
    - Cohesion: The cohesion for the soils within the selected layer.
    - Table of X and Y Coordinates: Using the hand sketch as a guide, the user sequentially enters the coordinates of selected problem. At this stage, the user can observe the slope geometry being constructed.

- **Surcharge**: The user has the opportunity to place point loads or line loads as surcharges anywhere on the top surface. The loads can be vertical or inclined with respect to the vertical.

- **Water Level**: A single water table (or phreatic surface) can be considered in ReSSA. This surface can be horizontal or "sloped", where the attitude of the surface is controlled by a series of line segments defined by their x and y coordinates. On this screen the user also has the opportunity to select whether a total or effective stress analysis will be performed. Guidelines for selection of the analysis type is beyond the scope of the course.

- **Tension Crack**: ReSSA gives the opportunity for the user to select a tension crack at the ground surface. The user can indicate the location and depth of the crack, as well as whether water will be considered to act on the crack. For purposes of analysis, the shear strength of this zone is not considered.

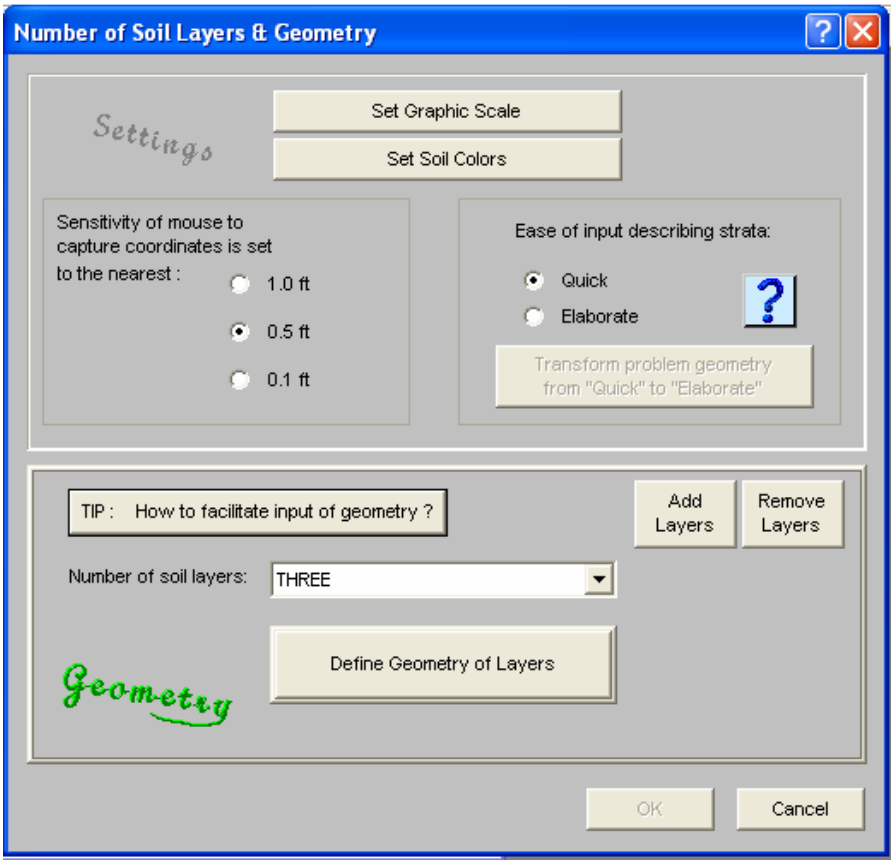

Figure D-5. Screen used to define soil layer geometry.

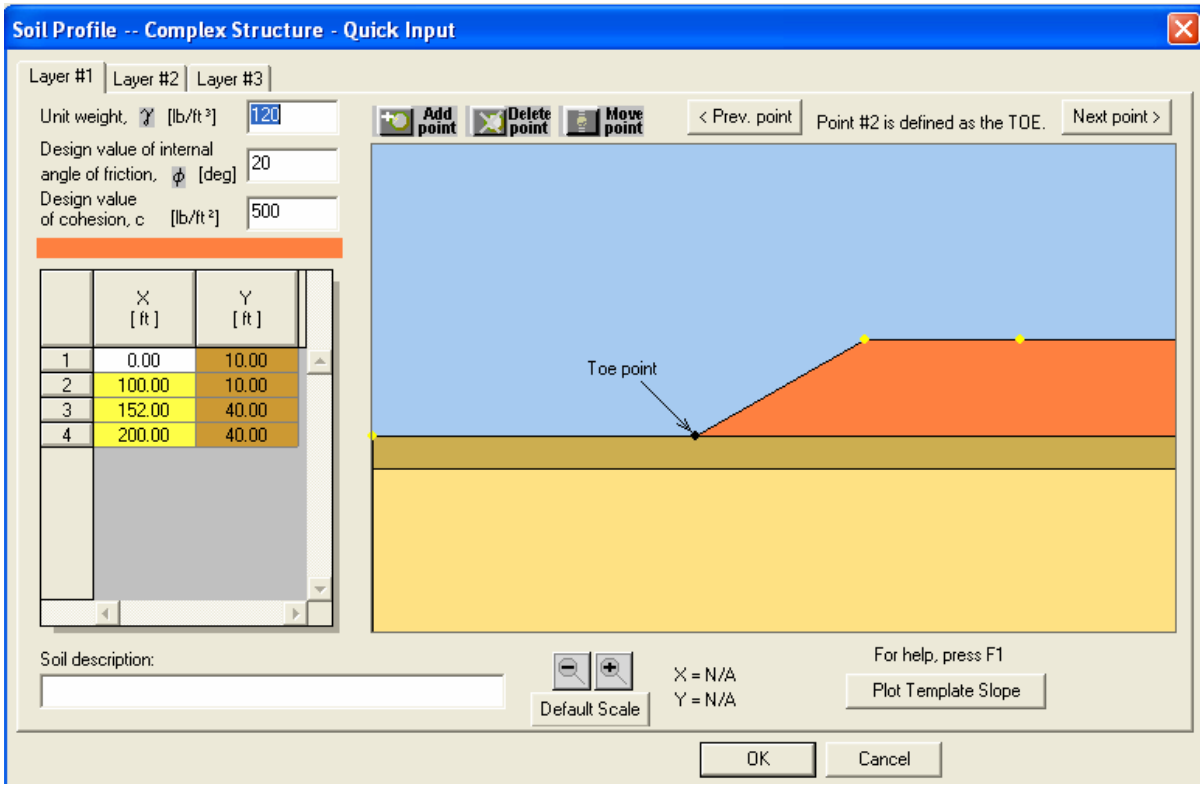

Figure D-6. Screen used to establish soil profile.

- **Seismic Parameters**: If a pseudo-static analysis is considered, the user can select the horizontal ground acceleration coefficient, A_o, as a specific percentage of the gravitational acceleration "g". Procedures and guidelines for selecting an appropriate value of A_o is beyond the scope of this course.

- **Reinforcement**: Finally, the type of reinforcement considered in the analysis is selected. The user will note that the option "No Reinforcement Used" is selected to overwrite the previous selection when unreinforced slopes are considered.

At this point, the problem is ready to solve. It is recommended to double check all of the input screens to assure that the appropriate values and options are selected. Once this has been completed, the user will note that ReSSA offers the following three analysis options:

- **Rotational Failure Mode**: This option is selected when performing a circular or rotational analysis in assessing global slope stability. Additional discussion follows.

- **Translational Failure Mode**: This failure mode is limited to reinforced slopes and will not be used for general slope stability of unreinforced slopes. No additional discussion is presented in this document.

- **Three-Part Wedge Failure Mechanism**: This option is selected to assess the potential for sliding along the base, also referenced as a "block sliding" mode. Additional discussion follows.

Before an analysis can be performed, the user needs to select one of the two options. Regardless of the option selected, this first step of the analysis allows the user to select the controls that will be used to assess either rotational or sliding failure modes. For each of these, the user selects the "locations" where the analyses will be conducted. For the rotational failure mode, ReSSA accomplishes this by selecting a range of "Start" points at the top of the slope, the "Exit" points at the bottom of the slope, and the number of start and exit points within the selected range (Figure D-7). ReSSA makes it very easy for the user to select and modify the selected points by use of either: (i) coordinate selection; or (ii) drag and click using the mouse. For the three-part wedge failure mechanism, the user selects "boxes" in the subsurface where the base of the wedge will pass through (Figure D-8). Like the rotational failure mode, the box location can be selected using specific coordinates or by dragging the corners of the boxes using the mouse. The user can select a fairly wide range of potential surfaces in the initial runs and then "fine tune" the selection after preliminary review of the analysis results.

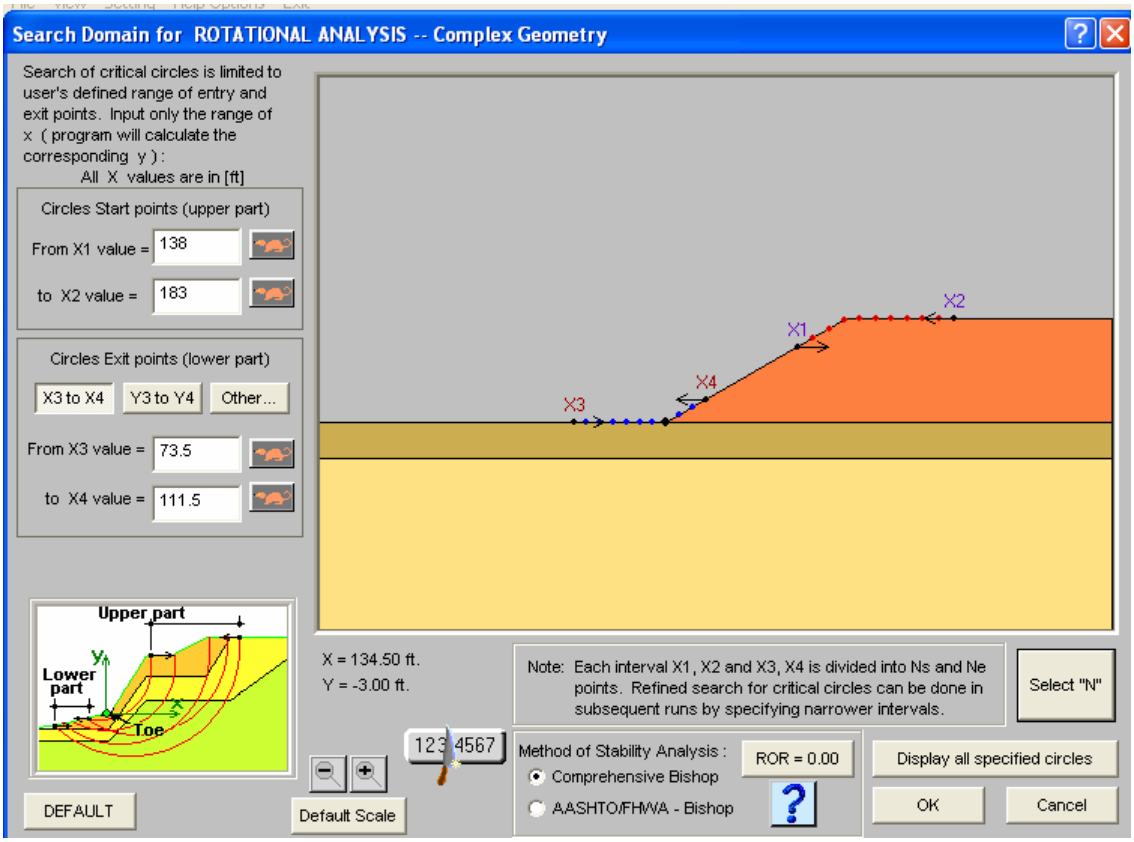

Figure D-7. Selection of Start and Exit analysis points (Rotational failure mode).

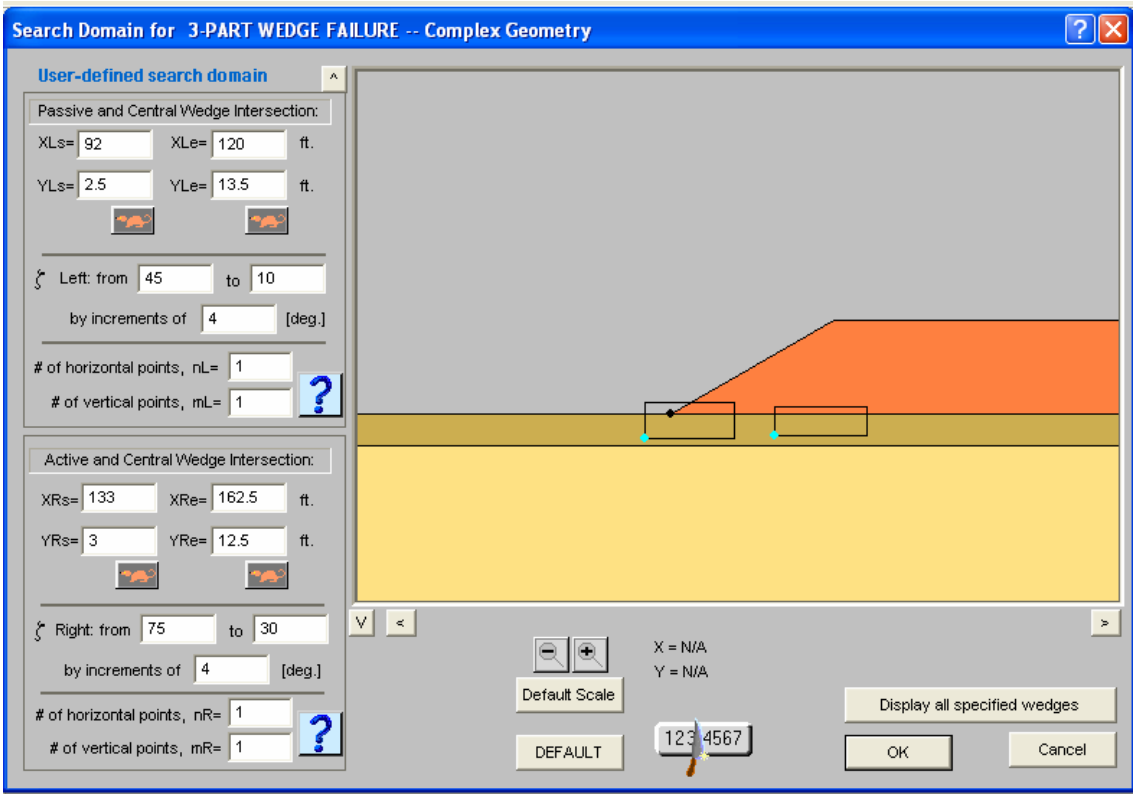

Figure D-8. Selection of Boxes for Three-Part Wedge (Sliding Block analysis).

After all of this preliminary work has been completed, it is now possible to actually conduct the analysis. This is accomplished by simply hitting the "Run" button. In a few seconds, the calculated lowest factor of safety, the most critical failure surface, and the center of the critical circle for the specific user-selected controls are displayed (Figure D-9). At this point, the user can perform additional analyses by narrowing the selection windows, as displayed in Figures D-7 and D-8 to assure that the computer is converging on the correct critical surface. With regards to the rotational failure mode, ReSSA provides the user with several useful options to help assess the calculated results. The following three options presented in Figure D-10 are particularly helpful and can be accessed using the "Results" tab on the toolbar.

- **Display 10 Most Critical Circles**: Although the program returns the analysis results for the single most critical calculation result, there is an option to display the surfaces that exhibit the 10 most critical (i.e., lowest calculated FS) surfaces. This option allows the user to assess whether there may be additional failure surfaces that need to be investigated.

- **FS Distribution**: This option is particularly helpful and is displayed at the top of Figure D-10. It shows the lowest calculated factor of safety at each of the "Start" and "Exit" points selected by the user. As shown on this figure, the selected range of start and exit points should results in a local minimum calculated factor of safety (FS). If the distribution indicates multiple local low values or low values at the edge of one of the start/exit points, it is recommended that the user "fine tune" the analysis to assure that the most critical condition(s) are identified and assessed.

- **Display Safety Map**: This option allows the user to observe all of the surfaces that were analyzed by the computer. Furthermore, using a user selected sensitivity scale bar, the calculation results are essentially "color coded" to indicate the relative sensitivity of the calculated FS. The safety map is a diagnostic tool that can indicate how efficient the reinforcement is utilized considering both its strength and length.

Using other options of the taskbar the user can observe the number of slices used in the analysis and assess the orientation of calculated forces, etc. on each slice. Importantly, a tabulated summary of results can be obtained for review by the user. Finally, a summary report can be presented. It is recommended that once an analysis has been completed, the user print a hard copy of the report for the project files and to assure that the problem solved by the computer is, in fact, the one desired by the user.

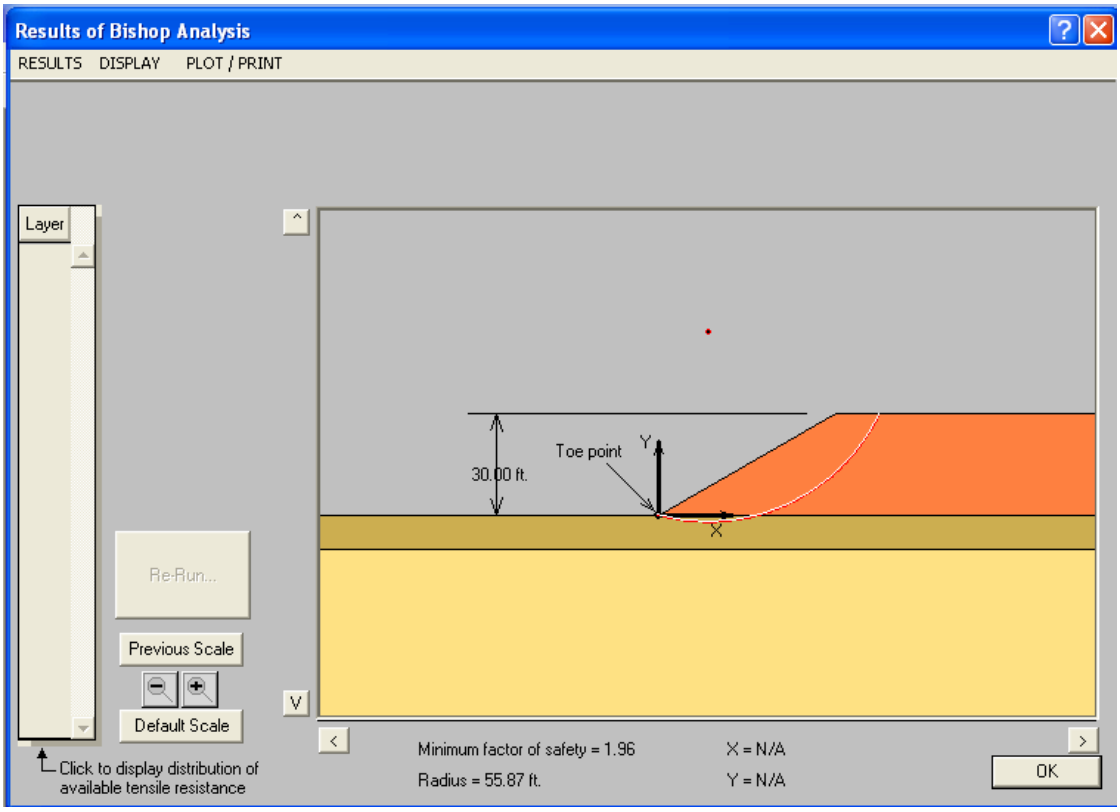

Figure D-9. Critical failure surface (Rotational analysis).

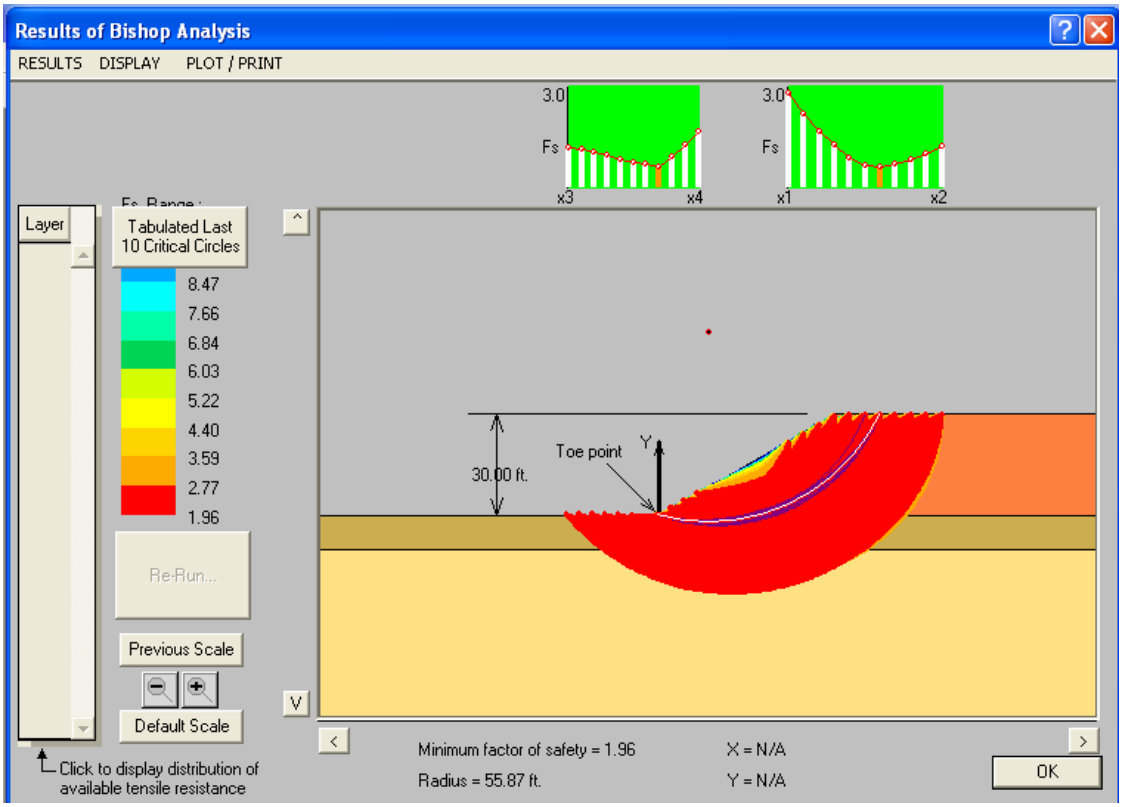

Figure D-10. Factor of safety distribution and Safety Map.

As can be seen in this narrative summary and the selected screen shots, ReSSA is a powerful analysis tool that can greatly aid the geotechnical specialist in assessing slope stability. One of the biggest advantages of ReSSA (and other computer programs) is that the "learning curve" for the program is not very steep, implying that users can be "up and running" fairly quickly. Most commercial programs are user-friendly and provide analysis/display options to help the user perform several "what-if" sensitivity analyses, which can be tremendously beneficial for a given project. In term of advice to the user, the authors recommend that they refer to the example programs provided by the software developers and try to re-create the published solutions. Most commercial slope stability software programs have extremely helpful example programs, Help Screens, and Users Manuals to help the user increase competence and confidence in assessing slope stability.

Finally, it is always recommended that a selected solution be verified or validated using independent resources (i.e., other computer codes, chart solutions, etc.) and that final results be reviewed by an experienced peer and senior reviewer.

APPENDIX E

USE OF THE COMPUTER PROGRAM FoSSA

[THIS PAGE INTENTIONALLY BLANK]

APPENDIX E
USE OF THE COMPUTER PROGRAM FoSSA

E.1 INTRODUCTION

The computer program Foundation Stress and Settlement Analysis (FoSSA), version 2.0 was developed by ADAMA Engineering, Inc. (ADAMA), Newark, Delaware under contract to FHWA. The following description of the program is provided by ADAMA:

> *"FoSSA(2.0) is an interactive program for computing the stress and settlement resulting from an embankment loading. It can consider the effects of staged construction and PVD's."*

FoSSA(1.0), the first released version, is a user-friendly, Windows-based program that is provided free-of-charge (but in a limited number of licenses) to each state DOT for their use to assess stress distribution and to calculate settlements beneath embankments. FoSSA(2.0) has additional features that were added in response to users comments. As indicated in the above description, FoSSA can also address partial consolidation under staged loading conditions and the beneficial effects of prefabricated vertical drains (PVDs). There is also a provision in FoSSA to address the stress distribution and settlement beneath multiple footings. As FoSSA is used in the Soils and Foundations course primarily to assess and understand the stress distribution beneath embankments, this narrative focuses on this component of the program. The other components (i.e., staged loading, PVDs, multiple footings) are considered beyond the scope of the course and will not be addressed. An excellent introduction regarding the program capabilities related to these other topics is provided on the opening screen taskbar titled 'Help Topics" (Figure E-1).

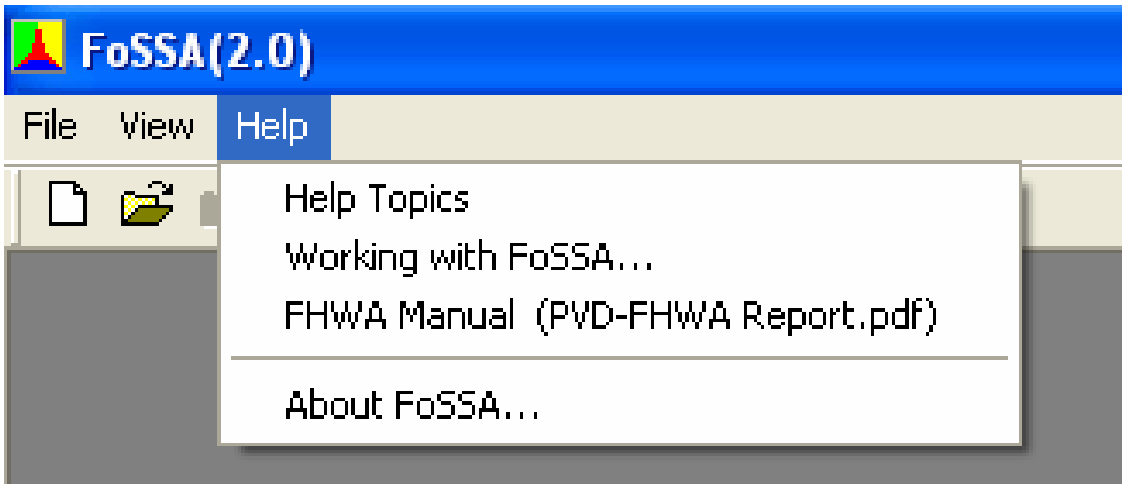

Figure E-1. Opening screen to learn capabilities of the program (Help Topics).

With regards to embankment stress distribution and settlement, FoSSA represents an advancement of the DOS-based program titled EMBANK (version 2.00), a program developed for FHWA by Prototype Engineering, Inc. in 1991. FoSSA can also be used to confirm the validity of the chart solutions regarding stress distribution beneath embankments attributed to the New York State DOT as presented in Figure 7-6 in the Reference Manual.

This appendix was prepared to provide a narrative summary of some of the specific features of FoSSA. It is recognized that this document is provided in lieu of a hands-on demonstration of the program capabilities as part of the course. The instructor can demonstrate FoSSA if there is interest among individual participants. It is important to note, however, that this summary was never intended to serve as or replace the Users Manual and the supporting technical documentation provided with the FoSSA program by ADAMA. The remainder of this appendix is organized to provide several screen shots from FoSSA and will demonstrate the use of the program for the case of an embankment on clay deposit.

E.2 PREPARING FOR INPUT TO THE COMPUTER PROGRAM

Before the analysis can be performed using a computer, it is essential that the user/designer prepare a hand sketch using an "unexaggerated" x-y scale (i.e., the same scale in the x and y directions). This sketch should show the geometry of embankment, geometry of the loads, the subsurface stratigraphy, and the location of the water table. It will be necessary to assign coordinates to the various points on this sketch so that information regarding the geometry can be input to the computer. Remember that the computer will only solve the problem that the user asks it to solve, so the user needs to be sure that the geometry developed in the hand sketch matches the geometry presented on the computer screen. Once the hand sketch is developed, it is possible to now enter the information into the computer. This initial step of developing a hand sketch is absolutely essential, particularly for complex embankment geometries and subsurface conditions. If the subsurface conditions change across the actual project site, it is necessary to develop multiple cross-sections for analysis so that the most critical cross-section can be identified and reported.

E.3 WORKING WITH FoSSA

The opening screens for FoSSA are similar to the opening screens for the program ReSSA presented previously in Appendix D. Under the "File" tab on the initial screen, the user opens an existing file or selects "New." At this step, the user has the option to: (i) re-run the program using an existing file; (ii) modify the input of an existing file and re-run the program; or (iii) establish a new program. For whichever option is selected, the next screen (Figure E-2) allows the user to select: (i) 2D geometry represented by a long rectangular

embankment of uniform cross section (i.e., plane strain); (ii) 3D geometry for representing relatively square embankment or footing loadings; or (iii) multiple foundations to simulate the interaction of foundation loading. Only the 2D case is discussed for the course. When the user selects "2D" and "Input Data," Figure E-3 is presented. The user can "Select Units" and provide "General Information" in a manner similar to that used previously for ReSSA.

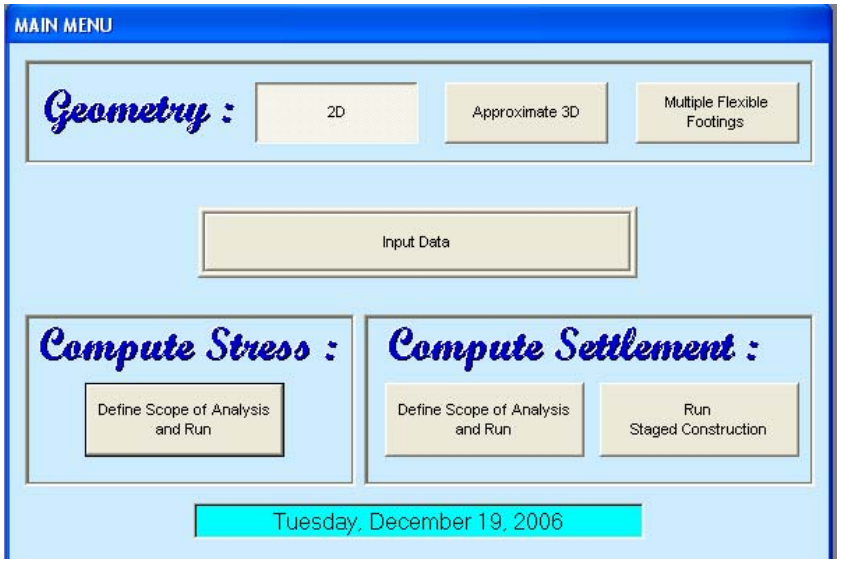

Figure E-2. Launch screen for computing stress and settlement.

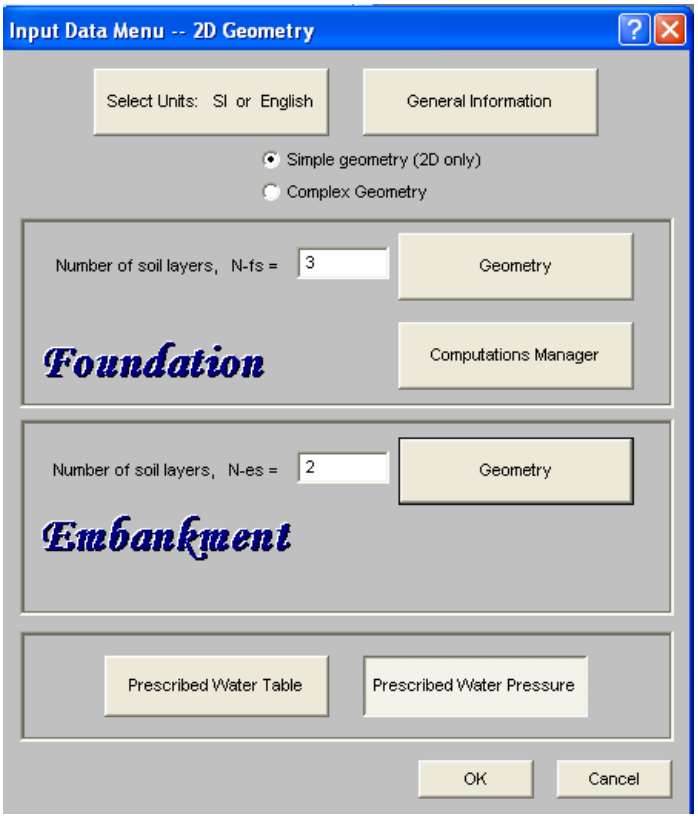

Figure E-3. Input Data Menu (2D Geometry).

After the initial general information is provided, the problem geometry is ready to be input to the computer. As mentioned in Section E.2 earlier, it is imperative that the user first sketch the analysis cross-section by hand and assign coordinates to all of the relevant foundation and embankments layers. For this example problem, Figure E-3 indicates that the user can select an option to consider a "Simple" (i.e., horizontal subsurface stratigraphy that will used herein) or a "Complex" 3D geometry (i.e., plane strain geometry assuming soil layers of non-uniform thickness in the cross-section. For the purpose of this demonstration, select "Simple Geometry" which will then give the opportunity to develop the profile by selecting the "Foundation" and "Embankment" tabs. An example of a "Simple" stratigraphy is presented in Figure E-4, while an example of a "Complex" stratigraphy is provided in Figure E-5. Note that for the Simple stratigraphy, only the vertical elevation is required, while for the Complex model data for the subsurface are entered as lines exhibiting x-y coordinates similar to the procedure used in ReSSA (Appendix D).

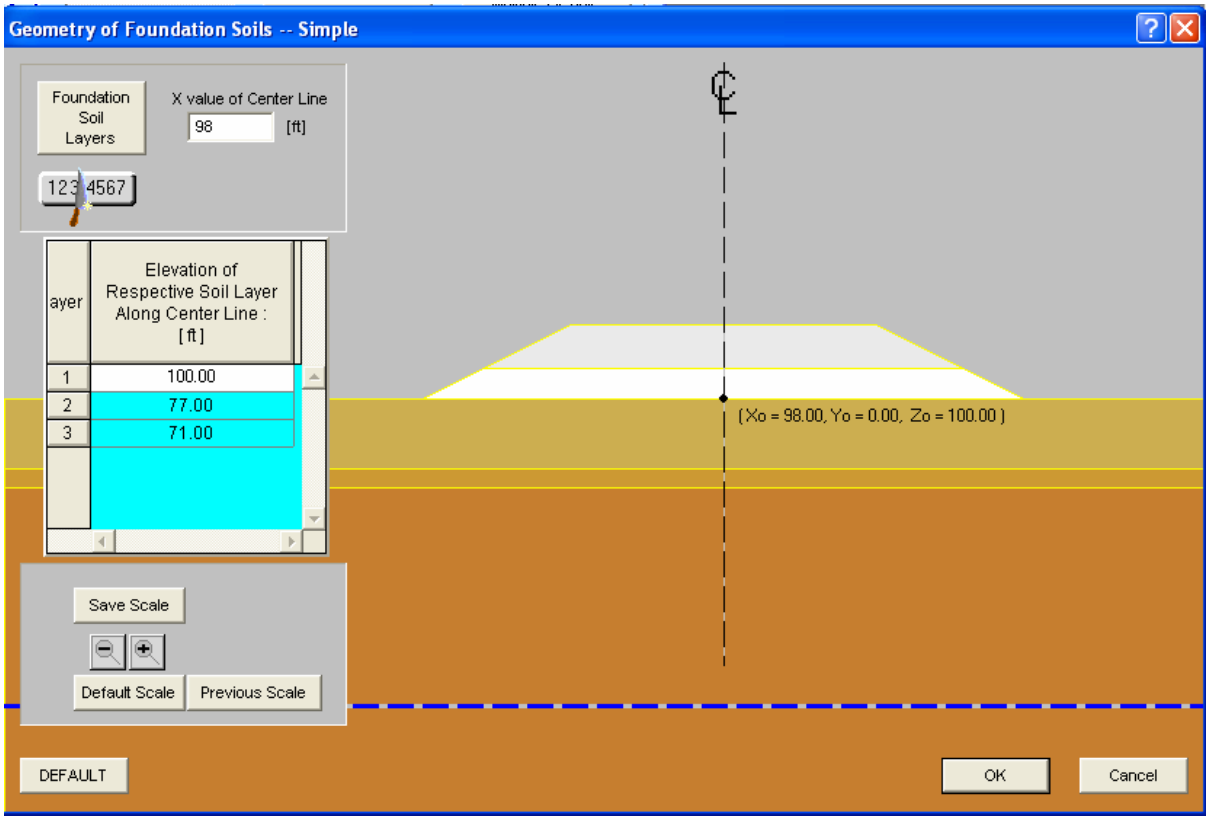

Figure E-4. Example problem with "Simple" horizontal geometry.

From Figure E-4 the user provides information regarding the geometry of the Foundation soils and the Embankment soils by accessing the relevant "Geometry" tabs. For the "Foundation" layer, there is a tab designated "Computations Manager" where input regarding the analysis are provided (Figure E-6). At this tab, the user can identify the following analysis conditions: (i) primary consolidation; (ii) effects of PVDs; (iii) calculation of increased shear strength due to consolidation; (iv) secondary consolidation; and (v) elastic or immediate settlement.

By accessing the "Modify Input" button on this screen, the user is provided the opportunity to input the consolidation (and time rate of consolidation) properties of the foundation soils (Figure E-7). With regards to the "Embankment" layer, the "Geometry" tab allows the user to provide information regarding the geometry and properties of the embankment (Figure E-8). In FoSSA, it is assumed that the embankment provides the loading for the foundation soils. Internal settlement of the embankment is explicitly not considered. From the "Input Data" button shown in Figure E-2, the user can also locate the water table using x and y coordinates (Figure E-9).

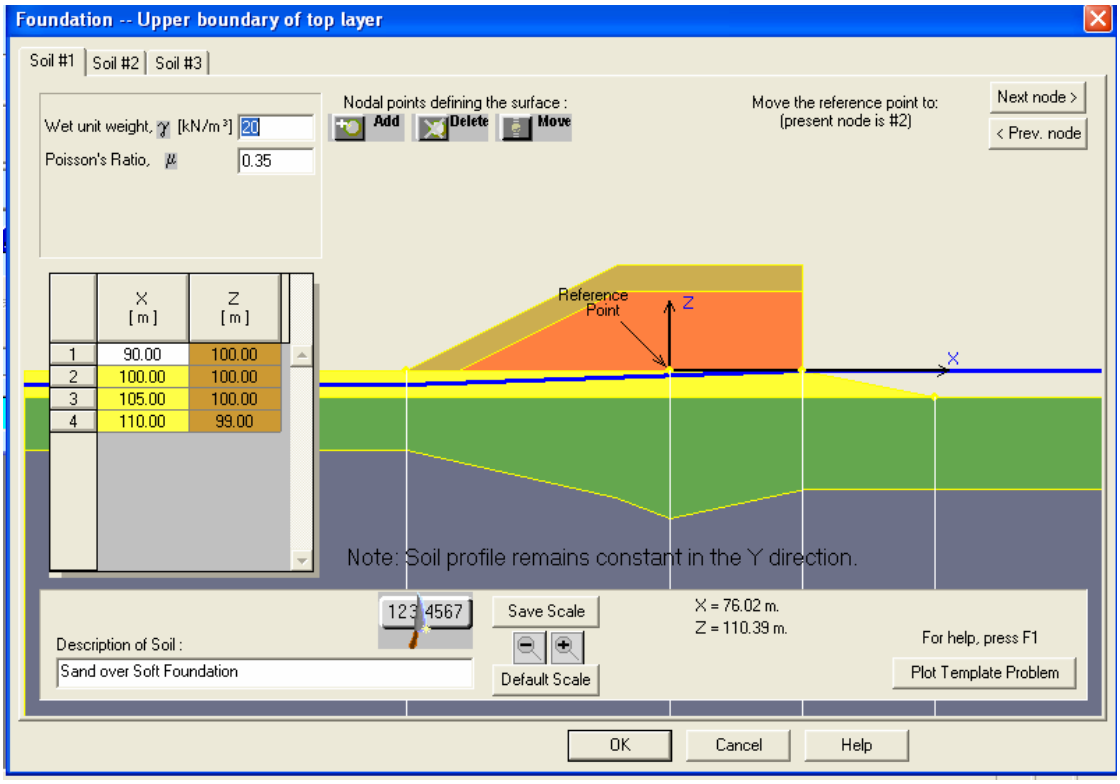

Figure E-5. Example of 2D "Complex" subsurface stratigraphy.

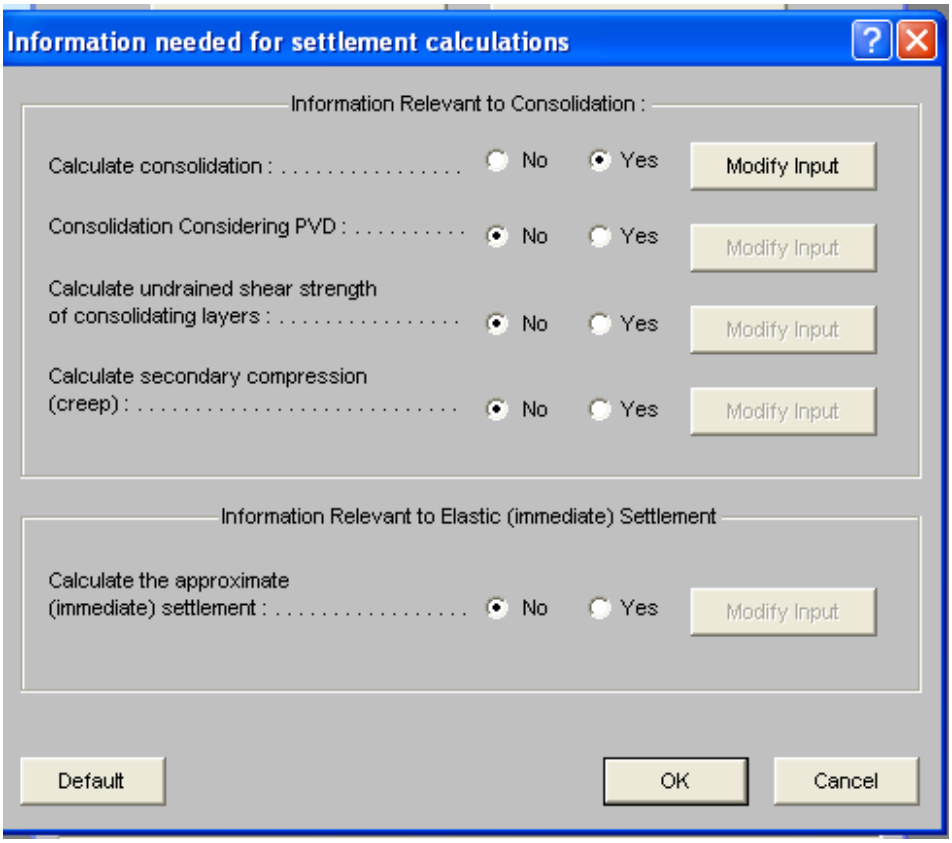

Figure E-6. Computation Manager Tab for defining the analysis case.

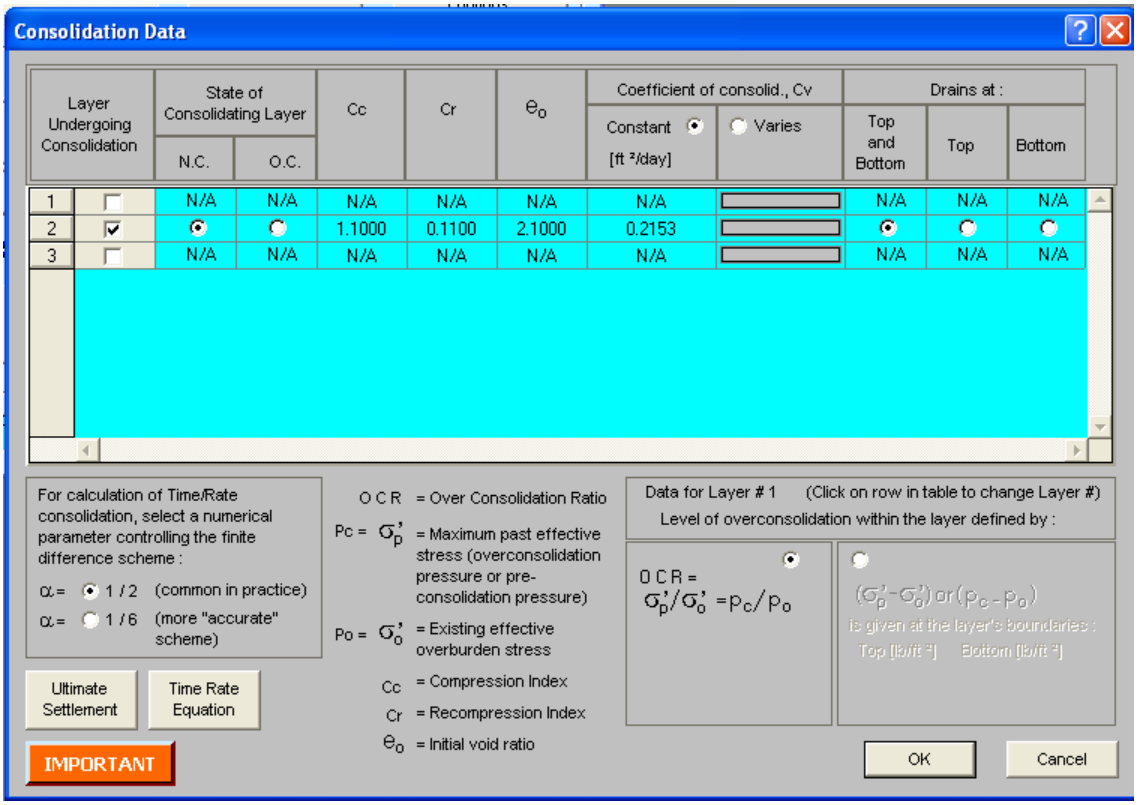

Figure E-7. Screen to provide foundation soil properties.

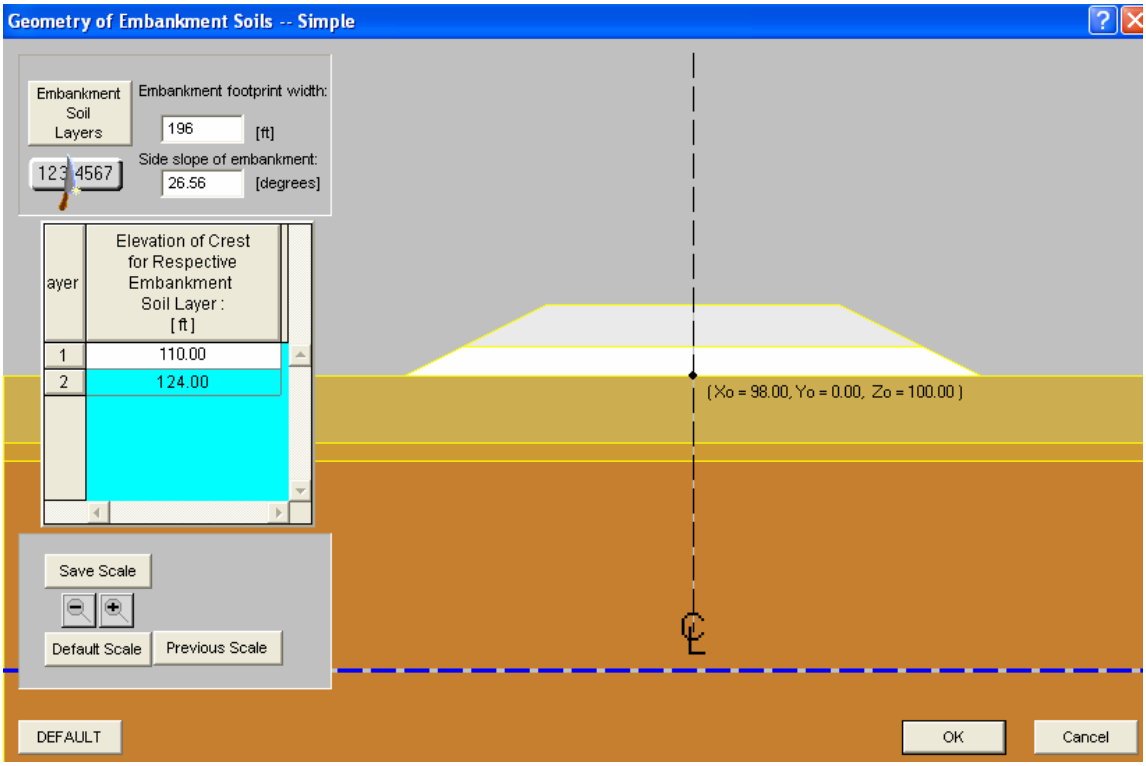

Figure E-8. Screen for embankment properties and geometry.

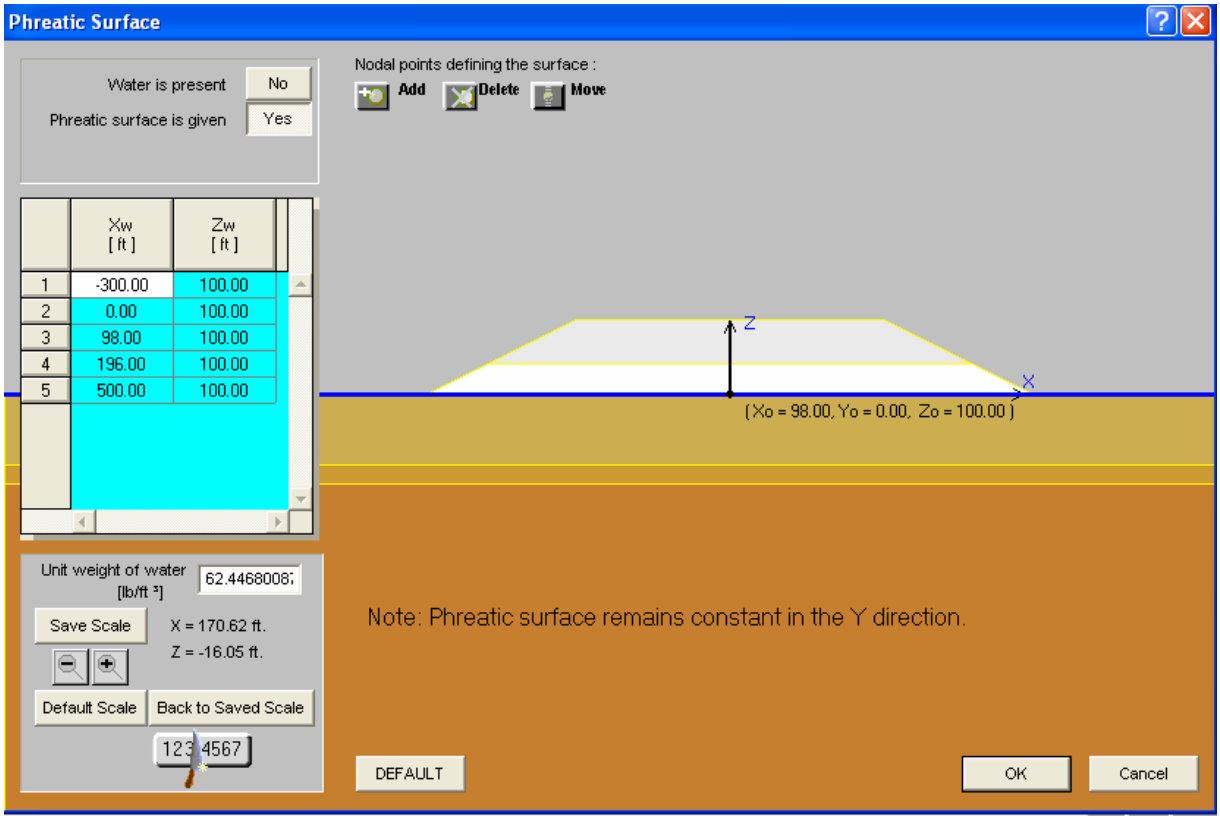

Figure E-9. Input of water table.

At this point, the program goes back to the screen (Figure E-2) and is ready to "Compute Stress" or "Compute Settlement" that would be induced in the foundation soils by the overlying embankment. Under each computation section is the launch tab titled "Define Scope and Analysis of Run." For the "Compute Stress" analysis, the user is directed to the taskbar, where there are several options to define the analysis limits and the results display format (Figure E-10). Of major importance are the "Define" task and the "Define Domain" option under this task (Figure E-11). At this screen, the user can select whether the analysis results (and display) will be presented along vertical or horizontal profiles, at a single point, or at selected grid points. The user selects the number of analysis and display points. Example outputs are presented in: (i) Figure E-12 for the vertical incremental stress distribution at 50 different depths beneath the centerline of the embankment to a depth of 400 ft below the embankment; and (ii) Figure E-13 for the contour of vertical incremental stresses using an analysis grid. Figure E-14 shows the analysis grid used for the contours presented in Figure E-13. As shown in the lower right hand corner of Figures E-10 through E-14, the user has the option to display the incremental vertical, horizontal and/or shear stresses on the display. Finally, by selecting the "Results" tab on the Taskbar after a specific analysis is complete, a tabulated summary of results is produced for export to Excel. This tabulated summary can include the vertical overburden stress or all of the incremental stress calculation results not just the displayed results (Figure E-15).

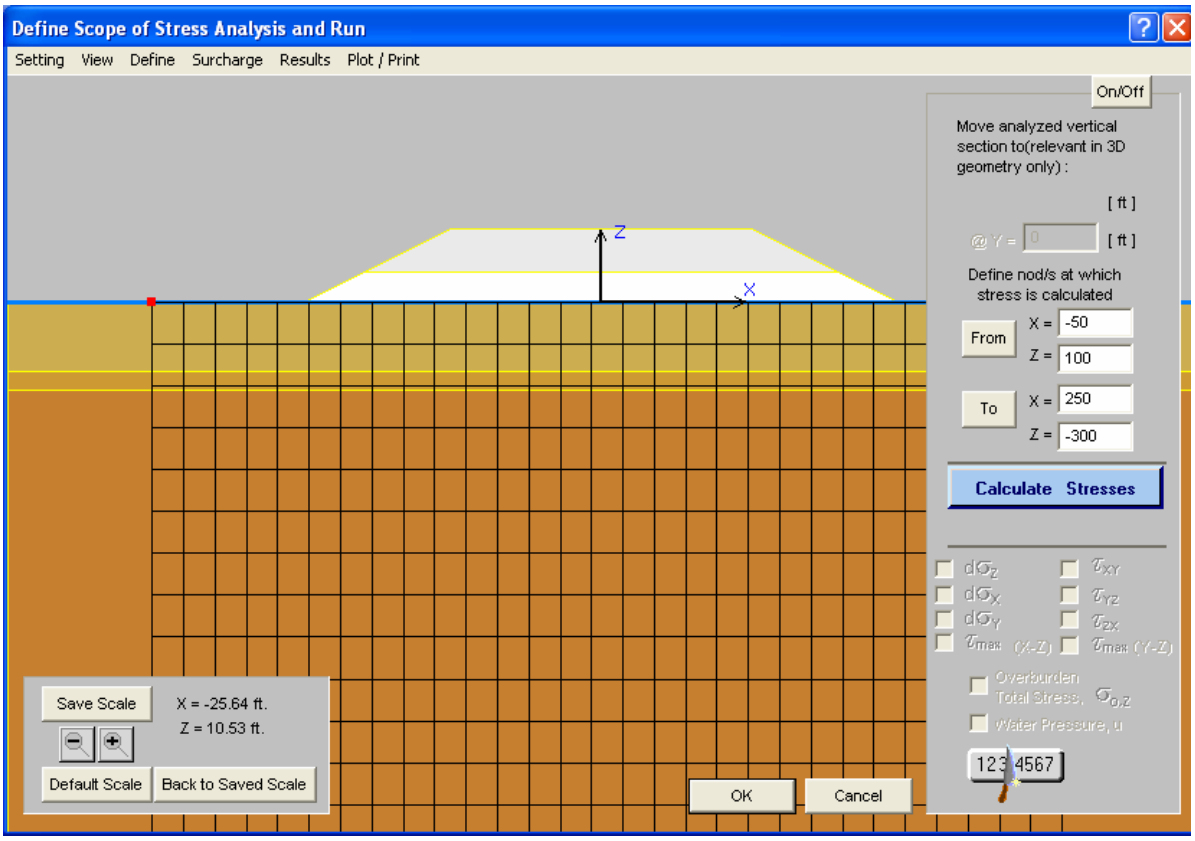

Figure E-10. Defining scope of stress analysis

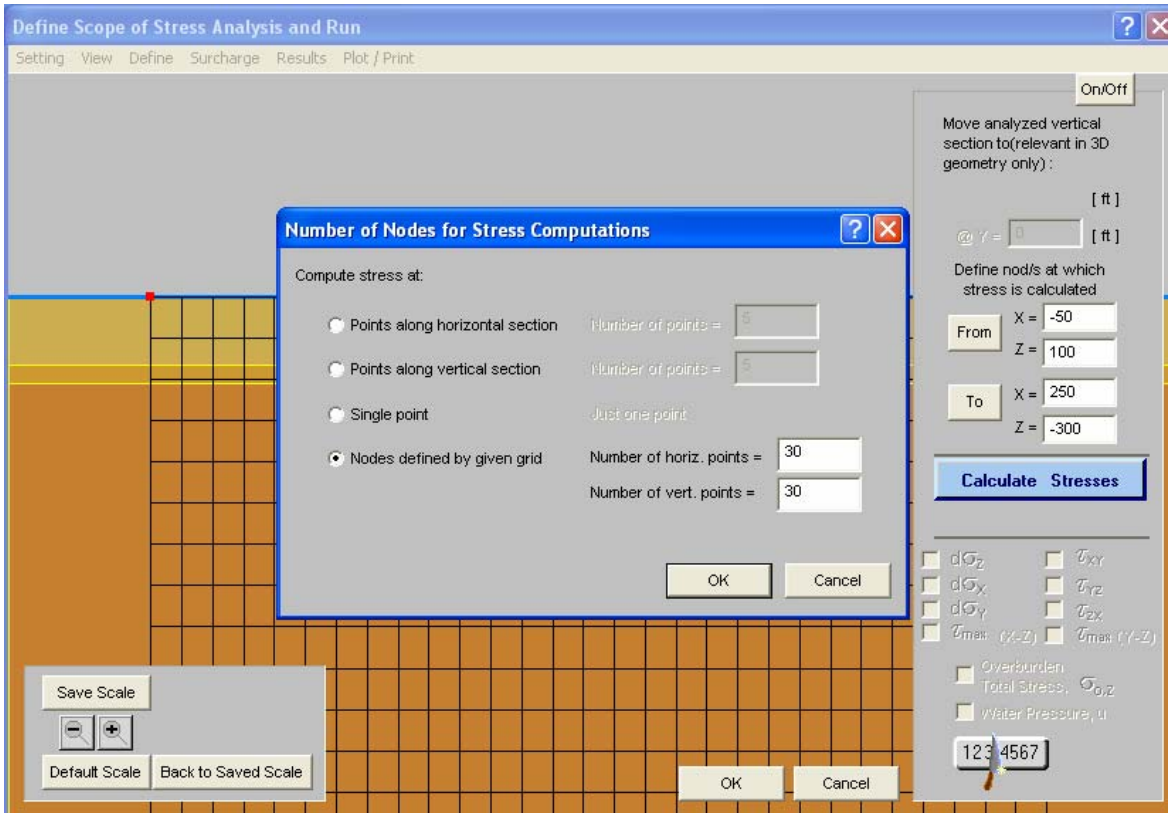

Figure E-11. Defining scope of stress analysis using Define Domain on Taskbar.

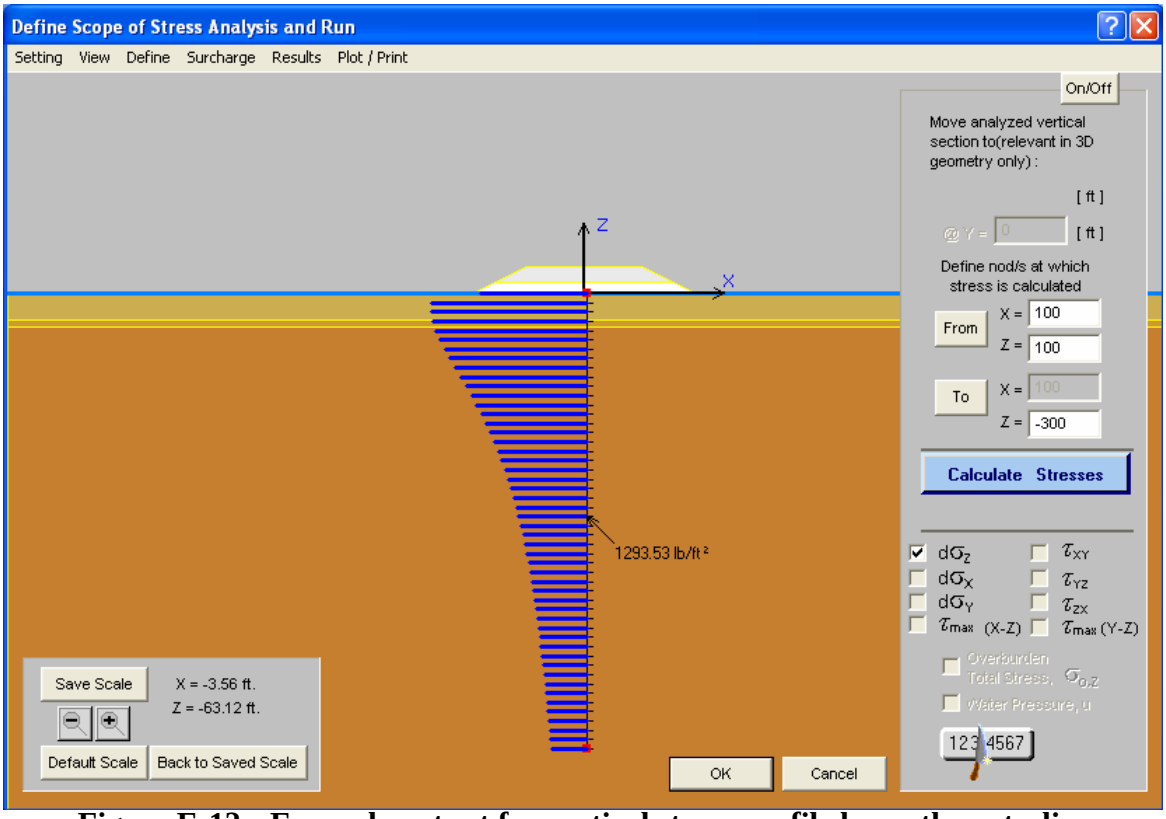

Figure E-12. Example output for vertical stress profile beneath centerline.

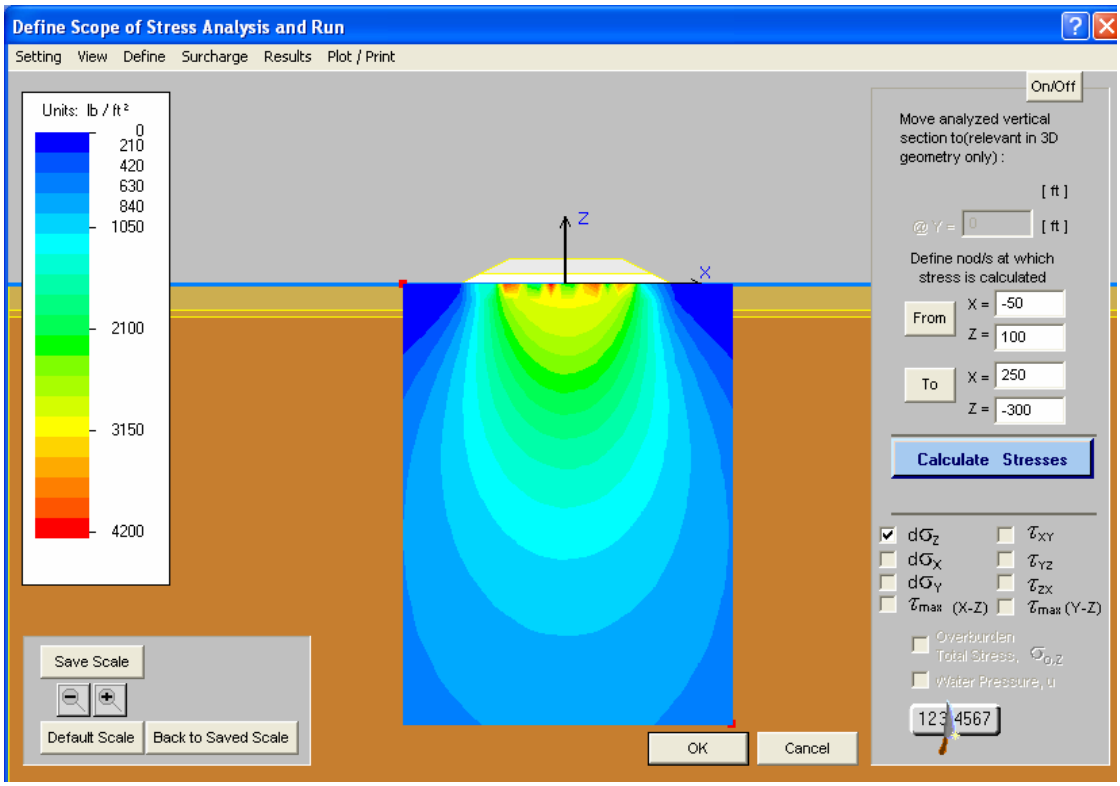

Figure E-13. Example contour plot of incremental vertical stress increase.

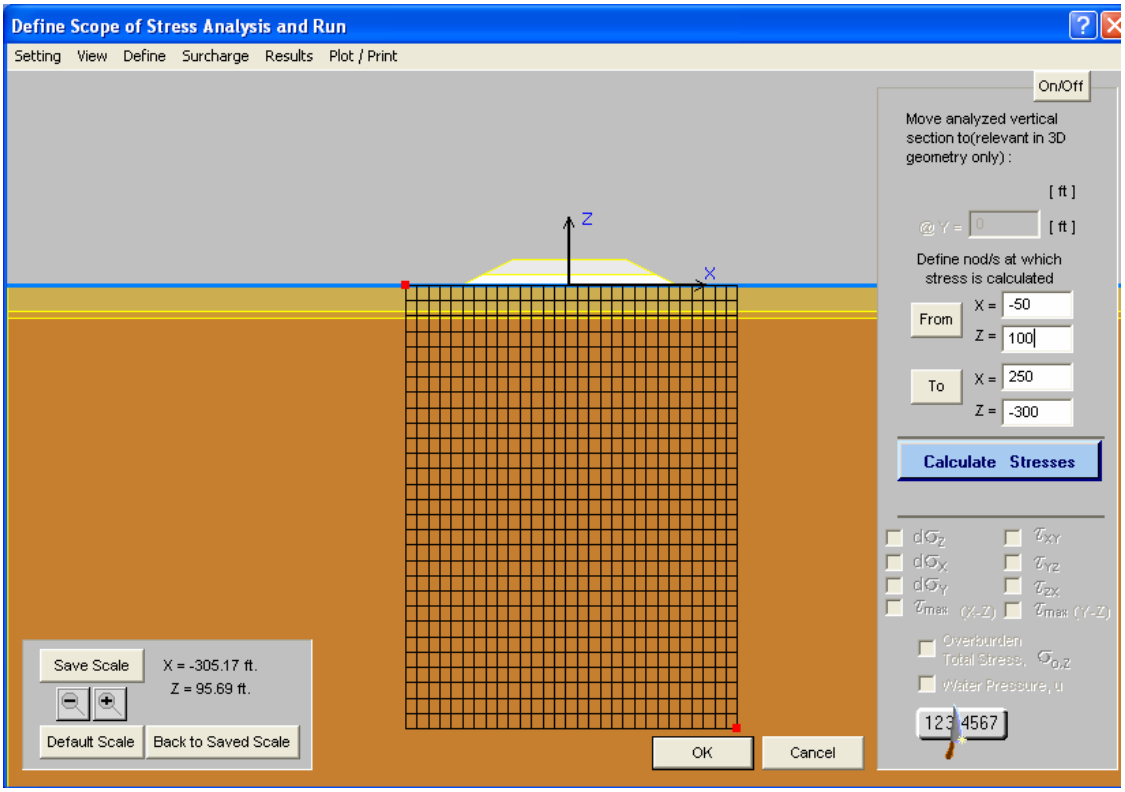

Figure E-14. Example of analysis grid used to produce Figure E-13.

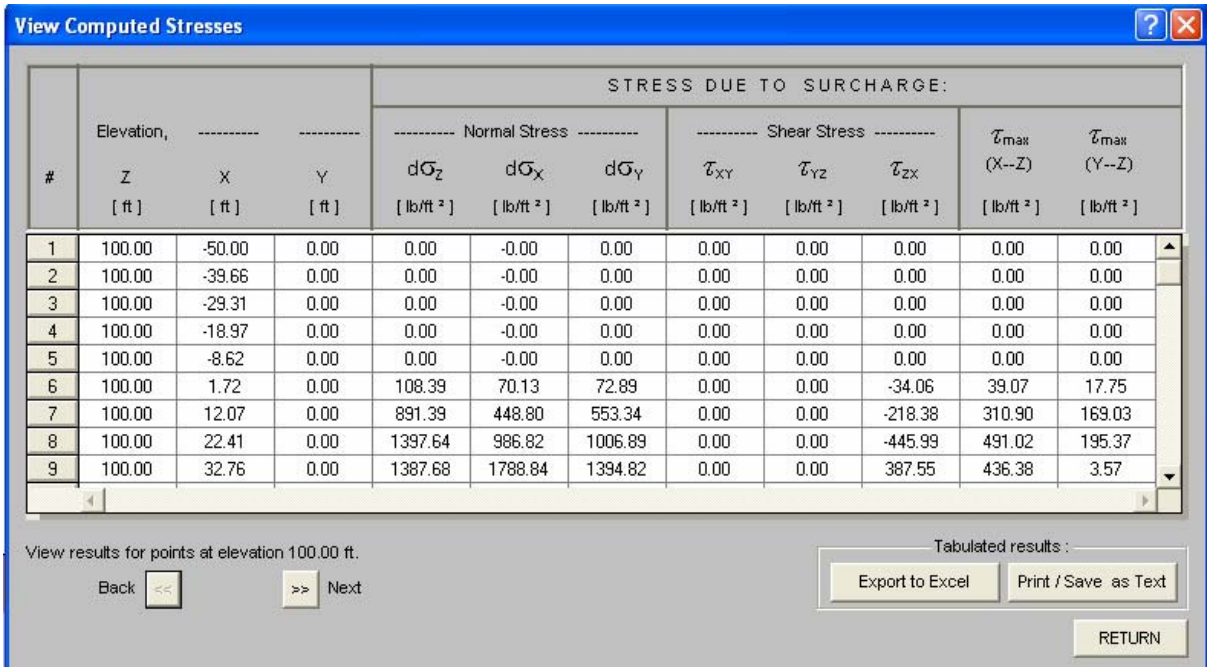

Figure E-15. Examples of results in a tabulated output format.

With regards to settlement calculations, the user can launch the "Compute Settlement" analysis independent of the stress calculations on the screen shown in Figure E-9. The resulting display from the launch is shown on Figure E-16. Calculated settlements at the base of the embankment are calculated. The user has the option to define the horizontal limits of the presented results and the number of analysis points that will be displayed. After launching "Calculate Ultimate Settlement," the user has the option to display results on a true axis or on an exaggerated vertical axis (Figure E-17). By accessing the "Results" option on the taskbar, a tabulated summary of results is presented in an Excel format similar to that previously shown in Figure E-15. Time rate of settlement calculations can also be performed, but are limited to a single horizontal location. After selecting the analysis location and performing an ultimate settlement calculation, the user launches the "Time Rate of Consolidation" button. The user selects either the time of the percent consolidation criteria for controlling the analysis, as displayed in the upper right hand corner, and then launches the analysis by selecting "Calculate" on the displayed screen. Results are presented as isochrones (Figure E-18). Results can also be presented in a tabulated format by selecting the "Tabulated Results for approximately "x days," where x was previously selected by the user (Figure E-19).

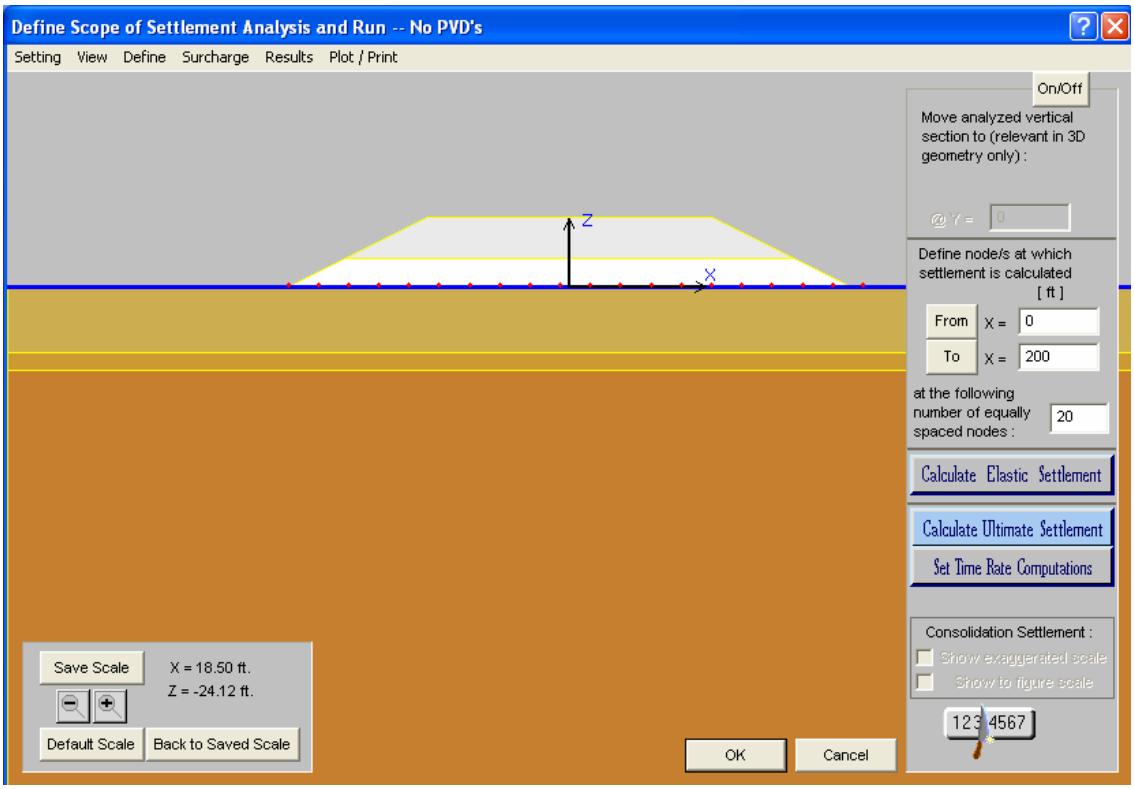

Figure E-16. Resulting screen from Launch to compute settlement.

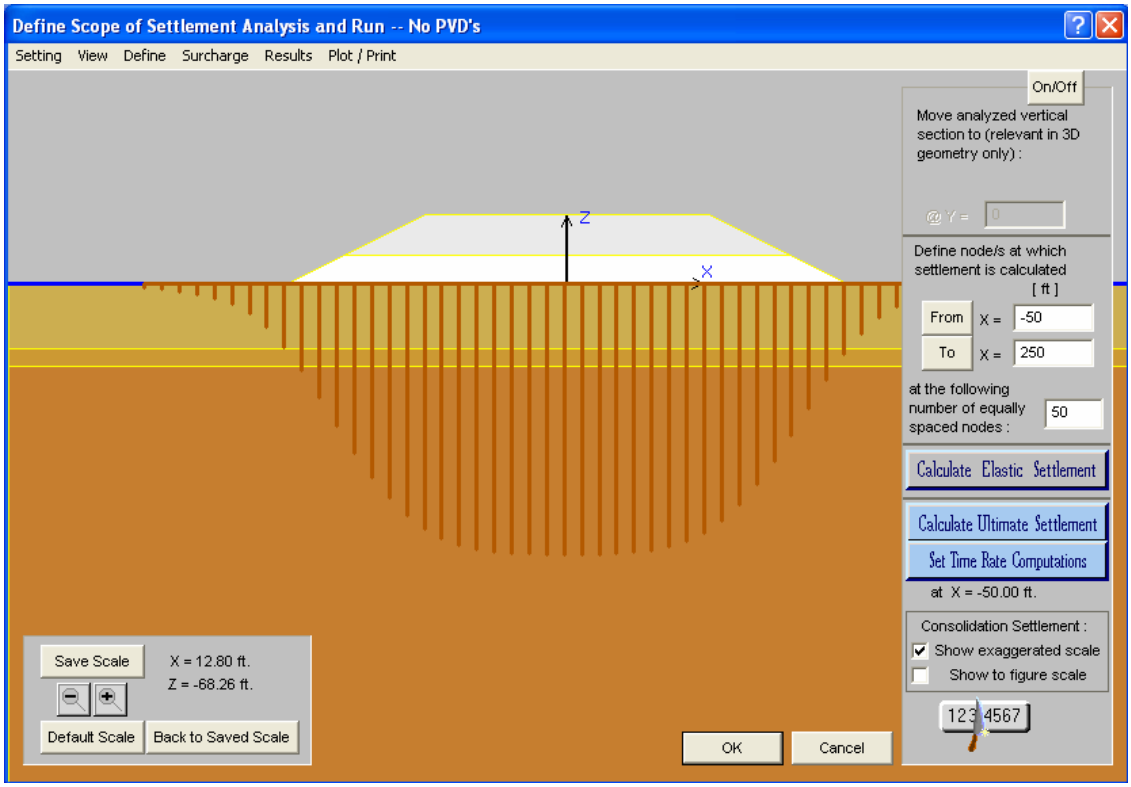

Figure E-17. Settlement results presented on exaggerated vertical axis.

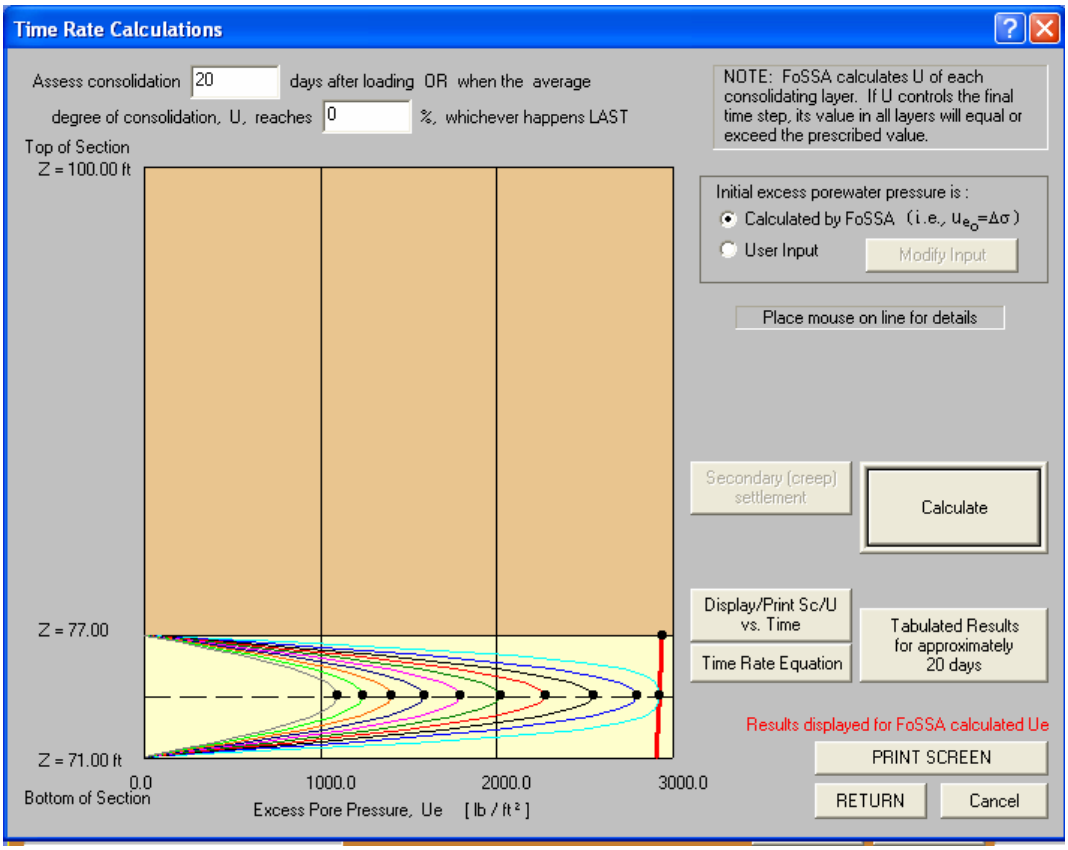

Figure E-18. Example of time rate of consolidation results.

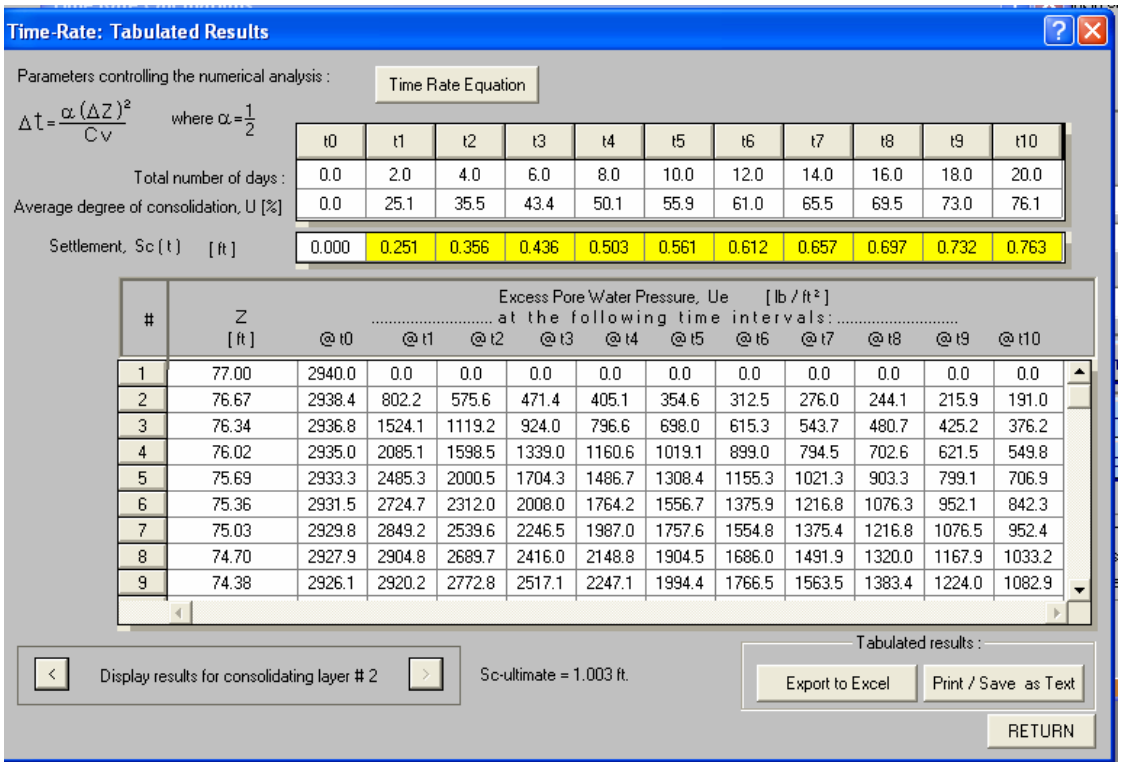

Figure E-19. Tabulated time rate of consolidation results.

FoSSA provides a significant advancement in capabilities relative to its predecessor (i.e., the DOS program EMBANK). As can be seen in this narrative summary and the selected screen shots, FoSSA is a powerful analysis tool that can greatly aid the geotechnical specialist in assessing stress distribution and settlement induced in foundation soils subjected to embankment loading. Like its sister program, ReSSA, the computer program FoSSA enjoys a fairly modest "learning curve," in that the user can be "up and running" fairly quickly. FoSSA is user-friendly and provides analysis/display options to help the user perform several "what-if" sensitivity analyses, which can be tremendously beneficial for a given project. In term of advice to the user, the authors recommend that they refer to the example programs provided by the software developers and try to re-create the published solutions. FoSSA has an extremely helpful range of example problems, Help Screens, and Users Manual to help the user increase competence and confidence in using and understanding the program.

Finally, it is always recommended that a selected solution be verified or validated using independent resources (i.e., hand calculations for approximate stress distribution and settlement or chart solutions) and that final results be reviewed by an experienced peer and senior reviewer.